Pyridine-Based 1,2,3-Triazoles: A New Class of Potential KAT2A Inhibitors and Scaffolds for C-H Activation and Catalysis

AUTHOR(S)

Roberta Pacifico

CITATION

Pacifico, Roberta (2023): Pyridine-Based 1,2,3-Triazoles: A New Class of Potential KAT2A Inhibitors and Scaffolds for C-H Activation and Catalysis. Royal College of Surgeons in Ireland. Thesis. https://doi.org/10.25419/rcsi.21104152.v1

DOI

10.25419/rcsi.21104152.v1

Pyridine-Based 1,2,3-Triazoles: a new class of potential KAT2A inhibitors and scaffolds for C-H activation and catalysis

A thesis submitted to the School of Postgraduate Studies, Department of Chemistry,

Royal College of Surgeons in Ireland, in fulfilment of the degree of

Doctor of Philosophy

By

Roberta Pacifico

Supervisor Prof. Mauro F. A. Adamo

PhD 2022

Scholar's thesis declaration

I declare that this thesis, which I submit to RCSI for examination in consideration of the award of a higher degree of Doctor of Philosophy (PhD) is my own personal effort. Where any of the content presented is the result of input or data from a related collaborative research programme this is duly acknowledged in the text such that it is possible to ascertain how much of the work is my own. I have not already obtained a degree in RCSI or elsewhere on the basis of this work. Furthermore, I took reasonable care to ensure that the work is original, and, to the best of my knowledge, does not breach copyright law, and has not been taken from other sources except where such work has been cited and acknowledged within the text.

Signed 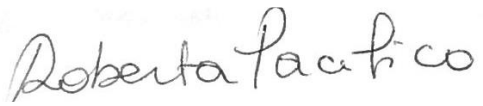

Scholar Number 181963473

Date 28/02/2022

Table of contents

Chapter 2

Pyridine-based 1,2,3-triazoles as potential lead compounds for drug discovery: Docking screening, Fluorescence Tests and Biological Evaluation.

Chapter 3

Pyridine- and proline-based 1,2,3-triazoles' applications in organic chemistry for C-H functionalisation and organocatalysis.

List of abbreviations

AchE	Acetylcholinesterase
AcOEt	Ethyl acetate
AcOH	Acetic acid
ACN	Acetonitrile
Ag(OAc)	Silver acetate
AML	Human Myeloid Leukemia
aq	Aqueous solution
Ar	Aryl
BINOL	1,1'-bi-2,2'-naphthol
Boc	*tert*-butylcarbonyl
BQ	Benzoquinone
bQSAR	Binary Quantitative Structure-property relationship
Bu_4NOAc	Tetrabutylammonium acetate
CAN	Cerium ammonium nitrate
CB1	Cannabinoid receptor 1
CDI	Carbonyldiimidazole
CML	Chronic Myelogenous Leukemia
CoA	Acetyl Coenzime A
CT	Charge transfer
Cu	Copper
CuAAC	Copper-Catalysed Azide-Alkyne Cycloaddition

$Cu(OAc)_2$	Copper acetate
$Cu(OTf)_2CH_3{*}C_6H_4$	Copper trifluoromethane sulfonate toluene complex
CuTc	$Copper_{(I)}$ thiophene 2-carboxylate
DBU	1,8-Diazabicyclo(5.4.0)undec-7-ene
DCC	*N*,*N*′-Dicyclohexylcarbodiimide
DCE	1,2-Dichloroethane
DCM	Dichloromethane
DCU	Dicyclohexylurea
DDQ	2,3-Dichloro-5,6-dicyano-1,4-benzoquinone
DMAP	*N,N*-dimethylaminopyridine
DMEDA	1,2-Dimethylethylenediamine
DMSO	Dimethylsulfoxide
EA	Electrophilic addition
ECL	Enhanced Chemiluminescence
EDG	Electron-donating group
EDTA	Ethylenediamine tetraacetic acid
ee	Enantiomeric eccess
EEDQ	*N*-ethoxycarbonyl-2-ethoxy-1,2-dihydroquinoline.
EPR	Electron paramagnetic resonance
equiv.	Molar equivalents
er	Enantiomeric ratio
ESC	Embryonic stem cell

EtOH	Ethanol
EWG	Electron withdrawing group
FG	Functional group
FMO	Frontier molecular orbital theory
GCN5	General control non-depressible 5
GNAT	GCN5-related *N*-acetyltransferase
HAT	Histone acetyl transferase
HCS	High content screening
HDAC	Histone deacetylases
HOMO	Highest occupied molecular orbital
HPLC	High Performance Liquid Chromatography
HTS	High-throughput screening
IL-2	Interleukin-2
i-Pr	*iso*-propyl
IR	Infra-red
KAT2A	Lysine Acetyltransferase 2°
KBr	Potassium bromide
KSO_4	Potassium sulfate
LUMO	Lowest unoccupied molecular orbital
Me	Methyl
MeCN	Acetonitrile
mmol	Millimoles

$NaHCO_3$	Sodium bicarbonate
Na_2SO_4	Sodium sulfate
NHC	*N*-heterocyclic carbene
NMP	*N*-methyl pyrrolidone
NMR	Nuclear magnetic resonance
OA	Oxidative addition
PA	Picolinic acid
Pd	Palladium
$Pd(OAc)_2$	Palladium acetate
PE	Petroleum ether
Ph	Phenyl
$PhI(OAc)_2$	(Diacetoxyiodo)benzene
PMA	Phorbol-12-myristate-13-acetate
Pt	Platinum
Py	Pyridine
Py-TA	Pyridine-triazole acid
QA	Quinaldic acid
Rh	Rhodium
RT	Room temperature
Ru	Ruthenium
RuAAc	Ruthenium-Catalyzed Azide-Alkyne Cycloaddition
$Ru(Cp)Cl_2$	Pentamethylcyclopentadienyl ruthenium dichloride

SAHA	Suberanilic hydroxamic acid
SET	Single-electron transfer
TAA	1,2,3-triazole-4-carboxylic acid
TA-Py	Triazole-pyridine amide
TBP	Tert-butyl peroxide
TCR	T-cell receptor
TEA	Triethylamine
TEB	Triton extraction buffer
THF	Tetrahydrofuran
TLC	Thin layer chromatography
$TMSN_3$	Trimethylsilyl azide
Tosyl	*p*-toluenesulfonyl
XPhos	2-Dicyclohexylphosphino-2′,4′,6′-triisopropylbiphenyl
5-FITC	Fluorescein isothiocyanate
P300/CBP	CREB-binding protein p300
σ-BM	σ-bond metathesis
H3K9	Histone H3 lysine 9

Aim

This thesis is focused on the synthesis of new pyridine-based 1,2,3-triazoles to be employed as potential scaffolds for drug discovery and for diverse applications in organic chemistry such as C-H activation and organocatalysis. In particular, this thesis will focus on the biological importance of the synthesised pyridine-based triazoles as potential inhibitors of the KAT2A protein and on their transformations through copper- and palladium- catalysed C-H activations into potentially active compounds. Moreover, it is also described the attempted synthesis of proline-based organocatalysts, enclosing a triazole moiety in their backbone, that will be further evaluated for future applications in organocatalytic reactions such as aldol condensations, Mannich and Michael reactions.

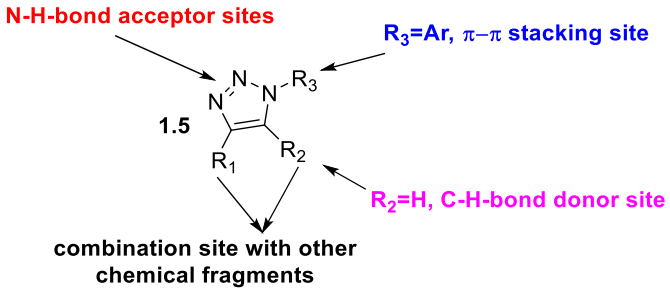

Abstracts

Chapter 1

In this chapter, the synthesis of new pyridine-based 5-hydroxy-triazoles was attempted. The reaction protocol adopted has been already successfully employed in the Adamo's group for the synthesis of aryl-based 5-hydroxy-triazoles and takes advantage of a free-catalyst cycloaddition occurring between active methylene compounds and pyridyl azides. Pyridine moieties are well known as ligands, organocatalysts and templates for fragment-based drug discovery, therefore the scope for this study was to include the pyridine unit in hydroxy-triazoles.

Chapter 2

The triazole pharmacophore is one of the most important well-known heterocycles which is a common and integral feature of a variety of natural products and medicinal agents. It is present as a core structural component in an array of drug categories such as antimicrobial, anti-inflammatory, analgesic, antiepileptic, antiviral, antineoplastic agents etc. In this chapter 1,4-disubstituted pyridine-based triazoles were turned into a small library of compounds that were

docked with a range of important biological targets (enzyme and proteins). This study allowed the identification of specific molecule/target selective interactions. The highest compound-protein binding scores proved our molecules to be quite selective and specific for a particular protein. Therefore, appropriate fluorescence tests were set up to quantify their activity against the target chosen, and biological evaluation followed for the final assessment.

N.B. Chapter 2 experiments have been performed either in RCSI and in collaboration with other institutions in Italy under the supervision of the PhD candidate.

Chapter 3

C-H functionalisation has been known for decades as one of the most efficient methods to create new C-X bonds allowing production of new molecules to be used in a pletora of fields including medicinal chemistry, material chemistry and agriculture. The possibility to selectively activate a specific C-H bond through metal coordination, has been hugely explored as a powerful tool to overcome the many synthetic steps a classic cross-coupling reaction requires. Furthermore, C-H activation allows the potential to develop new compounds of biological interests by simply substituting one single C-H bond with another functional group that may better fit the pharmacological target. For this reason, we attempted the C-H functionalisation of triazoles **2.80a-e** with linear or cyclic aliphatic amines and substituted phenyl compounds to form either new C-N or C-C bonds. Given the activity showed by triazole **2.80b** against KAT2A (see *Chapter 2*), we hypothesised the possibility to create new biologically active molecules by introducing different moieties through C-H functionalisation. Additionally, we also attempted to the synthesis of new potential triazole-based catalysts that incorporate a proline moiety within the backbone. Proline is renowed for being a powerful catalytic source, given its nature as bifunctional aminoacid, and 1,2,3-triazoles, bearing diverse activation sites, which are known to be excellent metal-coordinators.

Acknowledgements

I am delighted to acknowledge the institution and all the people that contributed to this unforgettable journey that is the PhD. Firstly, I would like to thank the Royal College of Surgeons in Ireland and, particularly, the Department of Chemistry, for having been my home these past 4 years and for having provided me with everything I needed to achieve my PhD. I also thank the Irish Research Council (project GOIPG/2018/3165) for funding my PhD project and my supervisor, Prof. Mauro F.A. Adamo, for having been my mentor during these years and for all his advice that let me build my professional skills.

I also particularly enjoyed building connections and collaborations with different groups outside RCSI that contributed to realising some of the experiments in my thesis. In particular, I would like to thank Prof. Gabriele Cruciani and Dr. Lydia Siragusa from Molecular Horizon Srl, Bettona, Italy and from the Laboratory for Chemometrics and Molecular Modeling, Department of Chemistry, Biology, and Biotechnology, University of Perugia, Perugia (PG), Italy, for their precious help with the docking screening of my compounds. I also acknowledge Prof. Lucia Altucci, Dr. Nunzio del Gaudio, Dr. Menotti Ruvo, and Guglielmo Bove from the Department of Precision Medicine, University of Campania Luigi Vanvitelli, and Institute of Biostructures and Bioimaging, Consiglio Nazionale delle Ricerche, Naples, Italy for their invaluable contribution to my work by performing the *in vitro* assays of my compounds against leukemia cell lines.

A huge thanks to all the beautiful people I met during this fulfilling experience for having become my best friends and my family for 4 years. I would also like to thank my best friends from all over the world who never failed to make me feel loved, understood, and supported, even if thousands of miles were between us. Finally, a massive thanks to my family, who has always supported and encouraged me, and to my boyfriend, who has always been by my side at every step of this journey and has never let me fall in the darkest moments.

Chapter 1

Synthesis of pyridine-based 1,2,3-triazoles *via* DBU-promoted cycloaddition and copper catalysis.

1.1 Introduction

1.1.1 1,2,3-triazoles: electronic features

Triazoles belong to the organic chemistry class of five-membered ring heterocycle containing three nitrogens. Generally, 1,2,3-triazoles derive from the replacement of one or two methines groups in pyrroles, thiophenes or furans with nitrogens. The insertion of one or more nitrogen atoms decreases the energy levels of the π-orbitals making 1,2,3-triazoles less "π-electron rich".[1] They exist as two isomeric forms namely 1,2,3-triazole (Figure 1, **1.1a-c**) and 1,2,4-triazole (Figure 1, **1.2a-c**). Both isomers share the possibility to exist each in three tautomeric forms (tautomers are structural isomers of chemical compounds that rapidly interconvert): 1*H*-1,2,3-triazole **1.1b** and 3*H*-1,2,3-triazole **1.1a**, formally being the same tautomer, and 2*H*-1,2,3-triazole **1.1c**, with regards to 1,2,3-triazoles, plus 1*H*-1,2,4-triazole **1.2a**, 2*H*-1,2,4-triazole **1.2b** and 4*H*-1,2,4-triazole **1.2c**, with regards to 1,2,4- triazoles (Figure 1).[2]

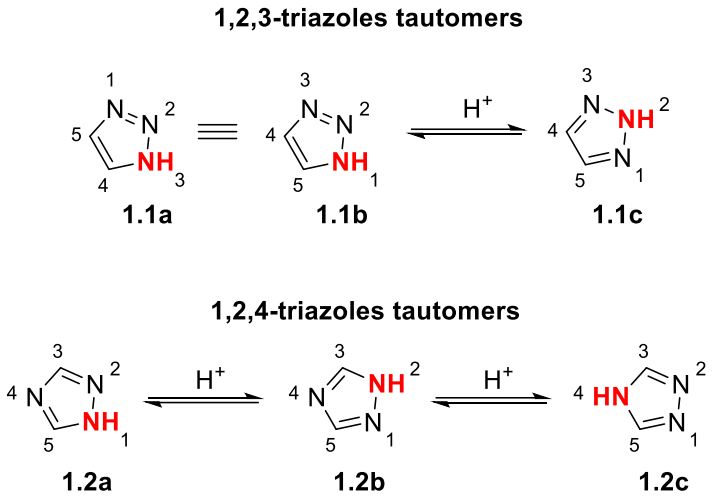

Figure 1: 1*H* (3*H*) and 2*H*-1,2,3-triazoles **1.1a-c** versus 1*H,* 2*H* and 4*H*-1,2,4-triazoles **1.2a-c** tautomerism.

The relative stability of the tautomers is influenced by the interactions between the substituents and the proton delocated on the three nitrogens. With regards to 1,2,4-triazoles, when electron withdrawing substituents are present, the 1*H* tautomer **1.2a** is favoured, whereas with electron donating substituents, the 2*H* tautomer **1.2b** is favoured. Considering, instead, the electronic nature of 1,2,3- triazole tautomers **1.1a-c**, the three of them exist in equilibrium with each other given the low energies requirements for the intermolecular proton transfer.[3] The 2*H*-1,2,3 triazole **1.1c** can be assumed as the most stable tautomer in gas phase, whereas the 1*H*- tautomer **1.1b** is mostly stable in solution, because of dipole interactions with the solvent.[4,5] Furthermore, 1*H*

tautomer's **1.1b** stability is increased by the *N*-2 character of both pyridine-type (Figure 2 in blue) and pyrrole-type (Figure 2 in red) nitrogens due to the absence of electrostatic repulsion between the adjacent σ lone pairs (Figure 2).[6] Since 1,2,3-triazoles display both pyridine and pyrrole type nitrogens atoms, frontier molecular orbitals also reflect different energy levels depending on the nitrogen atom-type involved in the reaction. More specifically, the pyrrole-like nitrogen acts as π-donating and σ-accepting, given the inclusion of the *NH* lone pair in the aromatic π sextet. On the other hand, the pyridine-like nitrogen displays an additional σ lone pair, giving greater π deficiency thus its strongly π –accepting behavior, while being weakly σ-donating.[7] Accordingly, the HOMO (Highest Occupied Molecular Orbital) and LUMO (Lowest Unoccupied Molecular Orbital) orbitals are, respectively, stabilised and destabilised when looking at the alternation of the π-accepting pyridine-type nitrogen and π-donating pyrrole-type nitrogen of the 1*H*- and 2*H* tautomers of 1,2,3-triazoles (Figure 2).[8]

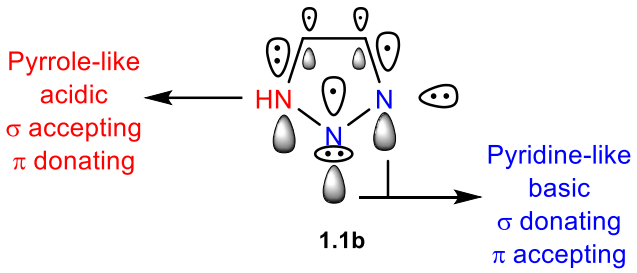

Figure 2: Features of the electronic structure of 1*H*-1,2,3-triazole **1.1b**.

1,2,3-triazoles can be further subdivided into two other main classes, namely, 1,2,3-benzotriazoles **1.3a,b** and 1,2,3-triazolium salts **1.4a,b** (Figure 3).

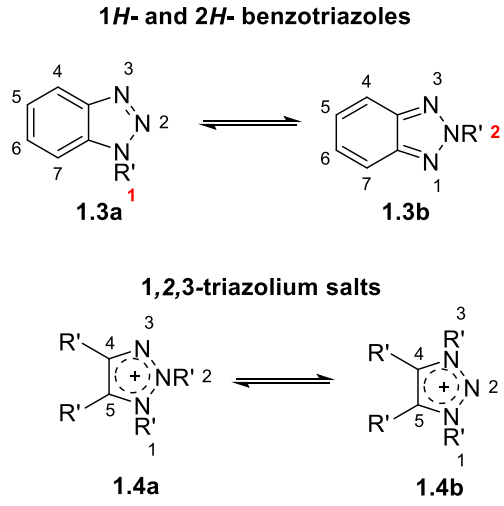

Figure 3: 1*H*- and 2*H*- benzotriazoles **1.3a,b** and 1,2,3-triazolium salts **1.4a,b** classes.

Monocyclic 1,2,3-triazoles **1.1** and benzotriazoles **1.3** are undoubtedly the most stable towards hydrolysis, oxidative conditions and enzymatic degradation.[5] Additionally, alkylation of the nucleophilic nitrogen allows for the formation of triazolium salts **1.4**. When subjected to pyrolysis or photolysis, 1,2,3 triazoles **1.5** can produce very reactive species because of the extrusion of nitrogen. This results in the formation of a wide range of compounds like nitriles **1.6**, ketenimines **1.7**, azirines **1.8**, etc (Figure 4).

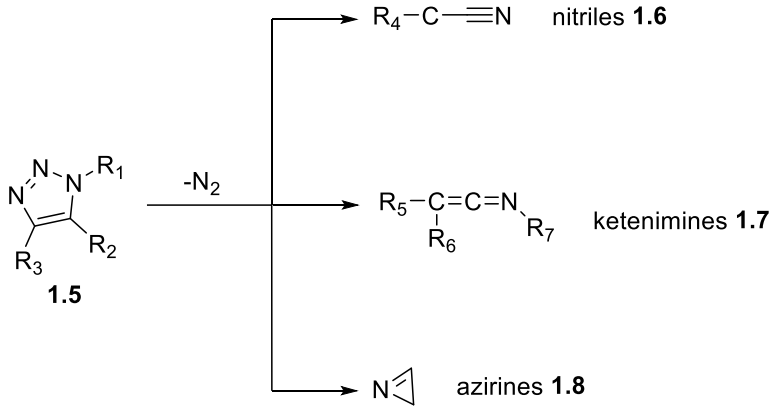

Figure 4: Decomposition products **1.6-1.8** of 1,2,3-triazole **1.5**.

Furthermore, the triazole nucleus benefits from its aromatic nature to increase its stability. Specifically, a cross conjugation, defined by Phelan as "a system possessing three unsaturated groups, two of which, although conjugated to a third unsaturated center, are not conjugated to each other",[9] occurs in these molecules rather than a proper π conjugation. This can be explained when considering that the lone pair on the pyrrole-type nitrogen (*N*1 position) cannot be delocalized to create consecutive "single bonds".[10] Consequently, an aromatic sextet **1.9b** and **1.10b** is formed by donation of one π electron from each atom connected by double bonds, in addition to the remaining two electrons from a nitrogen atom (Figure 5)[11]. This aromaticity in triazoles is evidently shown in the much shorter C-C, C-N and N-N bonds than the corresponding normal single bonds.[12] The same analysis can be carried out on triazolium salt **1.10** which bond distances and reactivity can be explained by limit formulas **1.10b**-**1.10d** (Figure 5).

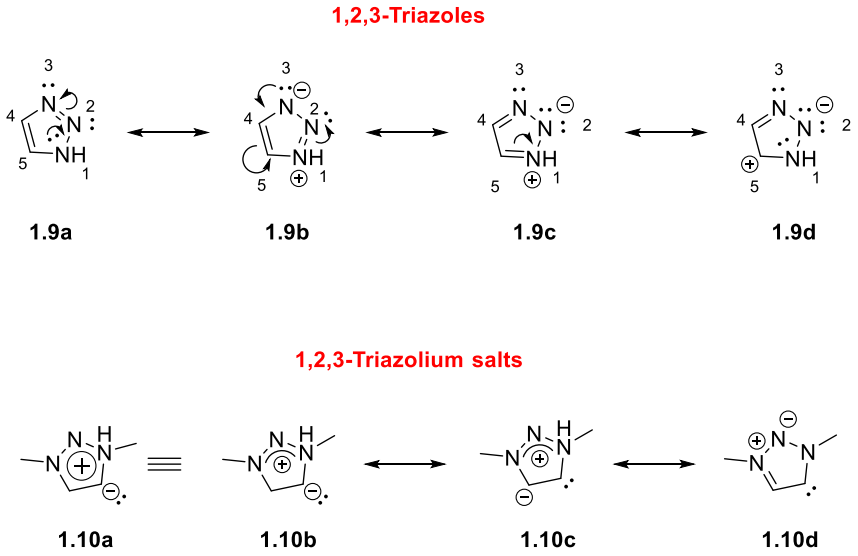

Figure 5: Resonance structures of 1,2,3-triazoles and 1,2,3-triazolium salts (**1.9** and **1.10** respectively) and their contribution to aromaticity.

1.1.2 1,2,3-triazoles: acid-base behavior

1,2,3-triazoles benefit from being either acidic or basic due to the pyridine/pyrrole-type nitrogens presence. Generally, the basicity of 1,2,3-triazoles is, for the most part, connected to the pyridine-like nitrogen and decreases with additional pyrrole-type nitrogens in adjacent positions.[13] In particular, the 1*H*- tautomer **1.1b** (Figure 1) shows two basic centers corresponding to the two pyridine-type nitrogens at position 2 and 3 while the 2*H*- tautomer **1.1c** (Figure 1) exhibits a weaker basic strength connected to the two pyridine-like basic centers, at positions 1 and 3 because of the *N*2 position in between.[14] Usually, 5-membered heterocyclic compounds containing oxygen or sulfur, possess a stronger acidity compared to nitrogen-based 5-membered heterocycles like triazoles due to the greater ability of oxygen and sulfur of stabilising negative charges. Consequently, carbanions formed in the adjacent positions will have higher stability. On the other hand, nitrogen-based 5-membered heterocycles' acidity is, typically, related to the hydrogen position (in case of 1,2,3-triazole, crucial is the close proximity to the pyrrole- or pyridine-type nitrogens) and to the nature of eventual *N*-substituents. The greater the substituent electron withdrawing character, the stronger the acidity of the heterocyclic proton.[15] Undoubtedly, 1,2,3-triazoles most acidic proton is the one related to the *CH* position close to the pyrrole-type nitrogen. As consequence, deprotonation pK_a values reach 35.0 for the C4 position and 27.8 for the C5 position (when considering deprotonation of 1-methyl-1*H*-1,2,3-triazole in DMSO, Table 1). These values are significantly lower than the ones showed for benzene **1.11**, which pK_a deprotonation values are only set at 44.7 in DMSO (Table 1).[16]

Table 1: pK_a values comparison of different aromatic and heterocyclic compounds.

Compound	pK_a (azole, CH, DMSO)	pK_a (azole, NH, water)	pK_a (azolium, water)
Benzene 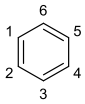 **1.11**	44.7	-	-
Pyridine 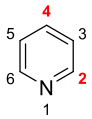 **1.12**	40.3 (C4), 43.6 (C2)	-	-
Pyrrole 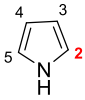 **1.13**	38.8 (C2)	16.5	-
Pyrazole 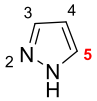 **1.14**	33.8 (C5)	14.2	2.5
1H-1,2,3 Triazole 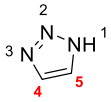 **1.15**	35.0 (C4), 27.8 (C5)	9.3	1.3

The acidity of the C-H position offers, also, the possibility to use 1,2,3-triazoles as versatile scaffolds for C-H activation and consequent substitution with various electrophiles (*Chapter 3*).[17] Diversely, the N-H acidity contribution is mainly visible in solution and depends on the number of total nitrogen ring atoms.[14]

1.2 Synthesis of 1,2,3-triazoles

1.2.1 Huisgen 1,3-dipolar cycloaddition

The synthesis of 1,2,3-triazoles has been a challenging and attractive topic for many years and several strategies are available for their preparation. 1,3-dipolar cycloaddition, better known as Huisgen cycloaddition, has been known as one of the first synthetic method through which 1,2,3-triazoles started to be produced. This procedure can be classified as an innovative and important system to synthesise heterocyclic species by creation of new σ-bonds at the expense of the π-ones (Figure 6).

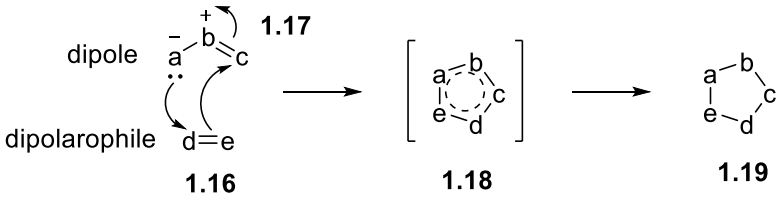

Figure 6: General mechanism of Huisgen 1,3-dipolar cycloaddition.

The species that participate at the reaction are known as 1,3-dipoles **1.17** and dipolarophiles **1.16**. 1,3-dipoles **1.17** are characterized by the presence of an atom with an incomplete sextet and a formal positive charge (electrophilic site), and an atom with an electron octet and a negative formal charge (nucleophilic site).[18] Furthermore, this chemical moiety can exist as either an allyl-type **1.21** or as propargyl/allenyl type **1.20** zwitterionic sextet/octet structures.1,2,3-triazoles can be considered as propagyl-allenyl type (**1.20**) of 1,3-dipoles, thus, possessing almost a linear configuration (Figure 7).[19]

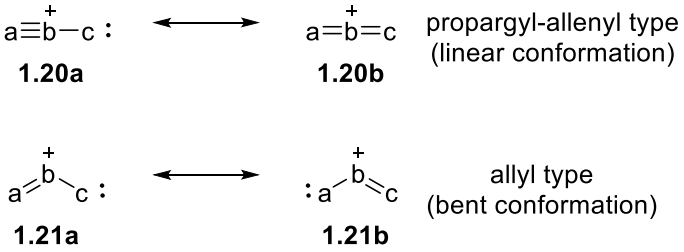

Figure 7: Allyl and propargyl-allenyl type conformations **1.20** and **1.21** respectively.

On the other hand, the dipolarophile **1.16** is a chemical entity that contains a multiple bond system capable of interacting with the 1,3-dipole **1.17** towards a cycloaddition reaction. Usually a dipolarophile is represented by alkenes and alkynes but heteroatomic molecules such as carbonyls or imines can also be considered capable of participating in 1,3-cycloaddition reactions.[18] The concept of 1,3-dipolar cycloaddition was first discovered by Michael in 1893.[20] He reacted phenyl azide **1.22** with dimethyl

acetylenedicarboxylate **1.23** discovering one of the first synthetic approach for the formation of 1,2,3-triazoles **1.24** (Scheme 1).[21,22]

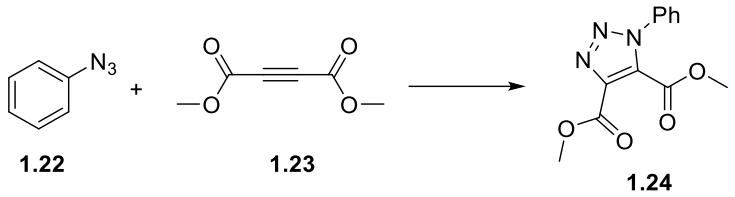

Scheme 1: Michael's first attempt to the synthesis of phenyl substituted 1,2,3-triazole **1.24**.

Huisgen later identified Michael's discovery as a [3+2] 1,3-dipolar cycloaddition of a 1,3-dipole to a multiple bond. According to Huisgen, the 1,3-dipolar cycloaddition proceeds through a concerted pericyclic mechanism in which the 1,3-dipole allyl-type molecule **1.21** acts with a π_4 fashion while the dipolarophile **1.20** acts as π_2 reactant,[18,23–25] in accordance with what also Woodward and Hoffman proposed few years later.[26] In spite of that, reaction rates and regioselectivity were still inexplicable until Sustmann *et al*.[27] and Houk *et al*.[28] proposed to justify this behavior through the Frontier Molecular Orbital theory (FMO). According to the FMO theory, three types of HOMO-LUMO overlapping possibilities exist. Furthermore, the FMO theory predicts that the concerted mechanism only occurs with the smallest HOMO-LUMO energy gap. Therefore, the superimposition can happen as:

a) **HOMO-controlled dipole**, in which the 1,3-dipole **1.25** has a high-lying HOMO that overlaps with the dipolarophile **1.26** LUMO (Type I, Figure 8).

b) **HOMO-LUMO controlled dipole**, in which the HOMO of the 1,3-dipole **1.25** can pair with the dipolarophile **1.26** LUMO and vice versa. The small energy gap between the two orbitals is given by the chance of both EWGs and EDGs on the dipolarophile **1.26** and the 1,3-dipole **1.25** to accelerate the reaction reducing the activation energy gap (Type II, Figure 8).

c) **LUMO-controlled dipole**, in which the 1,3-dipole **1.25** low-lying LUMO pairs with the dipolarophile **1.26** HOMO (Type III, Figure 8).[29]

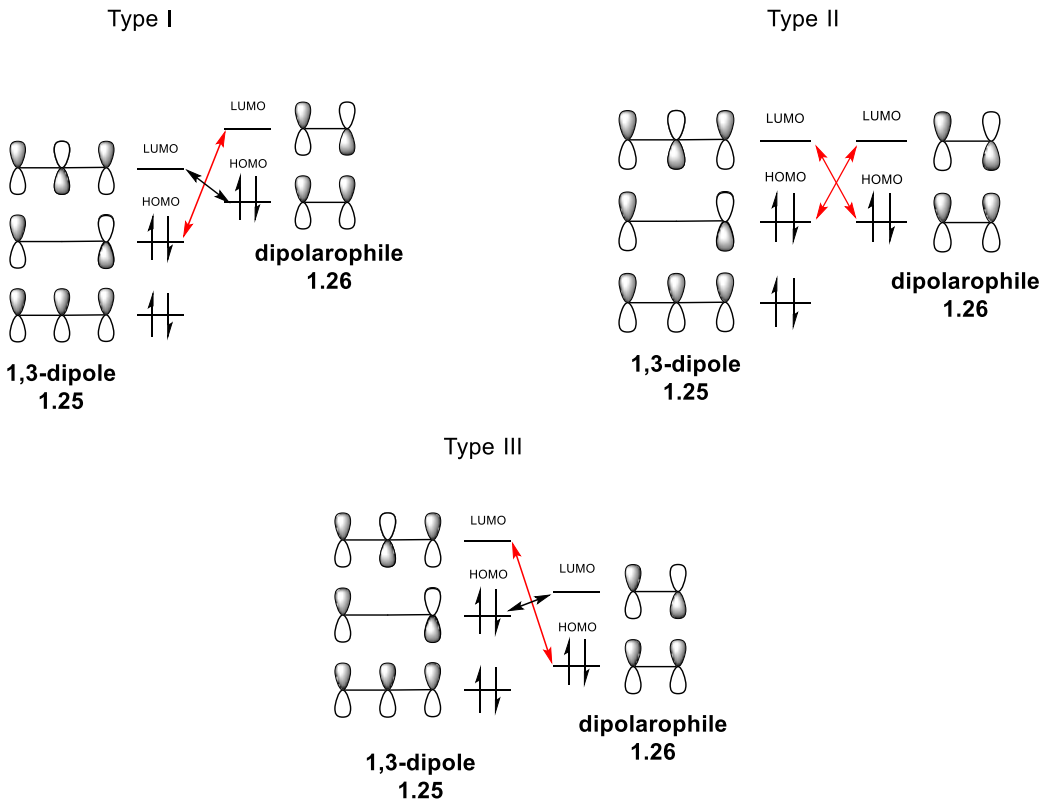

Figure 8: Sustmann's classification of 1,3-dipolar cycloadditions and Houk's terminology.

In line with a concerted mechanism, it seems that the 1,3-dipolar cycloaddition proceeds *via* LUMO-controlled dipole. The reaction rate appears to be independent from the solvent chosen as well as from the nature of the substituents (that also does not influence the formation of a specific regioisomer). Therefore, a HOMO-raising electron-donating group (EDG) as well as LUMO- lowering electron-withdrawing group (EWG) enhance the rate of reaction. Moreover, these groups polarise the π-system that affects the regioselectivity due to the interaction occurring between orbitals with the largest coefficient of overlap.[30] Notably, EWG groups at position C5 of 1,2,3-triazoles cause a reversible ring opening at the *N*1-*N*2 bond: in particular, when the C5 substituent is represented by a primary amine **1.27a**, an interconversion between triazole's exocyclic **1.27b,c** and cyclic form **1.27a,d** occurs (known as Dimroth's rearrangement, Scheme 2).[31]

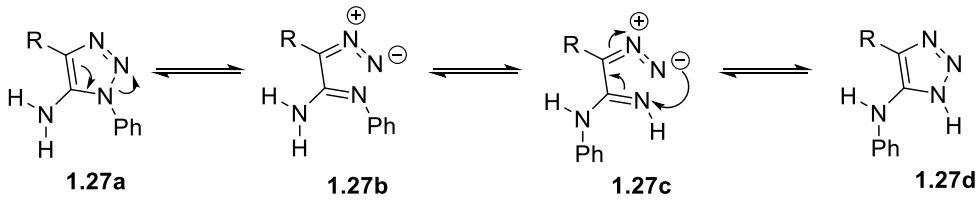

Scheme 2: Dimroth's rearrangement.

On the other hand, Firestone envisaged a completely different pathway. Their proposal involved a two-step reaction in which the rate determining step produces a spin paired di-radical species. This intermediate is formed when 1,3-dipoles **1.21**, according to Firestone, lose their allylic resonance energy when reacted with dipolarophiles. Given that, Firestone claimed that a di-radical mechanism (**1.28**) corroborates the similar reactivity of olefins and acetylenes (Figure 9).[32] Nowadays, after much debate, the Huisgen version is the only accepted mechanistic proposal.

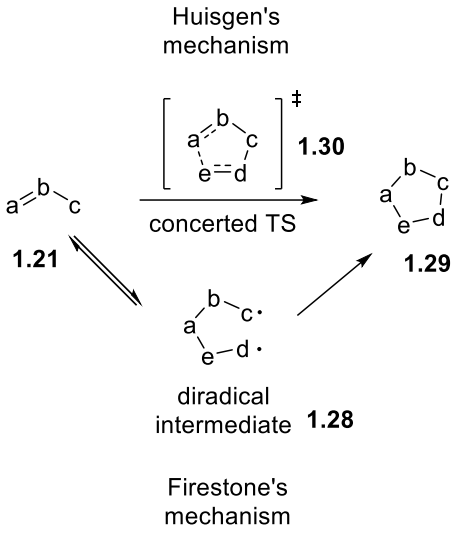

Figure 9: Huisgen's and Firestone's proposed mechanism for 1,3-dipolar cycloaddition.

1.2.2 Copper catalysed azide-alkyne cycloaddition (CuAAC)

The copper$_{(I)}$- catalysed azide-alkyne cycloaddition (CuAAC) strategy to synthesise 1,2,3-triazoles was discovered, independently, by Sharpless *et al*.[33] and Meldal *et al*.[34] Sharpless demonstrated that an uncatalysed reaction between organic azides and alkynes proceeded slowly following the fundamentals of the Huisgen 1-3 dipolar cycloaddition. Furthermore, it required high temperatures and the overall process was unselective: this means that the Huisgen cycloaddition produced equimolar mixtures of both 1,4- and 1,5- 1,2,3-triazole regioisomers. Copper$_{(I)}$ (Cu) is capable of drastically improving the reaction rate as well as the regioselectivity towards the 1,4 regioisomer. Generally, $Cu_{(II)}$ salts are the most used copper catalysts in CuAAC reactions; however, only $Cu_{(I)}$ is known to be the active species promoting this reaction. Indeed, if $Cu_{(II)}$ salts are used alone, they are incapable of forming the copper-acetylide complex that initiates the cycloaddition. For this reason, Sharpless and Fokin introduced a reducing agent, sodium ascorbate, to the standard procedure. The latter had the enormous advantage to be performed in aqueous media with, eventually, organic co-solvents like alcohols or DMSO to improve reagents solubility. An aqueous solution of sodium ascorbate, in conjunction with $Cu_{(II)}$ salts, prevents the $Cu_{(I)}$ intermediate from

disproportionation to $Cu_{(II)}$ and $Cu_{(0)}$ and from re-oxidation to $Cu_{(II)}$ through contact with air.[33,34] It is also possible to introduce $copper_{(I)}$ sources straight to the reaction mix, without having them being formed *in situ,* as aforementioned. Despite the advantages of having $copper_{(I)}$ species ready to be used (mostly represented by copper iodide (CuI), copper triflate benzene complex ($CuOTf*C_6H_6$) and $copper_{(I)}$ tetrakis(acetonitrile) hexafluorophosphate $[Cu(H_3CCN)_4][PF_6]$), this latter strategy requires inert atmosphere and anhydrous conditions. Furthermore, co-solvents like acetonitrile and auxiliary bases, such as 2,6-lutidine and triethylamine, are also required. Mechanistically speaking, CuAAC proceeds through the following steps: in the first instance a $Cu_{(I)}$ (Scheme 3, **1.31**) species binds an alkyne through a π-coordination (Scheme 3, **1.33**). This bond substantially increases the CH-acidity of the terminal alkyne allowing the formation of a σ-coordinated $Cu_{(I)}$-acetylide (Scheme 3, **1.34**).[35] An azide (Scheme 3, **1.35**), then, coordinates the copper metal center generating a π-coordinated $Cu_{(I)}$ complex (Scheme 3, **1.36**). Coordination of the azide **1.35** can occur at either the terminal or substituted nitrogen.[36] Nevertheless, the substituted nitrogen is the one preferred for the reaction to happen because of its π-donating features that increase the electron density on the metal center. The affinity of $Cu_{(I)}$ towards the α-carbon of the alkyne **1.32**,[37] which is responsible for the nucleophilic attack of the alkyne β-carbon at the terminal electrophilic nitrogen,[38] can explain the high selectivity for the 1,4- regioisomer **1.39** produced from the copper-catalysed cycloaddition (Scheme 3).[39] Finally, copper extrusion *via* reductive elimination (**1.37**) and subsequent protonolysis of the copper-triazolide complex (**1.38**), generate the desired 1,2,3-triazole (**1.39**) and allow copper to re-enter the catalytic cycle (Scheme 3). Based on these premises, many scientists have speculated whether or not the CuAAC proceeds *via* a mononuclear or dinuclear pathway. Sharpless firstly proposed a mononuclear fashion that evolved towards the product (Scheme 3, **1.39**) *via* the formation of a six-membered $Cu_{(III)}$ metallacycle (Scheme 3, **1.37**). **1.37** then undergoes ring contraction to release the product (Scheme 3, **1.39**).[33]

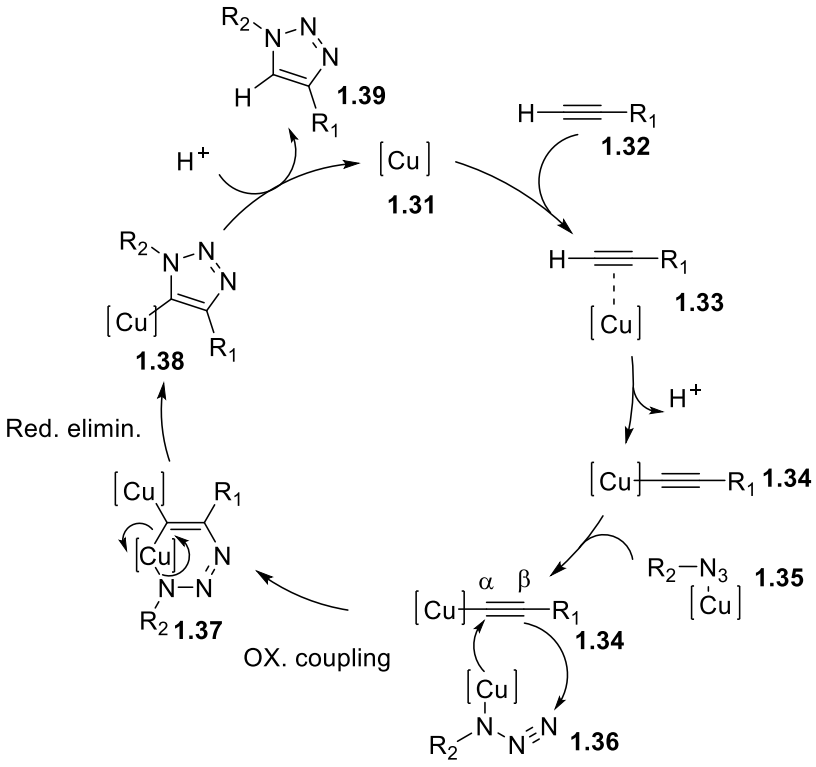

Scheme 3: General scheme of CuAAC cycloaddition.

A couple of years later, Fokin and Finn proposed a dinuclear fashion after reacting different heterocyclic ligands with dansyl azide **1.45** (Scheme 4). They found that the rate of reaction was second order with respect to $Cu_{(I)}$ concentration, suggesting the presence of a dinuclear intermediate species (Scheme 4, **1.40** and **1.41**).[40] It is believed that, once the alkyne-copper$_{(I)}$ complex is formed (Scheme 4, **1.43**), a neighbouring $Cu_{(I)}$ can attract another acetylide ligand. This sets up an equilibrium between intermediate **1.44** and **1.43**. This equilibrium, however, is unproductive as only when the azide (Scheme 4, **1.45**) coordinates a neighbouring copper, does the reaction benefit from the active intermediate formed (Scheme 4, **1.46**) and proceed further to completion of the cycloaddition mechanism (Scheme 4, **1.49**). Following this hypothesis, acetylide **1.43** does not bind to the azide **1.45** but, instead, to another copper center. According to Fokin and Finn, after formation of **1.46**, the reaction proceeds straight to ring contraction and formation of the product (Scheme 4, **1.49**).[40] On the other hand, van Maarseeven proposed a revised formulation for this mechanism introducing a potential intermediate (Scheme 4, **1.50**) that could be considered similar to the six-membered metallacycle described by Sharpless. According to Maarseeven, **1.50** is believed to be the dinuclear species formed before the transition from **1.46** to **1.47** (Scheme 4).[41] Throughout the years, others sustained and proved the existence of a dinuclear mechanism for the CuAAC rather than a mononuclear one such as Ahlquist and Fokin,[37] Cantillo[42] and Heaney.[43] All agreed on the impossibility for the CuAAC proceeding *via* a

mononuclear pathway due to a high energy barrier belonging to the ring strain in the cyclic $Cu_{(III)}$ intermediate (**1.37**, Scheme 3). The *sp* carbon in the Cu=C=C fragment prefers a 180°C angle that is impossible to recreate in a six-membered cycle. It is more plausible to accept the existence of two $Cu_{(I)}$ centers that bind the acetylide molecule (**1.50**, Scheme 4).

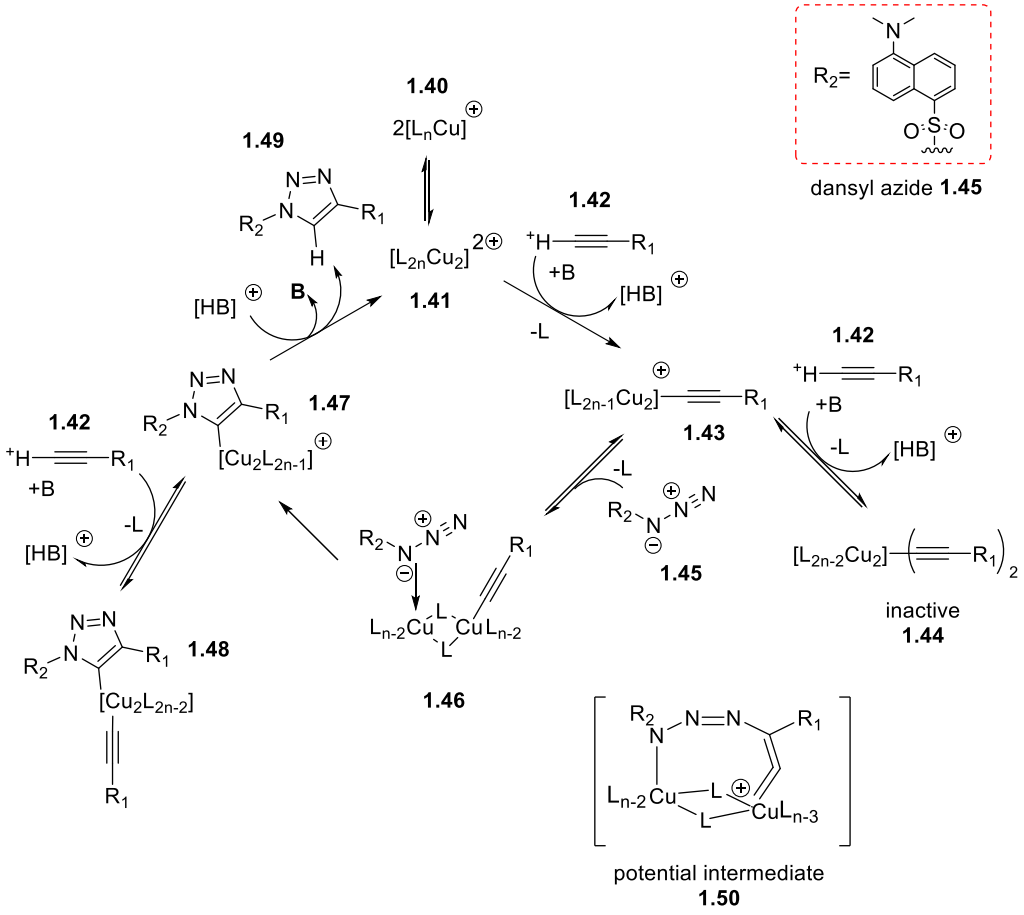

Scheme 4: Proposed mechanism for the CuAAC dinuclear pathway by Fokin, Finn and Maarseeven.

1.2.3 Ruthenium catalysed azide-alkyne cycloaddition (RuAAC)

Even though CuAAC represents the preferred method for the 1,2,3-triazole synthesis, many other approaches have been developed to afford this important chemical moiety. Ruthenium-catalysed azide- alkyne cycloaddition (RuAAC), initially introduced by Lin, Jia, Fokin *et al.*[44], takes advantage of strong electron-donating ruthenium complexes, such as pentamethylcyclopentadienyl ruthenium dichloride ($Ru(Cp)Cl_2$), capability to catalyse alkyne cyclotrimerization and direct the reaction to the sole formation of the 1,5-regioisomer.[44–46] Furthermore, RuAAC is a novel strategy that can be applied to either terminal and internal alkynes, despite CuAAC, where there are only few examples reported of 1,4-regioisomers

synthesised from internal alkynes.[47,48] The interaction between ruthenium **1.51** and the alkyne **1.32** proceeds through an addition/elimination sequence in which the π-coordinated alkyne **1.52** reacts with the terminal nitrogen of the azide **1.53** producing a six-membered ruthenacycle **1.55**, *via* oxidative coupling. Subsequently, **1.54** evolves into the product **1.59** through reductive elimination intermediates **1.56a,b** and **1.57** with extrusion of ruthenium (Scheme 5).[49]

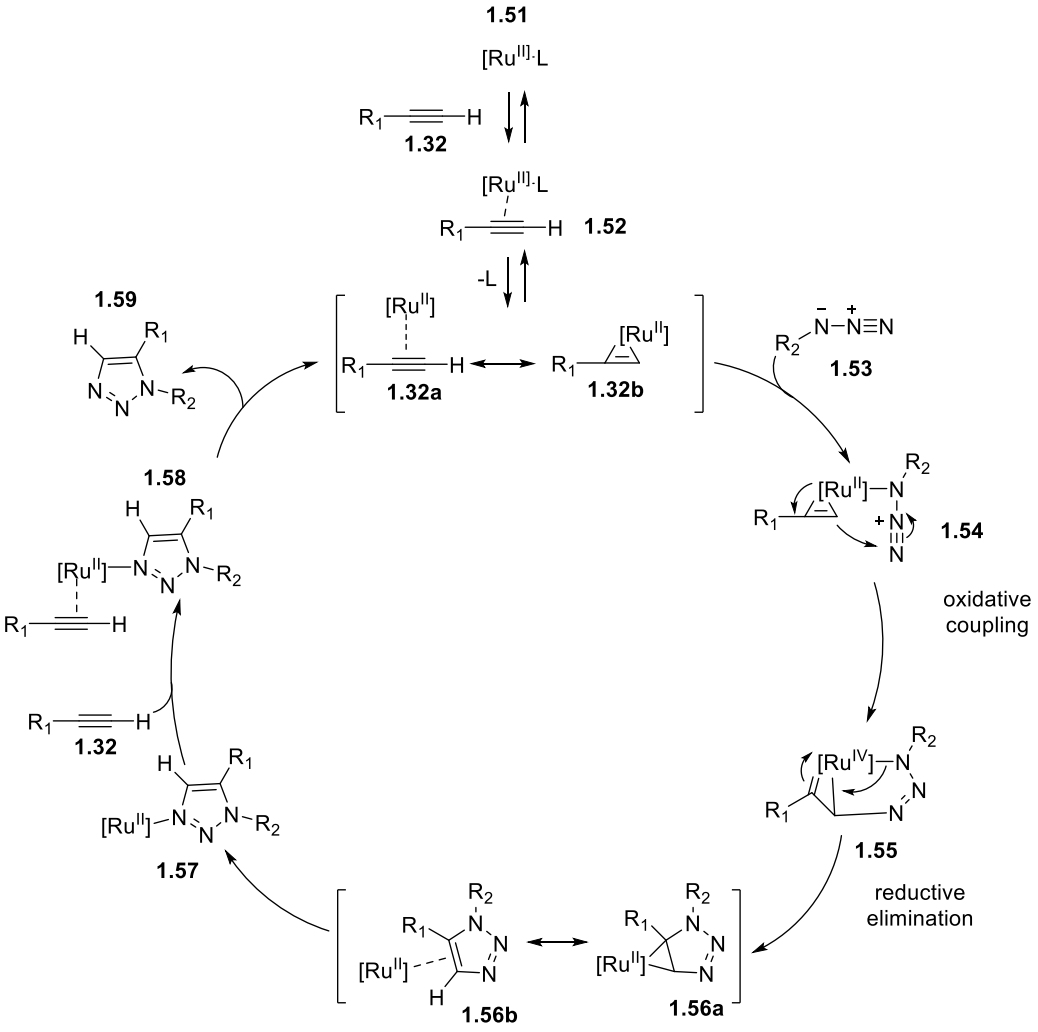

Scheme 5: General scheme of RuAAC cycloaddition.

It is pivotal to note that while the 1,5-regioisomer is completely afforded when reacting terminal alkynes, this exclusive regioselectivity does not fully occur when internal alkynes are used in the reaction. This issue mainly depends on how bulky the internal alkyne is. Electron-donating groups enhance the reactivity of the alkyne β-nucleophilic carbon that will attack the electrophilic nitrogen of the azide resulting in the formation of the 1,5-regioisomer exclusively.[44,49,50] Conversely, electron-withdrawing groups reduce the β-nucleophilicity of the alkyne, thus resulting into an α-carbon attack of the alkyne to the azide leading to the formation of 1,4-regioisomer instead.[50]

Nevertheless, the synthetic route using RuAAC still presents huge limits. In particular, when the ruthenium catalyst reacts with the sole azide **1.53**, in absence of the alkyne species **1.32**, side reactions can take place forming inactive and stable complexes (Figure 10, **1.60** or **1.61**) that do not evolve towards the formation of the free triazole.[44,49] On the contrary, if the alkyne **1.32** is the only species present in the reaction mix, then the ruthenium catalyst will form a ruthenacyclopentatriene complex **1.62** that is catalytically inactive (Figure 10).[51] Furthermore, RuAAC hardly tolerates azides requiring high steric hindrance as well as aryl azides and strong π-accepting substituents.[45]

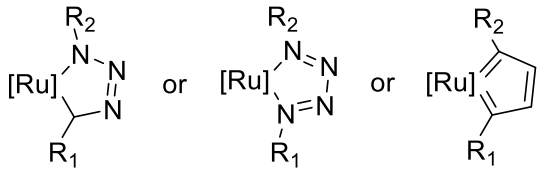

1.60 **1.61** **1.62**

Figure 10: Possible side products **1.60**-**1.62** arising from the RuAAC strategy.

1.2.4 1,2,3-triazole synthesis *via* organocatalysis

In the past few years, the organocatalytic approach for the synthesis of 1,2,3-triazoles has been notably preferred to the expensive and environmentally less ideal copper/ruthenium synthetic strategies.[52,53] Organocatalysts are, indeed, environmental-friendly, easy to synthesise and straightforward to produce. Furthermore, organocatalysis does not require metals to be present for the reaction and can also provide diverse 1,2,3-triazoles, impossible to synthesise with traditional methods, in high yields, high regioselectivity and of significant pharmaceutical interest.[54] Scientists agree on assuming Dimroth to be the very first one to apply organocatalysis to the synthesis of 1,2,3-triazoles *via* the condensation of organic azides and active methylene compounds.[31] In 2008, Ramachary *et al.*[55] proposed the first proline catalysed reaction between aryl azides **1.64** and Hagermann's ester **1.63,** *via* the formation of a dienamine intermediate **1.65** species, resulting in the corresponding fused 1,2,3-triazole **1.66** in high yields (Scheme 6).

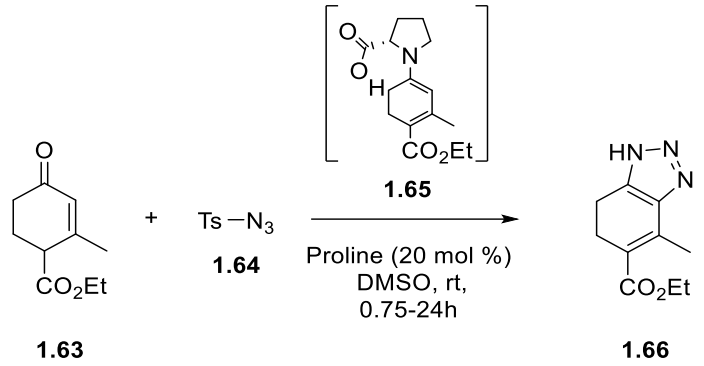

Scheme 6: Synthesis of fused 1,2,3-triazoles **1.66** *via* dienamine intermediate.

Ramachary *et al*.[56] also contributed to the synthesis of 1,4-disubstituted triazoles **1.70** using enolisable aldehydes **1.67** and azides **1.68**, *via* DBU catalysis which proceeded *via* formation of enolate intermediate **1.69** (Scheme 7).

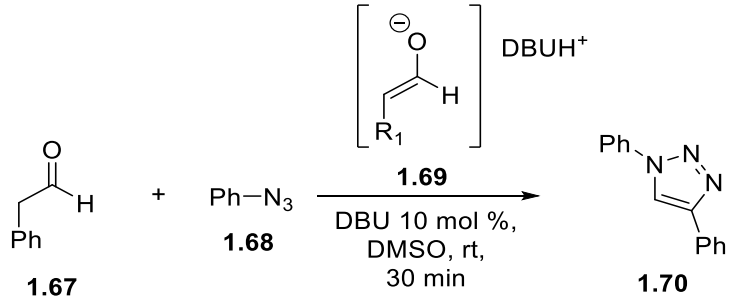

Scheme 7: Synthesis of 1,4-disubstituted triazole **1.70** *via* enolisable aldehydes.

Research was then extended to the synthesis of trisubstituted 1,2,3-triazoles **1.74** by reacting enolisable ketones **1.71** and a variety of aryl azides **1.72** with either electron-donating or electron-withdrawing groups, that progressed *via* similar intermediate **1.73** (Scheme 8) as highlighted before (**1.69**, Scheme 7).[57]

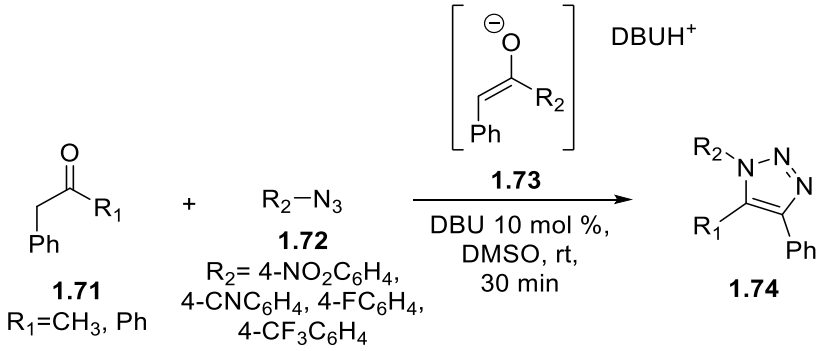

Scheme 8: Synthesis of fully decorated 1,2,3-triazoles **1.74** *via* enolisable ketones **1.71**.

Wang *et al*.[58] also deeply studied the reaction between active methylene compounds **1.75** and organic azides **1.72**, making use of diethylamine **1.76**, to achieve the regiospecific synthesis of trisubstituted 1,2,3-triazoles **1.77** in high yields. Wang's strategy worked perfectly with a wide range of enolisable aldehydes as well as various azides, both aromatic and aliphatic, with a wide range of substituents tolerated (Scheme 9).[58]

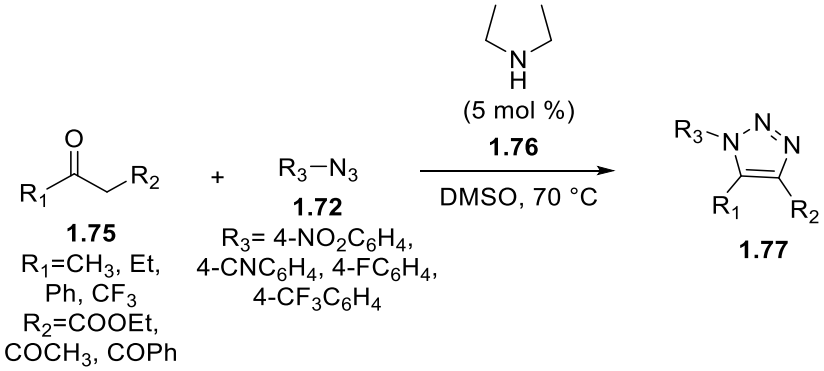

Scheme 9: Synthesis of trisubstituted 1,2,3-triazoles **1.77** *via* active methylene compounds **1.75**.

Wang *et al*. also developed an efficient method for the synthesis of trisubstituted 1,2,3-triazoles starting from ketoesters **1.79** under the catalysis of pyrrolidine **1.80**. This new approach let Wang and his group build an important CB1 cannabinoid receptor antagonist intermediate **1.81** (Scheme 10).[59]

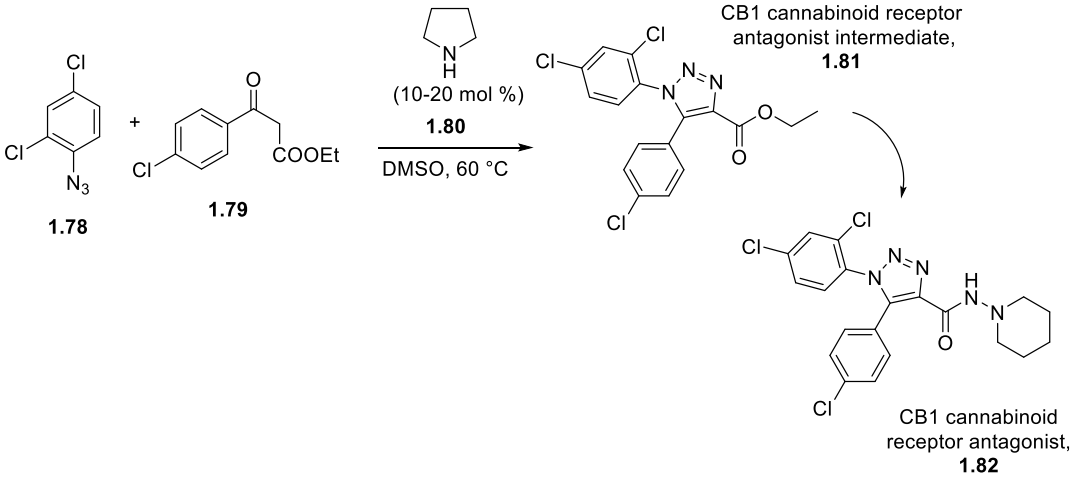

Scheme 10: Synthesis of the CB1 cannabinoid receptor antagonist intermediate **1.81** *via* organocatalytic approach starting from unactivated ketones **1.79**.

Furthermore, Wang *et al*.[60] can also be considered as the first to have attempted the organocatalytic synthesis of substituted 1,2,3-triazoles in water. They designed a catalyst with the unique properties of possessing specific hydrophobic groups (**1.85**) that allowed the reaction to happen in hydrophobic pockets (Scheme 11). The yields obtained with this greener method were comparable to the ones resulting from the same reactions carried out in organic solvents.[60] Therefore, a range of ketones **1.83** were reacted with aromatic azides **1.84** to provide relevant triazoles **1.86** in moderate to very good yields.

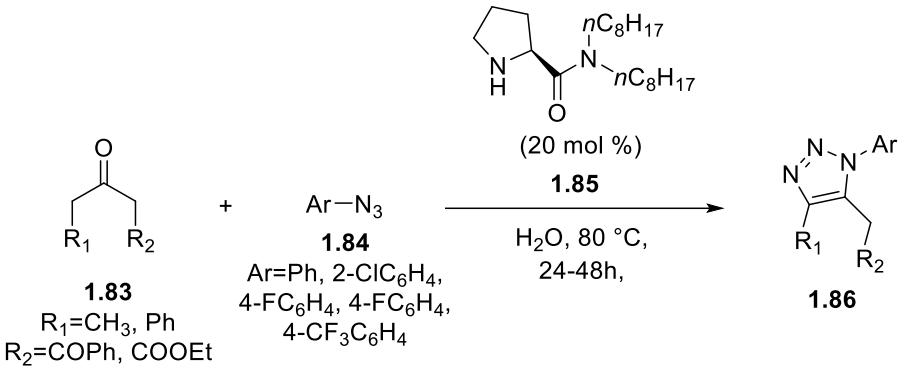

Scheme 11: Green approach to the synthesis of substituted 1,2,3-triazole **1.86**.

The Adamo's lab also investigated the versatility of Wang's and Ramachary's approaches to organocatalysis to synthesise enantioenriched amides **1.89** from enolisable aldehydes **1.87** and aromatic azides **1.84** under basic conditions *via* formation of a triazoline intermediate **1.88** (Scheme 12).[61]

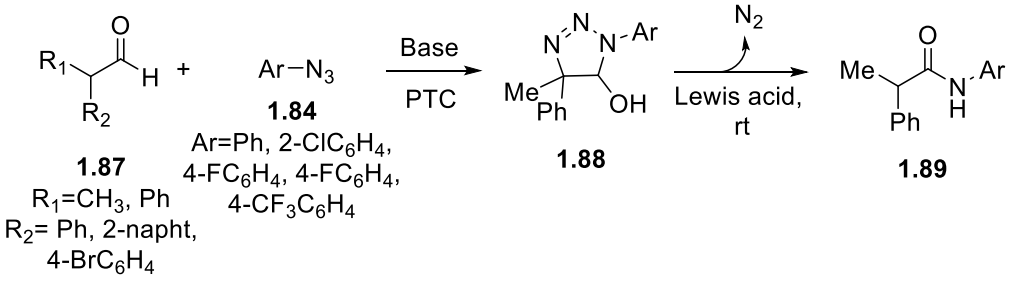

Scheme 12: Synthesis of enantioenriched amides **1.89** *via* triazoline intermediate **1.88** formation.

1.2.5 Introduction to hydroxyazoles and 5-hydroxy-1,2,3-triazoles

Hydroxyazoles, like 1,2,3-triazoles, belong to the azole heterocyclic class identified by the presence of a nitrogen involved in a double bond and, at least, another heteroatom in the same 5-membered ring **1.90**-**1.95** (Figure 11).

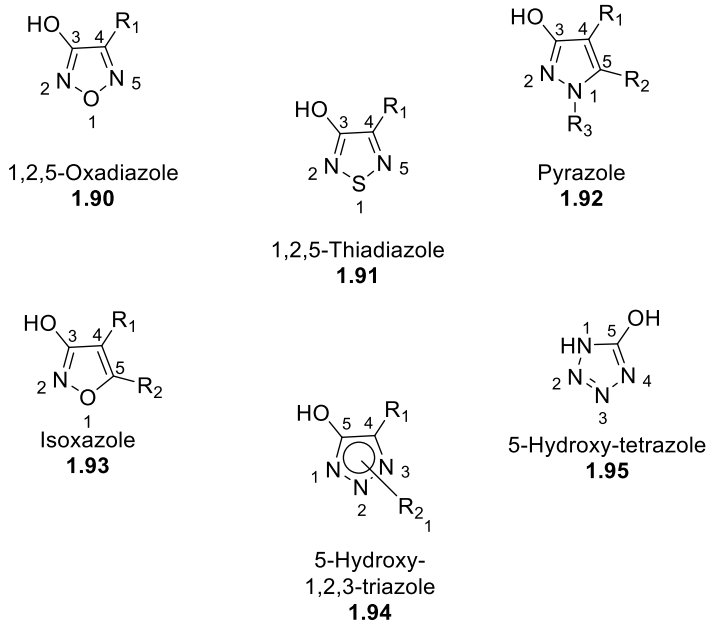

Figure 11: Some examples of 5-membered hydroxyazoles.

In particular, hydroxy-1,2,3-triazoles bear a hydroxyl-group with an *ortho* orientation with respect to the pyrrole-like nitrogen. The hydroxyl group allows these compounds to delocalise the negative charge, arising from the deprotonation of the hydroxyl group itself, over both the oxygen and nitrogen atoms. For this reason, hydroxyazoles are, predominantly, weak acids and their pK_a values is much lower than phenols as it strictly depends on the nature of the azole ring substituents. However, classifying hydroxyazoles only according to their pK_a is not suitable because of the lactam-lactim (**1.96** and **1.97** respectively) tautomerism that occurs between the hydroxyl group and the adjacent nitrogen. Specifically, the lactam-lactim tautomerism is a particular type of amide-imidol tautomerism that occurs when a hydrogen migrates between the oxygen and nitrogen atoms during the interconversion (Figure 12).[62]

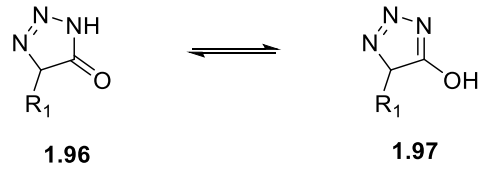

Figure 12: Lactam-lactim tautomerism in 5-hydroxy-1,2,3-triazoles.

The lactam-lactim tautomerism is greatly influenced by (i) the position of the heteroatom involved; (ii) the shape of the electronic density of the system after deprotonation of the hydroxyl moiety and, (iii), finally, by the reactivity towards electrophiles since both oxygen and nitrogen can intervene in creating new bonds.[63]

1.2.5.1 Synthesis of 5-hydroxy-1,2,3-triazoles

5-hydroxy-1,2,3-triazoles synthesis has been firstly described by Dimroth in 1902. He reacted ethyl acetoacetate **1.98** with phenyl azide **1.22** in the presence of sodium ethoxide **1.100** to provide 5-hydroxy-1,2,3-triazole **1.99** in poor yields (Scheme 13).[31]

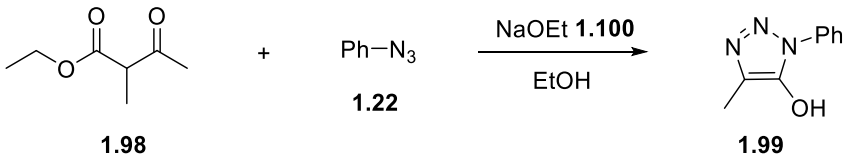

1.98 **1.22** **1.99**

Scheme 13: Dimroth's synthetic strategy to yield 5-hydroxy-1,2,3-triazole **1.99**.

Throughout the years, the base-catalysed reaction between aryl azides and active methylene compounds remained the general method of election for the synthesis of variously substituted 5-hydroxy-1,2,3-triazoles. Begtrup and Pedersen, in 1964, demonstrated that, when methylmalonamide **1.101a** (R_1=H, R_2=CH_3) reacted with phenyl azide **1.22** in the presence of sodium ethoxide **1.100**, the sole product observed was 1-phenyl-4-methyl-5-hydroxy-1,2,3-triazole **1.103a**. They obtained analogous results with *N*,*N*'-dimethyl methylmalonamide **1.101b** (R_1=R_2=CH_3), phenylmalonamide **1.101c** (R_1=H, R_2=Ph) and *N*,*N*'-dimethyl phenylmalonamide **1.101d** (R_1= CH_3, R_2=Ph) proposing the following synthetic pattern to justify the products obtained. The reaction between malonamides **1.101a-d** and phenyl azide **1.22** produced the triazene intermediate **1.102** and was followed by the attack of the negatively charged terminal nitrogen of the azide on the amide-carbon group. Simultaneous loss of the carboxamido group brought to products **1.103a-d** (Scheme 14).[64]

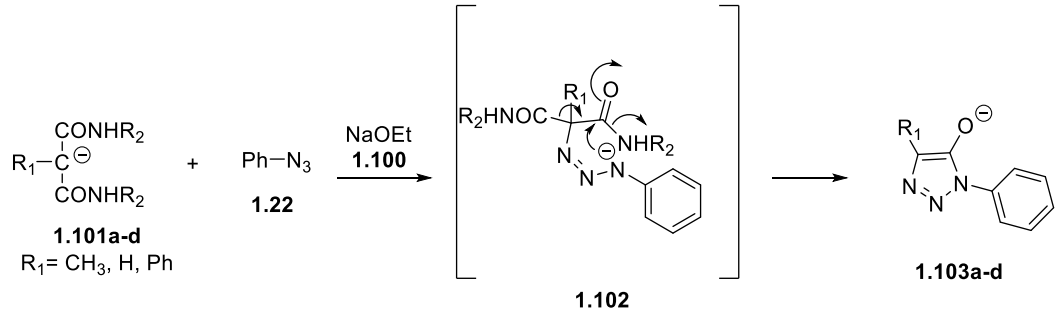

Scheme 14: Begtrup and Pedersen's synthetic pathway for the synthesis of 5-hydroxy-1,2,3-triazoles **1.103a-d**.

Olesen *et al.*[65] took advantage of the 5-hydroxy-1,2,3-triazoles synthesis, to form a new versatile compound (**1.106**), bearing a chlorine at position C5 and an aldehyde moiety at position C4 of the triazole ring *via* the Vilsmeier-Haack reaction (Scheme 15).

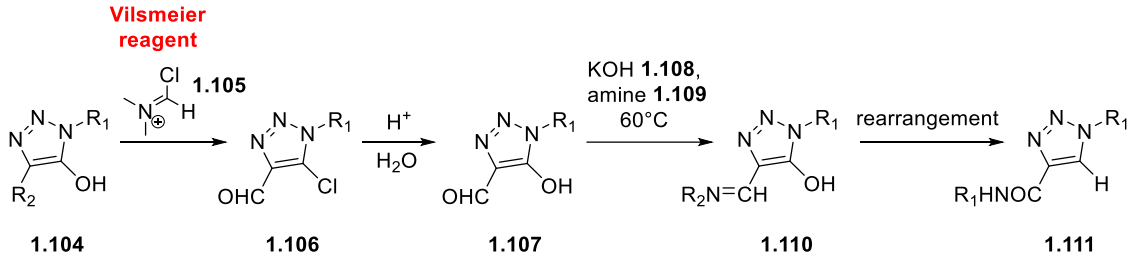

Scheme 15: Olesen approach for the synthesis of *N*-substituted-1*H*-1,2,3-triazole-4-carboxamides **1.111**.

The Vilsmeier-Haack reaction allows the formylation of electron-rich arenes **1.112** to produce aryl aldehydes **1.116** starting from aromatic amines **1.113** and phosphorous oxychloride **1.114** (Scheme 16).[65]

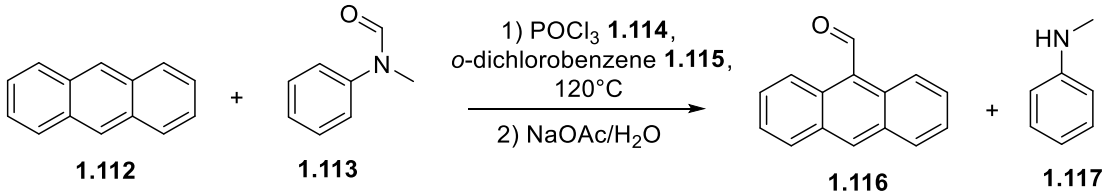

Scheme 16: Vilsmeier-Haack reaction for the synthesis of aryl aldehydes **1.116**.

Olesen, then, turned the 5-chlorotriazole-4-carboxyaldhehyde **1.106** into the corresponding 5-hydroxy-1,2,3-triazole **1.107** with a simple work-up with acidic aqueous media and finally reacted **1.107** with an appropriate primary amine **1.109** to give **1.110** that, upon heating beyond the

melting point, rearranged into the resulting carboxamide **1.111** (Scheme 15) presumably following the Dimroth rearrangement (Scheme 17).[31,66] This involves the relocation of two heteroatoms (**1.110**) in heterocyclic systems via ring opening (**1.118**) and ring closure (**1.119**) processes.[31]

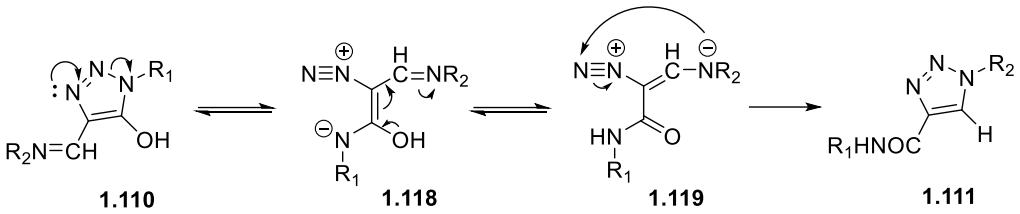

Scheme 17: Olesen Dimroth's rearrangement proposed mechanism for the synthesis of **1.111.**

Cottrel *et al.*[67] also obtained substituted 5-hydroxy-1,2,3-triazoles **1.123a-f**. In this study, diethyl malonate **1.121a** (R_1=COOEt), ethyl benzylacetate **1.121b** (R_1=Bn), ethyl fluoroacetate **1.121c** (R_1=F) and ethyl nitroacetate **1.121d** (R_1=NO_2) were reacted with benzyl azide **1.120a** or substituted benzyl azides **1.120b-c**, bearing both EWGs (**1.120b**, Ar=1,3-dichlorobenzene) and EDGs (**1.120c**, Ar=anisole). While compounds **1.123a** (Ar=Bn, R_1=COOEt), **1.123b** (Ar=1,3-dichlorobenzene, R_1=Bn), **1.123c** (Ar=anisole, R_1=Bn), **1.123d** (Ar=Bn, R_1=Bn) were obtained in 77-96% yields, compounds **1.123e** (R_1=F) and **1.123e** (R_1=NO_2) were not afforded (Scheme 18).[67]

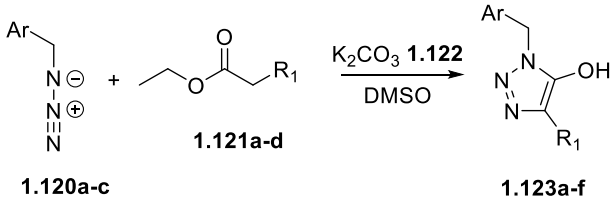

Scheme 18: Cottrel's strategy for the synthesis of 1-benzyl 5-hydroxy-1,2,3-triazoles **1.123a-f**.

The Adamo's lab provided a high-yielding cycloaddition reaction of β-ketoesters **1.124a** (R_1=H) and **1.98** (R_1=CH_3) with aryl azides **1.125a-g** to yield 5-hydroxy-1,2,3-triazoles **1.127a-g**.[68] The reaction was promoted by 1.2 equiv. of DBU **1.126** in acetonitrile (ACN) at 50 °C for 18 h and provided 5-hydroxy-1,2,3-triazoles **1.127a-g** in moderate to good yields (Scheme 19). The reaction was, however, sensitive to the electronic effects of substituents on the azide, where electron-neutral azides **1.125a** (Ar=Ph), **1.125b** (Ar=4-BrC_6H_4), **1.125d** (Ar=2-PhC_6H_4), **1.125e** (Ar=1-naphthyl) gave highest yields. Electron-rich azide **1.125c** (Ar=4-$OMeC_6H_4$) reacted well, albeit yields were lower. Aromatic azides **1.125f** (Ar=4-$NO_2C_6H_4$)**, 1.125g** (Ar=2-NO_2-4-MeC_6H_3) bearing strong electron-withdrawing groups provided corresponding 5-hydroxy-1,2,3-triazoles **1.127f–g** only in moderate yields. Steric hindrance from aryl-substituents of aryl azides **1.125** was not found to affect the reaction yield.

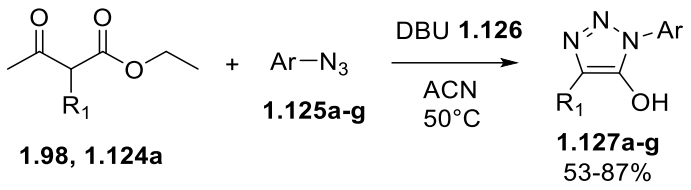

Scheme 19: Synthesis of 5-hydroxy-1,2,3-triazoles **1.127a-g** *via* DBU catalysis.

Since compound **1.127a** (R_1=CH_3) behaved as a relatively strong Brønsted acid, a titration experiment was carried out, to better characterise its properties. The pK_a of **1.127a** was found to be 4.2, which is comparable to that of a carboxylic acid (Figure 13).[69]

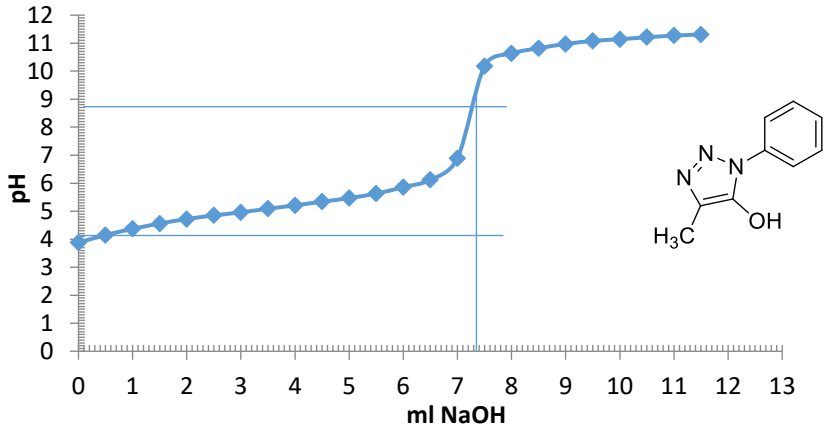

Figure 13: Potentiometric titration of 5-hydroxy-1,2,3-triazole **1.127a**. Equivalence point: pH = 8.4, pK_a = 4.2.

This result was very unexpected if compared to the pK_a values of related 4-hydroxy-1,2,3-triazoles, found to be significantly less acidic as reported by Pippione and co-workers.[70] This intriguing finding allowed the Adamo's group to synthesise long chain 5-hydroxy-1,2,3-triazoles **1.132**[68] (Scheme 20) to be potentially used as bioisosteres of hydroxamic acids (Figure 14), such as suberanilohydroxamic acid **1.133** (SAHA), known as potent HDAC (histone deacetylase) inhibitor.[71,72]

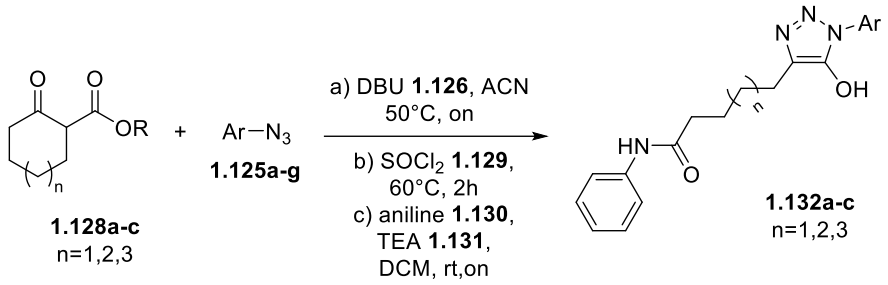

Scheme 20: Preparation of long chain 5-hydroxy-1,2,3-triazoles **1.132** *via* DBU catalysis.

A literature search highlighted the structural similarity of 5-hydroxy-1,2,3-triazoles **1.132** to hydroxamic acids.[73] Hydroxamic acids and 5-hydroxy-1,2,3-triazoles share similar pK_a and amide-like bioisosterism, which makes them excellent ligands for enzyme-bound metals. Compounds **1.127a–g** reacted with Fe^{2+} and Cu^{2+} salts providing blue-violet and red colored solutions, indicating a similar ligand-like behavior as hydroxamic acids. Suberanilohydroxamic acid **1.133** (SAHA) is an hydroxamic acid which is active as histone deacetylase (HDAC) inhibitor.[71,72] The structural and functional similarities between **1.133** and 5-hydroxy-1,2,3-triazoles **1.132** are highlighted in Figure 14 and include: (i) nominally similar scaffolds and chemical functionalities (i.e OH groups circled in blue); (ii) analogous lone pairs (circled in red) of the carbonyl oxygen of the hydroxamic acid and pyridyl-like nitrogen of the triazole system;[74] (iii) hydrophobic backbones (circled in green), essential for interaction with active sites of HDAC isoforms, e.g. zinc-binding groups; and (iv) aromatic rings (circled in pink), essential for the correct positioning in the enzyme active site via π-π stacking.[75]

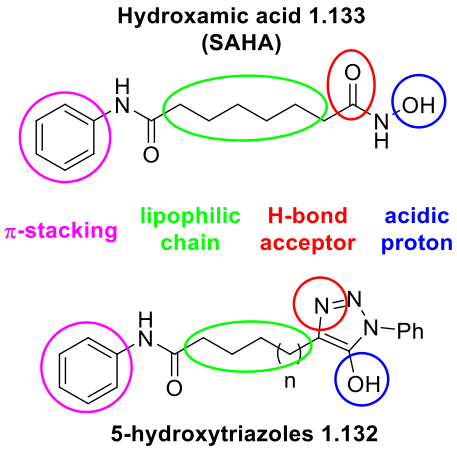

Figure 14. Structural similarities between HDAC inhibitor SAHA **1.133** and long-chain 5-hydroxy-1,2,3-triazoles **1.132**.

A more detailed description of 1,2,3-triazoles' properties in medicinal chemistry as hydroxamic acid biososteres will be discussed in *Chapter 2*.

1.3 Results and Discussion

The possibility to synthesise long-chain 5-hydroxy-1,2,3-triazoles as potential hydroxamic acid bioisosteres worked as driving force for the start of this project that was, initially, laying the groundwork for an important question: what if the reaction of β-ketoesters with pyridyl azides, instead of aryl azides, could lead to an even more active substrate to test as potential candidate in drug discovery? Consequently, this project focused, in the first part, on the synthesis of 5-hydroxy-1,2,3-pyridyl triazoles *via* the DBU promoted protocol followed for the synthesis of 5-hydroxytriazoles **1.127**. The reaction was carried out in ACN at 50 °C for 18 hours but did not provide the desired product except recovering of the starting materials. For this reason, different types of bases, either organic or inorganic, were used instead of DBU as well as solvents other than acetonitrile (Table 2). Additionally, β-ketoesters **1.98** and **1.124a** were reacted with diverse pyridyl azides (**1.134a,b**) all bearing the azido group N_3 in an *ortho* position, to prove the reaction to be, eventually, more favored in presence of EW or ED groups. Unfortunately, none of these approaches led to obtain the desired pyridyl-based 5-hydroxytriazoles **1.135a,b** (Table 2) in spite of the extensive attempts that were made.

Table 2: Reaction conditions: **1.124a** and **1.98** (1.2 equiv.,0.8 mmol), **1.134a,b** (1 equiv., 0.67 mmol), base (1.2 equiv., 0.80 mmol), solvent (0.3 M).

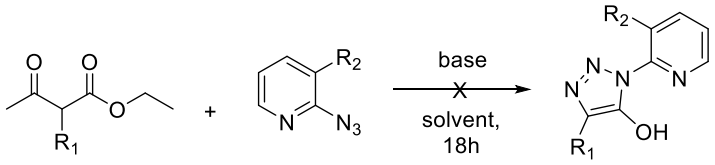

1.124a,R_1=H
1.98,R_1=CH_3

1.134a,R_2=H
1.134b,R_2=OCH_3

1.135a,b

Entry	Ketoester	Azide	Base	Solvent	Temperature
1	**1.124a**	**1.134a**	DBU	DMSO	Reflux
2	**1.124a**	**1.134b**			
3	**1.98**	**1.134a**			
4	**1.98**	**1.134b**			

Entry	Ketoester	Azide	Base	Solvent	Temperature
5	**1.124a**	**1.134a**	NaOEt	EtOH	rt
6	**1.124a**	**1.134b**			
7	**1.98**	**1.134a**			
8	**1.98**	**1.134b**			
9	**1.124a**	**1.134a**	NaH	THF dry	0°C to rt
10	**1.124a**	**1.134b**			
11	**1.98**	**1.134a**			
12	**1.98**	**1.134b**			
13	**1.124a**	**1.134a**	Diethylamine	Toluene dry	Reflux
14	**1.124a**	**1.134b**			
15	**1.98**	**1.134a**			
16	**1.98**	**1.134b**			
17	**1.124a**	**1.134a**	Proline	DCM dry	Reflux
18	**1.124a**	**1.134b**			
19	**1.98**	**1.134a**			
20	**1.98**	**1.134b**			

Hence, we thought of avail of a catalyst that, by lowering the energy barrier required to start the cycloaddition reaction, could act as a promoter. Different catalysts were tested to try to afford the desired products (Table 3). $Copper_{(II)}$- and $copper_{(I)}$- based catalysts were investigated in the first instance, due to the efficient role of copper in CuAAC reactions.[33] Notably, only when $copper_{(I)}$ trifluoromethane sulfonate toluene complex ($Cu(OTf)_2*C_6H_5CH_3$) was employed, with DMSO as solvent (Table 3, entry 3), the reaction succeeded, although affording a different triazole from the desired 5-hydroxy pyridine-based 1,2,3-triazole. The triazole obtained (**1.136a**) retained the ester moiety at the C4 position of the ring and a methyl at position C5. Surprisingly, when reacting azide **1.134b** with β-ketoesters **1.124a** and **1.98** (Table 3, entry 2 and 4) the only process observed was

the reduction of the azido group into an amino group (**1.137**). We explained the reduction step to be accelerated by the simultaneous presence of a copper source and an electron-donor group adjacent to the azido group, which was precedented in the literature.[76] In addition to that, when azide **1.134a** reacted with 2-substituted β-ketoester **1.98**, TLC of the reaction after 24 hours showed no conversion of the starting materials in all of the reaction conditions attempted. We assumed that the absence of substituents at position 2 of β-ketoester **1.124a** was essential to provide the optimal orientation for the azide to complete the cycloaddition. Bulky copper sources, like bromotris(triphenylphosphine)copper [$Cu(PPh_3)_3$,Table 3, entries 5-8], $copper_{(II)}$ species, like copper sulfate ($CuSO_4$, Table 3, entries 9-12), and other bases stronger than DBU (pK_a=13.5), like diethylamine (pK_a= 11.09, Table 3, entries 5-8), *N*,*N*'-dimethylethylendiamine (DMEDA, pK_a=9.5, Table 3, entries 9-12) and proline (pK_a=10.96, Table 3, entries 9-12), also did not bring to the formation of the desired pyridine-based 5-hydroxy-1,2,3-triazole **1.135**.

Table 3: [a]Reaction conditions: **1.124a** and **1.98** (1.2 equiv.,0.80 mmol), **1.134a,b** (1 equiv., 0.67 mmol),base (1.2 equiv., 0.80 mmol), copper source (0.1 equiv., 0.067 mmol), solvent (0.3 M). [b]Only starting materials recovered.

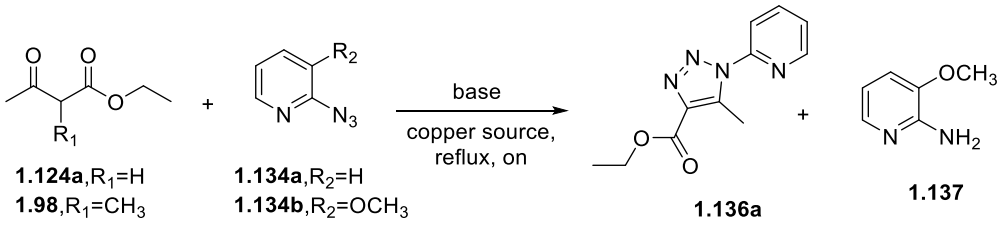

1.124a,R_1=H
1.98,R_1=CH_3
1.134a,R_2=H
1.134b,R_2=OCH_3
1.136a
1.137

Entry[a]	Ketoester	Azide	Base	Solvent	Catalyst	Product	Yield[b]
1	**1.124a**	**1.134a**	DBU	DMSO	$Cu(OTf)_2$* $C_6H_5CH_3$	**1.136a**	60%
2	**1.124a**	**1.134b**				**1.137**	55%
3	**1.98**	**1.134a**				**-**	**-**
4	**1.98**	**1.134b**				**1.137**	58%
5	**1.124a**	**1.134a**	Diethylamine	Toluene dry	$CuBr(PPh_3)_3$	-	-[b]
6	**1.124a**	**1.134b**					
7	**1.98**	**1.134a**					
8	**1.98**	**1.134b**					

Entry[a]	Ketoester	Azide	Base	Solvent	Catalyst	Product[b]	Yield
9	**1.124a**	**1.134a**	DMEDA or Proline	EtOH/ H_2O (7:3)	$CuSO_4$/ Na ascorbate	-	-[b]
10	**1.124a**	**1.134b**					
11	**1.98**	**1.134a**					
12	**1.98**	**1.134b**					

Supported by a similar mechanism described by Pedersen and Begtrup for the reaction of phenyl azides and amides of malonic acids,[64] we hypothesised that the terminal nitrogen of pyridyl-azide **1.134a** does not possess enough energy to promote the nucleophilic addition to the electrophilic ester carbonyl. We believed the strong EW effect of the adjacent pyridine nitrogen to have undermined the reaction success, contrary to what has been demonstrated in the past in our lab for the synthesis of 5-hydroxy-1,2,3-triazoles **1.127a-g** (Scheme 19) and **1.132a-c** (Scheme 20).[68] Based on the reactivity observed, two reaction mechanisms have been proposed (Figure 15) leading to distinct products *via* analogous intermediates **1.139a** and **1.140a**. These intermediates arise from the reaction of enolate **1.138,** formed by the base-promoted deprotonation of the corresponding β-ketoester, with aryl azides **1.125a,b** or **1.134a,b** (pathway **a** or pathway **b**), respectively. In pathway **a**, species **1.139a** evolves towards cyclic amide **1.139b**, containing no enolisable proton, with concomitant elimination of ethoxide. Subsequent attack of ethoxide to the acetoxy group in **1.139c** will lead to elimination of ethylacetate and formation of **1.127**. Conversely, in the presence of an enolisable proton such as in **1.140a** (pathway **b**), the following cyclisation to **1.140b** and its subsequent protonation will generate **1.140c** which will provide compounds **1.136a** after dehydration.

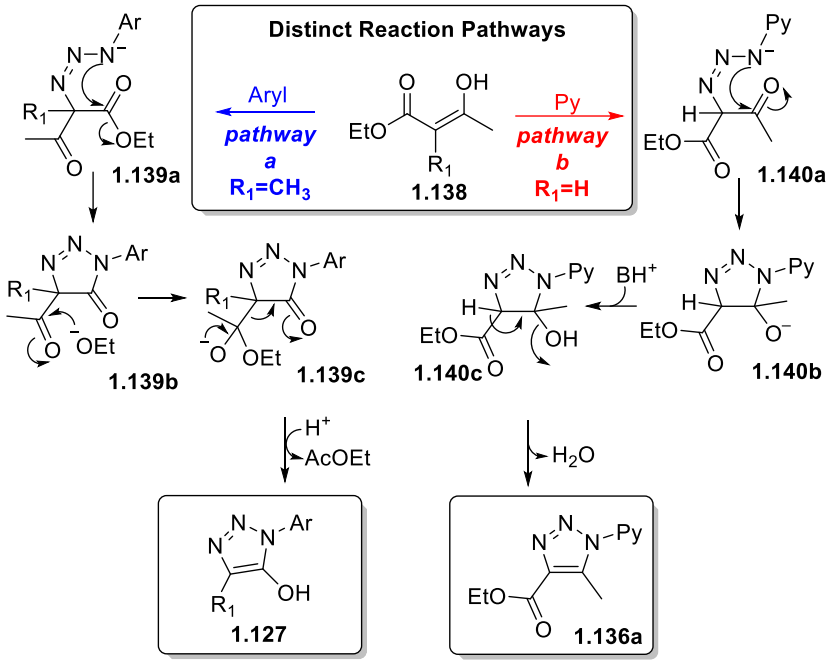

Figure 15: Different proposed pathways for the synthesis of aryl-based 5-hydroxy-1,2,3-triazoles **1.127** and pyridyl-based 5-methyl-1,2,3-triazoles **1.136a**.

In view of that, we tried to overcome the low reactivity of the nucleophilic azide by reacting 2-azidopyridines **1.134a,b** with different active methylene compounds, different bases and different solvents with the purpose of forcing the terminal nitrogen to interact with the ester carbonyl to give the desired pyridine-based 5-hydroxy-1,2,3-triazoles **1.135a,b**. Thus, we started the new cycloadditions with active methylene compounds bearing two ester moieties (**1.124b,c**, Table 4, entries 1 and 2), with one of them replacing the keto group, or with transforming the ester group of **1.98** into an activated and more electrophilic function (**1.124d**, Table 4, entry 3), making use, for this purpose, of hexafluoroisopropanol ester. Is it well known that the trifluoromethyl group is a strong EW moiety and, when attached to a carbonyl function, increases its electrophilicity providing an enhanced positive charge lying on the carbonyl carbon.[77] We also attempted to protect the keto-group with cyclic acetals (**1.124e**, Table 4, entry 5) or to enclose it into a cyclic constraint (**1.124f**, Table 4, entry 4), in order to make the ketone function less available to be attacked by the azide. Unfortunately, all these attempts met with no success.

Table 4: Different active methylene compounds reacting with azides **1.134a,b** [a]Reaction conditions: **1.124b-f** (1.2 equiv.,0.80 mmol), **1.134a,b** (1 equiv., 0.67 mmol), base (1.2 equiv., 0.80 mmol), copper source (0.1 equiv., 0.067 mmol), solvent (0.3 M).

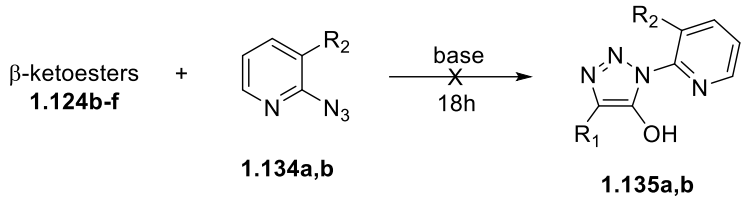

Entry[a]	β-ketoester	Base	Catalyst	Solvent	Temperature
1	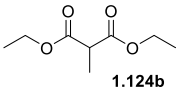 1.124b	a) DBU b) NaOEt c) NaH d) K_2CO_3	a) $Cu(OTf)_2$* $C_6H_5CH_3$ b) none c) none d) $Cu(OTf)_2$* $C_6H_5CH_3$	a) DMSO b) EtOH c) THF dry d) DMSO	a) reflux b) rt to 60°C c) 0°C to rt d) reflux
2	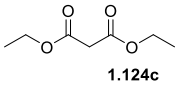 1.124c				
3	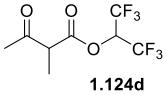 1.124d				
4	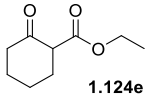 1.124e				
5	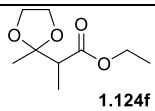 1.124f				

Acknowledging the possibility that also the presence of copper as catalytic source might have played a negative role for the synthesis of 1,2,3-triazoles **1.135a,b**, we decided to introduce different catalysts to the reaction process. According to literature, copper easily coordinates oxygen and nitrogen ligands.[78,79] A deep study on metal-ligands geometrical coordination has been disseminated by Mohamed. As reported by his review (Figure 16), copper can coordinate the azide moiety with three different spatial conformations: (i) the azide can link one metal center only (Figure 16, **1.141a**, square-planar arrangement), (ii) the azide can bridge two metal centers through the same nitrogen (Figure 16, **1.141b**, four-membered ring) or (iii) can bridge two metal

centers that are, in turn, linked to two terminal nitrogens of another azido-group (Figure 16, **1.141c**, eight-membered ring).[80,81]

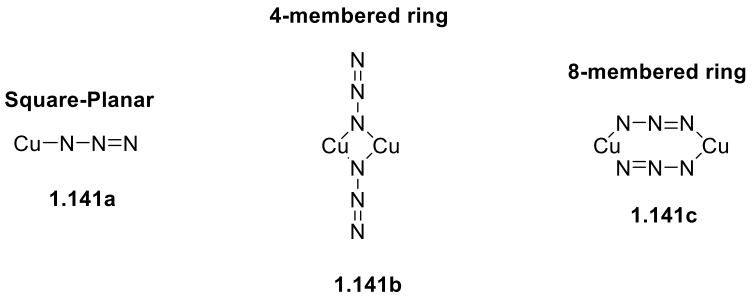

Figure 16: Copper spatial conformation when complexed with azides.

Based on these findings, we hypothesised that a possible competition of copper sources bridging either the carbonyl groups of β-ketoesters **1.98** and **1.124a** or the terminal nitrogen of azides **1.134a,b** might have reduced the reactivity of both reagents leading to product **1.136a** instead of **1.135a,b**. We therefore performed the only successful reaction again, which occurred between 2-azidopyridine **1.134a** and β-ketoester **1.124a** (Table 3, entry 3) in the presence of two catalysts diverse from copper: cerium chloride heptahydrate ($CeCl_3$*$5H_2O$) and scandium triflate ($Sc(OTf)_3$) for their higher affinity for oxygen rather than nitrogen. The reaction produced the same compound obtained with $Cu(OTf)_2$ toluene complex, triazole **1.136a**, proving our hypothesis wrong about a potential negative effect of the catalyst employed on the reactivity of the reagents. Finally, we decided to investigate whether or not the position of the azido group might have also influenced the outcome of the reaction. For this reason, we reacted β-ketoester **1.124a** with regioisomers of 2-azidopyridine **1.134a**, in which the azido group is in *meta* or *para* position respectively (**1.134c,d**), in the presence of DBU **1.126** as the base and ACN as the solvent. Once more, the products obtained, **1.136b** and **1.136c**, kept the ester function at position C4 of the triazole ring without evolving to the 5-hydroxytriazole **1.135** (Scheme 21).

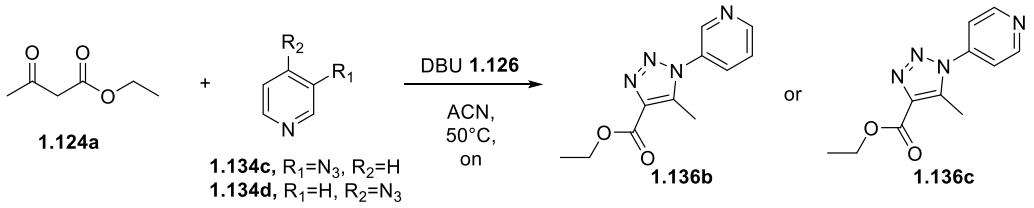

Scheme 21: Reaction conditions: **1.124a** (1.2 equiv.,0.80 mmol), **1.134c,d** (1 equiv., 0.67 mmol), DBU **1.126** (1.2 equiv.,0.80 mmol), ACN (0.3 M)

Despite not having obtained the desired pyridine-based 5-hydroxy-1,2,3-triazole **1.135**, we decided, anyway, to investigate the ability of triazole **1.136a** to act as potential interesting fragment

for fragment-based drug discovery. *Chapter 2* will describe the docking tests performed on some triazoles, including **1.136a**, and the results obtained.

1.4 Conclusions

In conclusion we have attempted to synthesise a new class of pyridine-based 5-hydroxy-1,2,3-triazoles **1.135** *via* a mild and catalyst-free reaction protocol, already validated in the Adamo's lab, between pyridyl azides **1.134a-d** and β-ketoesters **1.98** and **1.124a-f**. Unfortunately, the only result obtained was the formation of triazoles **1.136a-c** in which the ester function is retained and did not evolve towards the formation of the hydroxyl-group at position *C*5 of the triazole ring. It was clear that the withdrawing effect of the pyridine nitrogen had an important impact on the reactivity of the azido group of **1.134a-d**; the nucleophilic attack of the azide to the ketone carbonyl was energetically more favored than the one towards the ester group, despite all the attempts to make the ester function of β-ketoesters **1.98** and **1.124a** more electrophilic. Nevertheless, given the importance of the triazole nucleus in medicinal chemistry as amide bioisostere, we decided to perform docking tests on triazole **1.136a**, along with other 5-hydroxytriazoles previously synthesised in our group, to better evaluate their potential application in biological systems.

1.5 Experimental Section

^{1}H and ^{13}C NMR spectra were recorded on a Bruker 400 spectrometer. Chemical shifts (δ) are reported in ppm relative to residual solvent signals (^{1}H NMR: 7.26 ppm for $CDCl_3$; ^{13}C NMR: 77.16 ppm for $CDCl_3$). ^{13}C NMR spectra were acquired with ^{1}H broad band decoupled mode. Coupling constants (*J*) are in Hz. Melting points were measured using a Stuart scientific melting point apparatus and are uncorrected. Infrared spectra (IR) were recorded with KBr discs using a Bruker Tensor27 FT-IR instrument. High-resolution mass spectra were obtained on a Waters Micromass GCT PremierMS spectrometer or on a Bruker microTOF-Q III LC-MS spectrometer (APCI method). Analytical grade solvents and commercially available reagents were used as received. Dry DCM, dry toluene, dry THF and anhydrous DMSO were purchased from Sigma Aldrich. Reactions were monitored by TLC (Merck, silica gel 60 F254). Flash column chromatography was performed using silica gel 60 (0.040-0.063 mm, 230-400 mesh). Substituted pyridyl azides **1.134a-f** were prepared according to reported procedures[82,83] from the corresponding commercially available bromides. β-ketoesters **1.98 and 1.124b,c,e** were purchased from Sigma Aldrich and used without further purifications.

N.B. pyridyl azides **1.134e,f** synthesis is reported here but both compounds will be used for the synthesis of 1,2,3-triazoles **2.80d** and **2.80e** in *Chapter 2.*

1.5.1 General procedure for the synthesis of substituted 2-azidopyridines 1.134a-c,e,f (GP1)

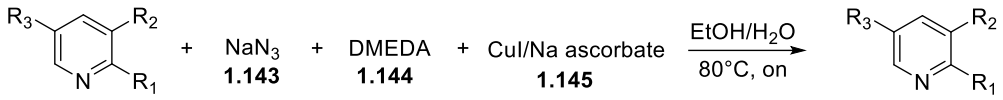

1.142a, R_1=Br,R_2,R_3=H
1.142b, R_1=Br,R_2=OCH_3,R_3=H
1.142c, R_1,R_3=H,R_2=Br
1.142e, R_1=Br,R_2=H,R_3=CH_3
1.142f, R_1=Br,R_2=H,R_3=Cl

1.134a, R_1=N_3,R_2,R_3=H
1.134b, R_1=N_3,R_2=OCH_3,R_3=H
1.134c, R_1,R_3=H,R_2=N_3
1.134e, R_1=N_3,R_2=H,R_3=CH_3
1.134f, R_1=N_3,R_2=H,R_3=Cl

Sodium azide **1.143** (1.54 mmol, 2 equiv.) was dissolved in a solution of EtOH/H_2O (7:3) in a round bottom flask equipped with a magnetic stirring bar. Commercially available 2-bromopyridines **1.142a-c,e,f** (0.77 mmol, 1 equiv.), dimethylethylendiamine **1.144** (DMEDA, 0.11 mmol, 0.15 equiv.), copper iodide **1.145** (CuI, 0.077 mmol, 0.01 equiv.) and sodium ascorbate **1.145** (0.038 mmol, 0.05 equiv.) were then added to the reaction mix. The reaction stirred at 80°C overnight. The day after, TLC showed complete consumption of the starting material (PE/AcOEt 70:30). The crude was washed with DCM/H_2O three times, the organic phases collected and dried over anhydrous sodium sulfate (Na_2SO_4). Hence the solvent was removed by rotary evaporation to afford products **1.134a,b,e** in almost quantitative yields (>95%) without further purification. Azides **1.134c,f** were, instead, obtained by column chromatography (DCM/AcOEt 80:20 and DCM/AcOEt 90:10 respectively) in 40% and 70% yields respectively.

2-azidopyridine 1.134a

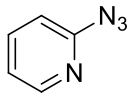

Prepared according to GP1. Yellow solid, 95% yield, 262 mg. ^{1}H NMR (400 MHz, $CDCl_3$) δ 8.86 (dt, *J* = 6.9, 1.0 Hz, 1H), 8.08 (d, *J* = 9.0 Hz, 1H), 7.70 (ddd, *J* = 9.0, 6.8, 1.1 Hz, 1H), 7.24 (dd, *J* = 6.8, 0.8 Hz, 1H).^{13}C NMR (101 MHz, CDCl3) δ 148.5, 131.8, 125.5, 116.6, 116.1. All analytical data are consistent with those reported in the literature.[82]

2-azido-3-methoxypyridine 1.134b

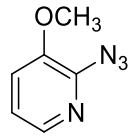

Prepared according to GP1. Orange solid, 98% yield, 156 mg. ^{1}H NMR (400 MHz, $CDCl_3$) δ 8.46 (d, *J* = 6.8 Hz, 1H), 7.14 (t, *J* = 7.2 Hz, 1H), 6.87 (d, *J* = 7.6 Hz, 1H), 4.14 (s, 3H).^{13}C NMR (101 MHz, $CDCl_3$) δ 148.4, 144.3, 117.7, 117.1, 107.3, 56.9. All analytical data are consistent with those reported in the literature.[82]

3-azidopyridine 1.134c

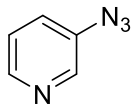

Prepared according to GP1. Yellow oil, 40% yield, 36.1 mg. ^{1}H NMR (400 MHz, $CDCl_3$) δ 8.40 (d, *J* = 4.4 Hz, 1H), 8.38 (s, 1H), 7.39 – 7.33 (m, 1H), 7.30 (dd, *J* = 8.2, 4.7 Hz, 1H).^{13}C NMR (101 MHz, $CDCl_3$) δ 146.1, 141.4, 137.1, 125.9, 124.1. All analytical data are consistent with those reported in the literature.[82]

2-azido-5-methylpyridine 1.134e

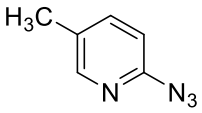

Prepared according to GP1. Yellow solid, 84% yield, 86.7 mg. ^{1}H NMR (400 MHz, $CDCl_3$) δ 8.61 (s, 1H), 7.93 (d, *J* = 11.0 Hz, 1H), 7.52 (d, *J* = 9.1 Hz, 1H), 2.50 (s, 3H). ^{13}C NMR (101 MHz, $CDCl_3$) δ 147.6, 135.0, 127.2, 122.9, 115.1, 18.1. IR (KBr, cm^{-1}): 2960, 2135, 1645, 1288. m.p. 98 °C. HRMS (ESI) m/z: $[M+H]^+$ calcd for $C_6H_7N_4$ 135.0671; found: 135.0693.

2-azido-5-chloropyridine 1.134f

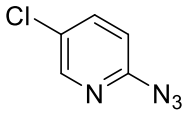

Prepared according to GP1. Yellow solid, 70% yield, 83 mg. ^{1}H NMR (400 MHz, $CDCl_3$) δ 8.89 (s, 1H), 8.03 (d, *J* = 9.5 Hz, 1H), 7.66 (d, *J* = 9.5 Hz, 1H). ^{13}C NMR (101 MHz, $CDCl_3$) δ 146.7, 133.7, 125.4, 123.5, 116.2. IR (KBr, cm^{-1}): 2153, 1644, 1328, 728. m.p. 102 °C. HRMS (ESI) m/z: $[M+H]^+$ calcd for $C_5H_4ClN_4$ 155.0124; found: 155.0158.

1.5.2 Synthesis of 4-azidopyridine 1.134d

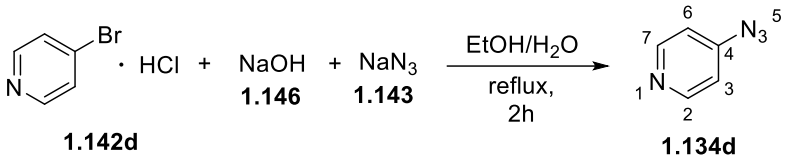

1.142d **1.134d**

To a solution of 4-bromo-pyridine hydrochloride **1.142d** (500 mg, 2.6 mmol, 1 equiv.) in a mix of ethanol:water 1:1 (5.2 mL) NaOH **1.146** (52 mg, 1.3 mmol, 0.5 equiv.) and NaN_3 **1.143** (390 mg, 6 mmol, 2.3 equiv.) were added. The reaction mixture was refluxed at 110 °C for 2 h. After completion of the reaction, monitored by TLC (PE/AcOEt 70:30), the mixture was extracted with DCM three times. The collected organic layers were then washed with brine and saturated $NaHCO_3$ and dried over anhydrous Na_2SO_4. The solvent was evaporated to afford product **1.134d** without further purification as yellow oil in high yields (75%, 235 mg). ^{1}H NMR (400 MHz, $CDCl_3$) δ 8.55 (d, *J* = 4.2 Hz, 2H), 6.96 (d, *J* = 6.0 Hz, 2H).^{13}C NMR (101 MHz, $CDCl_3$) δ 151.2 (C2-C7), 148.7, 114.1 (C3-C6). All analytical data are consistent with those reported in the literature.[83]

1.5.3 Hydrolysis of β-ketoester 1.98 to obtain 2-methyl-3-oxobutanoic acid 1.147, precursor for the synthesis of β-ketoester 1.124d

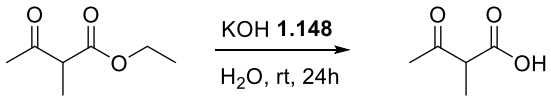

1.98 **1.147**

To an aqueous solution (20 mL, 0.5 M) of β-ketoester **1.98** (3 mL, 21 mmol, 1 equiv.), KOH **1.148** (1.18 g, 21 mmol, 1 equiv.) was added. The reaction mix stirred at room temperature for 24 hours. After complete consumption of the starting material, monitored by TLC analysis (PE/AcOEt 60:40), the reaction mix was quenched with sodium bicarbonate. The crude was extracted with

AcOEt and the organic phase discarded. The aqueous phase was then acidified with HCl 1N and washed with AcOEt twice. The organic phases were dried over anhydrous Na_2SO_4 and the solvent removed by rotary evaporation to afford the product **1.147** as yellow oil in moderate yields (41%, 1g). ^{1}H NMR (400 MHz, $CDCl_3$) δ 10.20 (s, 1H), 3.58 (q, *J* = 7.2 Hz, 1H), 2.31 (s, 3H), 1.39 (d, *J* = 7.2 Hz, 3H). ^{13}C NMR (101 MHz, $CDCl_3$) δ 203.7, 175.9, 36.9, 28.7, 12.8. All analytical data are consistent with those reported in the literature.[84]

1.5.4 Synthesis of modified β-ketoester 1,1,1,3,3,3-hexafluoropropan-2-yl 2-methyl-3-oxobutanoate 1.124d

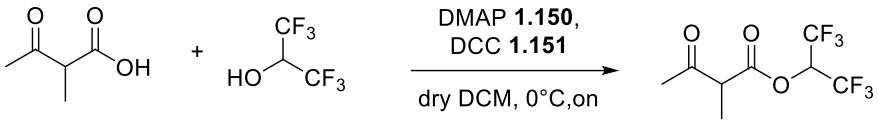

1.147 **1.149** **1.124d**

In a round bottom flask equipped with a magnetic stirring bar, a solution of **1.147** (668.3 mg, 5.75 mmol, 1 equiv.) in dry DCM (19 mL, 0.3 M) was prepared and cooled to 0°C. Afterwards, dimethylaminopyridine **1.150** (DMAP, 70 mg, 0.575 mmol, 0.1 equiv.), 1,1,1,3,3,3-hexafluoro-2-propanol **1.149** (0.65 mL, 6.32 mmol, 1.1 equiv.) followed by *N*,*N*′-dicyclohexylcarbodiimide **1.151** (DCC,1.3 g, 6.32 mmol, 1.1 equiv.) were added to the reaction mix. The reaction stirred at 0°C overnight. The day after a white precipitate was observed, corresponding to the dicyclohexyl urea (DCU) produced as DCC by-product, while TLC (DCM/MeOH 99:1) showed complete consumption of the starting material. The solid was filtered and washed carefully with petroleum ether. The solution collected was evaporated and purified by column chromatography (DCM 100%) to afford the product **1.124d** as colorless oil in moderate yields (64%,445 mg).^{1}H NMR (400 MHz, $CDCl_3$) δ 5.78 (m, 1H), 3.72 (q, *J* = 7.2 Hz, 1H), 2.28 (s, 3H), 1.45 (d, *J* = 7.2 Hz, 3H). ^{13}C NMR (101 MHz, $CDCl_3$) δ 201.0, 167.6, 120.2, 66.8 (average for the two CF_3), 52.8, 28.3, 12.7. All analytical data are consistent with those reported in the literature.[85]

1.5.5 Synthesis of modified β-ketoester ethyl 2-(2-methyl-1,3-dioxolan-2-yl)propanoate 1.124f

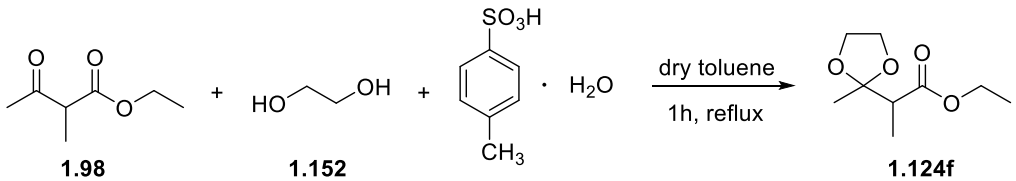

1.98 **1.152** **1.153** **1.124f**

A mixture of **1.98** (1 mL, 7.07 mmol, 1 equiv.)**,** ethylene glycol **1.152** (1.2 mL, 21.21 mmol, 3

equiv.) and *p*-toluensulfonic acid monohydrate **1.153** (4mg, 0.02 mmol, 0.003 equiv.) in anhydrous toluene (4 mL, 1.7 M), was refluxed using a distillation kit trap until the theoretical amount of water (1 mL for 1 mmol of starting material) was collected. After 1 hour, the reaction mix was cooled down and the crude extracted with sodium bicarbonate, water and brine three times. The organic phases were dried over anhydrous Na_2SO_4 and the solvent removed by rotary evaporation. The compound obtained was distilled again in order to separate the product (recovered at 150°C, 1 atm) from residuals of starting material. Product **1.124f** was obtained as colorless oil in poor yields (15%,195 mg). ^{1}H NMR (400 MHz, $CDCl_3$) δ 4.16 (q, *J* = 7.1 Hz, 2H), 4.03 – 3.90 (m, 2H), 2.76 (q, *J* = 7.1 Hz, 1H), 1.41 (s, 3H), 1.27 (t, *J* = 7.1 Hz, 3H), 1.22 (d, *J* = 7.1 Hz, 3H).^{13}C NMR (101 MHz, $CDCl_3$) δ 173.3, 109.8, 64.9, 60.5, 47.9, 21.4, 14.2, 12.9. All analytical data are consistent with those reported in the literature.[86]

1.5.6 Synthesis of ethyl 5-methyl-1-(pyridin-2-yl)-1H-1,2,3-triazole-4-carboxylate 1.136a

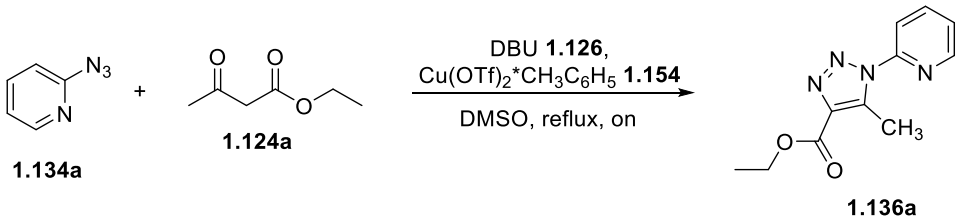

To a solution of 2-azido pyridine **1.134a** (80 mg, 0.67 mmol, 1 equiv.) in DMSO (0.3 M, 2 mL), β-ketoester **1.124a** (0.102 mL, 0.80 mmol, 1.2 equiv.), DBU **1.126** (0.120 mL, 0.80 mmol, 1.2 equiv.) and copper triflate toluene complex **1.154** ($Cu(OTf)_2$*$C_6H_5CH_3$, 48 mg, 0.067 mmol, 0.1 equiv.) were added. The reaction turned from light brown to black upon addition of the catalyst and stirred overnight at reflux. The day after, TLC (DCM/AcOEt 90:10) showed complete consumption of **1.134a**. The reaction mix was then cooled to room temperature, extracted with DCM/H_2O three times and the collected organic phases filtered through a celite pad, to eliminate solid copper triflate toluene complex. The crude was then purified by column chromatography (DCM/AcOEt 90:10) to afford product **1.136a** as a yellow oil in moderate yields (60%, 93 mg). ^{1}H NMR (400 MHz, $CDCl_3$) δ 8.60 (d, *J* = 4.6 Hz, 1H), 8.03 – 7.90 (m, 2H), 7.48 – 7.38 (m, 1H), 4.48 (q, *J* = 7.1 Hz, 2H), 2.93 (s, 3H), 1.46 (t, *J* = 7.1 Hz, 3H).^{13}C NMR (101 MHz, $CDCl_3$) δ 161.8, 150.2, 148.5, 139.8, 139.1, 137.4, 124.1, 118.4, 61.2, 14.4, 11.1. All analytical data are consistent with those reported in the literature.[68a,b]

1.5.7 General procedure for the synthesis of pyridine-based triazoles 1.136b,c (GP2)

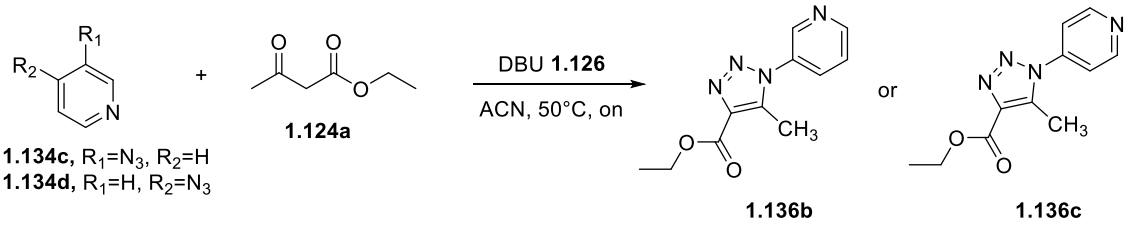

To a solution of 2-azido pyridines **1.134c,d** (0.5 mmol, 1 equiv.) and β-ketoester **1.124a** (0.6 mmol, 1.2 equiv.) in ACN (0.2 M) was added DBU **1.126** (0.6 mmol, 1.2 equiv.) and the reaction was stirred at 50 °C in an oil bath, overnight. The crude mixture was evaporated under vacuum and purified *via* flash column chromatography (MeOH/DCM/AcOH 90:10:0.1) to afford title compounds **1.136b,c** in moderate to high yields (50% and 86% respectively).

Ethyl 5-methyl-1-(pyridin-3-yl)-1H-1,2,3-triazole-4-carboxylate 1.136b

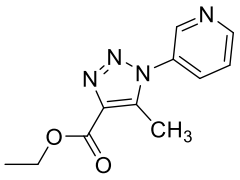

Prepared according to GP2. Yellow oil, 50% yield, 24.5 mg. ^{1}H NMR (400 MHz, $CDCl_3$) δ 8.83 (d, *J* = 4.7 Hz, 1H), 8.78 (s, 1H), 7.89 (d, *J* = 8.1 Hz, 1H), 7.58 (dd, *J* = 8.1, 4.9 Hz, 1H), 4.48 (q, *J* = 7.1 Hz, 2H), 2.65 (s, 3H), 1.46 (t, *J* = 7.1 Hz, 3H).^{13}C NMR (101 MHz, $CDCl_3$) δ 161.5, 151.2, 145.9, 139.1, 137.2, 132.7, 132.3, 124.3, 61.3, 14.4, 9.9. All analytical data are consistent with those reported in the literature.[68]

Ethyl 5-methyl-1-(pyridin-4-yl)-1H-1,2,3-triazole-4-carboxylate 1.136c

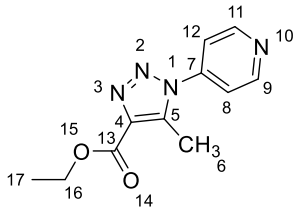

Prepared according to GP2. Orange solid, 86% yield, 84.4 mg. ^{1}H NMR (400 MHz, $CDCl_3$) δ 8.88 (d, *J* = 6.1 Hz, 2H), 7.51 (d, *J* = 6.1 Hz, 2H), 4.48 (q, *J* = 7.1 Hz, 2H), 2.72 (s, 3H), 1.46 (t, *J* = 7.1 Hz, 3H).^{13}C NMR (101 MHz, $CDCl_3$) δ 161.4, 151.7 (C11-C9), 142.5, 138.7, 137.6, 118.7 (C12-C8), 61.4, 14.4, 10.3. All analytical data are consistent with those reported in the literature.[68]

Chapter 2

Pyridine-based 1,2,3-triazoles as potential lead compounds for drug discovery: Docking screening, Fluorescence Tests and Biological Evaluation.

2.1 Introduction

In this chapter we report a study that, starting from synthetically available triazole **1.136a**, discussed in *Chapter 1*, identified a new lead compound, **2.80c**, for KAT2A inhibition. The study has been performed in collaboration with other institutions in Italy with frequent online meetings for the setting-up of the experiments and the comparison of the results. The PhD candidate has been supervising the entire process from the very first step while always interacting with the partner institutions to compare and analyse the results obtained from specific tests. In particular, the study involved the following activities:

A. Virtual screening of a small set of pyridyl-triazoles, including **1.136a** and its carboxylate analog **2.53**, performed in collaboration with Dr. Lydia Siragusa and Prof. Gabriele Cruciani of the Laboratory for Chemometrics and Molecular Modelling, Department of Chemistry, Biology and Biotechnology, University of Perugia, Italy.
B. Synthesis of a small library of pyridyl-triazoles following the results obtained from the virtual screening, performed here at RCSI by the PhD candidate.
C. Binding studies *via* fluorescence assays of the best candidates performed here at RCSI by the PhD candidate.
D. Biological evaluation *in vitro* following the results assessed through binding studies, performed in collaboration with Dr. Nunzio del Gaudio, Guglielmo Bove and Prof. Lucia Altucci of the Department of precision medicine, University of Campania Luigi Vanvitelli, Naples, Italy.

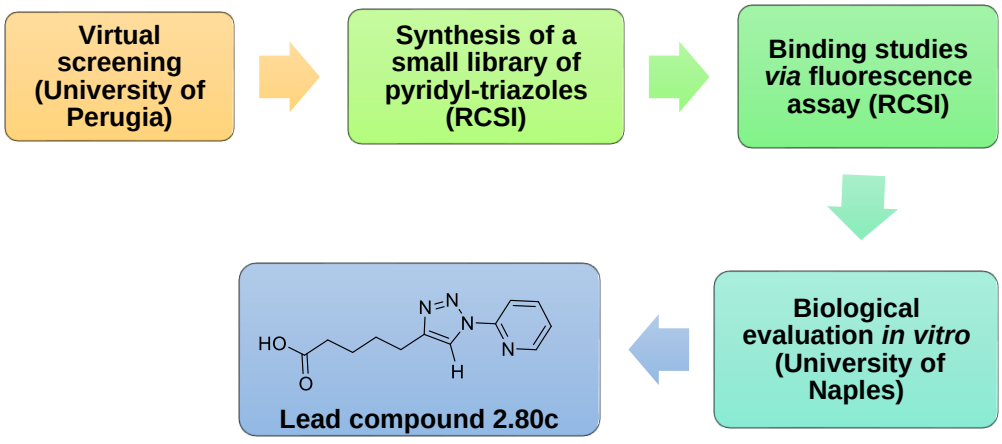

The contribution to science described in the Figures and Schemes of this Chapter is opportunely declared; when no indication is provided, it is assumed to be entirely work carried out by the PhD candidate at RCSI.

2.1.1 Bioisosteres definition and application in medicinal chemistry

Bioisosterism is defined as the replacement of a part of a bioactive molecule with another unit that shows similar biological properties.[87] The concept of bioisosterism was firstly described by Langmuir[88] and experimentally proved, in 1932[89] and 1933[90], by Erlenmeyer and his collaborators. They noticed that a group of antibodies, involved in recognising specific *ortho* substituents on tyrosines's scaffolds, were not able to distinguish between a phenyl and a thiophene ring or between O, NH and CH_2 in a linker element. Following this finding, in 1951, Friedman was able to attribute to this phenomenon the definition of bioisosterism as of compounds displaying similar biological activity.[91] Bioisosteric replacement is a powerful tool that has been and continues to be used by medicinal chemists to find new potential scaffolds for drug discovery. Moreover, bioisosteres can be useful to alter both parmacokinetic and pharmacodynamic profiles as well as toxicity and metabolic activation *in vivo* by simply modifying the electronic properties, the pK_a values or size and shape of the molecule (Figure 17).[92–98]

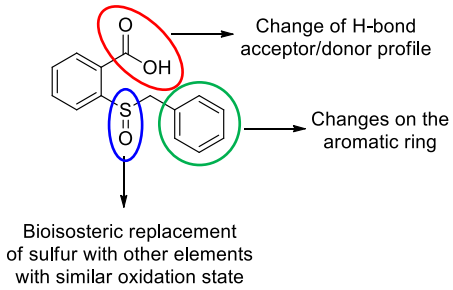

Figure 17: Some of the bioisosteric key-substitutions for new templates discovery.

Along with bioisosterism, scaffold hopping represents another important tool for searching for new drug candidates. Scaffold hopping involves the replacement of a core unit with another one that is structurally dissimilar but retains the original biological activity (Figure 18).[99–101] At the moment, diverse *in silico* methods are available to identify potential groups with similar properties such as chemoinformatic techniques (Principal Components Analysis, Self-Organising Maps, k-Means Clustering, Hierarchical Clustering)[102–104] that use specific descriptors to select similar bioisosteric pairs. In particular, two constants play an important role when looking for functional groups for bioisosteric replacement: Hammett's sigma constant, σ[105] and Hansch's parameter, π.[106] The σ parameter allows to screen for the electron-donating power of substituents while the π paramenter explores the hydrophobicity of the substituents.

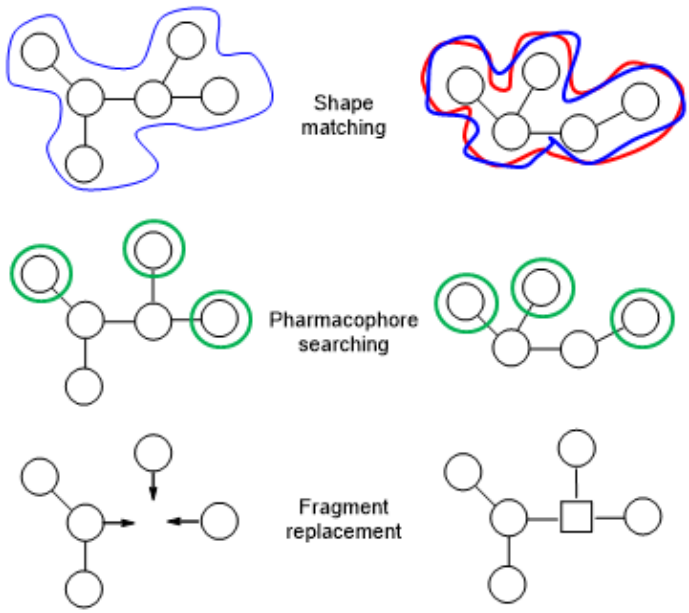

Figure 18: Scaffold hopping approach for the identification of new bioisosteres.

In spite of the terrific advances herein described, the identification of new bioisosteric replacements remains challenging and requires a deep chemical knowledge as well as multiple trials and error experiments to be performed, which is why there is urgent need for robust predictive models that furnish ideal conditions for bioisosteres development.

2.1.2 1,2,3-triazoles as bioisosteres in drug design

1,2,3-triazoles are commonly recognised as important chemical scaffolds as well as efficient molecules in the area of medicinal chemistry.[107,108] Throughout the years, many synthetic methods were developed to afford these compounds allowing for the disconnection of the triazole nucleus **1.5** in several directions and from diverse building blocks. Hence, from the first Huisgen 1,3-dipolar cycloaddition using **2.1** and **2.2**,[20,109] to the copper- or ruthenium- catalysed alkyne-azide cycloaddition developed by Sharpless and co-workers,[34,35,110] to finally end with greener and milder approaches explored by Wang[111] and Ramachary[49], who reacted active methylene compounds **2.4**[112] with organic azides **1.125** using secondary amines as catalysts **1.80** (Figure 19). Given 1,2,3-triazoles's versatile behavior as both soft Lewis acids and bases and considering the pyrrole-pyridine type characteristics of the three nitrogens,[12,113] they have been used as a core structural motif in a huge varieties of drug categories such as: antimicrobial,[114,115] anti-inflammatory,[116] antineoplastic,[117] antiviral,[118] antihypertensive[119] or as immunomodulatory agents[120].

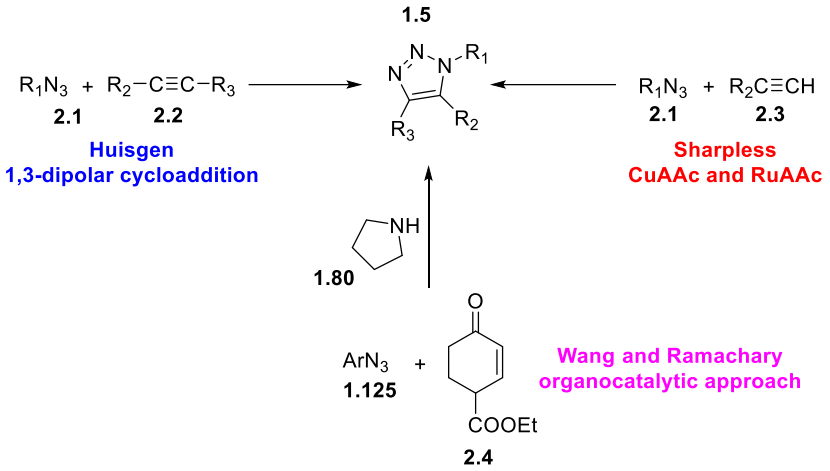

Figure 19: Different synthetic routes to afford 1,2,3-triazoles **1.5**.

1,2,3-triazoles owe their ability to be employed as bioisosteres, in particular, to the presence of a lone pair on one of the three nitrogens which provides a protonation site and imbues to 1,2,3-triazoles a unique capability of acting as both H-bond donors and acceptors.[121] For these reasons, 1,2,3-triazoles' solubility is increased *versus* other azoles along side their interaction with diverse biomolecular targets.[122] Furthermore, the 1,2,3-triazole nucleus is particularly stable to oxidation, hydrolysis or reduction, if compared to other organic compounds with three adjacent nitrogens.[123] Their unique chemical structure allows these compounds to bind enzymes and biological systems through weak interactions like coordination-bonds, H-bonds, π-π stacking, ion-dipole and so on.[124] Additionally, when combined with other active chemical fragments, the 1,2,3-triazole core turns into "lead compound" for the design of new pharmacophores, defined as parts of a molecular structure that are responsible for a particular biological or pharmacological interaction (Figure 20).[126,127]

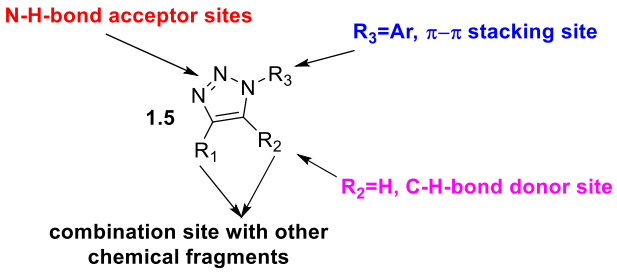

Figure 20. Sites potentially available for bioisosterism of 1,2,3-triazoles **1.5**.

For these reasons, *i.e.* H-bonding and solubility, the triazole core has been used to ameliorate the pharmacokinetic profile as in **2.5**, **2.7**, **2.8**, **2.9** or **2.10** or to become the pharmacophore as in antifungal **2.6**. (Figure 21). In this way the research of new potential candidates for drug discovery

is speeded up and optimised.[128]

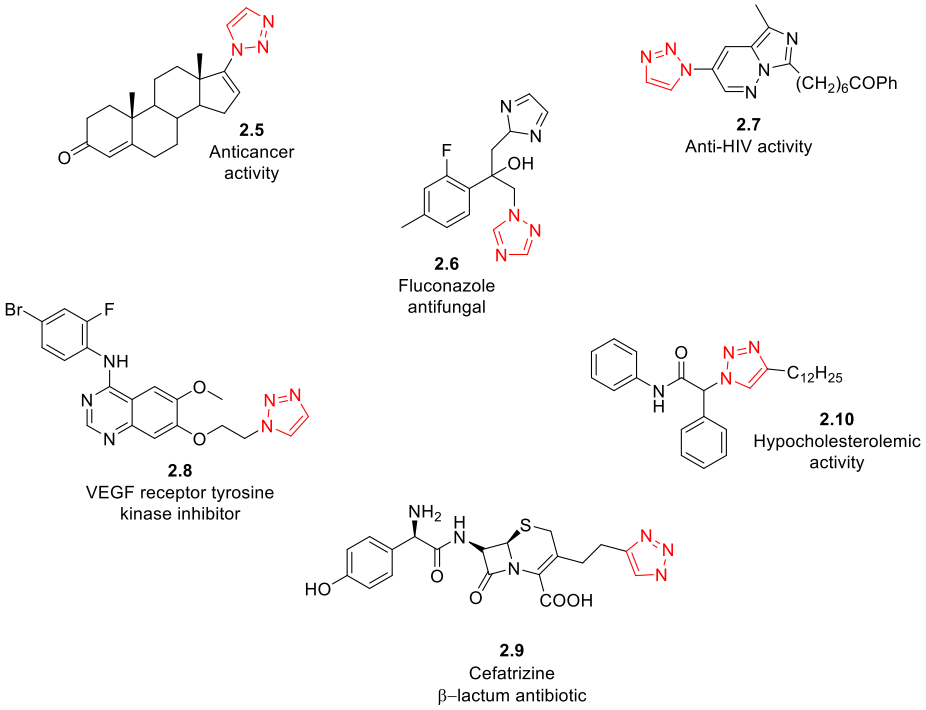

Figure 21: Examples of the 1,2,3-triazole scaffold in commercial drugs or bioactive compounds **2.5-2.10**.

2.1.2.1 1,2,3-triazoles as amide bond isosteres.

Among the most famous functional groups used for isosterism in medicinal chemistry, amides cover a huge variety of drugs that have been developed throughout the years. The amide function consists of two hydrogen bonding sites: i) the carbonyl function, that acts as hydrogen bond acceptor site, and ii) the amine group that acts as hydrogen bond donor site. The lone pair lying on the amine nitrogen cannot be employed as hydrogen bond acceptor site due to its involvement in stabilising the amide bond itself with resonance structures. For this reason, the amido group possesses a planar configuration that introduces a spatial rigidity that can either enhance or weaken any hydrogen bonds.[129] Erroneously, the peptide bond is considered as a synonym of the amide bond. The amide involved in a peptidic bond results from the linkage of the α-amino nitrogen of one aminoacid with the carbonyl carbon of a second aminoacid. The resulting amide-like bond can be considered as with partial double bond features (since the lone pair of the amido nitrogen can be delocalised for resonance structures) and, therefore, shares with amides a similar planar conformation.[130] Unfortunately, the amide bond is easily cleaved by enzymes, known as proteases, *in vivo* thus suffering from poor metabolic stability. Hence, bioisosteric replacement of the amide bond became imperative to build new pharmacophores more resistant to metabolic

cleavage and with an improved pharmacokinetic profile. 1,2,3-triazoles are commonly used as amide bioisosteres and are considered among the most efficient as they share an overlapping structure, in terms of dipole moment and substituents position. Specifically, 1,4-disubstituted 1,2,3-triazoles **2.14** present a similar superimposition with the *trans* conformer **2.13** (Figure 22) of the amide bond for the following reasons: i) carbon C4 possessing the same electrophilic power displayed by the carbonyl moiety of the amido group ii) *N*-3 lone pair featuring similar electronic properties to the oxygen lone pair of the amide carbonyl group.[130] On the other hand, 1,5-substituted 1,2,3-triazoles **2.12** possess high similarity in spatial conformation of the substituents, with regard to the *cis* amide conformer **2.11** keeping all the same electronic features of the 1,4-regioisomer.[130] Furthermore, the CH bond (at position 4 and 5 respectively) of both 1,4- **2.14** and 1,5-disubstituted **2.12** 1,2,3-triazoles exhibits a strong dipole moment and can be considered analogous of the amide *NH* function as H-bond donor site (Figure 22).[131]

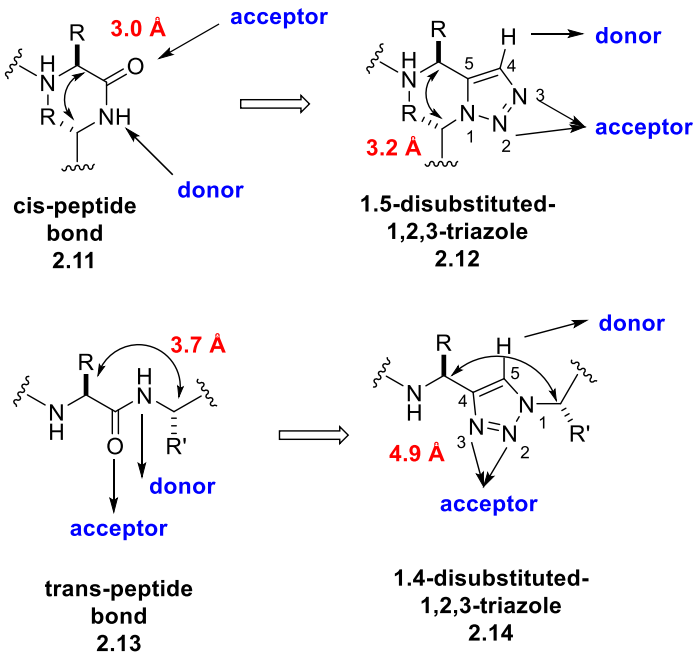

Figure 22: Electronic comparison of *cis*/*trans* amides **2.11** and **2.13** with 1.5-/1.4- substituted 1,2,3-triazoles **2.12** and **2.14**.

Contrary to amides, 1,2,3-triazoles are resistant to enzymatic cleavage and introduce a structural rigidity that can improve potency, selectivity, metabolic stability and pharmacokinetic properties.[132] Consequently, 1,2,3-triazoles are largely employed in drug discovery for amide bioisosteric replacements. Imatinib is the treatment of choice of an aggressive type of cancer known as chronic myelogenous leukemia (CML). This disease is caused by an unregulated growth of myeloid cells in the bone marrow and consequent accumulation of them in the blood. This enhanced proliferation, originated from the formation of the Bcr-Abl oncogene, results from the

traslocation of chromosomes 9 and 22 of the Philadelphia chromosome and follows overactivation of the tyrosine kinase linked to it. Nevertheless, mutations within and not the Bcr-Abl kinase domain conferred CML cancerogenic cells resistance to Imatinib.[133,134] Arioli *et al.*[135] developed 1,2,3-triazole FA030 **2.15** as potential triazole-based analog of Imatinib **2.16** (Figure 23) through CuAAc cycloaddition reaction. They proved **2.15** to be able to decrease phosphorylation of the Bcr-Abl tyrosine-kinase protein with a similar effect observed for Imatinib (0.9±0.1 μM *versus* 0.40±0.1 μM respectively); it is known that phosphorylation of the tyrosine 393 residue stabilises the open form of the activation loop of Bcr-Abl and prevents Imatinib from accessing the catalytic region.[136,137] Moreover, **2.15** showed a higher activity than Imatinib in the inhibition of the CDC25A in two diverse cell lines; dual specificity phosphatase CDC25A is a protein of the CDC25 phosphatase family that removes phosphate groups from phosphorylated tyrosine residues.[138]

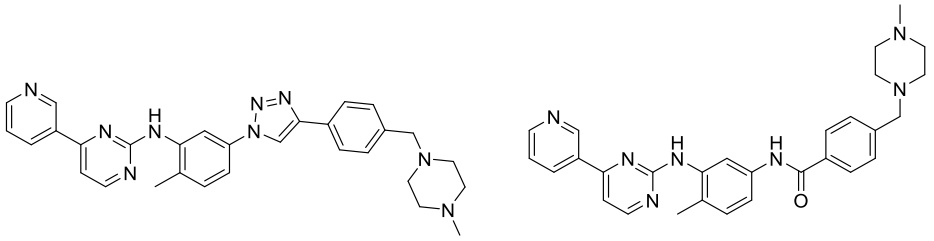

Figure 23: Arioli's compound FA030 **2.15** as potential Imatinib **2.16** triazole-based analog.

Among other important examples of 1,2,3-triazoles employed as amide bioisosteres, we can find several HIV-1 protease inhibitors developed by Mohammed *et al*.[139] They generated a new class of HIV-1 viral infectivity factor (vif) inhibitors, such as **2.17**, based on the structure of vif inhibitor RN-18 (**2.18**), and noticed that analogs containing a triazole nucleus (Figure 24) showed improved activity (IC_{50}=1.2μM against 6μM observed for RN-18).

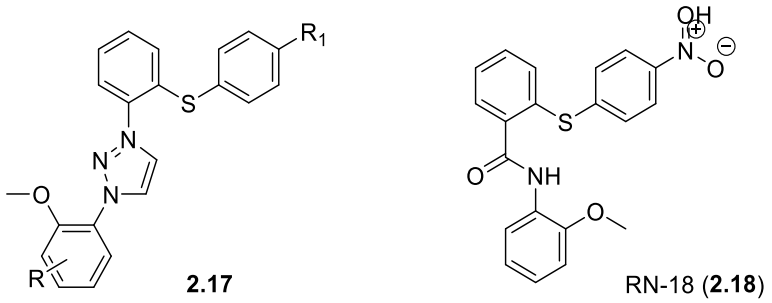

Figure 24: Mohammed's triazole analog **2.17** as potential HIV-1 vif inhibitors resembling approved drug RN-18 **2.18**.

On the other hand, Brik *et al*.[140,141] developed HIV-1 protease inhibitor Amprenavir (**2.21**) analogs

to overcome drug resistance. They proved two of the compounds synthesised, AB2 (**2.19**) and AB3 (**2.20**), both including a 1,2,3-triazole scaffold (Figure 25), possess nanomolar activity against HIV-proteases in both wild type and resistant models (6±0.5 nM and 13±0.5 nM respectively). Moreover, X-rays of AB2 and AB3, complexed with HIV-1 protease, found these molecules were bound in a similar binding position to the way Amprenavir relates with the protease thus confirming the 1,2,3-triazole scaffold to be a valid amide bioisosteric replacement.[142]

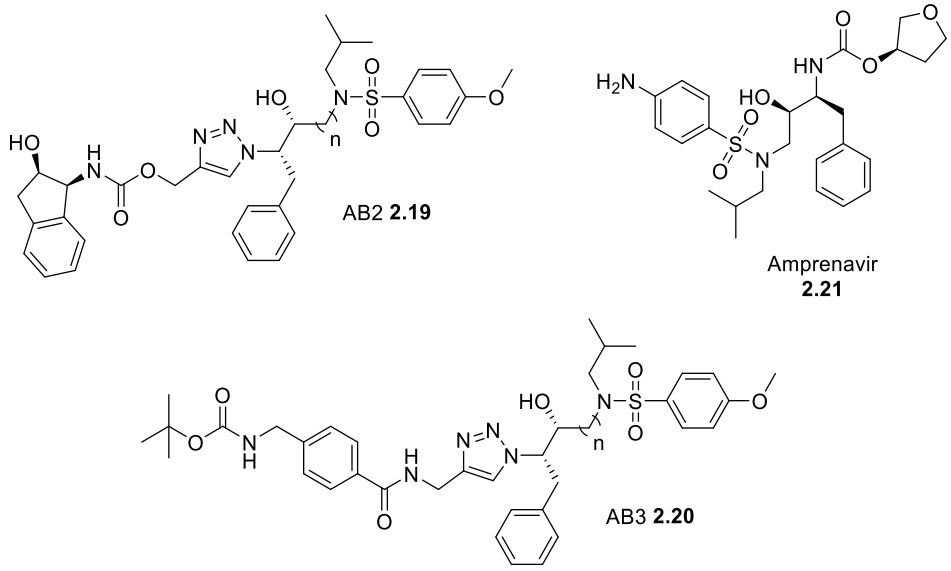

Figure 25: Brik's triazole analogs **AB2** (**2.19**) and **AB3** (**2.20**) as potential HIV-1 protease inhibitors resembling commercial drug Amprenavir **2.21**.

Additionally, diverse attempts have been performed to create 1,2,3-triazole-based bioisosteres of peptides, considering 1,2,3-triazoles resistance to proteolysis. Pioneers in this field were Meldal and Ghadiri. Meldal *et al.*[143] were the first to use the CuAAC strategy in solid support to couple small peptides **2.22** to 1,4-disubstituted-1,2,3-triazoles.[35] Meldal's team proved these peptides to be able to link with diverse azides **2.24** in high yields to generate a vast library of new peptidomimetics **2.25** with potential biological interest (Figure 26).

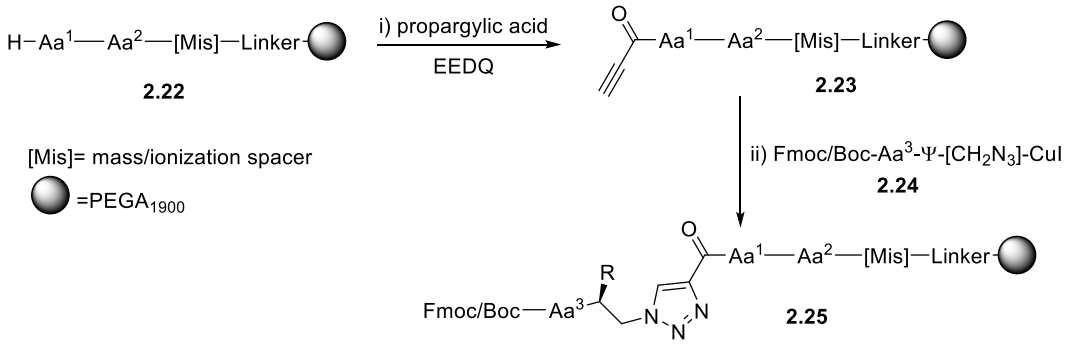

Figure 26: Meldal's strategy to incorporate 1,4-disubstituted-1,2,3-triazole unit into small peptides.

Ghadiri also worked on inserting the 1,4-disubstituted-1,2,3-triazole core into cyclic peptidomimetics with excellent results.[144,145] Mindt *et al.*[146,147] demonstrated peptidomimetics containing a 1,4-disubstituted-1,2,3-triazole unit were more efficient in tumor-targeting compared to the original peptides and also more stable to proteolysis, while keeping the same receptor-affinity properties. Inclusion of the 1,5-disubstituted-1,2,3-triazole scaffold has also been investigated by Beke-Somfai *et al.*[148] They noticed that peptidomimetics bearing a 1,4-disubstituted-1,2,3-triazole core could exist in a limited number of comformations while the same peptidomimetics including a 1,5-disubstituted-1,2,3-triazole scaffold were adopting a higher number of folded conformations such as torn, helix and zig-zag secondary structures.[149] Cao *et al*.[150] reported 1,2,3-triazole-based analog **2.26** of leucine-ureido conjugates to be roughly 100-fold more potent (Figure 27), compared to the positive control Bestatin **2.27**, in suppressing the activity of cell surface aminopeptidase N, APN, a membrane-bound ectoenzyme responsible for tumor cell expansion and mobility.[151]

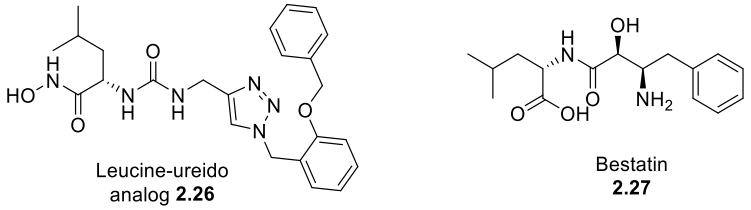

Figure 27: Cao's triazole analog **2.26** as potential cell surface aminopeptidase N inhibitor resembling commercial drug Bestatin **2.27**.

In summary, 1,2,3-triazoles can be employed as valid amides isosteres given their similar size and planar structure, their high dipolar moment (4.9Å and 3.1Å respectively for 1,4- and 1,5-substituted triazoles), their similar H-bonding capabilities and their resistance to cleavage by protease enzymes. Most importanty, more studies *in vivo* need to be performed to better characterise triazoles binding-mode with specific targets together with enhancing their

pharmacokinetic profile.

2.1.2.2 1,2,3-triazoles as ester bond isosteres.

Going further with the application of 1,2,3-triazoles as bioisosteres, an important role is covered by 1,2,3-triazoles employed as isosteres of the ester function. The ester moiety has the potential to act as H-bond acceptor site, thanks to the greater electron density on the carbonyl function, but its susceptibility to enzymatic degradation *in vivo* makes it a fragile scaffold to be employed in drug discovery. The triazole nucleus has been put to use as it offers the possibility to act as H-bond acceptor, enhancing the selectivity towards its target.[152,153] Notably, Imperio *et al*.[154] tried to synthesise 1,2,3-triazole-based analogs of Steganacin **2.30** and Podophyllotoxin **2.31**, two natural compounds with antitubuline effects. The replacement of the lactone moiety with a 1,2,3-triazole unit produced two analogs (Figure 28), **2.28** and **2.29**, that retained the antitubulin activity, displayed against neuroblastoma cells, while also keeping a high cytotoxicity, that is, although, inferior to the one possessed by their parental natural compounds **2.30** and **2.31**.

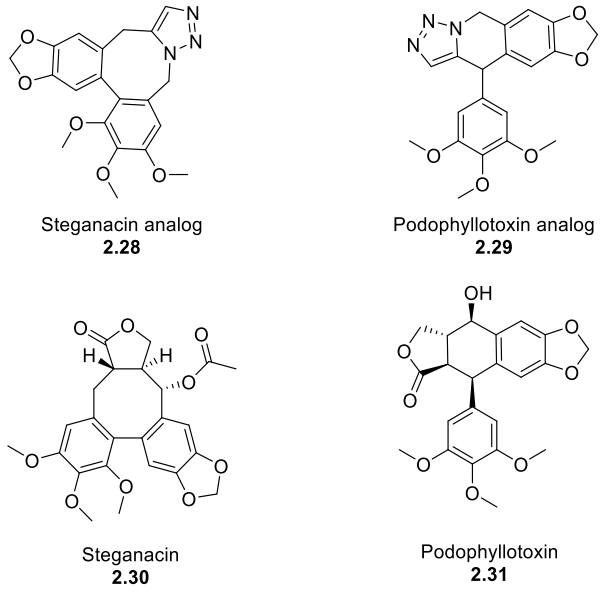

Figure 28: Imperio's triazole analogs **2.28** and **2.29** as potential antitubuline compounds resembling their parental compounds Steganacin **2.30** and Podophyllotoxin **2.31**.

Despite Podophyllotoxin toxicity, Yang *et al*.[155] revelead that 1,2,3-triazole analogs of Podophyllotoxin were efficiently employed against lung cancer (Figure 29). Compound **2.32** showed the best activity *in vitro* with an IC_{50} value of 5.49 μM, even higher than the one Etoposide **2.33** possesses, against KBvin (vincristine resistant nasopharingeal carcinoma)[156] cell line.

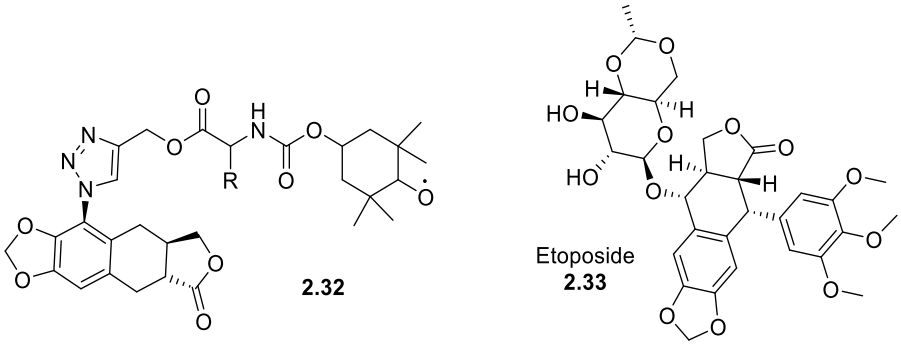

Figure 29: Yang's triazole analog **2.32** as potential anticancer compounds resembling commercial drug Etoposide **2.33**.

Currently, a significant effort towards finding new ester bond isosters is ongoing. 1,2,3-triazoles are being increasingly included as ester bond isosteres in drug discovery due to their versatility to act as hydrogen bond donors or hydrogen bond acceptors and, mostly, due to their stability towards hydrolysis by esterases.

2.1.2.3 1,2,3-triazoles as hydroxamic acid isosteres.

Hydroxamic acids can be considered valid bioisosteres of the carboxylic acid function with many advantages. Indeed, carboxylic acids suffer from metabolic instability, poor permeability across biological membranes and toxicity.[157] On the contrary, the stability of hydroxamic acids can be controlled towards hydrolysis by simply adding bulky substituents at the nitrogen atom of the hydroxylamine fragment.[158] Furthermore, they possess improved profiles of absorption, distribution, metabolism and excretion.[159] Above all, hydroxamic acids take their biological activity characteristics from their ability to chelate metals making them excellent candidates in targeting cancer, HIV, Alzheimer's disease etc.[160] 1,2,3-triazoles and, in particular, 4- and 5-hydroxy-1,2,3-triazoles share many common features with hydroxamic acids. More specifically, the Adamo's group already proved 5-hydroxytriazoles **1.127a** to be able to interact with metal ions, such as Fe^{3+} and Cu^{2+}, suggesting similar chelating properties as hydroxamic acids and display a similar pK_a value (4.2 against 7.6 respectively, Table 5).[68] Additionally, Pippione *et al*.[70] also demonstrated 4-hydroxy-1,2,3-triazoles **2.34** to be as acidic as hydroxamic acids (pK_a values of 5.54 against 7.6 respectively, Table 5).

Table 5: Comparison of the pK_a of 5- and 4-hydroxytriazoles **1.127a** and **2.34** with hydroxamic acids.

Triazole structure	Triazole pK_a	Hydroxamic acid pK_a
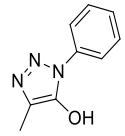 5-hydroxy-1,2,3-triazole **1.127a**	**4.20**	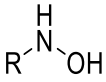 **7.6-10.3**
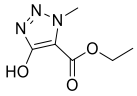 4-hydroxy-1,2,3-triazole **2.34**	**5.54**	

Hydroxamic acids are one of the most potent histone deacetylase (HDAC) inhibitory unit, often used as scaffold for the development of HDACs inhibitors. HDACs inhibitors, besides, are known to have a crucial impact on arresting cancer cell proliferation in most of the tumor types known.[161,162] He *et al*.[163] developed a potent 1,2,3-triazole-based HDAC inhibitor (**2.35**) with excellent activity profile (Figure 30) showed against five different pancreatic cell lines (at concentrations of 0.2μM, 0.4μM, 0.02μM, >0.5μM and 0.8μM respectively). Mwakwari *et al*.[164] also contributed to the discover of new HDAC triazole-based inhibitors by building a library of triazolyl analogs of tricyclic ketolide TE-802 **2.36**, a powerful mimetic of HDAC1 isoform peptide backbone (Figure 30). All their 1,2,3-triazole analogs produced high inhibitory activity against both HDAC isoforms 1 and 2 with nanomolar concentrations (for compound **2.37** they obtained concentrations of 1.17 nM, 0.82 nM and 1.26 nM against three different cell lines).

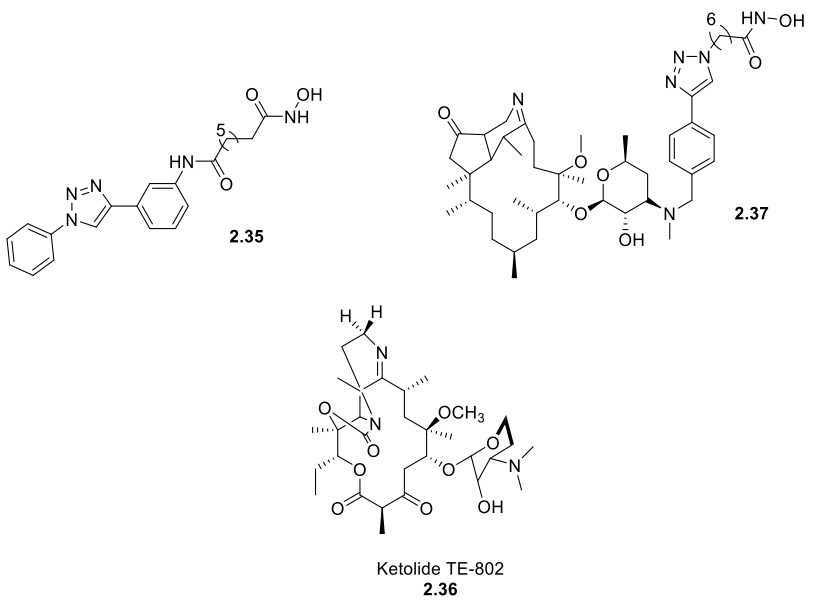

Figure 30: He's and Mwakawari's triazoles analogs **2.35** and **2.37** as potential HDAC inhibitors resembling commercial drug Ketolide TE-802 **2.36**.

Giraudo *et al*.[128] highlighted the importance of 4-hydroxy-1,2,3-triazoles as potential analogs of GABA inhibitors. The gamma-aminobutirric acid (GABA) is an important neurotransmitter involved in reducing neuronal excitability. A deficiency in GABA (**2.39**) activity can produce mental health conditions such as anxiety, schizophrenia and depression.[165] Giraudo noticed that 1,2,3-triazole analogs, bearing diphenylbutyl profiles within the backbone, like compound **2.38**, showed a higher K_i value concentration (1.6 μM) and that their alkylation on the *N*3 nitrogen might increase their inhibition power of the $GABA_A$ isoform (Figure 31).

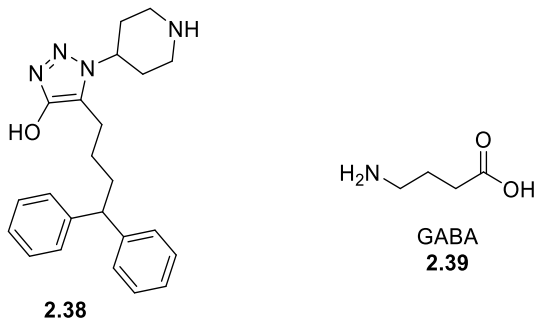

Figure 31: Giraudos triazole analog **2.38** as potential GABA **2.39** isoforms inhibitors.

1,2,3-triazoles are also efficiently employed as anti-inflammatory hydroxamic acids analogs. Kim *et al*.[166] illustrated a well-planned development of phenyl-1,2,3-triazoles **2.40** that produced a TNFα-induced COX2 expression higher than Diclofenac **2.41** when assessed at molecular level in ear edema model mice (Figure 32).

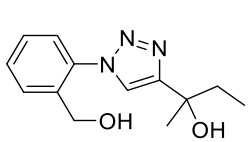

2.40

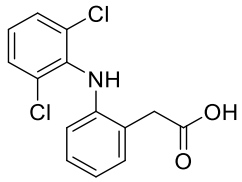

Diclofenac
2.41

Figure 32: Kim's triazole analog **2.40** as potential antinflammatory candidate based on Diclofenac's nucleus **2.41**.

Interestingly, Flieger *et al*.[167] demonstrated that Econazole derivatives with the 1*H*-triazole scaffold did not have any antifungal effect but, when the same derivative was converted into a 5-hydroxy-1,2,3-triazole, it turned out to have activity as an antitubercular. Compound **2.42** was found to be 2-fold more potent than Econazole **2.43** itself, suggesting the 1,2,3-triazole unit, in conjunction with the β-OH, to be very selective towards *M.Tubercolosis* (Figure 33).

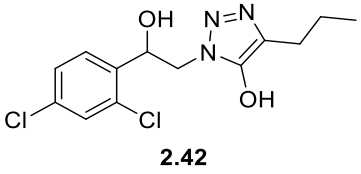

2.42

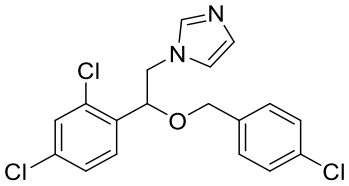

Econazole
2.43

Figure 33: Flieger's triazole analog **2.42** as potential antitubercular candidate resembling commercial drug Econazole **2.43**.

In summary, 1,2,3-triazoles can be efficiently employed as hydroxamic acid bioisosteres due to their similar pK_a and ability to coordinates metal ions. For this reason, we synthesised a small library of pyridine-based 1,2,3-triazoles bearing an acidic C-H proton at position 5 and evaluated, through docking studies, their potential as hydroxamic acids bioisosteres.

2.2 Docking studies: principles

Molecular docking was first described in 1982 by Kuntz *et al*.[168] They started to approach computational studies through the geometrical overlap of two structures, the receptor, with its "pockets" and "cavities", and the ligand, which fits into the receptor body through specific interactions. Kuntz's major challenge was the high degrees of freedom (3 translations and 3 orientations) that characterises each pair of objects interacting with each other in space. Therefore, he took advantage of Richard's[169] and Connolly's[170] algorithms to accelerate his screenings studies. According to Richards and Connolly, treating the ligand and the substrate as

a set of spheres, distributed on both surfaces, makes it easier to establish the binding energy affinity between the two systems. When the geometrical overlap is examined and a good fitting score is provided it can be stated that, within a specific error limit, the internal distances of both ligand and target spheres match with each other. This was the first example of molecules grouping through geometrical similarity in order to create clusters of selective compounds for that target.[171] Throughout the years, the term docking was introduced to incorporate all the techniques that were employed for drug discovery. Docking studies are commonly known as *in silico* virtual screening techniques (VS). Currently, virtual screening is extensively used to obtain fast and rapid affinity evaluations between substrates and enzymes or already existing protein crystal structures *via* computer programs that can screen up to 10^{60} potential hits simultaneously from fragment virtual libraries.[172] This new automated system can work synergistically with the high-throughput screening method (HTS). HTS, compared to the VS, can only screen from 10^3 to 10^6 compounds simultaneously against biological systems *via* a physical preparation of the test. The scientist loads microtiter plates, in 96-, 384-, or 1536-well formats, with the compounds to screen and then submits the microtiter plates to analysis through a specific machine.[172] Nevertheless, it is important to note that both HTS and VS share the same goal: the identification of novel hits.[173] More specifically, a typical workflow of HTS (Figure 34) starts with:

i) **Target identification**: this process starts with identifying the function of a possible therapeutic target (gene/protein) and its role in the disease. Target identification can be achieved using many different sources and approaches such as data mining bioinformatics, genetic association with the disease, expression profile (*i.e.* changes in mRNA/protein levels) and functional screening (knockdown/knockout models).[175]

ii) **Assay development**: once the target has been identified, the HTS process proceeds with the development of biological assays to assess and identify molecules with activity at the drug target. It is pivotal that, whatever is the assay selected, these factors are considered: a) pharmacological relevance of the assay; b) reproducibility of the assay; c) assay costs; d) assay quality; e) effects of compounds in the assay (*i.e.* assay sensitive to the concentration of the solvent used to dissolve/store the compound).[176]

iii) **Primary screen**: a primary screen is then run to examine direct binding measurements of selected molecules from the biological assays against the target by achieving a minimum number of false positives and a maximum number of confirmed hits. Generally, primary screening runs in multiplets of single compound concentrations and the results are expressed in terms of percentage activity as a negative (0%) and a positive (100%).[177]

iv) **Secondary screen**: a secondary screen is run when some hits from the primary screen display the same activities and to ensure that they can reliably proceed to further screenings and, eventually, become leads.[177]

v) **Lead optimisation**: intensive SAR investigations of the selected hits are then carried out via X-ray crystallography or NMR studies. If positive results are obtained, further preclinical pharmacology studies and clinical trials may follow to finally achieve the prototype of a drug.[177]

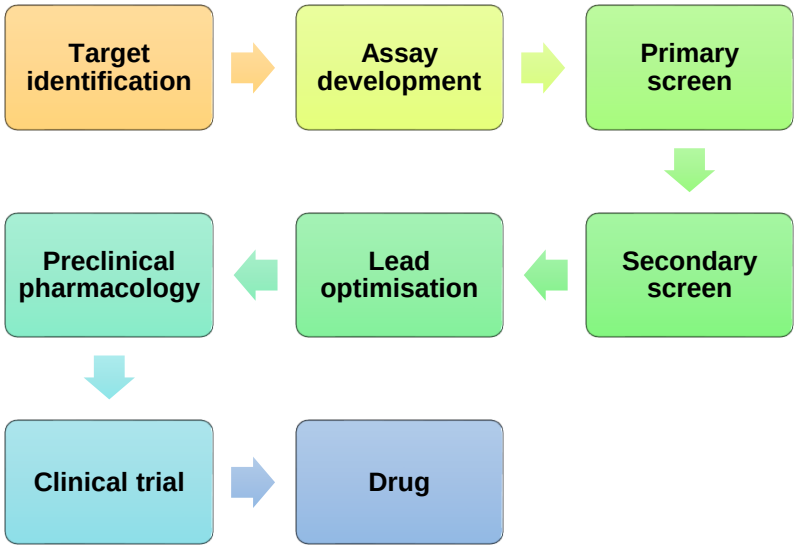

Figure 34: Example of high throughput screening workflow (HTS) for screening of new potential lead compounds.

On the other hand, VS can be run *via* both ligand-based and structure-based approach (Figure 36). VS ligand-based approach is performed by comparing the candidates ligand structure to the pharmacophore model according to shape similarities to known actives against that pharmacophore model.[178,179] VS structure-based approach is performed by using different computationl techniques, such as molecular docking or molecular dynamics simulations, that focus on the structure of the receptor as the molecualr target of the investigated active ligands.[180,181] A typical workflow of VS (Figure 36) starts with:

i) **Target identification**: the target is identified by 2D molecular databases (for ligand-based VS, Figure 36) or from protein structures of the PDB (protein data bank) database (for structure-based VS, Figure 36).[175]

ii) **Protein structure preparation**: is the most crucial step of virtual screening and

occurs once the target has been identified. Protein structure preparation can be achieved *via*:

a) *Protonation/charge assignment*: the protonation state refers to the exact locations of hydrogen atoms within the molecule.[182] Knowing where hydrogen atoms are revealed, allows for an accurate prediction of the affinity for the binding pocket.[183] An incorrect evaluation of the protonation state can lead to an increased number of false positives.[184] Moreover, the protonation state is crucial to understand how many H-bond donor/acceptor sites are present in both target and ligand (Figure 35).[185]

b) *Addition of explicit water molecules*: this operation is pivotal in determining the potential mediation that water molecules can establish between the compound and the receptor as well as their contribution to significant energetic changes.[186,187] Failing in the precise inclusion of necessary water molecules can lead to biased results.[188,189] Usually, water molecules are included in the docking algorithm in three cases: i) when their absence reduces the accuracy calculation,[190] ii) when they possess a maximum of three hydrogen bonds with the receptor.[191,192] and iii) when their presence is the only connection between the ligand and the target (Figure 35).[190]

c) *Dealing with mutations*. Often proteins are represented by a mutant form. It is very important to revert every mutant form to the wild-type form before performing a virtual screening particularly if the mutation affects the active site-compound binding (Figure 35).[193]

d) Considering proteins flexibility. Proteins flexibility represents one of the major challenges of virtual screening. Currently, two methods include proteins dynamic nature when producing scoring results: i) Flexible receptor docking incorporates lateral chains of residues within the active site despite very few aminoacidic side chains changing their conformation upong ligand binding.[194] ii) Ensemble docking is instead focused on the generation of an “ensemble” of target conformations by using molecular dynamic simulation (Figure 35).[195-200]

e) Incorporating pharmacophoric constraints. Pharmacophoric features can help to reduce the number of molecules to screen as well as to better identify a repeating scheme, for example, of a set of inhibitors towards the same protein/enzyme (Figure 35).[201]

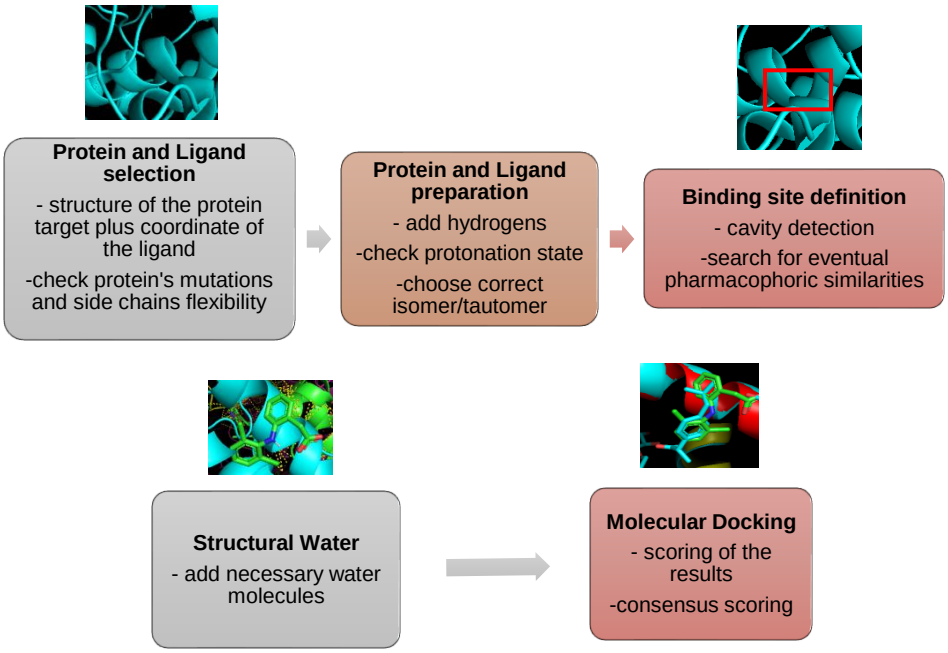

Figure 35: Structure-based virtual screening ligand/receptor preparation steps.

iii) **Docking**: this step of the workflow merges both ligand- and structure- based VS and consists in placing each molecule in a 3D small molecule database containing information about binding sites of a receptor/protein. The screening selects then molecules from the database that have the right orientation and conformation to possibly tightly bind to the protein (Figure 36).[175]

iv) **Scoring**: to each molecule is attributed a scoring function that is capable, theoretically, of predicting the binding affinity of a protein-ligand complex structure. Scoring functions can be mainly divided into three categories: a) force-field based, that takes into account the intermolecular van der Waals and electrostatic interactions between the ligand and the protein using a force field; b) empirical-based, that takes into account various types of interactions between ligand and protein such as number of atoms in contact or solvent accessible surface area difference in the complexed/uncomplexed ligand/protein set; c) knowledge-based, that takes into account statistical observations of intermolecular close contacts in large 3D databases (Figure 36).[175]

v) **Post-processing**: this stage includes ranking the ligands of a database, while the

docking simulation is running, and analysis of the drug-likeness to finally achieve a library of hit-candidates list (Figure 36).[175]

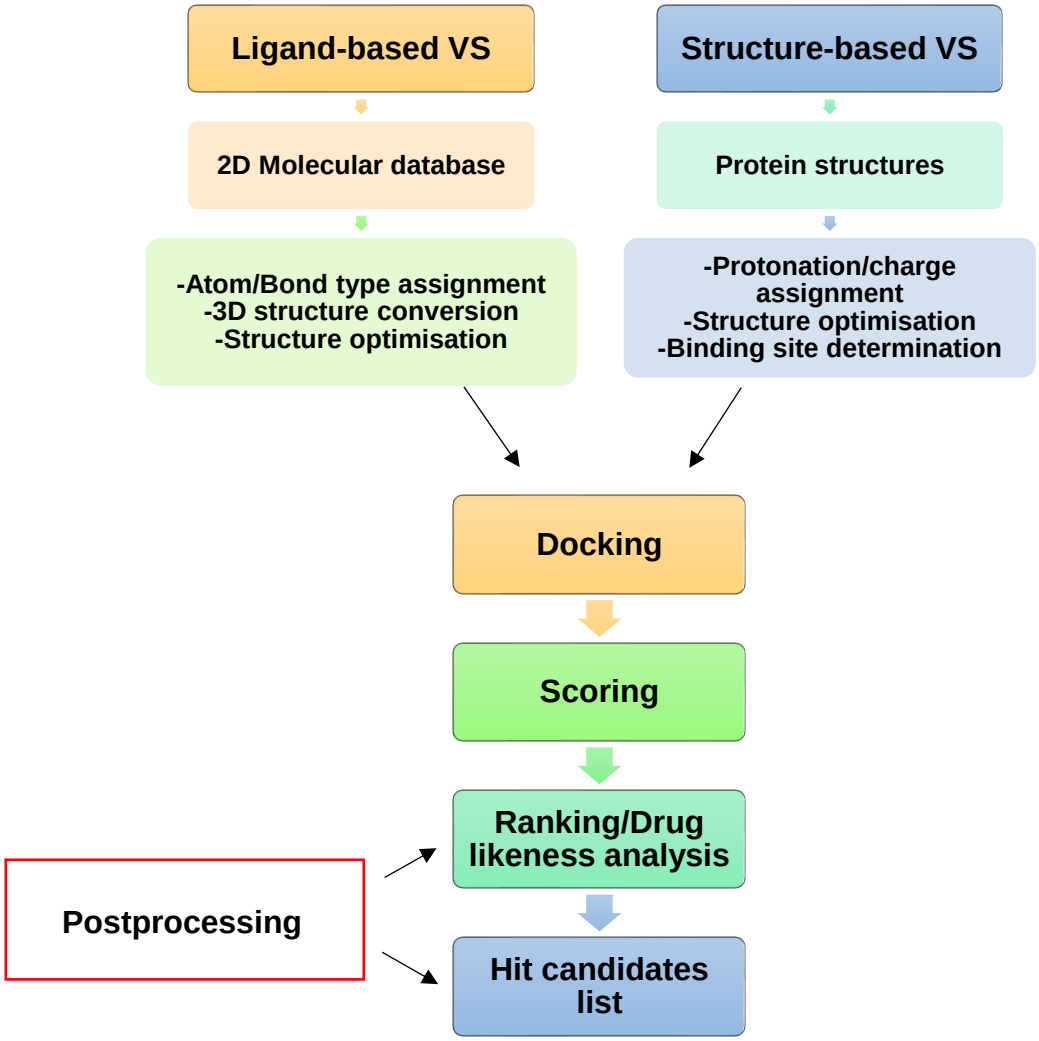

Figure 36: Example of virtual screening workflow (VS) for screening of new potential lead compounds.

2.2.1 Docking studies: virtual screenings techniques (VS)

VS aims to reduce the number of good candidates for a specific subject among millions of possible aspirants through a vast testing method that includes as many compounds as possible.[174] VS bases its screening on protein-structure[202,203] and chemical-similarity[204] approaches on small molecules and calculates binding affinity by applying specific descriptors as follows:

i) Structure- or descriptor-based queries: the easiest way to start screening potential candidates follows similarity-search calculations according to specific substructures.[205] Generally, these calculations require low-energy conformations of database compounds to be produced.[206] However, other specific descriptors can help the structure-based query such as the ones that compare similarities in molecular shape[207,208] or electronic characteristics[209] between the query and the candidates (**2.44**-**2.47**, Figure 37).

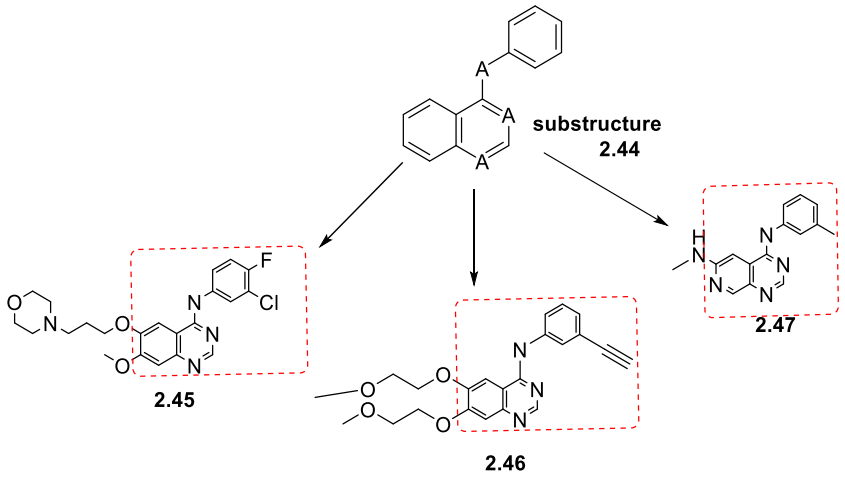

Figure 37: Substructure/Descriptors-based queries example: circled in red are the specific descriptor to look for in each molecule.

ii) Fingerprints: molecular fingerprints are better known as binary bit strings that connect diverse properties of molecular structures through a series of 1 or 0 characters that stands for the presence (1) or the absence (0) of a specific feature (Figure 38). Fingerprints are specifically used when single hits or leads are the only templates available for searching. When features of the template molecule find correspondence within the fingerprint database, an overlap occurs and is quantified by similarity measurements according to the similarity threshold values.[210,211] Fingerprints in VS can compare and screen candidates also according to more complex properties that make use of 2D and 3D tools. In particular, 2D fingerprints can scan possible connectivity pathway between molecules through the overlapping of thousands of bits while 3D fingerprints tracks all the possible settings of three- or four- point pharmacophores in a molecule.[212]

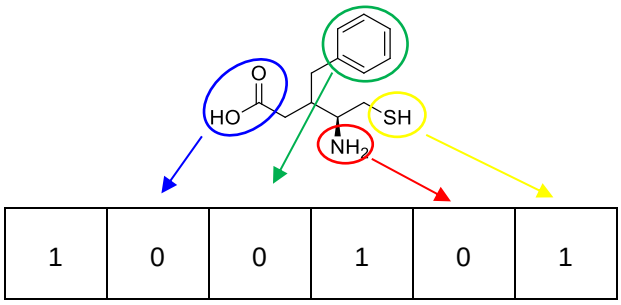

Figure 38: Example of a binary bit string matching specific functional groups and recognising them as peculiar fingerprints for that set of molecules.

iii) Clustering and Partitioning: Clustering is a VS technique that screens compounds according to the calculation of intermolecular distances in chemical reference spaces[213–215] whereas Partitioning involves building a solid frame that assigns specific coordinates to each molecule independently of others in different databases (Figure 39).[216] Clustering and partitioning are

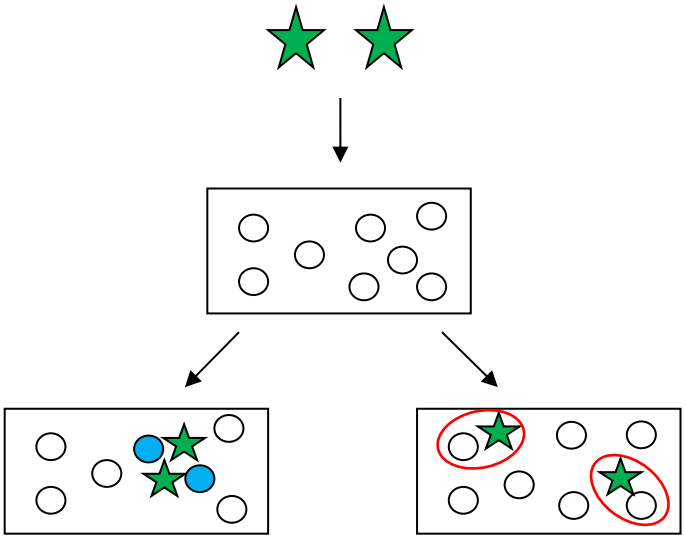

mainly used in VS when the screening starts from a set of active compounds available as starting point. Unfortunately, the increasing size of modern data set rendered clustering and partitioning methods more and more challenging.

Figure 39: Example of Clustering and Partitiong HTS screening: stars in **green** represent active compounds to screen against a source database. In Clustering, each **blue** ball represents a "similar" molecule to the one being analysed. Same happens for Partitioning, where similar feautures are grouped through **red** circles.

2.2.2 Docking studies: high-throughput screening techniques (HTS)

HTS, compared to VS, is more focused on largely examining compound-target bonds with the highest accuracy and is more prone to the presence of false positives or false negatives mainly occurring because of degradation of compounds on screening plates, purity issues or too low concentrations.[174] For this reason, different techniques have been implemented to minimise HTS issues such as:

i) Computational approaches: recursive partitioning (RP) is a computational approach that works by partitioning the data set according to a decision tree that has been adapted to recognise between active and inactive molecules by Rusinko *et al*.[217] Each branch of the tree encodes a specific descriptor (i.e. physical properties such as number of triple bonds, presence of nitrogen, chiral molecules etc) which separates potential candidates according to those descriptors. In this way, the candidates belonging to a specific branch will possess the desired number of properties to start screening for active biological compounds.[218] RP is a very fast and efficient method, as it screens large database of compounds and thousands of descriptors simultaneously, however it is also hugely impacted by the structural diversity of active compounds. It has been observed that active molecules with different scaffolds might end in different branches thus limiting the application of descriptors classifying for a specific chemotype. Recently, the phylogenetic-like tree algorithm has been addressing this issue by an iterative-like classification of compounds that allows for the association, in one single cluster, of diverse active molecules with different descriptors.[219,220]

ii) Binary Quantitative Structure-Property Relationship (bQSAR): based on Bayes' theorem and further developed by Labute,[221] this method determines associations between structural features and molecular properties of compounds and their biological activity through specific combinations of descriptors. In this way, each molecule will be linked to a determined probability value of biological activity.[222] bQSAR can work without requiring accurate activity data because of a binary system model that calculates all the possible predictions on activity-treshold values defined prior.[223] Furthermore, bQSAR can be employed to screen large data sets in which candidates share similar probability of activity. This is a key advantage in HTS screening as it is not only limited to biological activity prediction but involves any other feature that can be included in a binary scheme system.

2.2.3 Docking studies: problems and success of virtual screening

Unfortunately, even though VS is widely accredited as one of the best options for drug design, it still suffers from many disadvantages. First of all, the majority of chemical compounds are not of

any biological interest due to lack of selectivity or worse, acute toxicity. Secondly, receptors or enzymes or proteins are huge molecules made up of extremely high numbers of atoms that are more or less free to rotate and move in space. The consequence of this is that, as the number of possible rotations increases, the interaction prediction becomes more complicated and requires more computing resources.[224] Thirdly, calculations of the binding affinity is particularly hard when the solvation effect cannot be minimised.[225] Although the water effect can be reduced by thermodynamic integration methods, doing so is time consuming. However, many successes came from the application of either VS or HTS to drug discovery. Several molecules, binding more than 50 receptors of known structures, have been discovered through computational chemistry producing numerous libraries of compounds that resulted from patiently docking each organic molecule into various receptor structures, calculating their affinity and testing all of them experimentally.[226,227] The virtual screen "hit rate", defined as the number of compounds that bind a receptor at a specific concentration divided by the number of compounds tested, increased of 100- to 1000- fold with computational methods rather than empirical ones.[228,229] Furthermore, VS allows the restriction of research parameters for molecules matching only certain properties by, for example, introducing some sort of filters to meet specific standards, avoiding tedious experimental research.[230,231] Even though VS and HTS screenings may be affected by false-positive hits,[232] because of very large libraries of compounds screened, the progresses made through modern algorithms[233] to improve their potency are particularly impressive.

2.3 Results and Discussion

2.3.1 A) Virtual screening of pyridyl-triazoles 1.136a and 2.48-2.54

Given the importance of the pyridine scaffold in medicinal chemistry,[234-244] we decided to submit a number of pyridine-triazoles into a virtual screening study. Compounds **2.53** and **1.136a** were the only 1,2,3-triazoles that was possible to synthesise, using the synthetic methodology highlighted in *Chapter 1*, whereas for 1,2,3-triazoles **2.48**-**2.52** and **2.54**, the insufficient azide nucleophilic power impeded the generation of the hydroxyl function at position 5 of the triazole ring (see *Chapter 1, paragraph 1.2.4*).

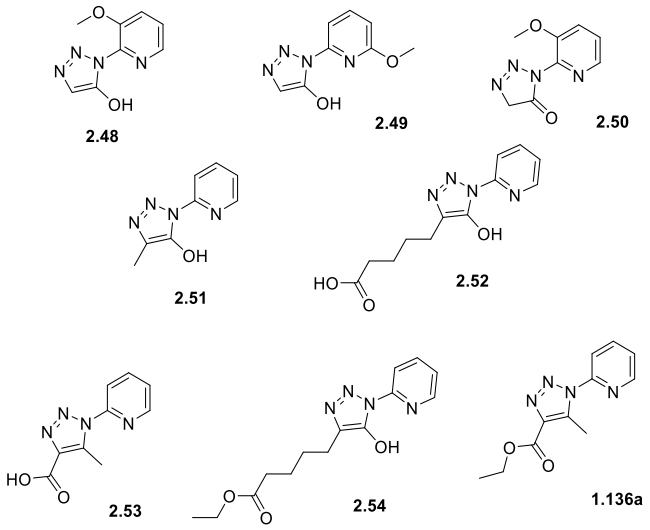

Figure 40: Pyridine-based 1,2,3-triazoles **2.48-2.54** and **1.136a** tested through docking screening against the BioGPS cavity database

In order to identify potential bioactivity of compounds **2.48**-**2.54** and **1.136a**, we established a collaboration with Prof. Gabriele Cruciani and Dr. Lydia Siragusa of the Laboratory for Chemometrics and Molecular Modeling, Department of Chemistry, Biology and Biotechnology, University of Perugia, Italy. They are both experts in the field of Molecular Modeling and owners of the BioGPS algorithm that has been used for the virtual screening of compounds **2.48**-**2.54** and **1.136a**. The BioGPS[245] is a new method implemented by Prof. Gabriele Cruciani that has the great advantage of comparing protein binding sites to each other by their ligand "image", derived from the GRID molecular interaction fields (MIFs), rather than according to rigid structural requirements such as protein/ligand shape similarity.[246,247] GRID is a computational procedure for determining energetically favorable binding sites on molecules of known structure, known as Molecular Interaction Fields (MIFs).[248,249] The BioGPS software has been already successfully employed by Prof. Cruciani's research group for i) the screening of new ligands for novel Thymidylate synthase (TS) inhibitors;[250] ii) for the retrieval of similar proteins with different structural folding to explain Sunitinib side effects;[250] iii) for the analysis of similarities between binding sites of two different ezymes by focusing on a multi-target therapy case.[250] In particular, the BioGPS workflow used for the docking screening of triazoles **2.48**-**2.54** and **1.136a** consisted of 5 parts:

i) Protein refinement, achieved by using an algorithm known as "Fixpdb" that enables the preparation of the protein structure obtained from the Protein Data Bank (PDB). Additionally, Fixpdb also processes potential solvent molecules, cocrystallised

ligands, cofactors or ions to be retained for consideration in subsequent analysis, if considered essential for the protein functionality.[245]

ii) Cavity detection, achieved by using an algorithm known as "Flapsite" that embeds the protein structure into a tridimensional grid and allows for the identification of pocket points located only within a distance of 4 Å maximum from the closest protein atom using the GRID probe H, that discriminates according to the "shape" parameter.[245]

iii) Cavity characterisation, achieved by the FLAP program (Fingerprints for Ligands And Proteins) that enables the identification of the potential complementary ligand pharmacophoric features for a protein binding site. The GRID probes H, DRY, O and N1 are used to calculate the shape, the hydrophobic interactions and the H-bond acceptor and donor interactions respectively for each cavity considered in the analysis. Generally, the minimum numbers of energetically favorable interactions between a ligand and a protein is equal or greater than 4. FLAP then generates all possible combinations of four of the representative points returning them as quadruplets. All quadruplets generated for a specific cavity form the so called "Common Reference Framework".[245,251]

iv) Cavities comparison, occurs via comparison of binding sites via superimposition of the "Common Reference Framework" of the cavity against one or more template structures. A good match between cavity and template occurs when a pair of quadruplets have their distances coupled within 1 Å from each other.[245]

v) Data analysis, in which each final superimposition, called "solution", is identified by a set of Tanimoto similarity scores,[252] inteded as a measure of the similarity of two sets of elements obtained by dividing the intersection of the two sets over the union of the two sets. The global pocket-pocket similarity is analysed by using the global scores that attribute to 0 no similarity and to 1 maximum similarity.[245]

Docking screening of compounds **2.48**-**2.54** and **1.136a** against the whole PDB returned a set of 20 proteins being able to bind, in their active site, the abovementioned triazoles (Table 6). In particular, distribution scores of compounds **2.48**-**2.54** and **1.136a** displayed a characteristic gaussian curve for each molecule that measured the probability the of these compounds to bind a protein's active site according to their shape similarities. Specifically, triazoles **2.59** and **1.136a** produced the highest global score of similarity against the 20 proteins returned by the docking screening against the PDB, with values close to 0.80 (the global score of similarity is a number comprised between 0, meaning "no similarity", and 1, meaning "maximum similarity", Figure 42).[245]

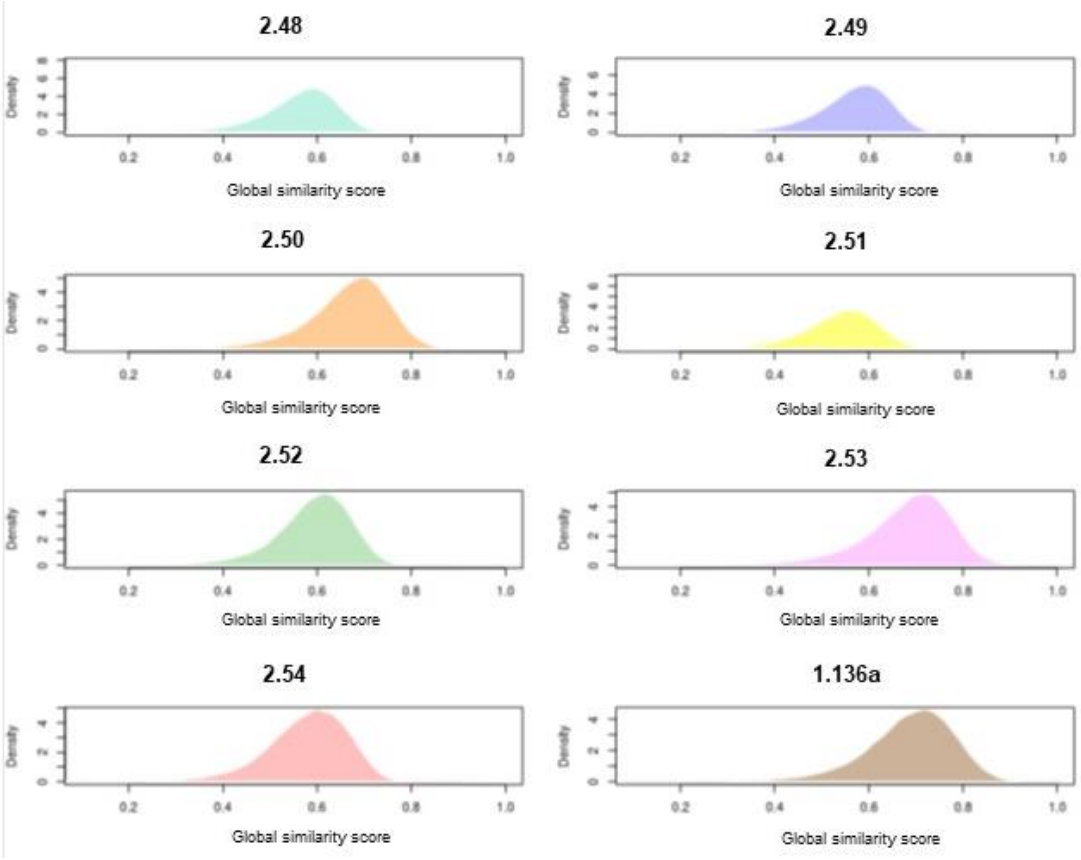

Figure 42: Distribution of scores of 1,2,3-triazoles **2.48-2.54** and **1.136a** against the BioGPS cavity database.

Table 6 describes the affinity of each triazole tested against the active site of the 20 proteins returned by the docking screening and it is expressed by an arbitrary score comprised between 0 and 100. From the results obtained, 1,2,3-triazoles **2.48,2.49** and **2.51**, bearing a hydroxyl group at position 5, as well as ketol triazole **2.50**, did not show significant binding scores with the 20 proteins screened, except for few pairs (Table 6). This latter phenomenon proved that the OH presence for these 1,2,3-triazoles was not crucial or did not increase the interaction between the compound and the protein target. Triazoles **2.52** and **2.54**, bearing a long chain at position C4 instead, displayed high binding scores with almost all of the proteins examined, thus suggesting lack of selectivity (Table 6). More interestingly, the docking analysis for 1,2,3-triazole **2.53** showed relatively high binding coefficient values only for a few proteins, including a binding score of 80.13 observed for KAT2A that caught our attention (Table 6, circled in black). Curiosly, triazole **1.136**, formally being **2.53** ester analog, also showed a relatively moderate binding score with KAT2A of 61.2 besides possessing a low binding-affinity with almost all of the 20 proteins.

Table 6: List of the 20 proteins examined and the compounds tested: **red cells** indicate bad fitting ligand-protein, **green cells** indicate medium fitting ligand-protein**, blue cells** indicate good fitting ligand-protein.

Protein name	2.48	2.49	2.50	2.51	2.52	2.53	2.54	1.136a
Carbonic anhydrase 2	51.62	47.49	39.22	42.64	53.03	53.65	48.18	26.41
Carboxypeptidase B2	50.19	53.3	55.71	49.04	71.82	56.12	61.97	43.01
Eukaryotic translational initiation factor 4E	37.3	40.34	44.97	54.65	48.68	51.6	53.76	41.71
Heparan sulfate glucosamine 3-O-sulfotransferase 3A1	43.76	45.09	44.65	43.65	78.9	54.62	48.1	47.98
Histone acetyltransferase KAT2A	44.25	54.84	47.54	47.97	76.47	80.13	72.29	61.2
Inositol-tetrakisphosphate 1-kinase	45.49	47.46	42.28	46.08	68.44	55.84	55.52	47.76
Lysine-specific demethylase 4C	47.58	46	54.22	47.21	65.45	58.89	70.85	44.04
Methionine aminopeptidase 1	55.43	56.44	51.82	46.12	76.33	63.55	59.14	45.68
Methionine aminopeptidase 2	46.83	48.25	45.71	40.11	43.77	54.88	30.94	23.54
Mitofusin-1	56.06	55.98	56.6	52.65	74.22	65.94	59.58	nd
NAD(P)H dehydrogenase [quinone] 1	48.01	55.78	50.22	48.23	78.42	62.74	55.66	45.84
Phosphoenolpyruvate carboxykinase, cytosolic [GTP]	49.82	46.77	50.86	41.29	67.21	50.96	63.36	43.08
Phospholipase A2, membrane associated	52.93	53.72	54.52	47.57	70.81	56.78	65.98	54.32
Polypeptide N-acetylgalactosaminyltransferase 2	59.69	57.76	56.42	51.96	76.42	66.87	65.06	56.17
Pyruvate kinase PKM	52.34	53.3	53.56	56.28	68.36	49.53	63.46	28.71
Ras-related C3 botulinum toxin substrate 1	50.34	55.33	49.56	50.44	68.85	54.05	71.79	54.26
Ras-related protein Rab7a	51.23	51.73	65.5	52	67.27	44.8	62	58.08
Serine/threonine- protein phophatase 5	51.42	46.91	65.49	42.42	64.87	50.57	51.54	33.99
Sulfotransferase 1e4	48.97	58.29	44.49	48.16	56.55	51.19	49.17	44.1
Sulfotransferase family cytosolic 1B member 1	49.44	52.89	46.34	45.75	67.75	58.64	64.66	51.8

These results were particularly intriguing since we noticed how the sole presence of a pyridine ring, instead of a phenyl residue at position *N*1 of the triazole ring, shifted the selectivity towards a protein, KAT2A, with opposite functions (acetylation of lysine residues from histones)[253,254] with respect to HDACs isoforms (deacetylation of lysine residues from histones)[255], contrary to what observed instead for 5-hydroxy-1,2,3-triazoles **1.132** (*Chapter 1*). According to the data collected, we hypothesised the presence of a carboxylic moiety at the C4 position would favor the interaction of 1,2,3-triazole **2.53** with the desired target (Figure 43), whereas the same 1,2,3-triazole displaying the ester function at position C4 (**1.136a**) showed a lower, but still moderate, binding score with KAT2A. We considered the absence of a hydrogen-bond donor site, either at position C4 or C5 of **1.136a**, to potentially reduce the interactions with the other proteins. To better understand the importance of **2.53**'s carboxylic group when interacting with KAT2A, we evidenced triazole's **2.53** structure connections with KAT2A active site using the PyMOL software (Figure 43). PyMOL is an open source for molecular visualisation system used to produce high-quality 3D images of small molecules and biological macromolcules, such as proteins.[256] KAT2A's structure was imported from the PDB database and **2.53**'s structure was drawn *via* the ChemDraw software and imported into PyMOL. **2.53**'s nitrogens atoms have been colored in blue, oxygen atoms in red and carbon atoms in green whereas polar contacts, with relative bond distance from the aminoacids of KAT2A active site, are expressed in angstrom values and represented with yellow dashes (Figure 43). In support of our hypothesis, polar contacts connecting **2.53** and KAT2A occurred mainly when **2.53**'s OH function of the carboxylic moiety and **2.53**'s *N*2-*N*3 atoms of the

triazole ring interacted with the NH functions of KAT2A Arg-558 residue (shown with blue and light blue sticks, Figure 43). In particular, **2.53**'s *N*2 and *N*3 atoms of the triazole ring coordinate arginine NH number 20289 (2.2 Å and 2.1 Å distance respectively, Figure 43) while the *N*3 atom of the triazole ring and the OH function of the carboxylic moiety coordinate arginine NH number 20292 (2.3 Å and 2.5 Å distance respectively, Figure 43).

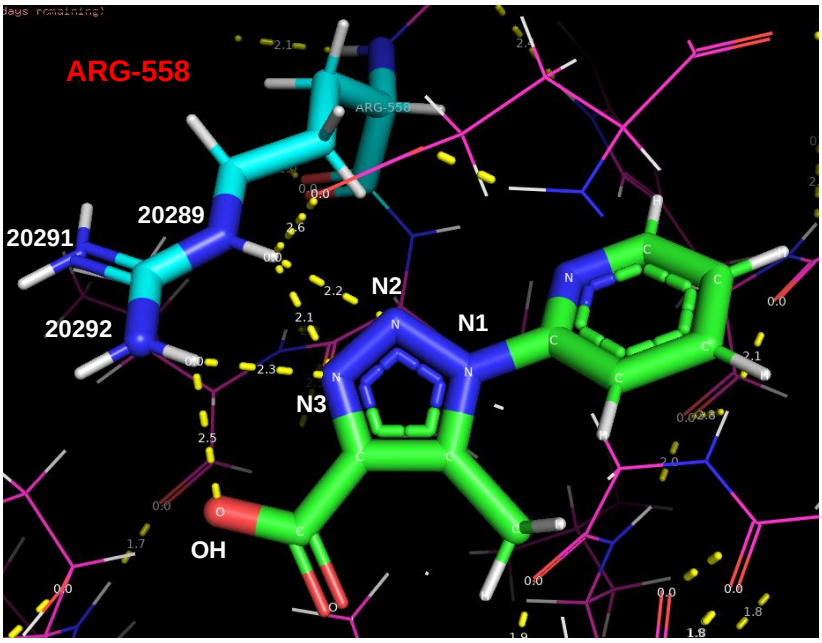

Figure 43: Pymol outlook of triazole **2.53** bound to KAT2A active site pocket. Triazole's **2.53** nitrogens are coloured in **blue**, carbons in **green** and oxygens in **red** while KAT2A active site is coloured in **pink**.

2.3.2 Importance of KAT2A gene: background and biological significance

We decided to focus our attention on the KAT2A protein for the crucial importance of this protein in several biological functions and, particularly, for its role in the surge of aggressive tumors such as renal carcinoma[257] or acute myeloid leukemia (AML)[258] when overexpressed or depressed. KAT2A, also known as GCN5 (general control nonderepressible 5), is part of the HAT (histone acetyltransferase) family and, more specifically, belongs to the GCN5-related *N*-acetyltransferase group.[259,260] HATs can be divided in two groups: type A and type B according to their localisation and function. HATs belonging to type A are located within the nucleus and include three main families: GNAT (Gcn5 related *N*-acetyltransferase), MYST (acronym for its four members: **M**OZ, **Y**bf2, **S**as2 and **T**ip60) and p300/CBP (**C**REB-**B**inding **P**rotein). HATs belonging to type B are located in the cytoplasm and, generally, modify new free histone proteins in order to transfer them

to the nucleus. KAT2A belongs to the GNAT family and promotes the acetylation of the ε-amino group of lysine residues of histones H3 and H4 thus preventing the positive charge on the amino group to negatively impact other proteins interaction. Histones acetylation is a primary epigenetic modification, intended as a chemical or physical modification that influences how genes are read and expressed, without changing the DNA sequence.[261] In particular, histones acetylation is responsible for genes accessibility or inaccessibility to transcriptional factors thus influencing chromatine structure, DNA replication, repair and recombination.[262] However, most of these histones modifications are reversible. KAT2A is mainly directing its acetylating activity to histones H3 and, to a lesser extent, to histone H4 despite each HAT being able to acetylate hundreds of targets.[263] It is noteworthy that KAT2A is also capable of acetylating non-histone targets such as CDC6 (cell division cycle 6) and cyclin A influencing, then, important biological functions such as the G1/S cell cycle transition (intended as a phase of the cell cycle in which the cell grows, phase G1, and the DNA is replicated, phase S)[264] and mitosis.[265,266] Furthermore, the neutralisation of lysine's positive charge leads to a weaker bond with DNA strands allowing transcriptional factors to penetrate DNA itself more easily.[267] KAT2A can also act as glutaryltransferase or succinyltransferase depending on the context. Succinylation[268] and glutarylation[269] are complementary functions as 2-oxoglutarate dehydrogenase is fundamental to provide succinyl CoA.[270] KAT2A is involved in numerous vital functions such as: i) long memory consolidation and synaptic plasticity;[271] ii) expression of a hippocampal gene network linked to neuroactive receptor signaling;[271] iii) regulation of embryonic stem cell (ECS) pluripotency and differentiation;[272] iv) positive regulation of T-cell activation upon T-cell receptor (TCR) stimulation and promotion of IL-2 (interleukin-2) expression.[273] KAT2A role in IL-2 expression is particularly important given that IL-2 is a type of cytokine that regulates white blood cells activity during infections and it is mainly expressed by activated $CD4^+$ and $CD8^+$ T-cells.[274] When KAT2A is repressed, T-cell growth is impared and so is the production of IL-2, given the dramatic reduction in both $CD4^+$ and $CD8^+$ T-cells production, thus drastically reducing the immune system response to infections.[272] Moreover, dysregulation of KATs' activity produces inhibition of the cell cycle and induces apoptosis. For this reason KAT's dysregulation is associated with numerous severe tumors such as small-cell lung cancer[275] or colon cancer[276], inflammatory disorders[277], type 2 diabetes[278] etc.

2.3.2.1 HATs inhibitors: classification and biological importance

So far, HATs inhibitors have been classified in three groups: i) bisubstrate inhibitors, ii) natural compounds and iii) synthetic compounds.

i) Bisubstrate inhibitors: Building bisubstrate chemical entities has been a widely used method to obtain effective and selective bioactive compounds.[279] HATs bisubstrate inhibitors can be, mainly, obtained according to two strategies: i) small organic molecules conjugated with CoA,

synthesised from corresponding bromo carboxamides, and subsequent coupling with CoASH; ii) peptide molecules conjugated with CoA, synthesised from corresponding Fmoc protected peptides by solid phase.

Cullis *et al.*[280], in 1982, reported the synthesis of Spd-CoA **2.55** and found this molecule to strongly inhibit histone activity with values below 10nM (Figure 44). Later, Lau *et al.*[281] synthesised Lys-CoA **2.56** and H3-CoA-20 **2.57** proving their selectivity towards p300 inhibition with IC_{50} value of 0.5μM (Figure 44). In 2011, Kwie *et al.*[282] investigated how specific conformational changes can modify the interactions of HATs inhibitors toward a specific member of HATs. In particular, they noticed that compound **2.58** displayed the most suitable chain length to interact with p300 with a 50% inhibitory activity of 0.07μM while a shorter chain length decreased the potency (Figure 44). Additionally, they observed that steric hindrance on constrained compounds also decreased HATs inhibitory activity highlighting the importance of size and chain length when interacting with the active site pocket.

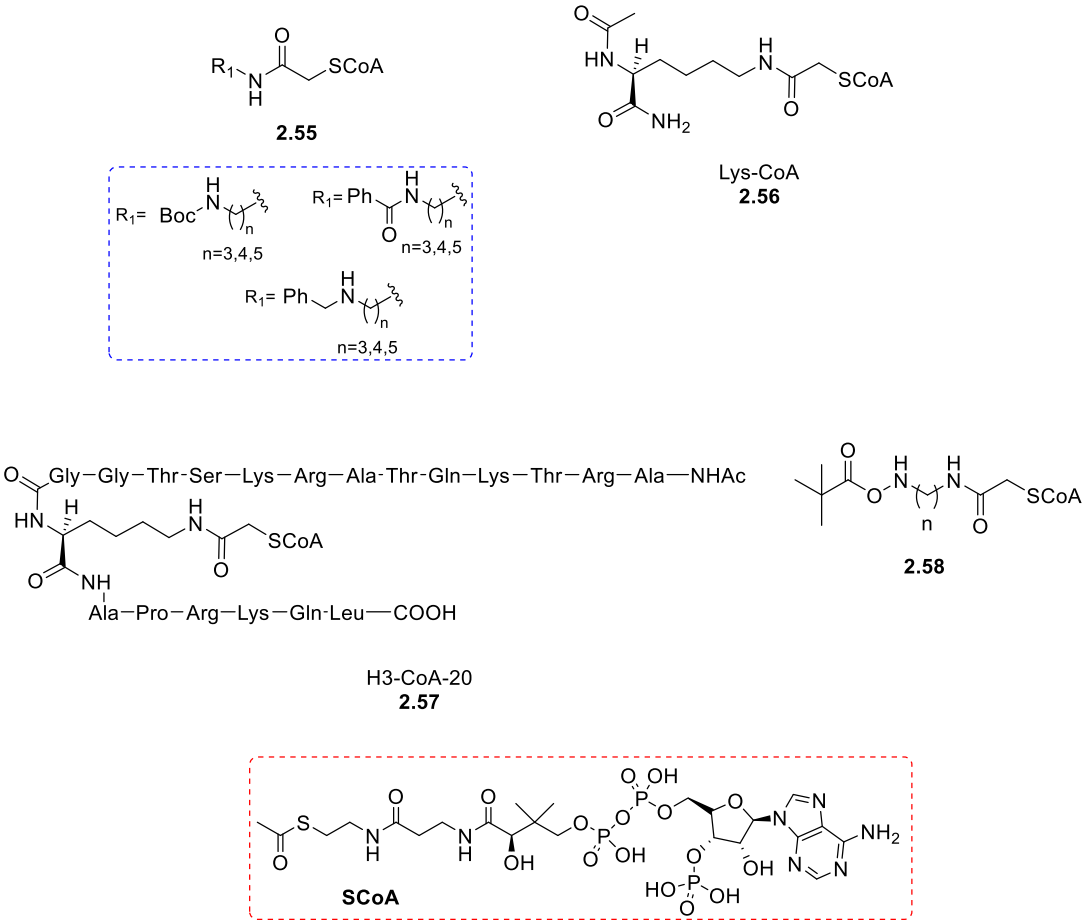

Figure 44: A few examples of active bisubstrate HATs inhibitors **2.56**, **2.57** and **2.58** and their reference compound **2.55**.

ii) Natural compounds:

a) ***Polyphenols***. *Garcinol*, **2.59**, is a polyisoprenylated benzophenone extracted from *Garcinia indica* and shows either p300 or PCAF (KAT2B) inhibitory activity in the low micromolar range (7 and 5μM respectively).[283] Even though garcinol's hydroxyl groups limit oxidative stress damage, due to the stability of the reduction products, being aspecific towards one of the HATs enzymes still remains the biggest issue.[284] For this reason, derivatives of isogarcinol **2.60**, resulting from the intramolecular cyclisation of garcinol, such as **2.61**, displayed absence of toxicity towards T-cells as well as a diminished reproduction of HIV through downregulation of p53 acetylation (Figure 45).[285]

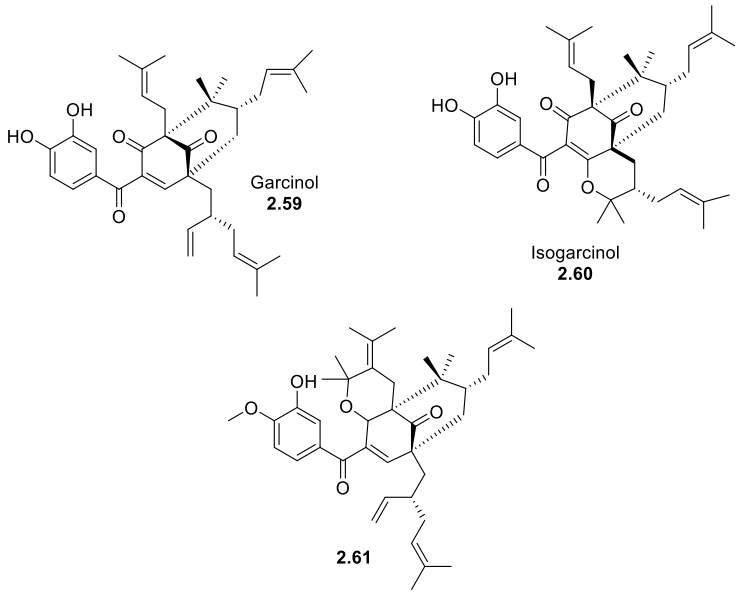

Figure 45: Garcinol **2.59** and its more active derivatives, isogarcinol **2.60** and **2.61**, as potential more specific HATs inhibitors.

Curcumin **2.62**, extracted from the rhizome of turmeric (*Curcuma longa*), is a non-competitive p300 inhibitor.[286] The inhibition occurs *via* formation of a covalent bond to the enzyme through curcumin's cynnamoil groups that work as Michael acceptors.[287] Curcumin, like garcinol, is a non selective KAT inhibitor and has been tested, for *in vivo* efficacy, in more than 120 clinical trials for different diseases.[288] Unfortunately, curcumin never showed a significant biological activity *in vivo* thus requiring the development of more potent analogs. In particular, compounds **2.63a,b**, in which the methoxy groups have been replaced with a carboxylic acid (**2.63a**) or bromine (**2.63b**), showed improved inhibition power towards p300 with an IC_{50} value of 33 μM and 21 μM respectively, suggesting the importance of an EW group to interact with the protein (Figure 46).[289]

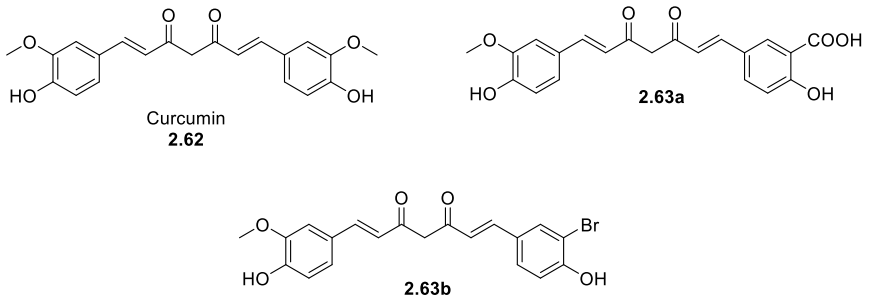

Figure 46: Curcumin **2.62** and analogs **2.63a,b** showing improved selectivity towards p300 protein.

b) ***Anacardic acid and derivatives***. *Anacardic acid*, **2.64**, is a 6-pentadecylsalicylic acid extracted from the cashew nut shell and is classified as a non-competitive and non-selective inhibitor of KAT enzymes.[290] Derivatives of anacardic acid, such as **2.65a-h**, proved the importance of long aliphatic tails to establish hydrophobic interactions with the target. Indeed, when substituting long chains with shorter ones or when introducing a hydroxyl group as a terminal modification, a complete activity loss was observed against p300 (Figure 47).[291]

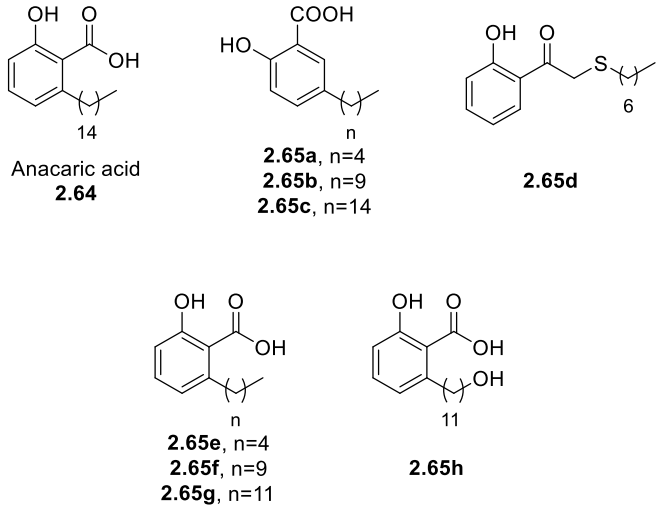

Figure 47: Anacardic acid **2.64** and analogs **2.65a-h** displaying different chain lengths and different electronic features.

c) ***Quinones***. *Plumbagin*, **2.66**, is a hydroxynaphtoquinone extracted from *Plumbago rosea* roots and acts with a non-competitive mechanism as KAT inhibitor against p300 and PCAF with IC_{50} values *in vitro* and *in vivo* of 20 µM and 50 µM respectively.[292] Docking studies on **2.66** highlighted how crucial the hydroxyl group is for the interaction with the target as it establishes a hydrogen

bond with Lys1358 residue which is fundamental for the inhibition activity. Derivatives of Plumbagin, such as Embelin **2.67**, with other moieties replacing the hydroxyl group and loss of the aromatic conjugation showed reduction of the inhibitory activity (Figure 48).[293]

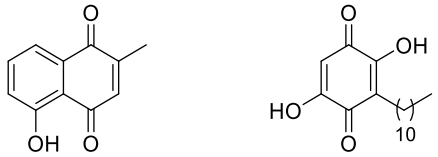

Plumbagin **2.66** Embelin **2.67**

Figure 48: Plumbagin **2.66** and its inactive derivative Embelin **2.67** showing how loss of the conjugated aromatic system eliminates KATs selectivity.

iii) Synthetic compounds:

a) ***Thiazole-based compounds*** have been identified by Filetici *et al.*[294] to be excellent p300 HAT inhibitor against a strain of yeast *Saccharomyces cerevisiae* holding a deletion of KAT2A. In particular, compound **2.68a**, bearing a fluorophenyl substitution at 4-thiazole, and compounds **2.68b,c**, with conjugated aromatic systems substituting the cyclopentelidene framework, displayed over 90% p300 HAT inhibition activity (Figure 49).[294]

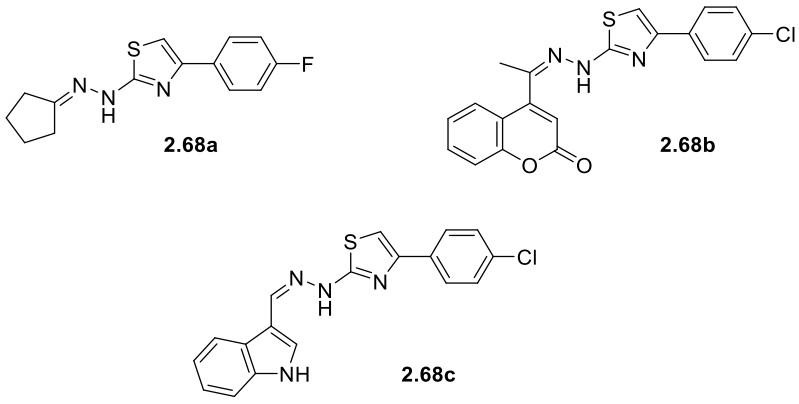

Figure 49: Thiazole-based compounds **2.68a-c** bearing EWG and conjugated aromatic systems inhibit p300 HAT activity in *Saccharomyces cerevisiae.*

b) ***Isothiazolone-based compounds*** have been recognised as excellent HAT inhibitors. Investigations of their inhibitory activity started in 2005 when it was clear that the cleavage of the S-N bond to form the disulfide bond was the key-point to engage with the target (Scheme 22).[295–299] Through this mechanistic rationale, thiols of proteins may react with **2.69** to form a transient species **2.71** which in turn reacts with a second thiol **2.70** to give reduced **2.72** and oxidised disulfide bond **2.73** (Scheme 22)**.**

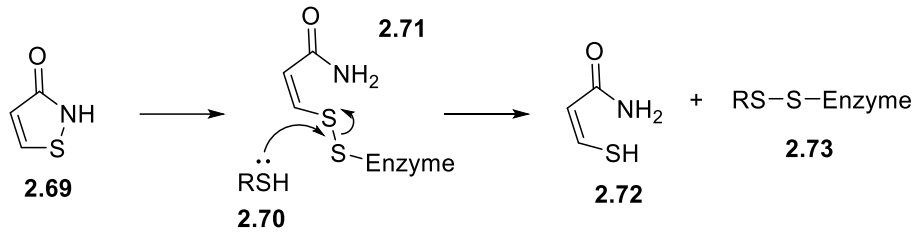

Scheme 22: Proposed mechanism of inhibition of HATs by S-N bond cleavage of isothiazolone-based compounds.

The S-N cleavage is positively influenced by the presence of free thiols groups onto the enzyme and by electrophilic substituents, such as EWG or less steric hindrance, in both position 4 and 5 of the isothiazolone nucleus whereas nucleophilic groups produce the opposite effect. In most cases, compounds bearing EWGs at position 5 (Figure 50, **2.74a** and **2.74b**) showed inhibitory activity against KAT2B below 20 μM (2.2 μM and 1.3 μM respectively)[295,299] while the introduction of a methyl group at position 4 (Figure 50, **2.74c**) decreased the potency bringing the inhibitory activity against KAT2B below 50% value at 10 μM concentration, proving the importance of the S-N bond cleavage to create a disulfide bridge with the target (Figure 50).[296]

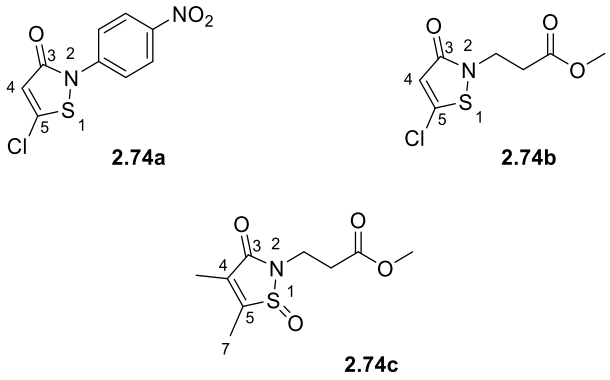

Figure 50: Isothiazolone- based compounds **2.74a-c** showing HATs inhibition power due to S-N bond cleavage.

c) ***pyrido- and benzisothiazolone- based compounds*** are mainly classified into 5 groups, according to the modification of the aromatic ring.[300,301] Compounds **2.75a,b** with a fluorine-group in the *para*-position, belonging to the **Type B** group of *N*-substituted pyridoisothiazolones (Figure 51), were found to be responsible for the hypoacetylation of H3K14 and H4K8 thus producing an anti-cancer effect against SK-N-SH neuroblastoma cell line (IC_{50} under 10 μM)[301]. Compounds **2.76a,b** with a flexible *N*-substituted linker, belonging to the **Type C** group of *N*-substituted pyridoisothiazolones (Figure 51), displayed decreased activity against HATs like KAT2B and KAT2A while still showing high selectivity towards HAT CBP.[300] *N*-alkyl derivatives with a

carboxylic acid function (**2.77a,b**), belonging to the **Type E** group of *N*-substituted pyridoisothiazolones (Figure 51), were found to be less potent against KAT2A, KAT2B and p300 while the same *N*-derivatives bearing an amido group showed an improved selectivity towards KAT2B (**2.78a** with IC_{50}=1.44 μM) and CBP (**2.78b** with IC_{50}=9.41 μM). Overall, pyrido- and benzoisothiazolones are known to be highly potent but, unfortunately, not very specific for a HAT enzyme in particular.

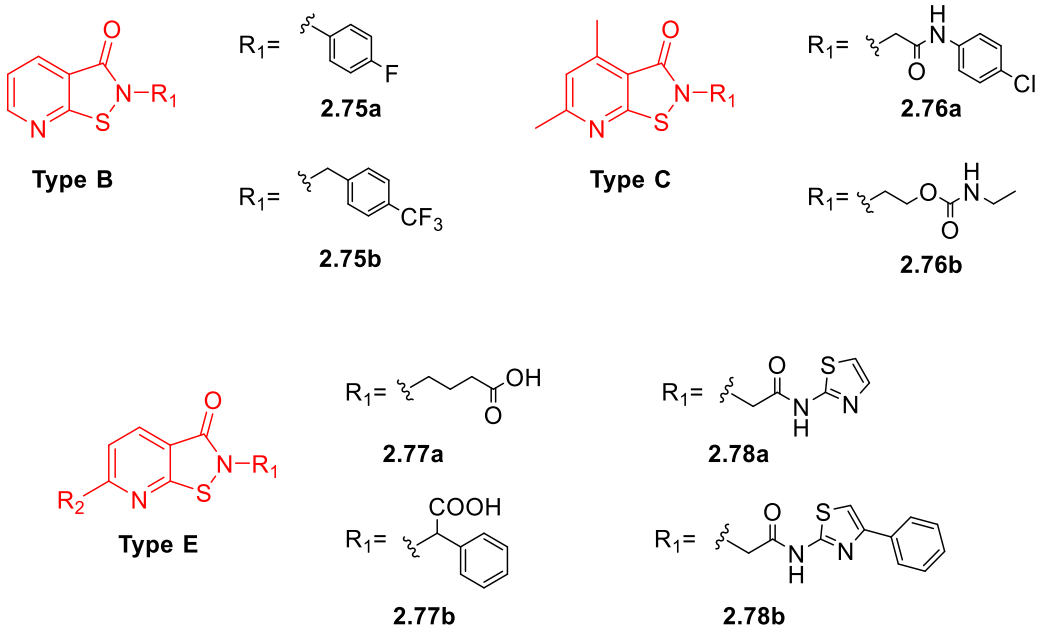

Figure 51: Pyrido- and benzoisothiazolone based compounds **2.75a,b**, **2.76a,b**, **2.77a,b** and **2.78a,b** displaying different electronic features thus different HATs selectivity.

Despite their high inhibition power, most of the HATs inhibitors known share a lack of selectivity and a pletora of side effects. Additionally, their mechanism of action remains unknown as well as how to increase their metabolic stability, potency, solubility and permeability without negatively affecting activity. For this reason, it is crucial to improve the efficiency and accuracy of screening methods such as HTS (high throughput screening), fluorometric assays and HCS (high content screening), in order to gather more data about KATs interaction with potential inhibitors.[302] Hence, the potential of triazole **2.53** (Figure 41) to selectively inhibit KAT2A isoform can dramatically contribute to the general knowledge of HATs inhibitors.

2.3.3 B) Synthesis of pyridyl-triazoles 2.80a-f undergoing biological tests against KAT2A

In order to confirm the results obtained *via* the virtual screening in relation to the activity of **2.53** (Figure 42) against KAT2A, two libraries of compounds **2.80a-f** and **2.81a-d** were prepared. Compounds **2.80a-f** included carboxylates or derivatives thereof, for example esters and amides. Based on the completely aspecific or negative binding scores obtained by docking screening for triazoles **2.48-2.52** and **2.54**, we thought that the hydrogen atom at position 5 could benefit from: i) a less polar behavior than the OH function, thus avoiding the resulting compound to be too hydrophilic to enter the external cells' membrane, ii) a smaller radius compared to the methyl group possessed by triazole **2.53**, thus producing a smaller molecule with an additional hydrogen-bond donor site. In addition to that, we also included, in the same library, the synthesis of long chain pyridyl-based triazole **2.80f** bearing an amide moiety to better investigate the role of diverse functional groups of our compounds when interacting with the target. However, **2.80f** synthesis was performed only after triazoles **2.53**, **2.80b** and **2.81a-d** were tested *in vitro* to investigate a possible different and better interaction with KAT2A when including an amide function (increased lipophilicity, facilitated passage through cell membrane) instead of a carboxylic one on the long-chain triazole **2.80b**; therefore, **2.80f** was not preliminary tested against KAT2A *via* fluorescence screening. The preparation of compound **2.53** has been carried out following the procedure previously reported in *Chapter 1 paragraph 1.3*. In particular, different pyridine-azides **1.134a,b,e,f** were reacted with an opportune alkyne (**2.79a-c**) to obtain triazoles **2.80a-f** *via* CuAAc cycloaddition protocol (Scheme 23).

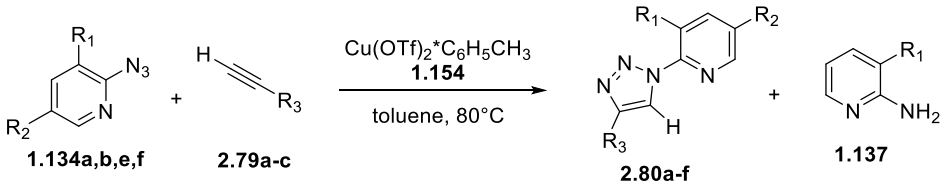

Scheme 23: Pyridyl-azides **1.134a,b,e,f** reacting with alkynes **2.79a-c** to obtain a small library of pyridine-based 1,2,3-triazoles **2.80a-f.**

Pyridine-based 1,2,3-triazoles **2.80a-f** were obtained in high yields (Table 7); however, when reacting pyridyl azide **1.134b** with terminal alkyne **2.79b**, the only compound recovered was the amino-product (**1.137**), deriving from the reduction of the azido group of pyridyl azide **1.134b** (Table 7 entry 4), similarly to what happened when reacting azide **1.134b** with β-ketoesters **1.98 and 1.124a** (Table 3, entries 2 and 4). We again proposed the presence of a copper source and an electron-donor group adjacent to the azido group to be responsible for promoting the reduction process rather than driving the reaction to completion.[75] The presence of EDG or EWG in *para*

position of the pyridine ring instead did not negatively impact the reaction but conversely produced very high yields (Table 7 entries 5,6) and fast reaction times (Table 7 entry 6). Finally, the long lateral chain of alkyne **2.79b**, bearing a carboxylic function, also did not affect the reaction yields except when reacting with azide **1.134b**, where the abovementioned reduction product **1.137** has been the only compound recovered.

Table 7: [a] Reaction conditions: **1.134a,b,e,f** (1 equiv.,0.8 mmol), **2.79a-c** (1.1 equiv., 0.9 mmol), catalyst (0.1 equiv., 0.08 mmol), solvent (0.25M).

Entry[a]	Azide	R_1	R_2	Alkyne	R_3	Time (h)	Product	Yield (%)
1	**1.134a**	H	H	**2.79a**	COOEt	17	**2.80a**	90
2	**1.134a**	H	H	**2.79b**	$(CH_2)_4COOH$	17	**2.80b**	89
3	**1.134b**	OCH_3	H	**2.79a**	COOEt	17	**2.80c**	78
4	**1.134b**	OCH_3	H	**2.79b**	$(CH_2)_4COOH$	17	**1.137**	80
5	**1.134e**	H	CH_3	**2.79a**	COOEt	24	**2.80d**	94
6	**1.134f**	H	Cl	**2.79a**	COOEt	1	**2.80e**	99
7	**1.134a**	H	H	**2.79c**	$(CH_2)_4CONHPh$	17	**2.80f**	75

Given the importance of a carboxylic group at position 4, as highlighted by the docking screening, we then proceeded with the hydrolysis of esters **2.80a,c-e** to reveal the corresponding acids **2.81a-d** (Scheme 24), hence generating a second small library of compounds.

N.B. Herein is also reported the synthesis of **2.81a-d** parental compound, triazole **2.53**.

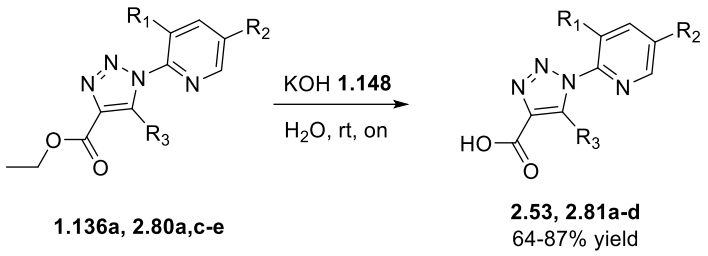

Scheme 24: Hydrolysis of pyridyl-based 1,2,3-triazoles **1.136a** and **2.80a,c-e** to obtain the corresponding carboxylic acids **2.53** and **2.81a-d**.

We then performed the preparation of amide **2.80f** by firstly reacting alkyne **2.79b** with aniline **1.130** in the presence of DCC **1.151** and DMAP **1.150** to achieve alkyne intermediate **2.79c**. Afterwards, we reacted alkyne **2.79c** with azide **1.134a**, following the same protocol described in scheme 2, to obtain 1,2,3-triazole **2.80f** in high yields (75%, Scheme 25).

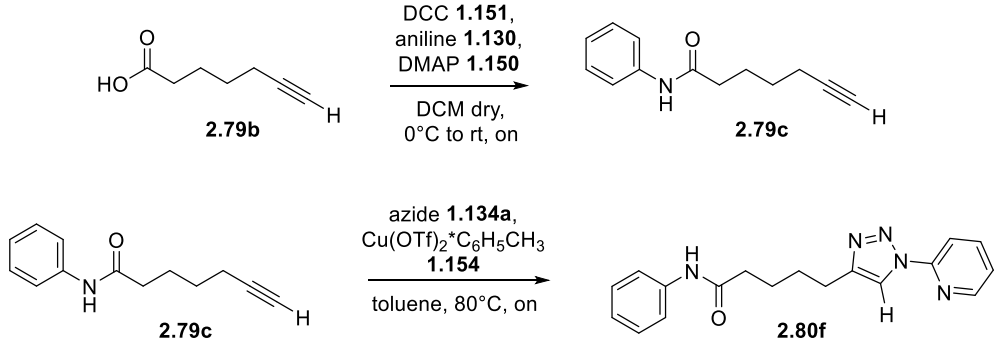

Scheme 25: Synthesis protocol of amide-based 1,2,3-triazole **2.80f**.

2.3.4 C) Preliminary binding studies through fluorescence analysis of pyridyl-triazoles 2.80a-e, 2.81a-d and 2.53 against KAT2A

The newly synthesised compounds **2.80a-e**, **2.81a-d** and **2.53** were tested against KAT2A, according to a validated pre-existing fluorescence protocol, to evaluate their effective binding properties. Fluorescence spectroscopy analyses fluorescence emitted from a sample by using a beam of light, generally UV light, that excites the electrons of the molecule which, in turn, emit light.[303] The emission of light is related to the excitation of the molecule from its ground state to an excited electronic state of higher energy. When the molecule collides with other molecules, it loses its vibrational energy until it reaches the lowest vibrational state emitting a photon in the process.[303] Fluorescence can be measured *via* instruments called fluorometers that exist as i) filter fluorometers, that use filters to isolate the incident light and the fluorescent light and ii)

spectrofluorometers, that use a diffraction grating monochromator to isolate the incident light and the fluorescent light. Anyway, both types of machines work *via* the same following scheme: the incident light passes through a filter or monochromator and hits the sample. Part of the incident light is absorbed by the sample and part of the sample's molecules fluoresce. The fluorescent light is then emitted in all directions and passes, eventually, through a second monochromator or filter before reaching the detector (Figure 52).[303]

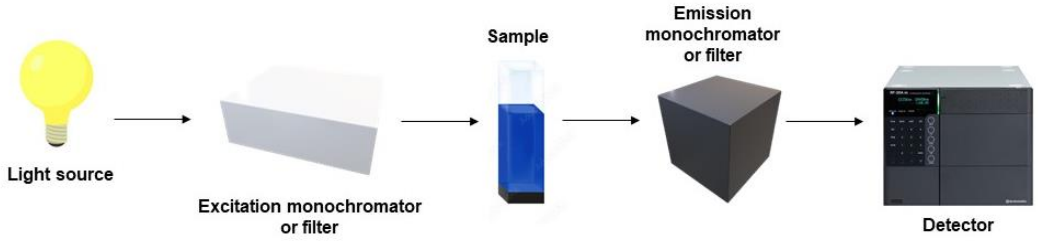

Figure 52: Example of fluorescence spectroscopy workflow.

KAT2A fluorogenic assay is based on the transfer of an acetyl group from acetyl-CoA (acetyl coenzyme A) to a peptide substrate, in this case represented by histone H3. The goal of this test is to detect the presence of potential inhibitors capable of reducing KAT2A acetylating activity by comparing the fluorescence levels of CoASH (intended as CoA without the acyl group) emitted, following the incubation of the enzyme with Acetyl CoA, the H3 histone and the potential inhibitors. The fluorogenic assay performed on 1,2,3-triazoles **2.53**, **2.80a-e** and **2.81a-d** against KAT2A was provided by West Bioscience protocol[304] and fluorescence of the abovementioned compounds was detected at excitation wavelength: 495 nm and emission wavelength: 519 nm on a Varian Cary Eclipse fluorescence spectrophotometer. Specifically, the assay was set up as follows:

- A positive control, to confirm the good quality of the enzyme purchased by testing its inherent acetylating activity on histone H3 when excluding the potential inhibitors from the test.

- An autoacetylation control, perfomed without the presence of either the inhibitors or the H3 histone. It is known that KAT2A, as well as all the other HATs of the GNAT family, can undergo autoacetylation with lysine residues within their catalytic subunit rather than with lysine residues of the original target, histone H3.[305]

- A negative control (blank), performed without the the presence of the KAT2A enzyme, to subtract from all other values when plotting the final graphs.

- And the proper test for screening the inhibition power of triazoles **2.53**, **2.80a-e** and **2.81a-d**, with all the components present.

The inhibition test was set up as follows (Table 8): Acetyl CoA (0.2 μM, 80 μL), the H3 histone (0.32 μM, 400 μL), the inhibitors **2.53**, **2.80a-e** and **2.81a-d** (dissolved in 1% *N*-methylpyrrolidone, 20 μL, in a range of 4 different concentrations: 1.5 μM, 5 μM, 10 μM and 15 μM) and the KAT2A protein (0.1 μM, 200 μL) were incubated in a water bath at 37°C for 30 minutes in 2 mL volume of TRIS HCL, (pH=8 buffer) in a glass vial. After incubation with acetyl CoA and the potential inhibitors, KAT2A generated acylated histone H3 and CoASH. After 30 minutes, the reaction was stopped by the addition of 50 μL of isopropanol (0.8 M) followed by introduction of 100 μL of fluoresceine isothiocyanate isomer I (5-FITC) in DMSO (0.4 μM) as fluorochrome to detect the fluorescence emitted by CoASH, given its reactivity towards nucleophiles including amine and SH groups on proteins.[255] Particularly, 5-FITC is capable of reacting with the SH group of CoASH to generate a fluorescent complex (Scheme 26).

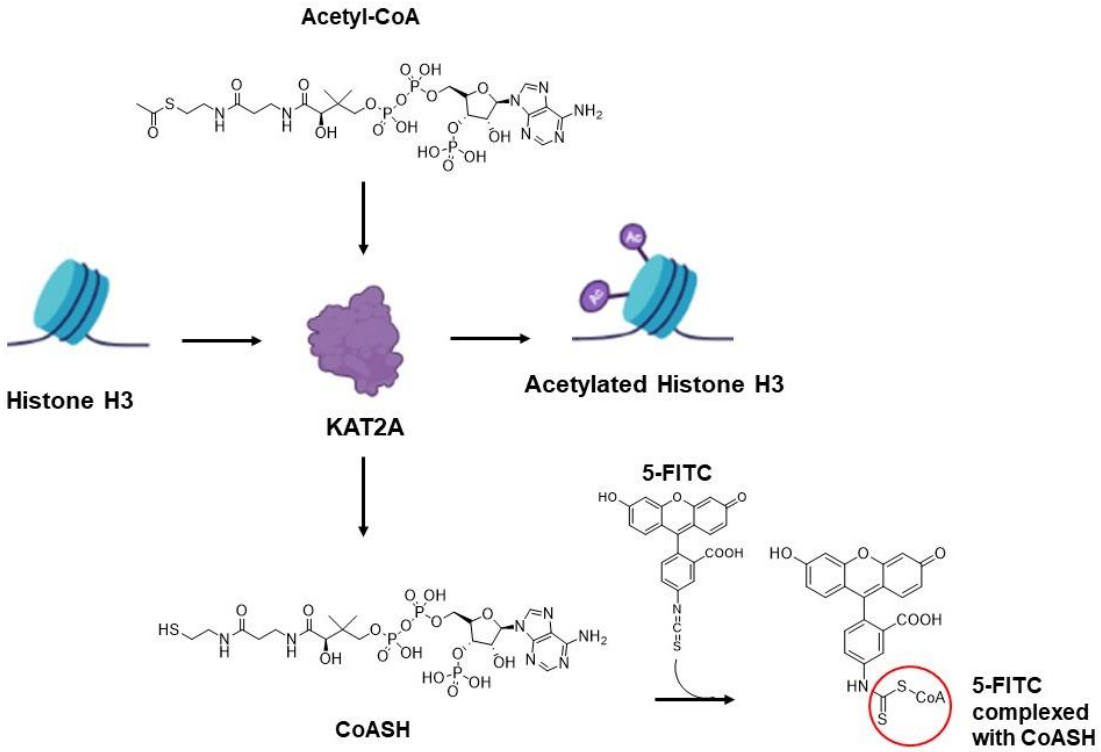

Scheme 26: KAT2A acetylation of histone H3 and generation of CoASH.

After 20 additional minutes of incubation with the fluorochrome at room temperature, the samples were analysed with a fluorescence spectrophotometer to quantify the actual fluorescence emitted. More specifically, the lowest the levels of CoASH complexed with 5-FITC were detected, the best was the inhibitory activity displayed by the specific triazole tested. Detection of the 5-FITC/CoASH complex occurred at absorption wavelength = 495 nm and emission wavelength = 525 nm,

whereas we were able to differentiate between free 5-FITC and 5-FITC bound to the CoASH by detecting the absence of CoASH inherent fluorescence emission at 258 nm. We performed each assay in triplicate at increasing concentrations of compounds **2.53, 2.80a-e** and **2.81a-d** while keeping constant the concentration of KAT2A (Table 8). We decided to perform this fluorogenic assay, specifically validated for the identification of KAT2A inhibitors,[304] because it allowed us to identify, with a rapid response (less than an hour), high specificity, by using small quantities of materials, and with the best cost-effective ratio, the triazole with the highest acetylation inhibition power. Other tests, such as immunofluorescence assays, would have required more time to occur and would have been less specific, given the frequent undesired fluorescence emitted by antigenic contaminants, and more expensive.

Table 8: Set-up of the fluorescence tests of 1,2,3-triazoles **2.53**, **2.80a-e** and **2.81a-d**

	Positive control	**Negative control (blank)**	**Autoacetylation Control**	**Test inhibitor**
Buffer	1.52 mL	1.70 mL	1.72 mL	1.50 mL
Acetyl-CoA	80 µL	80 µL	80 µL	80 µL
Histone H3	400 µL	400 µL	-	400 µL
KAT2A Enzyme	200 µL	-	200 µL	200 µL
Inhibitor	-	20 µL	-	20 µL

Each diagram has been plotted using the Prism software and shows the absolute value of fluorescence emitted by comparing the number of emitted photons with the number of absorbed photons. According to that, Figure 53 shows how the CoASH levels emitted changed according to the inhibitory power displayed by the specific triazole incubated with KAT2A. In particular, compounds **2.81a** and **2.81c** displayed a good inhibitory activity at as low as 5 µM concentration (colored as **blue line**, Figure 53) while higher concentrations for triazoles **2.53** and **2.80b** (15 µM and 10 µM respectively colored in black and **red**, Figure 53) were needed to start exhibiting inhibitory activity. Additionally, we observed that when electron-donor (methyl at C5 position of the pyridine ring for **2.81d**, Figure 53) and electron-withdrawing (chlorine at C5 position of the pyridine ring for **2.81e**, Figure 53) groups were added to the pyridine ring, the inhibition power was promising for **2.81d** only, which displayed a decreasing level of KAT2A activity at as low as

5 μM concentration (colored as **blue line**, Figure 53). Surprisingly, **2.81e** seemed to promote KAT2A acetylating activity as highlighted by the increasing level of CoASH produced despite possessing a very similar chemical structure to the other triazoles tested (Figure 53). No activity was detected for triazoles **2.80a,c-e**, bearing an ester group at position C4 of the triazole ring, thus proving the importance of an acidic functionality in that position for the engagement with the protein.

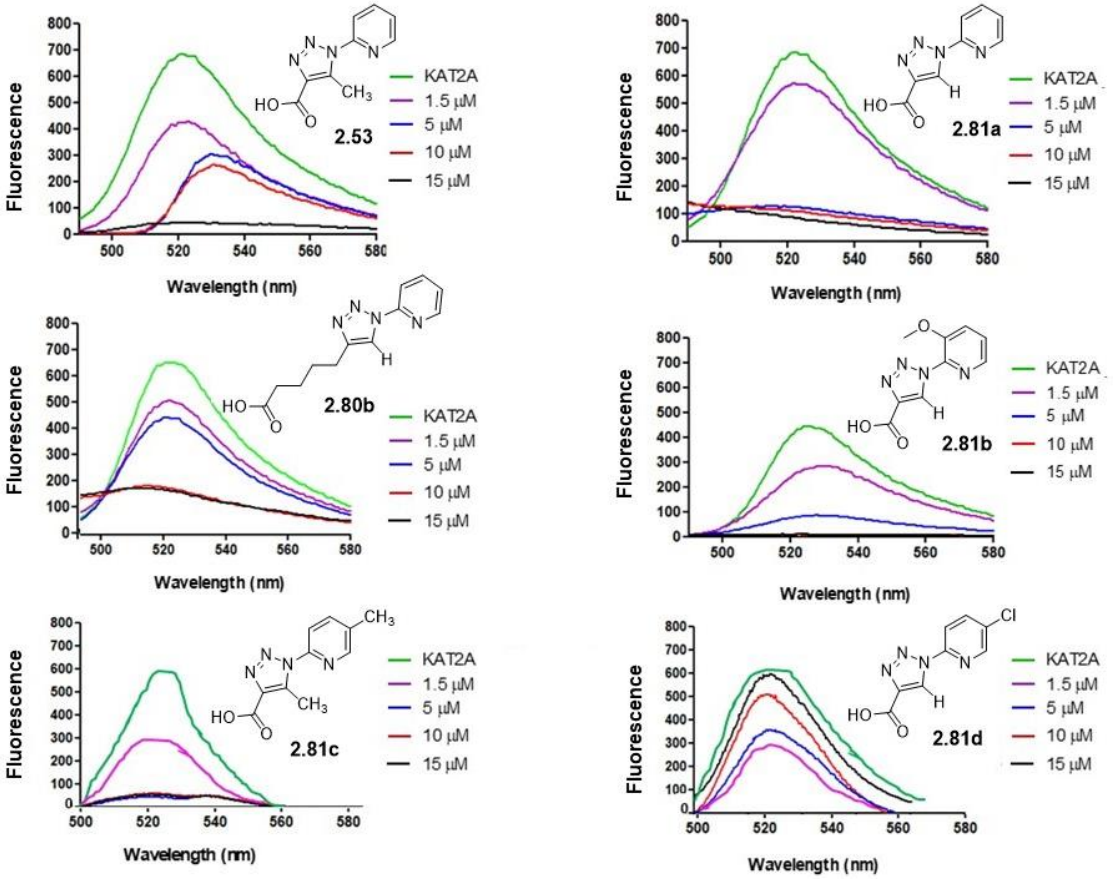

Figure 53: KAT2A fluorescence tests performed on triazoles **2.53**, **2.81a-d** and **2.80b** at different concentrations of 1.5 μM (**purple**), 5 μM (**blue**), 10 μM (**red**) and 15 μM (**black**) against KAT2A (**green**).

2.3.5 D) In *vitro* studies of pyridyl-triazoles 2.53, 2.81a-d, 2.80b and 2.80f against KAT2A

Compounds **2.53**, **2.81a-d**, **2.80b** and **2.80f** were tested against U937 cell cultures as potential KAT2A inhibitors. The U937 cell culture is a pro-monocytic human histiocytic lymphoma cell line (more specifically, human myeloid leukemia, AML).[306] These monocytic cells can differentiate into either macrophages or dendritic cells depending on the stimulus received upon treatment with chemical substances, such as DMSO, phorbol-12-myristate-13-acetate (PMA), retinoic acid, zinc ions and so on.[306] The KAT2A enzyme is known to be overexpressed in tumors like human acute myeloid leukemia (AML). More specifically, KAT2A in U937 tumor cell lines induces elevated acetylation levels of histones H3K9ac.[307] H3K9 is an epigenetic modification to the DNA packaging protein histone H3. H3K9 acts as a gene switch as when acetylated, gene activation is promoted, whereas when methylated, gene inhibition occurs.[308] Domingues *et al*.[309] demonstrated that knockout of KAT2A in retroviral-delivered MLL-AF9 model of AML produced a drastic reduction of AML cells ability to propagate and initiate the disease. Furthermore, KAT2A's absence in the abovementioned retroviral model impeded H3K9 acetylation thus reducing the binding level of trascriptional factors and impeding promoters to enhance AML cells proliferation. In order to tests triazoles **2.53**, **2.81a-d** and **2.80b** effective inhibition of KAT2A, a cell viability assay, namely thiazolyl blue tetrazolium bromide (MTT) assay, has been performed by treating U937 AML cells with the abovementioned compounds at different concentrations, starting from 200 μM. The MTT assay consists of a colorimetric assay for assessing cell metabolic activity and cytotoxicity.[310] The reaction of the NAD(P)H-dependent cellular oxidoreductase enzymes with the MTT dye produces an insoluble formazan which has a purple color detectable by a spectrofluorometer at 500-600 nm wavelenght and whose intensity is directly correlated with the amount of living/death cells detected.[310] We then plotted the results obtained from the MTT test in a bar chart graph that reports the drug concentration on the x axis and the % viability on the y axis. As shown in Figure 54, the test displayed a slight reduction in cell viability by all of the compounds tested by comparing their ability to induce cell death with a non-treated (NT) solution `(Figure 54).

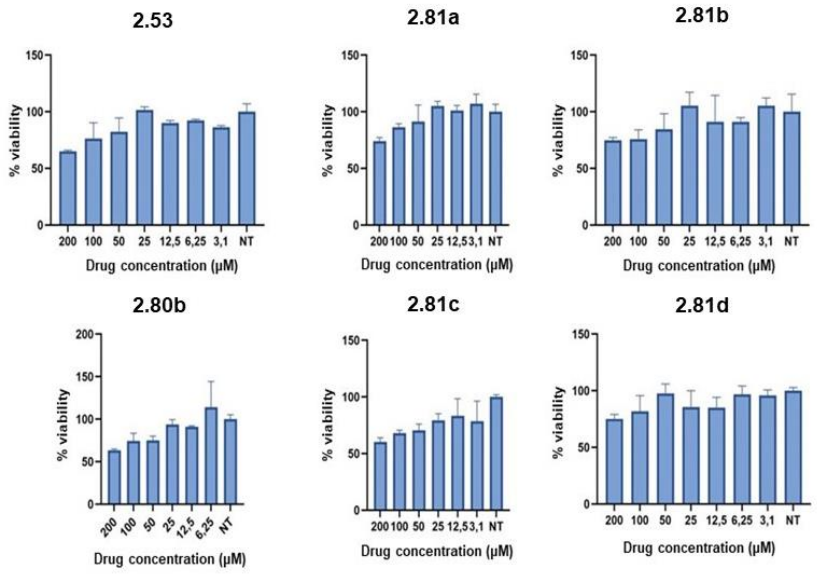

Figure 54: MTT assay performed on triazoles **2.53**, **2.81a-d**, and **2.80b.** NT=non treated. Dr. Nunzio del Gaudio developed the MTT assay and provided the data, which were interpreted and plotted on the graph by the PhD candidate using the Microsoft Excel program.

Given that KAT2A is specifically promoting the acetylation of histones H3 and H4, we focused our attention on the acetylation levels of histone H3K9/14ac when discussing compounds **2.53**, **2.81a-d**, and **2.80b** inhibition against KAT2A. To this end, U937 cells were treated with a 200 μM concentration of compounds **2.53**, **2.81a-d**, and **2.80b** for 24 hours, using SAHA (Suberoylanilide hydroxamic acid), a known histone deacetylase inhibitor, as positive control of acetylation at 5 μM concentration. Histone extraction and subsequent Western Blot (WB) analysis were carried out checking H3K9/14ac acetylation levels. Western Blot is a common technique used to identify specific proteins from a mixture of proteins extracted from cells. Generally, proteins are separated according to their molecular weight *via* gel electrophoresis. The results are transferred to a membrane of polyvinylidene fluoride (PDVF) that produces a band for each protein; the membrane is then incubated with a specific primary antibody to the target protein while the unbound antibody is washed out. The membrane is then exposed to a secondary antibody, conjugated with an enzyme, that can bind to the primary antibody bound to the target protein. Finally, a substrate reacts with the enzyme bound to the secondary antibody to produce a colored substance that indicates the densitometry and location of the target proteins. There are numerous detection methods, including colorimetric, chemiluminescent, and fluorescent detection, but the electrochemiluminescence system (ECL) is the most commonly used (more information about the specific antibodies used to perform WB on **2.80b** is described in the *Experimental Section paragraph 2.5.5.2*).[311] We then analysed WB assay results by plotting the data obtained into the Image*J* software. The data returned highlighted a 40% reduction of KAT2A acetylating activity

only for triazole **2.80b**, which displayed a less thick band compared to the other triazoles tested despite its higher concentration needed to start exhibiting KAT2A inhibition *via* fluorescence assay (Figure 55).

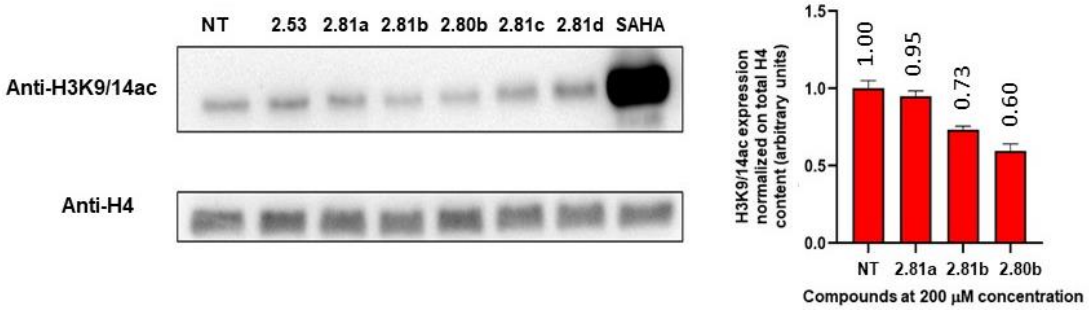

Figure 55: WB analysis (on the left) of **2.53**, **2.80b** and **2.81a-d** showing H3K9/14Ac levels in U937 cells following 24h treatment at the concentration of 200 µM; 5 µM SAHA treatment was used as positive control of acetylation. Densitometric analysis of WB is shown on the right. Dr. Nunzio del Gaudio provided the data, while the PhD candidate created the graph by plotting the densitometry raw data from the Image*J* software into Microsoft Excel.

From the results obtained, we observed that, despite all triazoles tested possessing a carboxylic moiety at the C4 position, only triazole **2.80b**, bearing the carboxylic function not directly attached to the triazole nucleus, produced a moderate inhibition of KAT2A of 40%. Therefore, we hypothesised that a lateral and flexible chain at position C4 of the triazole ring was necessary to properly interact with KAT2A as well as a carboxylic moiety not directly attached to the triazole scaffold. Despite a promising inhibition profile displayed by triazole **2.80b**, the high concentration of 200 µM needed to start displaying inhibitory activity, posed the question about wheter we could improve **2.80b**'s pharmacokinetic profile by rendering the molecule more lipophilic thus improving its permeability of cells' membrane and reducing the dose concentration to use. For this purpose, we decided to modify the terminal fragment of the C4-lateral chain by introducing an *N*-phenylacetamide moiety. We, then, tested the newly synthesised triazole **2.80f** directly in a CCK8 (Cell Counting Kit-8) assay skipping the MTT procedure due to the already assessed promising results of its parental compound **2.80b**. Moreover, the WST-8 formazan, employed in the CCK8 assay, is an upgraded replacement of the MTT dye, first because it generates a water-soluble product and secondly because it is more stable, has a wider linear range and higher sensitivity. Despite the CCK8 assay being more accurate and less toxic than the MTT one, we decided to perform both MTT and CCK8 assays to assess **2.80b** and **2.80f** inhibition power on KAT2A in order to compare the results obtained by two very similar tests. The CCK8 assay consists of a robust test that measures cell proliferation, allowing for accurate live cell counting.[312] The CCK8 assay, in particular, is based on the reduction of a water soluble tetrazolium salt, named Dojindo

WST-8, by dehydrogenase enzymes found in cells that convert NAD+ or NADP+ into NADH or NADPH.The resulting orange-colored formazan dye is formed *via* electron-transfer, following the abovementioned reduction reaction, mediated by 1-methoxyphenazine methosulfate (PMS), which is known to be a stable electron-transport mediator between NADPH and tetrazolium dyes.[312] The absorbance of the formazan dye produced is then measured by a spectrophotometer at 450 nm wavelength and is directly proportional to the number of living cells (Figure 56).[312]

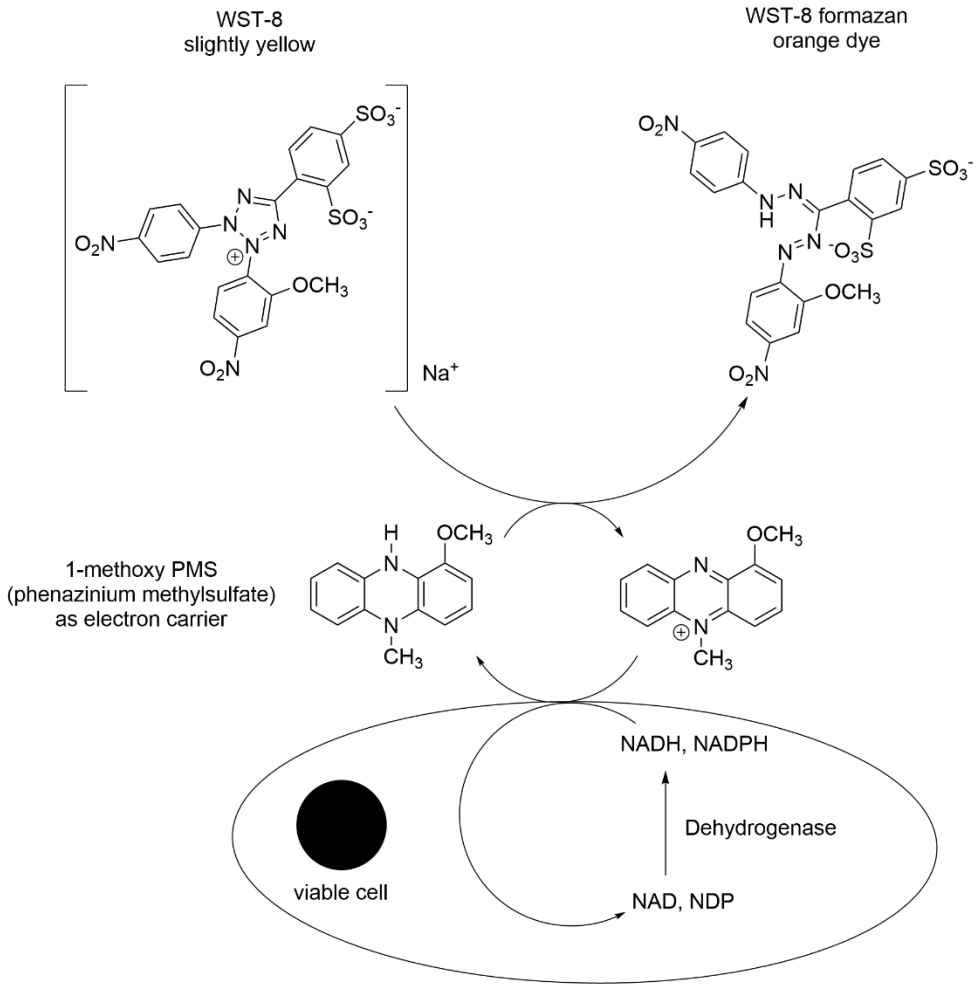

Figure 56: Principles of the CCK8 assay.

The results obtained from the CCK8 assay performed on triazole **2.80f** are shown in Table 9 which reports values of absorbance at different concentrations of **2.80f** matching a specific percentage of cell proliferation. In particular, **2.80f** displayed an improved inhibiting profile compared to **2.80b**, at even lower concentrations (30% cell proliferation inhibition at 50 μM against 200 μM of **2.80b**, Table 9).

Table 9: CCK8 assay absorbance values at different concentrations of **2.80f** matching a specific percentage of cell proliferation. Dr. Nunzio del Gaudio provided the data, while the PhD candidate organised the values for display.

Compound	Concentration	Absorbance	% Cell Proliferation
2.80f	400 μM	0.43	88
2.80f	200 μM	0.98	83
2.80f	100 μM	1.14	73
2.80f	50 μM	1.09	70
2.80f	25 μM	1.43	91
2.80f	12.5 μM	1.41	90
2.80f	6.25 μM	1.52	97

However, a WB of **2.80f** performed against U937 cells evidenced only a 15% reduction of KAT2A activity at 50 μM concentration when considering H3K9/14ac acetylations levels (Figure 57).

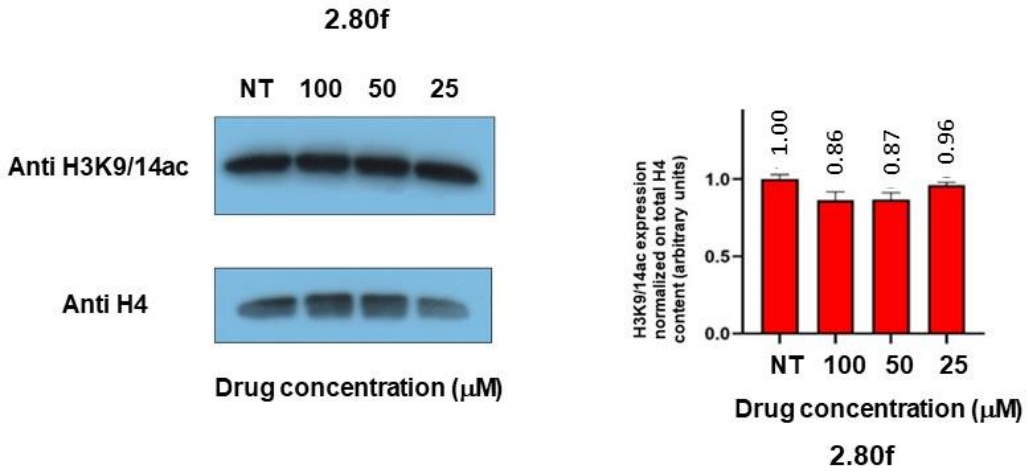

Figure 57: WB (on the left) of **2.80f** showing H3K9/14ac levels in U937 cells following 24h treatment at the concentrations of 100, 50 and 25 μM; Densitometric analysis of WB is shown on the right.
Dr. Nunzio del Gaudio provided the data, while the PhD candidate created the graph by plotting the densitometry raw data from the Image*J* software into Microsoft Excel.

Through consolidation of results, we considered the less flexible amide bond to negatively impact **2.80f** ability to bind the enzyme with the correct orientation, adding to the steric hindrance brought

by the aromatic portion. Nevertheless, object of future work will be **2.80b** modulation with either more lipophilic alternatives to the carboxylate group or functionalisation with other chemical fragments that can more favourably interact with the enzymatic pockets.

2.4 Conclusions

In conclusion, we evaluated triazoles **2.48-2.54** and **1.136a** potential biological importance through preliminar docking studies. The screening revealed these compounds to target 20 proteins and, in particular, highlighted a promising binding-score value (80.13) for **2.53** with KAT2A protein while accentuating the non-selective behavior of 5-hydroxy-triazole **2.52** and the low binding-score values for triazoles **2.48-2.51**, **2.54** and **1.136a.** Therefore, we proceeded to the synthesis of a small library of **2.53** analogs (**2.80a-f** and **2.81a-d**) bearing a hydrogen atom at position C5 rather than a hydroxy moiety, as shown by triazoles **2.48-2.52** and **2.54**. Fluorescence assays confirmed the activity of triazoles **2.53**, **2.81a-d** and **2.80b** only against KAT2A, pointing out the importance of a carboxylic function at position C4 of the triazole ring, while showing inactivity of triazoles **2.80a,c-e** bearing an ester group at position C4 instead. At this point, we tested activity of triazoles **2.53**, **2.81a-d**, **2.80b** and **2.80f** *in vitro* and found out that only triazole **2.80b** showed the best results, with a promising inhibition of KAT2A acetylation activity of 40%. Furthermore, the synthesis of a modified version of triazole **2.80b** bearing an amide function, instead of a carboxylic one (**2.80f**), proved the inhibitory activity of **2.80f** to slightly increase in CCK8 assay even though exhibiting only a 15% of H3K9/14ac reduction of acetylation levels when submitted to WB on U937 leukemia cells. These preliminary results proved a flexible lateral chain at position C4 to be fundamental to bind the enzyme as well as possessing an hydrogen-bond acceptor site to further engage with KAT2A. Future studies will focus on the structure-activity relationship (SAR) of **2.80b** in order to find the optimal chain length and substitution pattern at the end-chain fragment to correctly orientate the tested compound towards the enzyme.

2.5 Experimental Section

^{1}H and ^{13}C NMR spectra were recorded on a Bruker 400 spectrometer. Chemical shifts (δ) are reported in ppm relative to residual solvent signals (^{1}H NMR: 7.26 ppm for $CDCl_3$; 3.31 ppm for CD_3OD, ^{13}C NMR: 77.16 ppm for $CDCl_3$, 49.03 for CD_3OD). ^{13}C NMR spectra were acquired with ^{1}H broad band decoupled mode. Coupling constants (J) are in Hz. Melting points were measured using a Stuart scientific melting point apparatus and are uncorrected. Infrared spectra (IR) were recorded with KBr discs using a Bruker Tensor27 FT-IR instrument. High-resolution mass spectra were obtained on a Waters Micromass GCT PremierMS spectrometer or on a Bruker microTOF-Q III LC-MS spectrometer (APCI method). Purity of final products was verified by HPLC analysis and ^{1}H and ^{13}C NMR spectroscopy. Analytical grade solvents and commercially available reagents were used as received. Anhydrous toluene was purchased from Sigma Aldrich. Reactions were monitored by TLC (Merck, silica gel 60 F254). Flash column chromatography was performed using silica gel 60 (0.040-0.063 mm, 230-400 mesh). Alkynes **2.79a,b** were purchased from Tokyo Chemical Industry (TCI). Alkyne **2.79c** has been synthesised by reacting alkyne **2.79b** with aniline according to literature procedure.[313] 2-azidopyridines **1.134a,b,e,f** were synthesised from commercially available 2-bromopyridines according to literature procedure and following GP1 described in *Chapter 1*.[81] Pyridyl 1,2,3-triazoles **2.53**, **2.80a-f** and hydrolysed products **2.81a-d** were synthesised according to literature procedures (GP3 and GP4).[314–316] Recombinant Human KAT2A/GCN5 His Protein from E.Coli source (corresponding to the amino acids 411-837 of Human KAT2A/GCN5) was purchased from Novus Biological. Acetyl CoA and H3 histone peptide were purchased from Sigma Aldrich. For *in vitro* biological tests, fetal bovine serum (FBS) and SAHA were purchased from Sigma Aldrich, L-glutamine and antibiotics penicillin, streptomycin and amphotericin-B and U937 cell lines were purchased from Euroclone, KAT2A protease inhibitor cocktail was purchased from Roche, nitrocellulose membrane was purchased from Bio-Rad, α-tubulin was purchased from Cell Signal, antibodies anti-GADPH, anti-H4 and CCK8 assay kit were purchased from Elabscience and, finally, histones H3K9/14ac were purchased from Diagenode.

2.5.1 Synthesis of N-phenylhept-6-ynamide 2.79c

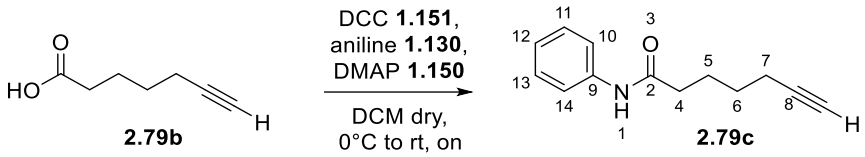

A solution of DCC **1.151** (410 mg, 2.0 mmol) in DCM (0.4 M, 5.0 mL) was added dropwise to a cooled (0°C) solution of alkyne **2.79b** (252 mg, 2.0 mmol), aniline **1.130** (1.82 mL, 2.0 mmol) and DMAP **1.150** (24 mg, 0.2 mmol) in DCM (0.4 M, 5.0 mL). Once the mixture reached room temperature, the mix was left to stir overnight. The progress of the reaction was monitored by TLC (PE/AcOEt 70:30). After disappearance of the starting material, the solid was filtered off and the mixture washed with 1N HCl, 5 mL, 5% solution of $NaHCO_3$, 5 mL and brine, 5mL. The organic layer was dried over anhydrous sodium sulfate Na_2SO_4 and the solvent evaporated. Then, the crude was further purified by flash chromatography (PE/AcOEt 70:30) to yield compound **2.79c** as yellowish solid in high yields (321.8 mg, 80%). ^{1}H NMR (400 MHz, $CDCl_3$) δ 7.52 (d, J = 7.9 Hz, 2H), 7.33 (t, J = 7.8 Hz, 2H), 7.22 (bs, 1H), 7.11 (t, J = 7.3 Hz, 1H), 2.40 (t, J = 7.4 Hz, 2H), 2.29 – 2.23 (m, 2H), 1.98 (s, 1H), 1.93 – 1.82 (m, 2H), 1.63 (dd, J = 13.4, 6.1 Hz, 2H). ^{13}C NMR (101 MHz, $CDCl_3$) δ 170.9, 137.9, 129.0 (C5-C6), 124.3, 119.8, 84.0, 68.7, 37.1, 27.8, 24.6, 18.2. All analytical data are consistent with those reported in the literature.[313]

2.5.2 General procedure for the synthesis of pyridine-based triazoles 2.80a-f (GP3)

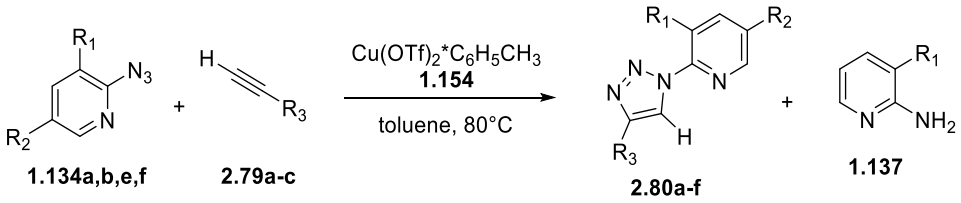

To a solution of 2-azidopyridines **1.134a,b,e,f** (0.8 mmol, 1 equiv.) and copper triflate toluene complex **1.154** (0.08 mmol, 0.1 equiv.) in dry toluene (0.25 M), alkynes **2.79a-c** (0.9 mmol, 1.1 equiv.) were added. The reaction mix stirred for 30min-24 hours at 80°C until complete consumption of the starting material, monitored by TLC (DCM/EtOAc 70:30). Once cooled to room temperature, the crude was washed with DCM/H_2O three times, the organic phases collected and dried over anhydrous Na_2SO_4. The crude was then further purified *via* column chromatography to afford the products **2.80a-f** (DCM/AcOEt 90:10 for **2.80a-e** and DCM/AcOEt 70:30 for **2.80f**) in good to excellent yields. Reaction of azidopyridine **1.134b** with alkyne **2.79b** did not afford the desired product but side compound **1.137** only.

Ethyl 1-(pyridin-2-yl)-1H-1,2,3-triazole-4-carboxylate 2.80a

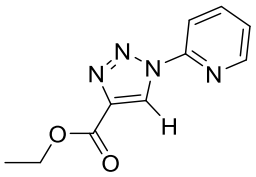

Prepared according to GP3, yellow/orange solid, 90%, 157 mg. ^{1}H NMR (400 MHz, $CDCl_3$) δ 9.10 (s, 1H), 8.55 (d, J = 4.7 Hz, 1H), 8.26 (d, J = 8.2 Hz, 1H), 7.97 (t, J = 7.8 Hz, 1H), 7.42 (dd, J = 7.3, 5.0 Hz, 1H), 4.48 (q, J = 7.1 Hz, 2H), 1.45 (t, J = 7.1 Hz, 3H). ^{13}C NMR (101 MHz, $CDCl_3$) δ 160.6, 148.8, 148.5, 140.5, 139.4, 124.8, 124.3, 114.2, 61.5, 14.3. All analytical data are consistent with those reported in the literature.[314,315]

5-(1-(pyridin-2-yl)-1H-1,2,3-triazol-4-yl)pentanoic acid 2.80b

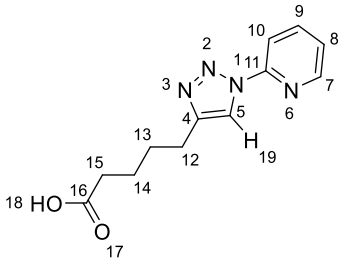

Prepared according to GP3, brown solid, 70%, 137.8 mg. ^{1}H NMR (400 MHz, $CDCl_3$) δ 8.49 (d, J = 4.4 Hz, 1H), 8.35 (s, 1H), 8.19 (d, J = 8.2 Hz, 1H), 7.91 (t, J = 7.8 Hz, 1H), 7.36 – 7.31 (m, 1H), 2.86 (t, J = 7.1 Hz, 2H), 2.44 (t, J = 7.0 Hz, 2H), 1.89 – 1.71 (m, 4H). ^{13}C NMR (101 MHz, $CDCl_3$) δ 177.6, 149.3, 148.4, 139.1 (C13-C14), 123.4, 118.4, 113.8, 28.6, 25.2, 24.2, 18.9. IR (KBr, cm-1): 3149, 2880, 1726, 1635, 1566. m.p. 172 °C. HRMS (ESI) m/z: $[M+Na]^+$ calcd for $C_{12}H_{14}N_4O_2Na$ 269,1114; found: 269,1141.

Ethyl 1-(3-methoxypyridin-2-yl)-1H-1,2,3-triazole-4-carboxylate 2.80c

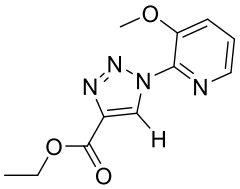

Prepared according to GP3, yellowish solid, 80%, 158.8 mg. ^{1}H NMR (400 MHz, $CDCl_3$) δ 8.73 (s, 1H), 8.26 (d, J = 4.4 Hz, 1H), 7.57 – 7.41 (m, 2H), 4.48 (q, J = 7.1 Hz, 2H), 2.93 (s, 3H), 1.45 (t, J = 7.1 Hz, 3H). ^{13}C NMR (101 MHz, $CDCl_3$) δ 160.9, 148.0, 140.5, 139.7, 138.1, 128.8, 126.0, 121.2, 61.5, 56.4, 14.4. IR (KBr, cm-1): 2860, 1735, 1625, 1528, 1189. m.p. 100 °C. HRMS (ESI) m/z: $[M+H]^+$ calcd for $C_{11}H_{13}N_4O_3$ 249,0288; found: 249.0299.

Ethyl 1-(5-methylpyridin-2-yl)-1H-1,2,3-triazole-4-carboxylate 2.80d

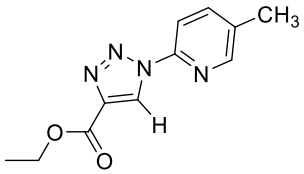

Prepared according to GP3, orange solid, 94%, 174.5 mg. ^{1}H NMR (400 MHz, $CDCl_3$) δ 9.05 (s, 1H), 8.34 (s, 1H), 8.13 (d, J = 8.3 Hz, 1H), 7.75 (d, J = 8.2 Hz, 1H), 4.47 (q, J = 7.1 Hz, 2H), 2.44 (s, 3H), 1.44 (t, J = 7.1 Hz, 3H). ^{13}C NMR (101 MHz, $CDCl_3$) δ 160.7, 148.8, 146.4, 140.4, 139.7, 134.4, 124.6, 113.6, 61.4, 18.1, 14.3. IR (KBr, cm-1): 2860, 1724, 1645, 1466. m.p. 105 °C. HRMS (ESI) m/z: $[M+H]^+$ calcd for $C_{11}H_{13}N_4O_2$ 233,2510; found 233,2870.

Ethyl 1-(5-chloropyridin-2-yl)-1H-1,2,3-triazole-4-carboxylate 2.80e

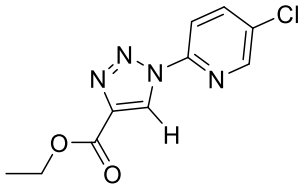

Prepared according to GP3, dark brown solid, 99%, 200 mg. ^{1}H NMR (400 MHz, $CDCl_3$) δ 9.04 (s, 1H), 8.50 (s, 1H), 8.23 (d, J = 8.7 Hz, 1H), 7.94 (dd, J = 8.7, 2.1 Hz, 1H), 4.48 (q, J = 7.1 Hz, 2H), 1.44 (t, J = 7.1 Hz, 3H). ^{13}C NMR (101 MHz, $CDCl_3$) δ 160.4, 147.6, 146.7, 140.7, 139.1, 132.3, 124.8, 114.9, 61.6, 14.3. All analytical data are consistent with those reported in the literature.[316]

N-phenyl-5-(1-(pyridin-2-yl)-1H-1,2,3-triazol-4-yl)pentanamide 2.80f

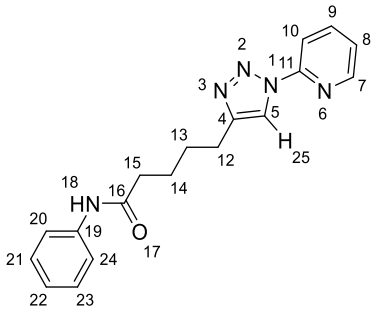

Prepared according to GP3, yellowish solid, 75%, 192.6 mg. ^{1}H NMR (400 MHz, $CDCl_3$) δ 8.49 (d, *J* = 3.6 Hz, 1H), 8.35 (bs, 1H), 8.18 (d, *J* = 8.2 Hz, 1H), 7.90 (t, *J* = 7.1 Hz, 1H), 7.55 (d, *J* = 7.9 Hz, 2H), 7.45 (bs, 1H), 7.32 (dd, *J* = 14.0, 6.4 Hz, 3H), 7.09 (t, *J* = 7.4 Hz, 1H), 2.88 (t, *J* = 5.5 Hz, 2H), 2.44 (t, *J* = 6.4 Hz, 2H), 1.87 (bs, 4H). ^{13}C NMR (101 MHz, $CDCl_3$) δ 171.5, 149.2, 148.5, 139.1, 138.3, 128.9 (C21-C23), 124.0, 123.4, 119.9 (C20-C24), 118.5, 113.71, 37.1, 28.6 (C13-C14), 25.2, 24.9. IR (KBr, cm^{-1}): 2875, 1680, 1643, 1338. m.p. 152 °C. HRMS (ESI) m/z: $[M+Na]^+$ calcd for $C_{18}H_{19}N_5ONa$ 344,3738; found: 344,3873.

3-methoxypyridin-2-amine 1.137

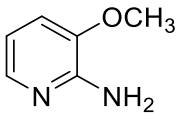

By-product obtained when reacting pyridyl-azide **1.134b** with terminal alkyne **2.85b**, yellow solid 80%, 79.3 mg. ^{1}H NMR (400 MHz, $CDCl_3$) δ 7.67 (bs, 1H), 6.90-6.92 (d, *J* = 7.8 Hz, 1H), 6.61 – 6.64 (m, 1H), 4.66 (bs, 2H), 3.84 (s, 3H). ^{13}C NMR (101 MHz, $CDCl_3$) δ 150.0, 142.4, 138.7, 115.1, 113.8, 55.2. All analytical data are consistent with those reported in the literature.[317]

2.5.3 General procedure for the synthesis of hydrolised pyridine-based triazoles 2.53 and 2.81a-d (GP4)

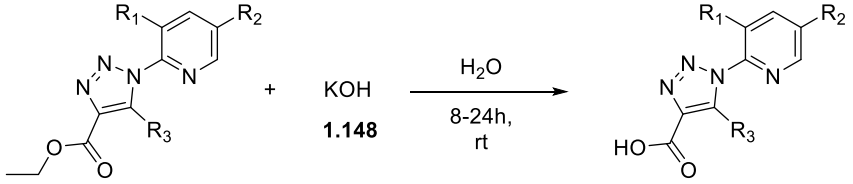

1.136a, R_1,R_2=H, R_3=CH_3
2.80a, R_1,R_2,R_3=H
2.80c, R_1=OCH_3, R_2,R_3=H
2.80d, R_1,R_3=H, R_2=CH_3
2.80e, R_1,R_3=H, R_2=Cl

2.53, R_1,R_2=H, R_3=CH_3
2.81a, R_1,R_2,R_3=H
2.81b, R_1=OCH_3, R_2,R_3=H
2.81c, R_1,R_3=H, R_2=CH_3
2.81d, R_1,R_3=H, R_2=Cl

To a solution of triazoles **1.136a** and **2.80a,c-e** (1 eq., 0.2 mmol) in water (1 M), potassium hydroxide **1.148** (1 eq., 0.2 mmol) was added. The reaction mix then stirred for 8 up to 24 hours at room temperature. Once TLC (DCM/MeOH 90:10) showed complete consumption of the starting triazoles, the crude was washed with AcOEt twice and the organic phases were discarded. The aqueous phases were collected and acidified with HCl 1M (20 mL) and washed with AcOEt twice. The collected organic phases were dried over anhydrous Na_2SO_4 and the solvent was removed by rotary evaporation to afford title compounds **2.53** and **2.81a-d** in good yields and without further purification.

5-methyl-1-(pyridin-2-yl)-1H-1,2,3-triazole-4-carboxylic acid 2.53

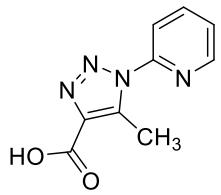

Prepared according to GP4, white solid, 68%, 27.8 mg. ^{1}H NMR (400 MHz, $CDCl_3$) δ 8.62 (d, *J* = 4.5 Hz, 1H), 8.01-7.99 (m, 2H), 7.47 (t, *J* = 4.6 Hz, 1H), 2.96 (s, 3H). ^{13}C NMR (101 MHz, $CDCl_3$) δ 171.3, 150.1, 148.6, 140.6, 139.2, 136.7, 124.3, 118.3, 21.1. All analytical data are consistent with those reported in the literature.[318]

1-(pyridin-2-yl)-1H-1,2,3-triazole-4-carboxylic acid 2.81a

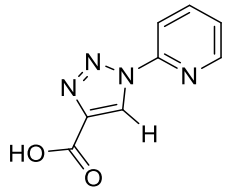

Prepared according to GP4, white solid, 87%, 33 mg. ^{1}H NMR (400 MHz, $CDCl_3$) δ 9.18 (s, 1H), 8.56 (d, J = 4.6 Hz, 1H), 8.26 (d, J = 8.2 Hz, 1H), 7.99 (t, J = 7.9 Hz, 1H), 7.44 (dd, J = 7.3, 5.1 Hz, 1H).^{13}C NMR (101 MHz, $CDCl_3$) δ 161.8, 148.9, 148.6, 140.5, 139.7, 124.8, 124.5, 113.8. All analytical data are consistent with those reported in the literature.[315]

1-(3-methoxypyridin-2-yl)-1H-1,2,3-triazole-4-carboxylic acid 2.81b

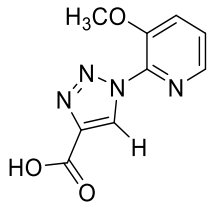

Prepared according to GP4, orange solid, 70%, 30.8 mg. %). ^{1}H NMR (400 MHz, MeOD) δ 8.93 (s, 1H), 8.20 (d, J = 4.9 Hz, 1H), 7.84 (d, J = 8.2 Hz, 1H), 7.64 (dd, J = 8.0, 4.5 Hz, 1H), 3.98 (s, 3H). ^{13}C NMR (101 MHz, MeOD) δ 162.0, 148.8, 139.7, 137.7, 129.3, 126.8, 122.0, 55.6, 53.4. IR (KBr, cm^{-1}): 3268, 2860, 1625, 1528, 1189. m.p. 160°C. HRMS (ESI) m/z: $[M+H]^+$ calcd for $C_9H_9N_4O_3$ 221,2248; found 221,2332.

1-(5-methylpyridin-2-yl)-1H-1,2,3-triazole-4-carboxylic acid 2.81c

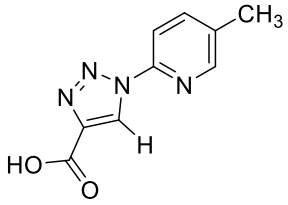

Prepared according to GP4, white powder, 71%, 29 mg. ^{1}H NMR (400 MHz, MeOD) δ 9.15 (s, 1H), 8.42 (s, 1H), 8.08 (d, J = 8.3 Hz, 1H), 7.91 (d, J = 8.1 Hz, 1H), 2.44 (s, 3H). ^{13}C NMR (101 MHz, MeOD) δ 161.8, 148.8, 146.4, 140.3, 139.9, 135.1, 124.7, 113.3, 16.6. IR (KBr, cm^{-1}): 3256, 2860, 1645, 1466. m.p. 125 °C. HRMS (ESI) m/z: $[M+H]^+$ calcd for $C_9H_9N_4O_2$ 205,0726; found 205,1057.

1-(5-chloropyridin-2-yl)-1H-1,2,3-triazole-4-carboxylic acid 2.81d

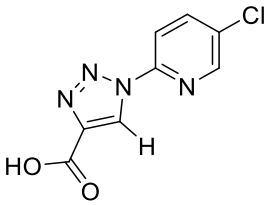

Prepared according to GP4, yellowish powder, 64%, 28.6 mg. ^{1}H NMR (400 MHz, MeOD) δ 9.19 (s, 1H), 8.60 (s, 1H), 8.22 (d, J = 8.7 Hz, 1H), 8.14 (d, J = 8.7 Hz, 1H). ^{13}C NMR (101 MHz, MeOD) δ 161.6, 147.5, 146.9, 140.5, 139.4, 132.2, 125.0, 114.9. All analytical data are consistent with those reported in the literature.[315]

2.5.4 Docking studies

The screening was launched on the AWS E2 cloud (Amazon Web Service EC2) using the following virtual centralized processing unit (VCPU): 36 RAM: 72 G HD: SSD (GP2 type) on a Scalable 2nd Gen Intel Xeon (Cascade Lake) with an all-core turbo frequency of 3.6 GHz and a single-core turbo frequency up to 3.9 GHz. Docking screening of 1,2,3-triazoles **2.48-2.54** and **1.136a** has been performed testing each of the candidate compounds against a precomputed database of human crystallographic protein pockets (BioGPS pocketome).[245] The BioGPS software combined GRID Molecular Interactions Fields (MIFs) and pharmacophoric fingerprints. The GRID probes H, DRY, O, and N1 were used to compute the shape, the hydrophobic interactions, the H-bond acceptor interactions and the H-bond donor interactions respectively for each cavity and for each compound considered in the analysis. Additionally, The GRID software calculated the MIFs complementarity returning a Tanimoto similarity score after each evaluation.[249] The 20 proteins identified by the screening have been chosen according to the best similarity score obtained for each protein pockets and the tested compounds. Each compound was docked within the selected pockets with the FLAPdock algorithm implemented in FLAP. FLAPdock is a program that enables flexible fragment-based docking, based on GRID MIF similarities, in combination with classical energetics.[249]

2.5.5 In vitro tests performed on pyridyl-triazoles 2.53, 2.81a-d, 2.80b and 2.80f against KAT2A overexpressed U937 leukemia cell lines.

2.5.5.1 Cell cultures

U937 cell line (DMSZ) was cultured in Roswell Park Memorial Institute (RPMI) 1640 Medium supplemented with 10% fetal bovine serum (FBS), 2 mM L-glutamine, and antibiotics (100 U/mL penicillin, 100 µg/mL streptomycin, and 250 ng/mL amphotericin-B). In all the experiments, the cells were treated with compounds **2.53**, **2.81a-d**, **2.80b** and **2.80f** at different concentrations and SAHA at a 5 µM concentration as positive control of acetylation.

2.5.5.2 Western Blot analysis

To determine the levels of H3K9/14ac, the histone protein lysates were quantified by Bradford assay using 1 mL Bradford reagent and 2 µL of each lysate in triplicate. Absorbance values were used to calculate protein concentration. 5 µg of proteins were then diluted in 6X Laemmli buffer (0.217 M Tris-HCl pH 8.0, 52.17% SDS, 17.4% glycerol, 0.026% bromo-phenol blue, 8.7% beta-mercapto-ethanol) + 50 mM DTT and subsequently boiled for 3 min at 99°C degrees; 5 µg of total protein extract was run and separated by SDS-polyacrylamide gel electrophoresis and then blotted on nitrocellulose membrane (Bio-Rad). The blotted membrane was blocked in 5% non-fat

milk dissolved in 1 X TBS-T for 1 hour and then incubated ON with the 1:1000 diluted H3K9/14ac antibody in 5% non-fat milk/TBS-T. The next day the membrane was washed 3 times with TBS-T 1X and incubated with anti-rabbit secondary antibody and washed again 3 times with TBS-T 1X for 5 min. Protein expression was detected by ECL chemiluminescence method (Bio-Rad). Normalization was performed with anti-H4 primary antibody and anti-mouse secondary antibody. The Image*J* software was used for the densitometric analysis of the bands.

2.5.5.3 Histones' extraction

Cells were harvested and washed twice with cold 1X PBS and lysed in Triton extraction buffer (TEB; PBS containing 0.5% Triton X 100 (v/v), 2 mM PMSF, 0.02% (w/v) NaN_3) at a cell density of 10^7 cells/mL for 10 min on ice, with gentle stirring. After centrifugation (2000 rpm at 4 °C for 10 min), the supernatant was removed, and the pellet was washed in half the volume of TEB and centrifuged as before. The pellet was suspended in 0.2 N HCl at a cell density of 4×10^7 cells/mL overnight at 4 °C on a rolling table. The samples were then centrifuged at 2000 rpm for 10 min at 4 °C and the supernatant for each of them was collected.

2.5.5.4 Cell Proliferation Assay (MTT Assay)

Thiazolyl blue tetrazolium bromide (MTT) assay was carried out as follows. Cells were collected and counted; 30.000 cells were seeded per well in a 48-well plate. The cells were treated with compounds **2.53**, **2.81a-d**, **2.80b** and **2.80f** at different concentrations and with SAHA and then kept at 37°C in 5% CO_2 for 24 hours. At this point, 50 µL of (5 mg/mL) MTT reagent was added to each well and the plate was placed at 37°C in the incubator for 4 hours. 300 µL of dimethyl sulfoxide (DMSO) was added to each well after aspirating the supernatant. Colored formazan product was assayed spectrophotometrically at 570 nm using TECAN infinite M200 plate reader.

2.5.5.5 Enhanced Cell Counting Kit 8 (WST-8/CCK8)

To assess viability of U937 cells after treatment with the compound, CCK8 assay Elabscience (cat num E-CK-A362) was performed. CCK8 is a colorimetric assay that employs WST-8 substrate, which is reduced by cellular NADH dehydrogenase, thus generating a yellow-colored formazan dye product correlated to the cell's metabolic activity. To perform CCK8 assay, the following protocol has been applied: 100 µL of cell suspension was added per well to the 96 well microplate (counting ca 5000 cells between control and treated cells) the day before and treated with 10 µL of compound **2.80f** at different concentrations; incubation for 24 hours 37°C, in a 5% CO_2 incubator then followed. The day after, 5 µL of CCK8 reagent was added to the wells and the plate was kept at 37°C in dark conditions for 4 hours to allow the reduction reaction of the WST-8 reagent into a colored formazan. The plate was then read in a Tecan Infinite M200 microplate reader at 450 nm. The background absorbance was subtracted, and the values were normalized

to the control cells.[319]

Chapter 3

Pyridine- and proline-based 1,2,3-triazoles' applications in organic chemistry for C-H functionalisation and organocatalysis.

3.1 C-H functionalisation of 1,2,3-triazoles in organic chemistry.

3.1.1 Introduction

The carbon-hydrogen bond functionalisation (C-H functionalisation) involves a set of reactions in which a carbon-hydrogen bond is replaced with a carbon-X bond, with X being an oxygen, carbon or nitrogen. Usually, the process requires the presence of a transition metal that creates a coordination state with the hydrocarbon to form an intermediate “alkane or arene complex” or “metal-carbon complex”. This requirement is necessary because of the non reactive nature of a scarcely acidic C-H bond and because of the large kinetic barrier to overcome when C-H cleavage occurs, considered the apolar nature of the C-H bond itself.[320,321] C-H functionalisation has been explored in the last years because of the vast number of applications that this synthetic strategy can access. In particular, C-H functionalisation has many advantages such as i) can synthetically work with almost all organic molecules known due to the presence of a C-H bond,[322] ii) reduction of the number of synthetic steps to achieve one chemical transformation[322] and iii) possibility to be a more environmentally green option compared to common cross-coupling reactions,[322] such as Negishi coupling,[323] Suzuki coupling,[324] Sonogashira coupling[325] and so on. The first reported example of C-H functionalisation dates back to Hoffman in 1883.[326] He performed a C-H functionalisation based on reactive nitrogen-containing radicals **3.2** under strongly acidic conditions (Scheme 27). This strategy was later applied successfully by Löffler and Freytag for the synthesis of *N*-containing heterocycles, such as nicotine (Scheme 27).[327] In this transformation, an *N*-centered radical performed “benzylic” C-H abstraction to give **3.3** as a transient species which then collapsed to bromide **3.4**. Final displacement of bromine provided pyrrolidine **3.5**.

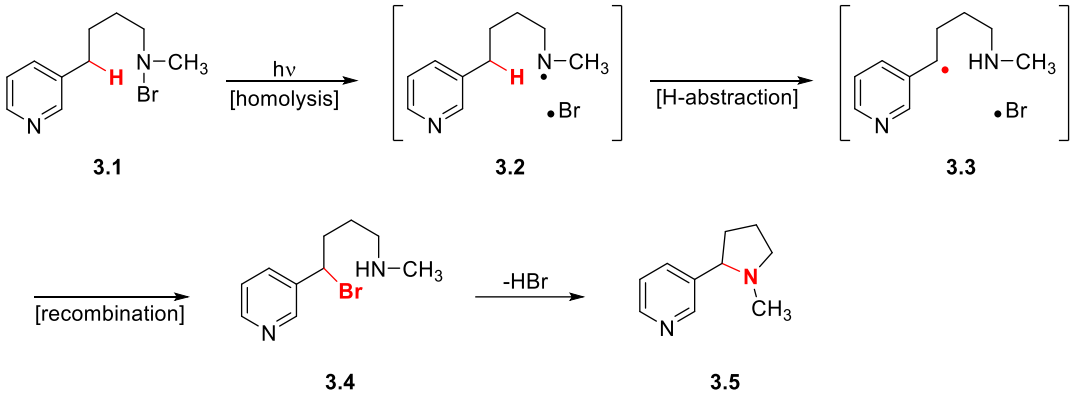

Scheme 27: The Hofmann-Loffler Freytag (HLF) first C-H functionalisation reaction.

On the other hand, the first metal-catalysed C-H activation was reported by Volhard in 1892 who reacted thiophene **3.6** and mercury(II)chloride to obtain chloromercurythiophene **3.7** (Scheme

28).[328] Even so, it is generally considered that Chatt is recognised as the pioneer of the metal-promoted C-H reactions with his successful first attempt to insert a ruthenium$_{(0)}$ (Ru$_{(0)}$) complex **3.8** into a C-H bond of naphtalene **3.9** in 1965 (Scheme 28),[328] a process that occurred *via* oxidative insertion of Ru$_{(II)}$ into a C-H bond (**3.10**).

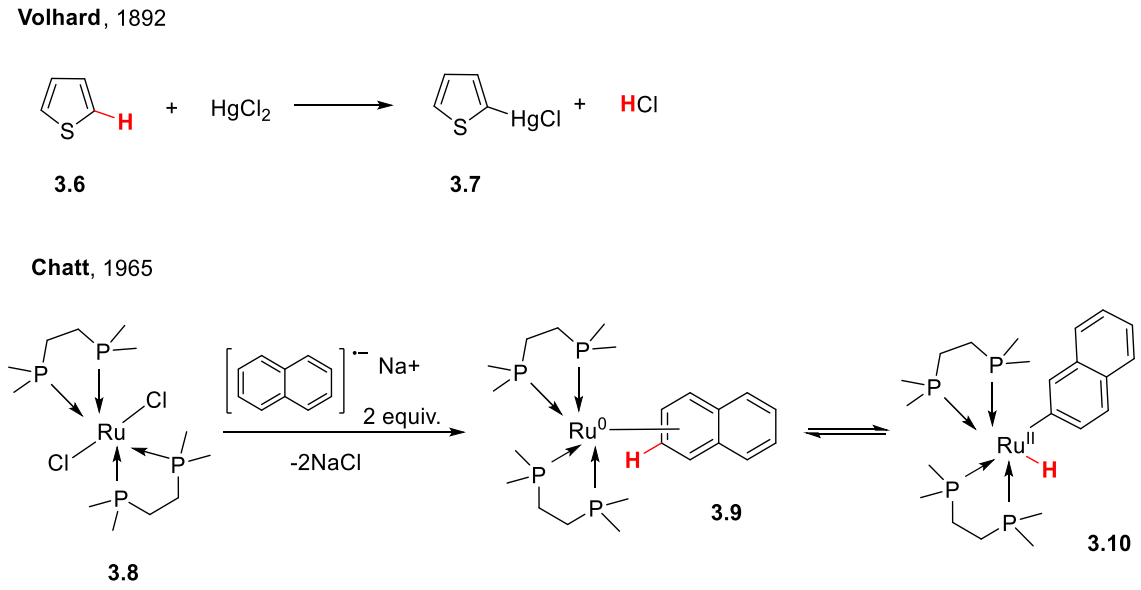

Scheme 28: Volhard's and Chatt's first proposed mechanisms for metal-catalysed C-H activation.

However, C-H bond activation suffers of a major issue: the selective activation of a specific C-H bond among others in the same molecule. Independent of the mechanism involved in the C-H activation, site selectivity can be conventionally achieved *via* substrate or innate control and reagent or guided control. The innate control takes advantage of the natural propensity of the substrate to react at one specific site while the guided control depends on the specific characteristics of the reagent that can overcome the inner control of the substrate.[329]

Additionally, C-H functionalisation can be also improved with regards to:

a) The design of directing groups to be easily removed thus facilitating the functionalisation not only of sp^2 C-H bonds but for sp^3 C-H bonds too.[330–333] A directing group (DG) is a substituent on a molecule or ion that facilitates reactions by interacting with a reagent.[334] DGs, used in C-H activation reactions, represent the most powerful strategy to control the reaction regioselectivity by allowing the catalyst to approach the C-H bond in the most suitable orientation, generally promoted by the presence of Lewis bases linked covalently to the substrate. Directing groups employed for C-H functionalisations include heteroatom-containing groups along with some alkenes molecules and usually possess the following characteristics: i) strong but reversible

coordination to the metal.[335] ii) being an intrinsic part of the starting reagent and of the desired product.[335] iii) if not intrinsic, to be formed *in situ*, readily available and easily removed.[336] Several directing groups have been designed throughout the years aiming for milder reaction conditions as well as for a facile disposal of them such as 5-methoxy-8-amidoquinoline. Bull *et al*.[337] took advantage of this 5-methoxy-8-amidoquinoline control site selectivity for one of the first sp^3 C-H functionalisation reaction reported between proline derivative **3.11** (intrinsic part of the DG) and aryl iodide **3.12** to achieve only the cis isomer **3.13**. The mechanism proposed for this reaction involved the oxidative addition of palladium$_{(II)}$ to form intermediate **3.15** that, upon addition of aryl iodide **3.12,** yielded Pd$_{(IV)}$ complex intermediate **3.16**, which, finally, evolved into product **3.13** following a reductive elimination process (Scheme 29). Furthermore, 5-methoxy-8-amidoquinoline can be removed upon treatment with cerium$_{(IV)}$ ammonium nitrate (CAN) to achieve product **3.14** thus fully respecting the need of an easily detachable DG.[337]

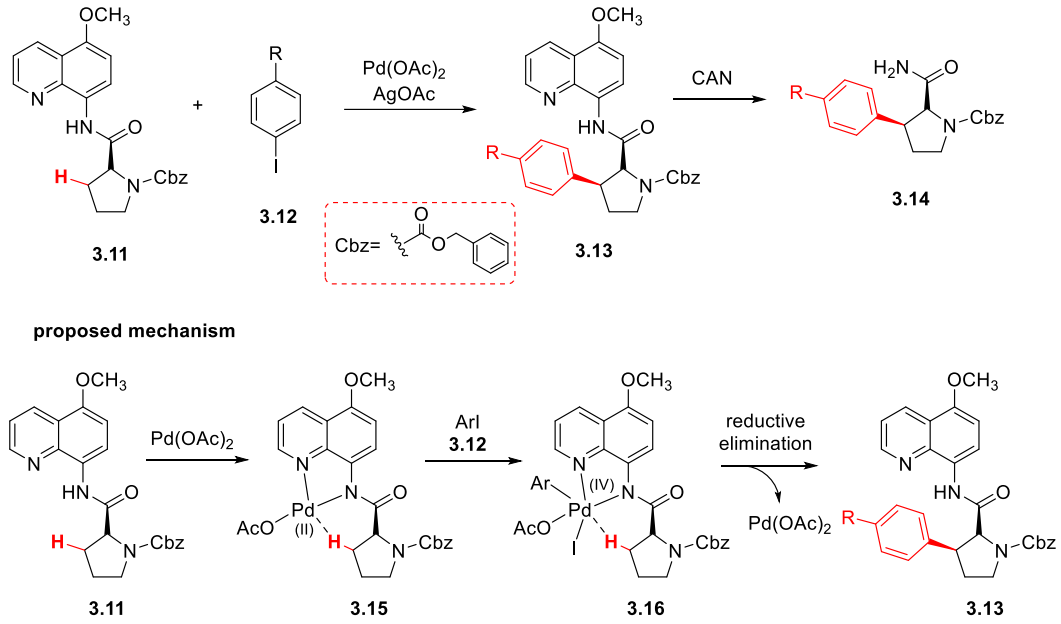

Scheme 29: Bull's use of the 5-methoxy-8-amidoquinoline moiety to stereo-direct the C-H activation of proline derivative **3.11** with different aryl iodides **3.12**.

Pyridine *N*-oxide **3.17** is also known to work as a powerful DG and to be smoothly removed by reaction with ammonium formate. Fagnov *et al*.[338] were the first to design **3.17** as a DG but Zeng and Lu[339] were the first to recognise its potential for the C(sp^3)-H functionalisation of acyclic systems **3.18** *via* palladium catalysis. They proved the amide nitrogen and the *N*-oxide could coordinate and orientate palladium to an ideal position to perform the C-H activation (Scheme 30).

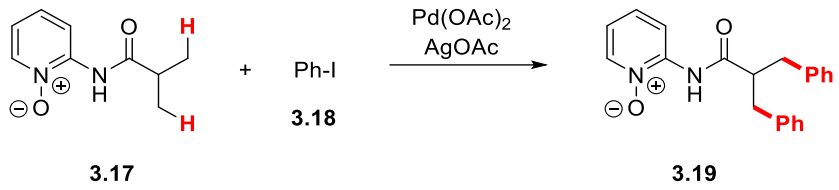

Scheme 30: Pyridine *N*-oxide as DG for the functionalisation of acyclic systems **3.17**.

b) the use of cheaper and greener catalysts.[340,341] Metal catalysed C-H activation often requires the employment of expensive and precious metals like rhodium, palladium, ruthenium or iridium. However, it is worthy of note how beneficial the use of first row transition metals instead could be for the environmental impact of traditional metal catalysed C-H activations. In 2014, Kumar *et al*.[342] proposed, for the first time, the use of potassium *tert*-butoxide (KO^{t}Bu) as the catalyst instead of a metal source to perform the C-H functionalisation of benzamide **3.20** into isoindoline **3.21** *via* a radical mechanism. Kumar proposed an electron transfer to occur between KO^{t}Bu and amide **3.20** to form radical anion **3.22**. Radical anion **3.22** furnished radical **3.23** upon release of iodide which, in turn, after a 1,5-hydrogen atom transfer (1,5-HAT), led to radical **3.24**. Radical **3.24** then attacked the aromatic ring of **3.20** through a 5-exo/endo-trig mechanism, intended as the formation of a 5-membered ring *via* both trigonal exocyclic and endocyclic new bonds formation, yielding intermediate **3.25**. **3.25**, after abstraction of a proton, furnished radical **3.26** which, finally, donated an electron to **3.20** and released the final product **3.21** (Scheme 31).

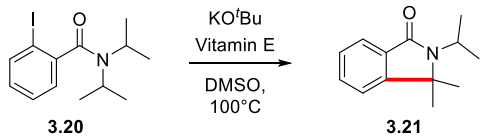

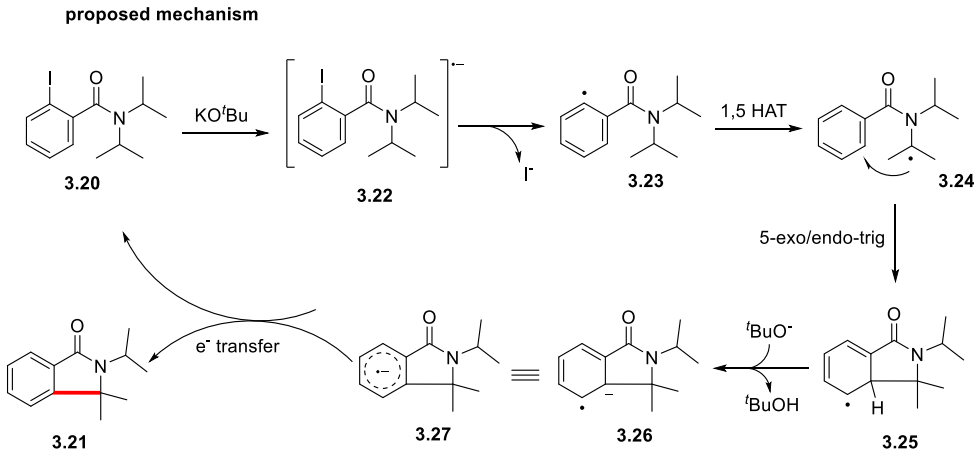

Scheme 31: Potassium *tert*-butoxide as valide alternative to metal source for the C-H functionalisation of **3.20** to obtain **3.21**.

c) the possibility to direct the C-H functionalisation also towards the meta and para position of the benzene ring rather than just the preferred ortho position. Referring to that, Yu *et al*.[343] designed nitrate-based templates **3.28** to achieve the activation of C-H bonds at the meta position. These templates were found to overcome the inherent *ortho*-activating moieties or steric biases for a vast number of substituted anilines, benzylic amines, toluene derivatives etc.[344–348] They hypothesised these C-H transformations proceeded *via* formation of a cyclophane-like-12-membered transition state **3.32** between the arene **3.28** and the catalyst (Scheme 32).

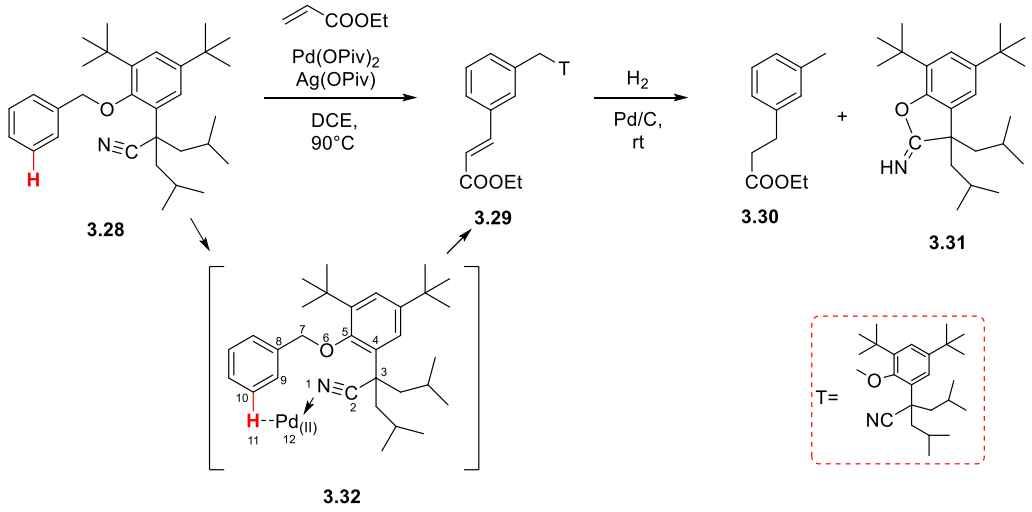

Scheme 32: Proposed cyclophane-like-12-membered transition state for meta selectivity of C-H activation reaction of **3.28**.

Yu and his collaborators also planned a strategy to obtain para selectivity by reacting substituted arenes **3.34** with aryl substitutents **3.33** in the presence of palladium acetate as the catalyst with the help of a pyridine-like ligand to enhance the para selectivity (Scheme 33).[349]

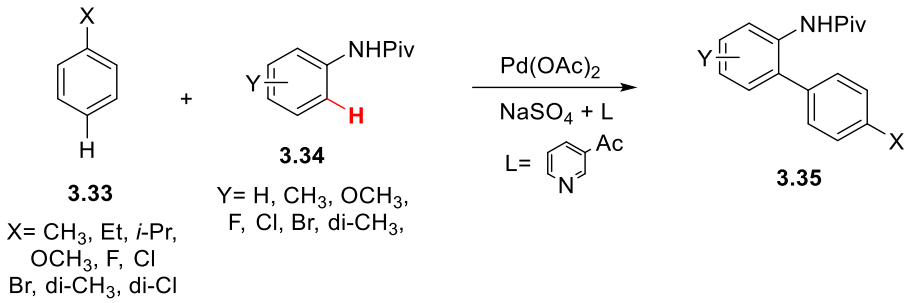

Scheme 33: Proposed scheme of reaction for the meta selectivity of C-H activation reaction of **3.34**

3.1.2 Reactivity of the C-H bond

Metals are often required for the C-H activation to occur, as the C-H bond has a very low reactivity. As previously mentioned, the cleavage of a C-H bond is particularly hard to perform due to the high kinetic barrier and its apolar nature.[320] The energy required to break any chemical bond is called bond dissociation energy (BDE). More specifically, BDE is defined as the energy required to break an A-B bond by homolysis to give fragments A and B which are usually radical species.[350] Therefore, we can consider BDE as directly related to free radical stability. Thus, the higher the number of alkyl substitutents, the weaker the C-H bond as the corresponding radical becomes the most stable species.[351] This means BDE decreases along the series C(sp)-H → C(sp^2)-H → C(sp^3)-H and also when going through 1°→2°→3°→allylic C(sp^3)-H bond, due to a longer C-C bond length that decreases the energy required to cleave the bond itself.[350] Additionally, C-H stability is also attributed to the hyperconjugation, defined as the interaction of the electrons in a σ orbital with an adjacent unpopulated non-bonding p or antibonding σ* or π* orbitals to give a pair of extended molecular orbitals. These interactions are usually from alkyl substituents **3.36** which possess a partially filled orbital with adjacent C-H or C-C bonds **3.37** (Figure 58).[352] However, there are concerns with this model as Gronert pointed out two important issues. Firstly, he stressed out the importance of the substituent effect on both the alkane and radical species. Throughout the years it has been assumed that the alkyl substitution did not impact the alkane stability and has been ignored when considering BDEs.[332] However, isomers of alkanes (i.e. *n*-butane *versus* isobutane heats of formation) proved the substitution to be crucial for alkane's stability.[353] Secondly, Gronert also showed that there are examples of many alkyl radicals species not following the BDE trend aforementioned, such as the BDE of water being greater than the one possessed by hydroxy groups in alcohols or carboxylic acids due to the stronger hydrogen-bond forces occurring in water.[354,355] Furthermore, geometrically and spatially speaking, when a hyperconjugation occurs, the C-H bond should lean towards the radical center. However, angles greater than 109.5° were observed for alkyl radicals' H-C-C bonds suggesting a repulsive rather than stabilising interaction. Given these instances, Gronert hypothesised a three-electron mechanism occurring during hyperconjugation in which the radical's orbital interacts with the σ and σ* orbitals of the adjacent bonds (**3.36**, **3.37**, Figure 58).[353-359]

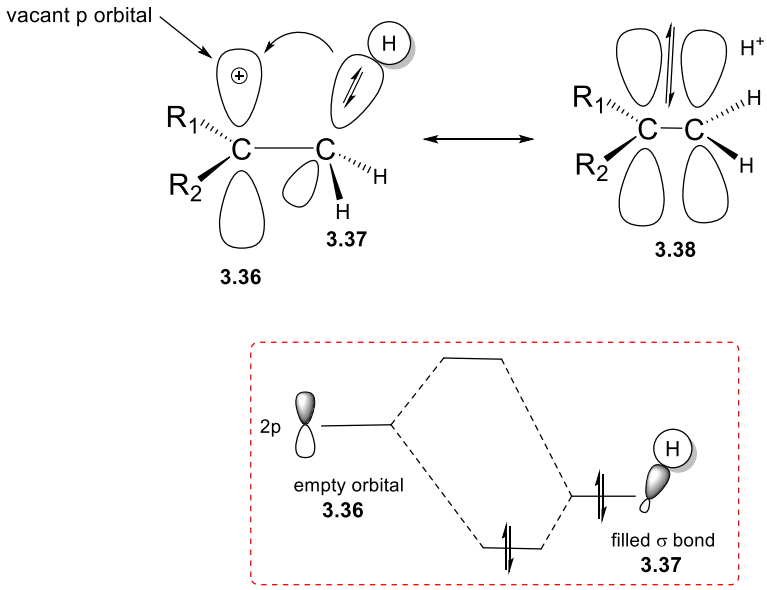

Figure 58: Hyperconjugation of alkyl substituents **3.36** partially filled orbital with adjacent C-H or C-C bonds **3.37**.

3.1.3 Metal-catalysed C-H activation

Undoubtedly, metal-catalaysed C-H activation is the most used strategy to produce new compounds, particularly functionalised arenes and heteroarenes,[360–364] owing to the coordination of the C-H bond with early or late stage transition metals. Specifically, mechanisms for C-H activation can be divided into two groups:

i) Outer sphere mechanism. The outer sphere mechanism is an electron transfer process occurring in coordination complexes in which the C-H bond is inserted into the ligand of a transition metal complex and its cleavage does not bring to a carbon-metal complex formation.[365–368] The outer sphere mechanism is mostly promoted by metal-oxo species through a metalloradical pathway known as the “rebound mechanism” in which the hydrogen radical is removed by the metal-species **3.41** (in which X is generally an oxo-, imido, or carbene species) from the alkane **3.42** and followed by the rebound of the same radical species to the metal hydroxo intermediate **3.44** (Scheme 34).[320] A clear example of this mechanism concerns the reactivity of metal-carbenes and metal-nitrenes. Once the former species react with C-H bonds to form metal-C-H and C-C (or N-H and C-N for nitrenes) complexes, a simultaneous dissociation of the metal species to furnish the desired product/s is observed.[320]

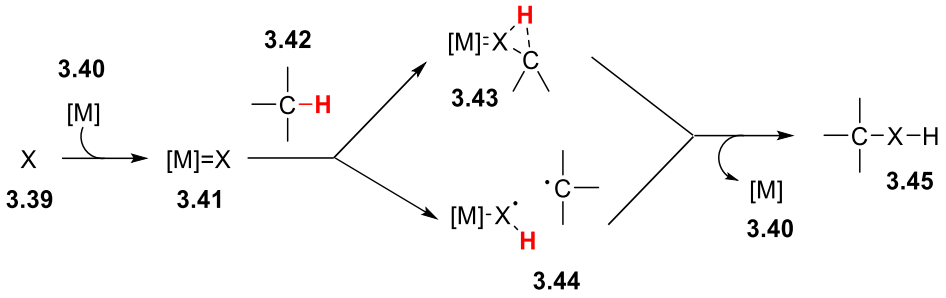

Scheme 34: Outer sphere mechanism of metal-catalysed C-H activation.

ii) Inner sphere mechanism: The inner sphere mechanism is an electron transfer process in which the C-H bond-metal complex **3.46** species remains in the inner-sphere during the activation (Scheme 35). In particular, the inner sphere process in C-H functionalisation reactions proceeds via two different steps: i) cleavage of the C-H bond **3.42** that leads to a transition metal allyl/aryl intermediate **3.46** and ii) functionalisation of **3.46** with an external oxo-, imido, or carbene species source (X=**3.39**) to yield product **3.47** (Scheme 35).[369]

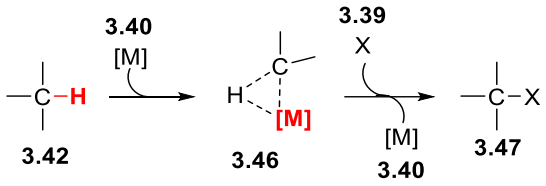

Scheme 35: Inner sphere mechanism of metal-catalysed C-H activation.

Three different classes belong to the inner sphere mechanism:

a) Oxidative Addition (OA) for low-valent electron-rich late transition metals, belonging to groups VIII to XI of the periodic table, that proceeds *via* low-valent metal insertion **3.48** into a C-H bond **3.42a** with subsequent formation of a C-H-metal coordination complex **3.49a** with a weak σ-donation and strong π-back bonding. In the OA process, the metal oxidation and coordination number increase of two units (Scheme 36).[370]

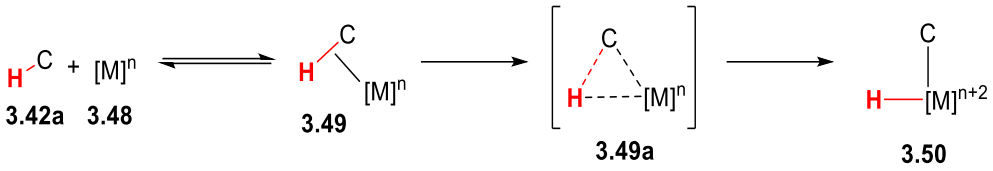

Scheme 36: Oxidative addition process for low-valent electron-rich late transition metals **3.48**.

Furthermore, good donor ligands promote the OA process while acceptor ligands suppress it.[371] OA can occur *via* many pathways depending on the metal center and the substrate involved: i) *concerted pathway*, for OA of nonpolar substrates such as hydrogen (H-H) or hydrocarbons (iodomethane, Me-I) A-B **3.52**. In this case, a σ-complex **3.53** is formed between the metal **3.51** and the substrate **3.52** followed by intramolecular cleavage of the bond to generate the oxidised complex **3.54** (Scheme 37).[372] ii) *S_N2-type pathway*, for OA of polar and electrophilic substrates such as alkyl halides and halogens (iodomethane, MeI). In this case, the metal center **3.55** attacks the less electronegative atom of the substrate to form a $[M\text{-}R]^+$ species **3.56**. This step is followed by the anion coordination with metal center **3.57** (Scheme 37).[372] iii) *radical pathway*, for OA, generally involving, alkyl halides **3.60a,b** reaction with $Pt(PPh_3)_3$ complexes **3.58**. In this case, we can distinguish two mechanisms, a non-chain type, in which the metal **3.58** transfers one electron to the R-X **3.60a,b** σ*-orbital to form cationic **3.61** and anionic **3.62** ($M^{+\bullet}$ and $RX^{-\bullet}$) radicals, and a chain-type, which mainly occurs for OA of ethyl bromide **3.60a** (EtBr) or benzyl bromide **3.60b** ($PhCH_2Br$) to the Vaska complex[373] **3.55** $(PMe_3)_2Ir(CO)Cl$, in which a radical initiator **3.64** is required (Scheme 37).[372]

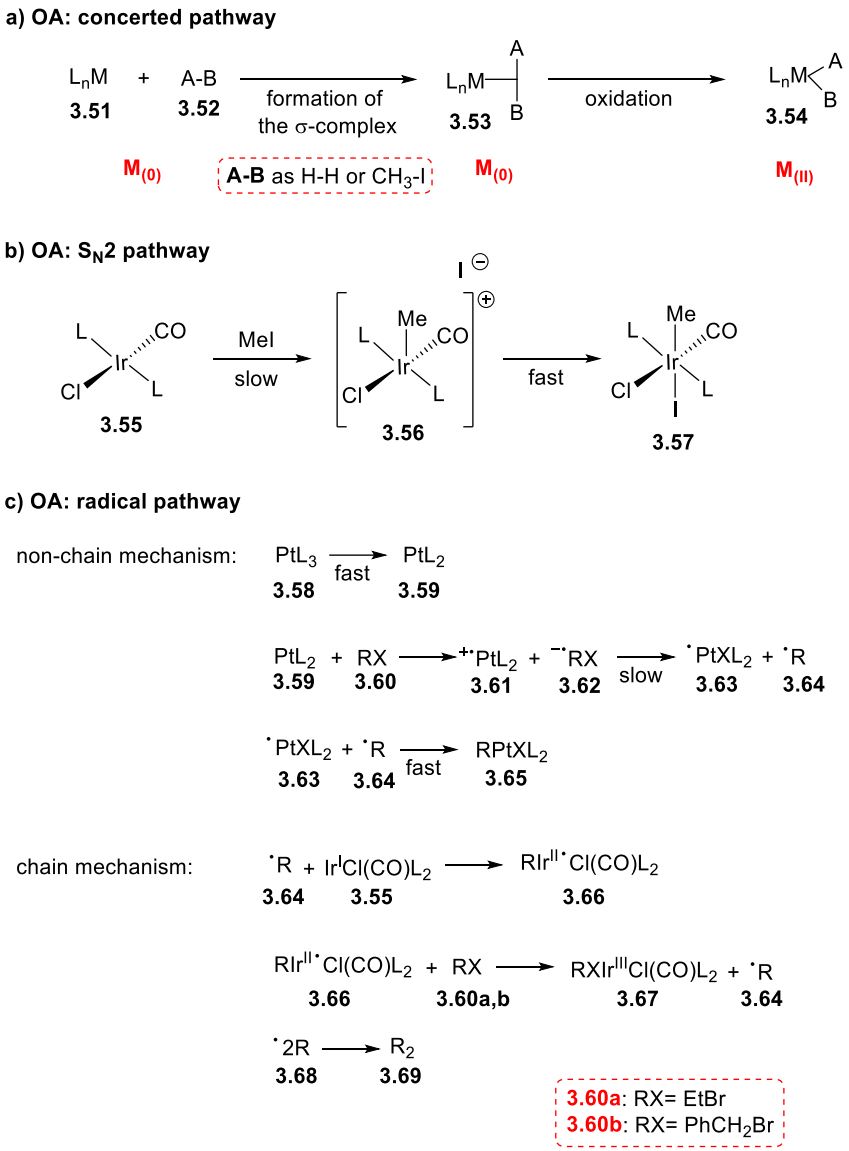

Scheme 37: OA's different pathways for metal-catalysed C-H activation.

b) σ-Bond Metathesis (σ-BM) for electrophilic early transition metals belonging to groups III to VII of the periodic table. σ-BM consists of a four-center concerted mechanism **3.76** without change of the metal transition state.[374–382] Generally, the transferring atom is a hydrogen atom **3.42a** that, with its spherical 1s orbital, is able to interact with the orbitals of the three other centers thus adding stability to the four-center transition state **3.72** (Scheme 38).[377] Despite early transition metals being the ones mostly undergoing σ-BM, studies from Morokuma *et al*.[383], concerning the hydrogenolysis reaction of palladium$_{(II)}$ or nickel$_{(II)}$ complexes [(diimine)M(R)(η^2-H_2)]$^+$→[(diimine)M(H)(η^2-HR)]$^+$, demonstrated a four-transition state **3.72** to exist also for late transition metals with low valency.

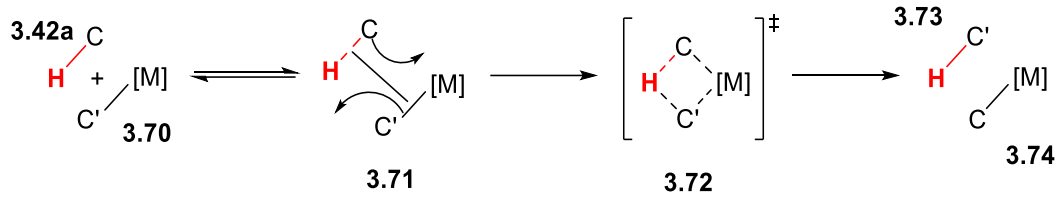

Scheme 38: σ-bond metathesis mechanism for electrophilic early transition metals.

c) Electrophilic Activation (EA) is typical of amido, alkylidene, alkoxy or alkylidyne complexes of early and middle transition metals bearing electron withdrawing ligands **3.75**.[384] This mechanism occurs *via* formation of a concerted four-center 1,2-addition **3.76** similar to σ-BM **3.72** but, in this case, the new X-H bond does not come from the metal complex but involves lone pairs or π-electrons instead of σ-bonds (Scheme 39). Moreover, in order to perform a 1,2-addition of a C-H bond to an M-X (X=O,N) metal center, a vacant site on the metal is needed. This requires the presence of a Lewis acidic/electron-deficient metal and a nucleophilic/basic heteroatom in close proximity to start the reaction.[369]

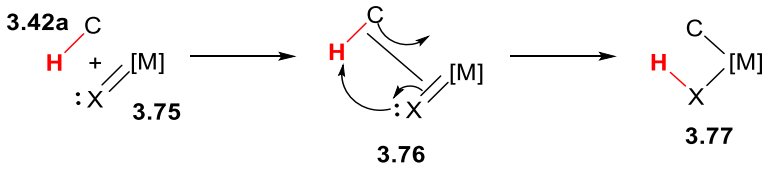

Scheme 39: Electrophilic activation 1,2-addition mechanism of amido, alkylidene, alkoxy or alkylidyne complexes of early and middle transition metals **3.75** bearing electron withdrawing ligands.

Depending on the oxidation state of the metal complex, the charge transfer (CT) during the C-H activation process can occur in two different ways: from the occupied dπ orbital of the metal to the σ* orbital of the C-H bond, in a fashion known as reverse CT, or from the σ orbital of the C-H group to an empty dσ orbital of the metal center, in a fashion known as forward CT (Figure 59).[385]

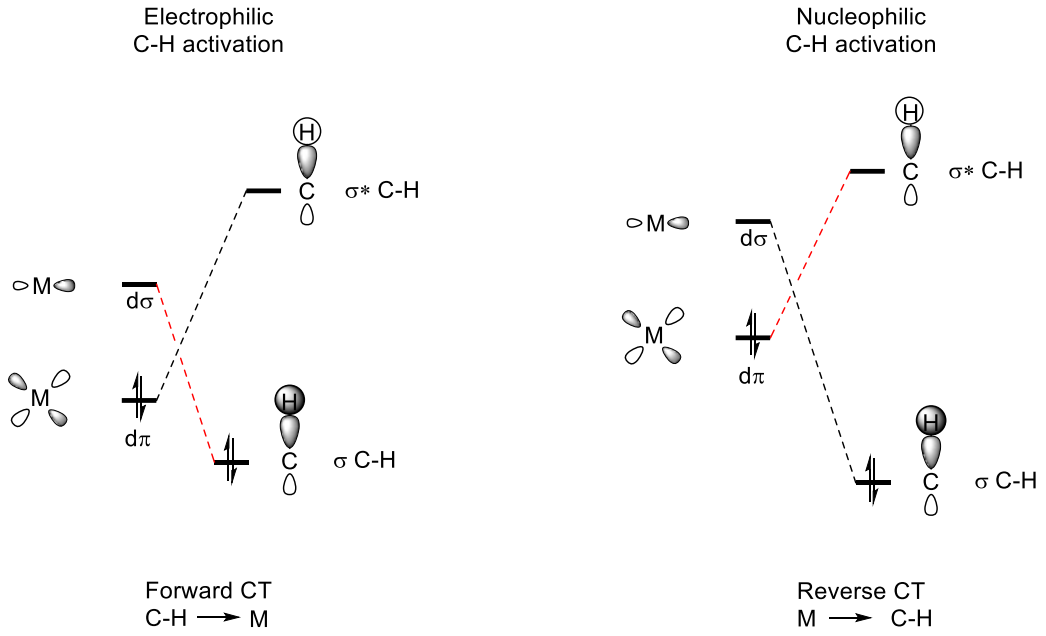

Figure 59: Electrophilic and nucleophilic C-H activation explained through forward and reverse charge transfer.

Furthermore, according to the electronic nature of the metal complex, we can distinguish between electrophilic and nucleophilic C-H activation.

i) Electrophilic C-H activation mainly occurs with electron-deficient transition metals, such as d^0 transition metals with high oxidation state, such as titanium or zirconium complexes (i.e $TiCl_4$ or $(C_5H_5)_2ZrHCl$). These metals possess low dπ and dσ energy thus interacting with C-H bonds only through the σ-BM mechanism (Figure 59).[354-356]

ii) Nucleophilic C-H activation occurs, instead, with electron-rich late transition metals (groups VIII to XI of the periodic table), prevalently in the d^8 configuration, in which the energetic barrier among the C-H bond break and the M-H bond d^6 configuration is not very high. Additionally, these metals possess a high dπ and dσ energy thus interacting with C-H bonds mainly through the OA mechanism (Figure 59).[320]

3.1.3.1 Palladium (Pd)-catalysed C-H activation

Palladium (Pd), along with ruthenium (Ru), rhodium (Rh) and platinum (Pt) transition metals, is known to undergo ligand-directed C-H activation reactions known as cyclometalations.[386,387] Palladium complexes employed in C-H activation reactions allow for the formation of different kind of bonds such as C-O, C-N, C-S and C-C. This is an exceptional characteristic given that only few other metals permit such a variety of bond creations.[388–390] Furthermore, Pd catalysts are compatible with many oxidants and grant functionalisation of diverse cyclopalladated intermediates. Pd also promotes both C-H activation of sp^2 and sp^3 C-H sites and its resistance to air and moisture is optimal for application in organic chemistry. Generally, Pd ligand directed C-H activations can take place according to two different mechanisms *via* a common cyclopalladated intermediate **3.81**. The first mechanism proceeds through a $Pd_{(II/0)}$ pathway in which a reductive process, which can be either reductive elimination or β-hydride elimination/deprotonation, generates the new C-functional group (FG) bond **3.83** and $Pd_{(0)}$ **3.84** which, in turn, is ready to be reoxidised to $Pd_{(II)}$ (Scheme 40, number 1). The second pathway involves an electrophilic reagent for the palladacycle intermediate **3.81** functionalisation. The addition of the electrophilic reagent **3.79** can occur *via* direct cleavage of the Pd-C bond without Pd changing its oxidation state (Scheme 40, number 2, mechanism a), *via* one-electron oxidation of intermediate **3.85** (Scheme 40, number 2, mechanism b) or *via* two-electron oxidation of intermediate **3.87** (Scheme 40, number 2, mechanism c) with $Pd_{(IV)}$ or $Pd_{(III)}$ dimeric species formation as an intermediate complex (Scheme 40, number 2).[391]

1) Reductive functionalisation mechanism: $Pd_{(II/0)}$ catalytic cycle.

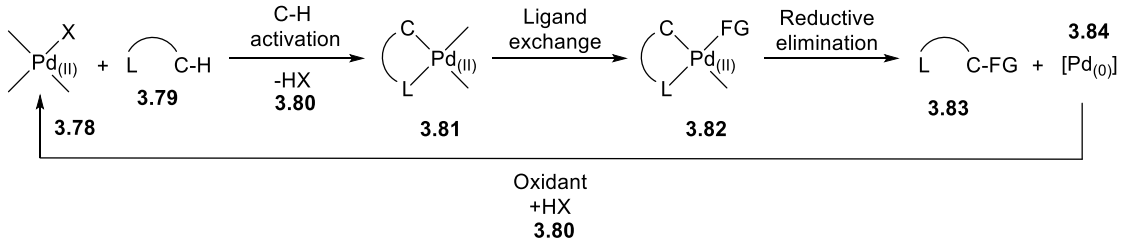

2) Electrophilic functionalisation (mechanism a): direct electrophilic functionalisation of palladacycle 3.81

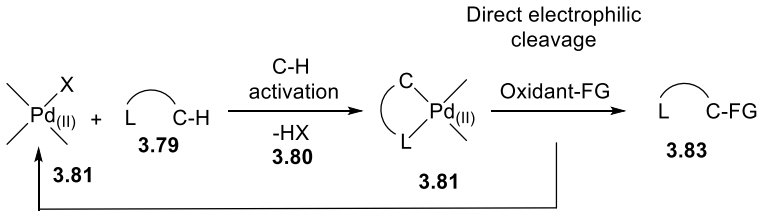

2) Electrophilic functionalisation (mechanism b): one-electron oxidation of palladacycle 3.81.

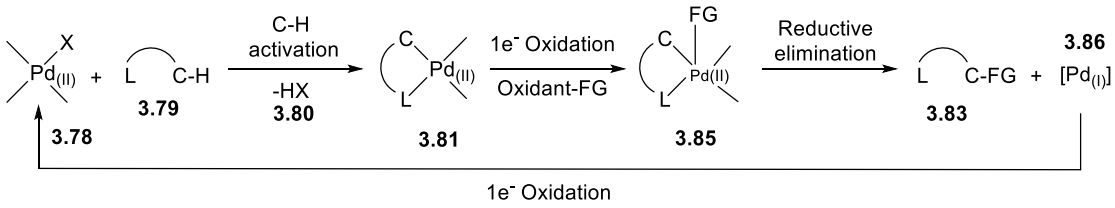

2) Electrophilic functionalisation (mechanism c): two-electron oxidation of palladacycle 3.81.

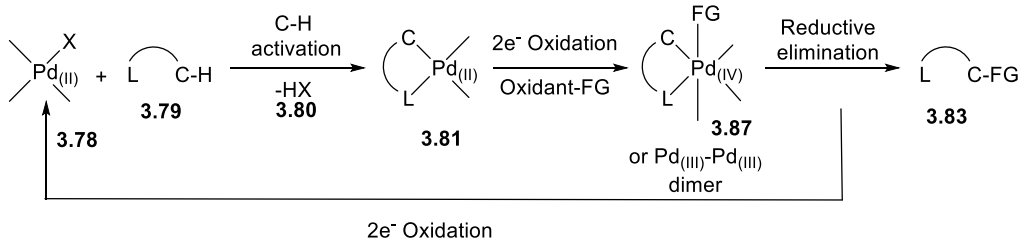

Scheme 40: Pd ligand directed C-H activation *via* reductive or electrophilic functionalisation mechanisms.

3.1.3.1.1 Pd-catalysed C-H activation for C-O bond formation

Dick *et al*. were the first to perform a Pd-catalysed sp^2 C-H activation to form a new C-O bond by using stoichiometric amount of (diacetoxyiodo)benzene **3.90**, $PhI(OAc)_2$, as the oxidant and palladium acetate **3.89**, $Pd(OAc)_2$, as palladium source. They tested a wide range of pyridine derivatives **3.88** as directing ligands and obtained ortho-acetoxylated products **3.91** between average and good yields (Scheme 41).[392] The same reaction performed with ketones or aldehydes as directing groups did not afford any product, presumably because of their poor engagement with $Pd_{(II)}$ species.[393,394]

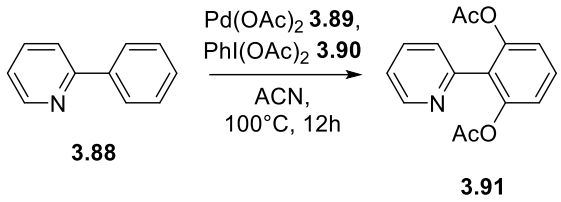

Scheme 41: Pd-catalysed sp^2 C-H activation using $PhI(OAc)_2$ **3.90** as the oxidant.

Moreover, it has been proved that $Pd_{(II)}$-catalysed sp^2 acetoxylation of *meta*-substituted aryl pyridines and aryl pyrrolidinones occurs at the less-hindered ortho site despite the electronic properties of the meta substitutent.[395] Polymer assisted-(diacetoxyiodo)aryl, $ArI(OAc)_2$, has also been introduced, later on, for $Pd_{(II)}$-catalysed acetoxylations, leading to results comparable to the ones obtained with $PhI(OAc)_2$. Furthermore, polymer assisted $ArI(OAc)_2$ is readily recovered from the reaction media and recycled for the next set of reactions.[396] $PhI(OAc)_2$ **3.90** has been also employed for the first Pd-catalysed sp^3 C-H functionalisation to form new C-O bonds. Many examples of benzylic[387] **3.92** and unactivated sp^3 C-H bonds[397] **3.92** have been successfully acetoxylated when incorporating pyridines or oximes as directing groups in their structures (Scheme 42).

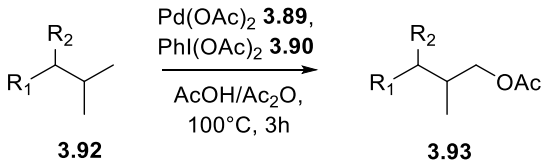

R_1=benzylic or unactivated sp^3 bond
R_2: oxime or pyridine

Scheme 42: Pd-catalysed sp^3 C-H activation using $PhI(OAc)_2$ as the oxidant.

3.1.3.1.2 Pd-catalysed C-H activation for C-S bond formation

Pd-catalysed C-H activation to form new C-S bonds remains still challenging. However, there is record of a first successful report of C-S bond formation provided by Inamoto *et al*.[398] They converted thioenols **3.94** to substituted benzothiophenes **3.96** through dichloro(1,5-cyclooctadiene)palladium$_{(II)}$ **3.95**, Pd(cod)Cl$_2$, catalysis and proposed this reaction proceeding *via* a disulfide intermediate, formed *in situ* by reaction of the starting material with DMSO (Scheme 43).[399–403] Once the disulfide has been formed, oxidative addition to Pd$_{(0)}$, cyclometalation at Pd$_{(II)}$ and reductive elimination to release the product followed.

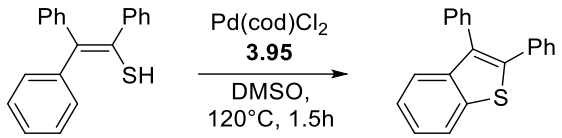

3.94 **3.96**

Scheme 43: Pd(cod)Cl$_2$ **3.95** catalysed C-H activation for the formation of a new C-S bond.

3.1.3.1.3 Pd-catalysed C-H activation for C-N bond formation

Pd-catalysed C-H activation to achieve new C-N bond has been crucial for the formation of several biologically active molecules.[404–407] Two different reaction pathways can occur for the Pd-catalysed C-N new bond formation:

a) <u>C-N bond formation intramolecularly</u>. Tsang reported the synthesis of carbazoles **3.99** from 2-phenylacetanilides **3.97** cyclisation catalysed by Pd(OAc)$_2$ **3.89** species in the presence of copper acetate/molecular oxygen, Cu(OAc)$_2$/O$_2$, or O$_2$ in DMSO as the oxidant/s species (Scheme 44).[408]

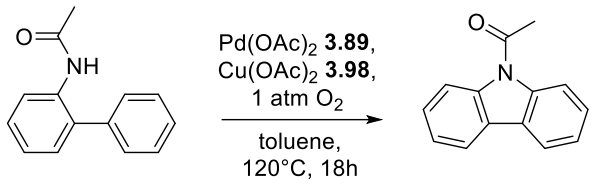

3.97 **3.99**

Scheme 44: Pd-catalysed intramolecular C-H amination of 2-phenylacetanilides **3.97** to form carbazoles **3.99.**

He reported this system to proceed either *via* coordination of palladium to the amide nitrogen followed by a Heck-type cyclisation and β-hydride elimination or *via* coordination of palladium to the amide nitrogen followed by a Wacker-type cyclisation and β-hydride elimination.[409]

b) <u>C-N bond formation intermolecularly</u>. To date, there is only one example, described by Thu *et*

al.[410], of Pd-catalysed C-N bond intermolecular formation and involves sp^2 or sp^3 C-H bonds of pyridine-based and oxime-based ethers. $Pd(OAc)_2$ **3.89** was selected, again, as the catalytic source along with potassium sulfate **3.112** (KSO_4) and an external source to provide the nitrogen atom, such as an electron-deficient primary amide like carbamates, acetamides or sulfonamides. They indicated the reaction to proceed through the formation of a cyclopalladate intermediate **3.113**, followed by nitrene insertion into the C-Pd bond (Scheme 45).[410]

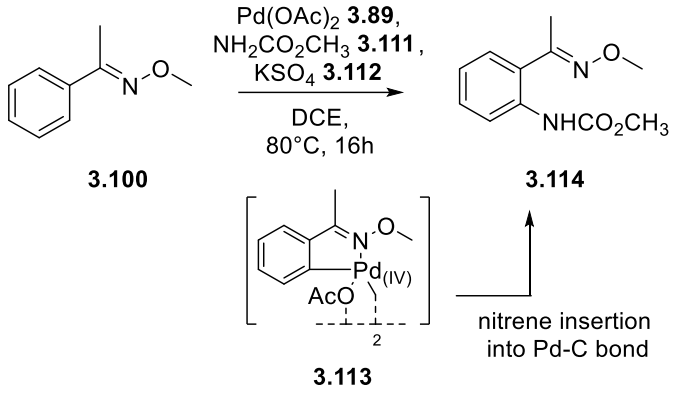

Scheme 45: Proposed mechanism for the intramolecular C-H amination of primary amide like carbamates, acetamides or sulfonamides via nitrene insertion.

3.1.3.1.4 Pd-catalysed C-H activation for C-C bond formation

Pd-catalysed C-H activation for the formation of new C-C bonds has been for decades the most used strategy to create new molecules. Extensive studies have been performed about ortho-arylation, alkenylation, alkylation and alkynylation reactions through Pd-species catalysis.

a) Pd-catalysed C-H arylation. Pd-catalysed C-H arylation reactions take place with coordination of $Pd(OAc)_2$ **3.89** with diphenyliodonium salts **3.116** to obtain *ortho*-functionalised 2-aryl pyridines, quinidines, pyrrolidinones, oxazolidinones and benzodiazepines **3.117** (Scheme 46).[411–414]

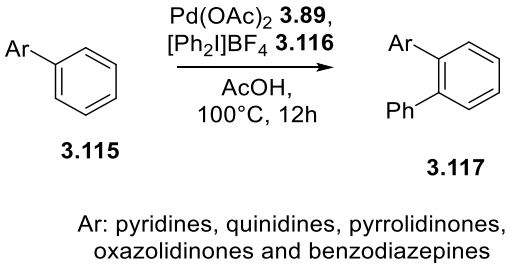

Scheme 46: Pd-catalysed C-H arylation in the presence of diphenyliodonium salts **3.116**.

Hull also proposed a C-H arylation reaction without the need for an auxiliary reagent to link to the catalytic source. He performed a $Pd(OAc)_2$-catalysed dimerisation of 2-arylpyridine derivatives

3.118 in presence of Oxone **3.119**, a potassium salt containing peroxymonosulfuric acid, as oxidant species to give substituted aryl pyridines **3.120** in good yields (Scheme 47).[415]

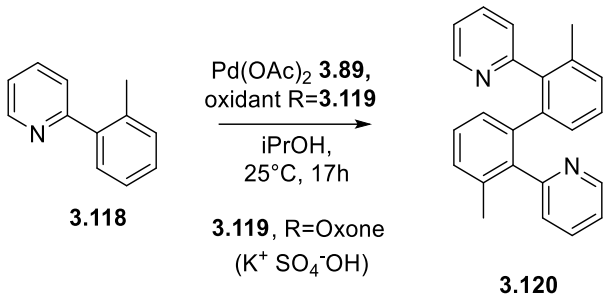

Scheme 47: Pd-catalysed C-H arylation reaction withouth an auxiliary reagent.

b) Pd-catalysed C-H alkenylation. In 2002, Boele proposed one of the first example of C-H alkenylation involving $Pd(OAc)_2$ **3.89** catalysis of acetanilides **3.121** coupling with acrylates **3.122** in the presence of benzoquinones **3.123** (BQ) as oxidant species. He was able to perform several *ortho*-substituted alkenylated products **3.125** with low yields only when reacting acrylates bearing EWGs (Scheme 48).[416] Wang, later, described comparably promising results while performing the same reaction but using O_2 as the oxidant and $Cu(OAc)_2$ as the catalyst.[417]

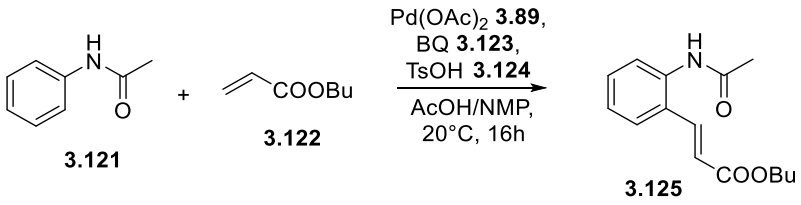

Scheme 48: Pd-catalysed C-H alkenylation in the presence of benzoquinone **3.123** as the oxidant species.

c) Pd-catalysed C-H alkylation. In 2006, Chen *et al*.[418] accomplished the $Pd(OAc)_2$-catalysed *ortho*-alkylation of aryl oxazolines **3.126** using stannane species **3.127** as methylating agent. They took advantage of $Cu(OAc)_2$ **3.99** as the oxidant species and benzoquinone (**3.123**, BQ) to speed-up the cyclopalladate intermediate formation and subsequent C-C new bond release (Scheme 49).

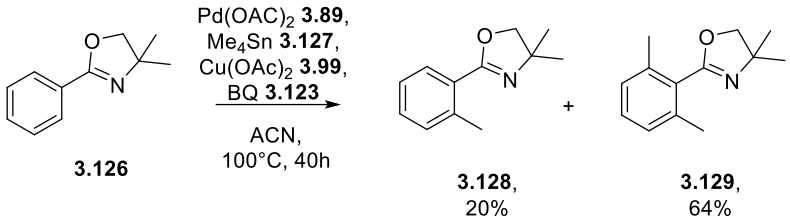

Scheme 49: Pd-catalysed C-H alkylation of oxazolines **3.126** using stannane species as auxiliary reagent.

Shi *et al*.[419] reported, in 2008, an asymmetric sp^2 C-H alkylation using monoprotected aminoacids **3.132** as chiral ligands. They reacted diverse (diarylmethyl)pyridines **3.130** in C-H alkylation of one prochiral aryl group with boronic acids **3.131** in good to excellent yields (96%, 88% ees, Scheme 50).

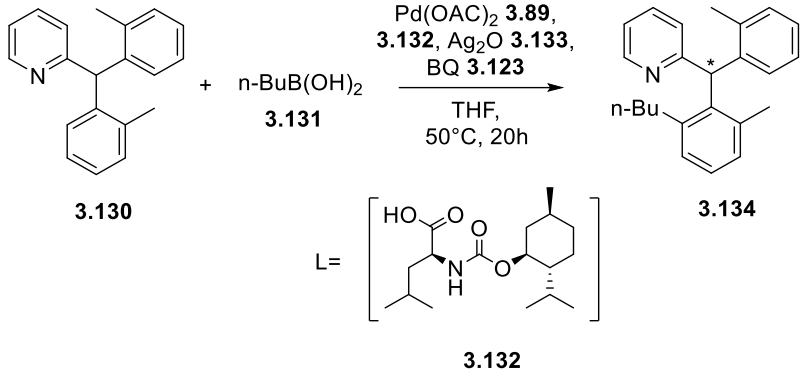

Scheme 50: Asymmetric sp^2 C-H alkylation of (diarylmethyl)pyridines **3.130** with boronic species **3.131**.

d) Pd-catalysed C-H alkynylation. The only example known so far of C-H alkynylation is attributed to Tobisu and his group. They reacted anilides **3.135** with bromoalkynes **3.136** in the presence of $Pd(OAc)_2$ **3.89** as catalytic source, silver triflate **3.137** (AgOTf) as the oxidant and potassium carbonate **3.138** (K_2CO_3) as the deprotonating base (Scheme 51).[420]

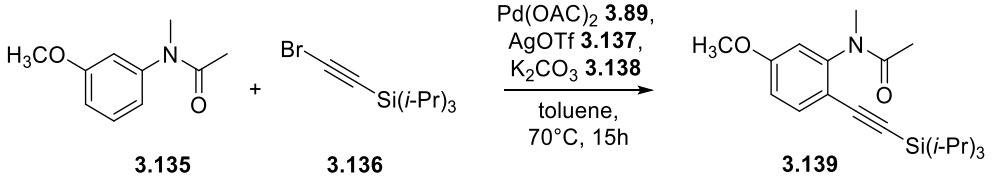

Scheme 51: Pd-catalysed C-H alkynylation of anilides **3.135** in the presence of AgOTf **3.137** as the oxidant species.

3.1.3.2 Copper (Cu)-catalysed C-H activation

Copper (Cu) species have been employed frequently in the last decades for C-H activation reactions to obtain several new C-N, C-O, C-C and C-S bonds with promising results.[421–423] Additionally, copper was the first transition metal identified to promote C-H bond arylation.[424] Generally, the mechanism involved in Cu-catalysed C-H activations is still very difficult to explain because of the several copper oxidation states involved. However, early studies proposed a single electron transfer (SET) for electron-rich substrates involved in the reaction. According to this proposal, it is believed that a Cu-catalysed C-H functionalisation may start with abstraction of one electron from the substrate **3.143** by $Cu_{(II)}$ **3.141** species to obtain a radical intermediate **3.144** (Scheme 52). At this point, the radical species can evolve through cyclisation, oxidation and formation of the product **3.145** or can proceed to the final result *via* further radical transformations **3.146** to **3.147**. $Cu_{(I)}$ species **3.142**, derived from $Cu_{(II)}$ **3.141** SET previously mentioned, is then oxidised to regenerate $Cu_{(II)}$ **3.141** that can enter a second $Cu_{(II)}/Cu_{(I)}$ catalytic cycle (Scheme 52).[425] A two-electron process has also been proposed involving a $Cu_{(I)}/Cu_{(III)}$ catalytic cycle. First, a $organocopper_{(III)}$ intermediate **3.150** is formed between $Cu_{(I)}$ **3.142** and a halogenated substrate **3.148**. Then, reductive elimination occurs to restore $Cu_{(I)}$ **3.142** and yield the desired product **3.151**. An alternative two-electrons process results from the formation of the $organocopper_{(III)}$ intermediate **3.150** in the presence of strong oxidants (Scheme 52).[425] Guo *et al*. also mentioned the possibility to, eventually, combine both one- and two-electron process to achieve improved results. The ideal $Cu_{(I)}/Cu_{(II)}/Cu_{(III)}$ catalytic cycle would proceed through the formation of an $organocopper_{(III)}$ intermediate **3.154** by a $Cu_{(II)}$ disproportionation. Reductive elimination would then follow to afford the product **3.155** and restore $Cu_{(I)}$ species **3.142**, which can be reoxidised and join a second catalytic cycle (Scheme 52).[425]

One-electron mechanism

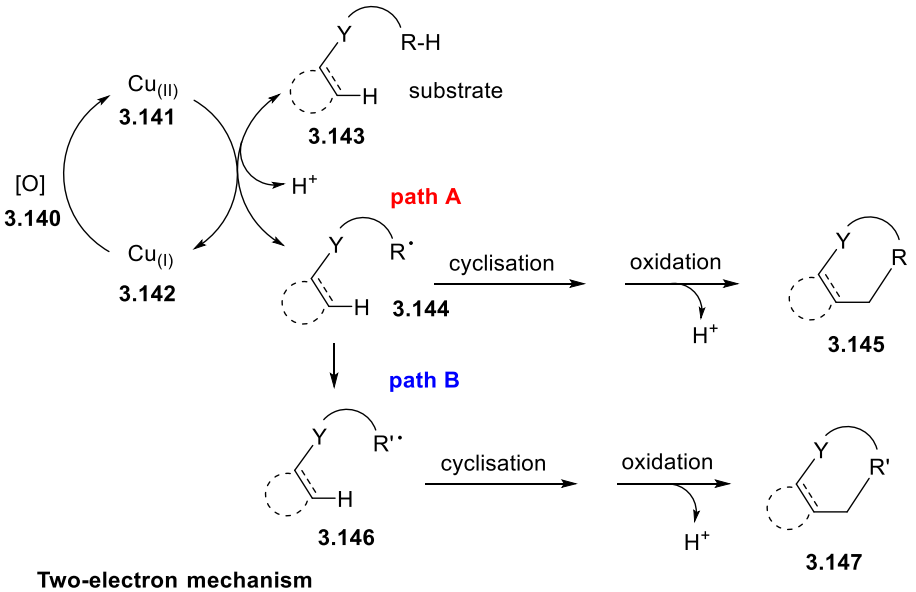

Two-electron mechanism

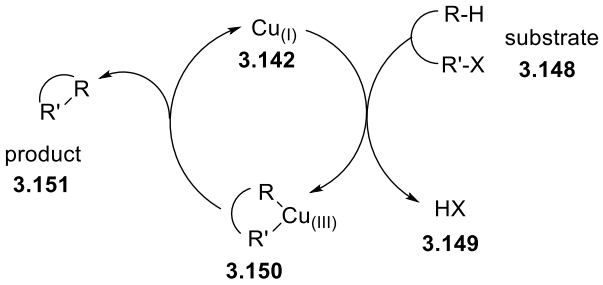

Combination of the one- and two-electron mechanism

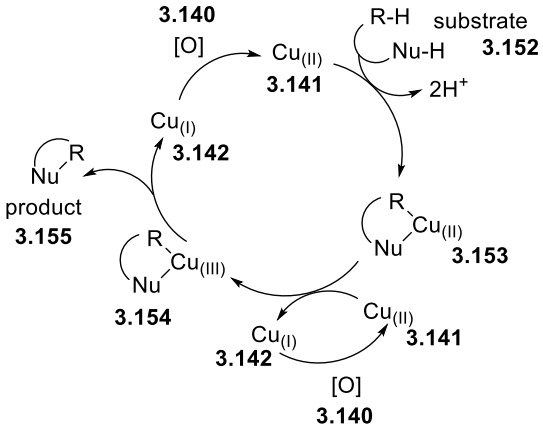

Scheme 52: Proposed mechanisms occurring for the Cu-catalysed C-H activation.

3.1.3.2.1 Cu-catalysed C-H activation for C-O bond formation

In 2013, Gooβen *et al*.[426] introduced a novel method for the formation of C-O new bonds *via* Cu-catalysis. They reacted benzoates **3.156** with boron alkoxides **3.167** in the presence of $Cu(OAc)_2$ **3.99** and silver carbonate **3.158** (Ag_2CO_3) to achieve good yields of aryl ethers products **3.159** proving Ag_2CO_3 to be fundamental for the decarboxylation step to obtain the desired compounds (Scheme 53, pathway a). In the same year, they also performed a successful C-O new bond formation of arenes **3.156** with alcohols **3.160** involving both sp^2 and sp^3 C-H bonds (Scheme 53, pathway b).[427]

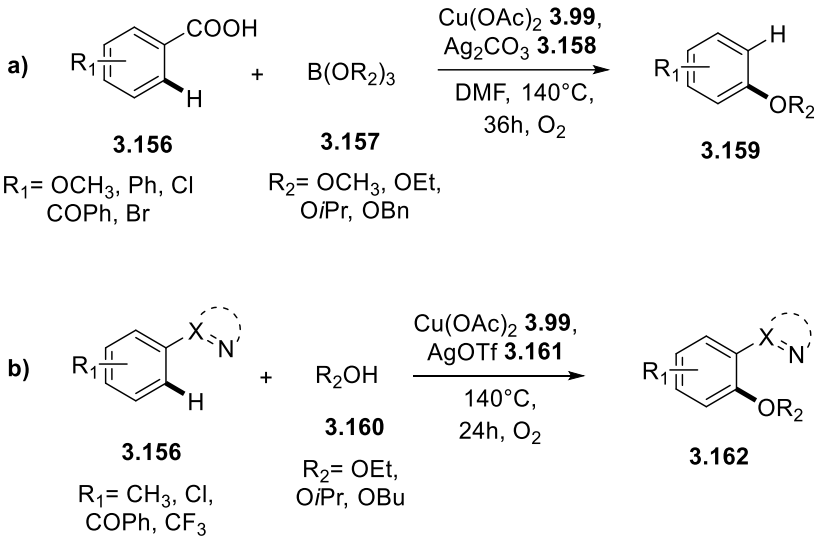

Scheme 53: Cu-catalysed C-H activation for the formation of new C-O bonds using either boron- **3.157** or alcohol- **3.160** based compounds as oxygen source.

Recently, carboxylic acids have also been employed as new C-O bond sources even though they are limited in use to stoichiometric amount of copper salts.[428,429] In 2017, Zhang *et al*.[430] reacted aryl amides **3.163** with carboxylic acids **3.164** in the presence of $Cu_{(I)}$ bromide **3.165** and Ag_2CO_3 **3.158** to achieve a broad range of acyloxy compounds **3.166**. This methodology was one of the most versatile given the vast types of acids that can be made use of such as benzoic acids, aliphatic acids or cinnamic acids (Scheme 54).

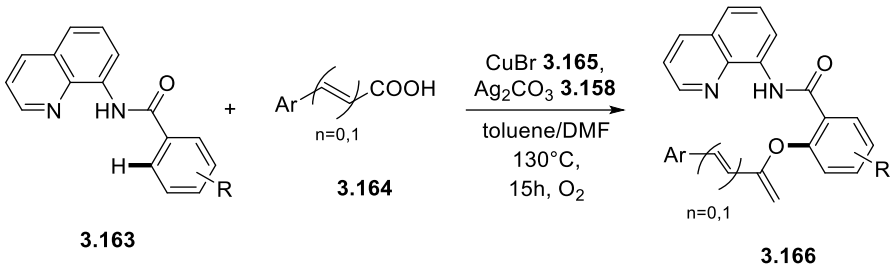

Scheme 54: Cu-catalysed C-H activation for the formation of new C-O bonds using carboxylic acids **3.164** as oxygen source.

3.1.3.2.2 Cu-catalysed C-H activation for C-S bond formation

Daugulis *et al*.[431] described a C-S new bond formation via Cu-catalysis by reacting amides **3.167** with disulfide reagents **3.168** in the presence of $Cu(OAc)_2$ **3.99** to give products **3.169** (Scheme 55).

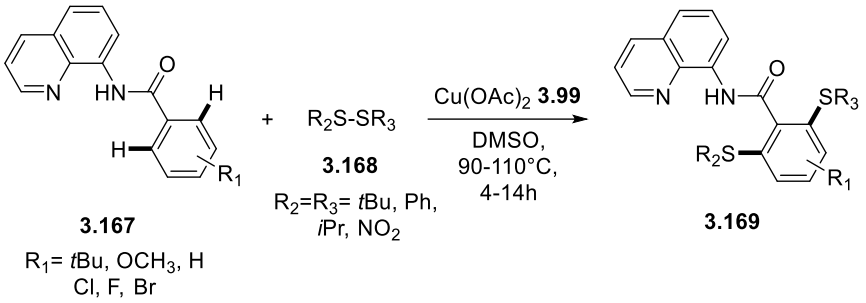

Scheme 55: Cu-catalysed C-H activation for the formation of new C-S bonds using disulfide reagents **3.168** as sulfur source.

Shi *et al*.[432] introduced sodium sulfinates **3.172** as sulfur source to achieve aryl sulfones **3.192** by reaction with benzamides **3.170**. They employed a removable DG, such as phosphatidylinositol **3.171** (PIP), a Cu catalytic source and Ag_2CO_3 **3.158** as the best oxidant among all the others tested (Scheme 56).

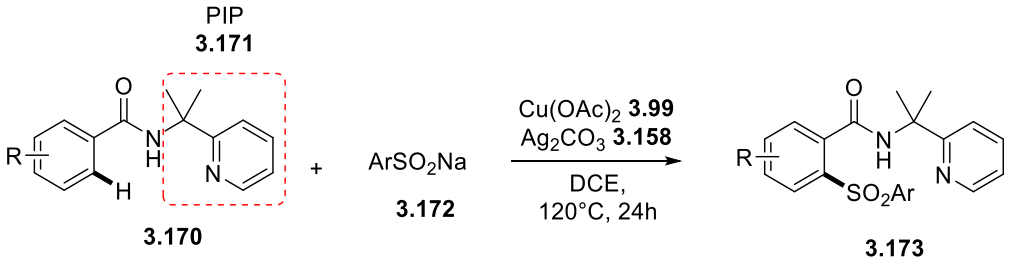

Scheme 56: Cu-catalysed C-H activation for the formation of new C-S bonds using sodium sulfinates **3.172** as sulfur source.

3.1.3.2.3 Cu-catalysed C-H activation for C-N bond formation

In 2010, Li *et al*.[433] proposed a Cu-catalysed C-N bond formation by reacting 2-arylpyridines **3.174** with secondary amides **3.175** in the presence of $Cu_{(I)}$ bromide **3.165** (CuBr) as catalytic source and *tert*-butyl peroxide **3.176** (tBuOOH or TBP) as the oxidant with no need of a base or ligands (Scheme 57).

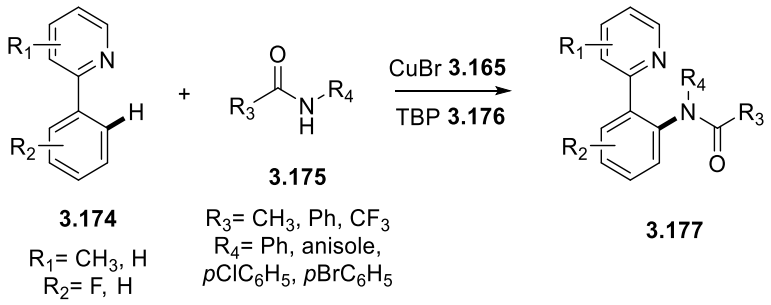

Scheme 57: Cu-catalysed C-H activation for the formation of new C-N bonds with no need for bases or ligands.

However, since primary amides produced very low yields, Nicholas *et al*.[434] presented an improved reaction scheme taking advantage of molecular oxygen as the oxidant, anisole as the solvent, DMSO as the additive and high temperatures. These factors allowed the successful coupling of primary sulfonamides, carboxamides and anilines **3.179** with 2-arylpyridines **3.178** to obtain amidation products **3.180**. DMSO was found to be crucial for the catalytic turnover as well as the addition of anisole for the positive outcome of the reaction (Scheme 58).

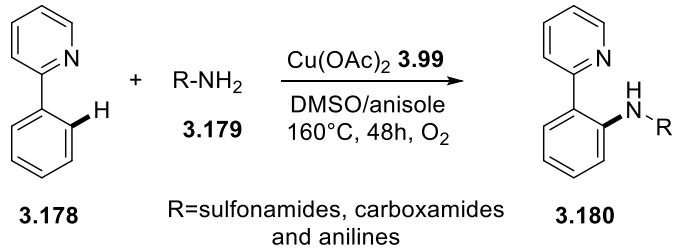

Scheme 58: Cu-catalysed C-H activation for the formation of new C-N bonds using DMSO as crucial additive.

Regardless of the good yields obtained for 2-arylpyridines amidation, the pyridine moiety still remained a powerful, non removable, directing group. To overcome this issue, Daugulis *et al*.[435] delineated a different directing group using a combination of 8-aminoquinoline and picolinic acid scaffolds, due to the easy removal process of aminoquinolines by basic hydrolysis. Unfortunately, expensive Ag_2CO_3 as cocatalyst, *N*-Methylmorpholine-*N*-Oxide **3.182** (NMO) as an oxidant and

the inclusion of primary and secondary aliphatic amines only, heavily limited the use of 8-aminoquinoline as DG (Scheme 59).

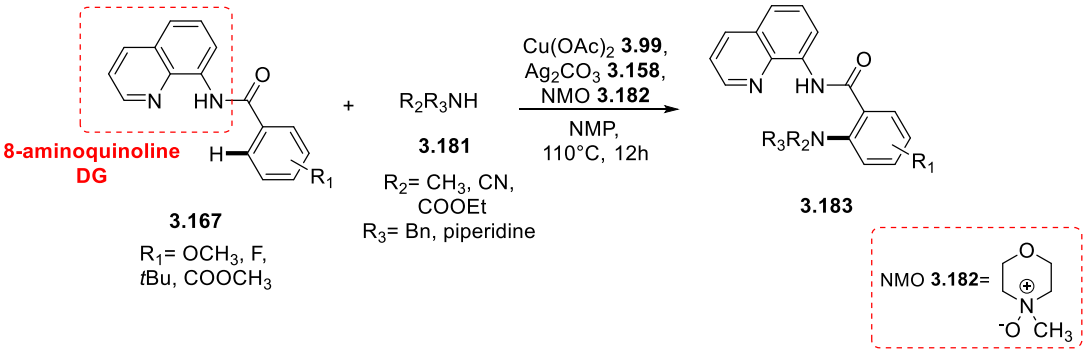

Scheme 59: Cu-catalysed C-H activation for the formation of new C-N bonds using **3.167** to replace pyridine as more versatile DG.

Recently, Wu and Cui attempted to perform a Cu-catalysed C-N bond formation by reacting quinoline *N*-oxides **3.184** with secondary amines **3.185** with copper$_{(I)}$ iodide **3.186** as the catalyst and air as the oxidant. Alas, the reaction failed for the amidation of quinoline *N*-oxide with primary amines, aromatic amines or amides. (Scheme 60).[436]

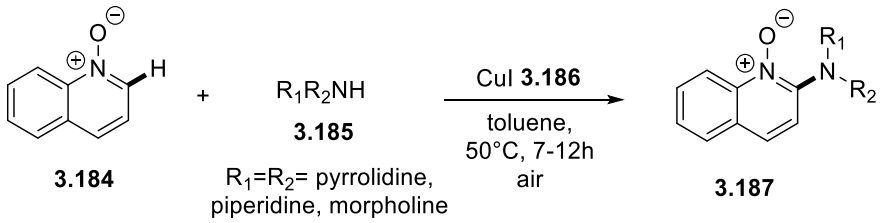

Scheme 60: Cu-catalysed C-H activation for the formation of new C-N bonds starting from quinoline *N*-oxides **3.184**.

In 2014, Zhu *et al*.[437] reported the synthesis in good yields of *N*-arylamides **3.191** using azides **3.189** as amino sources in the presence of copper$_{(I)}$ thiophene-2-carboxylate **3.190** (CuTc) as the catalyst and *N*-heterocycles **3.188** as directing groups (Scheme 61).

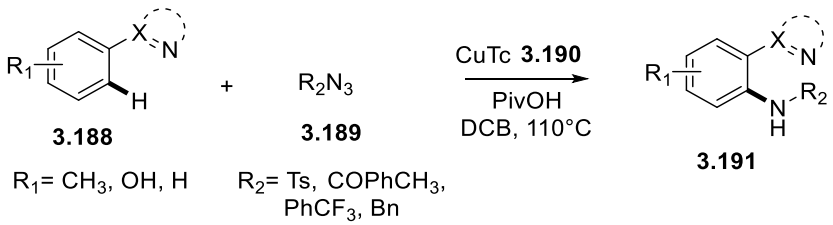

Scheme 61: Formation of new C-N bonds using azides **3.189** as amino source.

Ammonia has also been proposed as an amino source but suffers from a great disadvantage: it readily binds to metals to form stable complexes that impede the C-H activation. Chang *et al.*[438] tried to use aqueous ammonia **3.193** instead of ammonia in the presence of a low $Cu_{(I)}$ catalytic concentration to avoid its poisoning and by using 2-(4,5-dihydrooxazool-2-yl)aniline **3.196** as DG. In this way, they obtained several primary anilines **3.195** in good yields (Scheme 62).

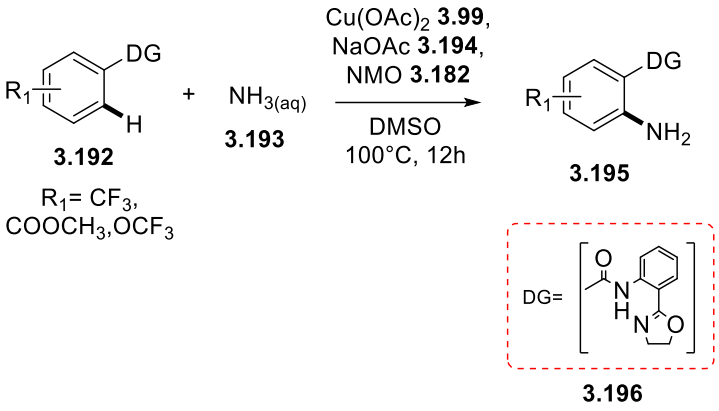

Scheme 62: Cu-catalysed C-H activation for the formation of new C-N bonds using aqueous ammonia **3.193** as amino source.

3.1.3.2.4 Cu-catalysed C-H activation for C-C bond formation

The most common C-H activation reactions catalysed by copper species concern, mainly, sp^2 and sp^3 C-H activation. Gaunt *et al.*[439] proposed, in 2008, a Cu-catalysed C-H activation of indoles **3.197** with diaryl-iodine$_{(III)}$ **3.198** in the presence of copper triflate **3.199**, $Cu(OTf)_2$, as the catalyst and 2,6-di-tert-butylpyridine **3.200** (dtbpy) as the base. They noticed how important was the directing power of the *N*-substituent of the indole: more specifically the free *NH*- and *N*-alkylindoles provided C3 selectivity while *N*-acetylindoles provided C2 selectivity (Scheme 63).

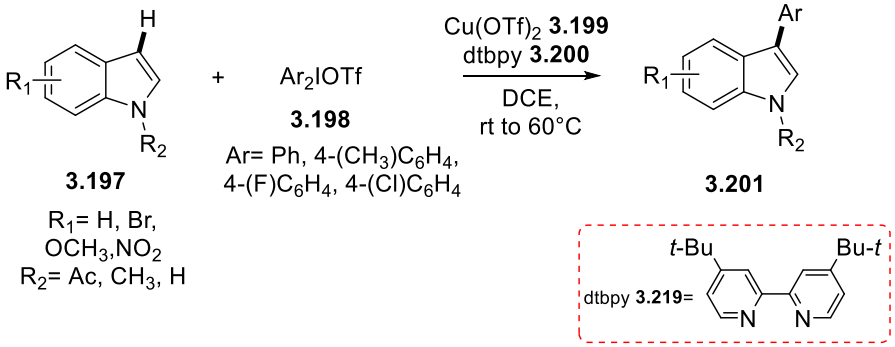

Scheme 63: Cu-catalysed C-H activation for the formation of new C-C bonds using *N*-substituted indoles **3.197** as DG.

Wang *et al.*,[440] taking advantage of previous studies conducted by Yang *et al.*,[441,442] began investigating the origins of C2, C3, C5 and C6 indole selectivity by specific types of directing group, using theoretical calculations and mass spectroscopy. They noticed that all of the tested directing groups induced a Heck-like four-membered ring mechanism (Scheme 64). However, indoles **3.204** bearing a strong DG, such as di-*tert*-butylphosphine-oxide P(O)*t*Bu$_2$, or a pivaloyl group in position C3 were shown to provide C5 and C6 indole arylation (**3.206** and **3.207** respectively) whereas a weak DG provides C2 or C3 indole arylation (**3.205**).

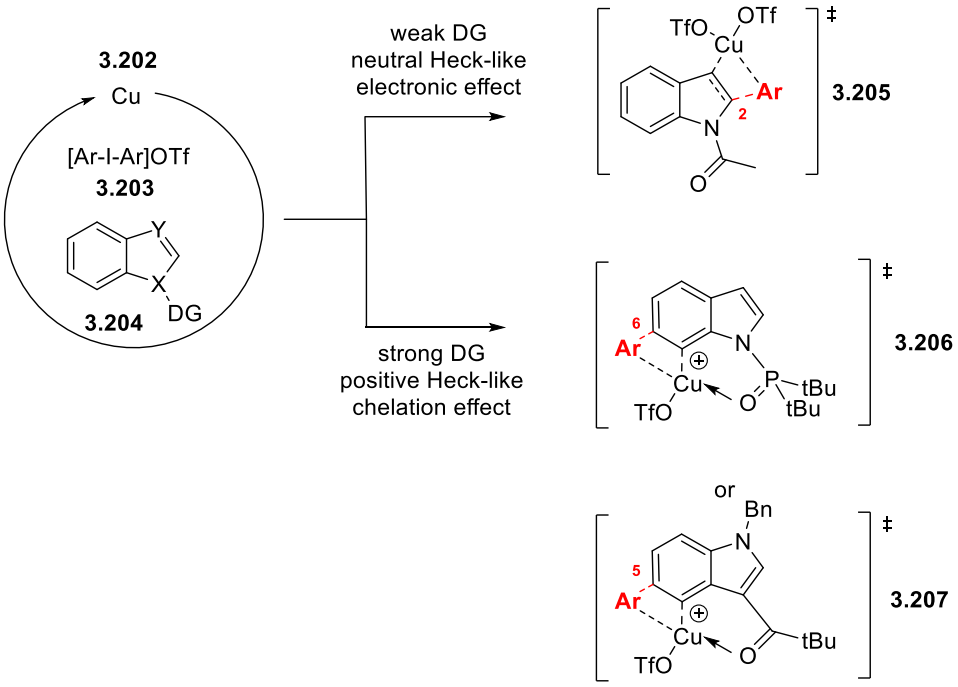

Scheme 64: Proposed mechanism for the Cu-catalysed C-H activation of indoles bearing EDGs or EWGs to explain a specific regioselectivity.

In 2014, Wang *et al.*[443] performed a C-H cyanation of tetrahydroisoquinolines **3.208** in the presence of trimethylsilyl azides **3.209** (TMSN$_3$), dichloroethane (DCE), 2,3-dichloro-5,6-dicyano-1,4-benzoquinone **3.210** (DDQ) as the oxidant and copper iodide **3.186** (CuI) as the catalytic source (Scheme 65).

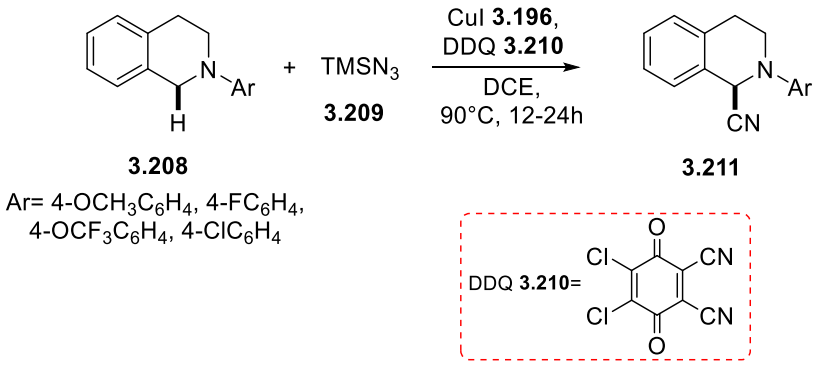

Scheme 65: Cu-catalysed C-H activation for the formation of new C-C bonds using cyanide as oxidant source.

Menche *et al*.[444] described a similar reaction to activate a C-H bond near a nitrogen atom using tetrahydroisoquinolines **3.208** and organo zinc reagents **3.212** (Scheme 66). The presence of copper species **3.213** in this reaction confirmed the process to follow a SET mechanism through investigation conducted *via* electron paramagnetic resonance spectroscopy (EPR).

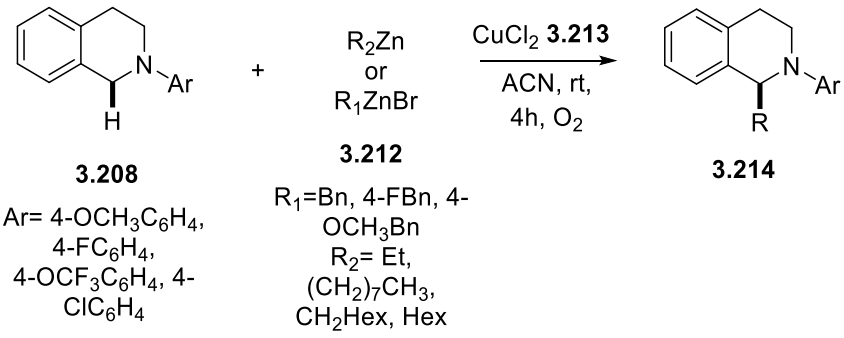

Scheme 66: Cu-catalysed C-H activation for the formation of new C-C bonds using organo zinc reagents **3.214**.

A Cu-catalysed sp^3 C-H activation of benzylic systems has also been described by Li *et al*.[445] They hypothesised a three-component intermolecular mechanism for the esterification of styrenes **3.215**, toluenes **3.216** and peroxyesters **3.217** to achieve new C-O bond formation (Scheme 67).

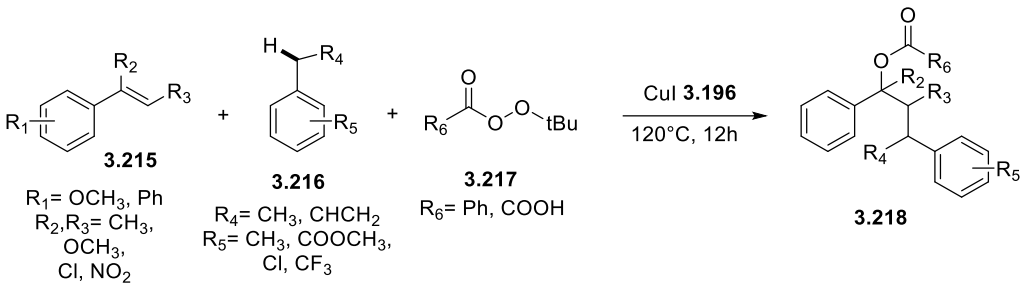

Scheme 67: Cu-catalysed C-H activation for the formation of new C-C bonds using a three-component intermolecular mechanism.

3.1.4 C-H activation of 1,2,3-triazoles

1,2,3-triazoles are known to be versatile scaffolds and unique chemical entities that found wide application in both medicinal chemistry and material science fields.[113-120] Unfortunately, given the particular conditions that 1,2,3-triazoles require for their synthesis, the C-H activation strategy was highlighted as an alternative approach to expensive catalysts or toxic starting materials. In fact, there are only a few examples of efficient C-H activation for 1,2,3-triazoles as they all have a demand for transition metals to occur.[446,447] Palladium, ruthenium and copper are among the most common transition metals used for direct arylation of the C5 position of the triazole ring. Ackermann *et al*.[448] attempted to use copper sources to perform the synthesis of fully substituted 1,2,3-triazoles **3.225** in a regioselective one-pot four-component reaction.[449] With this protocol in hands, they obtained both EWG and EDG-substituted 1,2,3-triazoles **3.225** by reacting either alkyl- or aryl-based alkynes **3.219** with sodium azide **3.221** and iodo-aryl based compounds **3.223** in high yields; additionally, bulky substituents were also tolerated. Notably, when using copper catalysts in combination with DMEDA **3.224** as stabilising ligand, 1,2,3-triazoles were produced using a one pot strategy to build simoultaneously one new C-C and three C-N bonds with high efficiency (Scheme 68).[448]

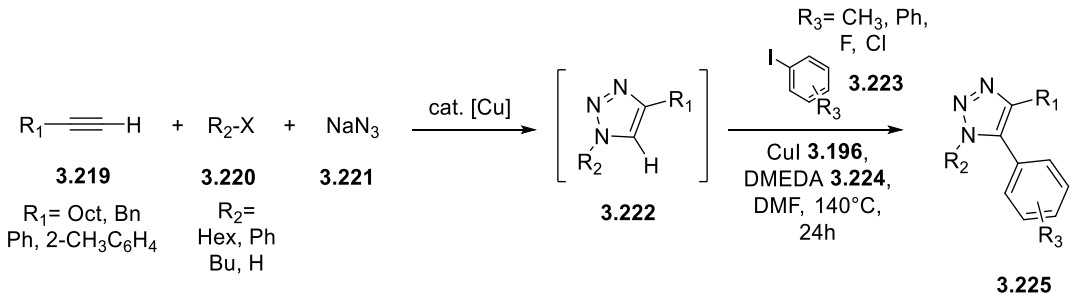

Scheme 68: One-pot four-component reaction protocol proposed for the synthesis of fully substituted 1,2,3-triazoles **3.225**.

Later on, Wei *et al*.[450] proposed a new Cu/Pd transmetalation to perform a C-H activation reaction with mild reaction conditions achieving trisubstituted 1,2,3-triazoles in good yields. The mechanism they proposed suggested a simultaneous formation of the cuprate-triazole intermediate **3.228**, by cycloaddition of copper$_{(I)}$ acetylide **3.227** and azide **3.221**, and the palladium intermediate **3.332**, by oxidative addition of the aryl halide **3.323** and Pd$_{(0)}$ **3.330**.[450,451] Subsequent transmetalation and reductive elimination would end the catalytic cycle with formation of the trisubstituted 1,2,3-triazole **3.324** and regeneration of Pd$_{(0)}$ (Scheme 69).

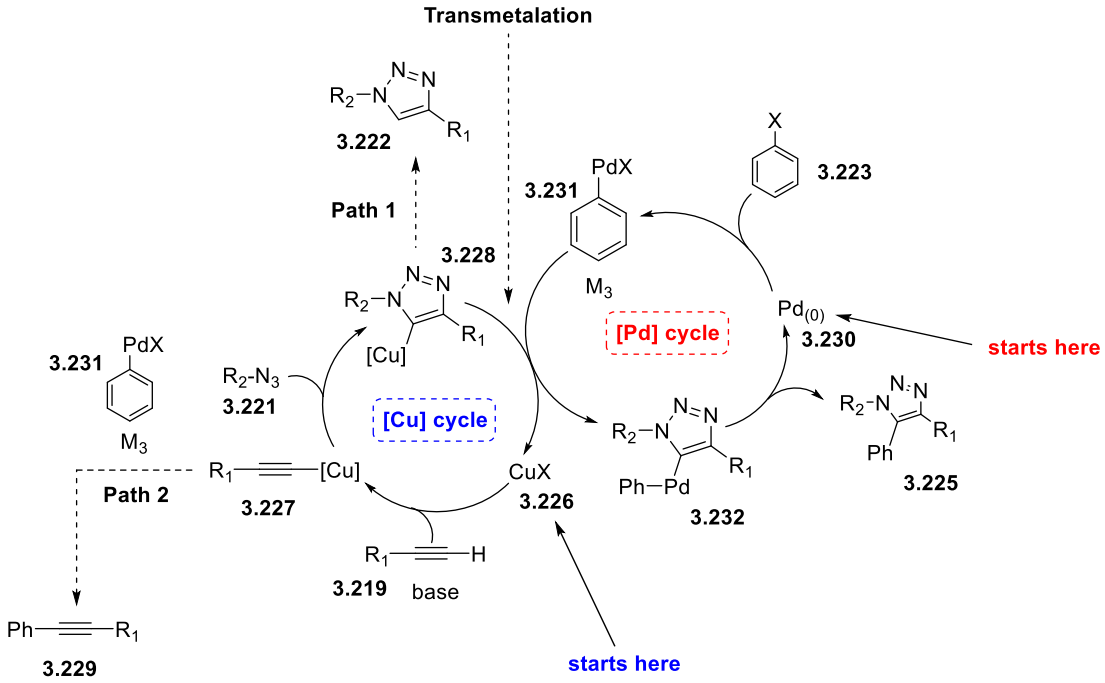

Scheme 69: Proposed mechanism for a Cu/Pd transmetalation to perform a C-H activation reaction yielding trisubstituted triazoles **3.225**.

Nevertheless, Wei envisaged two important issues arising from two potential side reactions: i) protonation of the cuprate intermediate **3.328** to give 1,4-disubstituted 1,2,3-triazole **3.322** and ii) transmetalation between copper$_{(I)}$ acetylide **3.327** and palladium intermediate **3.231** to give byproduct **3.229**, thus resembling a Sonogashira coupling reaction. According to Lei's group,[452] the Sonogashira product **3.229** has first-order kinetic dependance on both [Cu] and [Pd] whereas, according to Fokin's group,[453,454] the CuAAc reaction has second order kinetic dependance on [Cu] suggesting that high [Cu] species concentration would favor the cycloaddition product. Consequently, Wei disclosed a new reaction protocol using 2-dicyclohexylphosphino-2′,4′,6′-triisopropylbiphenyl **3.356** (XPhos) as ligand which was able to accelerate the [Pd] cycle over the [Cu] cycle, K_2CO_3 **3.138** as the base and DMF as the solvent to achieve in 93% yields the desired product (Scheme 70).

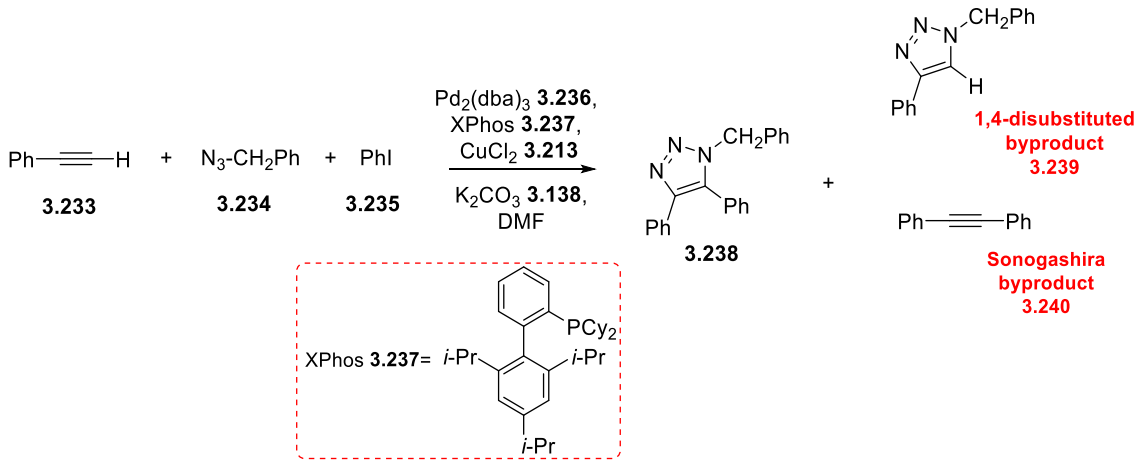

Scheme 70: Potential side reactions occurring when substituting 1,2,3-triazoles **3.238** *via* Cu/Pd C-H activation.

Chuprakov *et al*.[455] described an efficient C5 arylation of 1,4-disubstituted 1,2,3-triazoles **3.241** in good to excellent yields by using palladium catalysis, tetrabutylammonium acetate **3.243** (Bu_4NOAc) and *N*-methylpyrrolidone (NMP) as the solvent. Notably, this methodology allowed for the successful introduction of both electron-deficient and electron-rich aryl groups and bulky substitutents **3.242**. Furthermore, they proved this reaction scheme to be fruitful for the C5 regioselective arylation of 4,5-unsubstituted 1,2,3-triazoles **3.241** (R_1=H) too with the possibility to easily introduce aromatic EW substituents at the C5 position (Scheme 71).

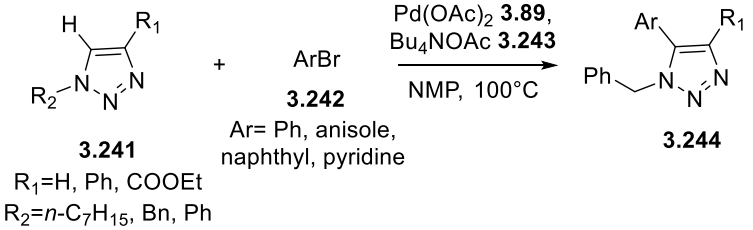

Scheme 71: C5 arylation of 1,4-disubstituted 1,2,3-triazoles **3.241** *via* palladium C-H activation.

In 2015, Zhu *et al*.[456] reported a Cu-catalysed direct amination of 2-aryl-1,2,3-triazoles *N*-oxides **3.245** with primary **3.246a** and secondary amines **3.246b** (Scheme 72).

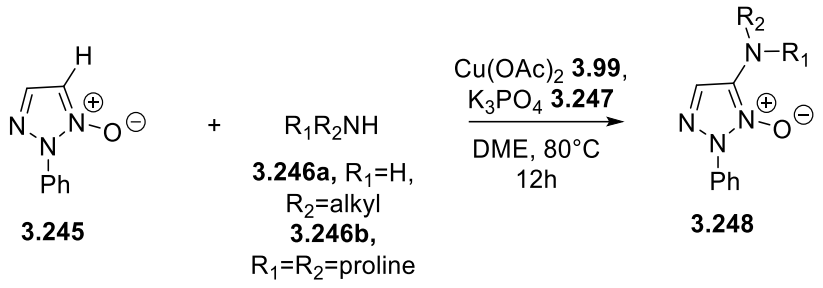

Scheme 72: Direct amination of 2-aryl-1,2,3-triazoles N-oxides **3.245** with primary and secondary amines **3.246**.

They demonstrated the crucial role of $Cu(OAc)_2$ as catalytic source in establishing a potential copper-catalysed cross-deprotonative mechanism going through the following steps: i) substitution of the C5 hydrogen atom of triazole **3.245** with copper, ii) reaction of the organocuprate intermediate **3.251** with amine **3.246**, iii) reductive elimination to yield the product **3.248** and a copper species **3.255** with lower oxidation state ready to be reoxidised to restore $copper_{(II)}$ **3.256** (Scheme 73). They also observed the importance of choosing a specific solvent: 1,2-dimethoxyethane (DME) achieved the best results while DMF showed to suppress the reaction. K_3PO_4 was, also, identified as the most suitable base over other inorganic bases.

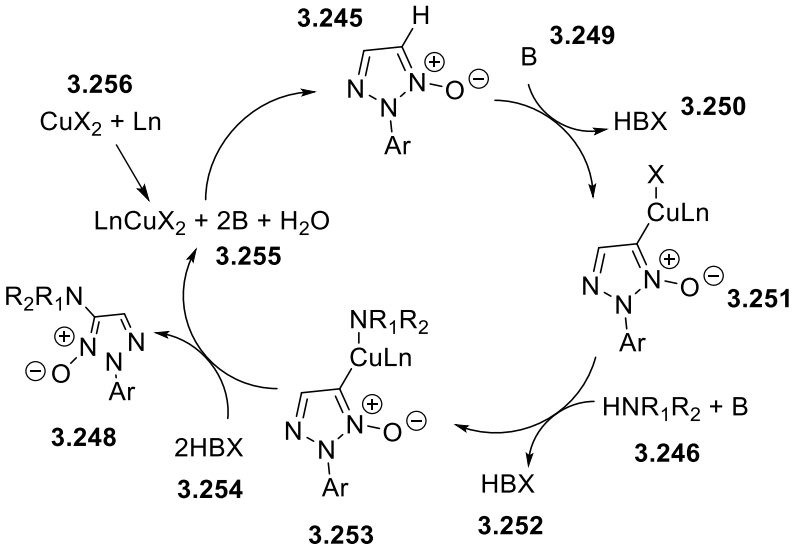

Scheme 73: Proposed mechanism for the direct amination of 2-aryl-1,2,3-triazoles N-oxides **3.245** with primary and secondary amines **3.246**.

With these optimised conditions, Zhu obtained various 4-substituted 2-aryl-1,2,3-triazoles **3.248** in up to 82% yields with triazoles bearing EWG, such as fluoro- or chloro- groups, giving the best results.1,2,3-triazoles have been widely exploited not only for their versatility in C-H activation

reactions to form new molecules, thus avoiding long reaction times and multiple steps, but have also become templates of interest as potential directing groups in new sp^2 and sp^3 C-H bond formations. Ye *et al*.[457] were among the first to propose 1,2,3-triazoles as directing group for C-H activation reactions. They started to investigate the potential of 1,2,3-triazole-4-carboxylic acid derivatives **3.258** (TAA) to be used as auxiliary reagents in Pd-catalysed C-H activations. They tested TAA activity for sp^2 and sp^3 C-H activations and noticed the reactions to effectively promote the formation of the desired cyclisation products in good to excellent yields in a similar fashion to picolinic acid (PA) or quinaldic acid (QA) directing groups performances (Scheme 74).

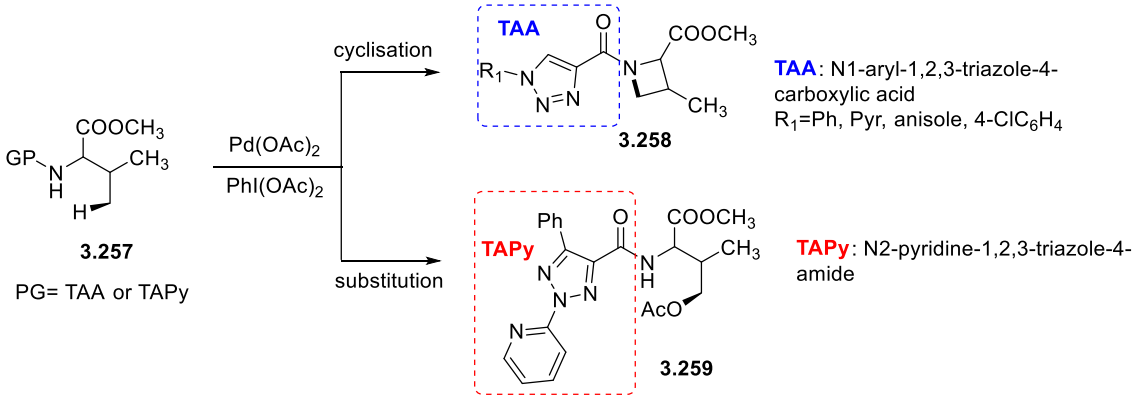

Scheme 74: 1,2,3-triazoles TAA **3.258** and TA-Py **3.259** applied as directing groups in the C-H activation of both sp^2 and sp^3 C-H bonds.

However, when they attempted to obtain only the substitution product, hence achieving the C-H activation goal via TAA, a tridentate directed group was needed. TAA, as well as PA and QA, was proved to favor the cyclisation reaction rather then the substitution pattern because of the more stable in-plane reductive elimination of palladium (Figure 60 pathway a, **3.260**). The introduction of a tridentate ligand, such as triazole-pyridine amide **3.259** (TA-Py) or pyridine-triazole acid **3.262** (Py-TA), produced an axial Pd-C bond orientation with an out-of-plane reductive elimination reaction favored (Figure 60, pathway b, **3.261**).[458–460] Nevertheless, only the combination of TA-Py **3.259** as directing group and silver acetate (AgOAc) as the oxidant directed towards the sole substitution product with no cyclisation occurring at all. So far, this is the only example known of Pd-catalysed C-H activation with 1,2,3-triazoles employed as directing group.

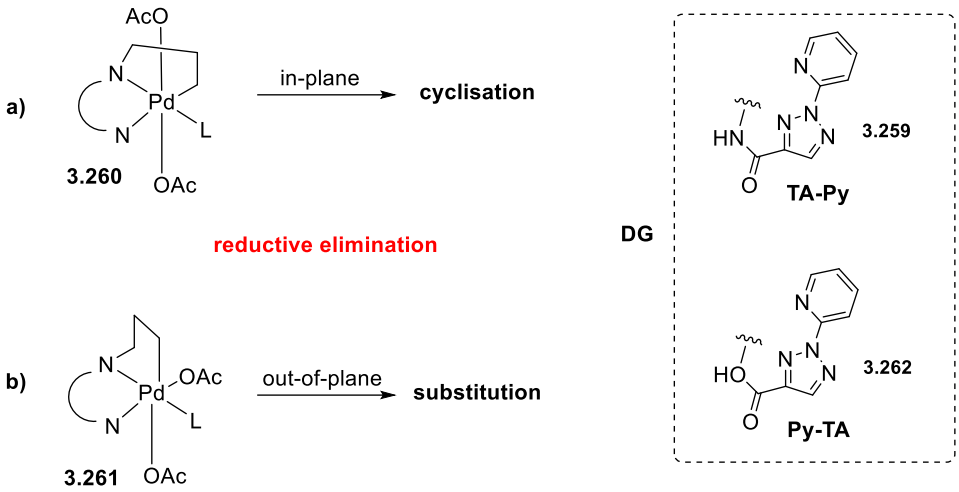

Figure 60: In-plane and out-of-plane proposed mechanisms involving $Pd_{(IV)}$ intermediates using TA-Py, **3.259**, and Py-TA, **3.262**, as DGs.

3.2 1,2,3-triazoles as organocatalysts

3.2.1 Organocatalysis: introduction and crucial role of proline- and pyridine-based organocatalysts in enantioselective reactions.

Organocatalysis is a form of catalysis reaction in which the catalyst is an organic molecule that does not contain a metal ion thus contributing to greener chemistry for more sustainable reaction conditions. Furthermore, when the organocatalyst involved is a chiral molecule, an asymmetric catalysis, also known as enantioselective reaction, occurs.[461] The enantioselective process allows for the formation of a specific enantiomer or diasteroisomer according to the properties of the catalyst employed.[462] Organocatalytic reactions can proceed *via* covalent bond interactions between the organocatalyst and the reactants or *via* a weaker bond interaction such as hydrogen bonding or ion pairing. The hydrogen-bonding interactions gained enormous attention in the last decade for their potential to furnish a greener pathway for alternatively metal-catalysed Diels-Alder reactions.[463-466] Generally, organocatalysts involved in organocatalytic reactions are represented by heteroatom-centerd Lewis bases (mainly N(O)-, P(O)- and S(O)- centered). However, Brønsted acids have been employed more and more often in asymmetric catalysis even in conjunction with other Lewis bases for synergic systems.[467] Organic molecules can catalyse a reaction with four different mechanisms: i) activation of the reaction based on the electrophilic/nucleophilic behavior of the catalyst, ii) formation of the reactive intermediates which consume the catalyst and require its regeneration, iii) phase-transfer catalysis in which the catalyst

forms a transient complex with the substrate and shuttles between the organic solvent of the reaction and a second phase, iv) molecular-cavity-accelerated asymmetric transformations in which the catalyst can select between competing reactants according to their size and structure.[468]

3.2.2 1,2,3-triazole-based organocatalysts: introduction

1,2,3-triazoles are extremely versatile ligands for metal coordination as they furnish the possibility to incorporate transition metals either at the *N*1 or the C4/C5 positions enabling the preparation of polydentate chelating systems.[469] Recently, metal-labelled 1,2,3-triazoles, such as technetium-labelled radiopharmaceuticals, have found wide applications in the field of diagnostics and therapeutics.[470] If conjugated with particles emitting radionuclides, such as α- and β-emitters, metal-labelled 1,2,3-triazoles have been proved to destroy some tumor species that cannot be reached by other therapies.[470,471] Generally, 1,2,3-triazoles can interact with transition metals through three different ways: i) via the *N*3 atom to form either a monodentate ligand **3.263** or a bi-/poly-dentate chelator **3.264** (Figure 61).[472,473] However, if more donor sites are present in proximity of the *N*3 atom, bi- or poly-dentate complexes can occur also at the *N*2 position **3.265** (Figure 61).[474] In both cases, transition metals complexed with the *N*2 or *N*3 nitrogen atom of 1,2,3-triazoles usually create bridging complexes with five or six terms (Figure 62, **3.266** and **3.267**).

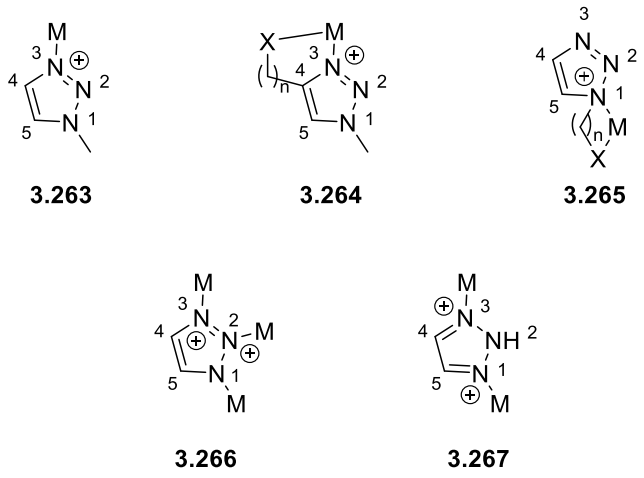

Figure 61: *N*2/*N*3 1,2,3-triazole-metal coordination binding modes.

ii) *via* C5 coordination of deprotonated triazolium salts to form *N*-heterocyclic carbenes (NHCs). NHCs are versatile ligands for transition metal catalysis given their strong electron-donating behavior as well as their improved stability to oxidation and easier possibility to undergo functionalisation.[475] Before the introduction of 1,2,3-triazolium salts in the synthesis of NHCs, the most common template used to create NHCs was represented by imidazolium salts. Imidazolium

salts are usually bounded at the C2 position to form the so-called normal NHCs (nNHCs), displaying a resonance structure with all neutral formal charges (Scheme 76, **3.284**). However, Crabtree *et al*.[476] also reported the existance of C4 bounded NHCs to form the so-called abnormal NHCs (aNHCs), possessing a mesoionic configuration instead (Scheme 75, **3.272**).[477] In 2008, Albrecht was the first to propose to use 1,3,4-substituted 1,2,3-triazolium salts, obtained by reacting alkynes **3.273** and azoles **3.274** *via* click reaction followed by nitrogen alkylation of the *N*3 position and complexation with metals like palladium **3.89** and silver **3.133**, as precursors for the synthesis of aNHCs **3.278** and **3.279** (Scheme 75).[478]

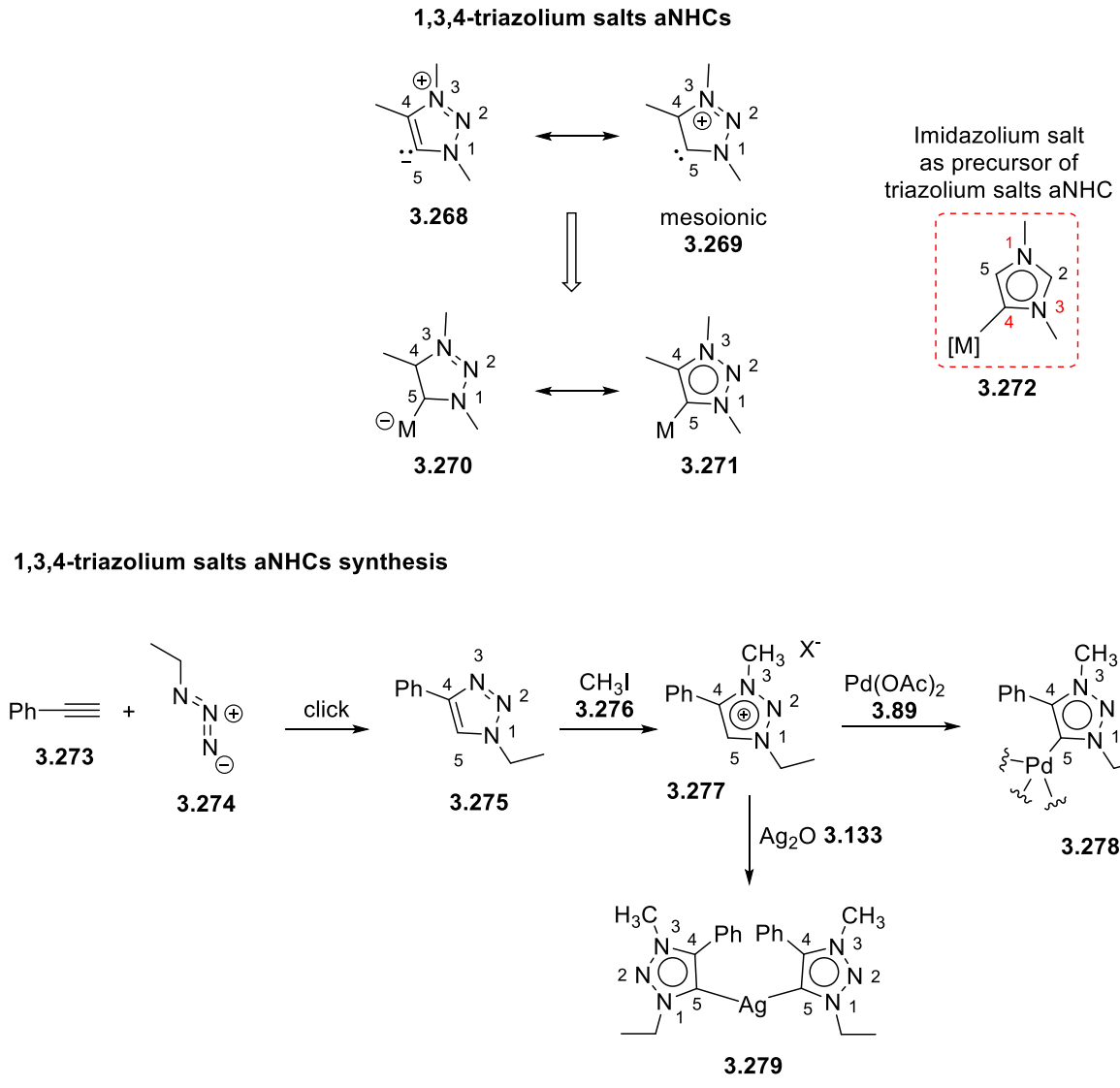

Scheme 75: Synthesis of 1,3,4-triazolium salts **3.277** as precursor for the formation of abnormal NHCs **3.278** and **3.279**.

On the other hand, Schaper proposed the synthesis of normal 1,2,3-triazolylidene carbenes with a 1,2,4-substitution fashion by reacting hydrazonoyl chlorides **3.285** with isocyanides **3.286** to form the precursor 1,2,4-triazolium salt **3.288** and by using ammonia adducts[479] **3.290** or transmetalation with silver oxide[480] **3.133** to form the final nNHC **3.291** and **3.292** (Scheme 76). He noticed that 1,2,4-substituted triazole-based nNHCs possessed an even higher donor strenght than the corresponding abnormal 1,3,4-substituted triazole-based NHCs.

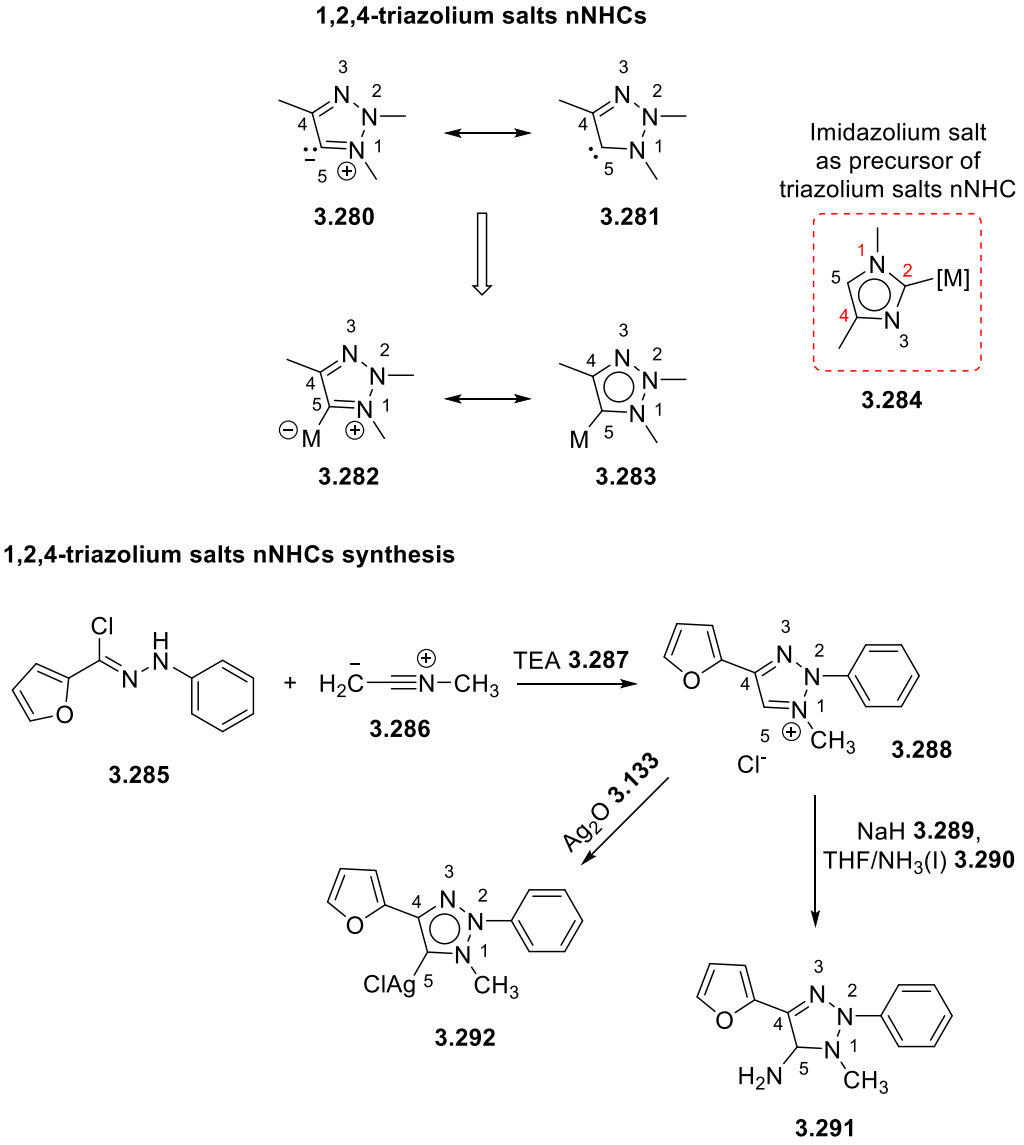

Scheme 76: Synthesis of 1,2,4-triazolium salts **3.288** as precursor for the formation of normal NHCs **3.291** and **3.292**.

iii) *via NH* deprotonation of 4,5-disubstituted triazoles (i.e. benzotriazoles or 4,5-disubstituted-*NH*-1,2,3-triazoles) to form anionic ligands in metal complexes. Generally, benzotriazoles bind metal

centers through the *N*1 position (Figure 62, **3.293**) whereas 4,5-disubstituted-*NH*-1,2,3-triazoles bind metal centers through the *N*2 position (Figure 62, **3.294**) despite the ability of the transition metal to also coordinate to the free neutral nitrogen to create diverse bridged complexes (Figure 62, **3.295**-**3.297**).[481]

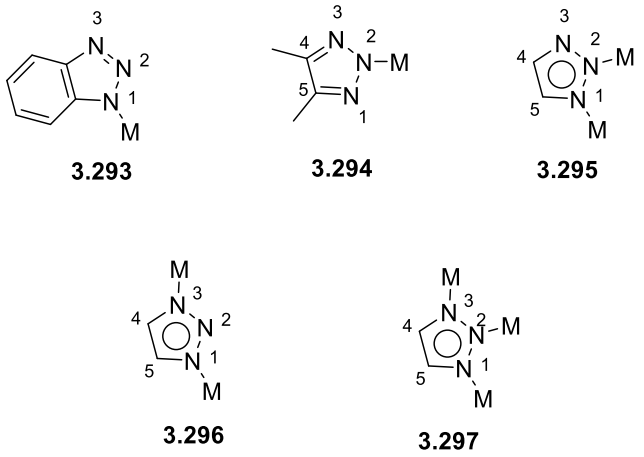

Figure 62: *N*2/*N*3 4,5- disubstituted 1,2,3-triazole-metal anionic coordination binding mode.

3.2.2.1 1,2,3-triazole-based organocatalysts: manganese, iron, copper, ruthenium and palladium metal complexes

Metal-based 1,2,3-triazoles complexes represent one of the most promising area of organic chemistry due to the high versatility of 1,2,3-triazoles in a plethora of organic reactions. The C5 proton acidity of 1,4-disubstituted 1,2,3-triazoles provides the opportunity to create new metal-coordinate complexes via C-H activation. In this way, mono-, bi- and poly-dentate 1,2,3-triazoles-based ligands can be obtained in a single step reaction and are ready to be linked to most transition metals (such as manganese, iron, copper, ruthenium and palladium) and, eventually, employed as organocatalysts.

i) Manganese (Mn) atoms usually form with 1,2,3-triazoles *N*4-tetradentate-like ligands **3.299** *via* nitrogen coordination. They have been covering an important role in the past years due to their versatile application in epoxidation reactions of terminal aliphatic olefines **3.298** with low catalyst loading and short reaction times (Scheme 77).[482]

ii) Iron (Fe) atoms are considered potent catalysts due to their dual reactivity as Lewis acids or as redox centers.[483,484] There are very a few examples of 1,2,3-triazoles complexed with iron atoms ligands, *via* nitrogen coordination, but a remarkable one (Scheme 77, **3.303a**) is furnished by Yan *et al*.[485] They described a successful 1,2,3-triazole-iron catalysed dehydration reaction of enyne

3.301 in propargyl alcohol **3.304** (Scheme 77). The presence of the triazole ligand was crucial for the success of the reaction; the addition of a triazole unit **3.303** to the iron catalyst, in a 2:1 ligand/Fe loading ratio, formed a more efficient bidentate ligand **3.303a** that greatly improved the yield of reaction.[485]

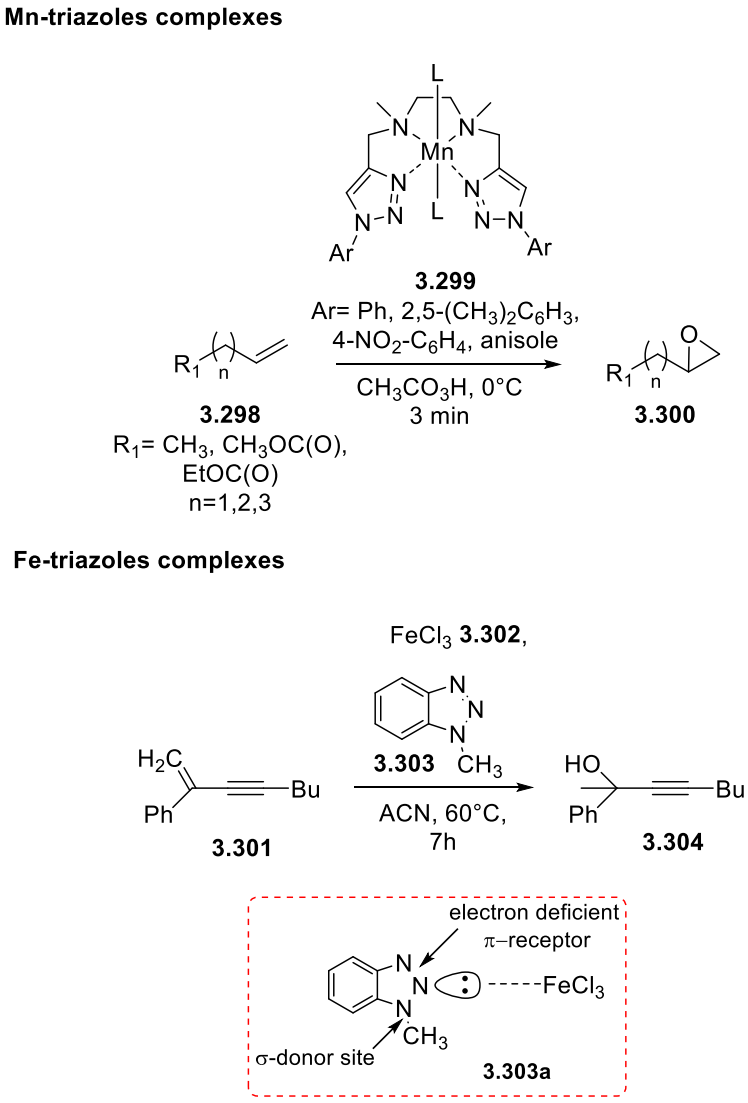

Scheme 77: Mn- and Fe- 1,2,3-triazole complexes **3.299** and **3.303a** catalysing epoxidation and dehydration reactions respectively.

iii) Cu-complexes of 1,2,3-triazoles are mainly formed *via* nitrogen coordination and have been used for the catalysis of CuAAc reactions. Chan *et al*.[486] reported the use of tris((1-benzyl-4-triazolyl)methyl)amine (**3.307**, TBTA) to stabilise, encapsulate and protect the $Cu_{(I)}$ center from disproportionation and oxidation while allowing the pendant triazole group to temporarily dissociate from the metal center and promote the formation of the $Cu_{(I)}$ acetylide intermediate

(Scheme 78).[486] Intriguely, William *et al*.[487] also reported the existance of TBTA complexes with $Cu_{(I)}$ in the presence of an opportune reducing agent such as sodium ascorbate.

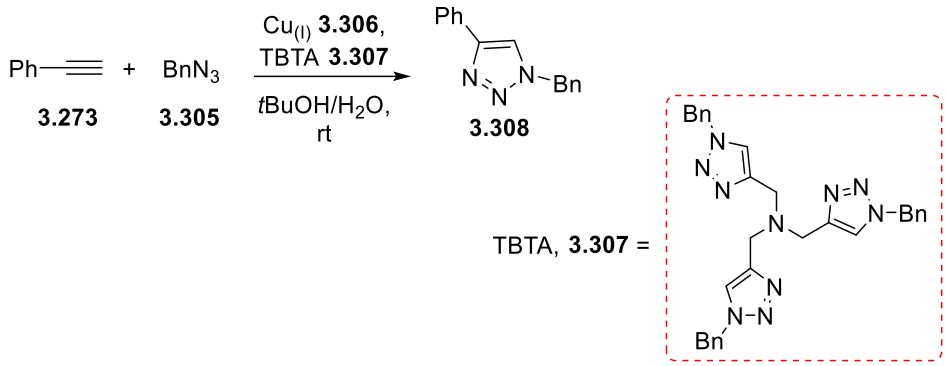

Scheme 78: Copper-1,2,3-triazole complex TBTA **3.307** as useful catalyst for CuAAc cycloaddition reactions.

Additionally, covalently immobilised catalysts for CuAAc reactions have been recently developed.[487] Tris(triazolyl) methanol ligands **3.312** supported on a Merrifield resin **3.311**, have been successfully employed in click reactions of various azides and alkynes in both aqueous and methanol-water systems to yield the corresponding triazoles with high yields (Scheme 79).[488]

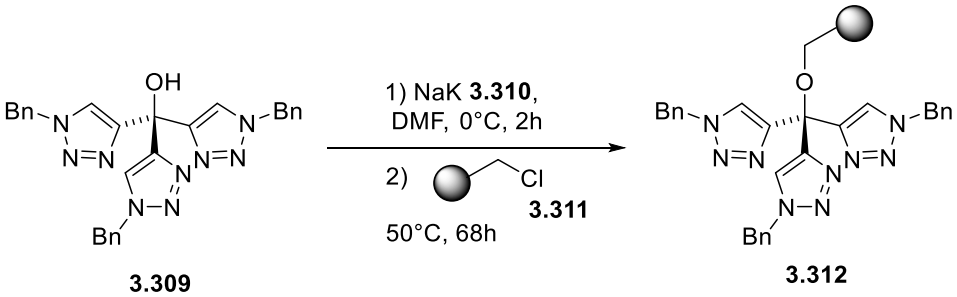

Scheme 79: Synthesis of the covalently immobilised tris(triazolyl) methanol ligand **3.312.**

Cu-carbene complexes with 1,2,3-triazoles have also been reported even though hardly used in CuAAc reactions because of the potential formation of byproducts arising from the reaction of the product-Cu-carbene bond with the catalyst-Cu-carbene bond. The only documented example of Cu-carbene complex with 1,2,3-triazole has been described by Nakamura *et al*.[489] They coupled copper with 1,4-diphenyl (**3.313**), 2,4,6-trimethylphenyl (Mes, **3.314**), 3,5-dimethylphenyl (Xyl, **3.315**) and 2,6-diisopropylphenyl (Dipp, **3.315**)-1,2,3-triazol-5-ylidene (aNHCs) to yield a new CuCl(aNHC) catalyst that gave excellent results when employed in CuAAc reactions between diverse alkynes and azides (Figure 63).

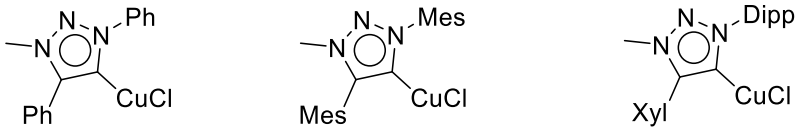

3.313 **3.314** **3.315**

Mes: 2,4,6-trimethylphenyl
Xyl: 3,5-dimethylphenyl
Dipp: 2,6-diisopropylphenyl

Figure 63: Nakamura's 1,4-diphenyl, 1,4-dimesityl and 2,6-diisopropylphenyl (Dipp)-1,2,3-triazol-5-ylidene (aNHCs) **3.313-3.315** employed in CuAAc reactions.

iv) Ruthenium (Ru) atoms complexes with 1,2,3-triazoles have been mainly synthesised in the low oxidation state $Ru_{(II)}$[490]. $Ru_{(II)}$ species are the most active for reactions like hydrogenation, reduction, cyclopropanation etc. Moreover, 1,2,3-triazole based NHC contributed to stabilise $Ru_{(II)}$ limited stability towards some substrates thus increasing $Ru_{(II)}$ catalytic activity.[490] Ru-complexes with 1,2,3-triazoles *via* nitrogen coordination have been introduced as active catalysts for both alcohol oxidation, in the presence of NMO, and for the hydrogenation of ketones to alcohols. Notably, Ru-*N*2 complexes **3.322** were proven to be more active than the Ru-*N*3 ones **3.321** (Scheme 80).[490]

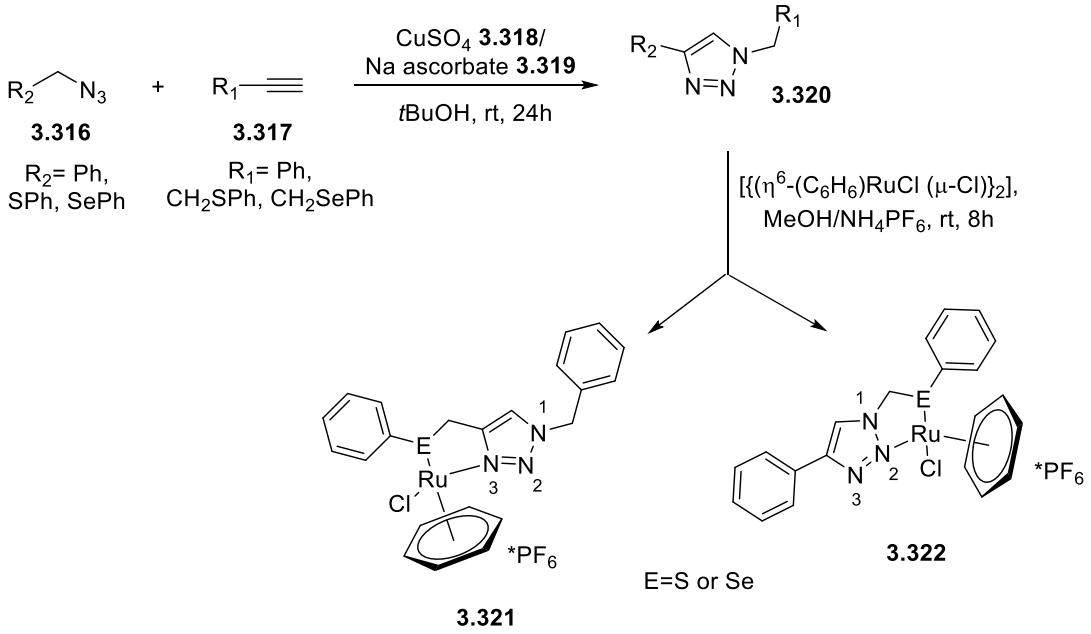

Scheme 80: Synthesis of Ru-complexes **3.321** and **3.322** with 1,2,3-triazoles *via* nitrogen coordination.

On the other hand, (η^6-arene) Ru-NHC complexes (**3.323**-**3.325**) are among the best catalyst sources used for the synthesis of amides starting from alcohols and amines (Figure 64).[491] Albrecht *et al*.[492] proved $Ru_{(II)}$ complexes with triazolium derivatives to be more active than the corresponding imidazolylidene systems.

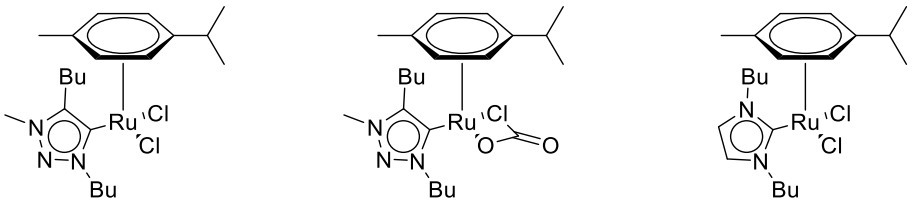

3.323 **3.324** **3.325**

Figure 64: (η^6-arene) Ru-NHC complexes as best catalyst source used for the synthesis of amides starting from alcohols and amines.

v) <u>Palladium (Pd)</u> is one of the most used metals in catalytic sources due to its exceptional versatility in a miriad of reactions such as oxidations, substitutions, cross-couplings etc.[493,494] 1,2,4-triazolylidene nNHC and 1,3,4- triazolylidene aNHC found large employment in forming less toxic and unstable Pd-complexes.[494] In particular, 1,3,4- triazolylidene aNHC were found to be more potent than the corresponding nNHC in catalysing Suzuki and Heck reactions due to their inherent stronger σ-donor ability.[495] Pd-metal complexes usually interact with 1,2,3-triazoles *via* nitrogen coordination of the *N*3 nitrogen[496] but *N*2 coordinated complexes have also been documented by Scrivanti *et al*.[497] (Scheme 81, **3.329**). He introduced them as active catalysts in Suzuki reactions between phenyl boronic acid **3.331** and aryl bromides **3.330** (Scheme 81).

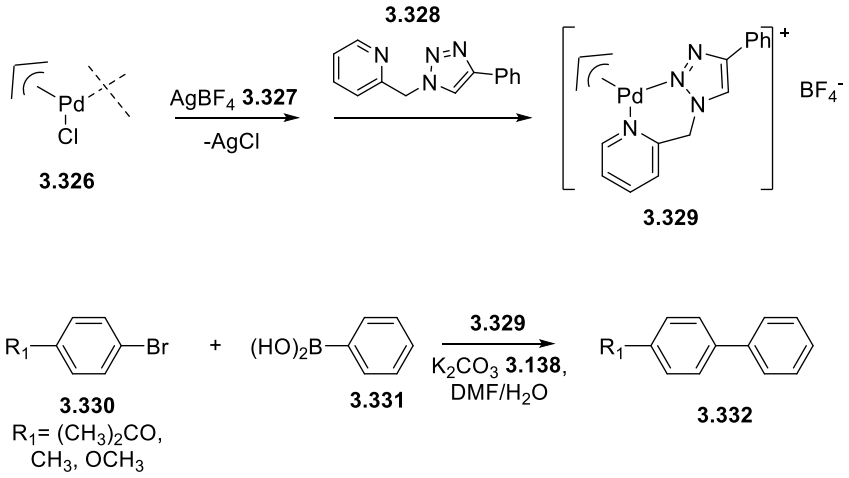

Scheme 81: Triazole chelated cationic palladium allyl complex **3.329** employed in Suzuki reactions between phenyl boronic acid **3.331** and aryl bromides **3.330**.

Verma *et al*.[498] designed an efficient *N*,*N*-type of bidentate ligand **3.334**, composed by an *N*3 substituted benzotriazole with a 2-pyridyl group, to be introduced in palladium catalysed C-C, C-N and C-S coupling reactions. The lone pair of the pyridyl nitrogen and the N=N bond of the benzotriazole contributed enhancing this bidentate ligand's donor properties (Scheme 82).

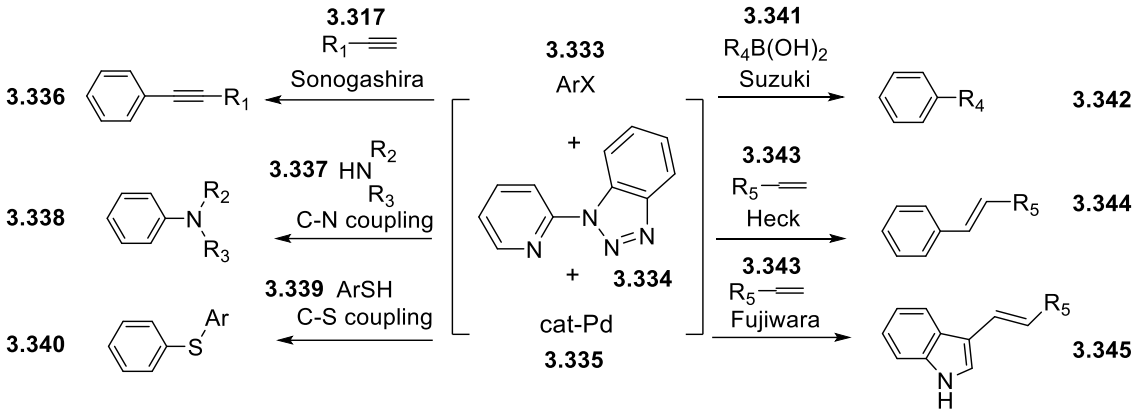

Scheme 82: *N*3 substituted benzotriazole **3.334** introduced in palladium catalysed C-C, C-N and C-S coupling reactions.

Recently, Zhang *et al*.[499] started to incorporate phosphine in 1,2,3-triazole scaffolds complexed with palladium species to obtain triazole-based monophosphine ligands **3.346** (ClickPhos) efficiently employed in amination and Suzuki reactions of unactivated aryl chlorides (Figure 65).

ClickPhos

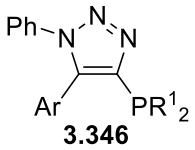

3.346

Ar= Ph, 2-MeO-Ph, 2-NMe_2-Ph,
2,6-dimethoxy-Ph
R_1= Ph, *t*Bu, Cy

Figure 65: Triazole-based monophosphine ligands (ClickPhos).

Sankararaman *et al*.[500] reported the first chiral palladium and palladium bis aNHCs **3.349** and **3.350** complexed with the C4 position of the 1,2,3-triazole scaffold to form a pair of catalysts that were introduced in Suzuki reactions with moderate yields only for the synthesis of biphenyl derivatives (Scheme 83). Therefore, they delineated a new 1,2,3-triazolylidene-based binuclear palladacycle complex with bridging acetate ligands **3.351** that found useful application in

hydroarylation reactions of alkynes **3.348** in the presence of trifluoroacetic acid (TFA, Scheme 83).[500]

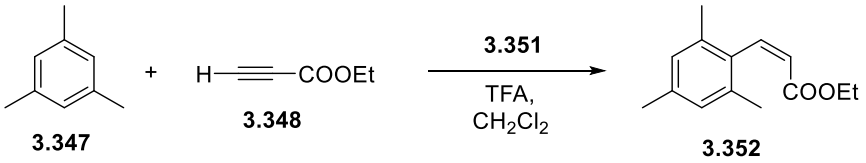

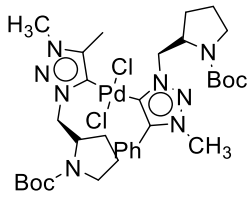

3.349

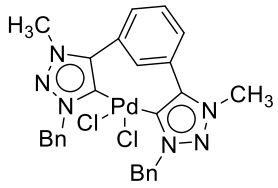

3.350

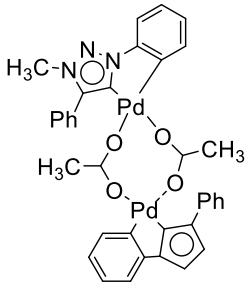

3.351

Scheme 83: Chiral palladium and palladium bis aNHCs **3.349-3.351** complexed with 1,2,3-triazoles employed as catalysts in Suzuki reactions.

In 2012, Albrecht *et al*.[501] described the synthesis of triazolylidene derived pyridine precatalyst preparation stabilisation and initiation (PEPPSI) palladium complexes **3.353**-**3.355** in conjunction with the 3-chloropyridine ligand (Figure 66). This group of catalysts found great applications in Suzuki reactions with the best yields obtained with less bulky substituents on the triazole portion. They proposed palladium atoms, generated from palladium nanoparticles of the catalyst, to be the active species catalysing the reaction and yielding the product.

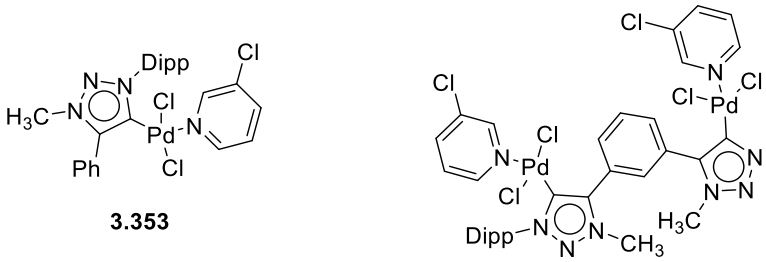

3.353

3.354

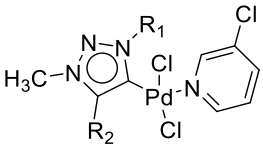

3.355
R_1=CH_3, Et, nBu, Mes
R_2=Ph, nBu, Mes

Figure 66: (PEPPSI) palladium complexes in conjunction with the 3-chloropyridine ligand.

Almost simultaneously, Crudden *et al*.[502] synthesised new PEPPSI complexes and observed high conversion yields when employed in Heck-like reactions involving aryl iodides and electron-deficient bromides in a similar palladium nanoparticles fashion described by Albrecht. Despite 1,2,3-triazoles forming, generally, aNHC with a 1,3,4-substitution pattern, Shaper *et al*.[479] outlined the existance of a Pd-complexed aNHC with 1,2,4-substitution **3.357**. They reported this catalyst to give moderate results when introduced to Suzuki reactions of aryl bromides and chlorides because of its instability despite following the same Pd-nanoparticles release mechanism described before (Scheme 84).[480]

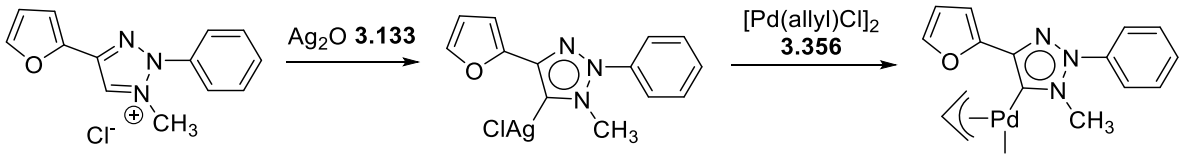

3.288 **3.292** **3.357**

Scheme 84: Synthesis of a Pd-complexed aNHC with 1,2,4-substitution pattern **3.357** to be used in Suzuki reactions of aryl bromides and chlorides.

3.2.2.2 1,2,3-triazoles in asymmetric reactions: BINOL- and triazole-based H-donor organocatalysts.

BINOL (1,1'-bi-2-naphtol) is an organic compound mostly used as a ligand for transition-metal catalysed asymmetric synthesis. BINOL has axial chirality and the two enantiomers are easy to separate and stable towards racemisation.[503] When bounded to 1,2,3-triazoles at the 3- and 3' position, they form important complexes that are crucial for selectivity and control of electronic and steric properties. BINOLs owe their chelating properties to the presence of two basic hydroxy moieties that can coordinate metal Lewis acids such as titanium ($Ti_{(IV)}$) or aluminium ($Al_{(III)}$) to generate chiral complexes. The addition of a second coordination portion, such as the 1,2,3-triazole core, greatly improves BINOL's catalytic activity.[504] BINOL's complexes with 1,2,3-triazoles **3.359**-**3.361** can be synthesised *via* click reaction of opportune azides and alkynes (click-BINOLs) or by *ortho*-lithiation of non-protected (*S*)-BINOLs followed by addition of the corresponding electrophile and methoxymethyl ether's (MOM) cleavage (Scheme 85).[505]

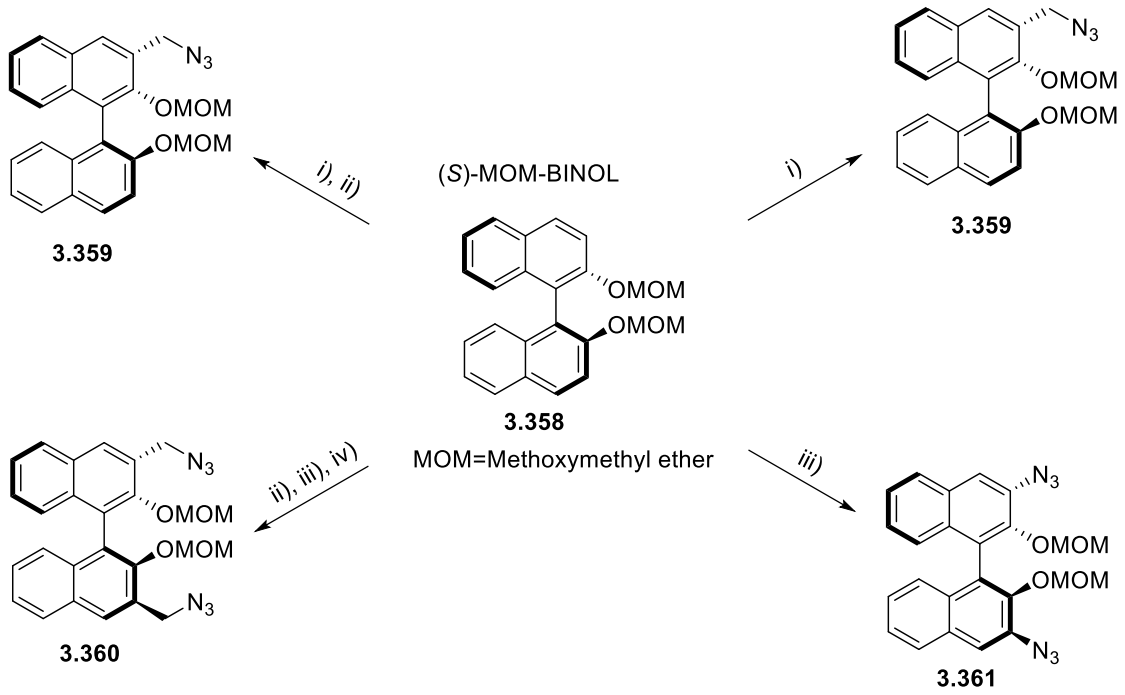

i) *t*-BuLi, -78°C, THF, 2h; ii) $MeSOCl_2$, TEA, toluene/EtOAc, 0°C, 1h and NaN_3, DMF, 0°C to rt; iii) *n*-BuLi, TMEDA, 0°C to rt; iv) $NaBH_4$, THF/EtOH, 0°C, 6h

Scheme 85: Synthesis of BINOL's complexes with 1,2,3-triazoles **3.359**-**3.361** *via* click reaction of opportune azides and alkynes or by *ortho*-lithiation of non-protected (*S*)-BINOLs.

Click-BINOL ligands **3.363** have been tested in the asymmetric addition of diethyl zinc to benzaldehyde **3.362** in the presence of titanium isopropoxide **3.364** ($Ti(O\text{-}iPr)_4$). These showed

the best activity with the 1,2,3-triazole scaffold directly bounded to the binaphtol moiety in position C2 (93:7 er) while bulky substituents in C4 position decreased the enantioselectivity (Scheme 86). Furthermore, when linking 1,5-disubstituted-1,2,3-triazoles a complete inversion of enantioselectivity was observed.[506]

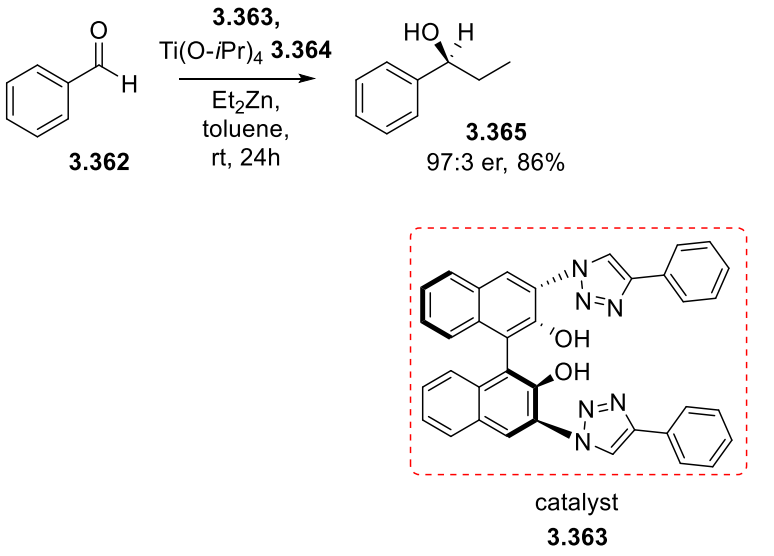

Scheme 86: Asymmetric addition of diethylzinc to benzaldehyde **3.362** *via* triazole-based BINOL catalyst **3.363**.

The catalytic complex responsible for the reaction protocol was found i) *via* coordination of the *N*2/*N*3 atom of the triazole unit by titanium as the organometallic species (**3.366**, Figure 67), i) *via* coordination of the triazole C5 position by titanium as the organometallic species (**3.367**, Figure 67) or iii) with a mixture of both coordination pathways (**3.368**, Figure 67).[472]

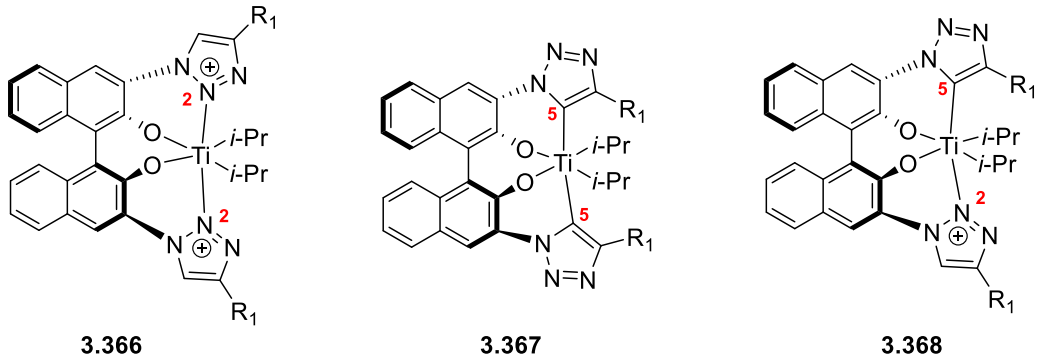

Figure 67: Potential triazole-based catalytic complexes involved in the asymmetric addition of diethylzinc to benzaldehyde **3.362.**

Toste *et al*.[507] described the synthesis of a triazole-based BINOL derivative **3.372** conjugated with phosphoric acid (PA) as organocatalyst. The corresponding bifunctional catalyst achieved high enantioselective yields in oxidative intramolecular C-N bond forming reactions (Scheme 87).

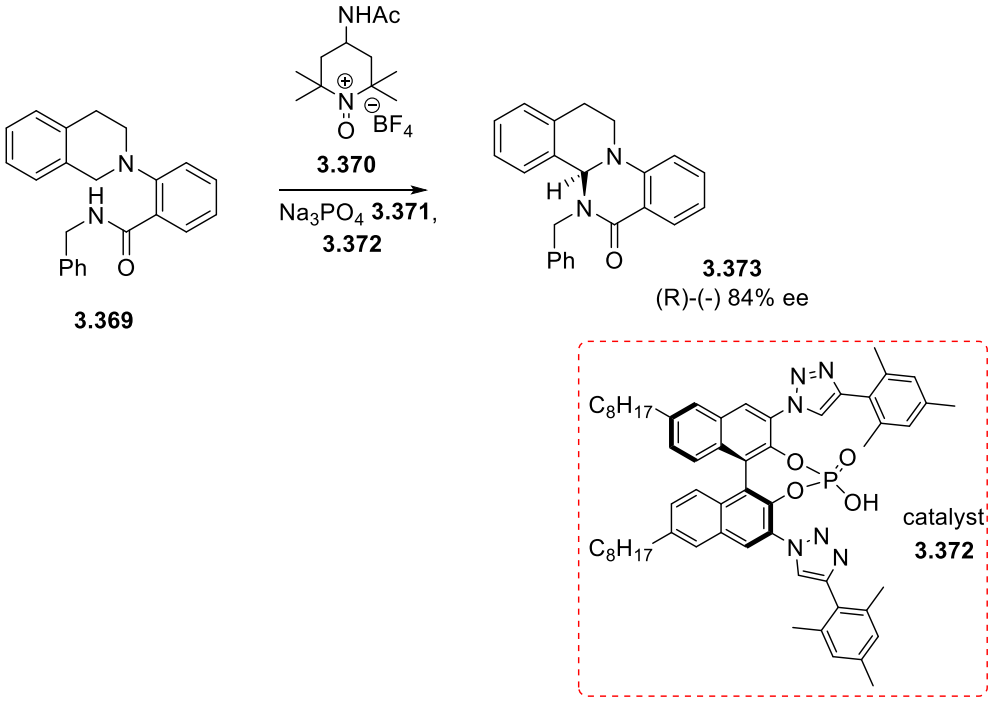

Scheme 87: Triazole-based BINOL derivative **3.372** as organocatalyst in oxidative intramolecular C-N bond forming reactions.

Very recently, the ability of triazoles to bind anions through hydrogen bonding has been applied to organocatalysis.[508] Anion-binding organocatalysis involves the activation of an ionic electrophile **3.374** by linkage of its counteranion **3.375** *via* H-bonding thus facilitating the attack of a nucleophile **3.378** (Scheme 88).[509]

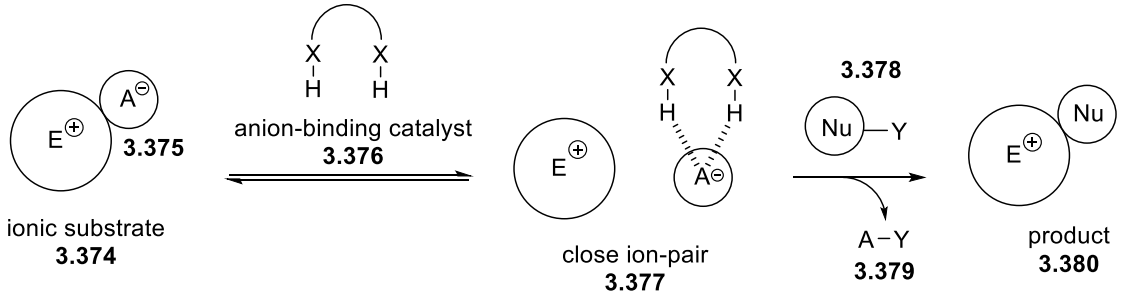

Scheme 88: Anion-binding organocatalysis.

Zurro *et al*.[510] designed novel bistriazole-based acceptors **3.381** for non covalent anion-binding by reacting a 1,3-bistriazolylbenzene motif with a 2-(methoxypropan-2-yl)acetylene group. NMR studies revealed weakly or non-coordinating anions, like the trifluoromethanesufonate anion (TfO^-) or the tetrafluoroborate anion (BF_4^-) not to link the acceptor molecule whereas moderate to good affinities were observed with chloride ions (Scheme 89).[511]

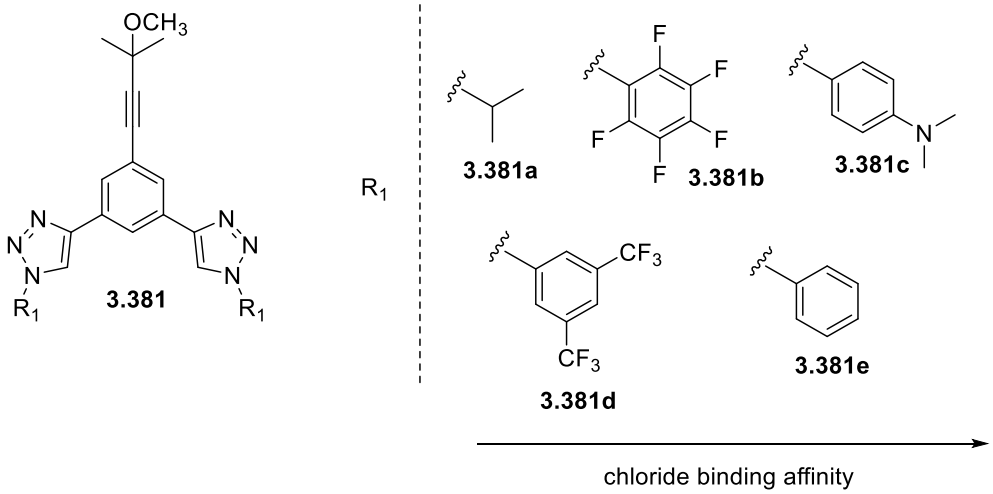

Scheme 89: Novel bistriazole-based acceptors **3.381** for non covalent anion-binding.

Chiral bis-triazoles have been also developed by Zurro *et al*.[505] by reaction of two- four- or six-triazoles groups with aryl electrophiles to obtain large and flexible structure organised in supramolecular patterns (Figure 68, **3.382**-**3.384**).[505] Chirality was introduced either at the backbone or at the end-chain and the anion-binding abilities were tested by circular dicroism (CD). CD revealed a strong chlorine ion binding with increasing amount of tetrabutylammonium chloride (TBACl) and suggested the existance of a more rigid catalyst-anion complex when the binding with chloride anions occurs.[512]

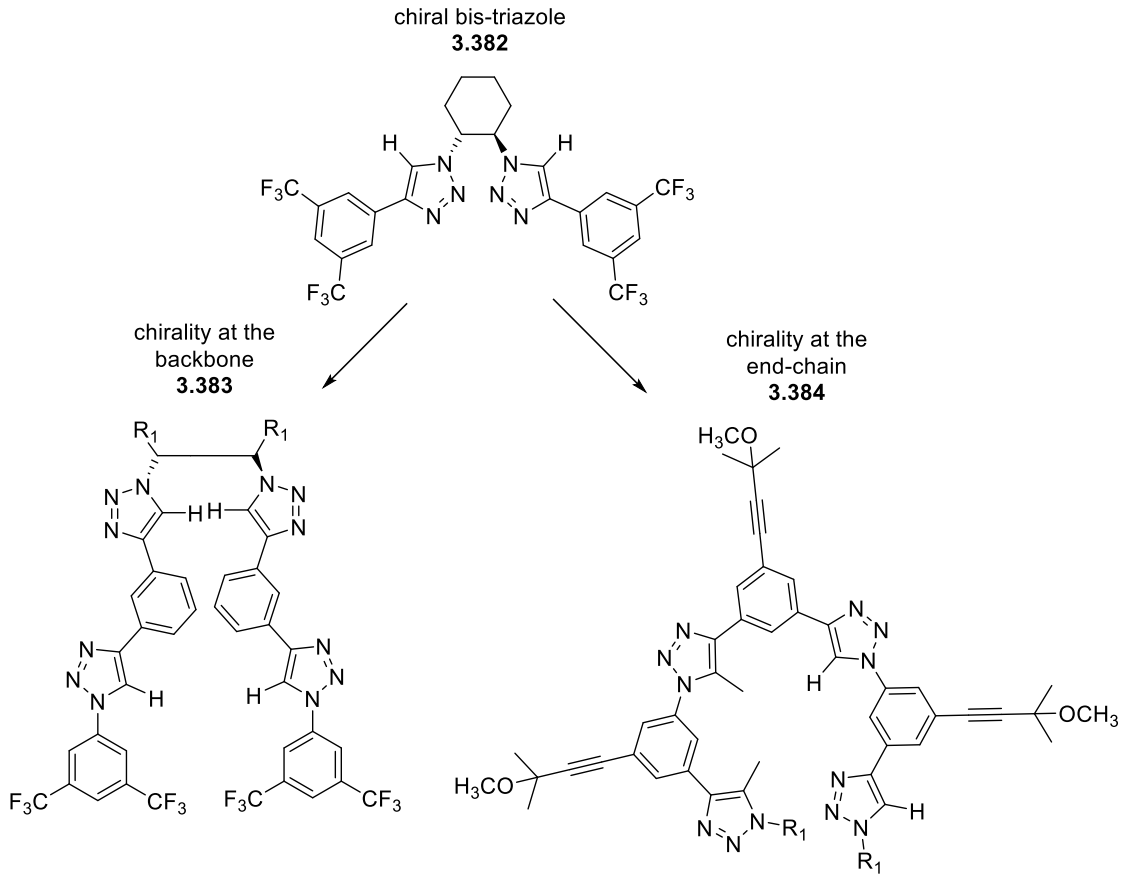

Figure 68: Chiral bis-triazoles **3.382**-**3.384** organised in supramolecular patterns.

In conclusion, a significant development has been made in the field of catalysis. With the increasing demand of non-renewable natural resources, chemicals and pharmaceuticals, catalysts will remain at the forefront of chemical research and development. Catalysts enabled us to synthesise complex molecules in fewer steps, and were crucial in the reduction in emission of CO, NOx, unburned hydrocarbons from the vehicles that operate on the combustion of petrol, diesel and jet fuel. Even though there are still issues associated with catalysts, including the cost, availability, toxicity of many of the precious metals and ligands needed to exploit the catalytic activity, a variety of organic transformations have been successfully accomplished by using metallorganocatalysis which were not achievable without the presence of a catalyst.

3.3 Results and discussion: C-H activation

3.3.1 Importance of the C-H activation in medicinal chemistry

C-H activation reactions have become a powerful and innovative tool for the incorporation of new chemical fragments that can potentially lead to the discovery of biologically active molecules.[513-515] Moreover, C-H activation can be directly used to functionalise known active drugs to enlarge libraries of known active compounds.[515] Yu *et al*.[516] produced analogs of the antinflammatory drug Celecoxib **3.385** *via* C-H activation of the sulfonamide ring, which is fundamental for celecoxib's activity. In this way, they were able to obtain new *ortho*-functionalised perfluoroaryl analogs **3.387** of Celecoxib in a single step with moderate yields (Scheme 90).

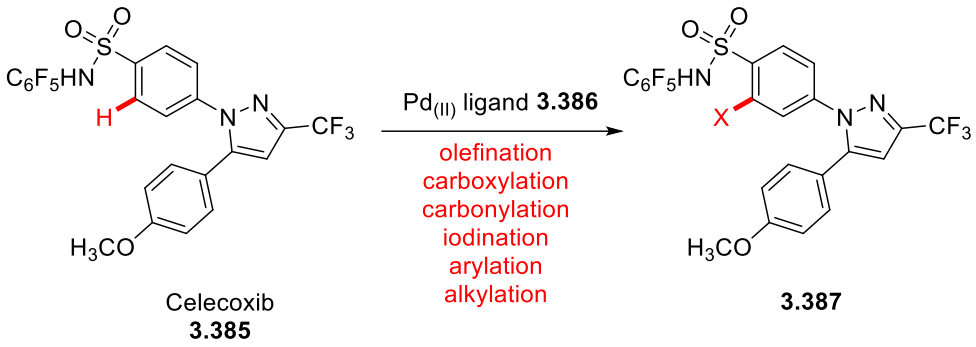

Scheme 90: Synthesis of Celecoxib's analogs **3.387** *via* C-H activation.

Itami and Wünsch used the inherent directing power of the thiophene ring α-position to selectively introduce an aryl residue *via* C-H activation.[517] When using palladium to catalyse the reaction, they obtained a library of α-arylated spirocyclic thiophenes **3.390** (Figure 69), starting from just two "parental" molecules (Figure 69, **3.388** and **3.389**) and test them for biological activity (Figure 69).[500,518]

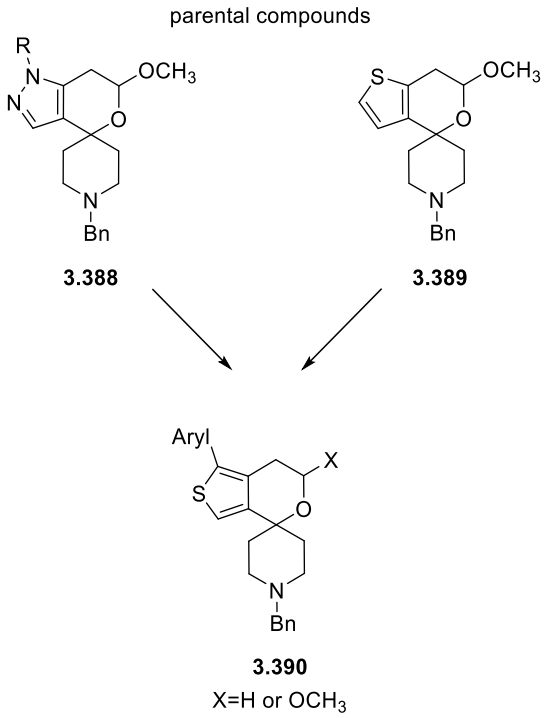

Figure 69: Synthesis of a library of α-arylated spirocyclic thiophenes **3.390** from parental compounds **3.388** and **3.389**.

3.3.2 Cu-catalysed C-H activation of pyridyl-triazoles 2.80a-e to form new C-N bonds.

Given the importance of C-H activation for the development of potential biologically active compounds and the promising results obtained against KAT2A for 1,2,3-triazole **2.80b**, we decided to perform C-H activation reactions on triazoles **2.80a-e** to prepare a small library of functionalised analogs to be eventually tested for further activity. Firstly, we attempted C-H activation of the triazoles' **2.80a-e** C5 position with either linear or cyclic primary and secondary amines **3.391-3.396** *via* copper catalysis **3.99** in the presence of an inorganic base such as potassium phosphate **3.247** (Scheme 91). The reaction produced eight new pyridine-based triazoles **3.397a-h**, not yet reported in literature.

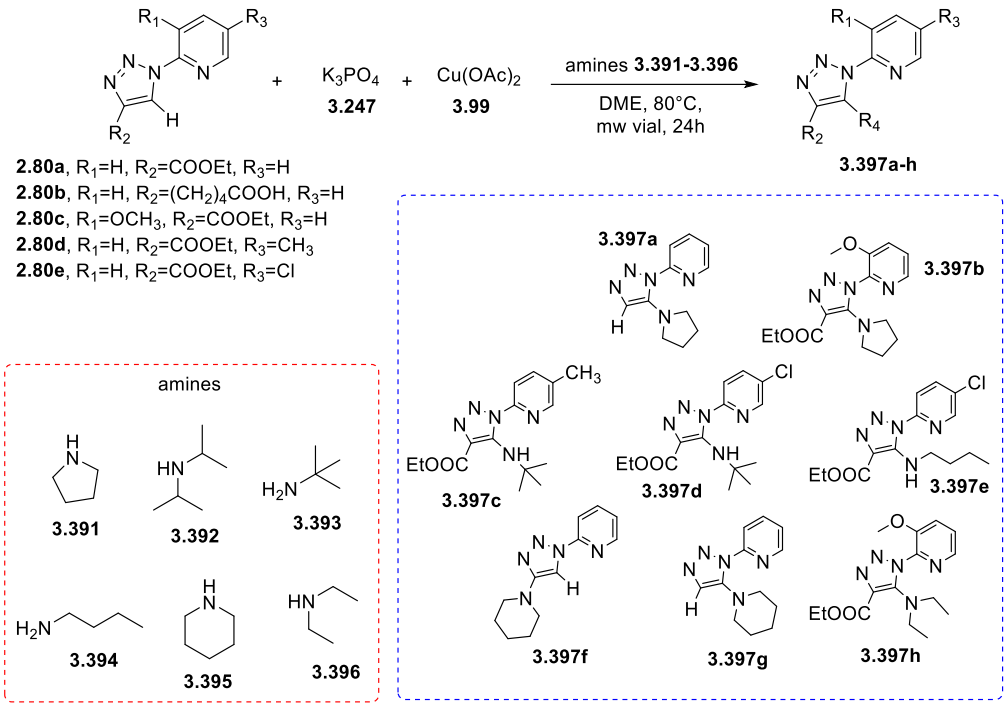

Scheme 91: Proposed reaction pathway for the Cu-catalysed C-H activation of pyridine-based 1,2,3-triazoles **2.80a-e**.

The reaction succeeded when triazoles **2.80a,c-e** were reacted with amines **3.391** and **3.393-3.396** whereas 1,2,3-triazole **2.80b** did not show any reactivity towards amines **3.391**-**3.396**. Notably, when reacting triazole **2.80a** with cyclic amine **3.391,** the reaction produced compound **3.397a**, whose NMR outlined loss of the ester group at the C4 position (R_2) and displayed the presence of a hydrogen atom instead, probably because of a decarboxylative side reaction occurring (Scheme 92). Additionally, when triazole **2.80a** was reacted with cyclic amine **3.395**, it was evident, by NMR analysis, that the formation of two different C-H activation products had occurred. These consisted of **3.397f**, in which the piperidine **3.395** substituted the ester group at the C4 position while retaining the hydrogen at C5, and **3.397g**, in which piperidine substituted the C5 hydrogen according to the traditional C-H activation pattern, albeit producing the same ester loss at C4. We hypothesised a decarboxylative side reaction to occur before the C-H activation process, thus leading to the loss of the ester group (**3.401**) at C4 and the activation of both C4 (**3.402a**) and C5 (**3.402b**) positions to achieve substituted triazoles **3.397f** and **3.397g** (Scheme 92).

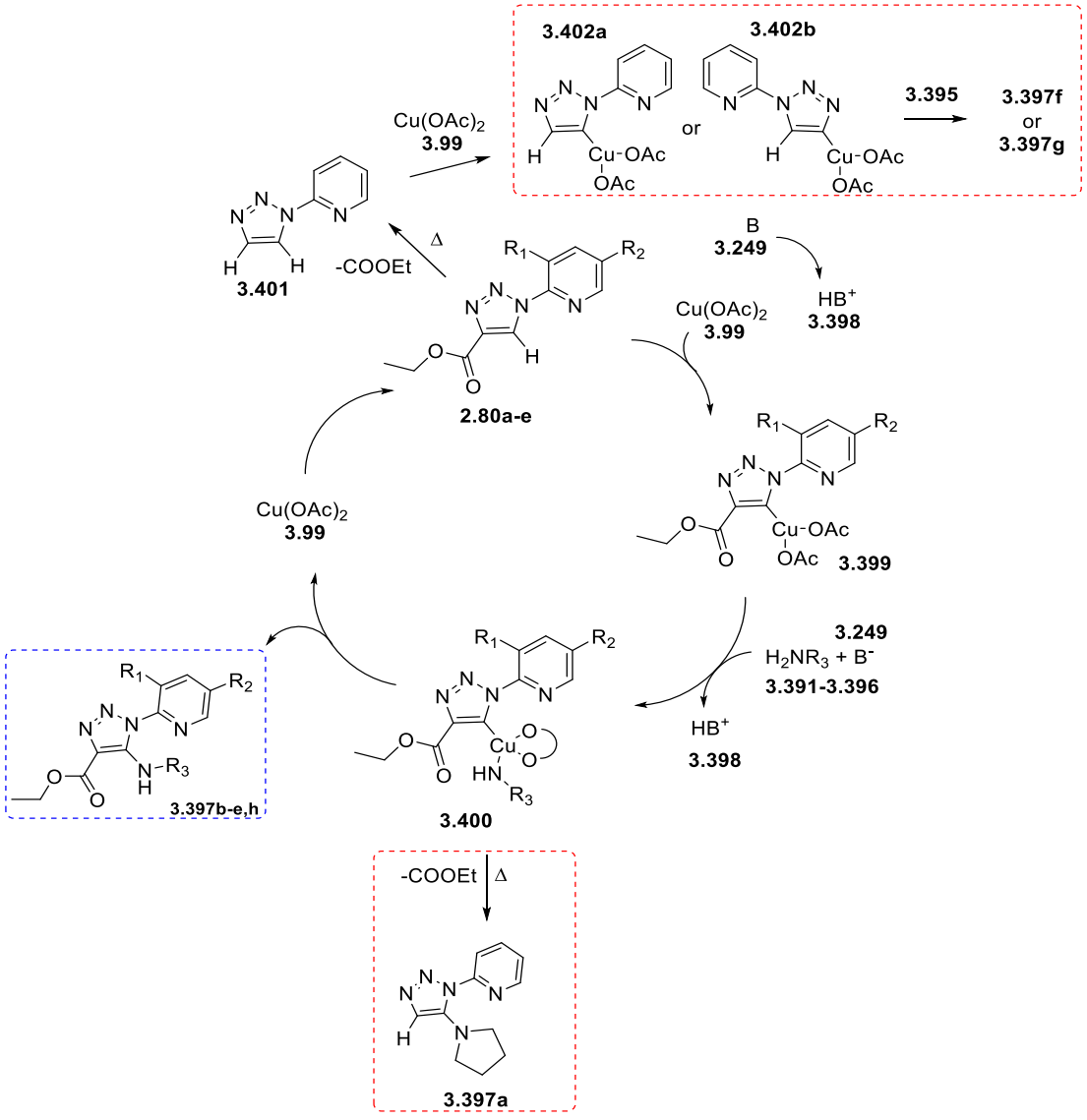

Scheme 92: Proposed mechanism for the Cu-catalysed C-H activation of 1,2,3-triazoles **2.80a-e.** C-H activation expected products **3.397b-e,h** are enclosed in the blue box while C-H activation products **3.397a,f,g** arising from a decarboxylative side reaction are enclosed in the red box.

2D NMR experiment HMBC (Heteronuclear Multiple-Bond Correlation), that establishes correlations between carbons and protons by two, three or four bonds, was needed to distinguish between triazoles **3.397f** and **3.397g**. In particular, HMBC of triazole **3.397f** showed a correlation between the proton at the C5 position (9.01 ppm, circled in red, Figure 70) and carbon C6 of the pyridine ring (144.52 ppm, circled in blue, Figure 70). This latter demonstrated the presence of a hydrogen atom at the C5 position, given the very downfield NMR signal of this proton matching

the ppm range value of all the other triazoles bearing this substitution, and the presence of the piperidine ring at the C4 position, given the long-range correlation existing between the proton at the C5 position and carbon C6, which is impossible to achieve if the piperidine ring was substituting the C5 (Figure 70).

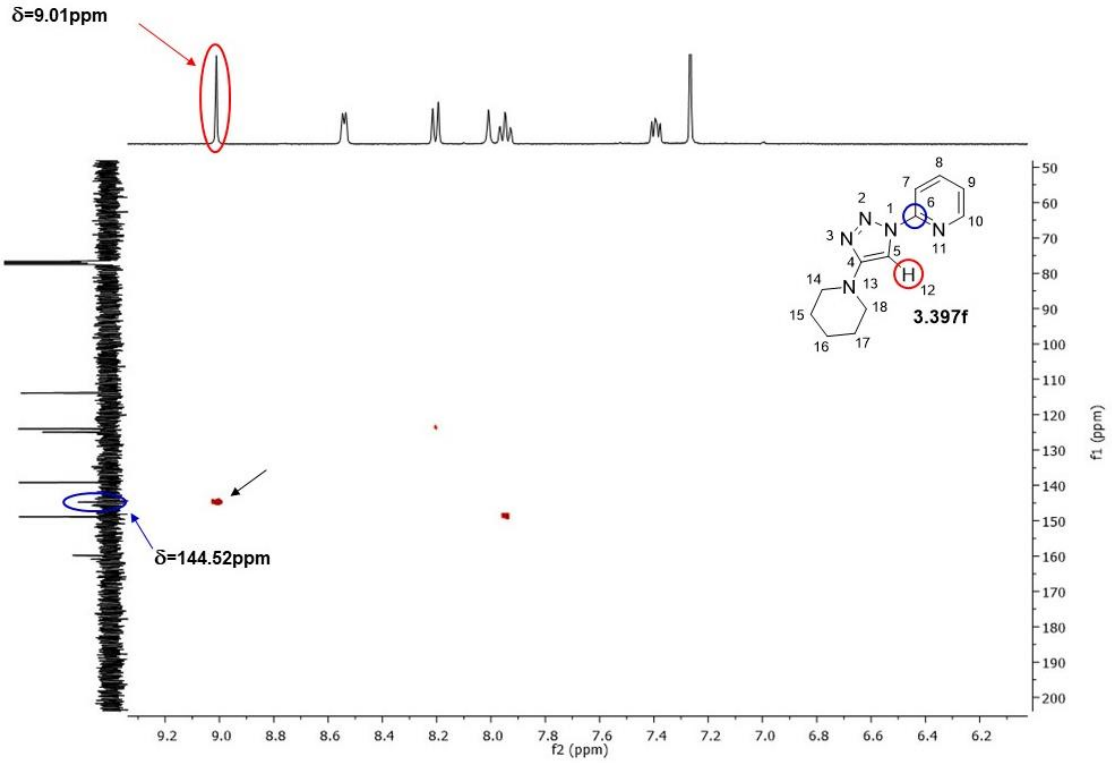

Figure 70: 2D NMR HMBC experiment to confirm triazole **3.397f** identity.

On the other hand, HMBC of triazole **3.397g** displayed no down-shifted singlet signal that could highlight the presence of a hydrogen atom at the C5 position. However, it revealed an upfield signal at 5.65 ppm (circled in red, Figure 71) that did not show any long-range correlation with the pyridine carbons, suggesting the presence, this time, of the piperidine ring at the C5 position and the hydrogen atom at the C4 position (Figure 71).

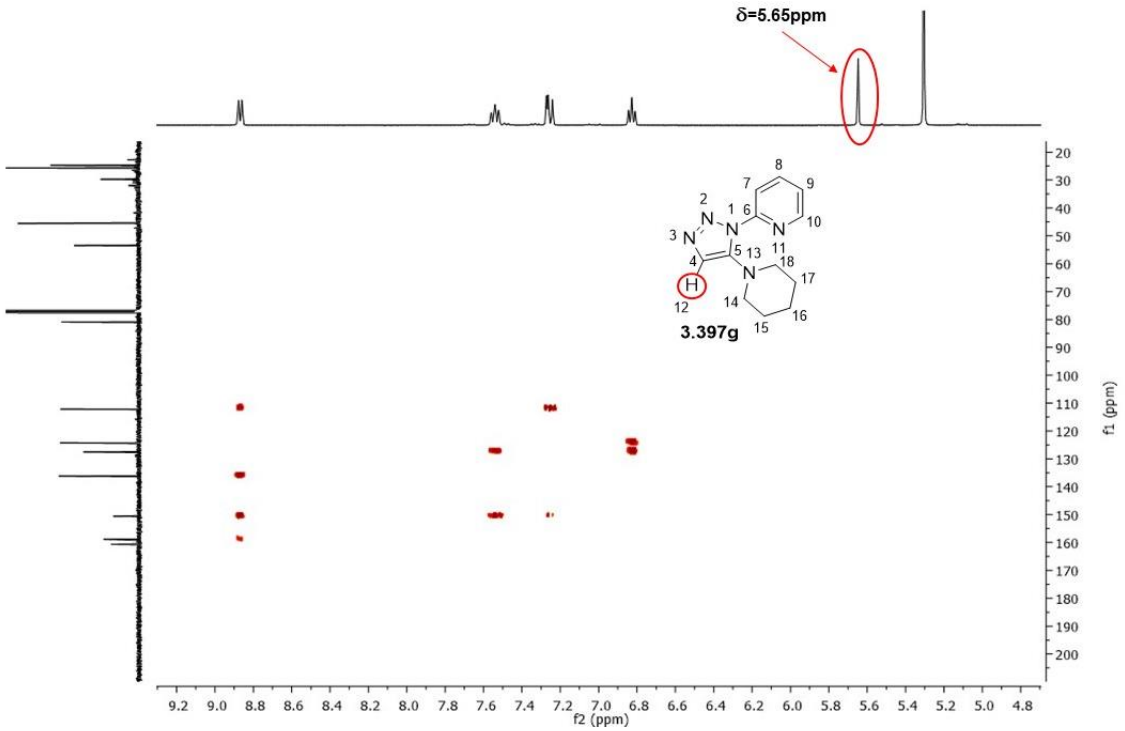

Figure 71: 2D NMR HMBC experiment to confirm triazole **3.397g** identity.

Triazoles **2.80a**-**d** were found unreactive towards linear amine **3.394** except for 1,2,3-triazole **2.80e** which afforded good yields of aminated product. Branched amine **3.393** gave modest to average results only when coupled with triazoles **2.80d** and **2.80e** while poor results arose from reaction of triazole **2.80c** and branched amine **3.396**. However, all of the 1,2,3-triazoles employed did not produce any results when reacted with amine **3.392**, due to the sterically hindered diisopropyl group not allowing copper to properly orientate for the C-H substitution (Table 10).

Table 10: [a]Reaction conditions: **2.80a-e** (1 equiv.,0.2 mmol), **3.391-3.396** (3 equiv., 0.6 mmol), $Cu(OAc)_2$ (0.2 equiv., 0.04 mmol), K_3PO_4 (2 equiv., 0.4 mmol), DME (0.2 M). [b]Only starting materials recovered.

Entry[a]	Triazole	Amine	Product	Yield (%)[b]
1	**2.80a**		**3.397a**	41
2	**2.80b**		-	-[b]
3	**2.80c**	**3.391**	**3. 397b**	10
4	**2.80d**		-	-[b]
5	**2.80e**		-	-[b]
6	**2.80a**		-	-[b]
7	**2.80b**		-	-[b]
8	**2.80c**	**3.392**	-	-[b]
9	**2.80d**		-	-[b]
10	**2.80e**		-	-[b]
11	**2.80a**		-	-[b]
12	**2.80b**		-	-[b]
13	**2.80c**	**3.393**	-	-[b]
14	**2.80d**		**3. 397c**	20
15	**2.80e**		**3. 397d**	40
16	**2.80a**		-	-[b]
17	**2.80b**		-	-[b]
18	**2.80c**	**3.394**	-	-[b]
19	**2.80d**		-	-[b]
20	**2.80e**		**3. 397e**	65

Entry[a]	Triazole	Amine	Product	Yield (%)[b]
21	**2.80a**		**3. 397f,g**	20,30
22	**2.80b**		-	-[b]
23	**2.80c**	**3.395**	-	-[b]
24	**2.80d**		-	-[b]
25	**2.80e**		-	-[b]
26	**2.80a**		-	-[b]
27	**2.80b**		-	-[b]
28	**2.80c**	**3.396**	**3. 397h**	10
29	**2.80d**		-	-[b]
30	**2.80e**		-	-[b]

We hypothesised this set of reactions to follow the same C-H amination pattern described by Zhu *et al*.[518], in which a $Cu_{(II)}$-$Cu_{(I)}$ catalytic cycle explained the oxidative addition and reductive elimination processes to afford aminated 1,2,3-triazoles *N*-oxide derivatives. We envisaged the reductive elimination to be the rate limiting step as influenced by the electronic nature of the substituents on the pyridine ring (Scheme 92). More specifically, we noticed the amination reaction happening only with electron-withdrawing groups present on the pyridine ring, such as chlorine in triazole **2.80e**, or with no substituents at all, in the case of triazole **2.80a**, in accordance with what has also been observed by Zhu *et al*.[518] The only electron-donating positive effect was displayed by triazole **2.80c,** whose reaction with branched amine **3.396** was the only successful one if compared to the failed reactions of triazoles **2.80a,b-d,e**, and by triazole **2.80d** when reacted with *tert*-butyl amine **3.393** (Scheme 92).

3.3.3 Pd-catalysed C-H activation of pyridyl-triazoles 2.80a-e to form new C-C bonds.

Although the average results obtained for the copper-catalysed C-H activation of 1,2,3-triazoles **2.80a-e**, we further investigated the reactivity of **2.80a-e** *via* palladium-catalysed C-H activation to obtain new C-C bonds. The addition of an auxiliary agent such as tetrabutylammonium acetate **3.243** (Bu_4NOAc) stabilised the palladium-intermediate complex during the C-H activation due to the presence of a quaternary ammonium cation species. Diverse palladium complexes have been screened, including phosphine-based Pd species, electron-rich and electron poor Pd-complexes and aNHC Pd-based compounds **3.89** and **3.406-3.409**. Unfortunately, only triazole **2.80a** successfully reacted with the sole aryl bromide **3.403** in the presence of palladium acetate $Pd(OAc)_2$ **3.89** to yield a new triazole **3.410a**, not yet reported in literature (Scheme 93 and Table 11).

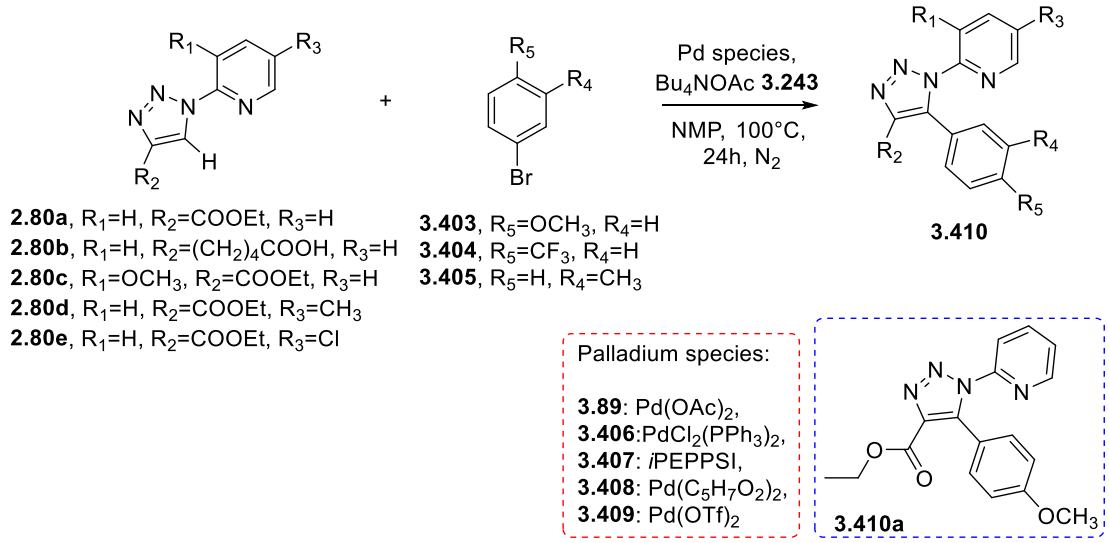

Scheme 93: Proposed reaction pathway for the palladium-catalysed C-H activation of pyridine-based 1,2,3-triazoles **2.80a-e**. Palladium species **3.89** and **3.406-3.409** employed as catalysts are enclosed in the red box while the only product achieved (**3.410a**) is enclosed in the blue box.

Table 11: [a]Reaction conditions: **2.80a-e** (1 equiv., 0.5mmol), Pd species (0.05 equiv., 0.025mmol), Bu_4NOAc (2 equiv., 1mmol), aryl bromides **3.403-3.405** (1.5 equiv., 0.75mmol), NMP (0.5M). [b]Only starting materials recovered.

Entry[a]	Triazole	Aryl bromide	Pd species	Product	Yield (%)
1	**2.80a**	**3.403**	**3.89** and **3.406-3.409**	**3.410a**	40
2	**2.80b**			-	-[b]
3	**2.80c**			-	-[b]
4	**2.80d**			-	-[b]
5	**2.80e**			-	-[b]
6	**2.80a**	**3.404**	**3.89** and **3.406-3.409**	-	-[b]
7	**2.80b**			-	-[b]
8	**2.80c**			-	-[b]
9	**2.80d**			-	-[b]
10	**2.80e**			-	-[b]
11	**2.80a**	**3.405**	**3.89** and **3.406-3.409**	-	-[b]
12	**2.80b**			-	-[b]
13	**2.80c**			-	-[b]
14	**2.80d**			-	-[b]
15	**2.80e**			-	-[b]

We hypothesised this reaction to follow a $Pd_{(II)}/Pd_{(0)}$ catalytic cycle with transmetallation of palladium-intermediate **3.412** with aryl bromide **3.403-3.405** to give **3.414** that, after reductive elimination, led to the formation of the product **3.410** and restored $Pd_{(II)}$ species **3.89**. Steric hindrance of the CF_3 group of aryl bromide **3.404** or conflicting interactions between EDGs and EWGs on the pyridine ring of 1,2,3-triazoles **2.80a-e** and on the phenyl ring of aryl bromides **3.403-3.405** probably played a negative role resulting in the absence of reactivity (Scheme 94).

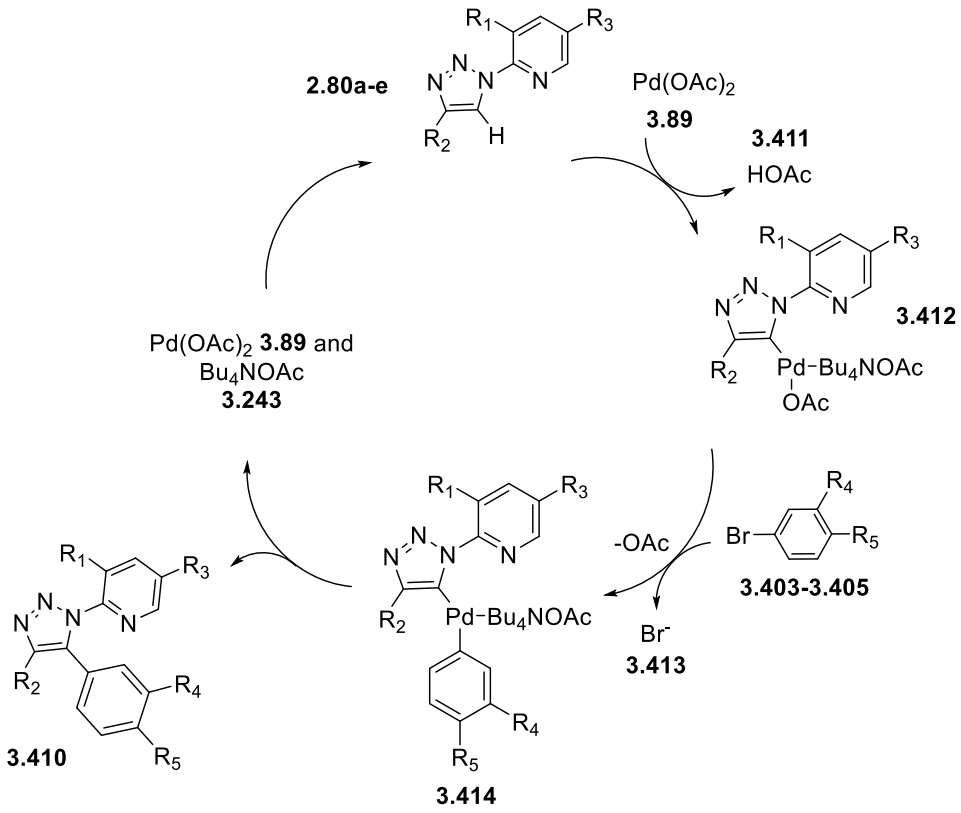

Scheme 94: Proposed mechanism for the Pd-catalysed C-H activation of pyridine-based 1,2,3-triazoles **2.80a-e**.

Moreover, not even when employing other reagents such as triphenyl phosphine **3.417** or tricyclohexylphosphine **3.418**, when using a stronger base such as potassium carbonate **3.138** (K_2CO_3), and when reacting only unsubstituted phenyl chloride **3.416** and phenyl bromide **3.415**, positive results were obtained (Scheme 95).

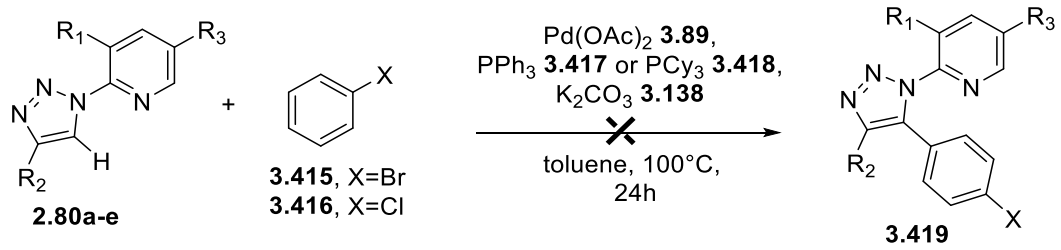

Scheme 95: Proposed alternative reaction pathway for the Pd-catalysed C-H activation of pyridine-based 1,2,3-triazoles **2.80a-e**.

3.3.4 Synthesis of proline-based organocatalysts from pyridyl azide 1.136a and 4-nitrophenyl azide 3.423b.

Proline-based organocatalysts have been proved to be fundamental for enantioselective reactions, such as aldol condensations, Mannich and Michael reactions.[519-528] Furthermore, there has been a significant increase in examples of 1,2,3-triazoles, conjugated with the proline moiety, employed in organocatalysis such as BINOLs complexes or bistriazole-based acceptors for non covalent anion-binding.[505,510] Previous attempts to build triazole-based organocatalysts with the insertion of the proline scaffold have been already exploited by the Adamo's lab (Scheme 96).

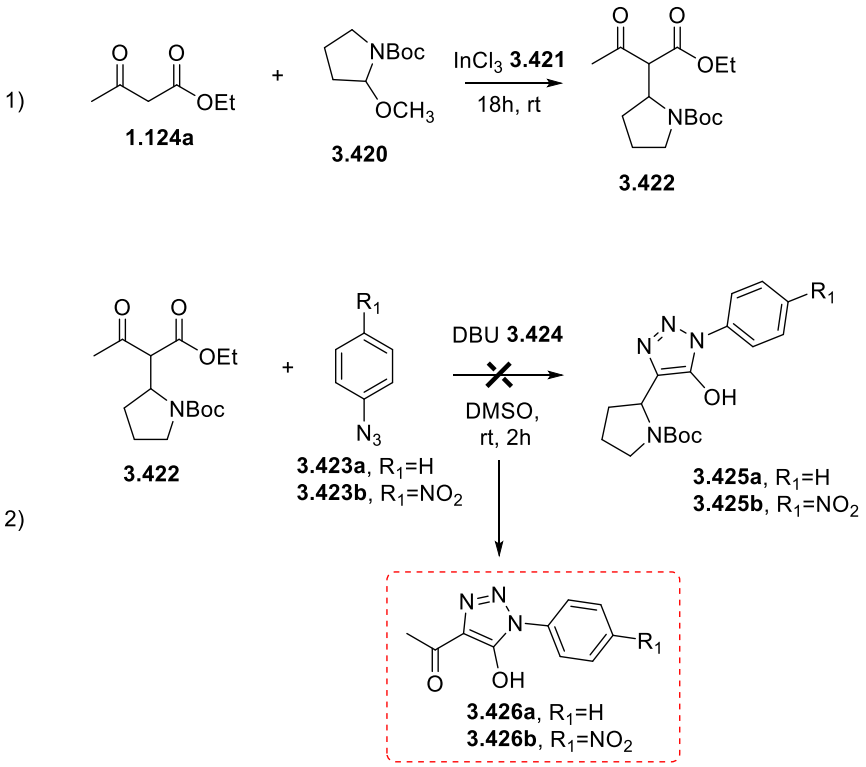

Scheme 96: Previous attempts for the synthesis of triazole-proline based organocatalysts **3.425**.

More specifically, β-ketoester **1.124a** was reacted with a Boc-protected proline functionalised with a methoxy group at position C2 (**3.420**) to obtain intermediate **3.422**. However, when intermediate **3.422** was coupled with phenyl azide **3.423a** and 4-nitrophenyl azide **3.423b**, the reaction produced only acylated compound **3.426** with loss of the proline fragment, probably due to the more stable imine **3.428** as the elimination product (Scheme 97).

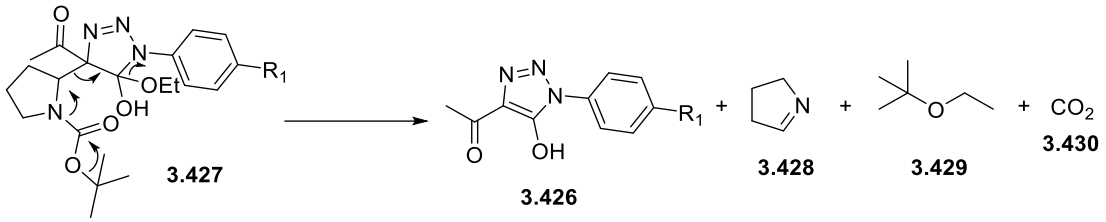

Scheme 97: Proposed mechanism for the formation of by-product **3.426**.

For this reason, we decided to insert a CH_2 spacer between the proline fragment and the triazole ring to avoid proline's elimination and push the reaction towards completion. Therefore, we approached the synthesis of new bifunctional triazole-based organocatalysts by employing the following reaction protocol. Firstly, we reacted D-prolinol **3.431** with Boc anhydride (Boc_2O) **3.432** in the presence of sodium hydroxyde (NaOH) to afford protected proline-Boc **3.433**. **3.433** was then coupled with the Dess-Martin reagent **3.434** in DCM for the oxidation of the alcohol group into aldehyde **3.435**. Reaction of **3.435** with β-ketoester **1.124a** afforded intermediate **3.437** that, after reduction in the presence of ammonium formate **3.438** (NH_4HCO_2) and palladium on carbon **3.439** (Pd/C), led to the final compound **3.440**. Notably, split ^1H NMR peaks of **3.437** and **3.440** suggested the existance of two stereoisomers **3.437a,b** and diasteroisomers **3.440** arising from the non-controlled stereoselectivity addition of Boc-prolinal **3.435** to β-ketoester **1.124a** as well as from Boc predisposition to the formation of multiple rotamers (Scheme 98).

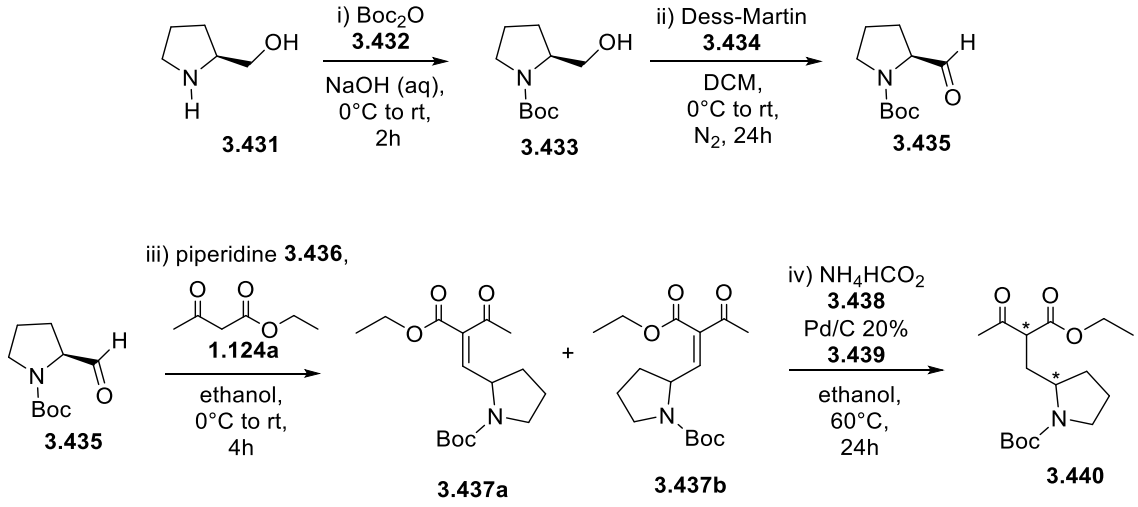

Scheme 98: Reaction flow for the synthesis of intermediates **3.440**.

At this point, pyridyl azide **1.136a** and 4-nitrophenyl azide **3.423b** were reacted with the *N*-Boc-proline β-ketoester **3.440** following the same DBU-catalysed cycloaddition process described in *Chapter 1* for the synthesis of 1,2,3-triazoles **1.136b,c.** Unfortunately, neither of the two aryl azides furnished the desired products, as they were collected unreacted, and the only observation

was degradation of the Boc-proline β-ketoester **3.440** with loss of the Boc protecting group. Consequently, we decided to perform the reaction in the presence of DMSO or ethanol as solvents, instead of ACN, sodium ethoxyde (EtONa) as the base, instead of DBU, and, eventually, a catalytic source, such as $Cu(OTf)_2*C_6H_5CH_3$ **3.442**, to push the reaction towards completion. Unfortunately, also these new reaction conditions did not lead to the formation of the desired triazole **3.441** as we only observed loss of the Boc protecting group and degradation of the starting materials (Scheme 99 and Table 12).

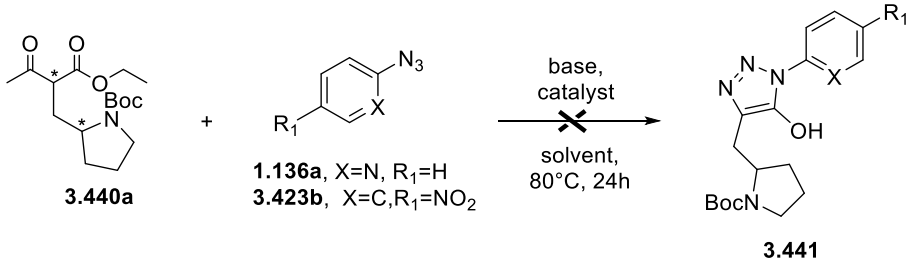

Scheme 99: Proposed reaction flow for the synthesis of a new proline-based 1,2,3-triazole organocatalyst **3.441**.

Table 12: [a]Reaction conditions: azides **1.136a, 3.423b** (1 equiv.,0.063 mmol), base (1.1 equiv., 0.07 mmol), catalyst (0.2 equiv., 0.0126 mmol), solvent (0.2 M).

Entry[a]	Azide	Base	Solvent	Catalyst
1	**1.136a**	DBU	ACN	-
2	**3.423b**			
3	**1.136a**	DBU	DMSO	-
4	**3.423b**			
5	**1.136a**	EtONa	Ethanol	-
6	**3.423b**			
7	**1.136a**	DBU	Neat	-
8	**3.423b**			
9	**1.136a**	DBU	DMSO	$Cu(OTf)_2*C_6H_5CH_3$ **3.442**
10	**3.423b**			

Given Boc protecting group instability and tendency to produce a high number of rotamers, we attempted to modify the nature of proline's nitrogen protecting group, by substituting the Boc fragment with a *p*-toluensulfonyl chloride moiety ($ClSO_2PhCH_3$), also known as tosyl group (Ts), which cleavage required more harsh conditions (*i.e.* reduction in the presence of lithium aluminiun hydride). Therefore, we approached the synthesis of *N*-tosyl-proline β-ketoester **3.447** following the same protocol abovementioned for *N*-Boc-proline β-ketoester **3.440**. It is important to note that also with the tosyl protecting group, two different steroisomers were visible from ^{1}H and ^{13}C NMR after coupling of *N*-tosyl prolinal **3.445** with β-ketoester **1.124a** and subsequent reduction to afford intermediate **3.447** (Scheme 100) due to the non-stereoselective reaction conditions. Final coupling with either pyridyl azide **1.136a** and 4-nitrophenyl azide **3.423b** did not bring, unfortunately, to the desired products **3.448**, despite attempting the same diverse reaction conditions used for the *N*-Boc protected intermediate **3.440** (Scheme 100). We supposed the steric hindrance of the tosyl group to have negatively impacted the nucleophilic addition of the azido-group to one of the two electrophilic carbonyls as well as the rigidity of its aromatic ring to have impeded *N*-tosyl-proline β-ketoester **3.447** flexibility during the reaction.

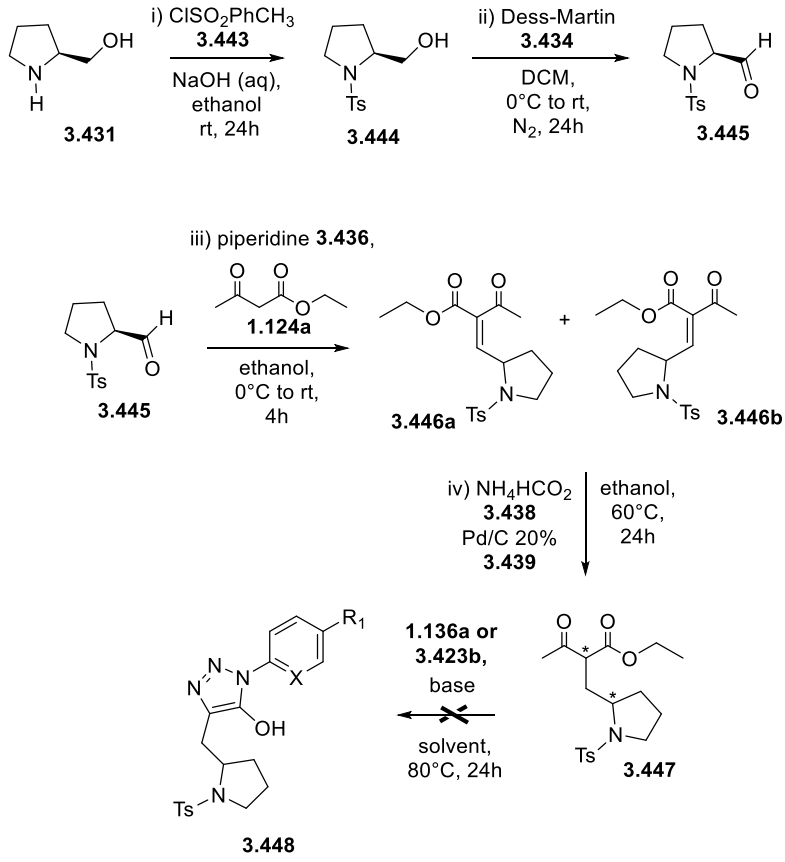

Scheme 100: Reaction protocol for the attempted synthesis of *N*-tosyl protected proline-triazole based organocatalysts **3.448**.

3.4 Conclusions

In conclusion, given the positive results obtained for 1,2,3-triazole **2.80b** against KAT2A and given the importance of C-H activation for the development of potential biologically active compounds, we built a small library of **2.80a-e** analogs *via* C-H activation reactions through either copper or palladium catalysis. In particular, copper-catalysed C-H activation led to the formation of new C-N bonds when reacting pyridine-based 1,2,3-triazole **2.80a-e** with both linear and cyclic primary and secondary amines **3.391-3.396** yielding analogs **3.397a-h**, not yet reported in literature, in average yields. On the other hand, palladium-catalysed C-H activation to form new C-C bonds was not successful. When reacting pyridine-based 1,2,3-triazole **2.80a-e** with both EW and ED substituted and unsubstituted aryl bromides and chlorides **3.403-3.405** and **3.415**,**3.416**, the sole product formed (**3.410a**), not yet reported in literature, arose from reaction of 1,2,3-triazole **2.80a** with 4-bromoanisole **3.403** in the presence of palladium acetate **3.89**. Unfortunately, when attempting to the development of a new prototype of proline-based triazole organocatalyst **3.441** or **3.448**, by reaction of β-ketoesters **3.440** or **3.447** with azides **3.423b** or **1.136a**, we observed no formation of the desired products either when employing the Boc or the tosyl protecting groups. When hypothesised the Boc instability as well as the tosyl group steric hindrance to have negatively impacted the outcome of the reactions, suggesting a more deeper investigation of how to optimise the reactions conditions.

3.5 Experimental Section

^{1}H and ^{13}C NMR spectra were recorded on a Bruker 400 spectrometer. Chemical shifts (δ) are reported in ppm relative to residual solvent signals (^{1}H NMR: 7.26 ppm for $CDCl_3$; 3.31 ppm for CD_3OD, ^{13}C NMR: 77.16 ppm for $CDCl_3$, 49.03 for CD_3OD). ^{13}C NMR spectra were acquired with ^{1}H broad band decoupled mode. Coupling constants (*J*) are in Hz. Melting points were measured using a Stuart scientific melting point apparatus and are uncorrected. Infrared spectra (IR) were recorded with KBr discs using a Bruker Tensor27 FT-IR instrument. High-resolution mass spectra were obtained on a Waters Micromass GCT PremierMS spectrometer or on a Bruker microTOF-Q III LC-MS spectrometer (APCI method). Purity of final products was verified by HPLC analysis and ^{1}H and ^{13}C NMR spectroscopy. Analytical grade solvents and commercially available reagents were used as received. Reactions were monitored by TLC (Merck, silica gel 60 F254). Flash column chromatography was performed using silica gel 60 (0.040-0.063 mm, 230-400 mesh). Amines **3.391-3.396**, aryl bromides **3.403-3.405**, phenyl chloride **3.416**, phenyl bromide **3.415** copper acetate **3.99**, palladium species **3.89** and **3.406**-**3.409**, D-Prolinol **3.431**, Boc_2O **3.432**, tosyl chloride **3.443** and Dess-Martin reagent **3.434** were purchased from Sigma Aldrich. Pyridine-based 1,2,3-triazoles' **2.80a-e** synthesis is described in *Chapter 2 Experimental Section*. C-H activation products **3.397a-h** and **3.410a** were synthesised according to literature protocols

applied on different substrates.[450,451,529] Proline-based aldehyde intermediates **3.435**, **3.445** together with β-ketoesters **3.437**, **3.446** and the corresponding reduced products **3.440**, **3.447** were synthesised according to existent literature procedures on similar substrates.[530-534] Attempted synthesis of proline-based triazole **3.441** and **3.448** was performed according to procedure GP2 already described in *Chapter 2 Experimental Section.*

3.5.1 General procedure for the C-H activation of triazoles 2.80a-e *via* copper catalysis (GP5)[451].

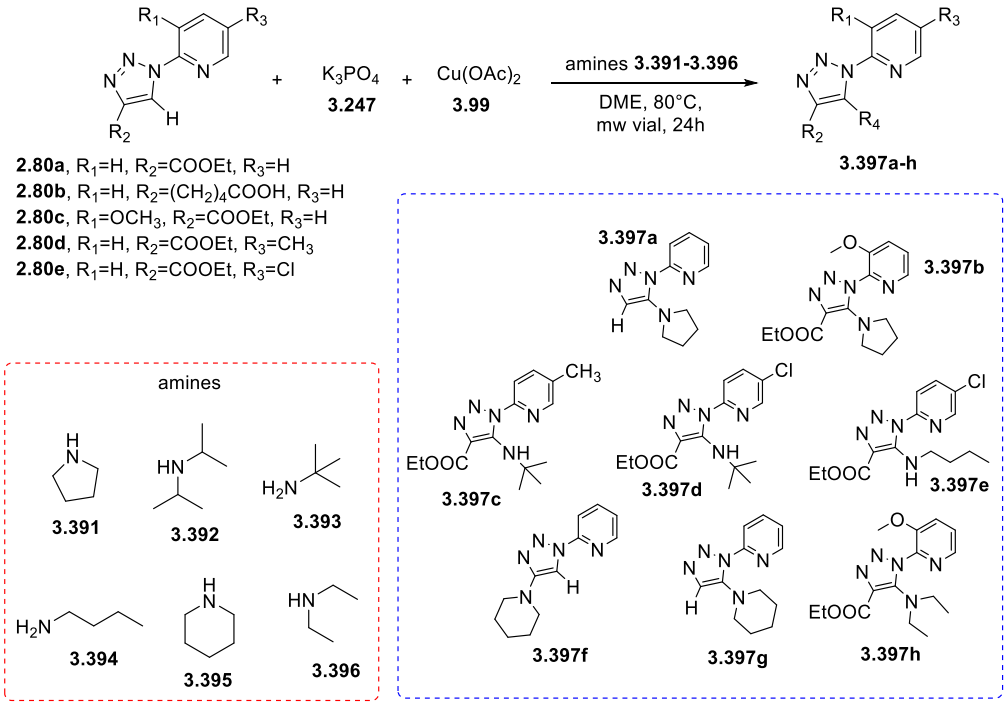

To a solution of triazoles **2.80a-e** (1 equiv., 0.2 mmol), copper acetate **3.99** (0.2 equiv., 0.04 mmol) and potassium phosphate **3.370** (2 equiv., 0.4 mmol) in DME (0.2 M), amines **3.391-3.396** (3 equiv. 0.6 mmol) were added. The reaction was set up at 80°C in a microwave vial under pressure given the solvent low boiling point (bp=85°C). After 24 hours, TLC (DCM/AcOEt 70:30) showed complete consumption of the starting materials only for the following reactions: triazole **2.80a** with amines **3.391** and **3.395**; triazole **2.80c** with amines **3.391** and **3.396**; triazole **2.80d** with amine **3.393**; triazole **2.80e** with amines **3.393** and **3.392**. Once cooled to room temperature, each crude was washed with DCM/H_2O three times, the organic phases collected and dried over anhydrous Na_2SO_4. Hence, the solvent was removed by rotary evaporation and further purification occurred *via* column chromatography to afford products **3.397a-h** in modest to average yields.

2-(5-(pyrrolidin-1-yl)-1H-1,2,3-triazol-1-yl)pyridine 3.397a

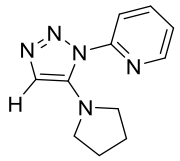

Prepared according to GP5, yellow solid (DCM/MeOH 95:05), 40% (21 mg). ^{1}H NMR (400 MHz, $CDCl_3$) δ 8.91 (d, *J* = 7.1 Hz, 1H), 7.62 – 7.46 (m, 1H), 7.29 (s, 1H), 6.83 (t, *J* = 6.8 Hz, 1H), 5.40 (s, 1H), 3.64 (bs, 2H), 3.37 (bs, 2H), 2.01 (bs, 4H). ^{13}C NMR (101 MHz, $CDCl_3$) δ 159.3, 158.0, 150.8, 136.2, 127.7, 124.1, 111.9, 81.0, 77.4, 77.1, 76.8, 46.7. IR (KBr, cm^{-1}): 2938, 1673,1636, 1285. m.p. 125°C. HRMS (ESI) m/z: $[M+H]^+$ calcd for $C_{11}H_{14}N_5$ 216.1249; found 216.2714.

Ethyl 1-(3-methoxypyridin-2-yl)-5-(pyrrolidin-1-yl)-1H-1,2,3-triazole-4-carboxylate 3.397b

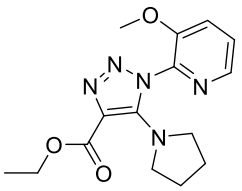

Prepared according to GP5, orange oil (DCM/ACOEt 80:20), 10% (5 mg). ^{1}H NMR (400 MHz, $CDCl_3$) δ 8.90 (d, *J* = 6.8 Hz, 1H), 6.75 (t, *J* = 7.3 Hz, 1H), 6.68 (d, *J* = 7.7 Hz, 1H), 4.40 (q, *J* = 7.1 Hz, 2H), 4.00 (s, 3H), 3.74 – 3.60 (m, 4H), 2.02 – 1.84 (m, 4H), 1.43 (t, J = 7.1 Hz, 3H). ^{13}C NMR (101 MHz, $CDCl_3$) δ 161.0, 157.6, 146.5, 139.5, 121.2, 111.5, 105.0, 100.1, 59.8, 55.9, 51.4, 29.7, 25.8, 14.7. IR (KBr, cm^{-1}): 3005, 1743, 1647, 1456, 1185. HRMS (ESI) m/z: $[M+H]^+$ calcd for $C_{15}H_{20}N_5O_3$ 318.4566; found 318.5346.

Ethyl 5-(tert-butylamino)-1-(5-methylpyridin-2-yl)-1H-1,2,3-triazole-4-carboxylate 3.397c

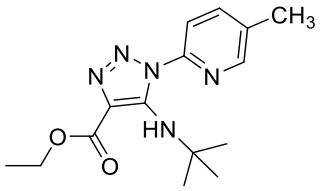

Prepared according to GP5, brown oil (PE/ACOEt 90:10), 20% (42mg). ^{1}H NMR (400 MHz, $CDCl_3$) δ 7.91 (s, 1H), 7.37 (d, *J* = 8.5 Hz, 1H), 6.68 (d, *J* = 8.4 Hz, 1H), 4.24 (s, 1H), 4.12 (q, *J* = 7.1 Hz, 2H), 2.22 (s, 3H), 1.43 (s, 9H), 1.29 (t, *J* = 7.1 Hz, 3H). ^{13}C NMR (101 MHz, $CDCl_3$) δ 157.5, 153.1, 145.10, 139.0, 125.3, 112.5, 65.9, 58.3, 53.4, 50.8, 29.7, 29.3, 17.6, 14.9. IR (KBr, cm^{-1}): 3428, 3061, 2918, 1739, 1650, 1646, 1485. HRMS (ESI) m/z: $[M+H]^+$ calcd for $C_{15}H_{22}N_5O_2$ 304.1773; found 304.2514.

Ethyl 5-(tert-butylamino)-1-(5-chloropyridin-2-yl)-1H-1,2,3-triazole-4-carboxylate 3.397d

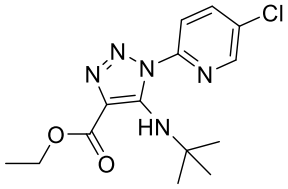

Prepared according to GP5, brown oil (PE/ACOEt 95:05), 40% (45 mg).^{1}H NMR (400 MHz, $CDCl_3$) δ 8.05 (s, 1H), 7.50 (dd, *J* = 8.9, 2.3 Hz, 1H), 6.71 (d, *J* = 8.8 Hz, 1H), 4.27 (s, 1H), 4.12 (q, *J* = 7.1 Hz, 2H), 1.43 (s, 9H), 1.29 (t, *J* = 7.2 Hz, 3H). ^{13}C NMR (101 MHz, $CDCl_3$) δ 156.8, 153.3, 144.1, 138.0, 123.3, 113.9, 66.8, 58.5, 51.0, 29.7, 29.2, 14.8. IR (KBr, cm^{-1}): 3438, 3021, 2917, 1736, 1651, 1636, 1455. HRMS (ESI) m/z: $[M]^+$ calcd for $C_{14}H_{18}ClN_5O_2$ 323.6227; found 323.6966.

Ethyl 5-(butylamino)-1-(5-chloropyridin-2-yl)-1H-1,2,3-triazole-4-carboxylate 3.397e

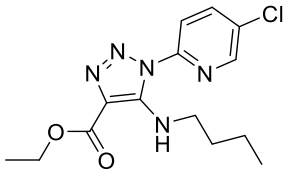

Prepared according to GP5, yellow solid (PE/ACOEt 95:05), 65% (50 mg).^{1}H NMR (400 MHz, $CDCl_3$) δ 8.07 (s, 1H), 7.54 – 7.47 (m, 1H), 6.73 (d, *J* = 8.8 Hz, 1H), 4.12 (q, *J* = 7.2 Hz, 3H), 3.11 (dd, *J* = 12.3, 6.6 Hz, 1H), 1.73 – 1.52 (m, 4H), 1.43 (td, *J* = 14.7, 7.3 Hz, 2H), 0.97 (t, *J* = 7.3 Hz, 3H). ^{13}C NMR (101 MHz, $CDCl_3$) δ 158.3, 153.2, 144.3, 138.1, 113.7, 63.8, 58.4, 41.8, 30.6, 29.7, 20.2, 14.7, 13.7. IR (KBr, cm^{-1}): 3438, 3021, 2917, 1736, 1651, 1636, 1455. HRMS (ESI) m/z: $[M]^+$ calcd for $C_{14}H_{18}ClN_5O_2$ 323.1149; found 323.5312.

2-(4-(piperidin-1-yl)-1H-1,2,3-triazol-1-yl)pyridine 3.397f

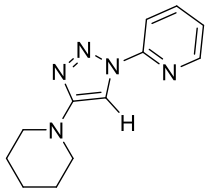

Prepared according to GP5, yellow oil (DCM/ACOEt 40:60), 20% (20 mg).^{1}H NMR (400 MHz, $CDCl_3$) δ 9.01 (s, 1H), 8.54 (d, *J* = 4.6 Hz, 1H), 8.20 (d, *J* = 8.2 Hz, 1H), 7.95 (t, *J* = 7.8 Hz, 1H), 7.42 – 7.35 (m, 1H), 4.09 (s, 3H), 3.76 (s, 3H), 3.58 – 3.39 (m, 2H), 3.35 – 3.22 (m, 2H). ^{13}C NMR (101 MHz, $CDCl_3$) δ 159.8, 148.8, 144.7, 139.2, 124.9, 124.0, 113.8, 48.1, 46.8, 43.8, 40.6. IR (KBr, cm^{-1}): 3425, 3027, 2927, 1475. HRMS (ESI) m/z: $[M+H]^+$ calcd for $C_{12}H_{16}N_5$ 230.1206; found 230.1292.

2-(5-(piperidin-1-yl)-1H-1,2,3-triazol-1-yl)pyridine 3.397g

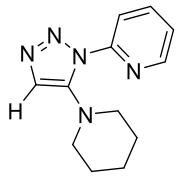

Prepared according to GP5, yellow oil (DCM/ACOEt 20:80), 30% (25mg).^{1}H NMR (400 MHz, $CDCl_3$) δ 8.87 (d, *J* = 7.1 Hz, 1H), 7.54 (t, *J* = 7.7 Hz, 1H), 7.27 (d, *J* = 3.5 Hz, 1H), 6.83 (t, *J* = 6.8 Hz, 1H), 5.65 (s, 1H), 3.66 (d, *J* = 5.2 Hz, 3H), 1.69 (d, *J* = 5.0 Hz, 3H), 1.63 (d, *J* = 4.8 Hz, 4H). ^{13}C NMR (101 MHz, $CDCl_3$) δ 160.6, 158.8, 150.5, 136.1, 127.5, 124.2, 112.1, 80.9, 45.5, 25.6, 24.6. IR (KBr, cm^{-1}): 3425, 3027, 2927, 1475. HRMS (ESI) m/z: $[M+H]^+$ calcd for $C_{12}H_{16}N_5$ 230.1206; found 230.1292.

Ethyl 5-(diethylamino)-1-(3-methoxypyridin-2-yl)-1H-1,2,3-triazole-4-carboxylate 3.397h

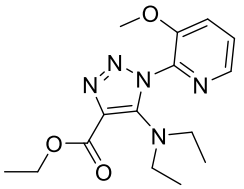

Prepared according to GP5, yellow oil (DCM/ACOEt 80:20), 10% (5mg). ^{1}H NMR (400 MHz, $CDCl_3$) δ 8.89 (d, *J* = 6.8 Hz, 1H), 6.75 (t, *J* = 7.2 Hz, 1H), 6.67 (d, *J* = 7.8 Hz, 1H), 4.41 (q, *J* = 7.2 Hz, 2H), 4.00 (s, 3H), 3.58 (q, *J* = 7.0 Hz, 4H), 1.41 (dd, *J* = 21.0, 13.9 Hz, 4H), 1.19 (t, *J* = 7.1 Hz, 3H). IR (KBr, cm^{-1}): 3436, 3017, 2917, 1475, 1123. HRMS (ESI) m/z: $[M+H]^+$ calcd for $C_{15}H_{22}N_5O_3$ 320.1723; found 320.2213.

N.B ^{13}C NMR was impossible to obtain due to the very low quantity of product arising from the reaction.

3.5.2 General procedure for the C-H activation of triazoles 2.80a-e *via* palladium catalysis (GP6).[455]

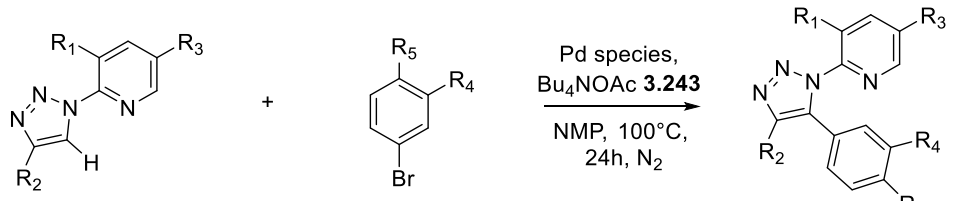

2.80a, R_1=H, R_2=COOEt, R_3=H
2.80b, R_1=H, R_2=$(CH_2)_4$COOH, R_3=H
2.80c, R_1=OCH_3, R_2=COOEt, R_3=H
2.80d, R_1=H, R_2=COOEt, R_3=CH_3
2.80e, R_1=H, R_2=COOEt, R_3=Cl

3.403, R_5=OCH_3, R_4=H
3.404, R_5=CF_3, R_4=H
3.405, R_5=H, R_4=CH_3

Palladium species:

3.89: $Pd(OAc)_2$,
3.406:$PdCl_2(PPh_3)_2$,
3.407: *i*PEPPSI,
3.408: $Pd(C_5H_7O_2)_2$,
3.409: $Pd(OTf)_2$

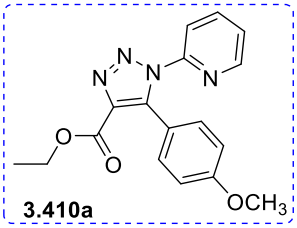

3.410a

To a round bottom flask equipped with a magnetic stirring bar were added the following: triazoles **2.80a-e** (1 equiv., 0.5 mmol), palladium species **3.89** and **3.406-3.409** (0.05 equiv., 0.025 mmol) and tetrabutylammonium acetate **3.243** (Bu_4NOAc, 2 equiv., 1 mmol) under nitrogen atmosphere. NMP (0.5 M) was then added, followed by the aryl bromides **3.403-3.405** (1.5 equiv., 0.75 mmol). The reaction mixture was stirred at 100°C for 24 hours. The day after, TLC (DCM/AcOEt 90:10) showed complete consumption of the starting material only when reacting triazole **2.80a** with aryl bromide **3.403**. The crude was then diluted with ethyl acetate, washed twice with H_2O/brine and dried over anhydrous sodium sulfate Na_2SO_4. Further purification occurred *via* column chromatography and the only product **3.410a** (DCM/AcOEt 90:10) was obtained in low yields.

Ethyl 5-(4-methoxyphenyl)-1-(pyridin-2-yl)-1H-1,2,3-triazole-4-carboxylate 3.410a

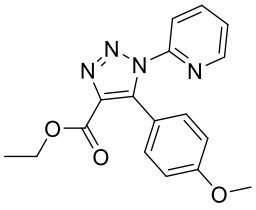

Prepared according to GP6, yellow oil (DCM/AcOEt 90:10), 5% (4mg). ^{1}H NMR (400 MHz, $CDCl_3$) δ 8.47 (d, *J* = 4.7 Hz, 1H), 7.86 (t, *J* = 7.8 Hz, 1H), 7.52 (d, *J* = 8.0 Hz, 1H), 7.37 (dd, *J* = 12.4, 5.2 Hz, 1H), 7.29 (d, *J* = 8.5 Hz, 2H), 6.88 (d, *J* = 8.6 Hz, 2H), 4.39 (q, *J* = 7.1 Hz, 2H), 3.82 (s, 3H), 1.39 – 1.35 (m, 3H). ^{13}C NMR (101 MHz, $CDCl_3$) δ 161.0, 160.6, 149.2, 140.3, 138.8, 135.3, 131.7, 128.8, 124.6, 120.1, 117.6, 113.6, 61.2, 55.2, 14.2. IR (KBr, cm^{-1}): 3436, 3017, 2917, 1436, 1075,

HRMS (ESI) m/z: $[M+H]^+$ calcd for $C_{17}H_{17}N_4O_3$ 325.3480; found 325.4199.

3.5.3 Synthesis of tert-butyl (R)-2-(hydroxymethyl)pyrrolidine-1-carboxylate 3.433.[530]

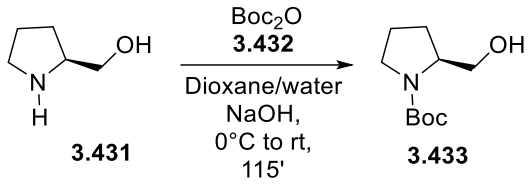

D-prolinol (**3.431**, 1 equiv., 10.4 mmol, 1.02 mL) was dissolved in a mixture of dioxane/water (20.8 ml and 15.6 ml respectively) and a 2 M solution of aqueous NaOH (5.2 mL). The solution was then cooled down to 0°C in an ice bath for 15 minutes and addition of Boc-anhydride **3.432** (1.1 equiv., 11.4 mmol, 2.5 g) then followed. After all the reagents dissolved, the ice bath was removed and the reaction stirred at room temperature until consumption of **3.431** (ca 100 min). Once TLC (DCM/AcOEt 70:30) showed complete consumption of **3.431**, the reaction was stopped and the solvent evaporated under reduced pressure. The crude was then washed with AcOEt/H_2O twice, the organic layers collected, dried over anhydrous Na_2SO_4 and concentrated upon removal of the solvent by rotary evaporation to yield the product **3.433** as colourless oil (98% yield, 1.97 g) without further purification needed. *N.B.* the product **3.433** solidified upon treatment with vacuum pump overnight and NMR double signals highlight the presence of two rotamers because of the Boc protecting group presence. ^{1}H NMR (400 MHz, $CDCl_3$) δ 4.78 (d, *J* = 6.1 Hz, 1H), 3.96 (s, 1H), 3.70 (s, 2H), 3.62 (dd, *J* = 18.8, 9.7 Hz, 3H), 3.52 – 3.38 (m, 1H), 3.39 – 3.21 (m, 2H), 2.07 – 1.94 (m, 2H), 1.80 (ddt, *J* = 18.9, 12.6, 6.3 Hz, 3H), 1.53 (s, 5H), 1.47 (s, 13H). ^{13}C NMR (101 MHz, $CDCl_3$) δ 157.1, 146.7, 85.1, 80.1, 67.6, 67.0, 60.1, 47.5, 28.6, 28.4, 27.7, 27.3, 24.0. All analytical data are consistent with those reported in literature.[530]

3.5.4 Synthesis of (R)-(1-tosylpyrrolidin-2-yl)methanol 3.444.[531]

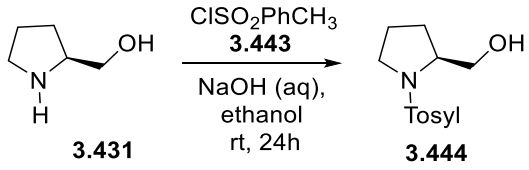

D-prolinol **3.431** (1 equiv., 10.1 mmol, 1 mL) was dissolved in ethanol (0.25 M, 40 mL) and a 1.5 M solution of aqueous NaOH (6.7 mL). Tosyl chloride **3.443** was then added and the reaction mix stirred at room temperature for 24 hours. The day after, TLC (PE/AcOEt 60:40) showed complete consumption of **3.431**. Therefore, the crude was washed with diethyl ether and water, the organic

phase collected and acidified with HCl 1 M until pH 2-3. A further extraction with AcOEt occurred to dissolve the product **3.444** in the organic phase. Further purification *via* column chromatography (100% AcOEt) occurred to yield the product as yellow oil in average yields (45%, 1.16 g). ^{1}H NMR (400 MHz, $CDCl_3$) δ 7.74 (d, *J* = 7.8 Hz, 1H), 7.34 (d, *J* = 7.8 Hz, 1H), 3.77 – 3.56 (m, 2H), 3.51 – 3.40 (m, 1H), 3.35 – 3.19 (m, 1H), 2.75 (s, 1H), 2.44 (s, 2H), 1.86 – 1.71 (m, 1H), 1.69 (dd, *J* = 13.1, 6.5 Hz, 1H), 1.50 – 1.36 (m, 1H). ^{13}C NMR (101 MHz, $CDCl_3$) δ 143.8, 133.9, 129.8, 127.6, 65.9, 61.8, 50.0, 28.9, 24.2, 21.5. All analytical data are consistent with those reported in literature.[531]

3.5.5 General procedure for the synthesis of proline-based aldehydes 3.435 and 3.445 (GP7).[532]

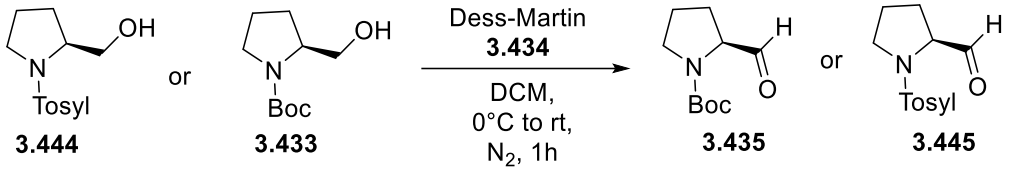

To a solution of **3.433** or **3.444** (1 equiv. 0.5 mmol and 2 mmol respectively) in DCM (0.5 M), previously cooled down to 0°C, the Dess-Martin reagent **3.434** (1.5 equiv., 3.75 mmol and 3 mmol respectively) was added under nitrogen atmosphere. The reaction stirred for 10 minutes at 0°C and for 1 hour at room temperature. After 1 hour, TLC (DCM/AcOEt 70:30) showed complete consumption of the starting materials **3.433** and **3.444**. The crude was then filtered through a celite pad, to separate the organic phase from the unreacted Dess-Martin reagent **3.434**, and further purified *via* column chromatography.

Tert-butyl (R)-2-formylpyrrolidine-1-carboxylate 3.435

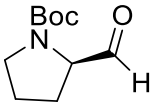

Prepared according to GP7, colorless oil (DCM/AcOEt 90:10), 82% (407.2 mg). ^{1}H NMR (400 MHz, $CDCl_3$) δ 9.56 (s, 1H), 9.46 (s, 2H), 4.23 – 4.17 (m, 1H), 4.05 (t, *J* = 5.2 Hz, 2H), 3.60 – 3.39 (m, 6H), 2.19 – 1.80 (m, 14H), 1.48 (s, 12H), 1.43 (s, 18H). ^{13}C NMR (101 MHz, $CDCl_3$) δ 200.6, 200.4, 171.1, 154.9, 153.9, 80.6, 80.2, 65.0, 64.8, 60.4, 53.4, 46.8, 46.7, 29.7, 28.4, 28.2, 28.0, 27.7, 26.7, 24.6, 23.9, 21.0, 14.2. All analytical data are consistent with those reported in literature.[532]

N.B. NMR double signals highlight the presence of two rotamers because of the Boc protecting group presence.

(R)-(1-tosylpyrrolidin-2-yl)methanol 3.445

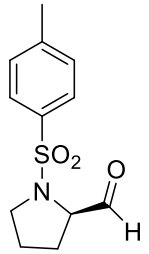

Prepared according to GP7, yellow oil (PE/AcOEt 40:60), 65% (330 mg). ^{1}H NMR (400 MHz, $CDCl_3$) δ 9.69 (s, 1H), 7.73 (d, *J* = 7.8 Hz, 2H), 7.35 (d, *J* = 7.9 Hz, 2H), 3.83 (t, *J* = 6.6 Hz, 1H), 3.64 – 3.50 (m, 1H), 3.19 (dd, *J* = 16.7, 7.5 Hz, 1H), 2.45 (s, 3H), 2.07 (td, J = 10.9, 5.1 Hz, 1H), 1.88 – 1.74 (m, 2H), 1.66 (dd, *J* = 11.6, 5.4 Hz, 1H). ^{13}C NMR (101 MHz, $CDCl_3$) δ 200.2, 144.1, 133.5, 129.9, 127.7, 66.5, 49.1, 27.5, 24.7, 21.6. All analytical data are consistent with those reported in literature.[532]

3.5.6 General procedure for the synthesis of proline-based β-ketoesters 3.437 and 3.446 (GP8).[533]

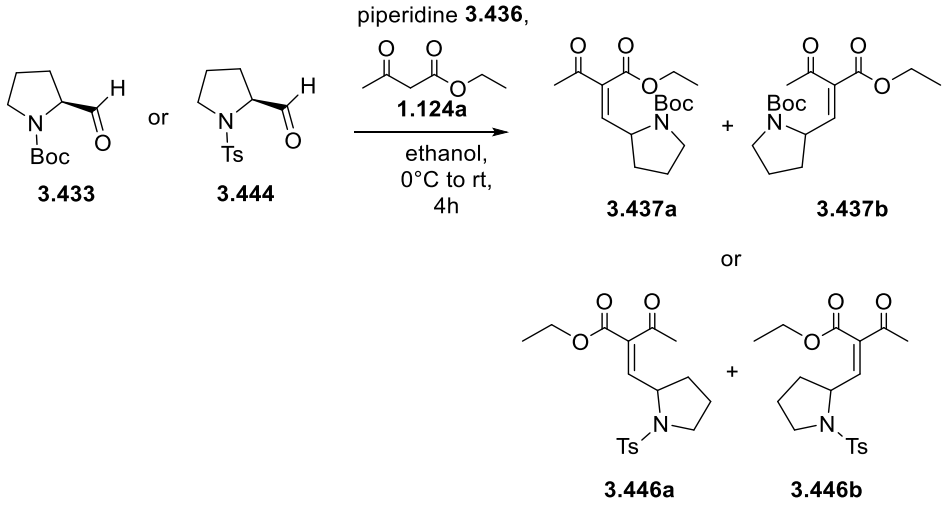

To a solution of β-ketoester **1.124a** (1 equiv., 0.5 mmol) in ethanol (1 M), previously cooled down to 0°C, piperidine **3.436** (0.05 equiv. 0.025 mmol) and aldehydes **3.435** or **3.445** (1 equiv., 0.5 mmol) were added. The reaction was monitored via TLC (DCM/AcOEt 70:30) analysis and showed complete consumption after 4 hours for both aldehydes **3.435** and **3.445**. The crude was, then, washed with diethyl ether and water three times. The organic phases were separated, collected and dried over anhydrous Na_2SO_4. Finally, the solvent was evaporated by rotary evaporation to yield product **3.437**, used directly in the next step of reaction due to the impossibility to separate the two Boc rotamers, and product **3.446** after further purification *via* column

cromatography (DCM/AcOEt 80:20).

Tert-butyl (R,E)-2-(2-(ethoxycarbonyl)-3-oxobut-1-en-1-yl)pyrrolidine-1-carboxylate 3.437

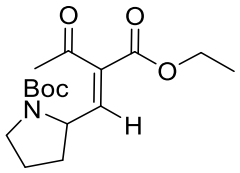

Prepared according to GP8, yellow oil, 75% (115.2 mg). ^{1}H NMR (400 MHz, $CDCl_3$) δ 6.76 (d, *J* = 7.9 Hz, 1H), 4.54 (d, *J* = 6.6 Hz, 1H), 4.31 (q, *J* = 6.6 Hz, 3H), 3.62 – 3.32 (m, 3H), 2.35 (s, 5H), 2.27 (d, *J* = 4.9 Hz, 2H), 2.01 – 1.71 (m, 5H), 1.42 (d, *J* = 14.1 Hz, 12H), 1.34 (t, *J* = 6.9 Hz, 3H). ^{13}C NMR (101 MHz, $CDCl_3$) δ 175.8, 165.7, 151.4, 134.4, 61.3, 56.4, 46.7, 32.9, 28.3, 27.5, 24.0, 14.1. IR (KBr, cm^{-1}): 3004, 1742, 1738, 1718, 1629; m.p. 157°C. HRMS (ESI) m/z: $[M+H]^+$ calcd for $C_{16}H_{26}NO_5$ 312.1811; found: 312.1835.

N.B. NMR double signals highlight the presence of two rotamers because of the Boc protecting group presence.

Ethyl (E)-3-oxo-2-((1-tosylpyrrolidin-2-yl)methylene)butanoate 3.446

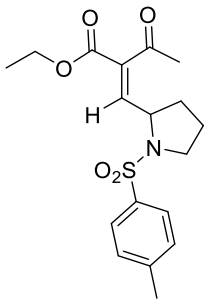

Prepared according to GP8, yellow oil (DCM/AcOEt 80:20) 60% (126 mg). ^{1}H NMR (400 MHz, $CDCl_3$) δ 7.62 (d, *J* = 7.7 Hz, 1H), 7.30 (d, *J* = 7.9 Hz, 1H), 4.83 (d, *J* = 10.1 Hz, 1H), 4.42 (d, *J* = 6.9 Hz, 1H), 4.31 – 4.17 (m, 1H), 4.05 (q, *J* = 7.1 Hz, 1H), 3.44 (t, *J* = 10.3 Hz, 1H), 3.08 (dd, *J* = 25.6, 9.4 Hz, 1H), 2.44 (d, *J* = 8.4 Hz, 3H), 2.15 – 2.05 (m, 1H), 1.66 – 1.52 (m, 3H), 1.39 – 1.22 (m, 2H), 1.16 (t, *J* = 7.1 Hz, 1H). ^{13}C NMR (101 MHz, $CDCl_3$) δ 177.1, 172.9, 168.4, 143.7, 134.3, 129.8, 127.4, 98.1, 62.2, 61.2, 61.1, 60.9, 48.0, 41.1, 30.6, 28.6, 23.6, 21.5, 20.0, 14.3, 14.0. IR (KBr, cm^{-1}): 3014, 1732, 1738, 1718, 1624,1420, 1368; m.p. 97°C. HRMS (ESI) m/z: $[M+H]^+$ calcd for $C_{18}H_{24}NO_5S$ 366.2365; found: 366.2635.

N.B. NMR double signals highlight the presence of both stereoisomer arising from the non stereospecific addition of β-ketoester **1.124a** to aldehyde **3.445.**

3.5.7 General procedure for the reduction of proline-based β-ketoesters 3.437 and 3.446 (GP9).[534]

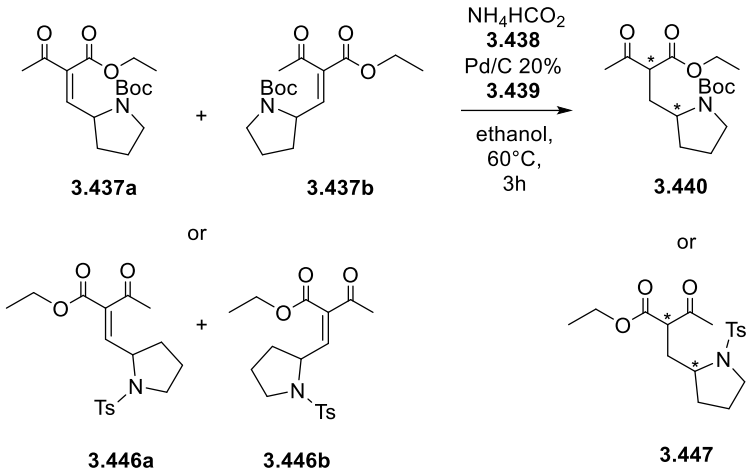

To a solution of proline-based β-ketoesters **3.437** and **3.446** (1 equiv. 0.37 mmol and 0.14 mmol respectively) in ethanol (0.3 M), palladium on carbon **3.439** (Pd/C 20% of the starting material weight) and ammonium formate **3.438** (NH_4HCO_2, 10 equiv. 3.7 mmol and 1.4 mmol respectively) were added. The reaction stirred at 60°C for 3 hours due to the complete consumption of the starting materials observed on TLC (PE/AcOEt 1:1). After cooling down the solution, the crude was filtrated to eliminate Pd/C and the solvent removed by rotary evaporation. Product **3.440** was used directly in the next step of reaction without further purification, due to the impossible separation of the two Boc rotamers, whereas product **3.447** was obtained after purification *via* column chromatography (DCM/AcOEt 70:30).

Tert-butyl 2-(2-(ethoxycarbonyl)-3-oxobutyl)pyrrolidine-1-carboxylate 3.440

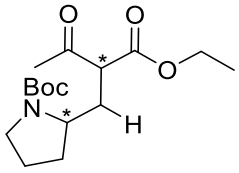

Prepared according to GP9, yellow oil, 78% (91 mg). ^{1}H NMR (400 MHz, $CDCl_3$) δ 4.29 – 4.07 (m, 4H), 3.95 (d, *J* = 9.7 Hz, 1H), 3.69 – 3.61 (m, 1H), 3.26 (t, *J* = 8.4 Hz, 1H), 2.35 (s, 3H), 1.95 – 1.78 (m, 2H), 1.41 (s, 9H), 1.33 – 1.23 (m, 6H). ^{13}C NMR (101 MHz, $CDCl_3$) δ 161.8, 142.0, 123.7, 82.8, 61.7, 53.4, 46.4, 32.9, 28.3, 28.0, 24.0, 17.4, 14.2. IR (KBr, cm^{-1}): 2851, 1731, 1737, 1728, 1368; m.p. 87°C. HRMS (ESI) m/z: $[M+H]^+$ calcd for $C_{16}H_{28}NO_5$ 314.1489; found: 314.1576.

N.B. NMR double signals highlight the presence of two rotamers because of the Boc protecting group presence

Ethyl 3-oxo-2-((1-tosylpyrrolidin-2-yl)methyl)butanoate 3.447

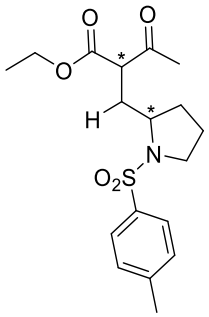

Prepared according to GP9, white solid (DCM/AcOEt 70:30) 72% (32.6 mg). ^{1}H NMR (400 MHz, $CDCl_3$) δ 7.63 (d, *J* = 7.4 Hz, 1H), 7.28 (dd, *J* = 16.4, 4.5 Hz, 1H), 4.32 – 4.13 (m, 3H), 3.64 (t, *J* = 7.4 Hz, 1H), 3.28 (t, *J* = 8.0 Hz, 1H), 3.09 (dd, *J* = 17.5, 8.5 Hz, 1H), 2.40 (t, *J* = 15.5 Hz, 3H), 2.32 (s, 2H), 1.90 (dd, *J* = 18.3, 10.4 Hz, 1H), 1.69 (d, *J* = 10.6 Hz, 1H), 1.48 (d, *J* = 7.1 Hz, 1H), 1.40 – 1.26 (m, 3H), 1.07 (dd, *J* = 20.1, 9.5 Hz, 1H). ^{13}C NMR (101 MHz, $CDCl_3$) δ 168.6, 168.0, 146.8, 145.5, 143.0, 135.3, 129.5, 127.4, 100.6, 100.1, 77.4, 77.1, 76.8, 64.0, 59.9, 59.7, 48.4, 37.1, 27.4, 23.8, 21.4, 19.6, 19.1, 14.4, 14.3. IR (KBr, cm^{-1}): 2861, 1731, 1737, 1736, 1368; m.p. 107°C. HRMS (ESI) m/z: $[M+H]^+$ calcd for $C_{18}H_{26}NO_5S$ 368.1532; found: 368.1783

N.B. NMR double signals highlight the presence of a mixture of diasteroisomers arising from the non-asymmetric reduction of **3.447**

Appendix: Copies of ^{1}H and ^{13}C Spectra

Compound 1.134a

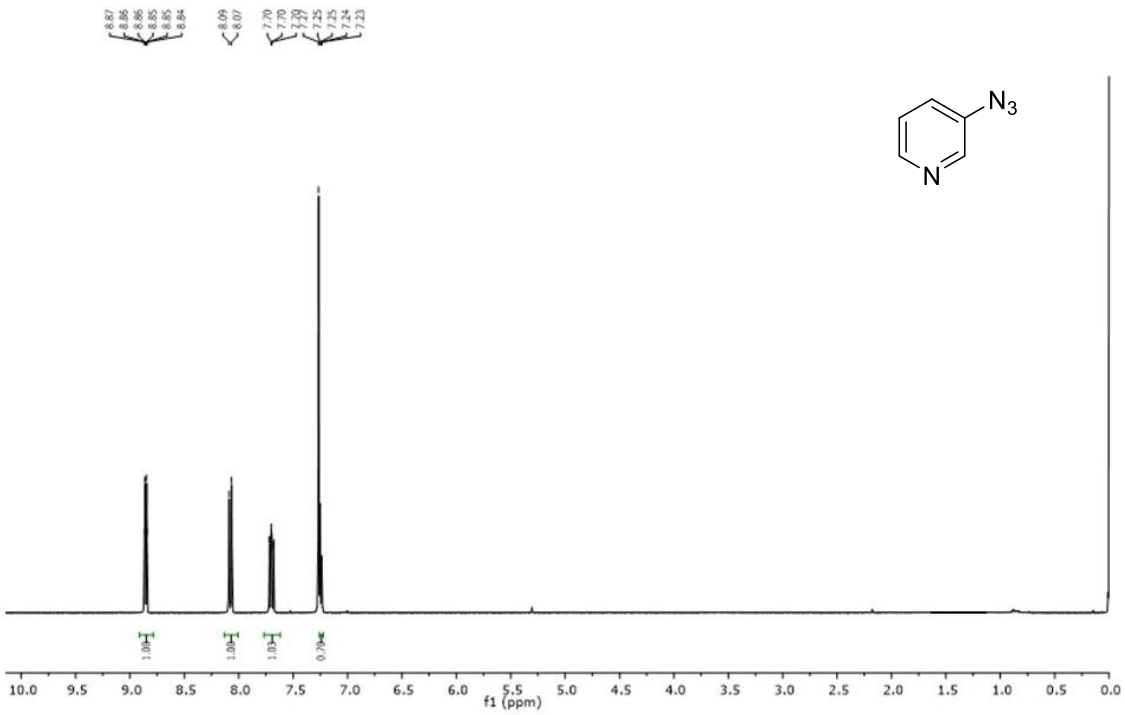

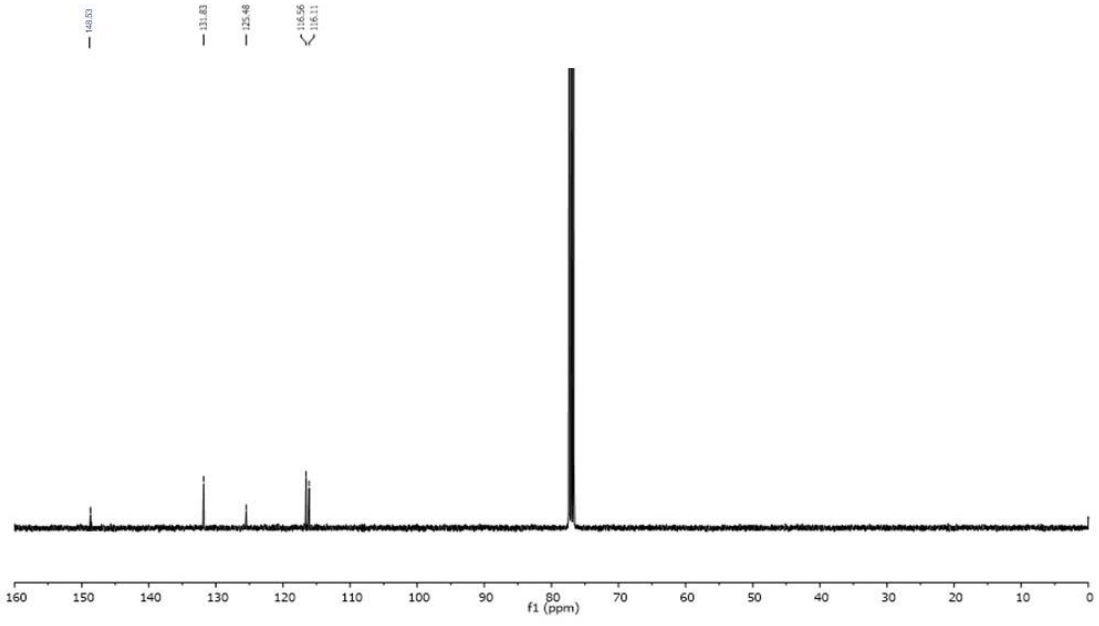

Compound 1.134b

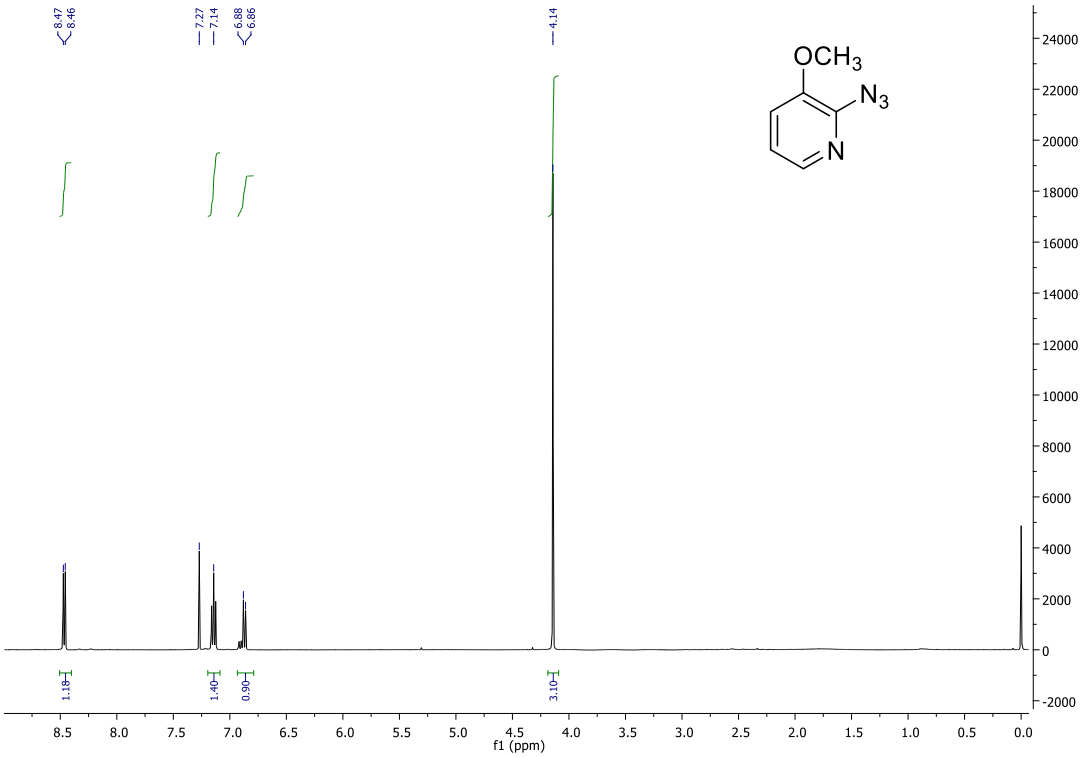

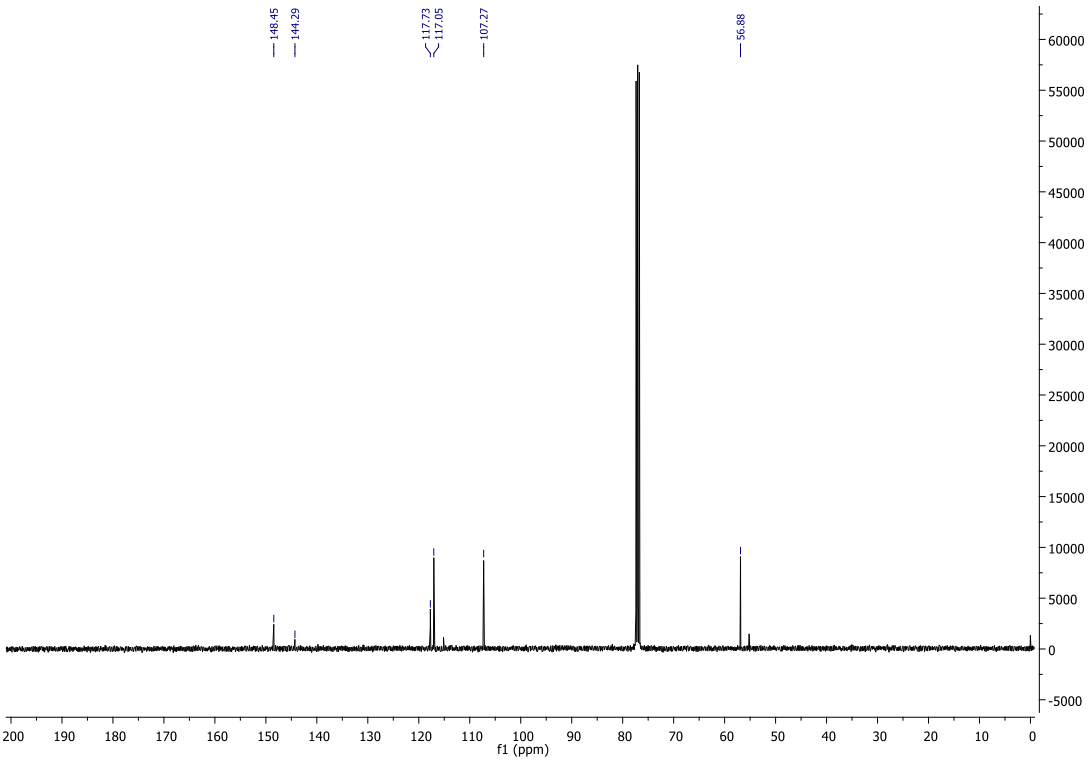

Compound 1.134c

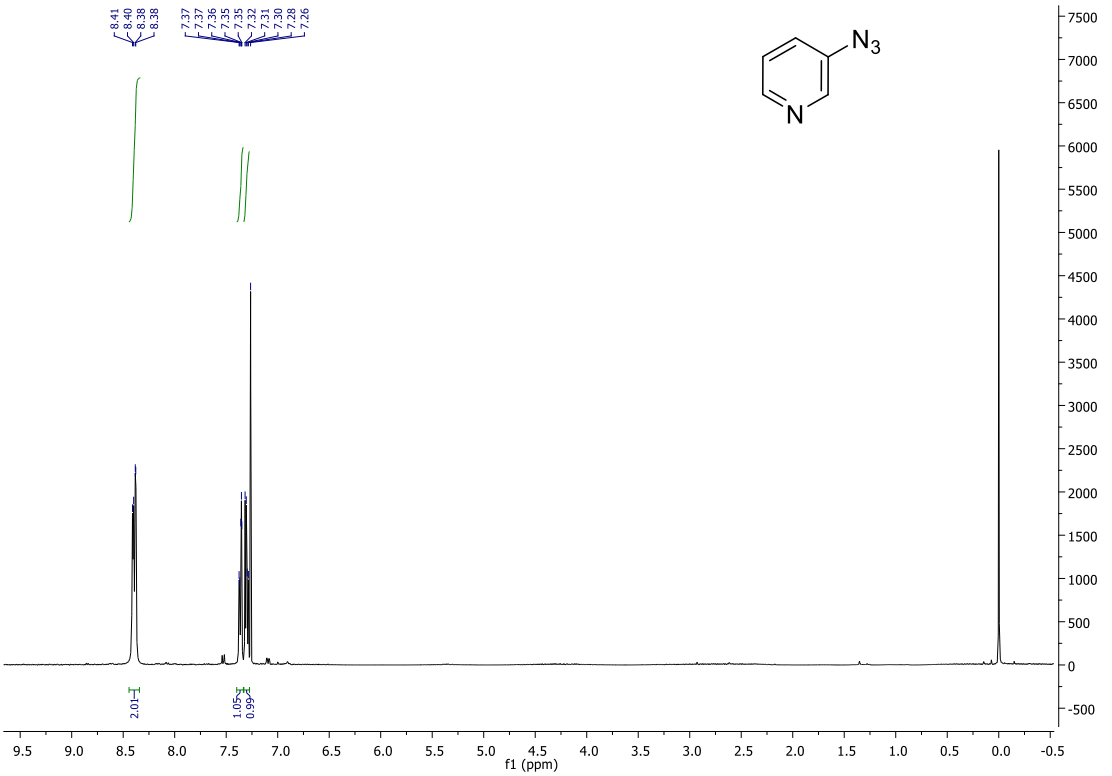

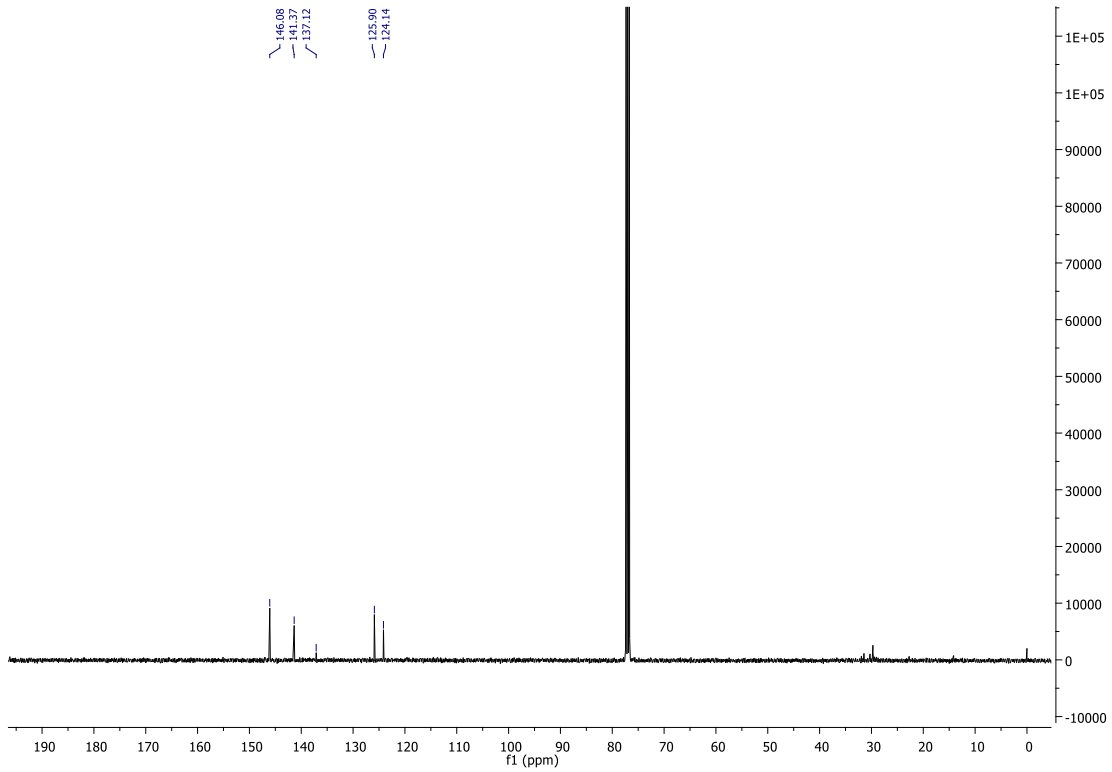

Compound 1.134d

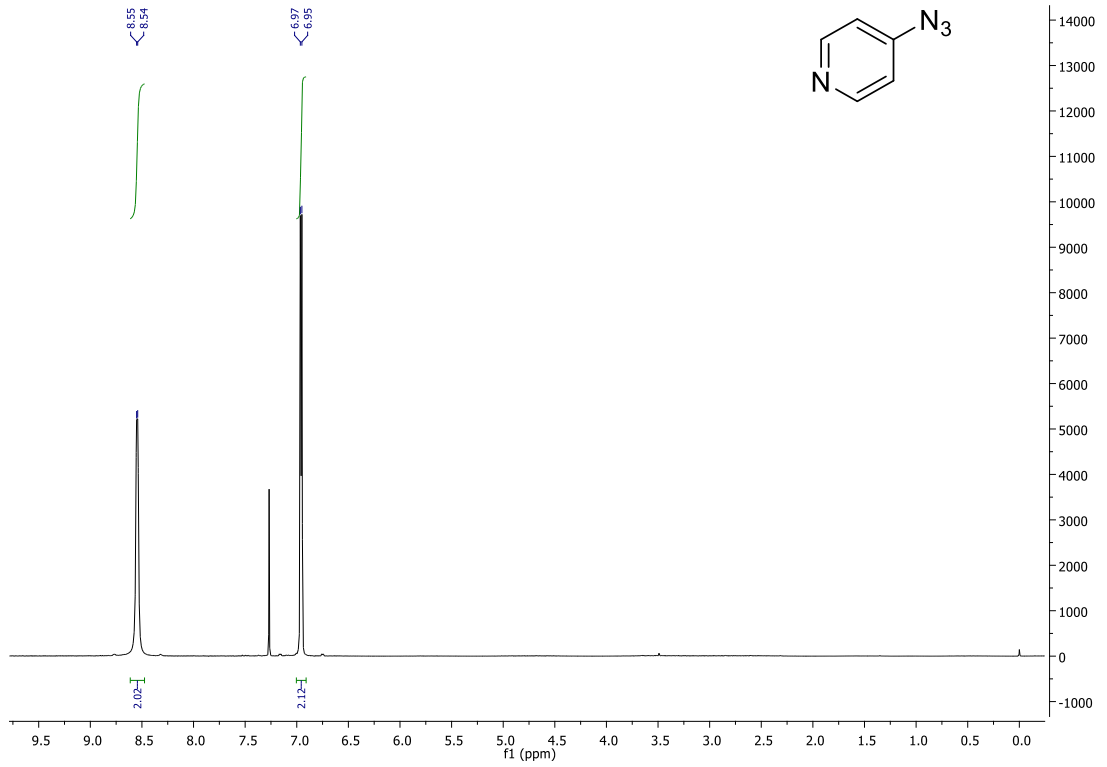

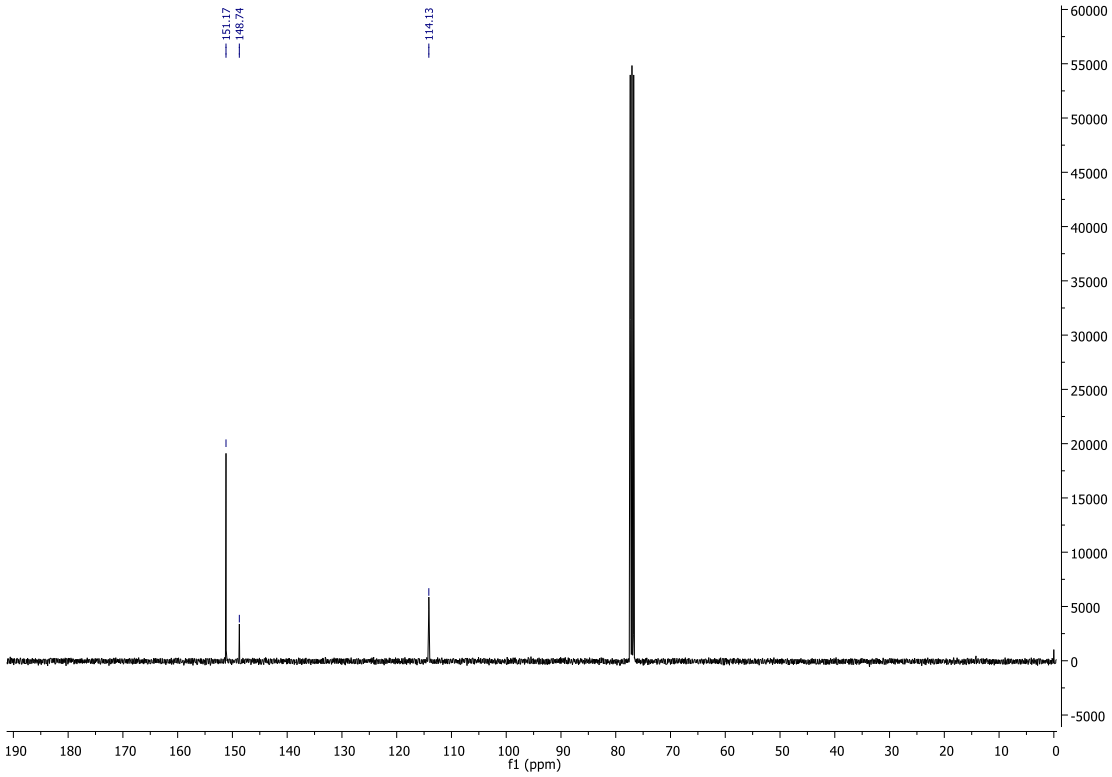

Compound 1.134e

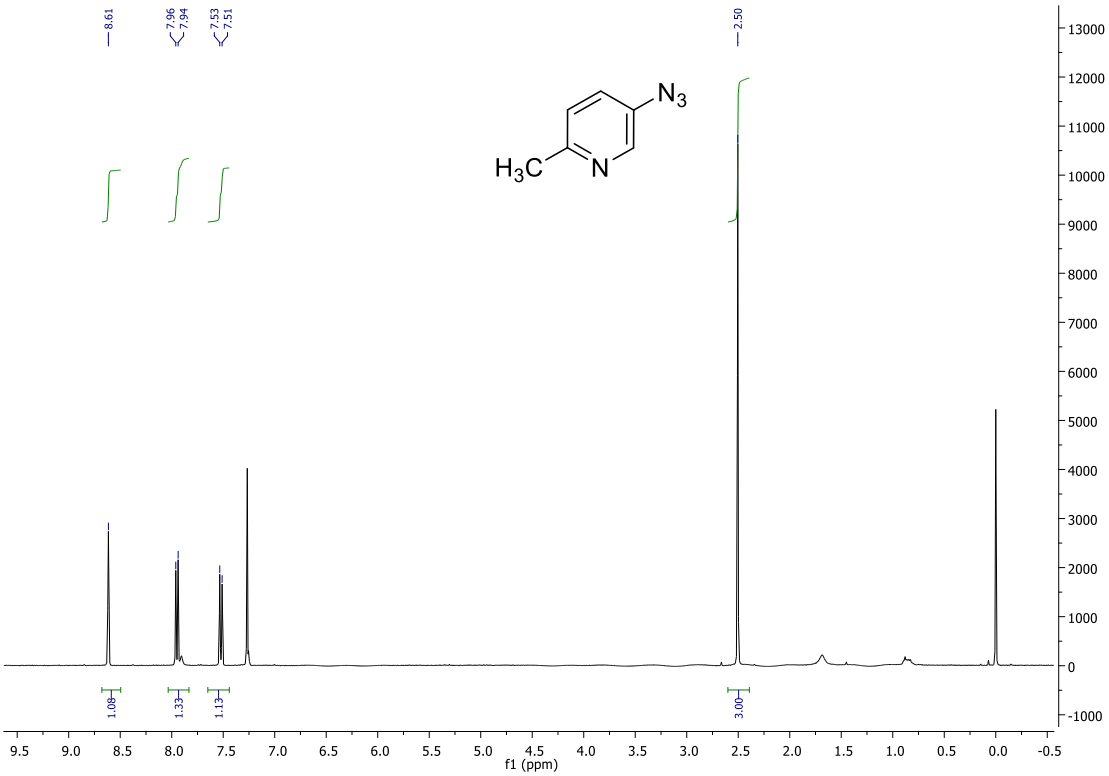

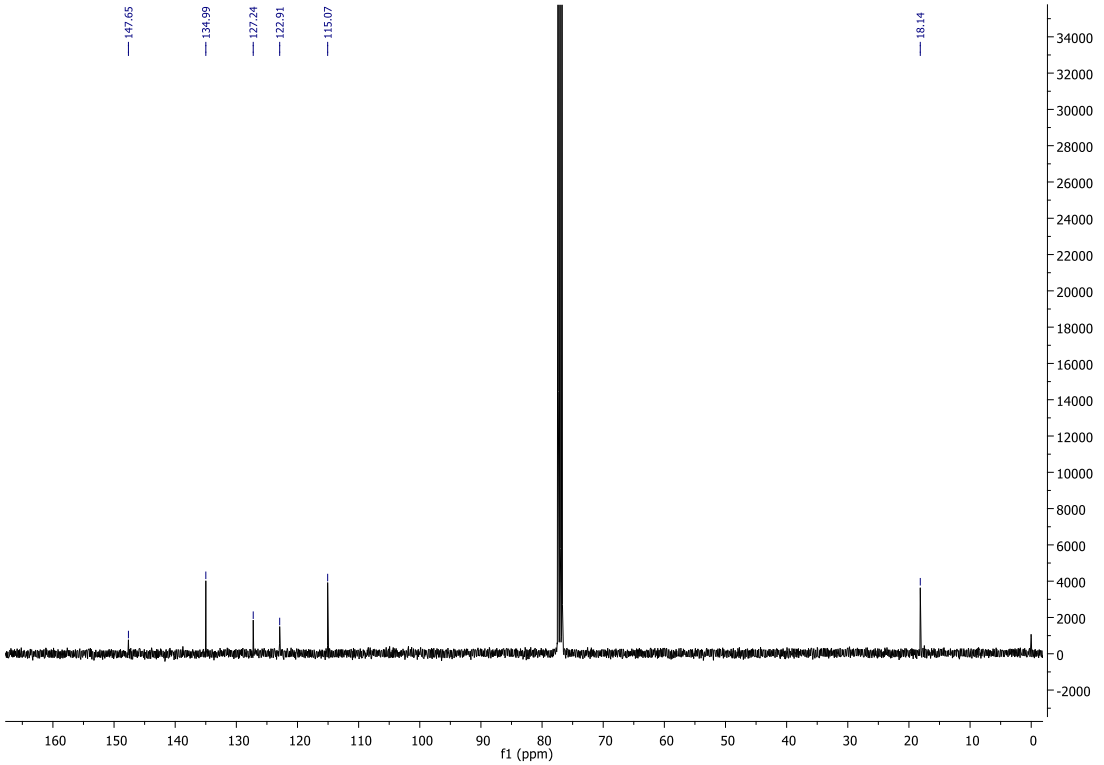

Compound 1.134f

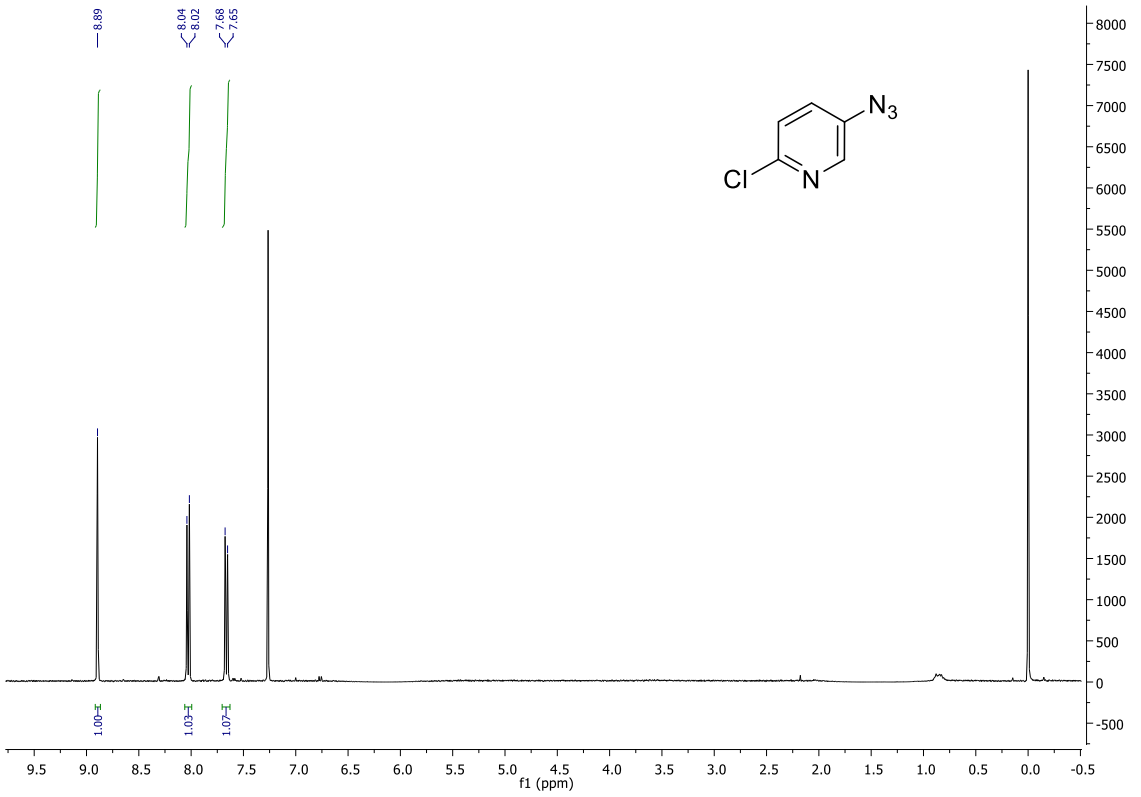

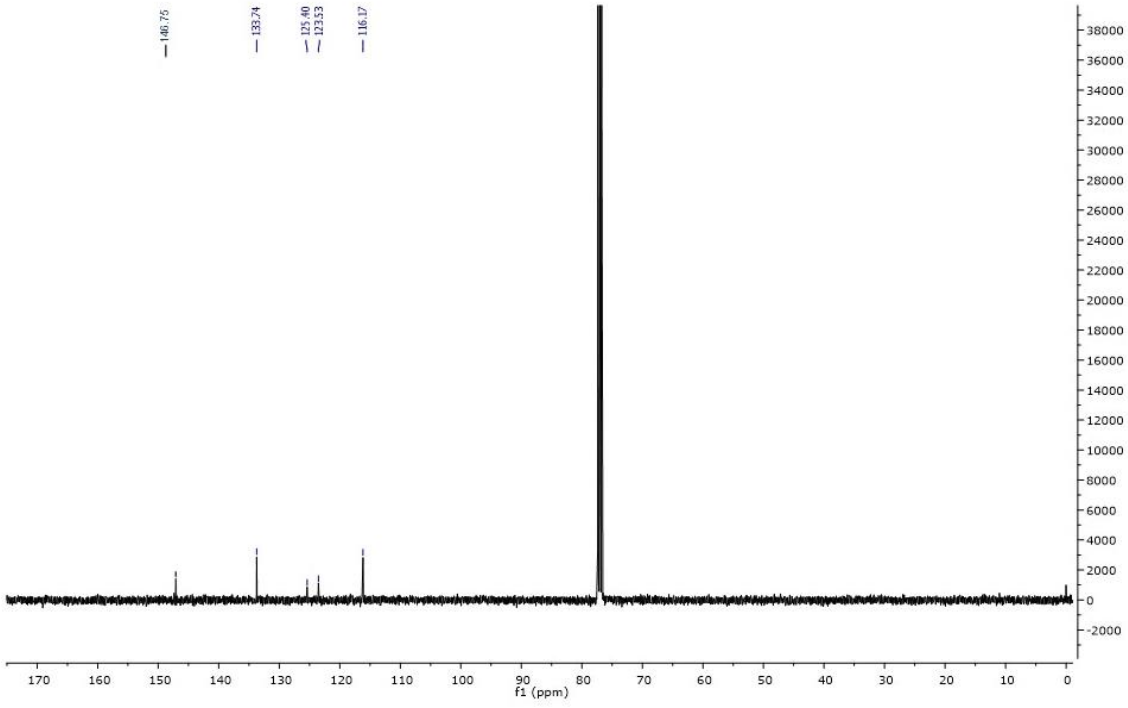

Compound 1.136a

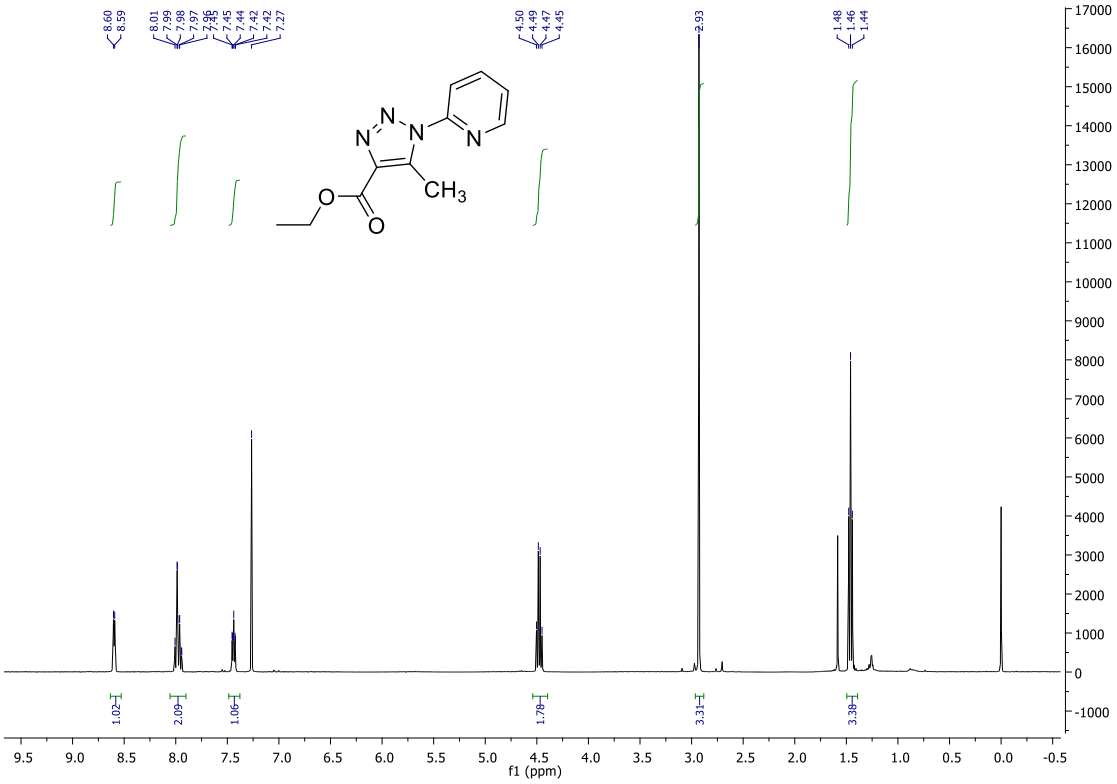

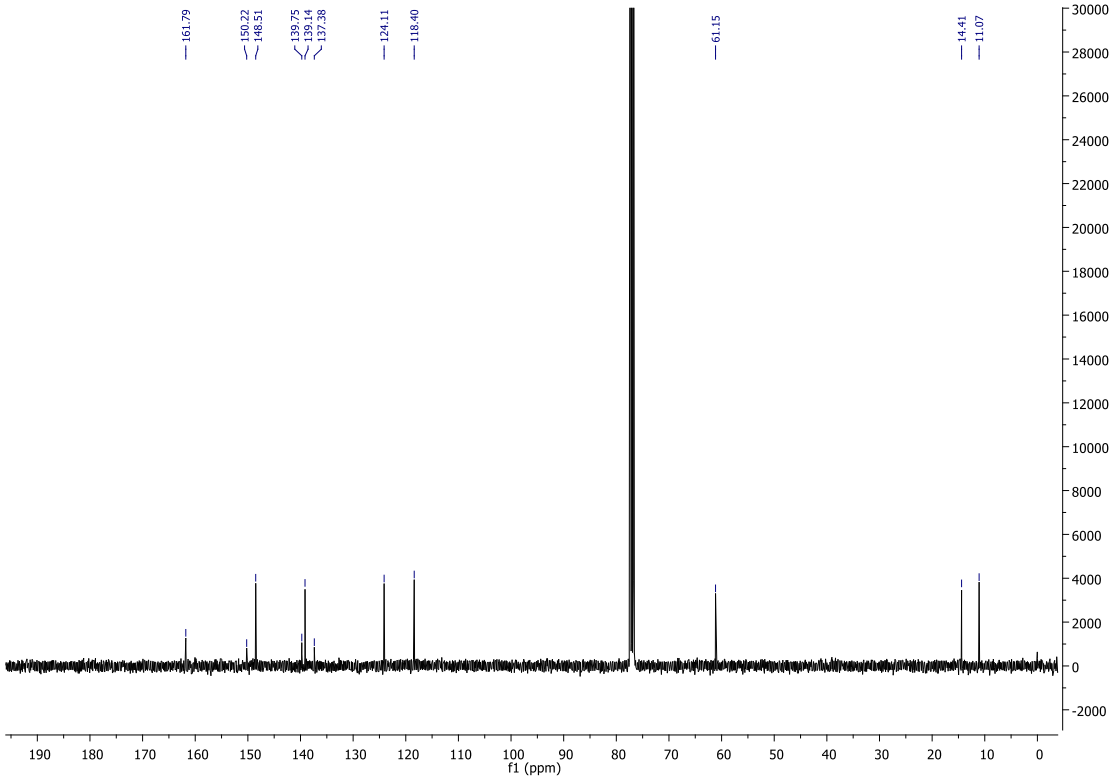

Compound 1.136b

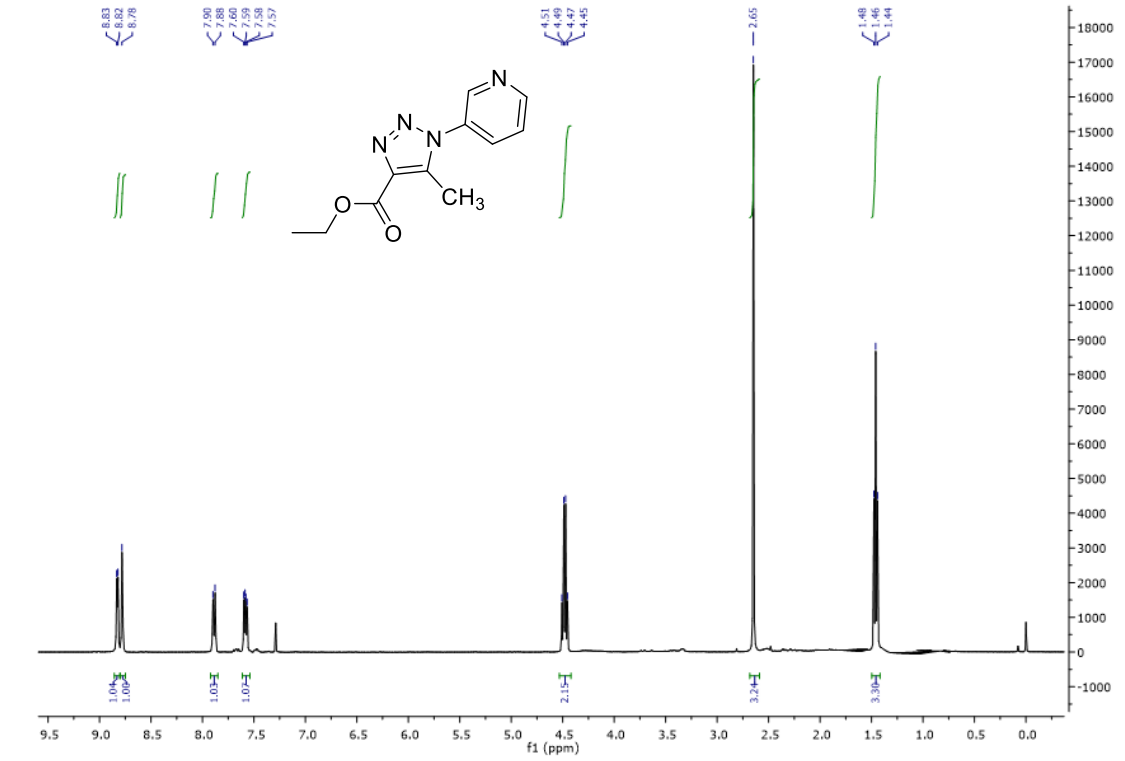

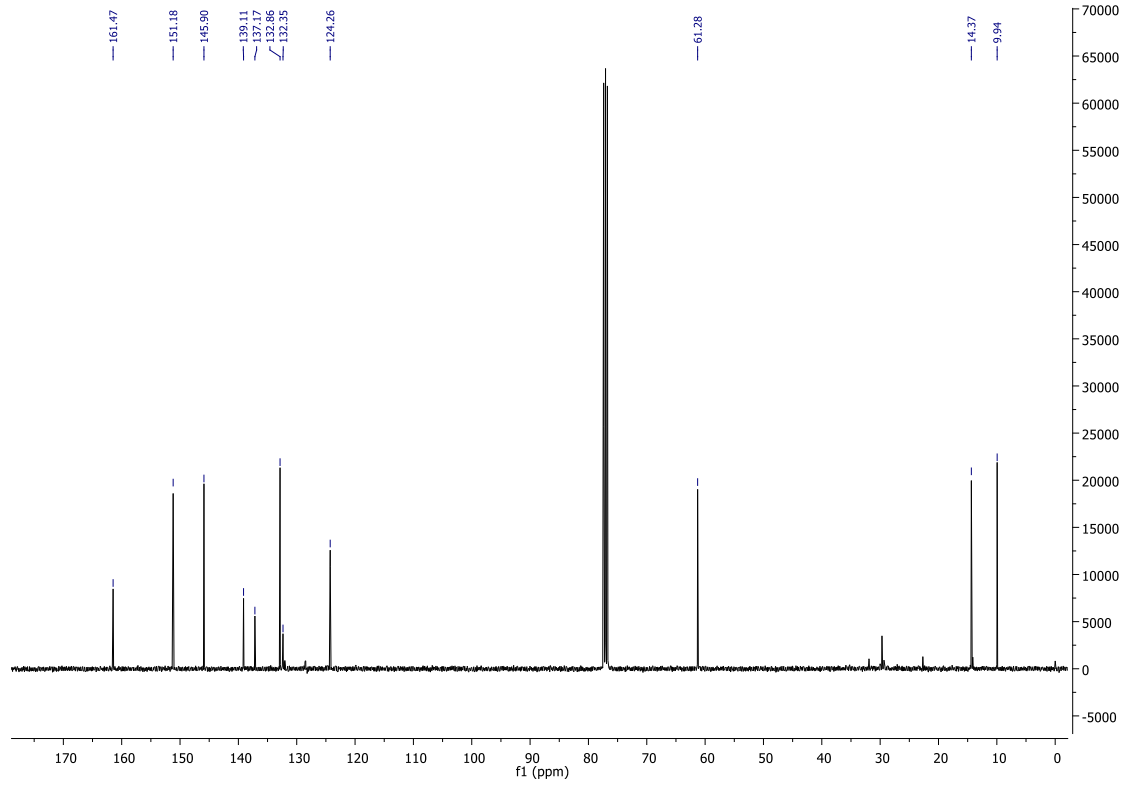

Compound 1.136c

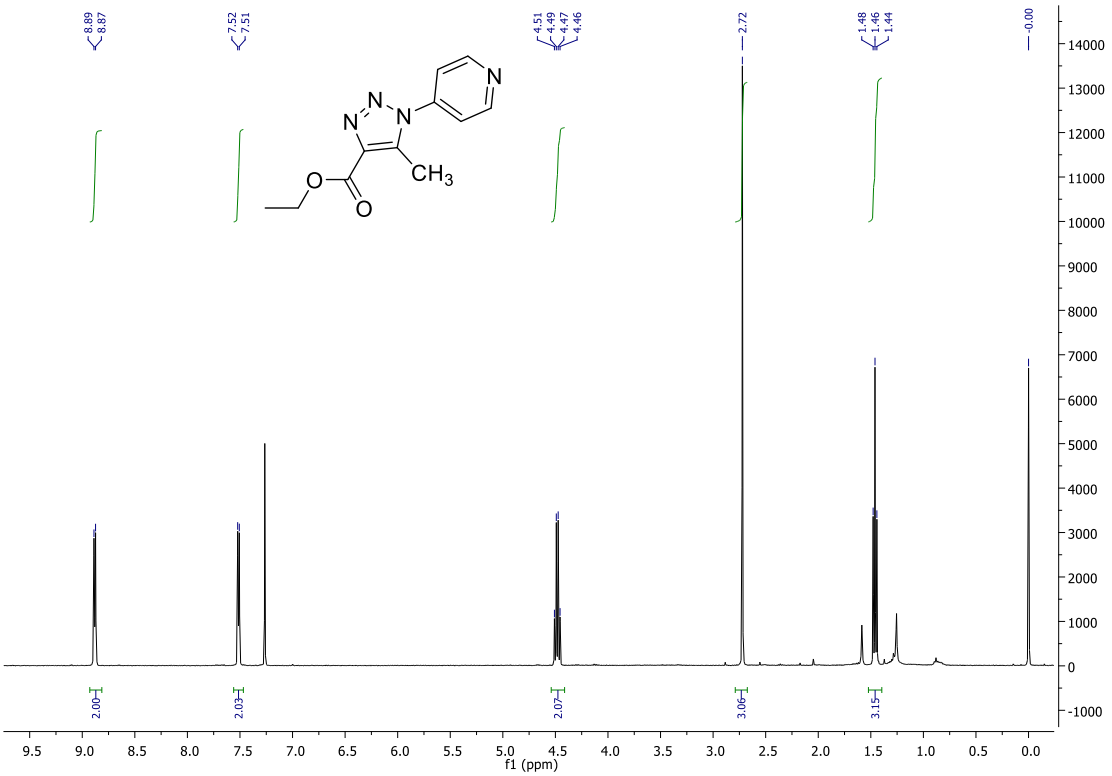

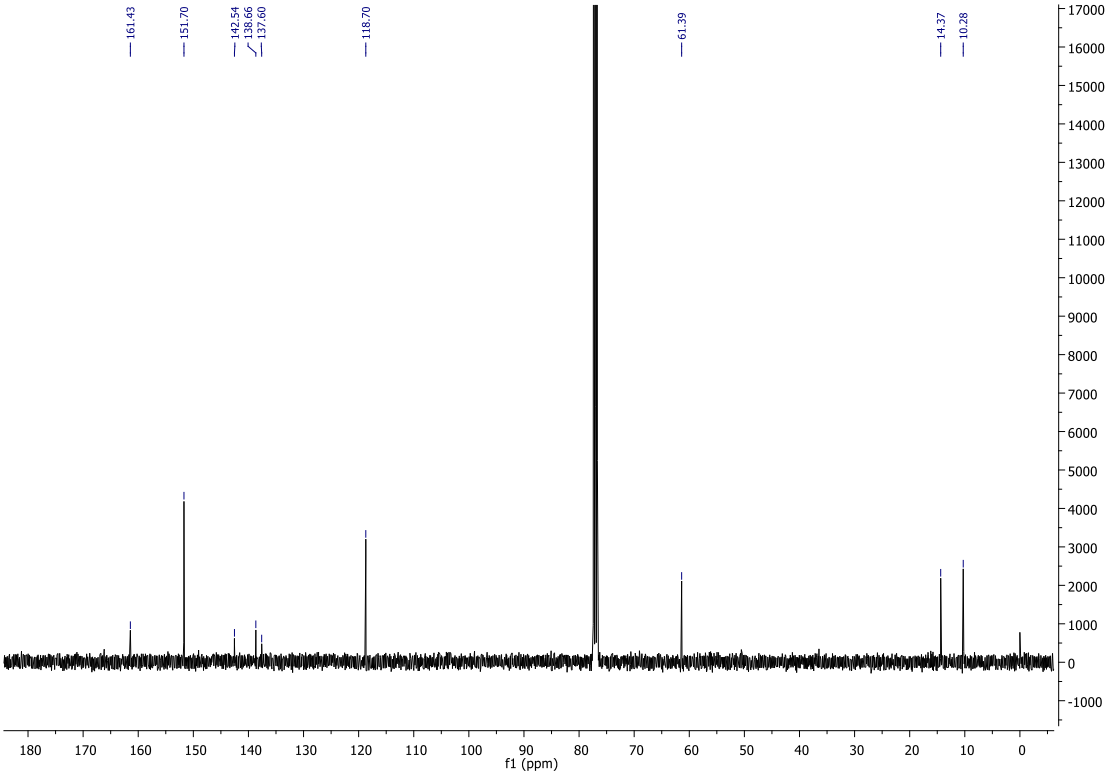

Compound 1.137

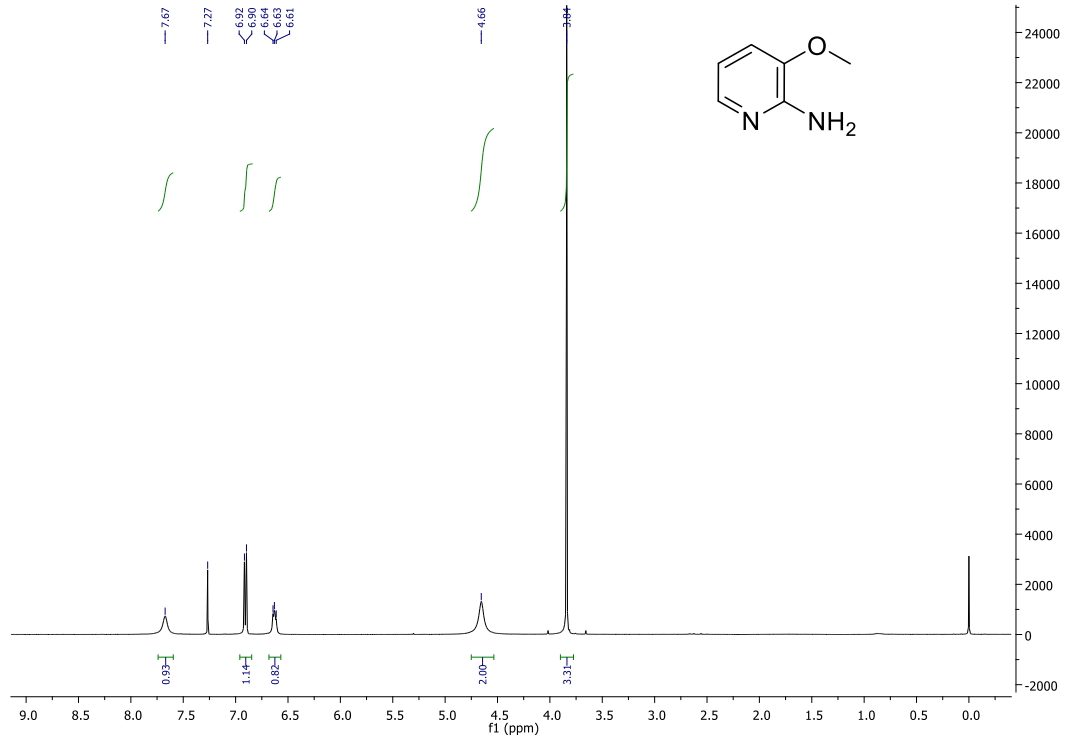

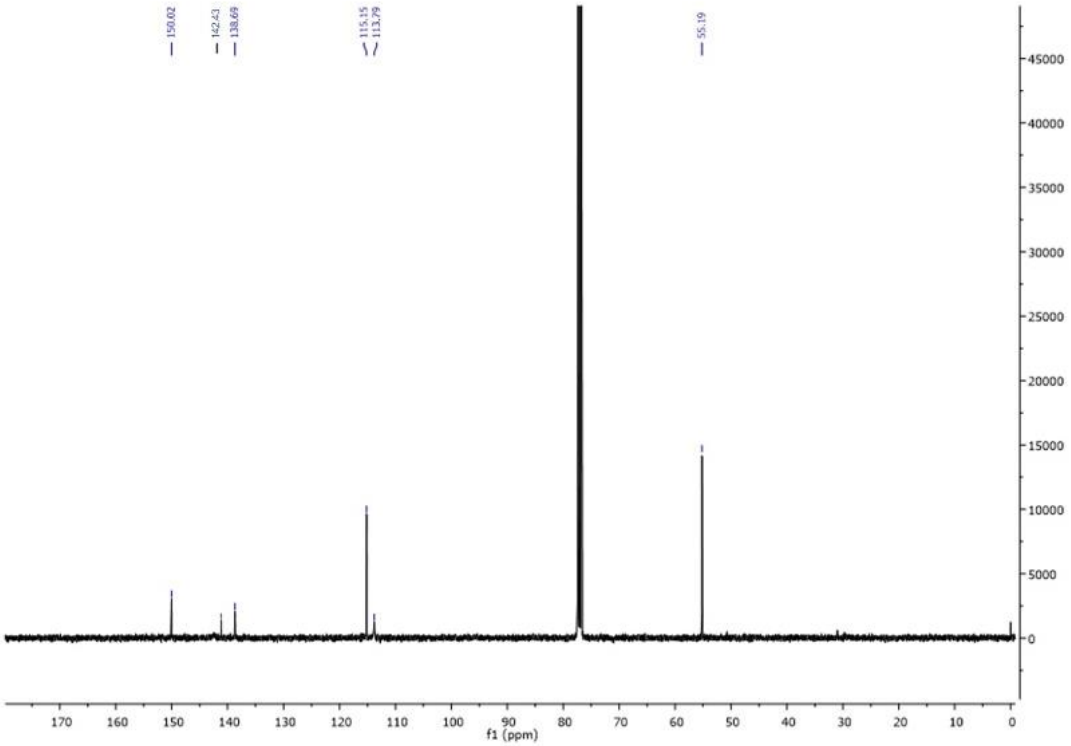

Compound 1.147

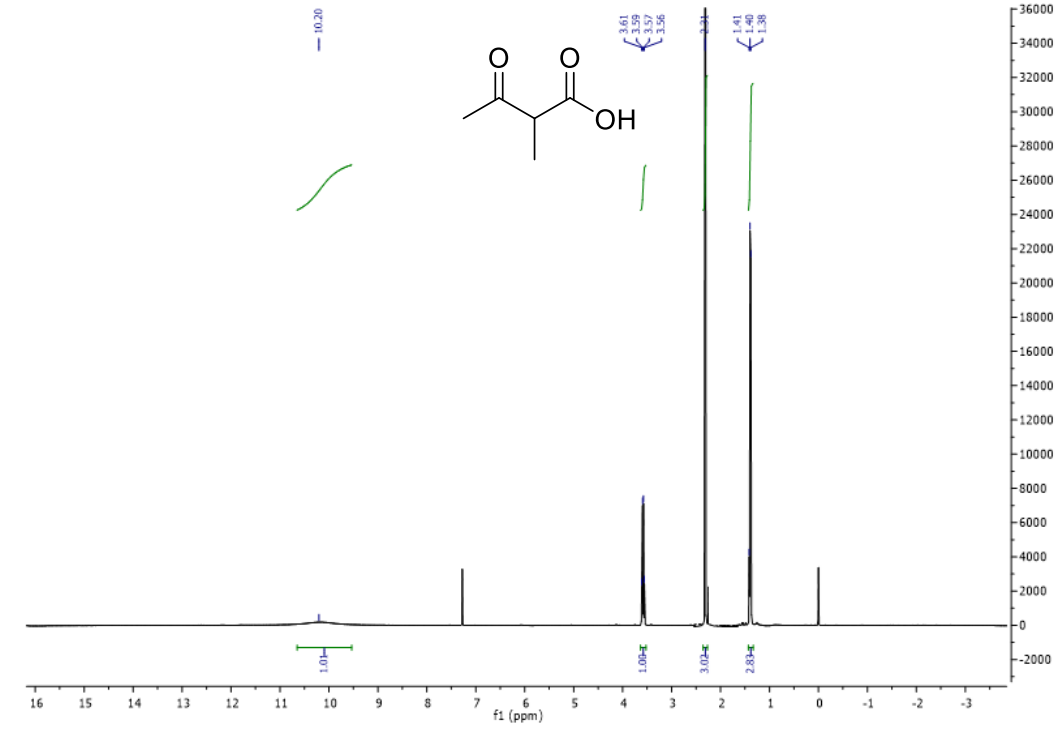

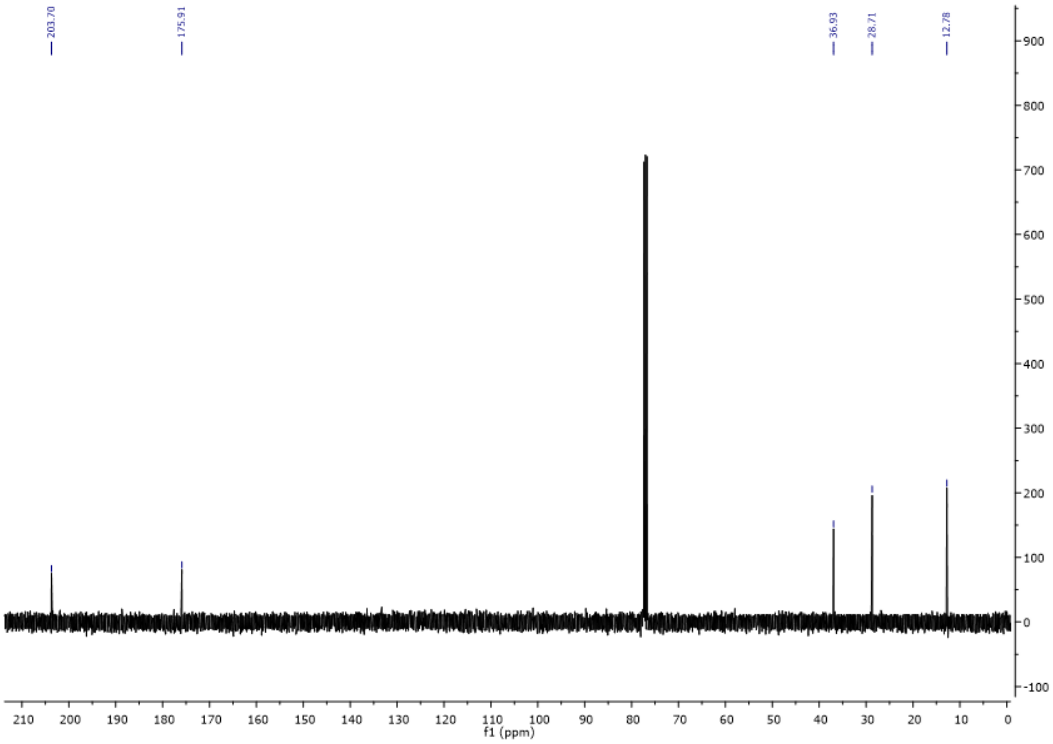

Compound 1.124d

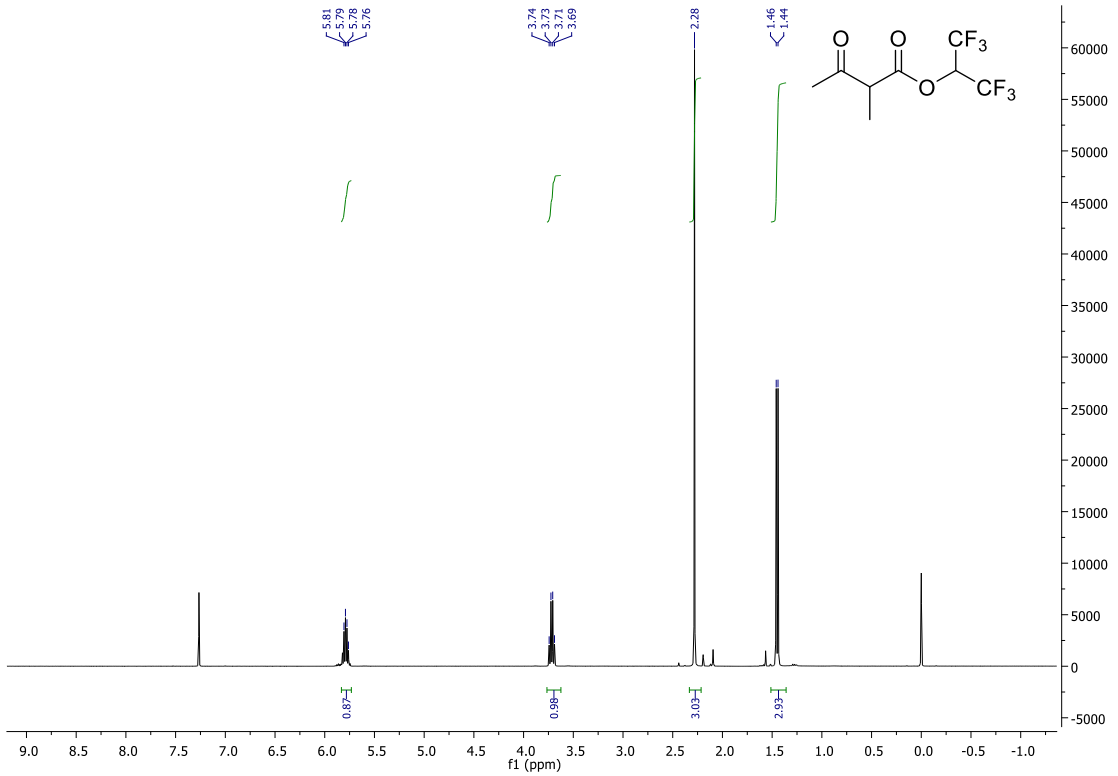

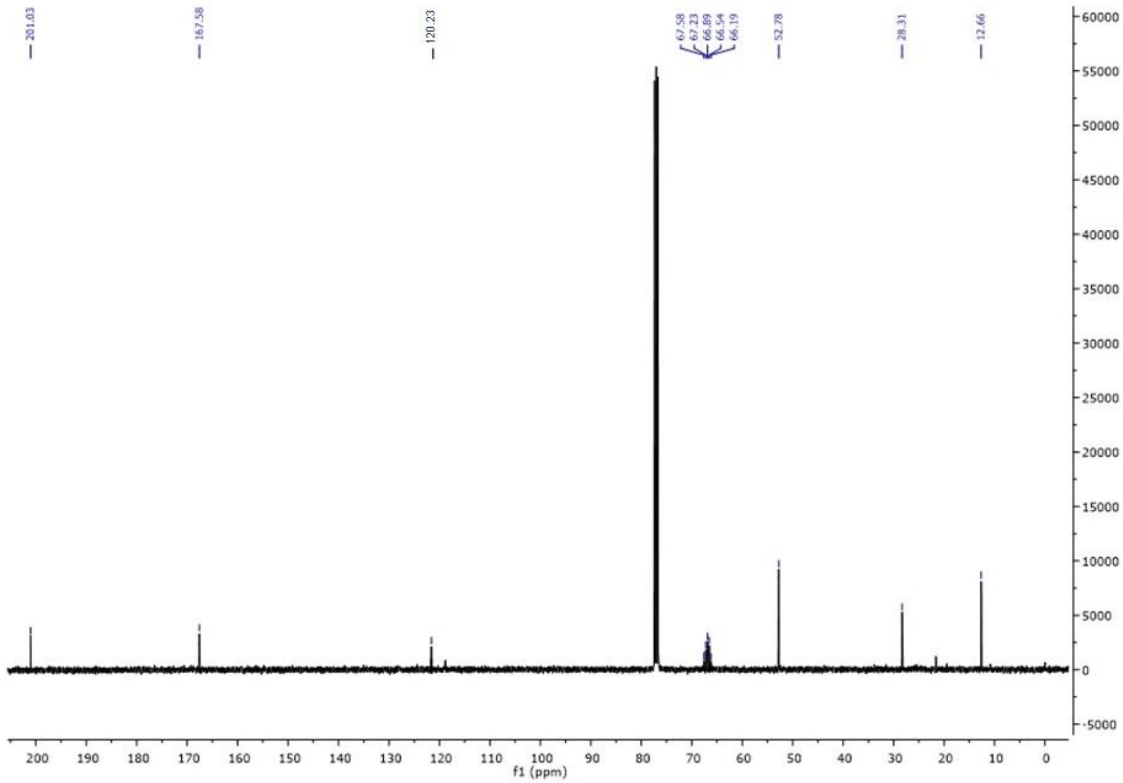

Compound 1.124f

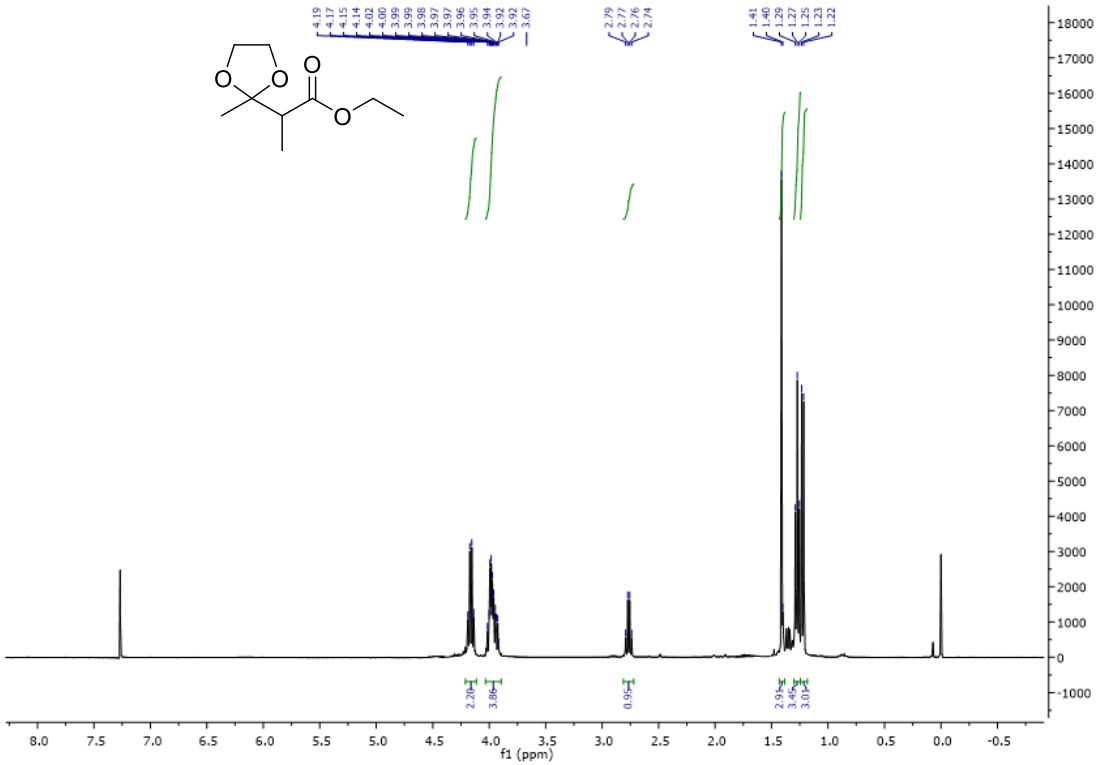

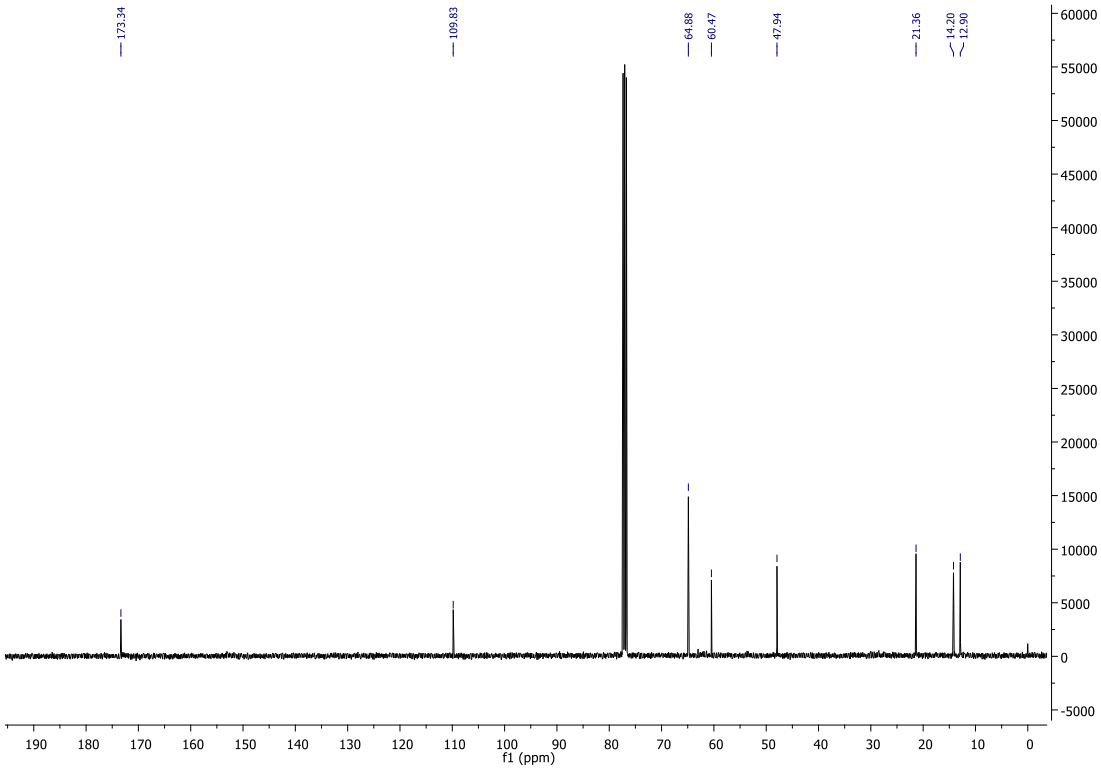

Compound 2.79c

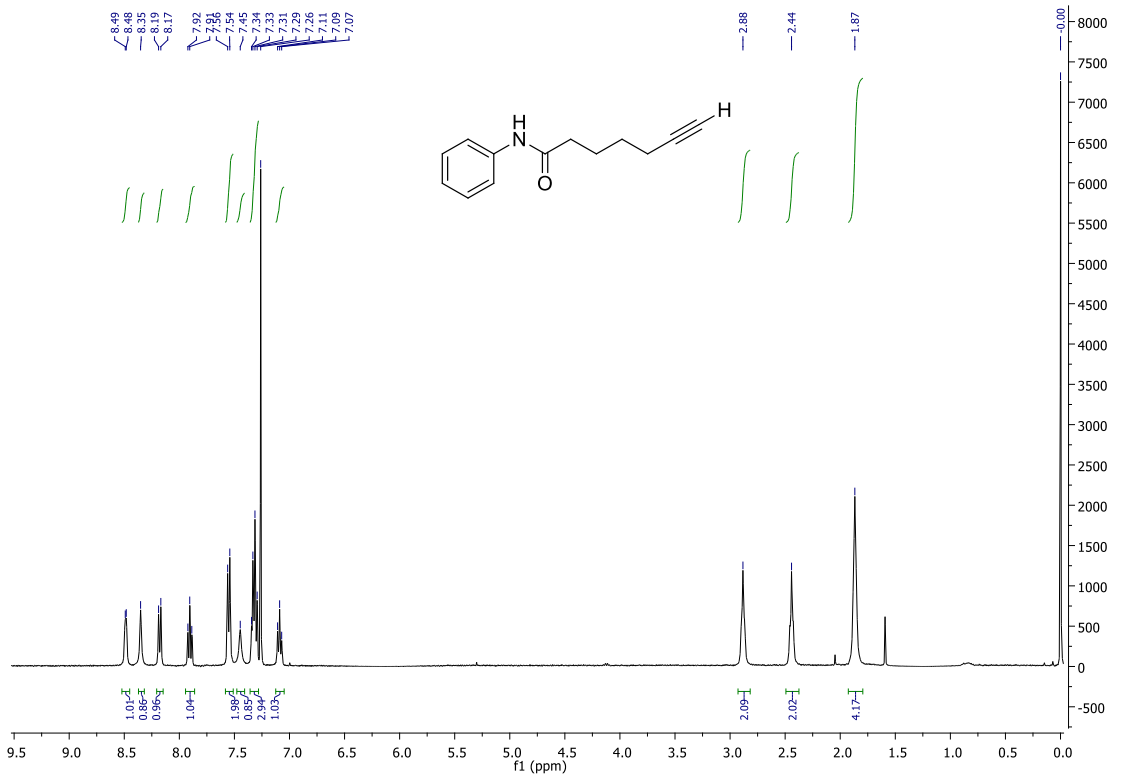

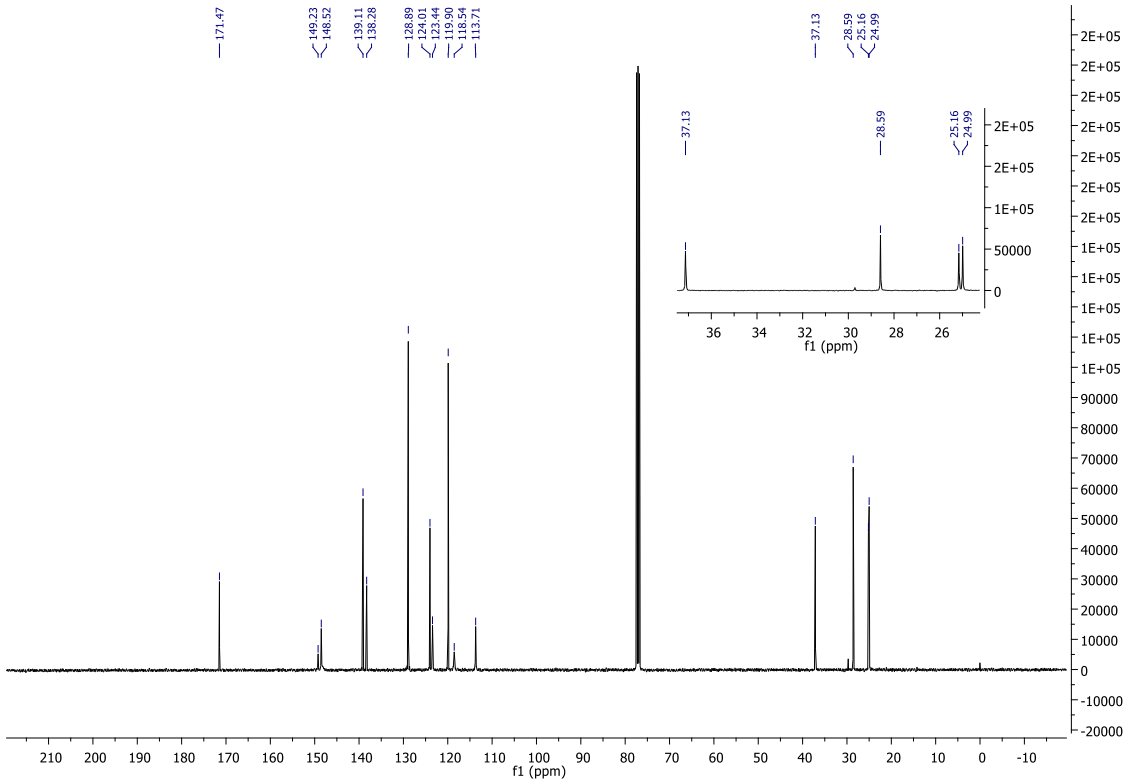

Compound 2.80a

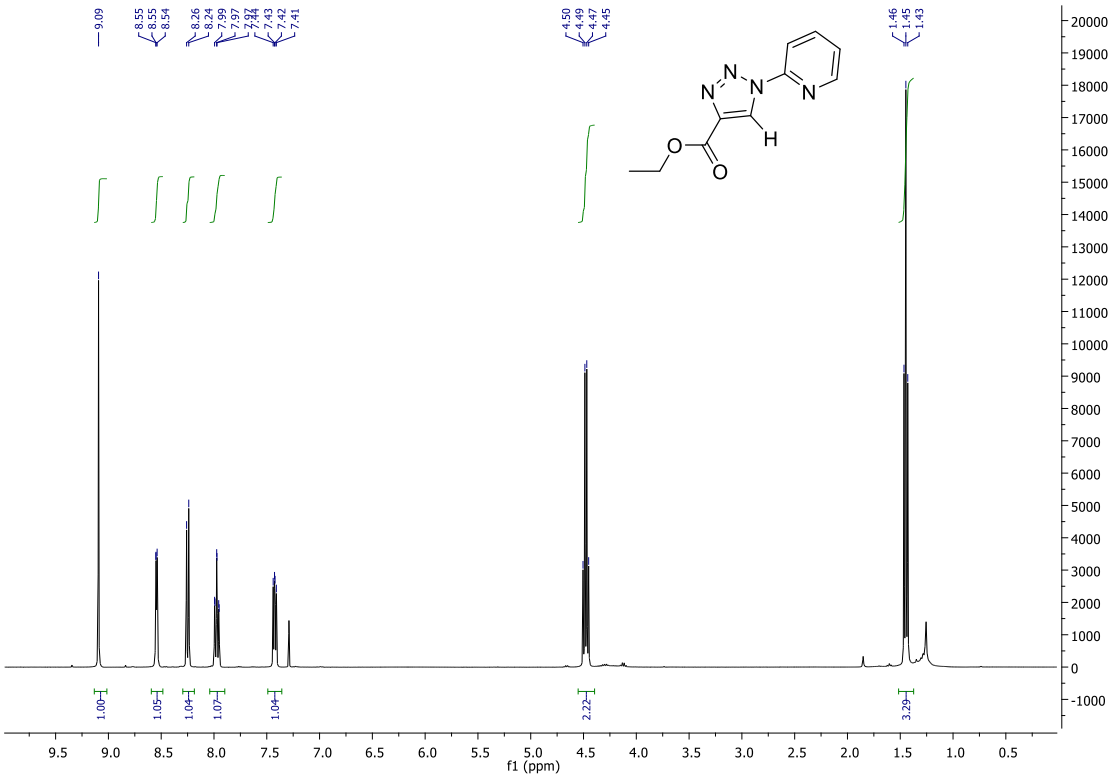

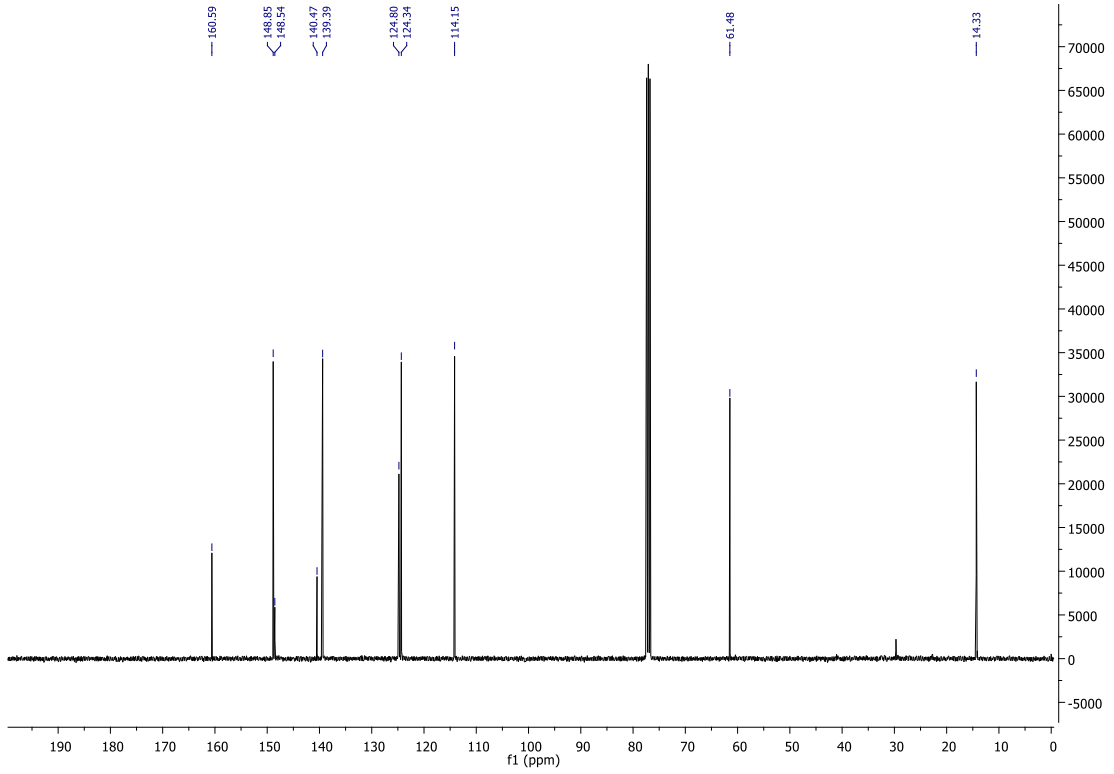

Compound 2.80b

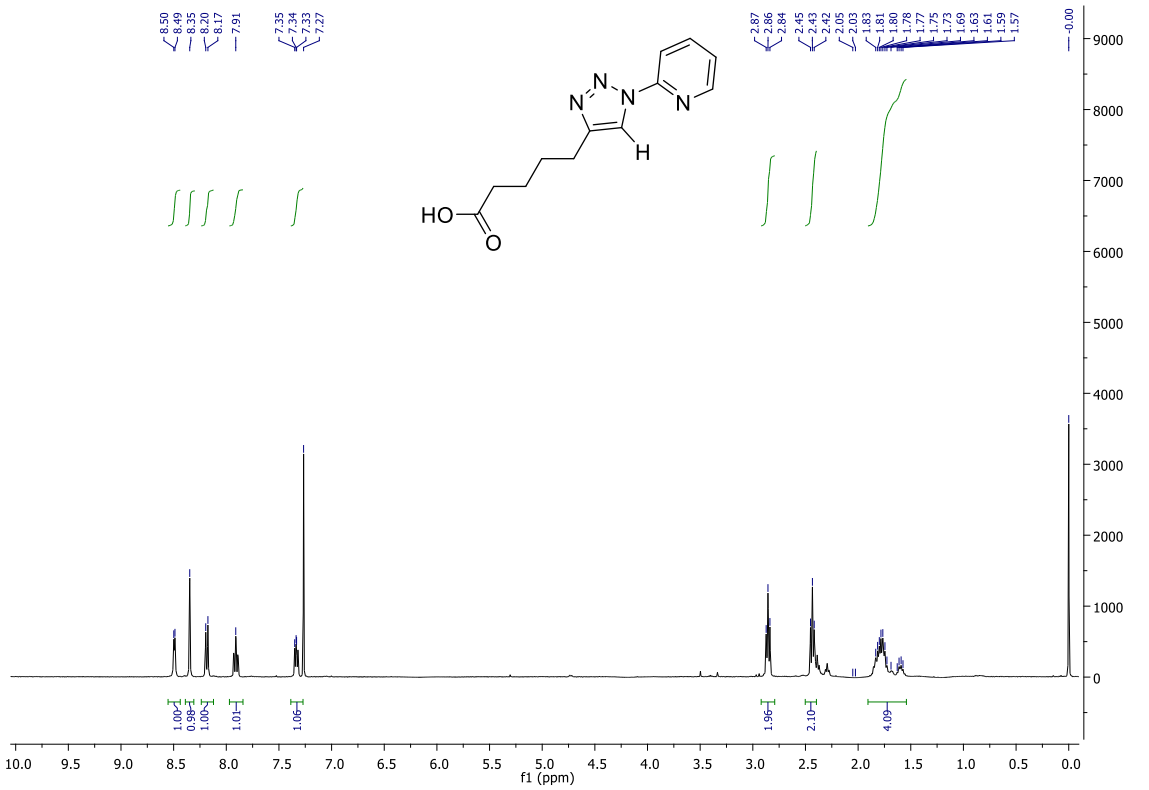

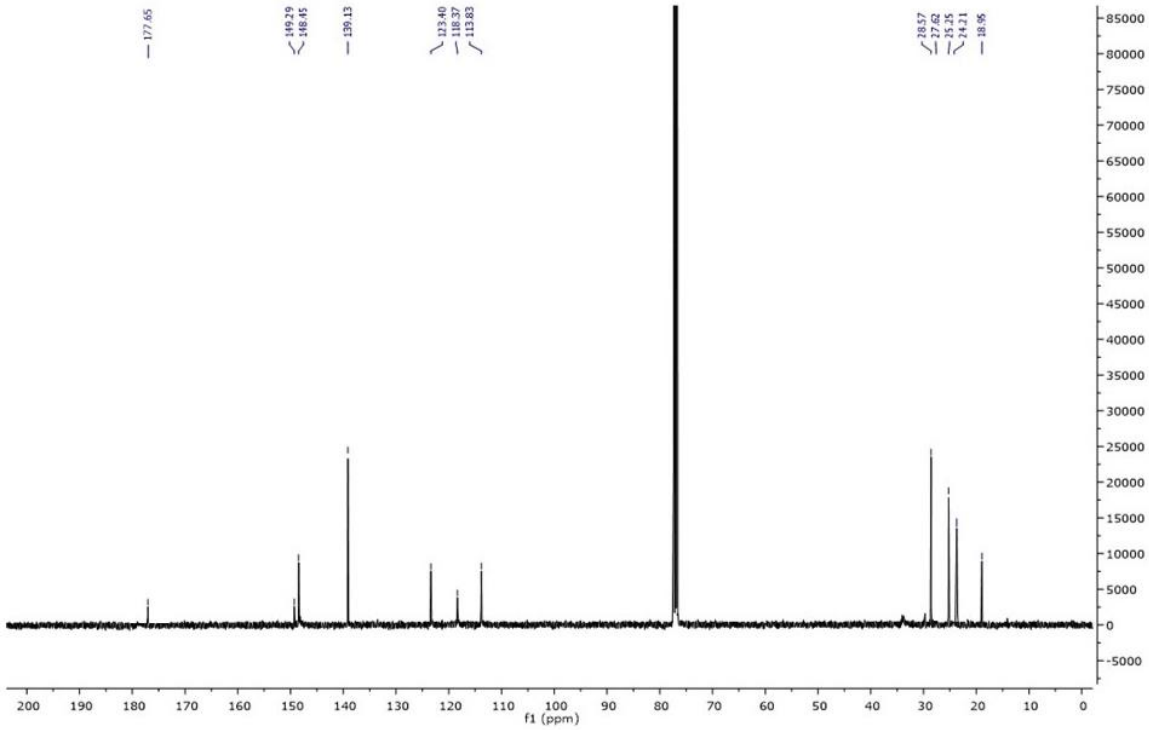

Compound 2.80c

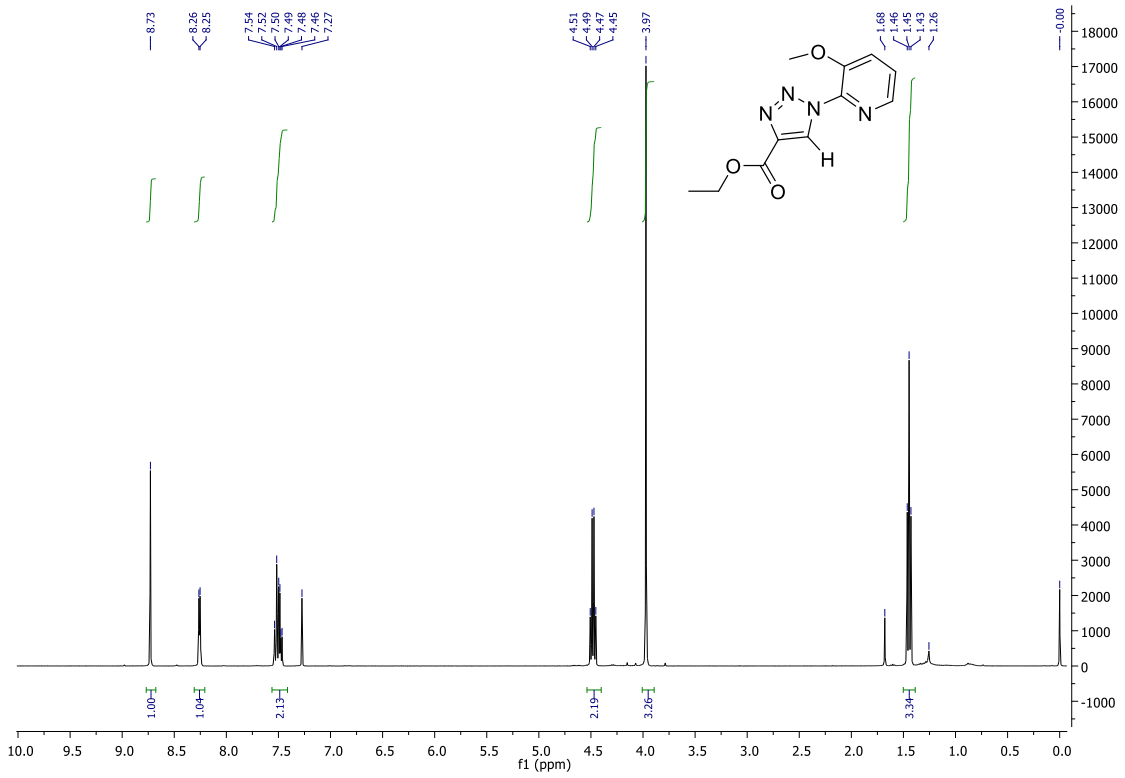

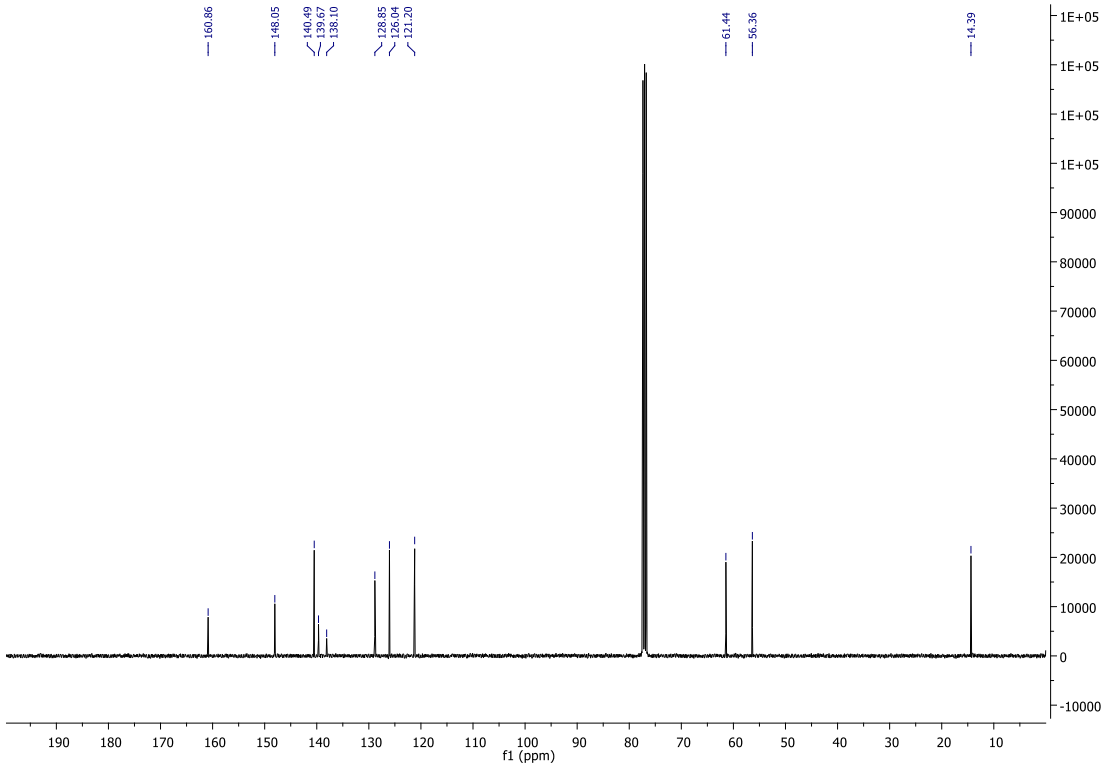

Compound 2.80d

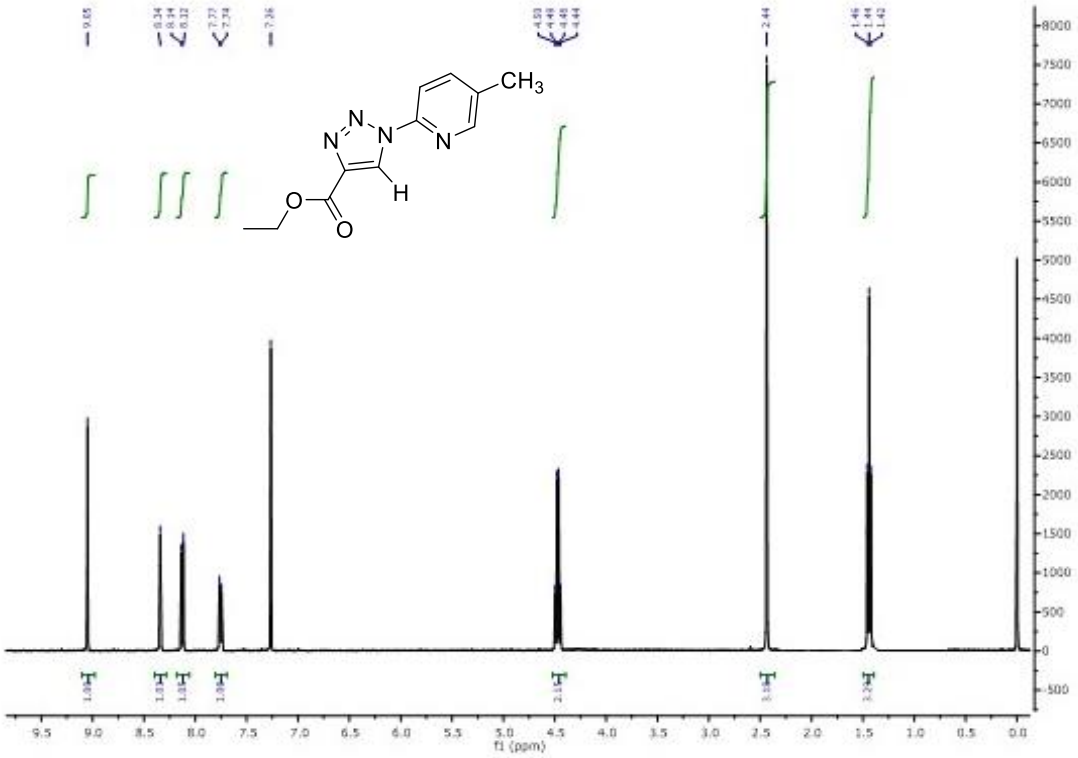

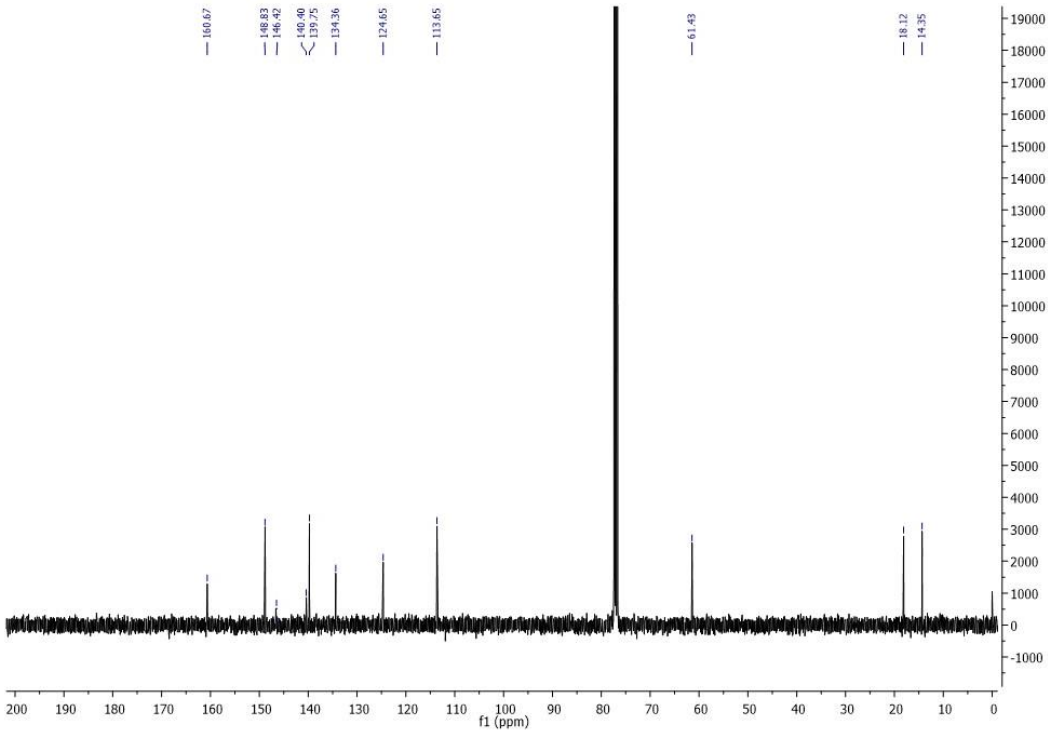

Compound 2.80e

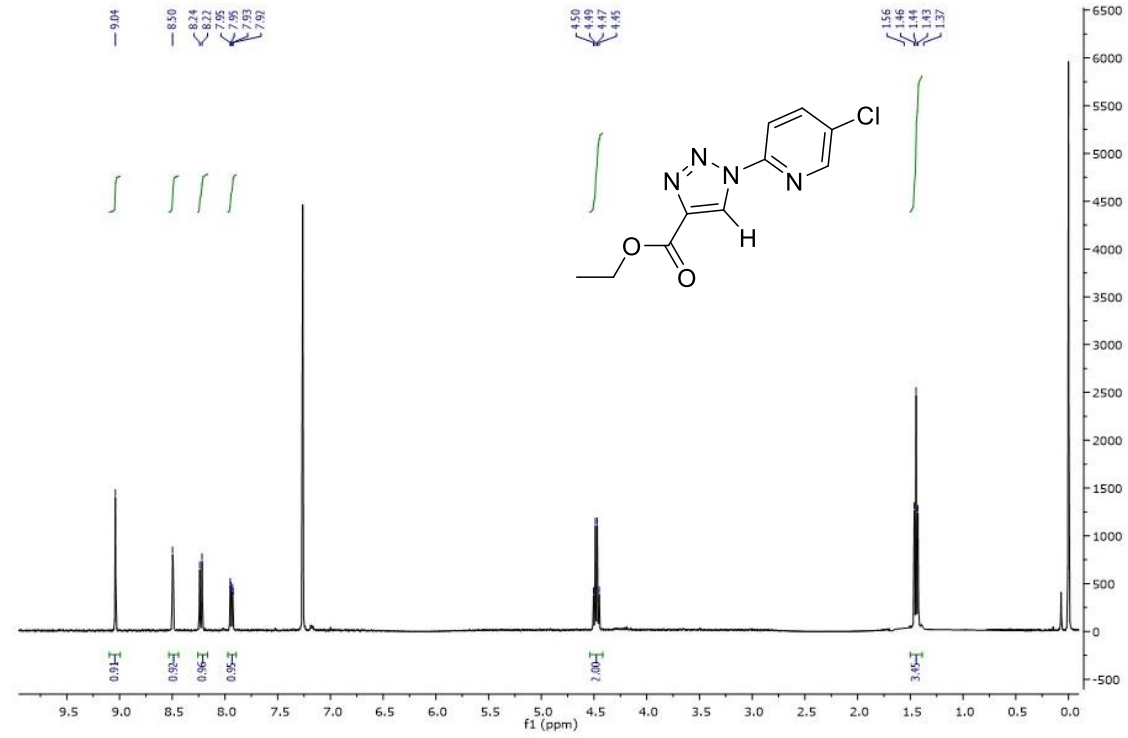

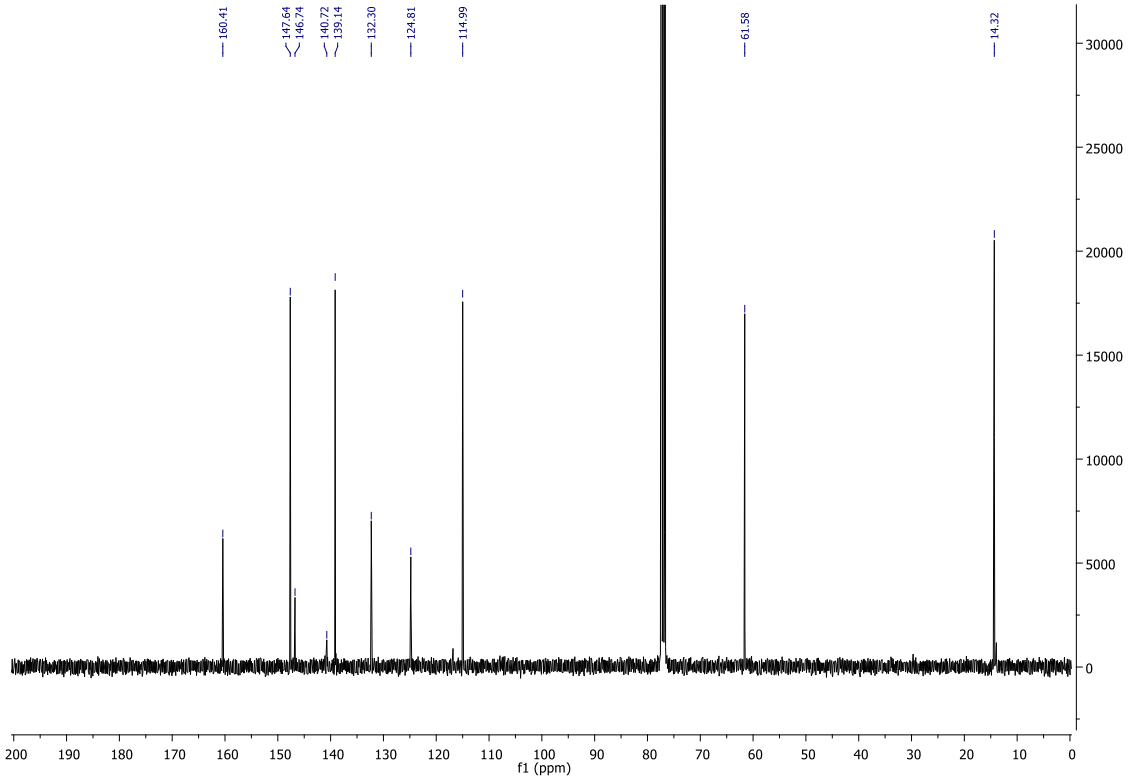

Compound 2.80f

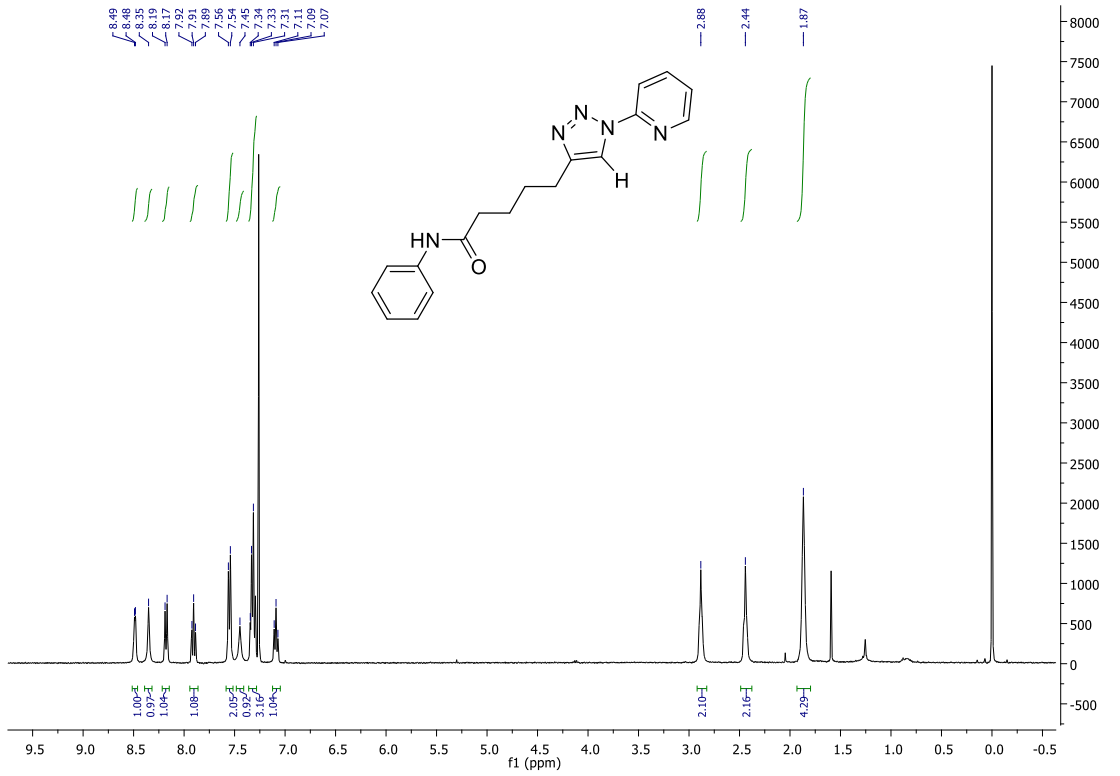

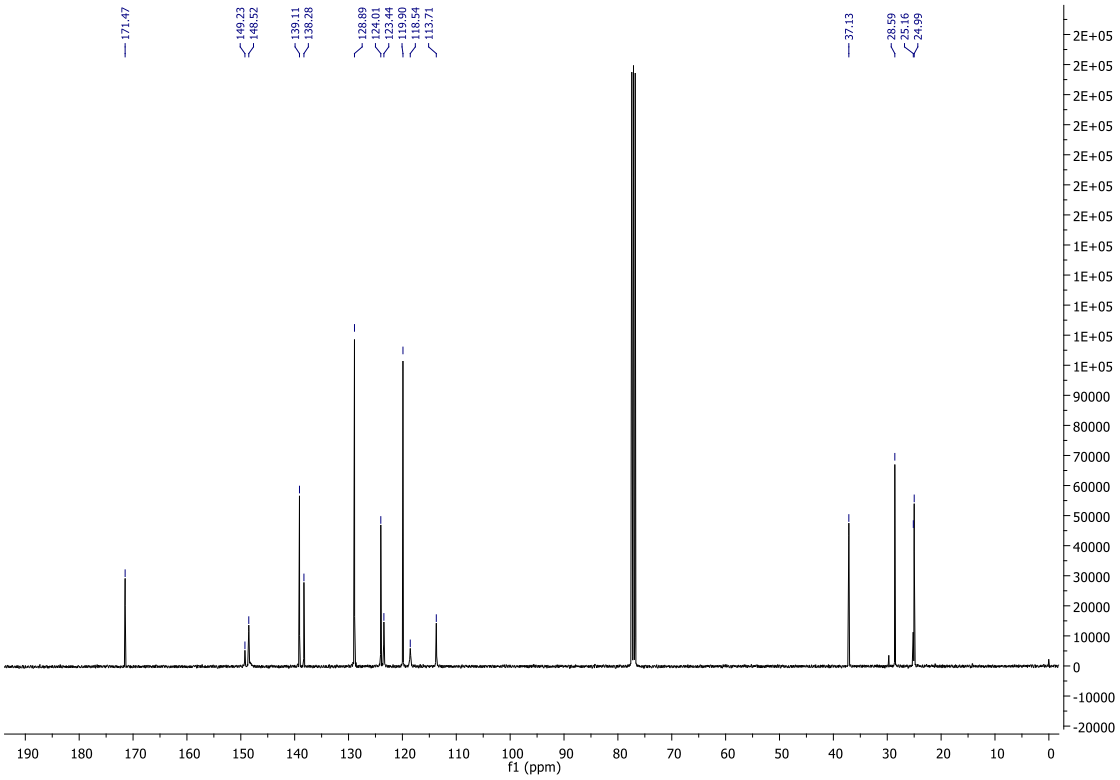

Compound 2.53

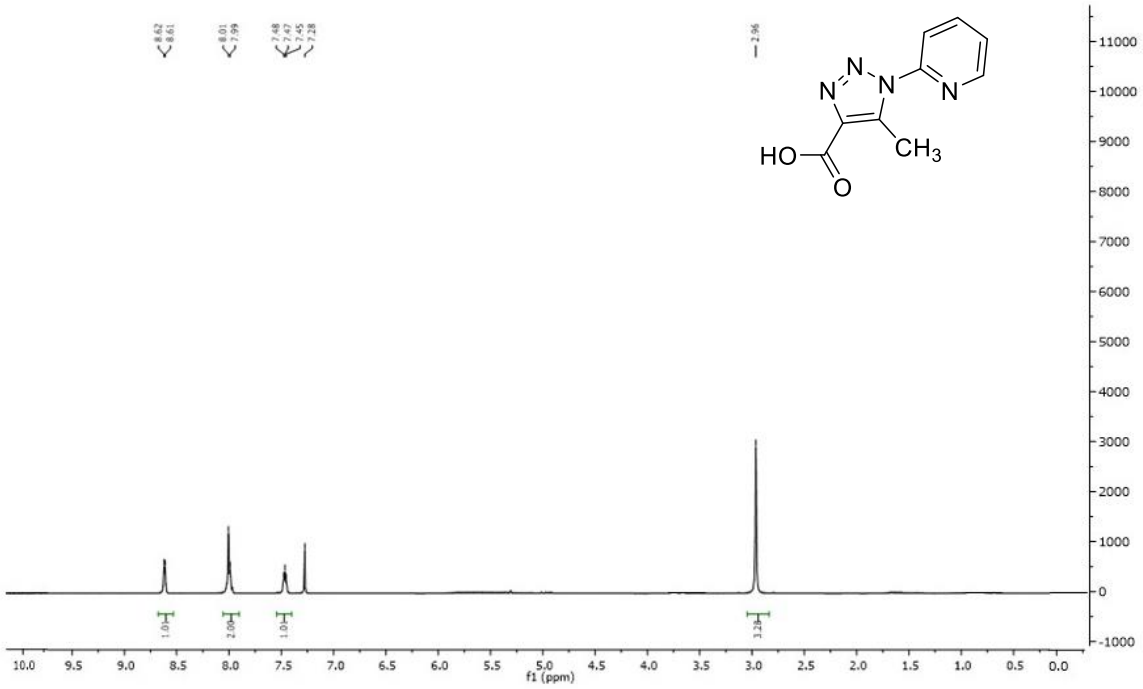

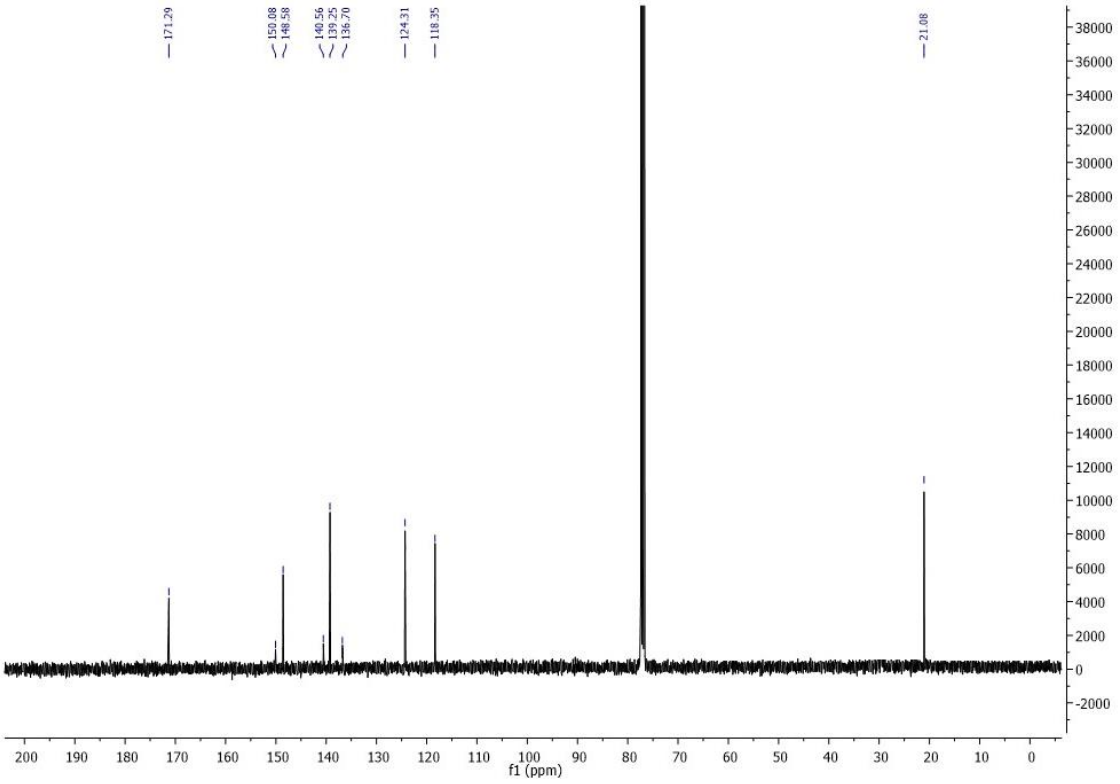

Compound 2.81a

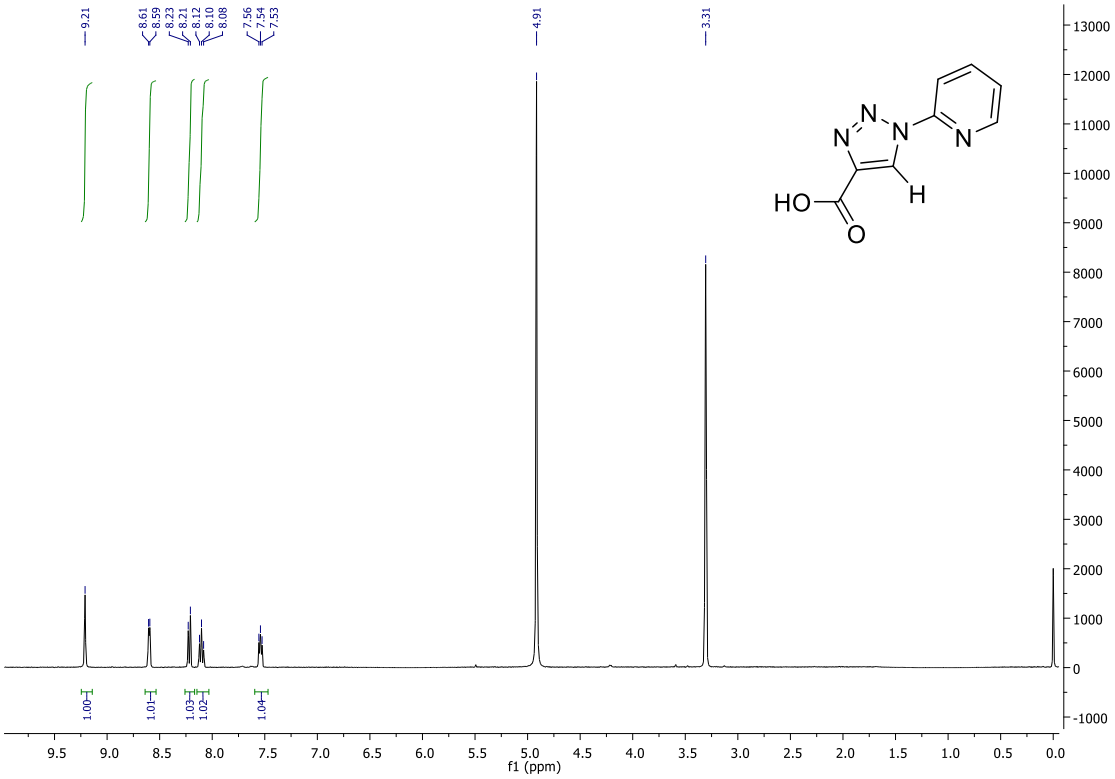

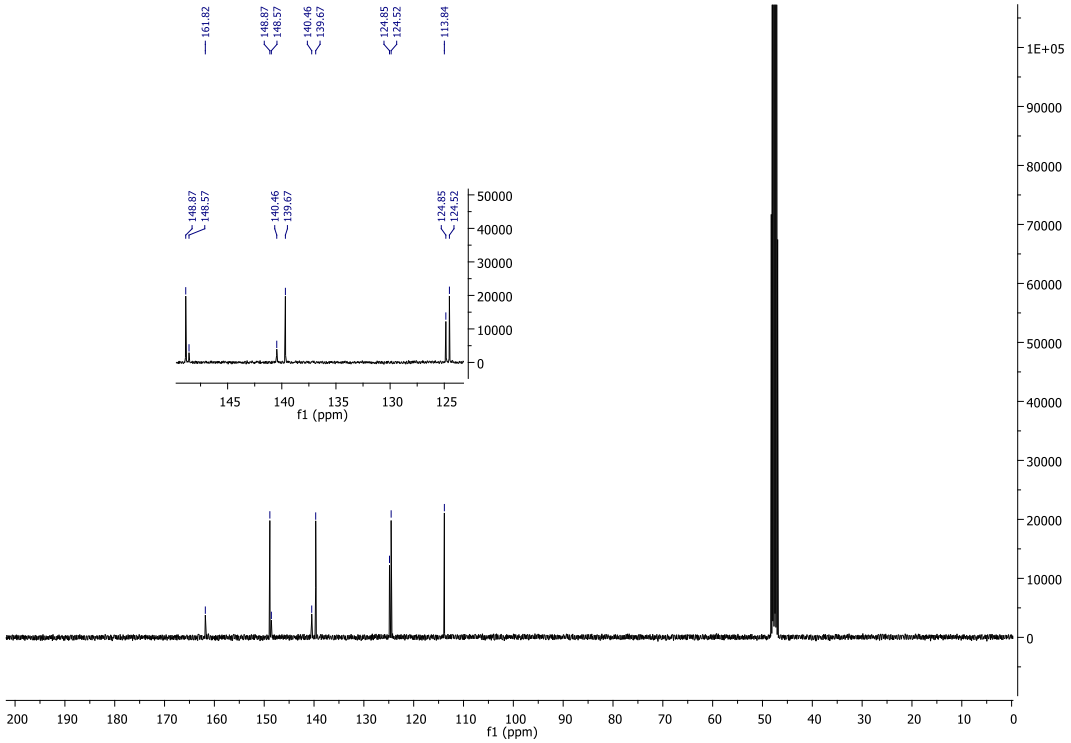

Compound 2.81b

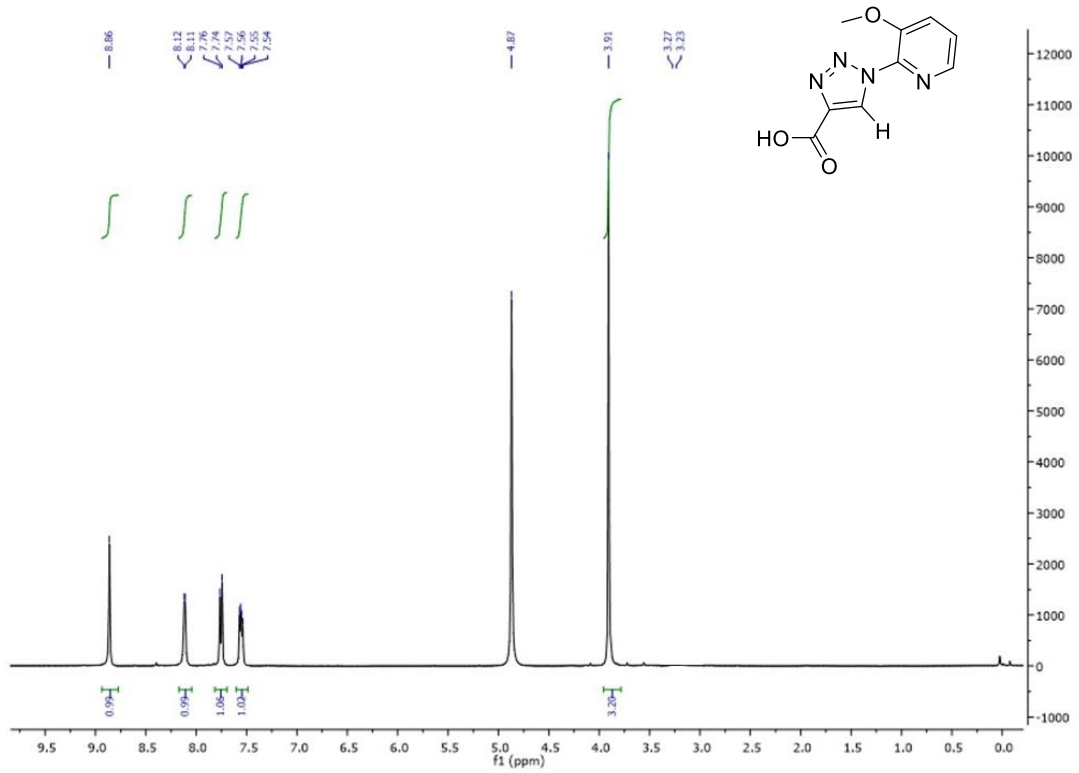

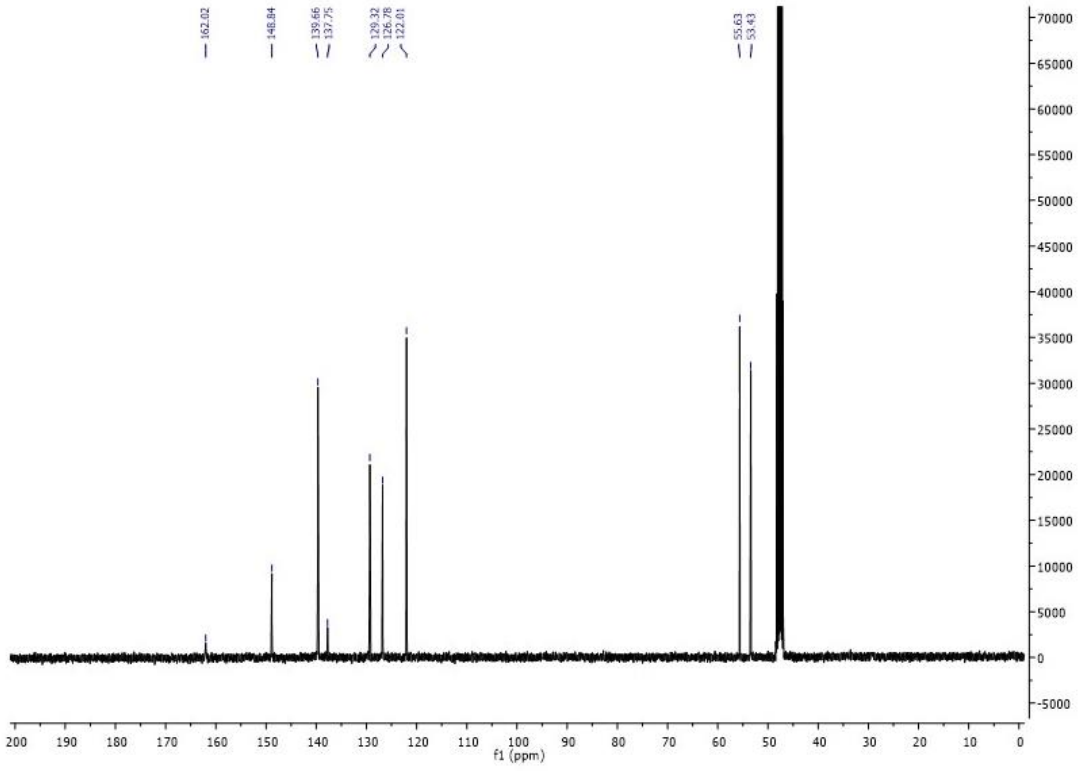

Compound 2.81c

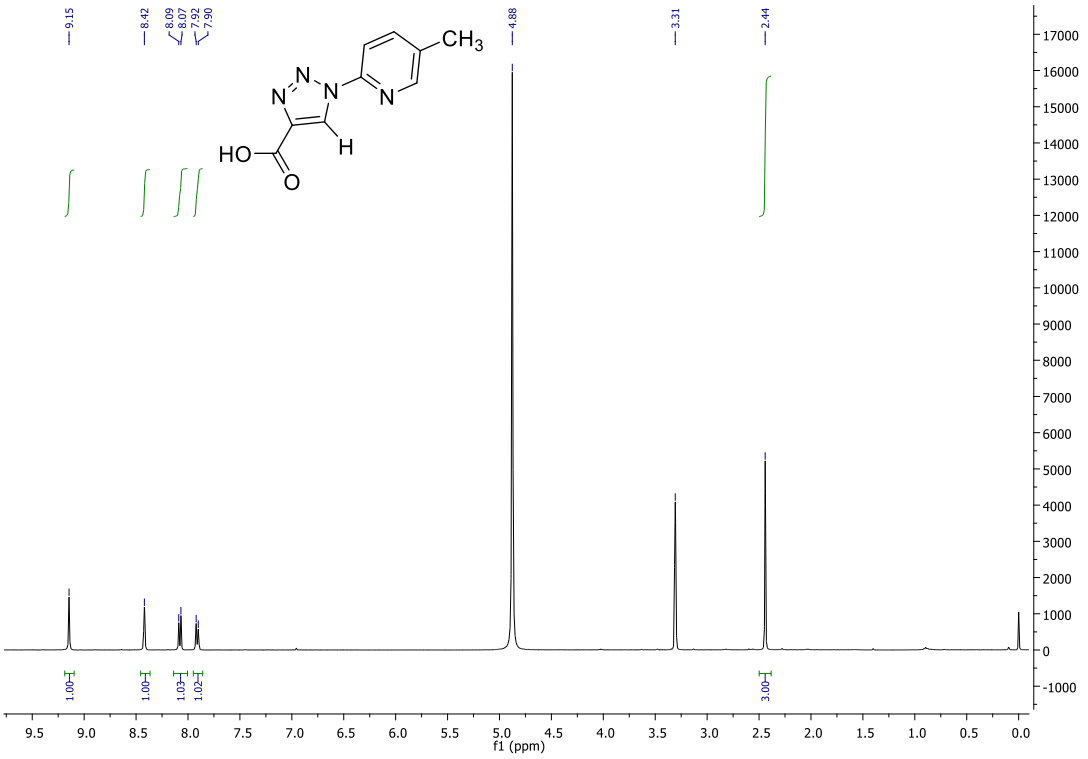

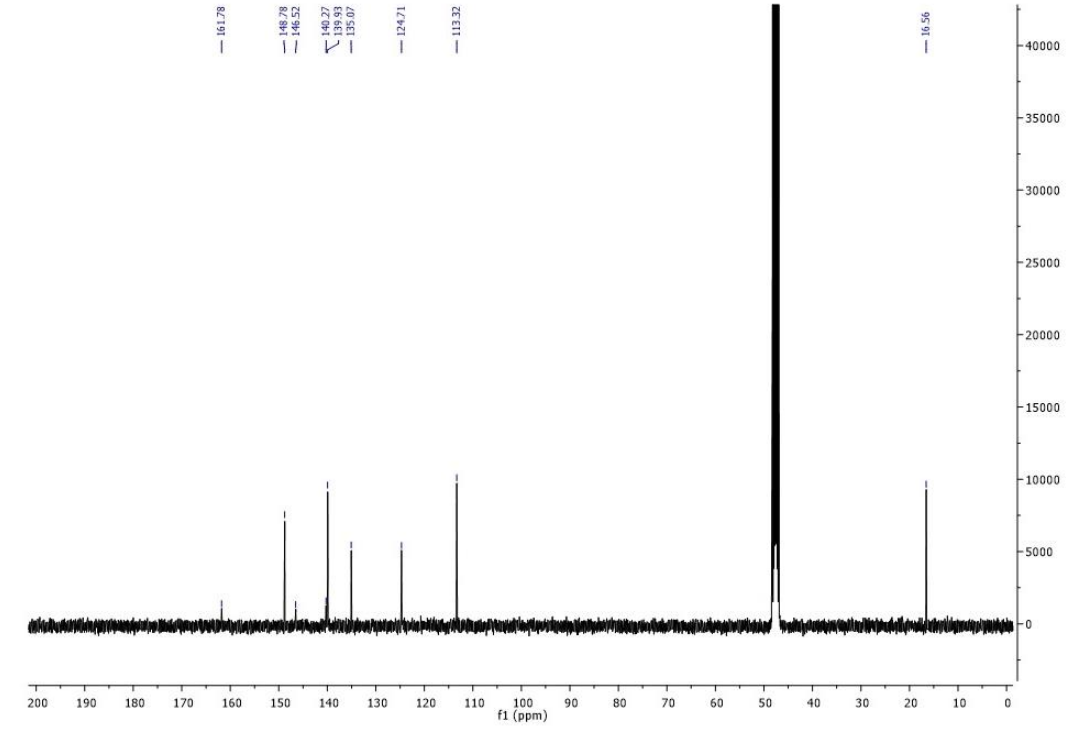

Compound 2.81d

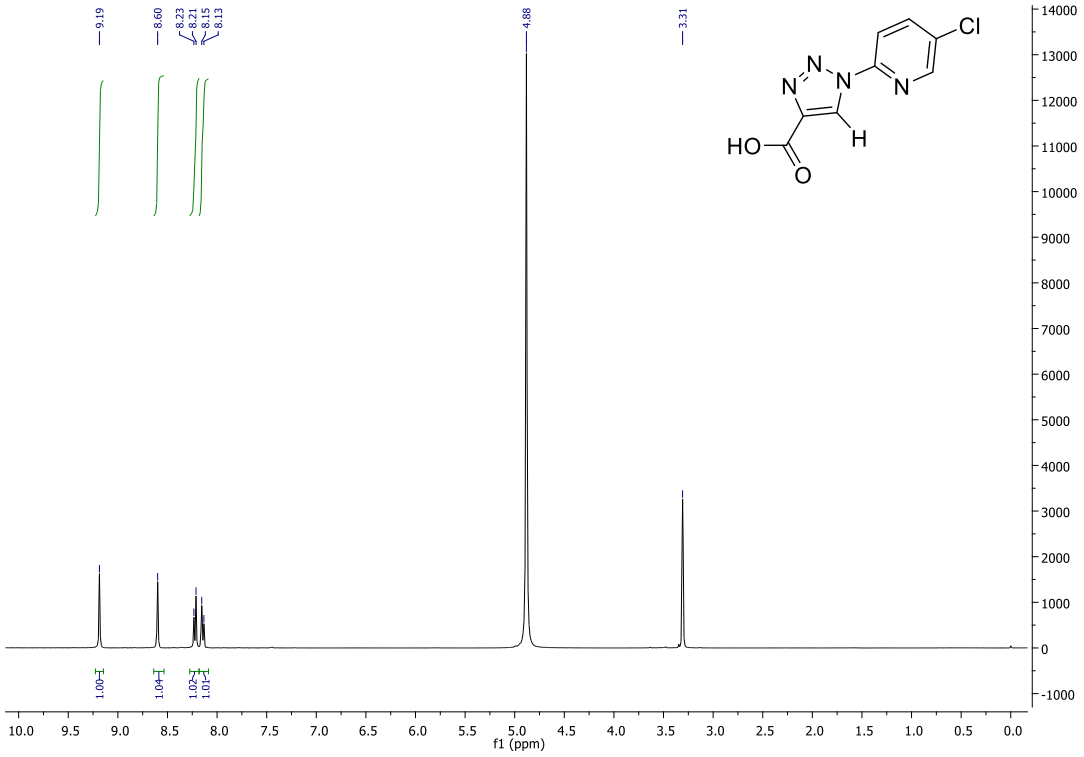

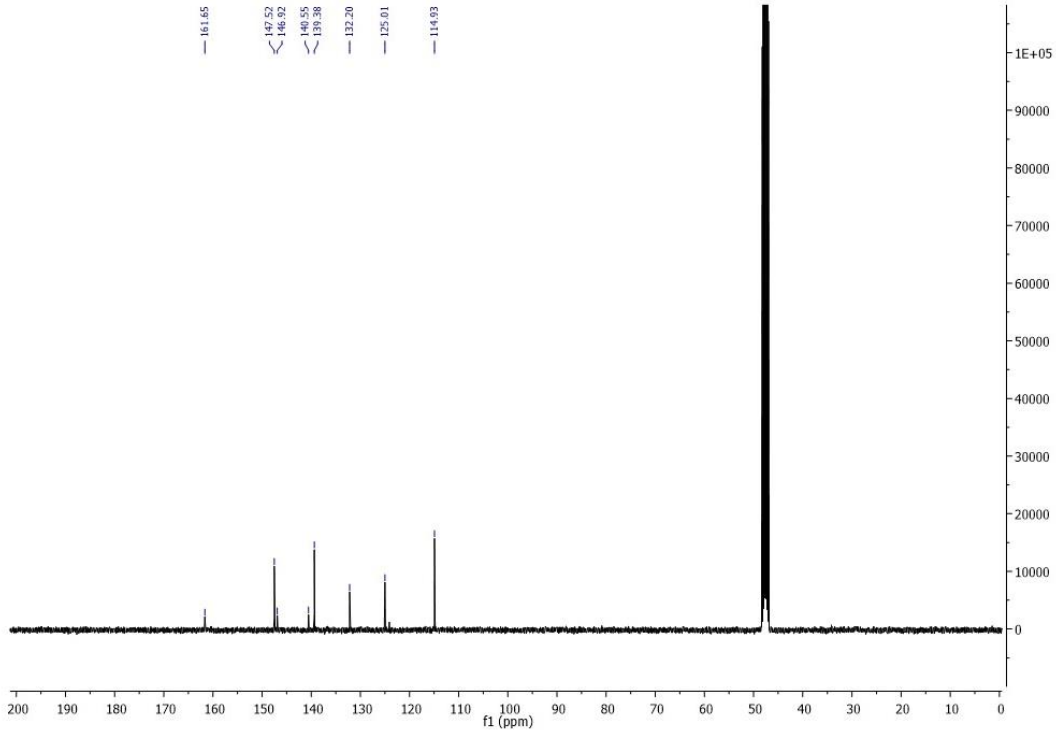

Compound 3.397a

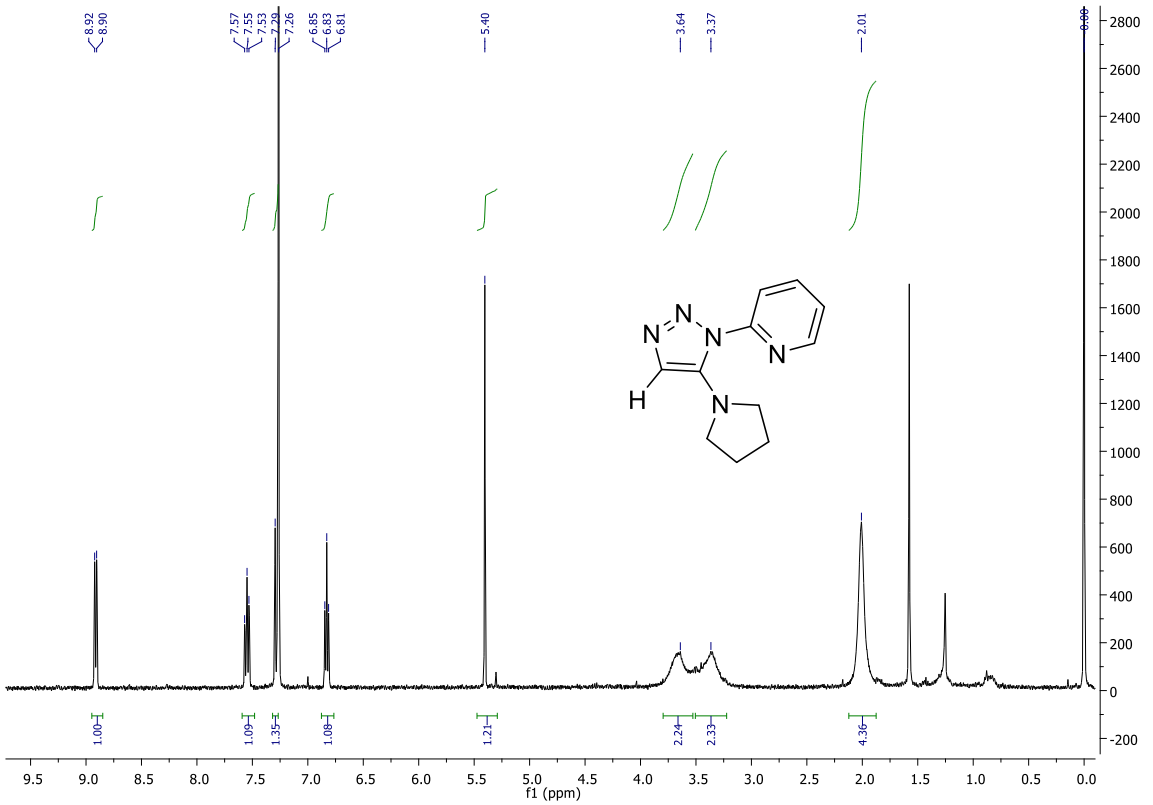

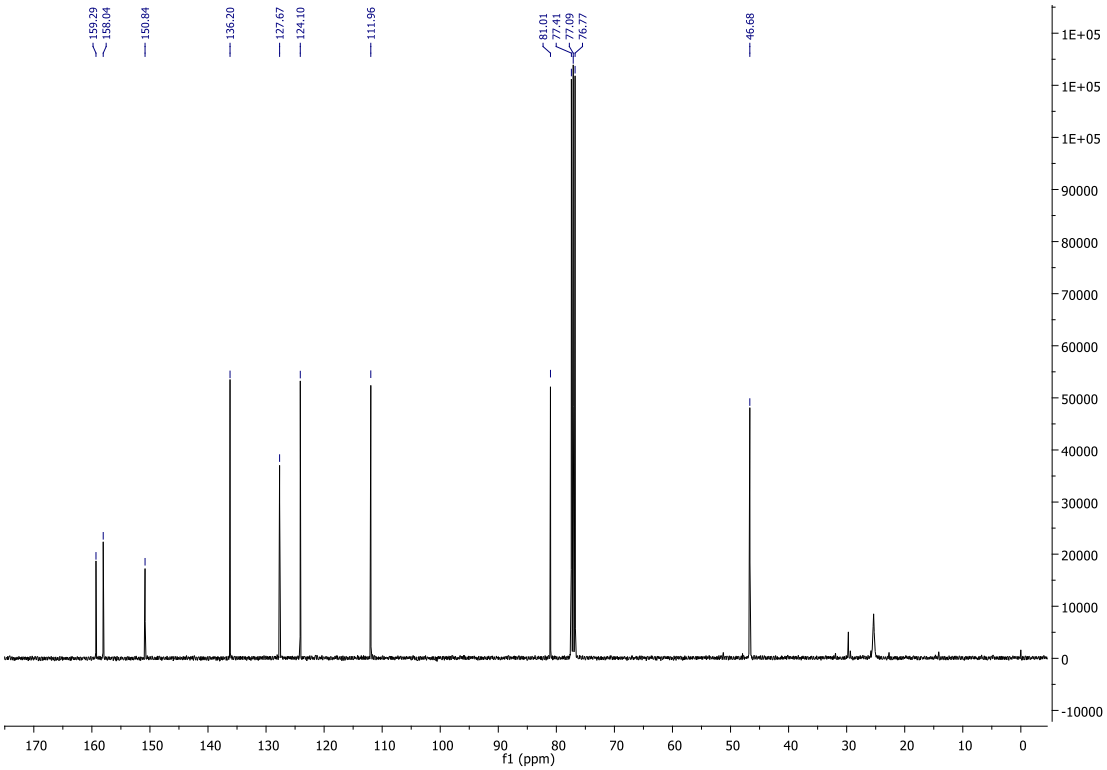

Compound 3.397b

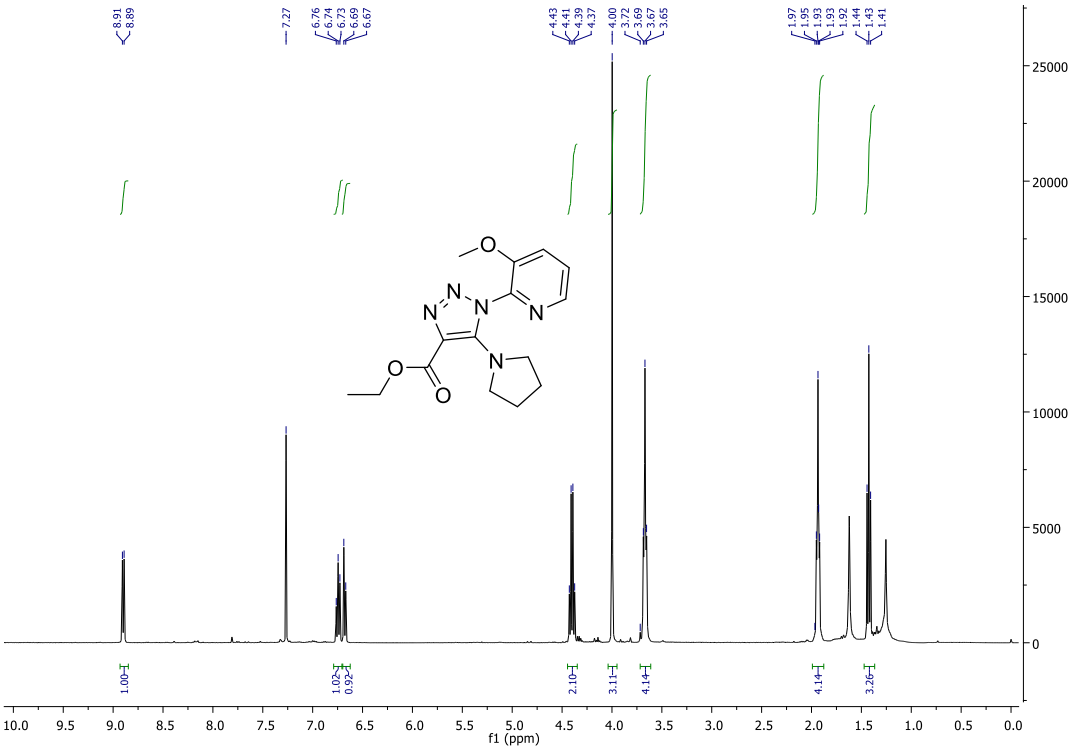

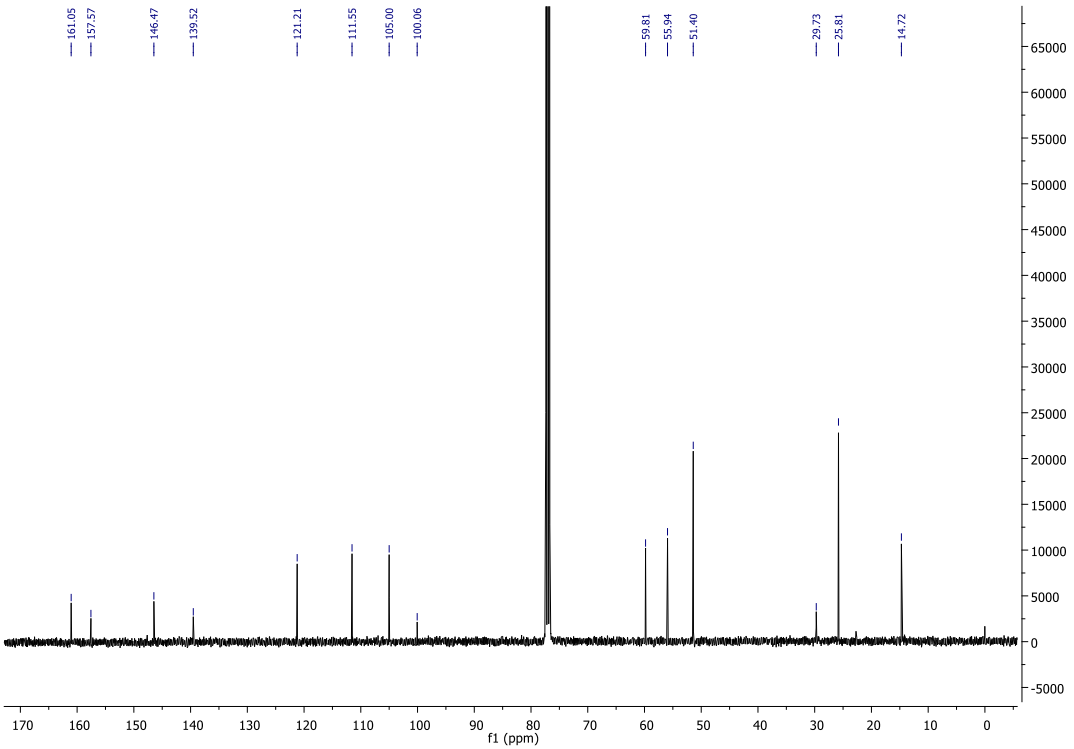

Compound 3.397c

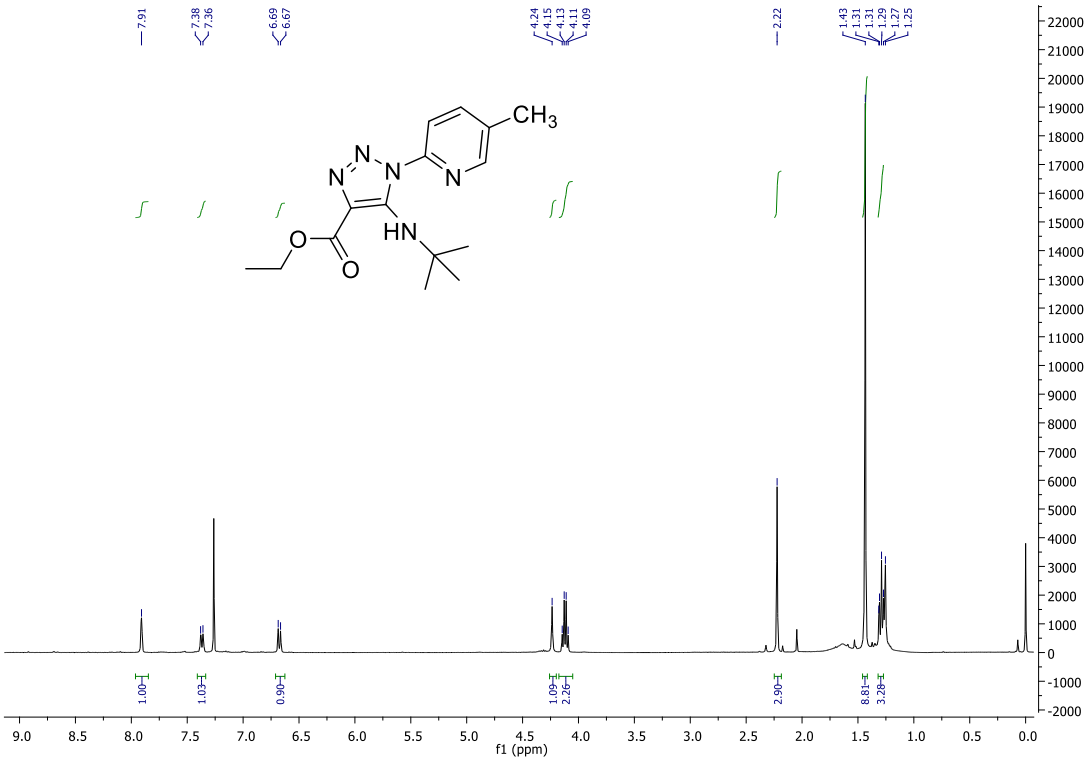

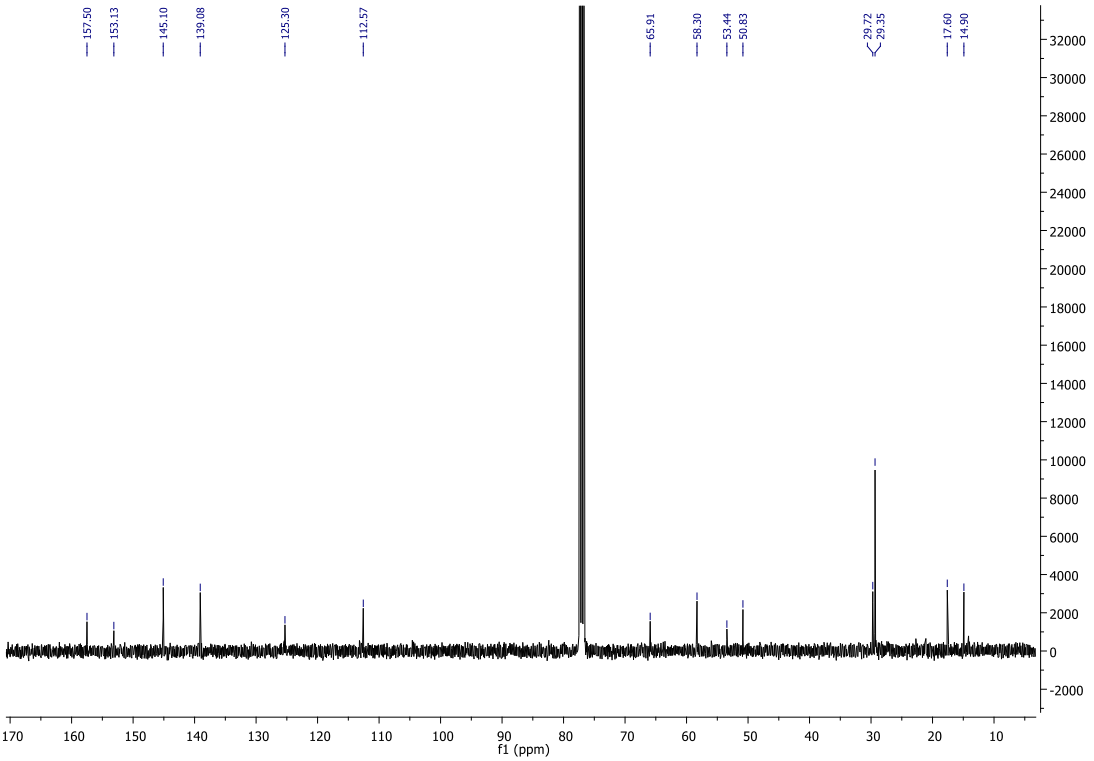

Compound 3.397d

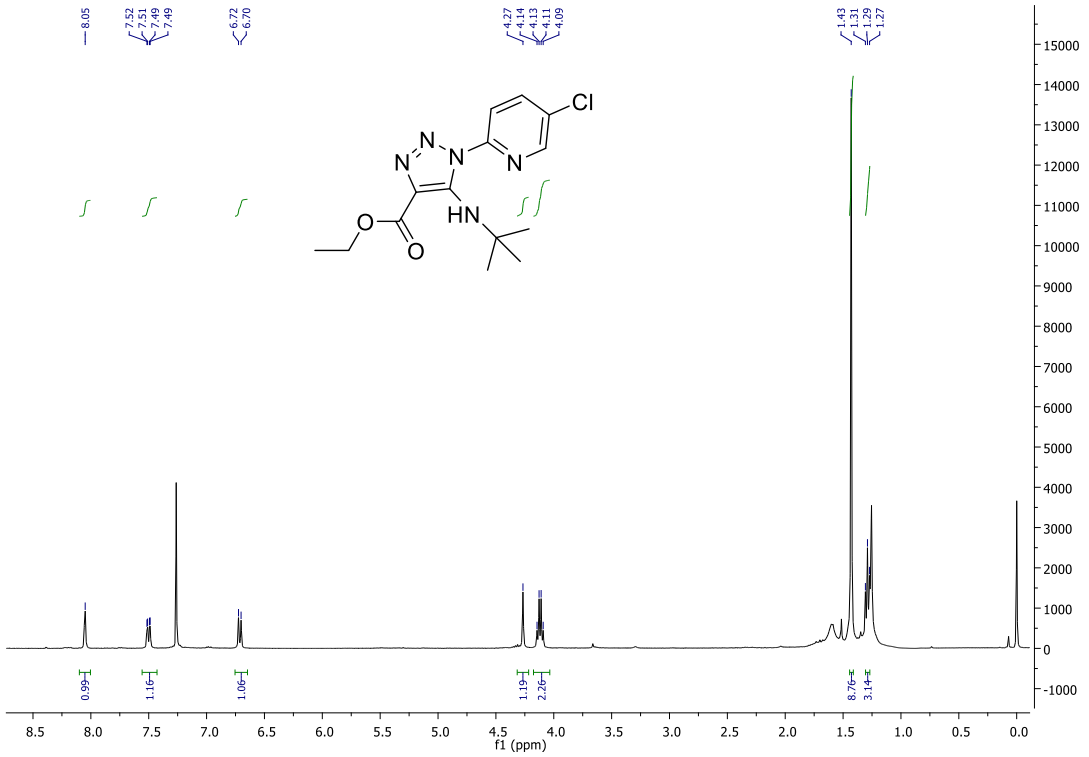

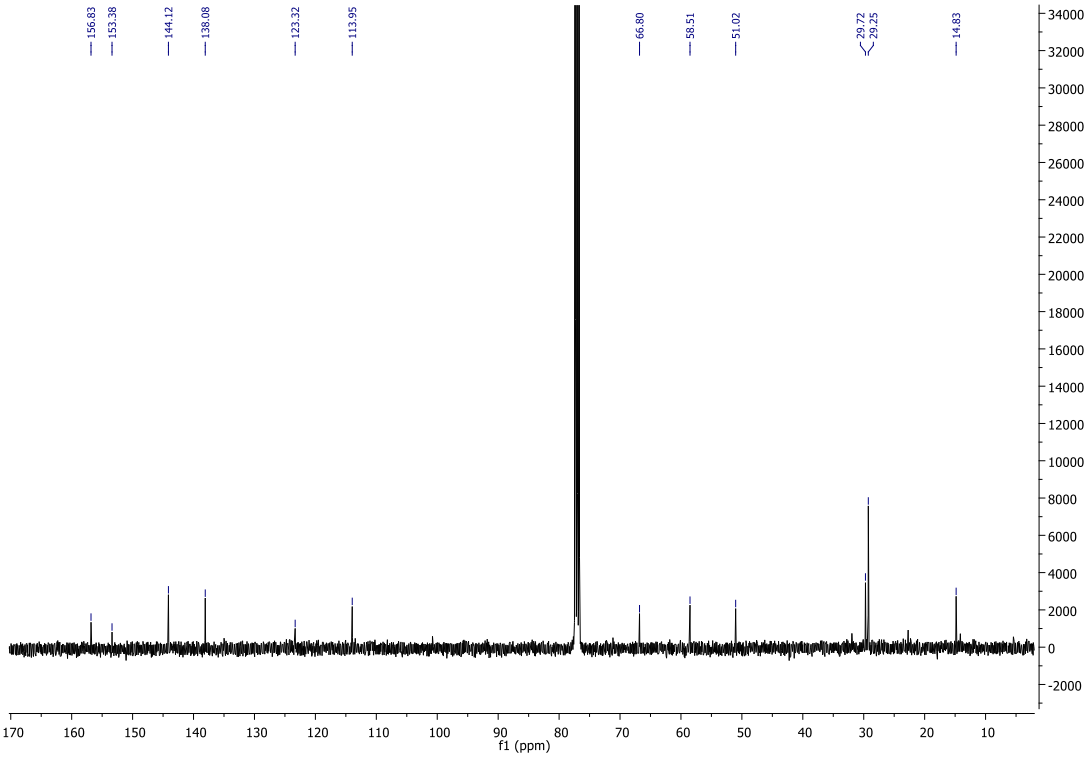

Compound 3.397e

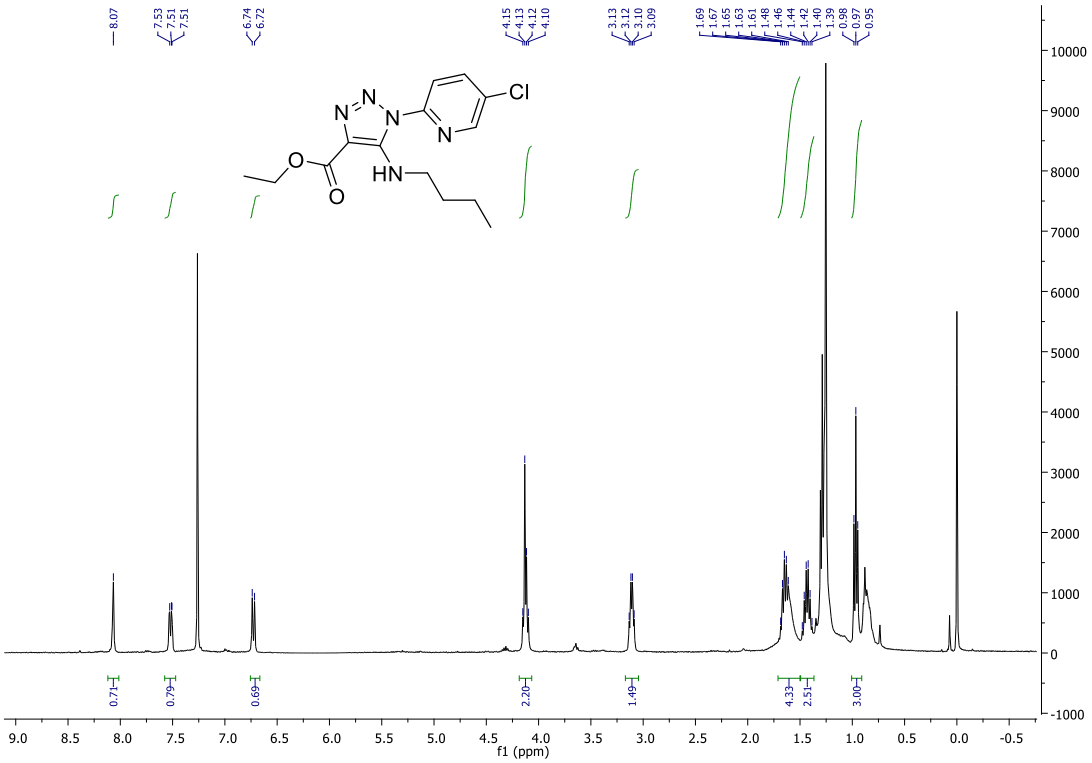

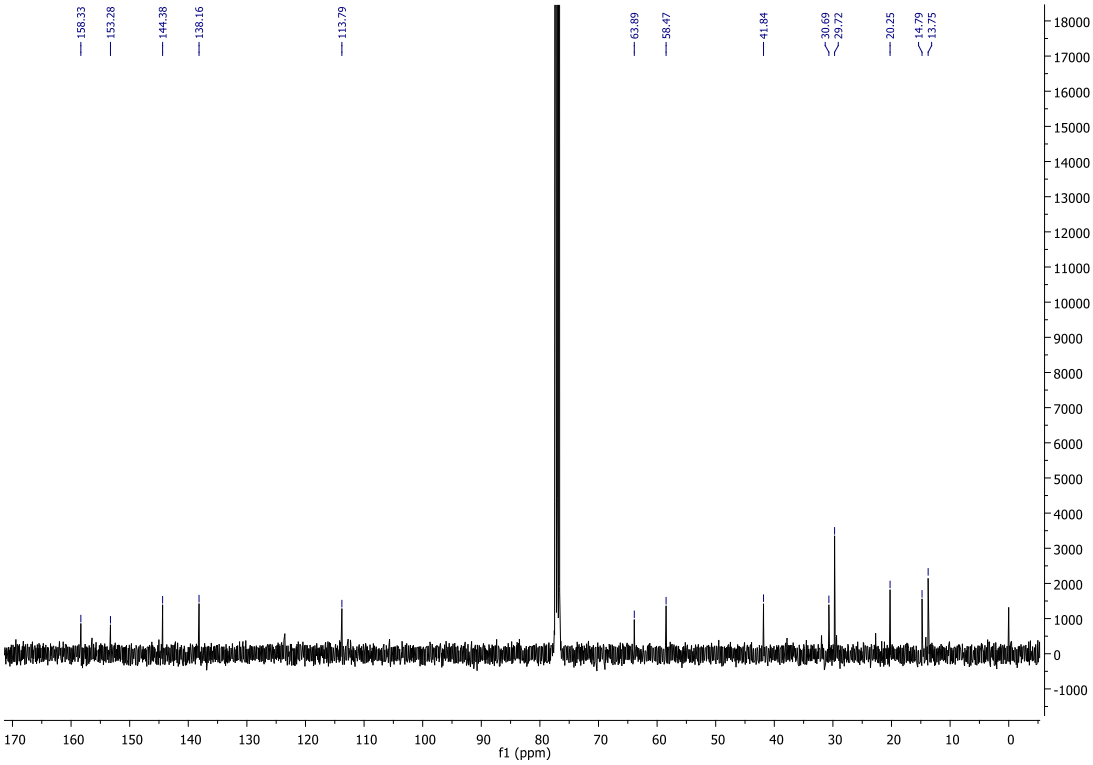

Compound 3.397f

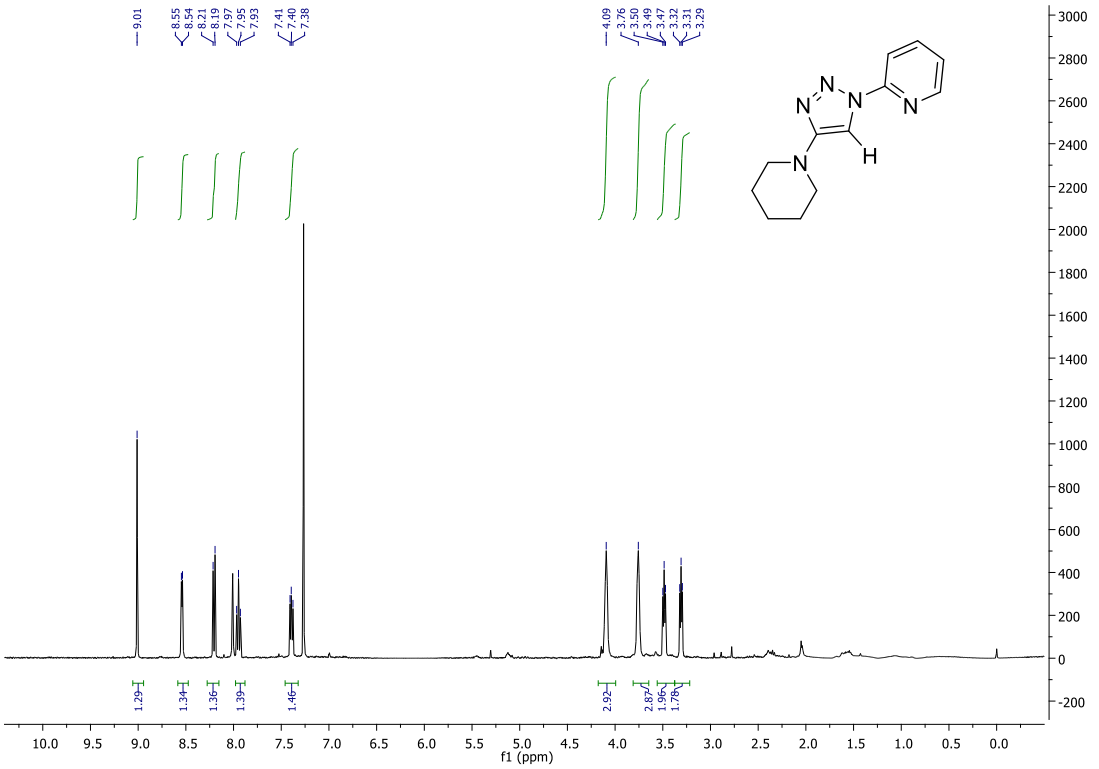

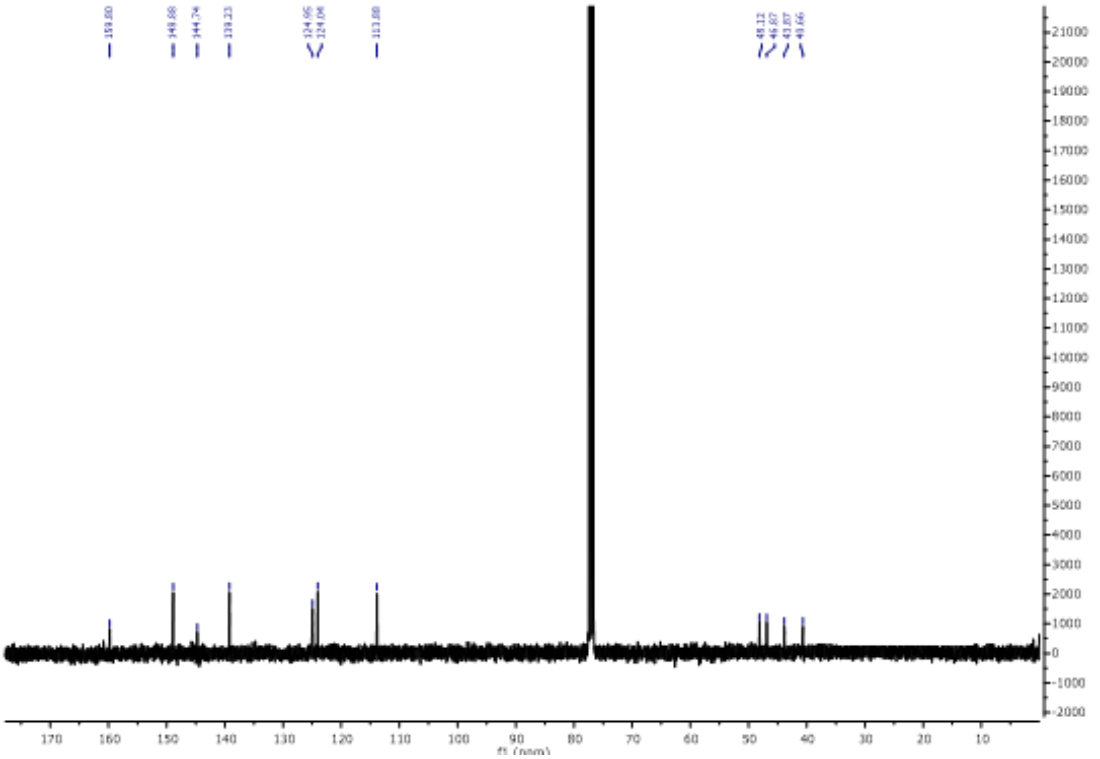

Compound 3.397g

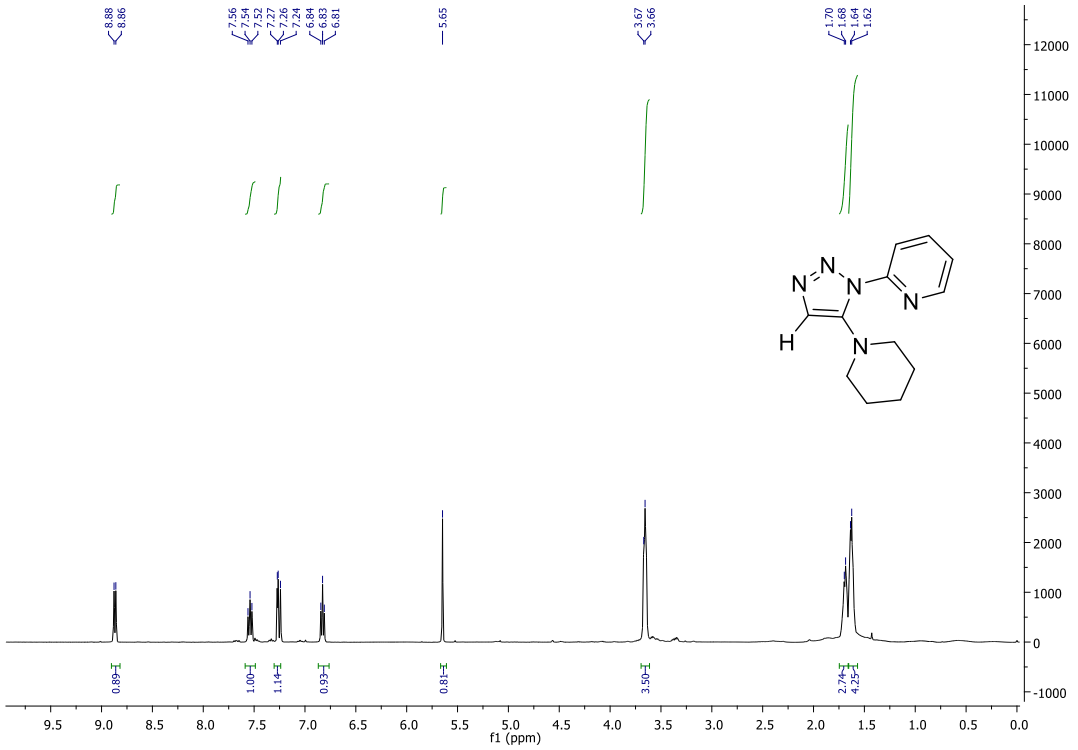

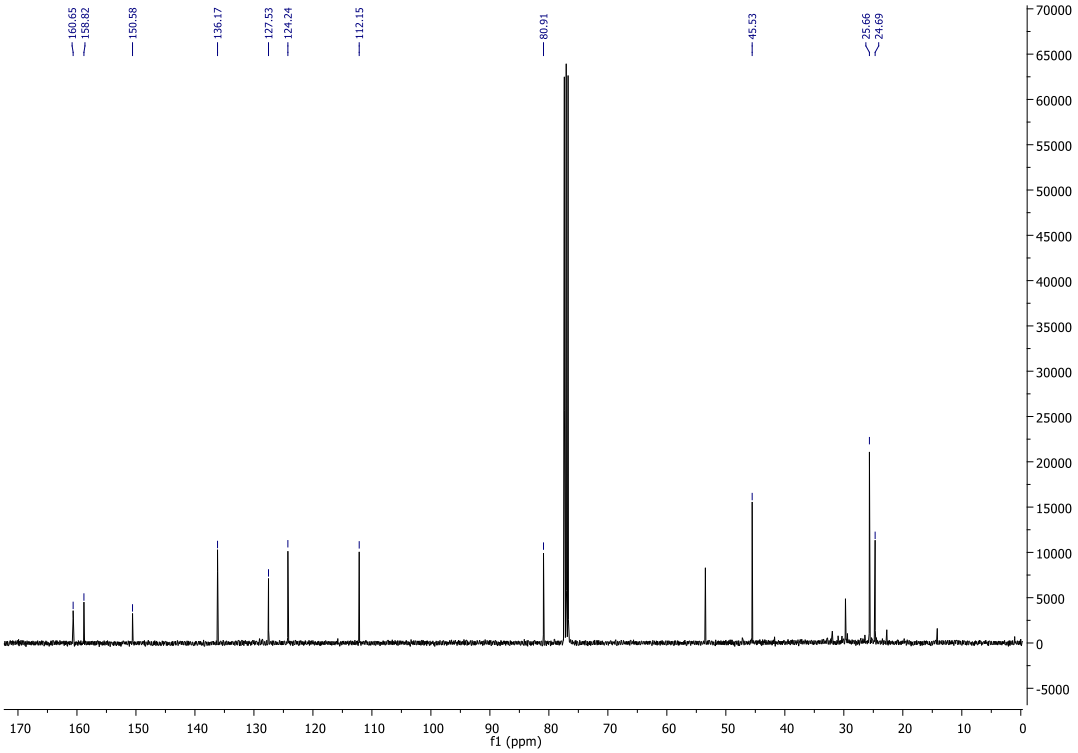

Compound 3.397h

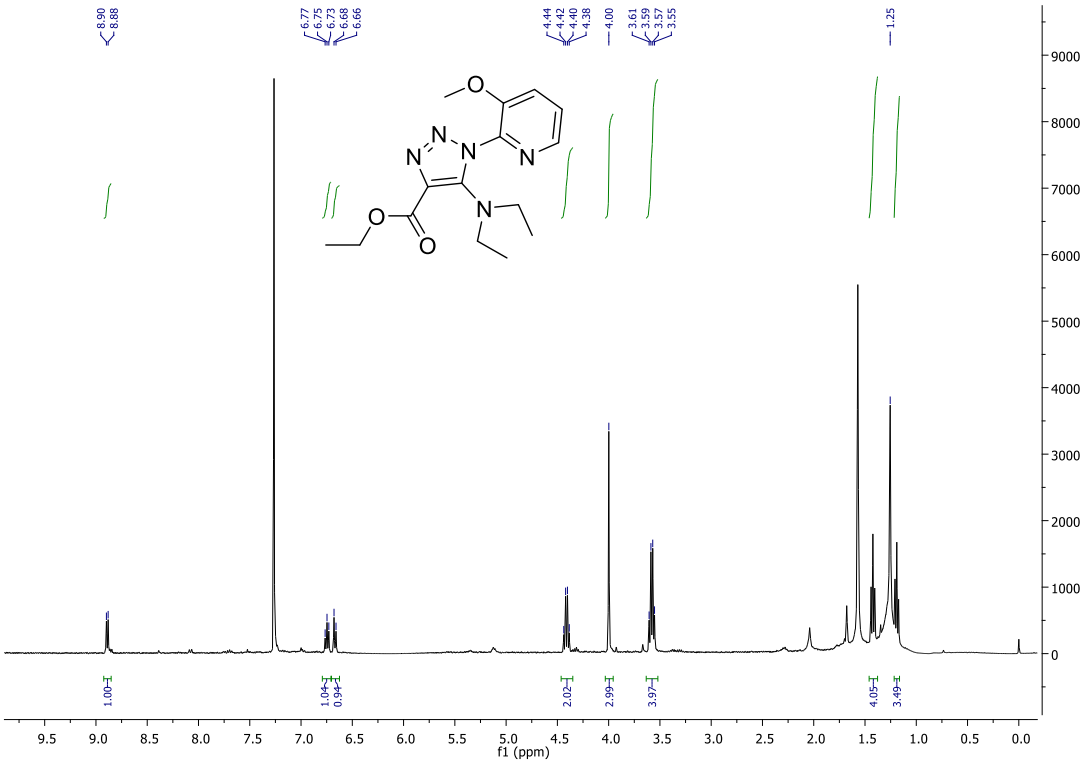

Compound 3.410a

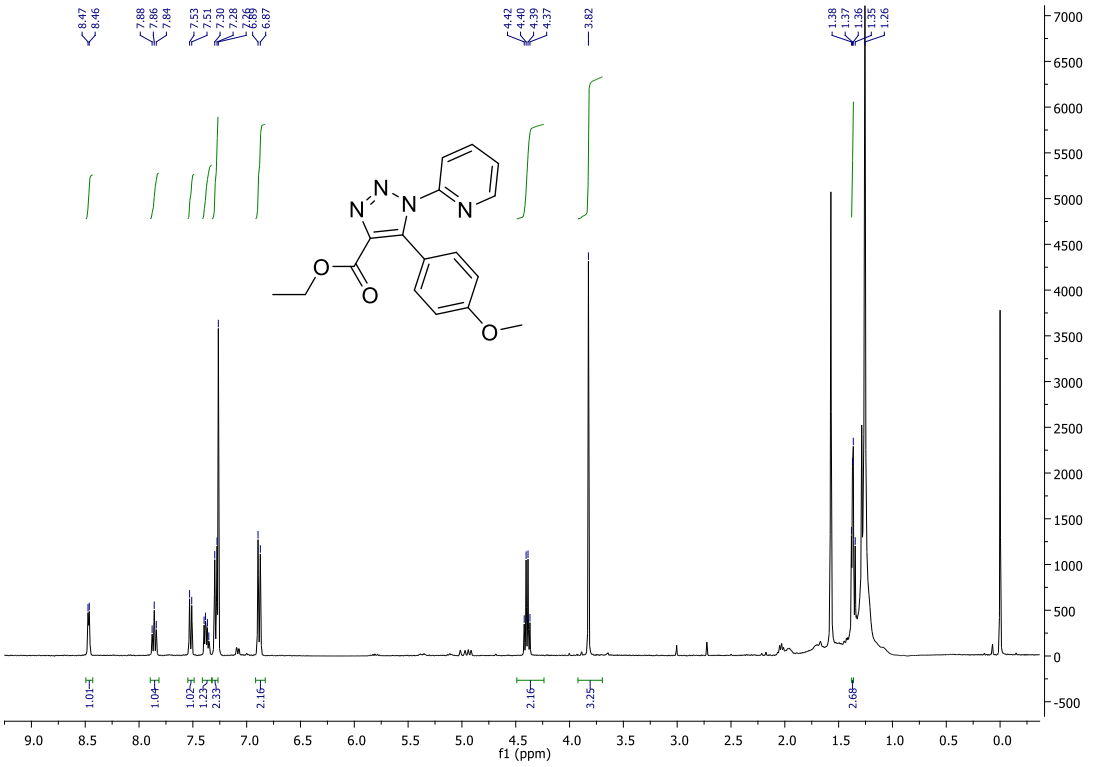

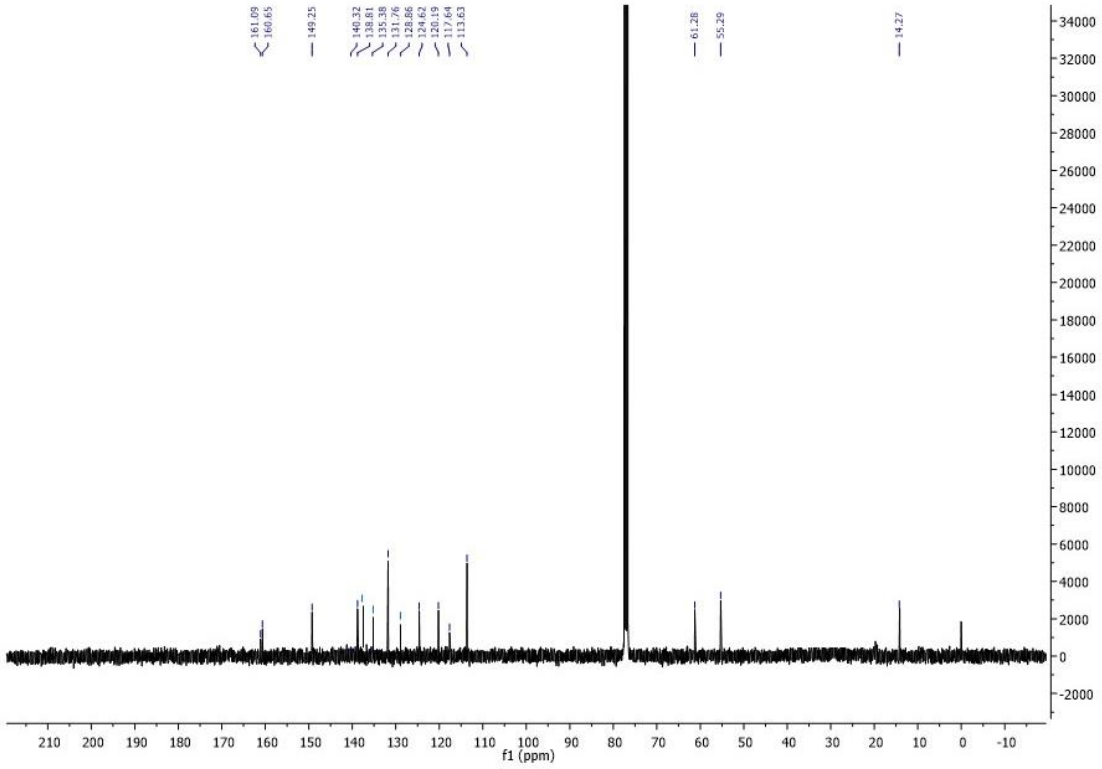

Compound 3.433

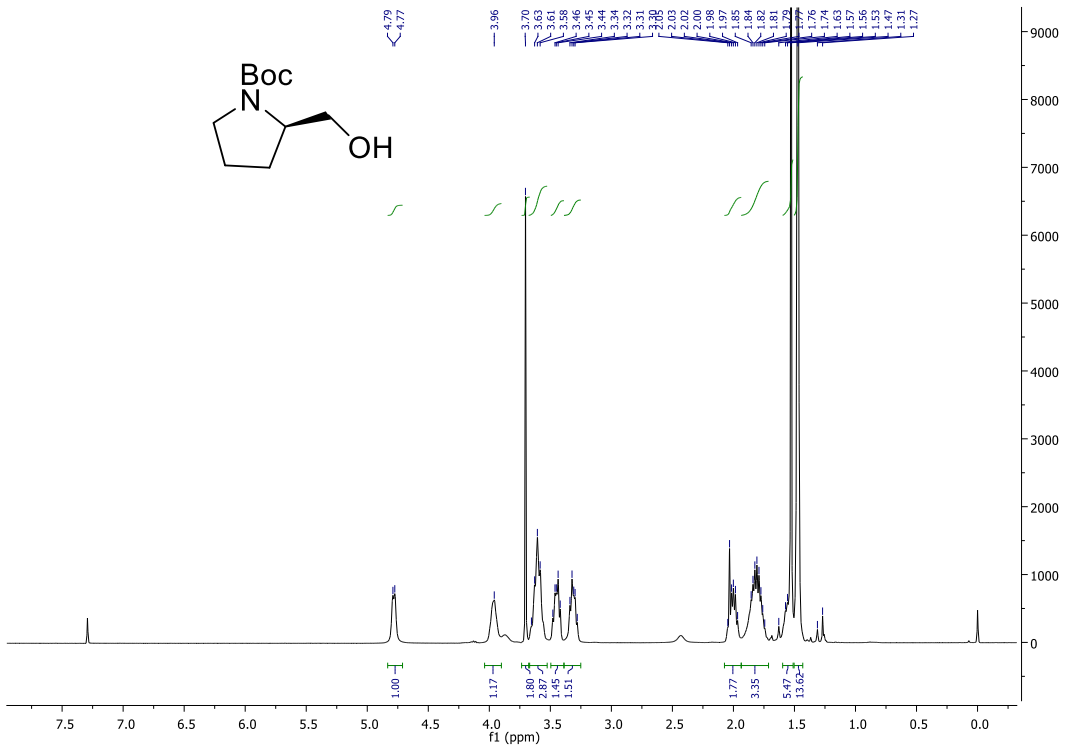

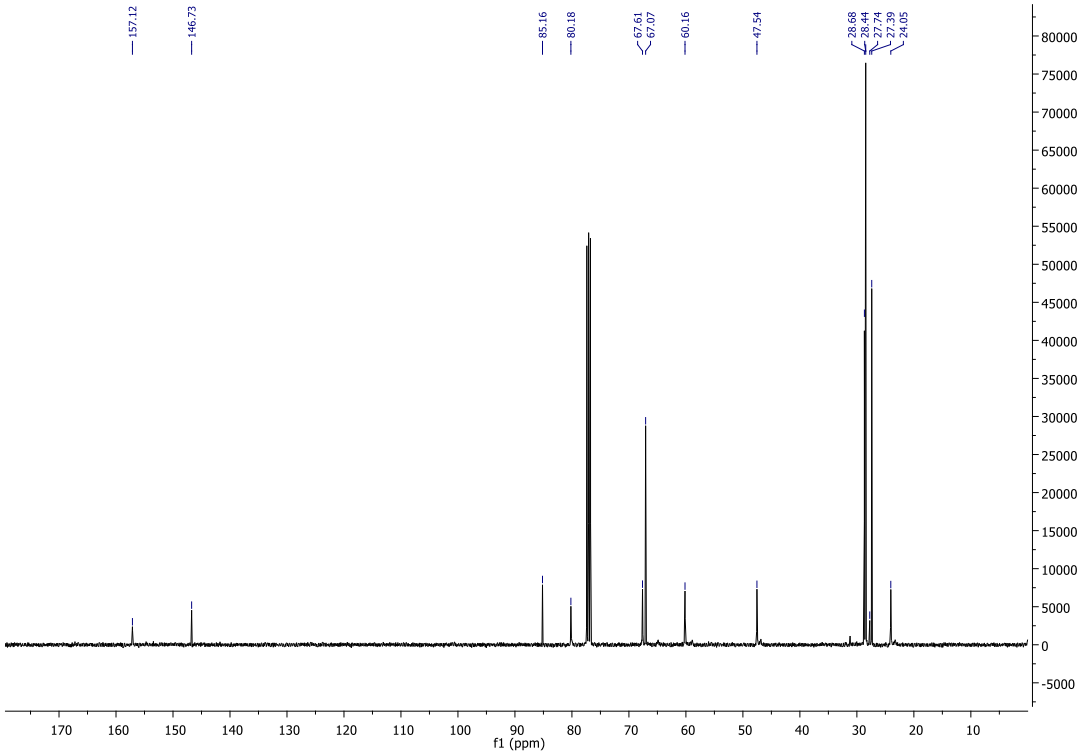

Compound 3.435

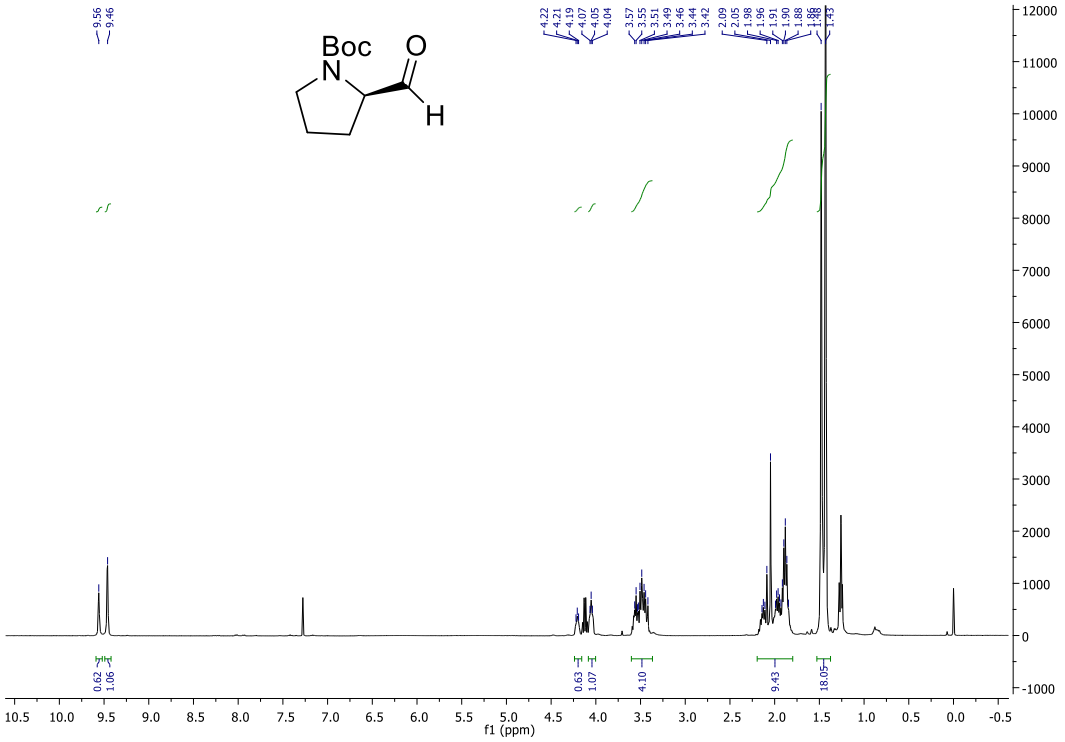

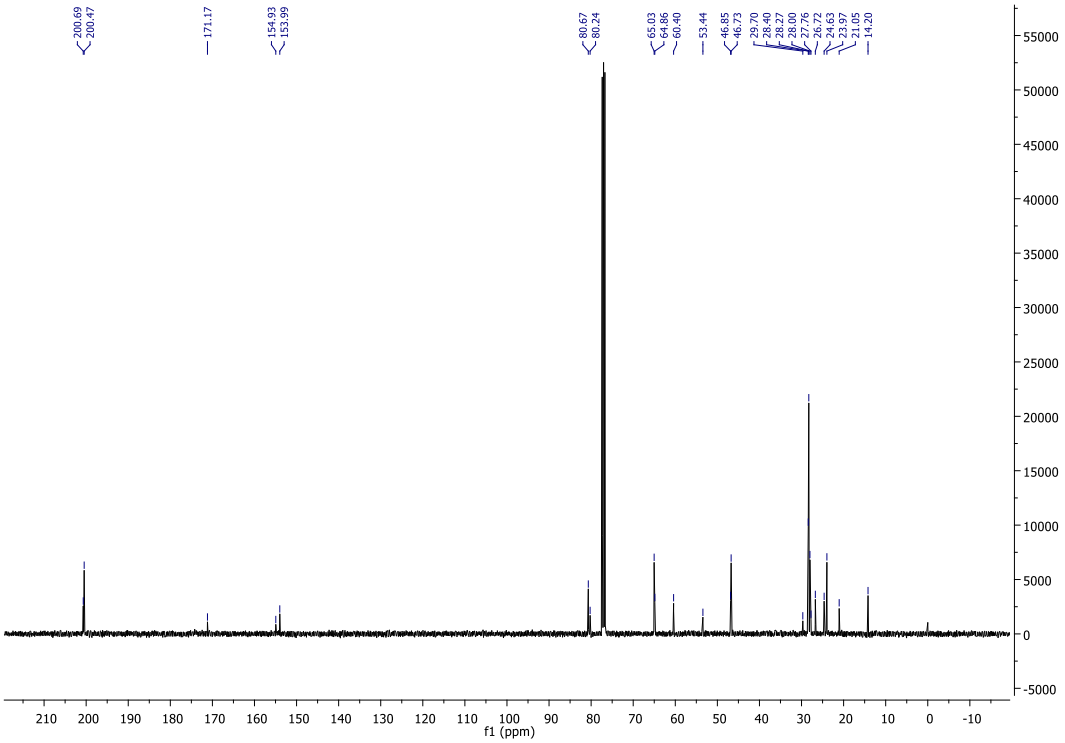

Compound 3.437

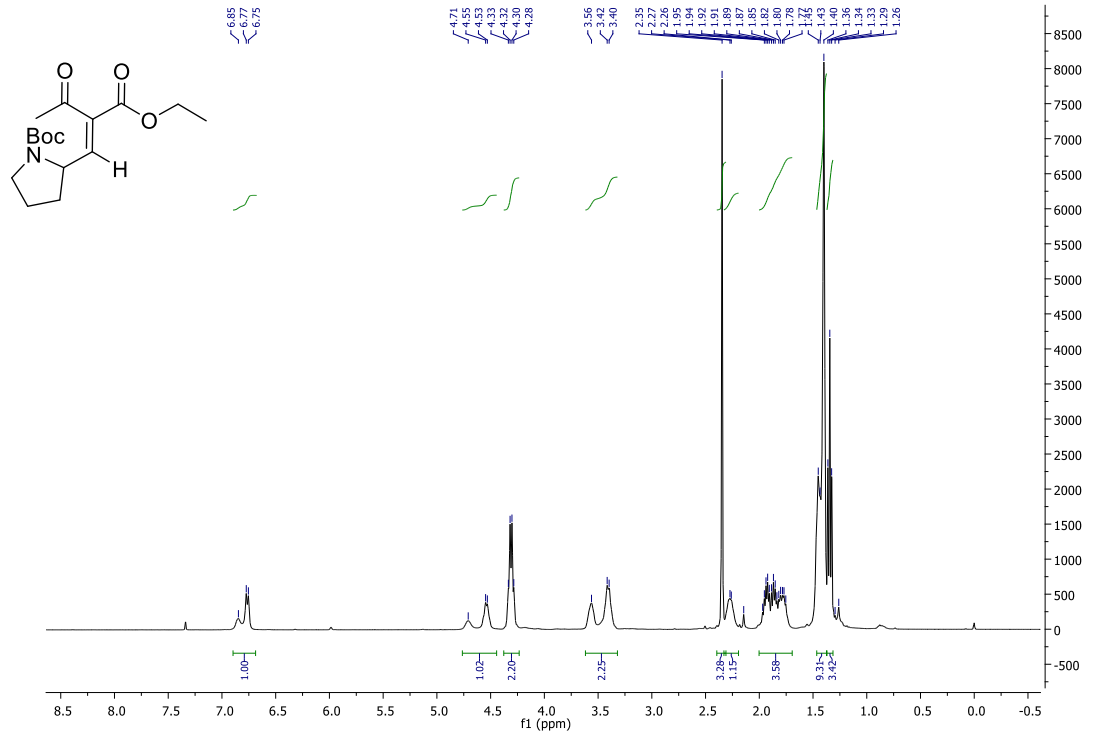

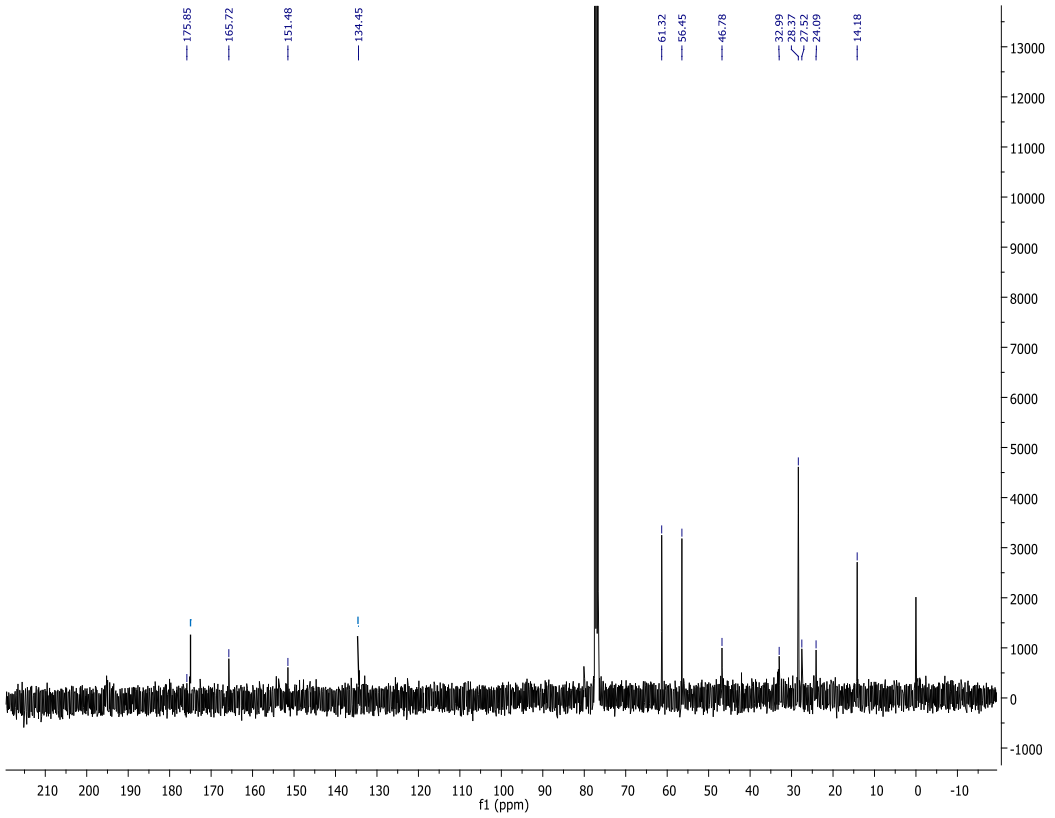

Compound 3.440

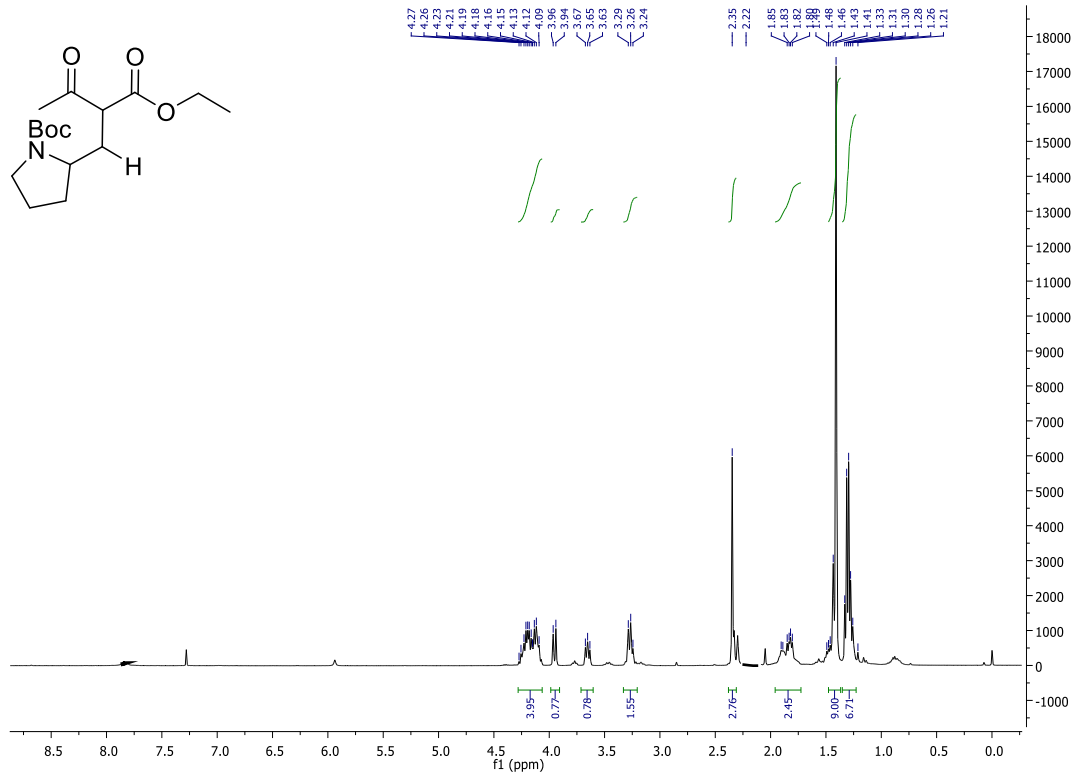

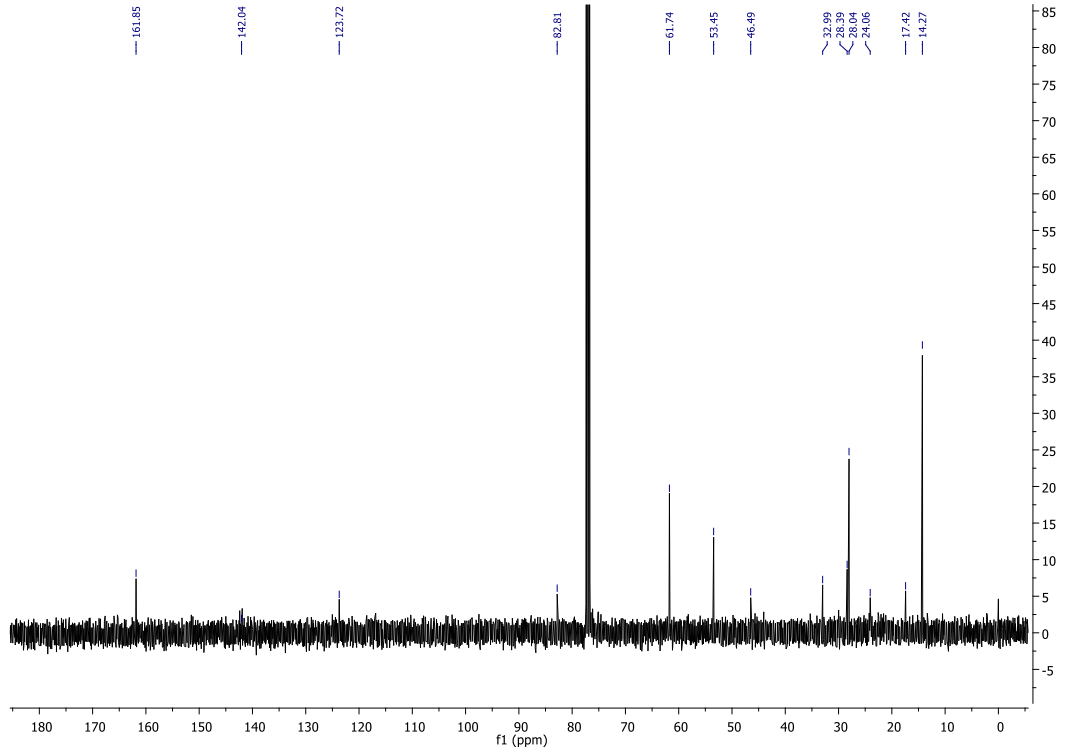

Compound 3.444

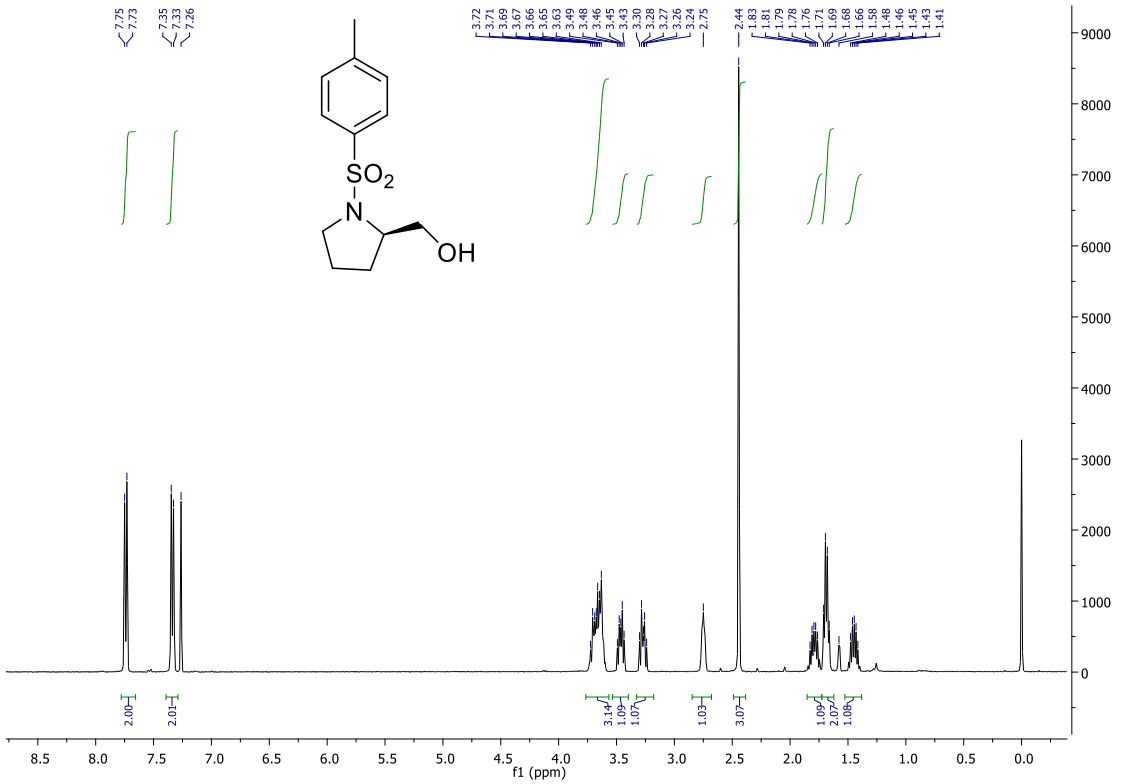

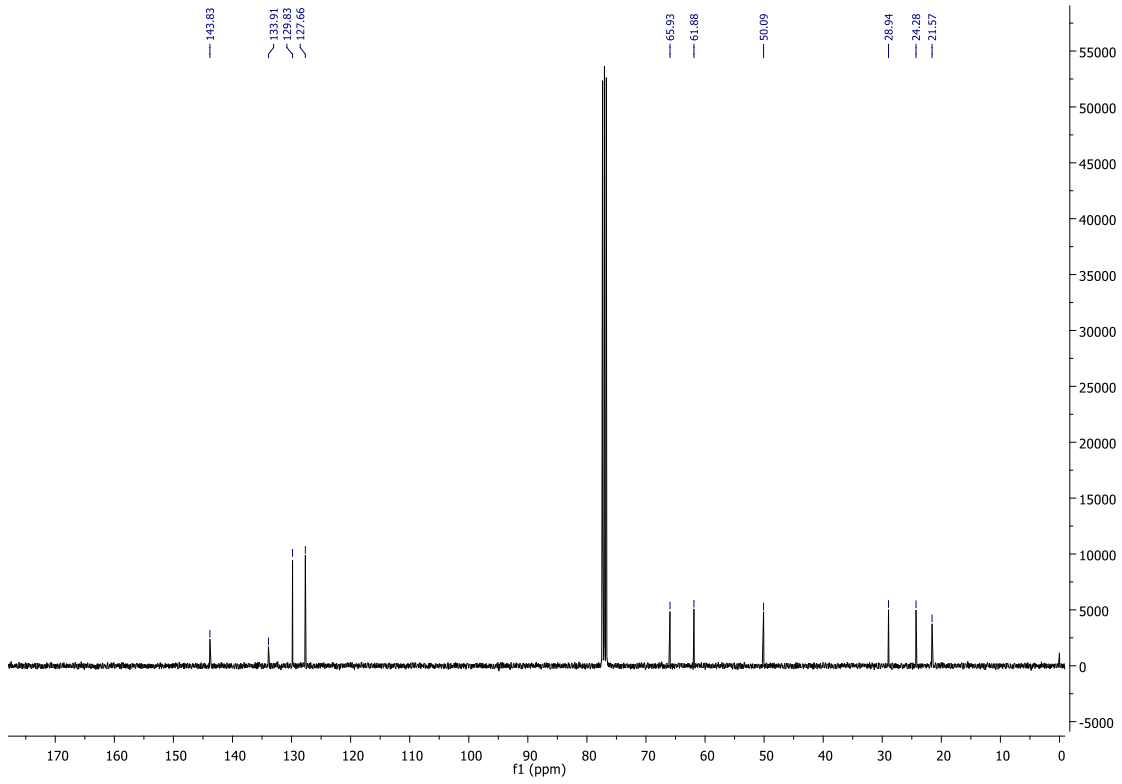

Compound 3.445

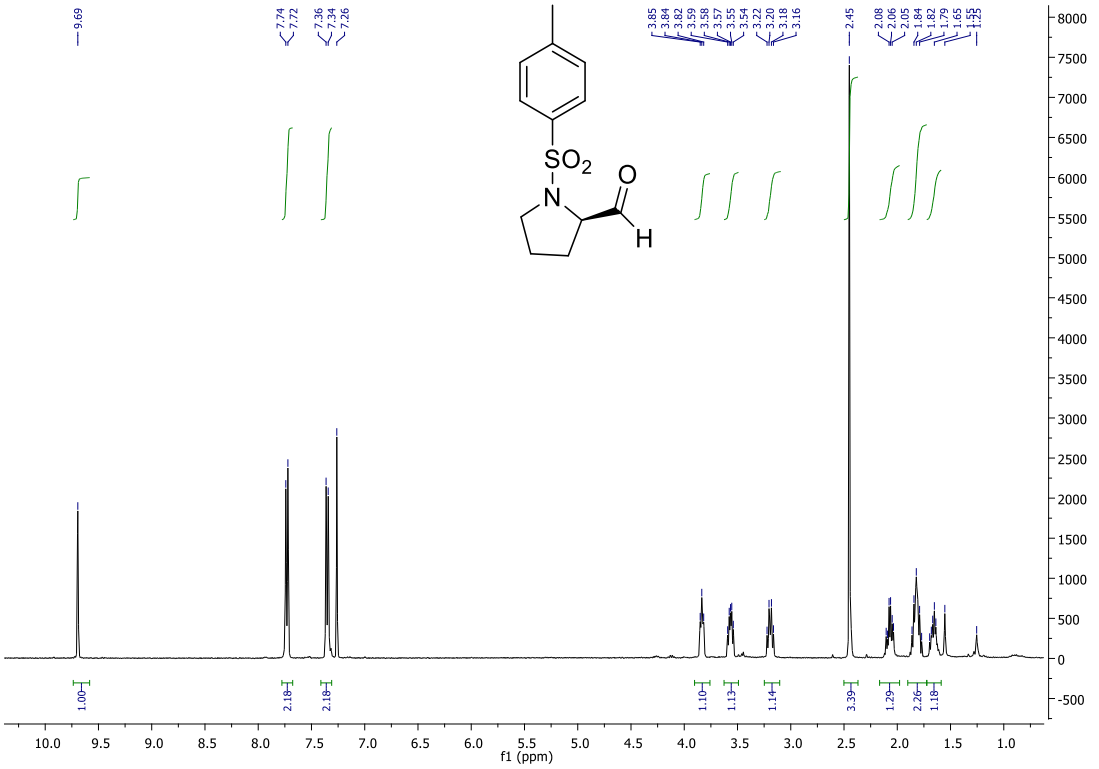

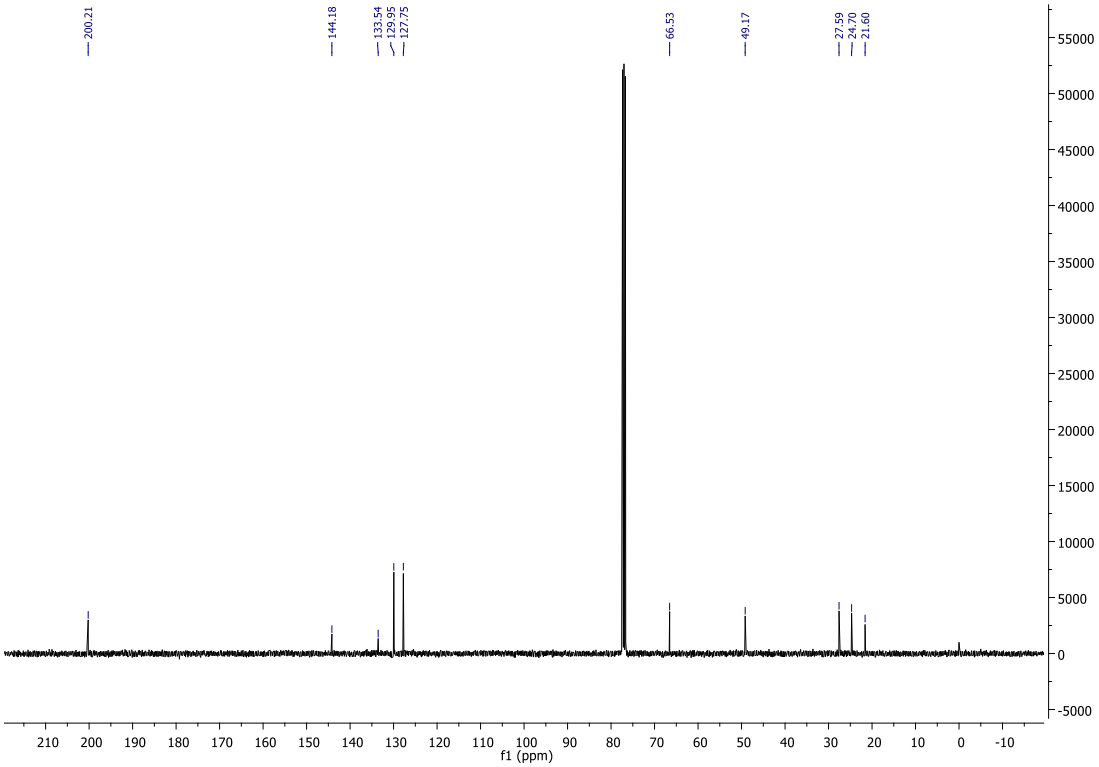

Compound 3.446

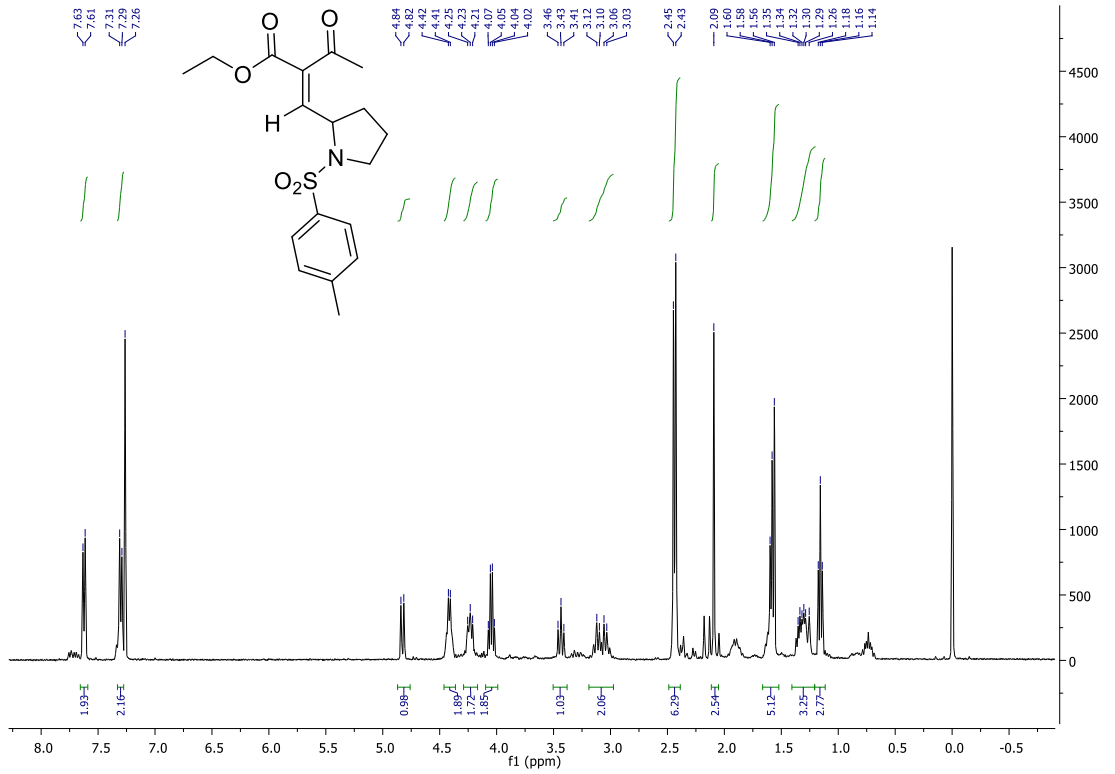

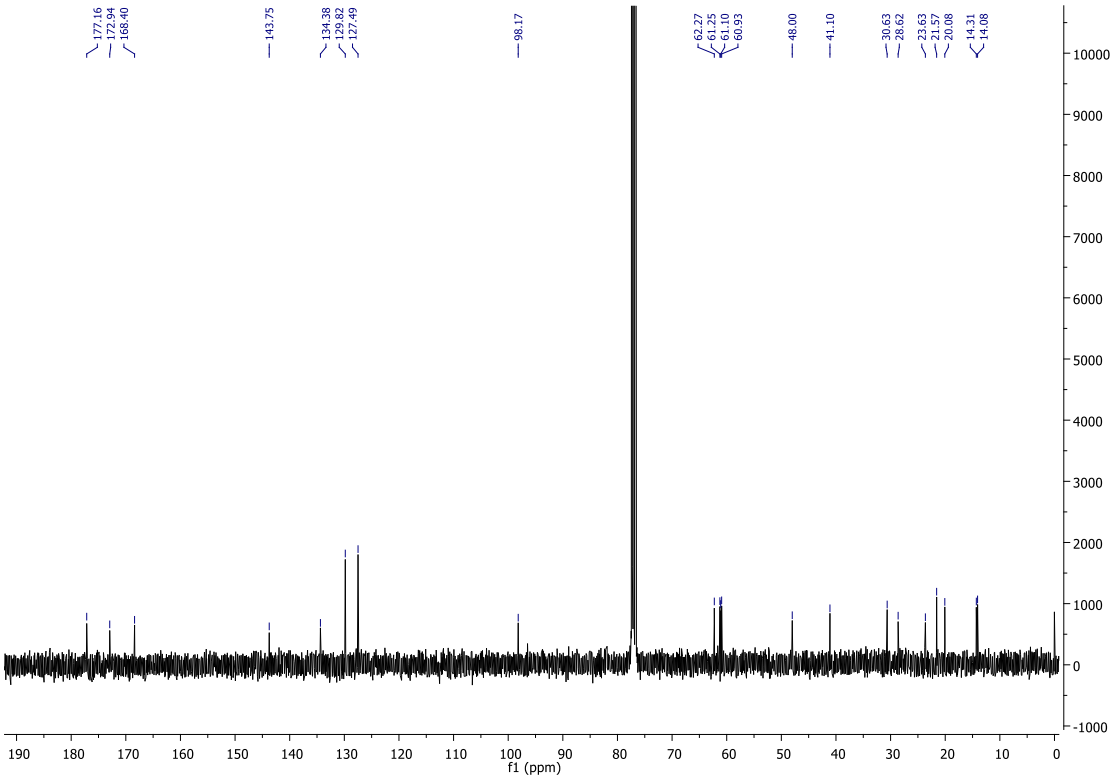

Compound 3.447

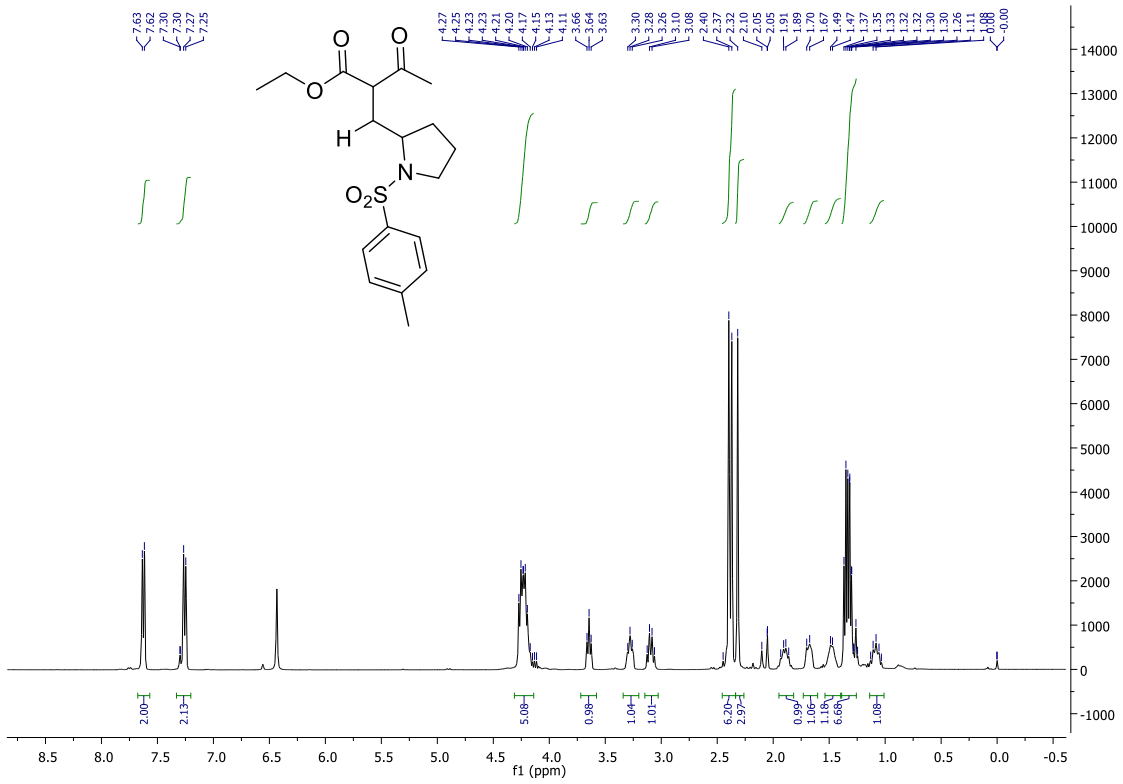

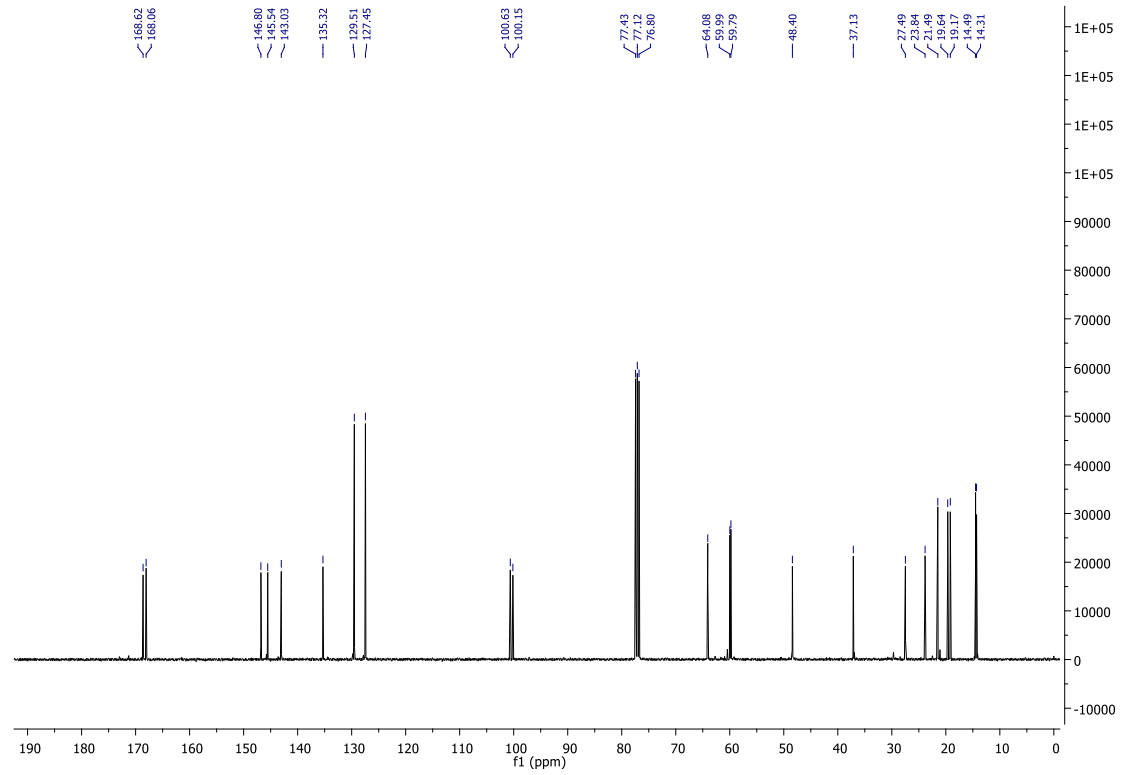

Conclusions

In summary, this thesis project has been focused on the synthesis of a novel small library of 1,4-disubstituted pyridine-based 1,2,3-triazoles **2.80a-f** *via* a mild and catalyst-free reaction protocol, already validated in the Adamo's lab, between pyridyl azides **1.134a-d** and β-ketoesters **1.98** and **1.124a-f**. Given the importance of the triazole pharmacophore in medicinal chemistry as amide bioisostere, we performed docking tests on triazoles **1.136a** and **2.80a-e**, along with other 5-hydroxytriazoles previously synthesised in our group, to better evaluate their potential application in biological systems. Notably, we found out these compounds to target 20 proteins and, in particular, the carboxylate derivative of **1.136a** (**2.53**) highlighted a promising binding-score value (80.13) with KAT2A protein. Therefore, we synthesised a small library of **2.53** analogs (**2.80a-f** and **2.81a-d**) bearing a hydrogen atom at position C5 rather than a hydroxy moiety. Fluorescence assays confirmed the activity of the sole triazoles **2.53**, **2.81a-d** and **2.80b** against KAT2A, pointing out the importance of a carboxylic function at position C4 of the triazole ring, while showing inactivity of triazoles **2.80a,c-e** bearing an ester group at position C4 instead. Following these results, we tested the activity *in vitro* of triazoles **2.53**, **2.81a-d, 2.80b** and **2.80f** and found out that only triazole **2.80b** displayed the best results, with a promising inhibition of KAT2A acetylation activity of 40%. Furthermore, the synthesis of a modified version of triazole **2.80b**, bearing an amide function instead of a carboxylic one (**2.80f**), proved the inhibitory activity to sligthly increase in CCK8 assay, even though exhibiting only a 15% H3K9/14ac reduction of acetylation levels when submitted to WB on U937 leukemia cells. These preliminary results proved the presence of a flexible lateral chain at position C4 to be crucial to bind the enzyme as well as possessing a hydrogen-bond acceptor site to further engage with KAT2A. We then also submitted triazoles **2.80a-e** to C-H activation and conjugation with prolinic scaffolds in order to test their potential in supramolecular organic chemistry and organocatalysis. We created a small library of **2.80a-e** analogs *via* C-H activation reactions through either copper or palladium catalysis. In particular, copper-catalysed C-H activation led to the formation of new C-N bonds when reacting pyridine-based 1,2,3-triazole **2.80a-e** with both linear and cyclic primary and secondary amines **3.391-3.396** yielding analogs **3.397a-h**, which are new compounds not yet reported in literature, in average yields. On the other hand, palladium-catalysed C-H activation to form new C-C bonds was successful only when reacting pyridine-based 1,2,3-triazole **2.80a** with 4-bromoanisole **3.403** in the presence of palladium acetate **3.89** yielding a new triazole-based compound **3.410a**, not yet reported in literature. We also tried to develope a new prototype of proline-based triazole organocatalyst by reacting *N*-Boc- and *N*-tosyl proline β-ketoesters **3.440** and **3.447** with azides **1.136a** and **3.423b** in the presence of various solvents and bases but none of these attempts succeeded. Therefore, future work will involve optimisation of the structure-activity relationship of **2.80b**, in order to find the optimal substitution pattern to correctly orientate

the tested compound towards KAT2A, and investigation of the best reaction conditions to attempt again to the synthesis of proline-based triazoles as organocatalysts.

References

(1) Dalvie D. K.; Kalgutkar A. S.; Khojasteh-Bakht S. C.; Obach R. S.; O'Donnell J. P., Biotransformation reactions of five-membered aromatic heterocyclic rings, *Chem Res Toxicol*., **2002**, *15* (3), 269-299.

(2) Dheer, D.; Singh, V.; Shankar, R. Medicinal Attributes of 1,2,3-Triazoles: Current Developments. *Bioorg. Chem.* **2017**, *71*, 30-54.

(3) Ozimiński, W. P.; Dobrowolski, J. C.; Mazurek, A. P. DFT Studies on Tautomerism of C5-Substituted 1,2,4-Triazoles. *J. Mol. Struct. THEOCHEM* **2004**, *680* (1-3), 107-115.

(4) Catalán, J.; Sánchez-Cabezudo, M.; De Paz, J. L. G.; Elguero, J.; Taft, R. W.; Anvia, F. The Tautomerism of 1,2,3-triazole, 3(5)-methylpyrazole and Their Cations. *J. Comput. Chem.* **1989**, *10* (3), 426-433.

(5) Tomas, F.; Abboud, J. M.; Laynez, J.; Notario, I.; Santos, L.; Nilsson, S. O.; Catalan, J.; Claramunt, R. M.; Elguero, J. Benzotriazole. **1989**, 7348-7353.

(6) Rauhut, G. Modulation of Reaction Barriers by Generating Reactive Intermediates: Double Proton Transfer Reactions. *Phys. Chem. Chem. Phys.* **2003**, *5* (5), 791-800.

(7) Adam, W.; Grimison, A. Sigma-Polarization in 5-Membered Heterocyclic Ring Systems. *Theor. Chim. Acta* **1967**, *7* (4), 342-351.

(8) Ramsden, C. A. The Influence of Aza-Substitution on Azole Aromaticity. *Tetrahedron* **2010**, *66* (14), 2695-2699.

(9) Phelan, N. F.; Orchin, M. Cross Conjugation. *J. Chem. Educ.* **1968**, *45* (10), 633-637.

(10) Curutchet, C.; Poater, J.; Solà, M.; Elguero, J. Analysis of the Effects of N-Substituents on Some Aspects of the Aromaticity of Imidazoles and Pyrazoles. *J. Phys. Chem. A* **2011**, *115* (30), 8571-8577.

(11) Schulze, B.; Schubert, U. S. Beyond Click Chemistry-Supramolecular Interactions of 1,2,3-Triazoles. *Chem. Soc. Rev.* **2014**, *43* (8), 2522-2571.

(12) Han, Y.; Huynh, H. V. Pyrazolin-4-Ylidenes: A New Class of Intriguing Ligands. *Dalt. Trans.* **2011**, *40* (10), 2141-2147.

(13) Jano, I. Comparison between Approximate Methods for Calculating Ionization Potentials and the Use of σ-Ionization Potentials as a Measure of Relative Basicity of Azoles. *J. Phys. Chem.* **1991**, *95* (20), 7694-7699.

(14) Marín-Luna, M.; Alkorta, I.; Elguero, J. A Theoretical Study of the Gas Phase (Proton Affinity) and Aqueous (PKa) Basicity of a Series of 150 Pyrazoles. *New J. Chem.* **2015**, *39* (4), 2861-2871.

(15) Shen, K.; Fu, Y.; Li, J. N.; Liu, L.; Guo, Q. X. What Are the PKa Values of C-H Bonds in Aromatic Heterocyclic Compounds in DMSO? *Tetrahedron* **2007**, *63* (7), 1568-1576.

(16) Matulis, V. E.; Halauko, Y. S.; Ivashkevich, O. A.; Gaponik, P. N. CH Acidity of Five-Membered Nitrogen-Containing Heterocycles: DFT Investigation. *J. Mol. Struct. Theochem.,* **2009**, *909* (1-3), 19-24.

(17) Ackermann, L.; Potukuchi, H. K. Regioselective Syntheses of Fully-Substituted 1,2,3-Triazoles: The CuAAC/C-H Bond Functionalization Nexus. *Org. Biomol. Chem.* **2010**, *8* (20), 4503-4513.

(18) Huisgen, R. 1,3-Dipolar Cycloadditions. Past and Future. *Angew. Chemie Int. Ed. English* **1963**, 565-598.

(19) Huisgen, R. The Concerted Nature of 1,3-Dipolar Cycloadditions and the Question of Diradical Intermediates. *J. Org. Chem.* **1976**, *41* (3), 403-419.

(20) Michael, A. Ueber Die Einwirkung von Diazobenzolimid Anf Herrn Stoehr Zur Erwidernng ; *J. für Prakt. Chemie* **1893**, *48* (1), 94-95.

(21) Benson, F. R.; Savell, W. L. The Chemistry of the Vicinal Triazoles. *Chem. Rev.* **1950**, *46* (1), 1-68.

(22) Katritzky, A. R.; Zhang, Y.; Singh, S. K.; Steel, P. J. 1,3-Dipolar Cycloadditions of Organic Azides to Ester Orbenzotriazolylcarbonyl Activated Acetylenic Amides. *Arkivoc* **2003**, *2003* (15), 47-64.

(23) Huisgen, R. *J. Org. Chem*., **1976**, 41, 403-419.

(24) Huisgen, R.; Mobius, L.B., *Chem. Ber*., **1967**, 100, 2494-2507.

(25) Huisgen, R., Kinetics and Mechanism of 1,3-Dipolar Cycloadditions. *Angew. Chem. Int. Ed. Engl.*, **1963**, *2*, 633-645

(26) Woodward, R. B.; Hoffmann, R. The Conservation of Orbital Symmetry. *Angew. Chemie Int. Ed. English* **1969**, *8* (11), 781-853.

(27) Sustmann, R. and Trill, H., *Angew. Chem., Int. Ed. Engl*.,**1972**, 11, 838-840.

(28) Houk, K. N. The Frontier Molecular Orbital Theory of Cycloaddition Reactions. *Acc. Chem. Res.* **1975**, *8* (11), 361-369.

(29) Ess, D. H.; Houk, K. N. Theory of 1,3-Dipolar Cycloadditions: Distortion/Interaction and Frontier Molecular Orbital Models. *J. Am. Chem. Soc.* **2008**, *130* (31), 10187-10198.

(30) Li, Z.; Seo, T. S.; Ju, J. 1,3-Dipolar Cycloaddition of Azides with Electron-Deficient Alkynes under Mild Condition in Water. *Tetrahedron Lett.* **2004**, *45* (15), 3143-3146.

(31) O. Dimroth, *Berichte der Dtsch. Chem. Gesellschaft*, **1902**, *35*, 1029.

(32) Firestone, R. A. On the Mechanism of 1,3-Dipolar Cycloadditions. *J. Org. Chem.* **1968**, *33* (6), 2285-2290.

(33) Rostovtsev, V. V.; Green, L. G.; Fokin, V. V.; Sharpless, K. B. A Stepwise Huisgen Cycloaddition Process: Copper(I)-Catalyzed Regioselective "Ligation" of Azides and Terminal Alkynes. *Angew. Chemie - Int. Ed.* **2002**, *41*(14), 2596-2599.

(34) Tornøe, C. W.; Christensen, C.; Meldal, M. Peptidotriazoles on Solid Phase: [1,2,3]-Triazoles by Regiospecific Copper(I)-Catalyzed 1,3-Dipolar Cycloadditions of Terminal Alkynes to Azides. *J. Org. Chem.* **2002**, *67* (9), 3057-3064.

(35) Himo, F.; Lovell, T.; Hilgraf, R.; Rostovtsev, V. V.; Noodleman, L.; Sharpless, K. B.; Fokin, V. V. Copper(I)-Catalyzed Synthesis of Azoles. DFT Study Predicts Unprecedented Reactivity and Intermediates. *J. Am. Chem. Soc.* **2005**, *127* (1), 210-216.

(36) Worrell, B.T., Malik, J.A, Fokin, V.V, Direct Evidence of a Dinuclear Copper Intermediate in Cu(I)-Catalyzed Azide-Alkyne Cycloadditions., *Science*, **2013**, *340* (I), 457-461.

(37) Ahlquist, M.; Fokin, V. V. Enhanced Reactivity of Dinuclear Copper(I) Acetylides in Dipolar Cycloadditions. *Organometallics,* **2007**, *26* (18), 4389-4391.

(38) Bräse, S.; Gil, C.; Knepper, K.; Zimmermann, V. Organic Azides: An Exploding Diversity of a Unique Class of Compounds. *Angew. Chemie - Int. Ed.* **2005**, *44* (33), 5188-5240.

(39) Selegue, J. P. Metallacumulenes: From Vinylidenes to Metal Polycarbides. *Coord. Chem. Rev.* **2004**, *248* (15-16 SPEC. ISS.), 1543-1563.

(40) Lewis, W. G.; Magallon, F. G.; Fokin, V. V.; Finn, M. G. Discovery and Characterization of Catalysts for Azide-Alkyne Cycloaddition by Fluorescence Quenching. *J. Am. Chem. Soc.* **2004**, *126* (30), 9152-9153.

(41) Bock, V. D.; Hiemstra, H.; Van Maarseveen, J. H. Cu I-Catalyzed Alkyne-Azide “Click” Cycloadditions from a Mechanistic and Synthetic Perspective. *European J. Org. Chem.* **2006**, No. 1, 51-68.

(42) Cantillo, D.; Ávalos, M.; Babiano, R.; Cintas, P.; Jiménez, J. L.; Palacios, J. C. Assessing the Whole Range of CuAAC Mechanisms by DFT Calculations - On the Intermediacy of Copper Acetylides. *Org. Biomol. Chem.* **2011**, *9* (8), 2952-2958.

(43) Buckley, B. R.; Dann, S. E.; Heaney, H. Experimental Evidence for the Involvement of Dinuclear Alkynylcopper(I) Complexes in Alkyne-Azide Chemistry. *Chem. - A Eur. J.* **2010**, *16* (21), 6278-6284.

(44) Boren, B. C.; Narayan, S.; Rasmussen, L. K.; Zhang, L.; Zhao, H.; Lin, Z.; Jia, G.; Fokin, V. V. Ruthenium-Catalyzed Azide-Alkyne Cycloaddition: Scope and Mechanism. *J. Am. Chem. Soc.* **2008**, *130* (28), 8923-8930.

(45) Zhang, L.; Chen, X.; Xue, P.; Sun, H. H. Y.; Williams, I. D.; Sharpless, K. B.; Fokin, V. V; Jia, G. Ruthenium-Catalyzed Cycloaddition of Alkynes and Organic Azides *J. Am. Chem. Soc.,* **2005**, *127*, 15998-15999.

(46) Rasmussen, L. K.; Boren, B. C.; Fokin, V. V. Ruthenium-Catalyzed Cycloaddition of Aryl Azides and Alkynes. *Org. Lett.* **2007**, *9* (26), 5337-5339.

(47) Candelon, N.; Lastécouères, D.; Diallo, A. K.; Ruiz Aranzaes, J.; Astruc, D.; Vincent, J. M. A Highly Active and Reusable Copper(I)-Tren Catalyst for the “Click” 1,3-Dipolar Cycloaddition of Azides and Alkynes. *Chem. Commun.* **2008**, *1* (6), 741-743.

(48) Diez-Gonzalez, S. The Use of Ligands in Copper-Catalyzed [3+2] Azide-Alkyne Cycloaddition: Clicker than Click Chemistry? *Curr. Org. Chem.* **2011**, *15* (16), 2830-2845.

(49) Lamberti, M.; Fortman, G. C.; Poater, A.; Broggi, J.; Slawin, A. M. Z.; Cavallo, L.; Nolan, S. P. Coordinatively Unsaturated Ruthenium Complexes as Efficient Alkyneazide Cycloaddition Catalysts. *Organometallics* **2012**, *31* (2), 756-767.

(50) Majireck, M.; Weinreb, S. Ru-Catalyzed [3+2] Cycloaddition of Azides with Alkynes to Form Triazoles. *Synfacts* **2007**, *2007* (3), 259.

(51) Kirchner, K.; Calhorda, M. J.; Schmid, R.; Veiros, L. F. Mechanism for the Cyclotrimerization of Alkynes and Related Reactions Catalyzed by CpRuCl. *J. Am. Chem. Soc.* **2003**, *125* (38), 11721-11729.

(52) Berkessel, A.; Gröger, H. Introduction: Organocatalysis - From Biomimetic Concepts to

Powerful Methods for Asymmetric Synthesis. *Asymmetric Organocatalysis* **2005**, 1-8.

(53) MacMillan, D. W. C. The Advent and Development of Organocatalysis. *Nature* **2008**, *455* (7211), 304-308.

(54) Ramasastry, S. S. V. Enamin/Enolat-Vermittelte Organokatalytische Azid-Carbonyl-[3+2]-Cycloadditionen Zur Synthese von Dicht Funktionalisierten 1,2,3-Triazolen. *Angew. Chemie* **2014**, *126* (52), 14536-14538.

(55) Ramachary, D. B.; Ramakumar, K.; Narayana, V. V. Amino Acid-Catalyzed Cascade [3+2]-Cycloaddition/Hydrolysis Reactions Based on the Push-Pull Dienamine Platform: Synthesis of Highly Functionalized NH-1,2,3-Triazoles. *Chem. - A Eur. J.* **2008**, *14* (30), 9143-9147.

(56) Ramachary, D. B.; Shashank, A. B.; Karthik, S. An Organocatalytic Azide-Aldehyde [3+2] Cycloaddition: High-Yielding Regioselective Synthesis of 1,4-Disubstituted 1,2,3-Triazoles. *Angew. Chemie - Int. Ed.* **2014**, *53* (39), 10420-10424.

(57) Shashank, A. B.; Karthik, S.; Madhavachary, R.; Ramachary, D. B. An Enolate-Mediated Organocatalytic Azide-Ketone [3+2]-Cycloaddition Reaction: Regioselective High-Yielding Synthesis of Fully Decorated 1,2,3-Triazoles. *Chem. - A Eur. J.* **2014**, *20* (51), 16877-16881.

(58) Danence, L. J. T.; Gao, Y.; Li, M.; Huang, Y.; Wang, J. Organocatalytic Enamide-Azide Cycloaddition Reactions: Regiospecific Synthesis of 1,4,5-Trisubstituted-1,2,3-Triazoles. *Chem. - A Eur. J.* **2011**, *17* (13), 3584-3587.

(59) Wang, L.; Peng, S.; Danence, L. J. T.; Gao, Y.; Wang, J. Amine-Catalyzed [3+2] Huisgen Cycloaddition Strategy for the Efficient Assembly of Highly Substituted 1,2,3-Triazoles. *Chem. - A Eur. J.* **2012**, *18* (19), 6088-6093.

(60) Yeung, D. K. J.; Gao, T.; Huang, J.; Sun, S.; Guo, H.; Wang, J. Organocatalytic 1,3-Dipolar Cycloaddition Reactions of Ketones and Azides with Water as a Solvent. *Green Chem.* **2013**, *15* (9), 2384-2388.

(61) Destro, D.; Sanchez, S.; Cortigiani, M.; Adamo, M. F. A. Reaction of Azides and Enolisable Aldehydes under the Catalysis of Organic Bases and: Cinchona Based Quaternary Ammonium Salts. *Org. Biomol. Chem.* **2017**, *15* (24), 5227-5235.

(62) Kosobutskii, V. A.; Kagan, G. I.; Belyakov, V. K.; Tarakanov, O. G. Amide-Imidol Tautomerism in Aromatic Polyamides. *J. Struct. Chem.* **1972**, *12* (5), 753-760.

(63) Pippione, A. C.; Sainas, S.; Boschi, D.; Lolli, M. L. *Hydroxyazoles as Acid Isosteres and Their Drug Design Applications—Part 2: Bicyclic Systems*, 1st ed.; Elsevier Inc., 2021.

(64) Begtrup, M., Pedersen, C., Reaction of Phenyl Azide with Amides of Malonic Acids and Phenylacetic Acid, *Acta Chem. Scand*.,**1964**, *18*(6), 1333-1336.

(65) Vilsmeier, A. and Haack, A. Über die Einwirkung von Halogenphosphor auf Alkyl-formanilide. Eine neue Methode zur Darstellung sekundärer und tertiärer *p*-Alkylamino-benzaldehyde. *Ber. dtsch. Chem. Ges. A/B*, **1927**, *60*, 119-122.

(66) Olesen, P.H., Nielsen, F.E., Pedersen, E.B. and Becher, J., Heterocyclic studies. 2. 5-Chloro-1*H*-1,2,3-triazole-4-carboxaldehydes, preparation and rearrangement reactions. *J. Heterocycl. Chem.*, **1984**, *21*,1603-1608.

(67) Cottrell, I. F.; Hands, D.; Houghton, P. G.; Humphrey, G. R.; Wright, S. H. B. An Improved Procedure for the Preparation of 1-benzyl-1H-1,2,3-triazoles from Benzyl Azides. *J. Heterocycl. Chem.*, **1991**, 301-304.

(68) a) Pacifico, R.; Destro, D.; Gillick-Healy, M. W.; Kelly, B. G.; Adamo, M. F. A. Preparation of Acidic 5-Hydroxy-1,2,3-Triazoles via the Cycloaddition of Aryl Azides with β-Ketoesters. *J. Org. Chem.* **2021**, *86*(17), 11354-11360. b) Mowbray, C.E.; Braillard, S., Glossop, P.A.; Whitlock, G.A.; Jacobs, R.T.; Speake, J.; Pandi, B.; Nare, B.; Maes, L.; Yardley, V.; Freund, Y.; Wall, R.J.; Carvalho, S.; Bello, D.; Van den Kerkhof, M.; Caljon, G.; Gilbert, I.H.; Corpas-Lopez, V.; Lukac, I.; Patterson, S.; Zuccotto, F.; Wyllie, S.; DNDI-6148: A Novel Benzoxaborole Preclinical Candidate for the Treatment of Visceral Leishmaniasis., *J. Med. Chem*., **2021**, *64* (21), 16159-16176.

(69) Tao, L.; Han, J.; Tao, F. M. Correlations and Predictions of Carboxylic Acid PKa Values Using Intermolecular Structure and Properties of Hydrogen-Bonded Complexes. *J. Phys. Chem. A,* **2008**, *112* (4), 775-782.

(70) Pippione, A. C.; Dosio, F.; Ducime, A.; Federico, A.; Martina, K.; Sainas, S.; Frølund, B.; Gooyit, M.; Janda, K. D.; Boschi, D.; Lolli, M. L. Substituted 4-Hydroxy-1,2,3-Triazoles: Synthesis, Characterization and First Drug Design Applications through Bioisosteric Modulation and Scaffold Hopping Approaches. *Medchemcomm,* **2015**, *6* (7), 1285-1292.

(71) Richon, V. M.; Webb, Y.; Merger, R.; Sheppard, T.; Jursic, B.; Ngo, L.; Civoli, F.; Breslow, R.; Rifkind, R. A.; Marks, P. A. Second Generation Hybrid Polar Compounds Are Potent Inducers of Transformed Cell Differentiation. *Proc. Natl. Acad. Sci. U. S. A.* **1996**, *93* (12), 5705-5708.

(72) Richon, V. M.; Emiliani, S.; Verdin, E.; Webb, Y.; Breslow, R.; Rifkind, R. A.; Marks, P. A. A Class of Hybrid Polar Inducers of Transformed Cell Differentiation Inhibits Histone Deacetylases. *Proc. Natl. Acad. Sci. U. S. A.* **1998**, *95* (6), 3003-3007.

(73) Ballatore, C.; Huryn, D. M.; Smith, A. B. Carboxylic Acid (Bio)Isosteres in Drug Design. *ChemMedChem,* **2013**, *8* (3), 385-395.

(74) Tsatsaroni, A.; Zoidis, G.; Zoumpoulakis, P.; Tsotinis, A.; Taylor, M. C.; Kelly, J. M.; Fytas, G. An E/Z Conformational Behaviour Study on the Trypanocidal Action of Lipophilic Spiro Carbocyclic 2,6-Diketopiperazine-1-Acetohydroxamic Acids. *Tetrahedron Lett.,* **2013**, *54* (25), 3238-3240.

(75) Marmion, C. J.; Griffith, D.; Nolan, K. B. Hydroxamic Acids - An Intriguing Family of Enzyme Inhibitors and Biomedical Ligands. *Eur. J. Inorg. Chem.* **2004**, *15*, 3003-3016.

(76) Stilling, R. M.; Rönicke, R.; Benito, E.; Urbanke, H.; Capece, V.; Burkhardt, S.; Bahari-Javan, S.; Barth, J.; Sananbenesi, F.; Schütz, A. L.; Dyczkowski, J.; Martinez-Hernandez, A.; Kerimoglu, C.; Dent, S. Y.; Bonn, S.; Reymann, K. G.; Fischer, A. K-Lysine Acetyltransferase 2a Regulates a Hippocampal Gene Expression Network Linked to Memory Formation. *EMBO J.* **2014**, *33* (17), 1912-1927.

(77) Kelly, C. B.; Mercadante, M. A.; Leadbeater, N. E. Trifluoromethyl Ketones: Properties, Preparation, and Application. *Chem. Commun.* **2013**, *49* (95), 11133-11148.

(78) Tetteh, S., Coordination Behavior of Ni^{2+}, Cu^{2+}, and Zn^{2+} in Tetrahedral-1-Methylimidazole Complexes: A DFT/CSD Study, *Bioinorg. Chem. Appl*., **2018**, 3157969-3157977.

(79) Elwell, C. E.; Gagnon, N. L.; Neisen, B. D.; Dhar, D.; Andrew, D.; Yee, G. M.; Tolman, W. B. Copper–Oxygen Complexes Revisited: Structures, Spectroscopy, and Reactivity *Chem. Rev.,* **2017**, 117 (3), 2059-2107.

(80) Mohamed, A. A. Advances in the Coordination Chemistry of Nitrogen Ligand Complexes of Coinage Metals. *Coord. Chem. Rev.* **2010**, *254* (17–18), 1918-1947.

(81) Benamara, N.; Setifi, Z.; Yang, C. I.; Bernès, S.; Geiger, D. K.; Kürkçüoğlu, G. S.; Setifi, F.; Reedijk, J. Coexistence of Spin Canting and Metamagnetism in a One-Dimensional Mn(Ii) Compound Bridged by Alternating Double End-to-End and Double End-on Azido Ligands and the Analog Co(Ii) Compound. *Magnetochemistry* **2021**, *7* (4), 50-66.

(82) Pagoti, S., Surana, S., Chauhan, A., Parasar, B., Dash, J.,Reduction of organic azides to amines using reusable Fe_3O_4 nanoparticles in aqueous medium, *Catal. Sci. Technol.*, **2013**,*3*, 584-588.

(83) Jia, Z.; Zhu, Q. “Click” Assembly of Selective Inhibitors for MAO-A. *Bioorganic Med. Chem. Lett.* **2010**, *20* (21), 6222-6225.

(84) Bertogg, A.; Hintermann, L.; Huber, D. P.; Perseghini, M.; Sanna, M.; Togni, A. Substrate Range of the Titanium TADDOLate Catalyzed Asymmetric Fluorination of Activated Carbonyl Compounds. *Helv. Chim. Acta,* **2012**, *95* (3), 353-403.

(85) Rigby, C. L.; Dixon, D. J. Enantioselective Organocatalytic Michael Additions to Acrylic Acid Derivatives: Generation of All-Carbon Quaternary Stereocentres. *Chem. Commun.* **2008**, *32*, 3798-3800.

(86) Shcherbakova, I., Balandrin, M., Huang, G., **2004**, Pyrimidinone compounds as calcilytics, **PCT: WO 2004/092120 A2**.

(87) Burger A., Isosterism and bioisosterism in drug design., *Prog Drug Res*., **1991**, *37*, 287-371

(88) Langmuir, I., Isomorphism, Isosterism and Covalence, *J. Am. Chem. Soc*., **1919**, *41*, 10, 1543-1559.

(89) Erlenmeyer, H.; E. Berger., Studies on the significance of structure of antigens for the production and the specificity of antibodies, *Biochem. Z*, **1932**, *252*, 22-36.

(90) Erlenmeyer, H.; Berger, E.; Leo, M., Beziehungen Zwischen Der Struktur Der Antigene Und Der Spezifität Der Antikörper. *Helv. Chim. Acta,* **1933**, *16* (1), 733-738.

(91) Friedman H. L.; Influence of isosteric replacements upon biological activity, *NASNRS*, **1951**, *206*, 295-358.

(92) Patani, G. A.; LaVoie, E. J., Bioisosterism: A Rational Approach in Drug Design, *Chem. Rev.,* **1996**, *96* (8), 3147-3176.

(93) Thornber, C. W., Isosterism and Molecular Modification in Drug Design, *Chem. Soc. Rev.,* **1979**, *8* (4), 563-580.

(94) Lipinski, C. A., Chapter 27. Bioisosterism in Drug Design, *Annu. Rep. Med. Chem.,* **1986**, *21* (C), 283-291.

(95) Sheridan, R. P., The Most Common Chemical Replacements in Drug-like Compounds, *J. Chem. Inf. Comput. Sci.,* **2002**, *42* (1), 103-108.

(96) Wermuth, C. G., Similarity in Drugs: Reflections on Analogue Design, *Drug Discov. Today*, **2006**, *11* (7–8), 348-354.

(97) Lima, L.; Barreiro, E., Bioisosterism: A Useful Strategy for Molecular Modification and Drug Design, *Curr. Med. Chem.,* **2012**, *12* (1), 23-49.

(98) Meanwell, N. A., Synopsis of Some Recent Tactical Application of Bioisosteres in Drug Design, *J. Med. Chem.,* **2011**, *54* (8), 2529-2591.

(99) Böhm, H. J.; Flohr, A.; Stahl, M., Scaffold Hopping, *Drug Discov. Today Technol.,* **2004**, *1* (3), 217-224.

(100) Brown, N.; Jacoby, E., On Scaffolds and Hopping in Medicinal Chemistry, *Mini-Reviews Med. Chem.,* **2006**, *6* (11), 1217-1229.

(101) Zhao, H., Scaffold Selection and Scaffold Hopping in Lead Generation: A Medicinal Chemistry Perspective, *Drug Discov. Today,* **2007**, *12* (3–4), 149-155.

(102) Anzali, S.; Gasteiger, J.; Holzgrabe, U.; Polanski, J.; Sadowski, J.; Teckentrup, A.; Wagener, M., The Use of Self-Organizing Neural Networks in Drug Design, *Perspect. Drug Discov. Des.,* **1998**, *9--11*, 273-299.

(103) Kohonen, T., Self-Organized Formation of Topologically Correct Feature Maps, *Biol. Cybern.,* **1982**, *43* (1), 59-69.

(104) Holzgrabe, U.; Wagener, M.; Gasteiger, J., Comparison of Structurally Different Allosteric Modulators of Muscarinic Receptors by Self-Organizing Neural Networks, *J. Mol. Graph.,* **1996**, *14* (4), 185-193.

(105) Hammett, L. P., The Effect of Structure upon the Reactions of Organic Compounds: Temperature and Solvent Influences, *J. Chem. Phys.,* **1936**, *4* (9), 613-617.

(106) Hansch, C.; Leo, A.; Taft, R. W., A Survey of Hammett Substituent Constants and Resonance and Field Parameters, *Chem. Rev.,* **1991**, *91* (2), 165-195.

(107) Angell, Y. L.; Burgess, K. Peptidomimetics via Copper-Catalyzed Azide-Alkyne Cycloadditions. *Chem. Soc. Rev.,* **2007**, *36* (10), 1674-1689.

(108) Kharb, R.; Sharma, P. C.; Yar, M. S. Pharmacological Significance of Triazole Scaffold. *J. Enzyme Inhib. Med. Chem.,* **2011**, *26* (1), 1-21.

(109) Al-Sader, B. H.; Kadri, M., Kinetics and mechanism of the 1,2-dipolar cycloaddition of phenyl azides to merhyl 3-pyrrolidinoacrylate, *Tetrahedron Lett*., **1985**, *26* (38), 4661-4664.

(110) Zhang, L.; Chen, X.; Xue, P.; Sun, H. H. Y.; Williams, I. D.; Sharpless, K. B.; Fokin, V. V.; Jia, G. Ruthenium-Catalyzed Cycloaddition of Alkynes and Organic Azides. *J. Am. Chem. Soc.* **2005**, *127* (46), 15998-15999.

(111) Ramachary, D. B.; Ramakumar, K.; Narayana, V. V. Amino Acid-Catalyzed Cascade [3+2]-

Cycloaddition/Hydrolysis Reactions Based on the Push-Pull Dienamine Platform: Synthesis of Highly Functionalized NH-1,2,3-Triazoles. *Chem. - A Eur. J.,* **2008**, *14* (30), 9143-9147.

(112) Swamer, F. W.; Hauser, C. R. Claisen Acylations and Carbethoxylations of Ketones and Esters by Means of Sodium Hydride. *J. Am. Chem. Soc.,* **1950**, *72* (3), 1352-1356.

(113) Palmer, M. H.; Parsons, S. 4-Methyl-1,2,4-Triazole and 1-Methyl-Tetrazole. *Acta Crystallogr. Sect. C Cryst. Struct. Commun.,* **1996**, *52* (11), 2818-2822.

(114) Sheremet, E. A.; Tomanov, R. I.; Trukhin, E. V.; Berestovitskaya, V. M. Synthesis of 4-Aryl-5-Nitro-1,2,3-Triazoles. *Russ. J. Org. Chem.,* **2004**, *40* (4), 594-595.

(115) Hafez, H. N.; Abbas, H. A. S.; El-Gazzar, A. R. B. A. Synthesis and Evaluation of Analgesic, Anti-Inflammatory and Ulcerogenic Activities of Some Triazolo- and 2-Pyrazolyl-Pyrido[2,3-d]-Pyrimidines. *Acta Pharm.,* **2008**, *58* (4), 359-378.

(116) Liu, K.; Shi, W.; Cheng, P. The Coordination Chemistry of Zn(II), Cd(II) and Hg(II) Complexes with 1,2,4-Triazole Derivatives. *Dalt. Trans.,* **2011**, *40* (34), 8475-8490.

(117) Passannanti, A.; Diana, P.; Barraja, P.; Mingoia, F.; Lauria, A.; Cirrincione, G. Pyrrolo[2,3-d][1,2,3]Triazoles as Potential Antineoplastic Agents. *Heterocycles,* **1998**, *48* (6), 1229-1235.

(118) Johns, B. A.; Weatherhead, J. G.; Allen, S. H.; Thompson, J. B.; Garvey, E. P.; Foster, S. A.; Jeffrey, J. L.; Miller, W. H. The Use of Oxadiazole and Triazole Substituted Naphthyridines as HIV-1 Integrase Inhibitors. Part 1: Establishing the Pharmacophore. *Bioorganic Med. Chem. Lett.,* **2009**, *19* (6), 1802-1806.

(119) Shalini, K.; Kumar, N.; Drabu, S.; Sharma, P. K. Advances in Synthetic Approach to and Antifungal Activity of Triazoles. *Beilstein J. Org. Chem.,* **2011**, *7*, 668-677.

(120) Lindstedt, R.; Ruggiero, V.; Alessio, V. D.; Manganello, S.; Santis, R. D. E.; Sigma-tau, D. S. A.; Superiore, I. Inhibits T Cell Activation By Reducing Nfat Nuclear Residency., **2009**, *22* (1), 29-42.

(121) Dheer, D.; Singh, V.; Shankar, R. Medicinal Attributes of 1,2,3-Triazoles: Current Developments. *Bioorg. Chem.,* **2017**, *71*, 30-54.

(122) Agard, N. J.; Prescher, J. A.; Bertozzi, C. R. A Strain-Promoted [3+2] Azide-Alkyne Cycloaddition for Covalent Modification of Biomolecules in Living Systems. *J. Am. Chem. Soc.,* **2004**, *126* (46), 15046-15047.

(123) Bonandi, E.; Christodoulou, M. S.; Fumagalli, G.; Perdicchia, D.; Rastelli, G.; Passarella, D.

The 1,2,3-Triazole Ring as a Bioisostere in Medicinal Chemistry. *Drug Discov. Today,* **2017**, *22* (10), 1572-1581.

(124) H. Zhou, C.; Wang, Y. Recent Researches in Triazole Compounds as Medicinal Drugs. *Curr. Med. Chem.,* **2012**, *19* (2), 239-280.

(125) Agalave, S. G.; Maujan, S. R.; Pore, V. S. Click Chemistry: 1,2,3-Triazoles as Pharmacophores. *Chem. - An Asian J.,* **2011**, *6* (10), 2696-2718.

(126) Bozorov, K.; Zhao, J.; Aisa, H. A. 1,2,3-Triazole-Containing Hybrids as Leads in Medicinal Chemistry: A Recent Overview. *Bioorganic Med. Chem.,* **2019**, *27* (16), 3511-3531.

(127) Wermuth, C. G.; Ganellin, C. R.; Lindberg, P.; Mitscher, L., Glossary for Chemists of Terms Used in Medicinal Chemistry,*Pure Appl. Chem.,* **1998**, *70* (5), 1129-1143.

(128) Giraudo, A.; Krall, J.; Nielsen, B.; Sørensen, T. E.; Kongstad, K. T.; Rolando, B.; Boschi, D.; Frølund, B.; Lolli, M. L,. 4-Hydroxy-1,2,3-Triazole Moiety as Bioisostere of the Carboxylic Acid Function: A Novel Scaffold to Probe the Orthosteric γ-Aminobutyric Acid Receptor Binding Site, *Eur. J. Med. Chem.,* **2018**, *158*, 311-321.

(129) Johansson, A.; Kollman, P.; Rothenberg, S.; McKelvey, J., Hydrogen Bonding Ability of the Amide Group, *J. Am. Chem. Soc.,* **1974**, *96* (12), 3794-3800.

(130) Tron G. C.; Pirali T.; Billington R. A.; Canonico P. L.; Sorba G.; Genazzani A. A.; Click chemistry reactions in medicinal chemistry: applications of the 1,3-dipolar cycloaddition between azides and alkynes, *Med. Res. Rev*., **2008**, *28* (2), 278-308.

(131) Chrysina, E. D.; Bokor, É.; Alexacou, K. M.; Charavgi, M. D.; Oikonomakos, G. N.; Zographos, S. E.; Leonidas, D. D.; Oikonomakos, N. G.; Somsák, L., Amide-1,2,3-Triazole Bioisosterism: The Glycogen Phosphorylase Case, *Tetrahedron Asymmetry* **2009**, *20* (6-8), 733-740.

(132) Sun, S.; Jia, Q.; Zhang, Z., Applications of Amide Isosteres in Medicinal Chemistry, *Bioorganic Med. Chem. Lett.,* **2019**, *29* (18), 2535-2550.

(133) Sawyers C. L., Chronic myeloid leukemia., *N. Engl. J. Med*., **1999**, *340* (17), 1330-1340.

(134) Schenone, S., Bruno, O., Radi, M., & Botta, M., New insights into small-molecule inhibitors of Bcr-Abl, *Med. Res. Rev*., **2011**, *31* (1), 1-41.

(135) Arioli, F.; Borrelli, S.; Colombo, F.; Falchi, F.; Filippi, I.; Crespan, E.; Naldini, A.; Scalia, G.; Silvani, A.; Maga, G.; Carraro, F.; Botta, M.; Passarella, D., N-[2-Methyl-5-(Triazol-1-

Yl)Phenyl]Pyrimidin-2-Amine as a Scaffold for the Synthesis of Inhibitors of Bcr-Abl, *ChemMedChem,* **2011**, *6* (11), 2009-2018.

(136) Miething, C.; Mugler, C.; Grundler, R.; Hoepfl, J.; Bai, R. Y.; Peschel, C.; Duystel, J., Phosphorylation of Tyrosine 393 in the Kinase Domain of Bcr-Abl Influences the Sensitivity towards Imatinib in Vivo, *Leukemia,* **2003**, *17* (9), 1695-1699.

(137) Skaggs, B. J., Gorre, M. E., Ryvkin, A., Burgess, M. R., Xie, Y., Han, Y., Komisopoulou, E., Brown, L. M., Loo, J. A., Landaw, E. M., Sawyers, C. L., & Graeber, T. G., Phosphorylation of the ATP-binding loop directs oncogenicity of drug-resistant BCR-ABL mutants, *Proceedings of the National Academy of Sciences of the United States of America*, **2006**, *103* (51), 19466-19471.

(138) Shen, T.; Huang, S., The Role of Cdc25A in the Regulation of Cell Proliferation and Apoptosis, *Anticancer. Agents Med. Chem.,* **2012**, *12* (6), 631-639.

(139) Mohammed, I.; Kummetha, I. R.; Singh, G.; Sharova, N.; Lichinchi, G.; Dang, J.; Stevenson, M.; Rana, T. M., 1,2,3-Triazoles as Amide Bioisosteres: Discovery of a New Class of Potent HIV-1 Vif Antagonists, *J. Med. Chem.,* **2016**, *59* (16), 7677-7682.

(140) Brik, A.; Muldoon, J.; Lin, Y. C.; Elder, J. H.; Goodsell, D. S.; Olson, A. J.; Fokin, V. V.; Sharpless, K. B.; Wong, C. H., Rapid Diversity-Oriented Synthesis in Microtiter Plates for in Situ Screening of HIV Protease Inhibitors, *ChemBioChem,* **2003**, *4* (11), 1246-1248.

(141) Brik, A.; Alexandratos, J.; Lin, Y. C.; Elder, J. H.; Olson, A. J.; Wlodawer, A.; Goodsell, D. S.; Wong, C. H., 1,2,3-Triazole as a Peptide Surrogate in the Rapid Synthesis of HIV-1 Protease Inhibitors, *ChemBioChem* **2005**, *6* (7), 1167-1169.

(142) Giffin, M. J.; Heaslet, H.; Brik, A.; Lin, Y. C.; Cauvi, G.; Wong, C. H.; McRee, D. E.; Elder, J. H.; Stout, C. D.; Torbett, B. E., A Copper(I)-Catalyzed 1,2,3-Triazole Azide-Alkyne Click Compound Is a Potent Inhibitor of a Multidrug-Resistant HIV-1 Protease Variant, *J. Med. Chem.* **2008**, *51* (20), 6263-6270.

(143) Tornøe, C. W., Sanderson, S. J., Mottram, J. C., Coombs, G. H., & Meldal, M., Combinatorial library of peptidotriazoles: identification of [1,2,3]-triazole inhibitors against a recombinant Leishmania mexicana cysteine protease, *J. Comb. Chem*., **2004**, *6* (3), 312-324.

(144) Horne, W. S.; Stout, C. D.; Ghadiri, M. R., A Heterocyclic Peptide Nanotube, *J. Am. Chem. Soc.,* **2003**, *125* (31), 9372-9376.

(145) Van Maarseveen, J. H.; Horne, W. S.; Ghadiri, M. R., Efficient Route to C2 Symmetric Heterocyclic Backbone Modified Cyclic Peptides. ,*Org. Lett.,* **2005**, *7* (20), 4503-4506.

(146) Valverde, I. E.; Bauman, A.; Kluba, C. A.; Vomstein, S.; Walter, M. A.; Mindt, T. L., 1,2,3-Triazoles as Amide Bond Mimics: Triazole Scan Yields Protease-Resistant Peptidomimetics for Tumor Targeting, *Angew. Chemie - Int. Ed,.* **2013**, *52* (34), 8957-8960.

(147) Valverde, I. E.; Vomstein, S.; Fischer, C. A.; Mascarin, A.; Mindt, T. L., Probing the Backbone Function of Tumor Targeting Peptides by an Amide-to-Triazole Substitution Strategy, *J. Med. Chem.,* **2015**, *58* (18), 7475-7484.

(148) Johansson, J. R.; Hermansson, E.; Nordén, B.; Kann, N.; Beke-Somfai, T., δ-Peptides from RuAAC-Derived 1,5-Disubstituted Triazole Units, *European J. Org. Chem.,* **2014**, *2014* (13), 2703-2713.

(149) Kann, N.; Johansson, J. R.; Beke-Somfai, T., Conformational Properties of 1,4- and 1,5-Substituted 1,2,3-Triazole Amino Acids-Building Units for Peptidic Foldamers, *Org. Biomol. Chem.,* **2015**, *13* (9), 2776-2785.

(150) Cao, J.; Ma, C.; Zang, J.; Gao, S.; Gao, Q.; Kong, X.; Yan, Y.; Liang, X.; Ding, Q.; Zhao, C.; Wang, B.; Xu, W.; Zhang, Y., Novel Leucine Ureido Derivatives as Aminopeptidase N Inhibitors Using Click Chemistry, *Bioorganic Med. Chem.,* **2018**, *26* (12), 3145-3157.

(151) Santiago, C.; Mudgal, G.; Reguera, J.; Recacha, R.; Albrecht, S.; Enjuanes, L.; Casasnovas, J. M., Allosteric Inhibition of Aminopeptidase N Functions Related to Tumor Growth and Virus Infection, *Sci. Rep.,* **2017**, *7*, 1-14.

(152) Morita, Y., Application of Bioisosteres in Drug Design, *Literature Seminar*, **2012**.

(153) Jalili-Baleh, L.; Forootanfar, H.; KüçükkılınÇ, T. T.; Nadri, H.; Abdolahi, Z.; Ameri, A.; Jafari, M.; Ayazgok, B.; Baeeri, M.; Rahimifard, M.; Abbas Bukhari, S. N.; Abdollahi, M.; Ganjali, M. R.; Emami, S.; Khoobi, M.; Foroumadi, A., Design, Synthesis and Evaluation of Novel Multi-Target-Directed Ligands for Treatment of Alzheimer's Disease Based on Coumarin and Lipoic Acid Scaffolds, *Eur. J. Med. Chem.,* **2018**, *152*, 600-614.

(154) Imperio, D.; Pirali, T.; Galli, U.; Pagliai, F.; Cafici, L.; Canonico, P. L.; Sorba, G.; Genazzani, A. A.; Tron, G. C., Replacement of the Lactone Moiety on Podophyllotoxin and Steganacin Analogues with a 1,5-Disubstituted 1,2,3-Triazole via Ruthenium-Catalyzed Click Chemistry, *Bioorganic Med. Chem.* **2007**, *15* (21), 6748-6757.

(155) Yang, L.; Nan, X.; Li, W. Q.; Wang, M. J.; Zhao, X. B.; Liu, Y. Q.; Zhang, Z. J.; & Lee, K. H.; Synthesis of novel spin-labeled podophyllotoxin derivatives as potential antineoplastic agents: Part XXV. Medicinal chemistry research: an international journal for rapid communications on design and mechanisms of action of biologically active agents, **2014**, *23* (11), 4926-4931.

(156) Hung, H. Y.; Ohkoshi, E.; Goto, M.; Bastow, K. F.; Nakagawa-Goto, K.; & Lee, K. H., Antitumor agents. 293. Nontoxic dimethyl-4,4'-dimethoxy-5,6,5',6'-dimethylenedioxybiphenyl-2,2'-dicarboxylate (DDB) analogues chemosensitize multidrug-resistant cancer cells to clinical anticancer drugs, *J. Med. Chem*., **2012**, *55* (11), 5413-5424.

(157) Carlo, B.; Donna, M. H.; Amos, B. Smith, L., Carboxylic Acid (Bio)Lsosteres in Drug Design, *ChemMedChem,* **2013**, *8* (3), 385-395.

(158) Summers, J. B.; Gunn, B. P.; Martin, J. G.; Mazdiyasni, H.; Stewart, A. O.; Young, P. R.; Goetze, A. M.; Bouska, J. B.; Dyer, R. D.; Brooks, D. W.; Carter, G. W., Orally Active Hydroxamic Acid Inhibitors of Leukotriene Biosynthesis, *J. Med. Chem.,* **1988**, *31* (1), 3-5.

(159) Barrett, S. D.; Bridges, A. J.; Dudley, D. T.; Saltiel, A. R.; Fergus, J. H.; Flamme, C. M.; Delaney, A. M.; Kaufman, M.; LePage, S.; Leopold, W. R.; Przybranowski, S. A.; Sebolt-Leopold, J.; Van Becelaere, K.; Doherty, A. M.; Kennedy, R. M.; Marston, D.; Howard, W. A.; Smith, Y.; Warmus, J. S.; Tecle, H., The Discovery of the Benzhydroxamate MEK Inhibitors CI-1040 and PD 0325901, *Bioorganic Med. Chem. Lett.,* **2008**, *18* (24), 6501-6504.

(160) Liebman, Z. R., The Chemistry of Hydroxylamines, Oximes and Hydroxamic Acids, **2003**.

(161) Kurdistani, S. K.; Grunstein, M., Histone Acetylation and Deacetylation in Yeast., *Nat. Rev. Mol. Cell Biol.,* **2003**, *4* (4), 276-284.

(162) Kelly, W. K.; O'Connor, O. A.; Marks, P. A., Histone Deacetylase Inhibitors: From Target to Clinical Trials, *Expert Opin. Investig. Drugs,* **2002**, *11* (12), 1695-1713.

(163) He, R.; Chen, Y.; Chen, Y.; Ougolkov, A. V.; Zhang, J. S.; Savoy, D. N.; Billadeau, D. D.; Kozikowski, A. P., Synthesis and Biological Evaluation of Triazol-4-Ylphenyl-Bearing Histone Deacetylase Inhibitors as Anticancer Agents, *J. Med. Chem.,* **2010**, *53* (3), 1347-1356.

(164) Mwakwari, S. C., Guerrant, W., Patil, V., Khan, S. I., Tekwani, B. L., Gurard-Levin, Z. A., Mrksich, M., & Oyelere, A. K., Non-peptide macrocyclic histone deacetylase inhibitors derived from tricyclic ketolide skeleton, *J. Med. Chem.*, **2010**, *53* (16), 6100-6111.

(165) Brambilla, P.; Perez, J.; Barale, F.; Schettini, G.; Soares, J. C., GABAergic Dysfunction in Mood Disorders, *Mol. Psychiatry,* **2003**, *8* (8), 721-737.

(166) Kim, T. W.; Yong, Y.; Shin, S. Y.; Jung, H.; Park, K. H.; Lee, Y. H.; Lim, Y.; Jung, K. Y., Synthesis and Biological Evaluation of Phenyl-1H-1,2,3-Triazole Derivatives as Anti-Inflammatory Agents, *Bioorg. Chem.,* **2015**, *59*, 1-11.

(167) Flieger, J.; Tatarczak-Michalewska, M.; Wujec, M.; Pitucha, M.; Świeboda, R., RP-HPLC

Analysis and in Vitro Identification of Antimycobacterial Activity of Novel Thiosemicarbazides and 1,2,4-Triazole Derivatives, *J. Pharm. Biomed. Anal.,* **2015**, *107*, 501-511.

(168) Kuntz, I. D.; Blaney, J. M.; Oatley, S. J.; Langridge, R.; Ferrin, T. E., A Geometric Approach to Macromolecule-Ligand Interactions. **1982**, *161*(2), 269-288.

(169) Richards, F. M., Areas, Volumes, Packing, and Protein Structure. **1977**, *6*, 151-176.

(170) Connolly, M. L., Analytical Molecular Surface Calculation, *J. Appl. Crystallogr.,* **1983**, *16* (5), 548-558.

(171) Shoichet, B. K.; Kuntz, I. D., Protein Docking and Complementarity, *J. Mol. Biol.,* **1991**, *221* (1), 327-346.

(172) Shoichet, B. K., Virtual Screening of Chemical Libraries, *Nature,* **2004**, *432* (7019), 862-865.

(173) Ripphausen, P.; Nisius, B.; Bajorath, J., State-of-the-Art in Ligand-Based Virtual Screening, *Drug Discov. Today,* **2011**, *16* (9–10), 372-376.

(174) Bajorath, J., Integration of Virtual and High-Throughput Screening, *Nat. Rev. Drug Discov.,* **2002**, *1* (11), 882-894.

(175) Shen, J.; Xu, X.; Cheng, F.; Liu, H.; Luo, X.; Shen, J.; Chen, K.; Zhao, W.; Shen, X.; Jiang, H., Virtual Screening on Natural Products for Discovering Active Compounds and Target Information., *Curr. Med. Chem*., **2005**, *10* (21), 2327-2342.

(176) Hughes, J. P.; Rees, S. S.; Kalindjian, S. B.; Philpott, K. L., Principles of Early Drug Discovery., *Br. J. Pharmacol*., **2011**, *162* (6), 1239-1249.

(177) Saxena, S. K., High-Throughput Screening for Drug Discovery., *IntechOpen*., Ed. **2022**.

(178) Sun H., Pharmacophore-based virtual screening., *Curr Med Chem*., **2008**, *15* (10), 1018-1024.

(179) Kumar, A.; Zhang, K. Y. J., Advances in the Development of Shape Similarity Methods and Their Application in Drug Discovery., *Front. Chem*., **2018**, *6*, 1-21.

(180) Toledo Warshaviak, D.; Golan, G.; Borrelli, K. W.; Zhu, K.; Kalid, O., Structure-Based Virtual Screening Approach for Discovery of Covalently Bound Ligands., *J. Chem. Inf. Model*., **2014**, *54* (7), 1941-1950.

(181) Maia, E. H. B.; Assis, L. C.; de Oliveira, T. A.; da Silva, A. M.; Taranto, A. G., Structure-

Based Virtual Screening: From Classical to Artificial Intelligence., *Front. Chem*., **2020**, *8*, 343-361.

(182) Brink, T. Ten; Exner, T. E., Influence of Protonation, Tautomeric, and Stereoisomeric States on Protein-Ligand Docking Results, *J. Chem. Inf. Model.,* **2009**, *49* (6), 1535-1546.

(183) Kalliokoski, T.; Salo, H. S.; Lahtela-Kakkonen, M.; Poso, A., The Effect of Ligand-Based Tautomer and Protomer Prediction on Structure-Based Virtual Screening, *J. Chem. Inf. Model.* **2009**, *49* (12), 2742-2748.

(184) Onufriev, A. V., Alexov, E. (). Protonation and pK changes in protein-ligand binding. Quarterly reviews of biophysics, **2013**, *46* (2), 181-209.

(185) Polgár, T.; Keserü, G. M., Virtual Screening for β-Secretase (BACE1) Inhibitors Reveals the Importance of Protonation States at Asp32 and Asp228, *J. Med. Chem.,* **2005**, *48* (11), 3749-3755.

(186) Thilagavathi, R.; Mancera, R. L., Ligand-Protein Cross-Docking with Water Molecules, *J. Chem. Inf. Model.,* **2010**, *50* (3), 415-421.

(187) Barillari, C.; Taylor, J.; Viner, R.; Essex, J. W., Classification of Water Molecules in Protein Binding Sites, *J. Am. Chem. Soc.,* **2007**, *129* (9), 2577-2587.

(188) Hartshorn, M. J.; Verdonk, M. L.; Chessari, G.; Brewerton, S. C.; Mooij, W. T. M.; Mortenson, P. N.; Murray, C. W., Diverse, High-Quality Test Set for the Validation of Protein-Ligand Docking Performance, *J. Med. Chem.,* **2007**, *50* (4), 726-741.

(189) Lie, M. A.; Thomsen, R.; Pedersen, C. N. S.; Schiøtt, B.; Christensen, M. H., Molecular Docking with Ligand Attached Water Molecules, *J. Chem. Inf. Model.,* **2011**, *51* (4), 909-917.

(190) Huang, N.; Shoichet, B. K., Exploiting Ordered Waters in Molecular Docking, *J. Med. Chem.,* **2008**, *51* (16), 4862-4865.

(191) Yang, H.; Bartlam, M.; Rao, Z., Drug Design Targeting the Main Protease, the Achilles Heel of Coronaviruses, *Curr. Pharm. Des.,* **2006**, *12* (35), 4573-4590.

(192) Hornak, V.; Okur, A.; Rizzo, R. C.; Simmerling, C., HIV-1 Protease Flaps Spontaneously Close to the Correct Structure in Simulations Following Manual Placement of an Inhibitor into the Open State, *J. Am. Chem. Soc.,* **2006**, *128* (9), 2812-2813.

(193) Bender, B. J.; Gahbauer, S.; Luttens, A.; Lyu, J.; Webb, C. M.; Stein, R. M.; Fink, E. A.; Balius, T. E.; Carlsson, J.; Irwin, J. J.; Shoichet, B. K., A Practical Guide to Large-Scale Docking, *Nat. Protoc.,* **2021**, *16* (10), 4799-4832.

(194) Meng, X. Y.; Zhang, H. X.; Mezei, M.; Cui, M. M.; Molecular Docking: A Powerful Approach for Structure-Based Drug Discovery, *Curr. Comput. Aided Drug Des.,* **2011**, *7* (2), 146-157.

(195) Amaro, R. E.; Baudry, J.; Chodera, J.; Demir, Ö.; McCammon, J. A.; Miao, Y.; Smith, J. C., Ensemble Docking in Drug Discovery, *Biophys. J.,* **2018**, *114* (10), 2271-2278.

(196) Yang, J. M.; Frank Hsu, D., Consensus Scoring Criteria in Structure-Based Virtual Screening, *J. Chem. Inf. Model.,* **2005***, 45,* 1134-1146*.*

(197) Warren, G. L.; Andrews, C. W.; Capelli, A. M.; Clarke, B.; LaLonde, J.; Lambert, M. H.; Lindvall, M.; Nevins, N.; Semus, S. F.; Senger, S.; Tedesco, G.; Wall, I. D.; Woolven, J. M.; Peishoff, C. E.; Head, M. S., A Critical Assessment of Docking Programs and Scoring Functions., *J. Med. Chem.* **2006**, *49* (20), 5912-5931.

(198) Wang, R.; Lu, Y.; Wang, S., Comparative Evaluation of 11 Scoring Functions for Molecular Docking, *J. Med. Chem.,* **2003**, *46* (12), 2287-2303.

(199) Teramoto, R.; Fukunishi, H., Supervised Consensus Scoring for Docking and Virtual Screening, *J. Chem. Inf. Model.,* **2007**, *47* (2), 526-534.

(200) Chang, M. W.; Ayeni, C.; Breuer, S.; Torbett, B. E., Virtual Screening for HIV Protease Inhibitors: A Comparison of AutoDock 4 and Vina, *PLoS One,* **2010**, *5* (8), 1-9.

(201) Yang, S. Y., Pharmacophore Modeling and Applications in Drug Discovery: Challenges and Recent Advances, *Drug Discov. Today,* **2010**, *15* (11–12), 444-450.

(202) Kuntz, I. D.; Blaney, J. M.; Oatley, S. J.; Langridge, R.; Ferrin, T. E., A geometric approach to macromolecule-ligand interactions, *J. Mol. Biol*., **1982**, *161* (2), 269-288.

(203) Halperin, I.; Ma, B.; Wolfson, H.; Nussinov, R., Principles of Docking: An Overview of Search Algorithms and a Guide to Scoring Functions, *Proteins Struct. Funct. Genet.,* **2002**, *47* (4), 409-443.

(204) Willett, P.; Barnard, J. M.; Downs, G. M., Chemical Similarity Searching, *J. Chem. Inf. Comput. Sci.,* **1998**, *38* (6), 983-996.

(205) Cramer, R. D.; Redi, G.; Berkoff, C. E., Substructural Analysis. A Novel Approach to the Problem of Drug Design, *J. Med. Chem.,* **1974**, *17* (5), 533-535.

(206) Gasteiger, J.; Rudolph, C.; Sadowski, J., Automatic Generation of 3D-Atomic Coordinates for Organic Molecules, *Tetrahedron Comput. Methodol.,* **1990**, *3*, 537-547.

(207) Cramer, R. D.; Poss, M. A.; Hermsmeier, M. A.; Caulfield, T. J.; Kowala, M. C.; Valentine,

M. T., Prospective Identification of Biologically Active Structures by Topomer Shape Similarity Searching, *J. Med. Chem.,* **1999**, *42* (19), 3919-3933.

(208) Andrews, K. M.; Cramer, R. D., Toward General Methods of Targeted Library Design: Topomer Shape Similarity Searching with Diverse Structures as Queries, *J. Med. Chem.,* **2000**, *43* (9), 1723-1740.

(209) Hall, L. H.; Kier, L. B., The E-State as the Basis for Molecular Structure Space Definition and Structure Similarity, *J. Chem. Inf. Comput. Sci.,* **2000**, *40* (3), 784-791.

(210) Xue, L.; Godden, J. W.; Bajorath, J., Evaluation of Descriptors and Mini-Fingerprints for the Identification of Molecules with Similar Activity, *J. Chem. Inf. Comput. Sci.,* **2000**, *40* (5), 1227-1234.

(211) Xue, L.; Stahura, F. L.; Godden, J. W.; Bajorath, J., Mini-Fingerprints Detect Similar Activity of Receptor Ligands Previously Recognized Only by Three-Dimensional Pharmacophore-Based Methods, *J. Chem. Inf. Comput. Sci.,* **2001**, *41* (2), 394-401.

(212) Mason, J. S.; Morize, I.; Menard, P. R.; Cheney, D. L.; Hulme, C.; Labaudiniere, R. F., New 4-Point Pharmacophore Method for Molecular Similarity and Diversity Applications: Overview of the Method and Applications, Including a Novel Approach to the Design of Combinatorial Libraries Containing Privileged Substructures, *J. Med. Chem.,* **1999**, *42* (17), 3251-3264.

(213) Brown, R. D.; Martin, Y. C., Use of Structure-Activity Data to Compare Structure-Based Clustering Methods and Descriptors for Use in Compound Selection, *J. Chem. Inf. Comput. Sci.*, **1996**, *36* (3), 572-584.

(214) Willett, P.; Winterman, V.; Bawden, D., Implementation of Nonhierarchic Cluster Analysis Methods in Chemical Information Systems: Selection of Compounds for Biological Testing and Clustering of Substructure Search Output, *J. Chem. Inf. Comput. Sci.,* **1986**, *26* (3), 109-118.

(215) Barnard, J. M.; Downs, G. M., Clustering of Chemical Structures on the Basis of Two-Dimensional Similarity Measures, *J. Chem. Inf. Comput. Sci.,* **1992**, *32* (6), 644-649.

(216) Pearlman, R. S.; Smith, K. M., Novel Software Tools for Chemical Diversity, *Perspect. Drug Discov. Des.,* **1998**, *9*, 339-353.

(217) Rusinko, A.; Farmen, M. W.; Lambert, C. G.; Brown, P. L.; Young, S. S., Analysis of a Large Structure/Biological Activity Data Set Using Recursive Partitioning, *J. Chem. Inf. Comput. Sci.,* **1999**, *39* (6), 1017-1026.

(218) Cho, S. J.; Frank Shen, C.; Hermsmeier, M. A., Binary Formal Inference-Based Recursive

Modeling Using Multiple Atom and Physicochemical Property Class Pair and Torsion Descriptors as Decision Criteria, *J. Chem. Inf. Comput. Sci.,* **2000**, *40* (3), 668-680.

(219) Nicolaou, C. A.; Tamura, S. Y.; Kelley, B. P.; Bassett, S. I.; Nutt, R. F., Analysis of Large Screening Data Sets via Adaptively Grown Phylogenetic-like Trees, *J. Chem. Inf. Comput. Sci.,* **2002**, *42* (5), 1069-1079.

(220) Tamura, S. Y.; Bacha, P. A.; Gruver, H. S.; Nutt, R. F., Data Analysis of High-Throughput Screening Results: Application of Multidomain Clustering to the NCI Anti-HIV Data Set, *J. Med. Chem.,* **2002**, *45* (14), 3082-3093.

(221) Labute, P., Binary QSAR: A New Method For The Determination Of Quantitative Structure Activity Relationships, Pacific Symposium on Biocomputing, **1999**, *4*, 444-455.

(222) Gao, H., Application of BCUT Metrics and Genetic Algorithm in Binary QSAR Analysis, *J. Chem. Inf. Comput. Sci.,* **2001**, *41* (2), 402-407.

(223) Gao, H.; Williams, C.; Labute, P.; Bajorath, J., Binary Quantitative Structure-Activity Relationship (QSAR) Analysis of Estrogen Receptor Ligands, *J. Chem. Inf. Comput. Sci.,* **1999**, *39* (1), 164-168.

(224) Perutz, M. F., The hemoglobine molecule, *Scientific American*, **1964**, *211* (5), 64-79.

(225) Van Gunsteren, W. F.; Berendsen, H. J. C., Computer Simulation of Molecular Dynamics: Methodology, Applications, and Perspectives in Chemistry., *Angew. Chemie Int. Ed. English,* **1990**, *29* (9), 992-1023.

(226) Schapira, M.; Raaka, B. M.; Das, S.; Fan, L.; Totrov, M.; Zhou, Z.; Wilson, S. R.; Abagyan, R.; Samuels, H. H., Discovery of Diverse Thyroid Hormone Receptor Antagonists by High-Throughput Docking, *Proc. Natl. Acad. Sci. U. S. A.,* **2003**, *100* (12), 7354-7359.

(227) Evers, A.; Klebe, G., Ligand-Supported Homology Modeling of G-Protein-Coupled Receptor Sites: Models Sufficient for Successful Virtual Screening, *Angew. Chemie - Int. Ed.,* **2003**, *43* (2), 248-251.

(228) Doman, T. N.; McGovern, S. L.; Witherbee, B. J.; Kasten, T. P.; Kurumbail, R.; Stallings, W. C.; Connolly, D. T.; Shoichet, B. K., Molecular Docking and High-Throughput Screening for Novel Inhibitors of Protein Tyrosine Phosphatase-1B, *J. Med. Chem.,* **2002**, *45* (11), 2213-2221.

(229) Paiva, A. M.; Vanderwall, D. E.; Blanchard, J. S.; Kozarich, J. W.; Williamson, J. M.; Kelly, T. M., Inhibitors of Dihydrodipicolinate Reductase, a Key Enzyme of the Diaminopimelate Pathway of Mycobacterium Tuberculosis, *Biochim. Biophys. Acta - Protein Struct. Mol. Enzymol.,* **2001**,

1545 (1–2), 67-77.

(230) Lipinski, C. A.; Lombardo, F.; Dominy, B. W.; Feeney, P. J., Experimental and Computational Approaches to Estimate Solubility and Permeability in Drug Discovery and Development Settings, *Adv. Drug Deliv. Rev.,* **2012**, *64*, 4-17.

(231) Oprea, T. I., Current Trends in Lead Discovery: Are We Looking for the Appropriate Properties?, *Mol. Divers.,* **2000**, *5* (4), 199-208.

(232) McGovern, S. L.; Caselli, E.; Grigorieff, N.; Shoichet, B. K., A Common Mechanism Underlying Promiscuous Inhibitors from Virtual and High-Throughput Screening, *J. Med. Chem.* **2002**, *45* (8), 1712-1722.

(233) Schneidman-Duhovny, D.; Nussinov, R.; Wolfson, H. J., Predicting Molecular Interactions In Silico: Protein-Protein and Protein-Drug Docking, *Front. Med. Chem.,* **2010**, *3*, 585-613.

(234) Ertl, P.; Rohde, B.; Selzer, P., Fast Calculation of Molecular Polar Surface Area as a Sum of Fragment-Based Contributions and Its Application to the Prediction of Drug Transport Properties, *J. Med. Chem.,* **2000**, *43* (20), 3714-3717.

(235) Hohenstein, E. G.; Sherrill, C. D., Effects of Heteroatoms on Aromatic π-π Interactions: Benzene-Pyridine and Pyridine Dimer, *J. Phys. Chem. A,* **2009**, *113* (5), 878-886.

(236) Huber, R. G.; Margreiter, M. A.; Fuchs, J. E.; Von Grafenstein, S.; Tautermann, C. S.; Liedl, K. R.; Fox, T., Heteroaromatic π-Stacking Energy Landscapes, *J. Chem. Inf. Model.,* **2014**, *54* (5), 1371-1379.

(237) Vitaku, E.; Smith, D. T.; Njardarson, J. T., Analysis of the Structural Diversity, Substitution Patterns, and Frequency of Nitrogen Heterocycles among U.S. FDA Approved Pharmaceuticals, *J. Med. Chem.,* **2014**, *57* (24), 10257-10274.

(238) Hsu K. H. K., Thirty Years After Isoniazid: Its Impact on Tuberculosis in Children and Adolescents, *JAMA*, **1984**, *251* (10),1283-1285.

(239) Pym, A. S.; Domenech, P.; Honoré, N.; Song, J.; Deretic, V.; Cole, S. T., Regulation of Catalase-Peroxidase (KatG) Expression, Isoniazid Sensitivity and Virulence by FurA of Mycobacterium Tuberculosis, *Mol. Microbiol.,* **2001**, *40* (4), 879-889.

(240) Morlock, G. P.; Metchock, B.; Sikes, D.; Crawford, J. T.; Cooksey, R. C., EthA, InhA, and KatG Loci of Ethionamide-Resistant Clinical Mycobacterium Tuberculosis Isolates, *Antimicrob. Agents Chemother.,* **2003**, *47* (12), 3799-3805.

(241) Wang, Z.; Vince, R., Design and Synthesis of Dual Inhibitors of HIV Reverse Transcriptase and Integrase: Introducing a Diketoacid Functionality into Delavirdine, *Bioorganic Med. Chem.,* **2008**, *16* (7), 3587-3595.

(242) Wang, L.; Bharti; Kumar, R.; Pavlov, P. F.; Winblad, B., Small Molecule Therapeutics for Tauopathy in Alzheimer's Disease: Walking on the Path of Most Resistance, *Eur. J. Med. Chem.,* **2021**, *209*, 112915-112944.

(243) Minami, J.; Numabe, A.; Andoh, N.; Kobayashi, N.; Horinaka, S.; Ishimitsu, T.; Matsuoka, H., Comparison of Once-Daily Nifedipine Controlled-Release with Twice-Daily Nifedipine Retard in the Treatment of Essential Hypertension, *Br. J. Clin. Pharmacol.,* **2004**, *57* (5), 632-639.

(244) Wang, J. G.; Kario, K.; Lau, T.; Wei, Y. Q.; Park, C. G.; Kim, C. H.; Huang, J.; Zhang, W.; Li, Y.; Yan, P.; Hu, D., Use of Dihydropyridine Calcium Channel Blockers in the Management of Hypertension in Eastern Asians: A Scientific Statement from the Asian Pacific Heart Association, *Hypertens. Res.,* **2011**, *34* (4), 423-430.

(245) Siragusa, L.; Cross, S.; Baroni, M.; Goracci, L.; Cruciani, G. BioGPS: Navigating Biological Space to Predict Polypharmacology, off-Targeting, and Selectivity., *Proteins Struct. Funct. Bioinforma.,* **2015**, *83* (3), 517-532.

(246) Goodford, P. J. A Computational Procedure for Determining Energetically Favorable Binding Sites on Biologically Important Macromolecules., *J. Med. Chem.,* **1985**, *28* (7), 849-857.

(247) Schmitt, S.; Kuhn, D.; Klebe, G. A New Method to Detect Related Function among Proteins Independent of Sequence and Fold Homology., *J. Mol. Biol.,* **2002**, *323* (2), 387-406.

(248) Artese, A.; Cross, S.; Costa, G.; Distinto, S.; Parrotta, L.; Alcaro, S.; Ortuso, F.; Cruciani, G. Molecular Interaction Fields in Drug Discovery: Recent Advances and Future Perspectives., *Wiley Interdiscip. Rev. Comput. Mol. Sci.,* **2013**, *3* (6), 594-613.

(249) Cross, S.; Baroni, M.; Carosati, E.; Benedetti, P.; Clementi, S. FLAP: GRID Molecular Interaction Fields in Virtual Screening. Validation Using the DUD Data Set., *J. Chem. Inf. Model.,* **2010**, *50* (8), 1442-1450.

(250) Siragusa, L.; Spyrakis, F.; Goracci, L.; Cross, S.; Cruciani, G. BioGPS: The Music for the Chemo- and Bioinformatics Walzer., *Mol. Inform.* **2014**, *33*(6–7), 446-453.

(251) Baroni, M.; Cruciani, G.; Sciabola, S.; Perruccio, F.; Mason, J. S. A Common Reference Framework for Analyzing/Comparing Proteins and Ligands. Fingerprints for Ligands and Proteins (FLAP): Theory and Application., *J. Chem. Inf. Model.* **2007**, *47* (2), 279-294.

(252) Bajusz, D.; Rácz, A.; Héberger, K. Why Is Tanimoto Index an Appropriate Choice for Fingerprint-Based Similarity Calculations?, *J. Cheminform.,* **2015**, *7* (1), 1-13.

(253) Voss, A. K.; Thomas, T., Histone Lysine and Genomic Targets of Histone Acetyltransferases in Mammals, *BioEssays,* **2018**, *40* (10), 1-16.

(254) Ud-Din, A. I. M. S.; Tikhomirova, A.; Roujeinikova, A., Structure and Functional Diversity of GCN5-Related n-Acetyltransferases (GNAT), *Int. J. Mol. Sci.,* **2016**, *17* (7), 1018-1063.

(255) Milazzo, G.; Mercatelli, D.; Di Muzio, G.; Triboli, L.; De Rosa, P.; Perini, G.; Giorgi, F. M., Histone Deacetylases (HDACs): Evolution, Specificity, Role in Transcriptional Complexes, and Pharmacological Actionability, *Genes (Basel).,* **2020**, *11* (5), 556-605.

(256) https://pymol.org/2/

(257) Guo, Y.; Liu, B.; Liu, Y.; Sun, W.; Gao, W.; Mao, S.; Chen, L. Oncogenic Chromatin Modifier KAT2A Activates MCT1 to Drive the Glycolytic Process and Tumor Progression in Renal Cell Carcinoma., *Front. Cell Dev. Biol.,* **2021**, *9*, 1-14.

(258) Arede, L.; Pina, C. Buffering Noise: KAT2A Modular Contributions to Stabilization of Transcription and Cell Identity in Cancer and Development., *Exp. Hematol.,* **2021**, *93*, 25-37.

(259) Roth, S.Y, Denu, J.M, Allis, C.D., Histone acetyltransferases., *Annu. Rev. Biochem*. **2001**, *70*, 81-120.

(260) Sternglanz, R., Schindelin, H., Structure and mechanism of action of the histone acetyltransferase Gcn5 and similarity to other N-acetyltransferases., *Proc. Natl. Acad. Sci. U S A*., **1999**, *96* (16), 8807-8808.

(261) Gujral, P.; Mahajan, V.; Lissaman, A. C.; Ponnampalam, A. P., Histone Acetylation and the Role of Histone Deacetylases in Normal Cyclic Endometrium. Reprod., *Biol. Endocrinol*., **2020**, *18* (1), 1-11.

(262) Bannister, A. J.; Kouzarides, T., Regulation of Chromatin by Histone Modifications., *Cell Res*., **2011**, *21* (3), 381-395.

(263) Riss, A.; Scheer, E.; Joint, M.; Trowitzsch, S.; Berger, I.; Tora, L., Subunits of ADA-Two-A-Containing (ATAC) or Spt-Ada-Gcn5-Acetyltrasferase (SAGA) Coactivator Complexes Enhance the Acetyltransferase Activity of GCN5., *J. Biol. Chem*., **2015**, *290* (48), 28997-29009.

(264) Bartek, J.; Lukas, J., Pathways Governing G1/S Transition and Their Response to DNA Damage., *FEBS Lett*., **2001**, *490* (3), 117-122.

(265) Paolinelli, R.; Mendoza-Maldonado, R.; Cereseto, A.; Giacca, M., Acetylation by GCN5 Regulates CDC6 Phosphorylation in the S Phase of the Cell Cycle., *Nat. Struct. Mol. Biol*., **2009**, *16* (4), 412-420.

(266) Orpinell, M.; Fournier, M.; Riss, A.; Nagy, Z.; Krebs, A. R.; Frontini, M.; Tora, L., The ATAC Acetyl Transferase Complex Controls Mitotic Progression by Targeting Non-Histone Substrates., *EMBO J*., **2010**, *29* (14), 2381-2394.

(267) Smith, B. C.; Denu, J. M., Chemical Mechanisms of Histone Lysine and Arginine Modifications, *Biochim. Biophys. Acta - Gene Regul. Mech.,* **2009**, *1789* (1), 45-57.

(268) Wang, Y.; Guo, Y. R.; Liu, K.; Yin, Z.; Liu, R.; Xia, Y.; Tan, L.; Yang, P.; Lee, J. H.; Li, X. J.; Hawke, D.; Zheng, Y.; Qian, X.; Lyu, J.; He, J.; Xing, D.; Tao, Y. J.; Lu, Z., KAT2A Coupled with the α-KGDH Complex Acts as a Histone H3 Succinyltransferase, *Nature,* **2017**, *552*, 273-277.

(269) Bao, X.; Liu, Z.; Zhang, W.; Gladysz, K.; Fung, Y. M. E.; Tian, G.; Xiong, Y.; Wong, J. W. H.; Yuen, K. W. Y.; Li, X. D., Glutarylation of Histone H4 Lysine 91 Regulates Chromatin Dynamics. *Mol. Cell,* **2019**, *76* (4), 660-675.

(270) Tretter, L.; Adam-Vizi, V., Alpha-Ketoglutarate Dehydrogenase: A Target and Generator of Oxidative Stress, *Philos. Trans., R. Soc. B Biol. Sci.,* **2005**, *360* (1464), 2335-2345.

(271) Xylaki, M.; Atzler, B.; Outeiro, T. F., Epigenetics of the Synapse in Neurodegeneration., *Curr. Neurol. Neurosci. Rep*., **2019**, *19* (10), 1-10.

(272) Moris, N.; Edri, S.; Seyres, D.; Kulkarni, R.; Domingues, A. F.; Balayo, T.; Frontini, M.; Pina, C., Histone Acetyltransferase KAT2A Stabilizes Pluripotency with Control of Transcriptional Heterogeneity, *Stem Cells,* **2018**, *36* (12), 1828-1838.

(273) Gao, B.; Kong, Q.; Zhang, Y.; Yun, C.; Dent, S. Y. R.; Song, J.; Zhang, D. D.; Wang, Y.; Li, X.; Fang, D., The Histone Acetyltransferase Gcn5 Positively Regulates T Cell Activation, *J. Immunol.,* **2017**, *198* (10), 3927-3938.

(274) Liao, W.; Lin, J. X.; Leonard, W. J., IL-2 Family Cytokines: New Insights into the Complex Roles of IL-2 as a Broad Regulator of T Helper Cell Differentiation., *Curr. Opin. Immunol*., **2011**, *23* (5), 598-604.

(275) Chen, L.; Wei, T.; Si, X.; Wang, Q.; Li, Y.; Leng, Y.; Deng, A.; Chen, J.; Wang, G.; Zhu, S.; Kang, J., Lysine Acetyltransferase GCN5 Potentiates the Growth of Non-Small Cell Lung Cancer via Promotion of E2F1, Cyclin D1, and Cyclin E1 Expression, *J. Biol. Chem.,* **2013**, *288* (20), 14510-14521.

(276) Yin, Y. W.; Jin, H. J.; Zhao, W.; Gao, B.; Fang, J.; Wei, J.; Zhang, D. D.; Zhang, J.; Fang, D., The Histone Acetyltransferase GCN5 Expression Is Elevated and Regulated by C-Myc and E2F1 Transcription Factors in Human Colon Cancer, *Gene Expr.,* **2015**, *16* (4), 187-196.

(277) Dekker, F. J.; Van Den Bosch, T.; Martin, N. I., Small Molecule Inhibitors of Histone Acetyltransferases and Deacetylases Are Potential Drugs for Inflammatory Diseases, *Drug Discov. Today,* **2014**, *19* (5), 654-660.

(278) Sun, C.; Wang, M.; Liu, X.; Luo, L.; Li, K.; Zhang, S.; Wang, Y.; Yang, Y.; Ding, F.; Gu, X., PCAF Improves Glucose Homeostasis by Suppressing the Gluconeogenic Activity of PGC-1α, *Cell Rep.,* **2014**, *9* (6), 2250-2262.

(279) Lavogina, D.; Enkvist, E.; Uri, A., Bisubstrate Inhibitors of Protein Kinases: From Principle to Practical Applications, *ChemMedChem,* **2010**, *5* (1), 23-34.

(280) Cullis, P. M.; Wolfenden, R.; Cousens, L. S.; Alberts, B. M., Inhibition of Histone Acetylation by N-[2-(S-Coenzyme A)Acetyl] Spermidine Amide, a Multisubstrate Analog, *J. Biol. Chem.,* **1982**, *257* (20), 12165-12169.

(281) Lau, O. D.; Kundu, T. K.; Soccio, R. E.; Ait-Si-Ali, S.; Khalil, E. M.; Vassilev, A.; Wolffe, A. P.; Nakatani, Y.; Roeder, R. G.; Cole, P. A., HATs off: Selective Synthetic Inhibitors of the Histone Acetyltransferases P300 and PCAF, *Mol. Cell,* **2000**, *5* (3), 589-595.

(282) Kwie, F. H. A.; Briet, M.; Soupaya, D.; Hoffmann, P.; Maturano, M.; Rodriguez, F.; Blonski, C.; Lherbet, C.; Baudoin-Dehoux, C., New Potent Bisubstrate Inhibitors of Histone Acetyltransferase P300: Design, Synthesis and Biological Evaluation, *Chem. Biol. Drug Des.,* **2011**, *77* (1), 86-92.

(283) Balasubramanyam, K.; Altaf, M.; Varier, R. A.; Swaminathan, V.; Ravindran, A.; Sadhale, P. P.; Kundu, T. K., Polyisoprenylated Benzophenone, Garcinol, a Natural Histone Acetyltransferase Inhibitor, Represses Chromatin Transcription and Alters Global Gene Expression, *J. Biol. Chem.,* **2004**, *279* (32), 33716-33726.

(284) Rama Rao, A. V.; Venkatswamy, G.; Pendse, D., Camboginol and Cambogin,*Tetrahedron Lett.,* **1980**, *21* (20), 1975-1978.

(285) Mantelingu, K.; Reddy, B. A. A.; Swaminathan, V.; Kishore, A. H.; Siddappa, N. B.; Kumar, G. V. P.; Nagashankar, G.; Natesh, N.; Roy, S.; Sadhale, P. P.; Ranga, U.; Narayana, C.; Kundu, T. K., Specific Inhibition of P300-HAT Alters Global Gene Expression and Represses HIV Replication, *Chem. Biol.,* **2007**, *14* (6), 645-657.

(286) Balasubramanyam, K.; Varier, R. A.; Altaf, M.; Swaminathan, V.; Siddappa, N. B.; Ranga,

U.; Kundu, T. K., Curcumin, a Novel P300/CREB-Binding Protein-Specific Inhibitor of Acetyltransferase, Represses the Acetylation of Histone/Nonhistone Proteins and Histone Acetyltransferase-Dependent Chromatin Transcription, *J. Biol. Chem.,* **2004**, *279* (49), 51163-51171.

(287) Neckers, L.; Trepel, J.; Lee, S.; Chung, E.-J.; Lee, M.-J.; Jung, Y.-J.; Marcu, M., Curcumin Is an Inhibitor of P300 Histone Acetylatransferase, *Med. Chem. (Los. Angeles),* **2006**, *2* (2), 169-174.

(288) Nelson, K. M.; Dahlin, J. L.; Bisson, J.; Graham, J.; Pauli, G. F.; Walters, M. A., The Essential Medicinal Chemistry of Curcumin, *J. Med. Chem.,* **2017**, *60* (5), 1620-1637.

(289) Costi, R.; Di Santo, R.; Artico, M.; Miele, G.; Valentini, P.; Novellino, E.; Cereseto, A., Cinnamoyl Compounds as Simple Molecules That Inhibit P300 Histone Acetyltransferase, *J. Med. Chem.,* **2007**, *50* (8), 1973-1977.

(290) Balasubramanyam, K.; Swaminathan, V.; Ranganathan, A.; Kundu, T. K., Small Molecule Modulators of Histone Acetyltransferase P300, *J. Biol. Chem.,* **2003**, *278* (21), 19134-19140.

(291) Wapenaar, H.; Van Der Wouden, P. E.; Groves, M. R.; Rotili, D.; Mai, A.; Dekker, F. J., Enzyme Kinetics and Inhibition of Histone Acetyltransferase KAT8, *Eur. J. Med. Chem.,* **2015**, *105*, 289-296.

(292) Vasudevarao, M. D.; Mizar, P.; Kumari, S.; Mandal, S.; Siddhanta, S.; Swamy, M. M. M.; Kaypee, S.; Kodihalli, R. C.; Banerjee, A.; Naryana, C.; Dasgupta, D.; Kundu, T. K., Naphthoquinone-Mediated Inhibition of Lysine Acetyltransferase KAT3B/P300, Basis for Non-Toxic Inhibitor Synthesis, *J. Biol. Chem*., **2014**, *289* (11), 7702-7717.

(293) Ravindra, K. C.; Selvi, B. R.; Arif, M.; Reddy, B. A. A.; Thanuja, G. R.; Agrawal, S.; Pradhan, S. K.; Nagashayana, N.; Dasgupta, D.; Kundu, T. K., Inhibition of Lysine Acetyltransferase KAT3B/P300 Activity by a Naturally Occurring Hydroxynaphthoquinone, Plumbagin., *J. Biol. Chem.* **2009**, *284* (36), 24453-24464.

(294) Secci, D.; Carradori, S.; Bizzarri, B.; Bolasco, A.; Ballario, P.; Patramani, Z.; Fragapane, P.; Vernarecci, S.; Canzonetta, C.; Filetici, P., Synthesis of a Novel Series of Thiazole-Based Histone Acetyltransferase Inhibitors, *Bioorganic Med. Chem.,* **2014**, *22* (5), 1680-1689.

(295) Dekker, F. J.; Ghizzoni, M.; van der Meer, N.; Wisastra, R.; Haisma, H. J., Inhibition of the PCAF Histone Acetyl Transferase and Cell Proliferation by Isothiazolones, *Bioorganic Med. Chem.,* **2009**, *17* (2), 460-466.

(296) Ghizzoni, M.; Haisma, H. J.; Dekker, F. J., Reactivity of Isothiazolones and Isothiazolone-

1-Oxides in the Inhibition of the PCAF Histone Acetyltransferase, *Eur. J. Med. Chem.,* **2009**, *44* (12), 4855-4861.

(297) Skehan, P.; Storeng, R.; Scudiero, D.; Monks, A.; McMahon, J.; Vistica, D.; Warren, J. T.; Bokesch, H.; Kenney, S.; Boyd, M. R., New Colorimetric Cytotoxicity Assay For Anticancer-Drug Screening, *J. Natl. Cancer Inst.,* **1990**, *82* (13), 1107-1112.

(298) Alvarez-Sánchez, R.; Basketter, D.; Pease, C.; Lepoittevin, J. P., Studies of Chemical Selectivity of Hapten, Reactivity, and Skin Sensitization Potency. 3. Synthesis and Studies on the Reactivity toward Model Nucleophiles of the 13C-Labeled Skin Sensitizers, 5-Chloro-2-Methylisothiazol-3-One (MCI) and 2-Methylisothiazol, *Chem. Res. Toxicol.,* **2003**, *16* (5), 627-636.

(299) Stimson, L.; Rowlands, M. G.; Newbatt, Y. M.; Smith, N. F.; Raynaud, F. I.; Rogers, P.; Bavetsias, V.; Gorsuch, S.; Jarman, M.; Bannister, A.; Kouzarides, T.; McDonald, E.; Workman, P.; Aherne, G. W., Isothiazolones as Inhibitors of PCAF and P300 Histone Acetyltransferase Activity, *Mol. Cancer Ther.,* **2005**, *4* (10), 1521-1532.

(300) Furdas, S. D.; Hoffmann, I.; Robaa, D.; Herquel, B.; Malinka, P.; Świątek, P.; Akhtar, A.; Sippl, W.; Jung, M., Pyrido- and Benzisothiazolones as Inhibitors of Histone Acetyltransferases (HATs), *Medchemcomm,* **2014**, *5* (12), 1856-1862.

(301) Gajer, J. M.; Furdas, S. D.; Gründer, A.; Gothwal, M.; Heinicke, U.; Keller, K.; Colland, F.; Fulda, S.; Pahl, H. L.; Fichtner, I.; Sippl, W.; Jung, M., Histone Acetyltransferase Inhibitors Block Neuroblastoma Cell Growth in Vivo, *Oncogenesis,* **2015**, *4* (2), 137-147.

(302) Gul, S., Epigenetic Assays for Chemical Biology and Drug Discovery,*Clin. Epigenetics*, **2017**, *9* (1), 1-19.

(303) Shahzad, A.; Köhler, G.; Knapp, M.; Gaubitzer, E.; Puchinger, M.; Edetsberger, M., Emerging Applications of Fluorescence Spectroscopy in Medical Microbiology Field., *J. Transl. Med*., **2009**, *7*, 1-6.

(304) https://westbioscience.com/acetyltransferase/assay-kit/gcn5-fluorogenic-assay-kit 3372.html.

(305) Albaugh, B. N.; Denu, J. M., Catalysis by Protein Acetyltransferase Gcn5., *Biochim. Biophys. Acta - Gene Regul. Mech*., **2021**, *1864* (2), 1-23.

(306) Sundström, C.; Nilsson, K., Establishment and Characterization of a Human Histiocytic Lymphoma Cell Line (U-937). *Int. J. Cancer*, **1976**, *17*, 565-577.

(307) Kikuchi, H.; Kuribayashi, F.; Kiwaki, N.; Takami, Y.; Nakayama, T. GCN5 Regulates the

Superoxide-Generating System in Leukocytes Via Controlling Gp91-Phox Gene Expression., *J. Immunol*., **2011**, *186*, 3015-3022.

(308) Xu, L.; Jiang, H., Writing and Reading Histone H3 Lysine 9 Methylation in Arabidopsis., *Front. Plant Sci*., **2020**, *11*, 1-10.

(309) Domingues, A. F.; Kulkarni, R.; Giotopoulos, G.; Gupta, S.; Vinnenberg, L.; Arede, L.; Foerner, E.; Khalili, M.; Adao, R. R.; Johns, A.; Tan, S.; Zeka, K.; Huntly, B. J.; Prabakaran, S.; Pina, C., Loss of KAT2A Enhances Transcriptional Noise and Depletes Acute Myeloid Leukemia Stem-like Cells., *Elife*, **2020**, *9*, 1-29.

(310) Stockert, J. C.; Horobin, R. W.; Colombo, L. L.; Blázquez-Castro, A., Tetrazolium Salts and Formazan Products in Cell Biology: Viability Assessment, Fluorescence Imaging, and Labeling Perspectives., *Acta Histochem*., **2018**, *120* (3), 159-167.

(311) Mahmood, T.; Yang, P. C., Western Blot: Technique, Theory, and Trouble Shooting., *N. Am. J. Med. Sci.*, **2012**, *4* (9), 429-434.

(312) Cai, L.; Qin, X.; Xu, Z.; Song, Y.; Jiang, H.; Wu, Y.; Ruan, H.; Chen, J., Comparison of Cytotoxicity Evaluation of Anticancer Drugs between Real-Time Cell Analysis and CCK-8 Method., *ACS Omega,* **2019**, *4* (7), 12036-12042.

(313) Kamijo, S.; Dudley, G.B; Tandem Nucleophilic Addition/Fragmentation Reactions and Synthetic Versatility of Vinylogous Acyl Triflates, *J. Am. Chem. Soc*., **2006**, *128* (19), 6499-6507.

(314) Sabater, S.; Müller-Bunz, H.; Albrecht, M., Carboxylate-Functionalized Mesoionic Carbene Precursors: Decarboxylation, Ruthenium Bonding, and Catalytic Activity in Hydrogen Transfer Reactions, *Organometallics,* **2016**, *35* (13), 2256-2266.

(315) Chattopadhyay, B.; Vera, C. I. R.; Chuprakov, S.; Gevorgyan, V., Fused Tetrazoles as Azide Surrogates in Click Reaction: Efficient Synthesis of N-Heterocycle-Substituted 1,2,3-Triazoles, *Org. Lett.,* **2010**, *12* (9), 2166-2169.

(316) Detrick, F., Toms, R., Forest, W., Alto, P., Richard, J., Place, T.I., (**2018**), WO 2018/160845 Al (51). 12.

(317) Fantasia, S., Windisch, J., Scalone, M., Ligandless Copper-Catalyzed Coupling of Heteroaryl Bromides with Gaseous Ammonia., *Adv. Synth. Catal*., **2013**, *355*, 627-631.

(318) Mowbray, C. E.; Braillard, S.; Glossop, P. A.; Whitlock, G. A.; Jacobs, R. T.; Speake, J.; Pandi, B.; Nare, B.; Maes, L.; Yardley, V.; Freund, Y.; Wall, R. J.; Carvalho, S.; Bello, D.; Van Den Kerkhof, M.; Caljon, G.; Gilbert, I. H.; Corpas-Lopez, V.; Lukac, I.; Patterson, S.; Zuccotto, F.;

Wyllie, S., DNDI-6148: A Novel Benzoxaborole Preclinical Candidate for the Treatment of Visceral Leishmaniasis., *J. Med. Chem*., **2021**, 64 (21), 16159-16176.

(319) https://www.elabscience.com/p-enhanced_cell_counting_kit_8_wst_8_cck8_-388417.html

(320) Roudesly, F.; Oble, J.; Poli, G., Metal-Catalyzed C-H Activation/Functionalization: The Fundamentals., *J. Mol. Catal. A Chem*., **2017**, *426*, 275-296.

(321) Altus, K. M.; Love, J. A. The Continuum of Carbon–Hydrogen (C–H) Activation Mechanisms and Terminology., *Commun. Chem*., **2021**, *4* (1), 1-11.

(322) Shamsabadi, A.; Chudasama, V. Recent Advances in Metal-Free Aerobic C-H Activation., *Org. Biomol. Chem*., **2019**, *17* (11), 2865–2872.

(323) King, A.O.; Okukado, N.; Negishi, E. I., Highly General Stereo-, Regio-, and Chemo-Selective Synthesis of Terminal and Internal Conjugated Enynes by the Pd-Catalysed Reaction of Alkynylzinc Reagents with Alkenyl Halides., *J. Chem. Soc. Chem. Commun*., **1977**, *19*, 683–684.

(324) Miyaura, N.; Yamada, K.; Suzuki, A., A new stereospecific cross-coupling by the palladium-catalyzed reaction of 1-alkenylboranes with 1-alkenyl or 1-alkynyl halides, *Tetrahedron Lett*., **1979**, *20* (36), 3437-3440.

(325) Sonogashira, K., Development of Pd-Cu Catalyzed Cross-Coupling of Terminal Acetylenes with Sp_2-Carbon Halides., *J. Organomet. Chem*., **2002**, *653* (1-2), 46-49.

(326) Hofmann, A. W., Effect of Basic Bromine Solution on Amines., *Ber. Dtsch. Chem. Ges*., **1883**, *16*, 558-560.

(327) Freytag, C.; Loffler, K., Über die Bildung des i-Nicotins aus N-Methyl-p-pyridyl-butylamin (Dihydrometanicotin), *Chem. Ber*., **1909**, *42*, 3427-3431.

(328) Volhard, J., Ueber Verbindungen Des Thiophens, Seiner Homologen Und Einiger Ketone Mit Quecksilberchlorid., *Justus Liebigs Ann. Chem*., **1892**, *267* (2–3), 172-185.

(329) Brückl, T.; Baxter, R. D.; Ishihara, Y.; Baran, P. S., Innate and Guided C-H Functionalization Logic., *Acc. Chem. Res*., **2012**, *45* (6), 826-839.

(330) Davies, H. M. L.; Morton, D., Recent Advances in C-H Functionalization. *J. Org. Chem.,* **2016**, *81* (2), 343-350.

(331) Xiao, K.J, Lin, D.W., Miura, M., Zhu, R.Y, Gong, W., Wasa, M., Yu, J.Q., Palladium(II)-Catalyzed Enantioselective C(sp_3)–H Activation Using a Chiral Hydroxamic Acid Ligand, *J. Am.*

Chem. Soc., **2014**, *136*, 8138-8142

(332) Li, S.; Chen, G.; Feng, C.; Gong, W.; Yu, J., Ligand-Enabled γ-C–H Olefination and Carbonylation: Construction of β-Quaternary Carbon Centers., *J. Am. Chem. Soc*., **2014**, *136*, 5267-5270.

(333) Giri, R.; Shi, B. F.; Engle, K. M.; Maugel, N.; Yu, J. Q. Transition Metal-Catalyzed C–H Activation Reactions: Diastereoselectivity and Enantioselectivity., *Chem. Soc. Rev*., **2009**, *38* (11), 3242-3272.

(334) Sambiagio, C.; Schönbauer, D.; Blieck, R.; Dao-Huy, T.; Pototschnig, G.; Schaaf, P.; Wiesinger, T.; Zia, M. F.; Wencel-Delord, J.; Besset, T.; Maes, B. U. W.; Schnürch, M. A Comprehensive Overview of Directing Groups Applied in Metal-Catalysed C-H Functionalisation Chemistry., *Chem. Soc. Rev*., **2018**, *47* (17), 6603-6743.

(335) Zhang, M.; Zhang, Y.; Jie, X.; Zhao, H.; Li, G.; Su, W., Recent Advances in Directed C-H Functionalizations Using Monodentate Nitrogen-Based Directing Groups., *Org. Chem. Front*., **2014**, *1* (7), 843-895.

(336) Rousseau, G.; Breit, B. Removable Directing Groups in Organic Synthesis and Catalysis., *Angew. Chemie - Int. Ed*., **2011**, *50* (11), 2450-2494.

(337) Affron, D. P.; Davis, O. A.; Bull, J. A., Regio- and Stereospecific Synthesis of C-3 Functionalized Proline Derivatives by Palladium Catalyzed Directed C(Sp_3)-H Arylation., *Org. Lett*., **2014**, *16* (18), 4956-4959.

(338) Campeau, L. C.; Fagnou, K., Palladium-Catalyzed Direct Arylation of Simple Arenes in Synthesis of Biaryl Molecules., *Chem. Commun*., **2006**, *12*, 1253-1264.

(339) Liu, J., Xie, Y., Zeng, W., Lin, D., Yuanfu Deng, Y., Lu, X., Pd(II)-Catalyzed Pyridine N-Oxides Directed Arylation of Unactivated Csp_3–H Bonds *J. Org. Chem*., **2015**, *80* (9), 4618-4626.

(340) Shang, R.; Ilies, L.; Asako, S.; Nakamura, E., Iron-Catalyzed C(Sp_2)-H Bond Functionalization with Organoboron Compounds., *J. Am. Chem. Soc*., **2014**, *136* (41), 14349-14352.

(341) Foo, K., Sella, E., Thomé, I., Eastgate, M.D., Baran, P.S., A Mild, Ferrocene-Catalyzed C–H Imidation of (Hetero)Arenes, *J. Am. Chem. Soc*., **2014**, *136*, 5279-5282

(342) Kumar, S.; Bhakuni, B. S.; Yadav, A.; Kumar, S.; Patel, S.; Sharma, S., KOtBu-Mediated Synthesis of Dimethylisoindolin-1-Ones and Dimethyl-5-Phenylisoindolin-1-Ones: Selective C-C Coupling of an Unreactive Tertiary Sp_3 C-H Bond., *J. Org. Chem*., **2014**, *79* (7), 2944-2954.

(343) Leow, D.; Li, G.; Mei, T. S.; Yu, J. Q., Activation of Remote Meta-C-H Bonds Assisted by an End-on Template., *Nature*, **2012**, *486* (7404), 518-522.

(344) Patra, T.; Watile, R.; Agasti, S.; Naveen, T.; Maiti, D., Sequential Meta-C-H Olefination of Synthetically Versatile Benzyl Silanes: Effective Synthesis of Meta-Olefinated Toluene, Benzaldehyde and Benzyl Alcohols., *Chem. Commun*., **2016**, *52* (10), 2027-2030.

(345) Shen, P.X., Wang, X.C., Wang, P., Zhu, R.Y., Yu, J.Q., Ligand-Enabled Meta-C–H Alkylation and Arylation Using a Modified Norbornene, *J. Am. Chem. Soc*., **2015**, *137*, 11574-11577.

(346) Bera, M.; Maji, A.; Sahoo, S. K.; Maiti, D., Palladium(II)-Catalyzed Meta-C-H Olefination: Constructing Multisubstituted Arenes through Homo-Diolefination and Sequential Hetero-Diolefination., *Angew. Chemie - Int. Ed.*, **2015**, *54* (29), 8515-8519.

(347) Wang, X. C., Gong, W., Fang, L. Z., Zhu, R. Y., Li, S., Engle, K. M., & Yu, J. Q., Ligand-enabled meta-C-H activation using a transient mediator., *Nature*, **2015**, *519* (7543), 334-338.

(348) Yang, G.; Lindovska, P.; Zhu, D.; Kim, J.; Wang, P.; Tang, R.; Movassaghi, M.; Yu, J. Pd(II) -Catalyzed Meta-C−H Olefination, Arylation, and Acetoxylation of Indolines Using a U-Shaped Template. *J. Am. Chem. Soc*., **2014**, *136*, 10807-10813.

(349) Xu, H.; Shang, M.; Dai, H. X.; Yu, J. Q. Ligand-Controlled Para-Selective C-H Arylation of Monosubstituted Arenes., *Org. Lett*., **2015**, *17* (15), 3830-3833.

(350) Calvert, J. G., Glossary of Atmospheric Chemistry Terms., *Pure Appl. Chem*., **1990**, *62* (11), 2167-2219.

(351) Poutsma, M. L., The Radical Stabilization Energy of a Substituted Carbon-Centered Free Radical Depends on Both the Functionality of the Substituent and the Ordinality of the Radical., *J. Org. Chem*., **2011**, *76* (1), 270-276.

(352) Hyperconjugation. *IUPAC Compend. Chem. Terminol*. **2008**, *1077*, 2924.

(353) Gronert, S.; Lee, J. M., Strain-Free Transition States in the Formation of Strained Rings: An Ab Initio Study of Thiirane, Thietan, and Tetrahydrothiophene., *J. Org. Chem*., **1995**, *60* (21), 6731-6736.

(354) Blanksby, S. J.; Ellison, G. B., Bond Dissociation Energies of Organic Molecules., *Acc. Chem. Res*., **2003**, *36* (4), 255-263.

(355) George, W. O.; Jones, B. F.; Lewis, R., Water and Its Homologues: A Comparison of

Hydrogen-Bonding Phenomena., *Philos. Trans. R. Soc. A Math. Phys. Eng. Sci*., **2001**, *359* (1785), 1611-1629.

(356) Wiberg, K. B., The Concept of Strain in Organic Chemistry., *Angew. Chemie Int. Ed. English*, **1986**, *25* (4), 312-322.

(357) Bauld, N. L.; Cessac, J.; Holloway, R. L., 1,3(Nonbonded) Carbon/Carbon Interactions. The Common Cause of Ring Strain, Puckering, and Inward Methylene Rocking in Cyclobutane and of Vertical Nonclassical Stabilization, Pyramidalization, Puckering, and Outward Methylene Rocking in the Cyclobutyl Cat., *J. Am. Chem. Soc*., **1977**, *99* (25), 8140-8144.

(358) Gronert, S., Lee, J.M., Strain-Free Transition States in the Formation of Strained Rings: An ab Initio Study of Thiirane, Thietan, and Tetrahydrothiophene., *J. Org. Chem*., **1995**, *60*, 6731-6736.

(359) Gronert, S.; Azizian, K.; Friedman, M. A., Cyclizations of 3-Chlorocarbanions to Cyclopropanes: “Strain-Free” Transition States for Forming Highly Strained Rings., *J. Am. Chem. Soc*., **1998**, *120* (13), 3220-3226.

(360) Hassan, J.; Sévignon, M.; Gozzi, C.; Schulz, E.; Lemaire, M., Aryl-Aryl Bond Formation One Century after the Discovery of the Ullmann Reaction., *Chem. Rev*., **2002**, *102* (5), 1359-1469.

(361) Kakiuchi, F.; Murai, S., Catalytic C-H/Olefin Coupling., *Acc. Chem. Res*., **2002**, *35*, 826-834.

(362) Goj, L.; Gunnoe, T., Developments in Catalytic Aromatic C-H Transformations: Promising Tools for Organic Synthesis., *Curr. Org. Chem*., **2005**, *9* (7), 671-685.

(363) Campeau, L.C., Fagnou, K., Palladium-catalyzed direct arylation of simple arenes in synthesis of biaryl molecules, *Chem. Commun*., **2006**, 1253-1264.

(364) Alberico, D.; Scott, M. E.; Lautens, M., Aryl-Aryl Bond Formation by Transition-Metal-Catalyzed Direct Arylation., *Chem. Rev*., **2007**, *107* (1), 174-238.

(365) Davies, H. M. L.; Beckwith, R. E. J., Catalytic Enantioselective C-H Activation by Means of Metal-Carbenoid-Induced C-H Insertion., *Chem. Rev*., **2003**, *103* (8), 2861-2903.

(366) Müller, P.; Fruit, C., Enantioselective Catalytic Aziridinations and Asymmetric Nitrene Insertions into C-H Bonds., *Chem. Rev*., **2003**, *103* (8), 2905-2919.

(367) Davies, H. M. L.; Dai, X.; Long, M. S., Combined C-H Activation/Cope Rearrangement as a Strategic Reaction in Organic Synthesis: Total Synthesis of (-)-Colombiasin A and (-)-Elisapterosin B., *J. Am. Chem. Soc*., **2006**, *128* (7), 2485-2490.

(368) Davies, H. M. L.; Manning, J. R., Catalytic C-H Functionalization by Metal Carbenoid and Nitrenoid Insertion., *Nature*, **2008**, *451* (7177), 417-424.

(369) Boutadla, Y., Davies, D.L., Macgregor, S.A., Poblador-Bahamonde, A.I., Mechanisms of C–H bond activation: rich synergy between computation and experiment, *Dalton Trans*., **2009**, 5820-5831.

(370) Labinger, J.A., Tutorial on Oxidative Addition, *Organometallics*, **2015**, *34* (20), 4784-4795.

(371) L. S. Hegedus, Transition metals in organic synthesis, *J. Organomet. Chem*., **1994**. *477* (1-2), 269-362.

(372) Crabtree, R.H., The Organometallic Chemistry of the Transition Metals, 6th Edition.

(373) Vaska, L., Di Luzio, J.W., Carbonyl And Hydrido-carbonyl Complexes of Iridium by Reaction with Alcohols. Hydrido Complexes by Reaction with Acid., *J. Am. Chem. Soc*., **1961**, *83*, 2784-2785.

(374) Watson, P. L., Ziegler-Natta polymerization: the lanthanide model, *J. Am. Chem. Soc*., **1982**, *104*, 337-339.

(375) Thompson, M. E.; Baxter, S. M.; Bulls, A. R.; Burger, B. J.; Nolan, M. C.; Santarsiero, B. D.; Schaefer, W. P.; Bercaw, J. E., Non involvement of the 7r System in Electrophilic Activation of Aromatic and Vinylic C-H Bonds., *J. Am. Chem. Soc*., **1987**, *3*, 203-219.

(376) Waterman, R., σ-Bond Metathesis : A 30-Year Retrospective., *Organometallics*, **2013**, *32*, 7249-7263.

(377) Ziegler, T., The 1994 Alcan Award Lecture Density functional theory as a practical tool in studies of organometallic energetics and kinetics. Beating the heavy metal blues with DFT., *Can. J. Chem*., **1995**, *73* (6), 743-761.

(378) Folga, E., Ziegler,T., A theoretical study on the activation of hydrogen–hydrogen and hydrogen–alkyl bonds by electron-poor early transition metals., *Can. J. Chem*., **1992**, *70* (2), 333-342.

(379) Barros, N.; Eisenstein, O.; Maron, L., DFT Studies of the Methyl Exchange Reaction between Cp2M–CH_3 or Cp*2M–CH_3(Cp = C_5H_5, Cp* = C_5Me_5, M = Y, Sc, Ln) and CH_4. Does M Ionic Radius Control the Reaction?, *J. Chem. Soc. Dalt. Trans*., **2006**, *3* (25), 3052-3057.

(380) Maron, L.; Eisenstein, O., DFT Study of H - H Activation by Cp2 L_nH D_0 Complexes., *J. Am. Chem. Soc.,* **2001**, *123* (6), 1036-1039.

(381) Perrin, L.; Maron, L.; Eisenstein, O.; Ii, M.; Cedex, M.; Physique, L. De; Sabatier, P.; Narbonne, D.; Cedex, T., A DFT Study of SiH 4 Activation by Cp 2 L_nH., *Inorg. Chem*., **2002**, *41*, 4355-4362.

(382) Musaev, D. G.; Froese, R. D. J.; Morokuma, K. Molecular Orbital and IMOMM Studies of the Chain Transfer Mechanisms of the Diimine - M(II)-Catalyzed (M = Ni, Pd) Ethylene Polymerization Reaction., *Organometallics*, **1998**, *17* (9), 1850-1860.

(383) Shilov, A.E., Shul'pin, G.B., Activation of C−H Bonds by Metal Complexes, *Chem. Rev*., **1997**, *97*, 2879-2932.

(384) Ess, D. H.; Goddard, W. A.; Periana, R. A., Electrophilic, Ambiphilic, and Nucleophilic C-H Bond Activation: Understanding the Electronic Continuum of C-H Bond Activation through Transition-State and Reaction Pathway Interaction Energy Decompositions., *Organometallics*, **2010**, *29* (23), 6459-6472.

(385) Dupont, J.; Consorti, C. S.; Spencer, J., The Potential of Palladacycles: More than Just Precatalysts., *Chem. Rev*., **2005**, *105* (6), 2527-2571.

(386) Cope, A.C., Siekman, R.W., Formation of Covalent Bonds from Platinum or Palladium to Carbon by Direct Substitution, *J. Am. Chem. Soc*., **1965**, *87*, 14, 3272-3273.

(387) Dick, A. R.; Hull, K. L.; Sanford, M. S., A Highly Selective Catalytic Method for the Oxidative Functionalization of C-H Bonds., *J. Am. Chem. Soc*., **2004**, *126* (8), 2300-2301.

(388) Chen, X.; Hao, X. S.; Goodhue, C. E.; Yu, J. Q., Cu(II)-Catalyzed Functionalizations of Aryl C-H Bonds Using O_2 as an Oxidant., *J. Am. Chem. Soc*., **2006**, *128* (21), 6790-6791.

(389) Dangel, B. D.; Johnson, J. A.; Sames, D. Selective Functionalization of Amino Acids in Water: A Synthetic Method via Catalytic C-H Bond Activation., *J. Am. Chem. Soc*., **2001**, *123* (33), 8149-8150.

(390) Lyons, T. W.; Sanford, M. S.; Palladium-Catalyzed Ligand-Directed C−H Functionalization Reactions, *Chem. Rev*., **2010**, *110*, 1147-1169.

(391) Dick, A. R.; Sanford, M. S., Transition Metal Catalyzed Oxidative Functionalization of Carbon-Hydrogen Bonds., *Tetrahedron*, **2006**, *62* (11), 2439-2463.

(392) Terao, Y.; Kametani, Y.; Wakui, H.; Satoh, T.; Miura, M.; Nomura, M., Multiple Arylation of Alkyl Aryl Ketones and α,β-Unsaturated Carbonyl Compounds via Palladium Catalysis., *Tetrahedron*, **2001**, *57* (28), 5967-5974.

(393) Gürbüz, N.; Özdemir, I.; Çetinkaya, B., Selective Palladium-Catalyzed Arylation(s) of Benzaldehyde Derivatives by N-Heterocarbene Ligands., *Tetrahedron Lett*., **2005**, *46* (13), 2273-2277.

(394)Kalyani, D.; Sanford, M. S. Regioselectivity in Palladium-Catalyzed C−H Activation/Oxygenation Reactions, *Org. Lett*., **2005**, *7*, 4149-4152

(395) Kalberer, E. W.; Whitfield, S. R.; Sanford, M. S., Application of Recyclable, Polymer-Immobilized Iodine(III) Oxidants in Catalytic C-H Bond Functionalization., *J. Mol. Catal. A Chem*., **2006**, *251* (1-2), 108-113.

(396) Desai, L.V., Hull, K.L., Sanford, M.S., Palladium-Catalyzed Oxygenation of Unactivated sp^3 C−H Bonds, *J. Am. Chem. Soc*., **2004**, *126*, 9542-9543.

(397) Yoneyama, T., Crabtree, R.H, Pd(II) catalyzed acetoxylation of arenes with iodosyl acetate, *J. Mol. Catal. A Chem*., **1996**, *108*, 35-40.

(398) Inamoto, K.; Arai, Y.; Hiroya, K.; Doi, T., Palladium-Catalysed Direct Synthesis of Benzo[b]Thiophenes from Thioenols., *Chem. Commun*., **2008**, *43*, 5529-5531.

(399) Fristad, W. E.; Peterson, J. R.; Ernst, A. B., Manganese(III) γ-Lactone Annulation with Substituted Acids., *J. Org. Chem*., **1985**, *50* (17), 3143-3148.

(400) Wallace, T.J., Reactions of Thiols with Sulfoxides. I. Scope of the Reaction and Synthetic Applications, *J. Am. Chem. Soc*., **1964**, *86*, 2018-2021.

(401) Yiannios, C. N., Karabinos, J. V., Oxidation of Thiols by Dimethyl Sulfoxide, *J. Org. Chem*., **1963**, *28*, 3246-3248.

(402) Wallace, T. J. Reactions of Thiols with Metals. II. Low Temperature Oxidation by Soluble Metal Salts, *J. Org. Chem*., **1966**, *31*, 3071-3074.

(403) Kirihara, M.; Okubo, K.; Uchiyama, T.; Kato, Y.; Ochiai, Y.; Matsushita, S.; Hatano, A.; Kanamori, K., Aerobic Oxidation of Thiols to Disulfides Catalyzed by Trichlorooxyvanadium., *Chem. Pharm. Bull*., **2004**, *52* (5), 625-627.

(404) Ley, S. V.; Thomas, A. W., Modern Synthetic Methods for Copper-Mediated C(Aryl)-O, C(Aryl)-N, and C(Aryl)-S Bond Formation., *Angew. Chemie - Int. Ed*., **2003**, *42* (44), 5400-5449.

(405) Beletskaya, I. P.; Cheprakov, A. V., Copper in Cross-Coupling Reactions: The Post-Ullmann Chemistry., *Coord. Chem. Rev*., **2004**, *248* (21–24), 2337-2364.

(406) Corbet, J. P.; Mignani, G. Selected Patented Cross-Coupling Reaction Technologies.,

Chem. Rev., **2006**, *106* (7), 2651-2710.

(407) Thansandote, P.; Lautens, M., Construction of Itrogen-Containing Heterocycles by C-H Bond Functionalization., *Chem. - A Eur. J*., **2009**, *15* (24), 5874-5883.

(408) Tsang, W. C. P.; Munday, R. H.; Brasche, G.; Zheng, N.; Buchwald, S. L., Palladium-Catalyzed Method for the Synthesis of Carbazoles via Tandem C-H Functionalization and C-N Bond Formation., *J. Org. Chem*., **2008**, *73* (19), 7603-7610.

(409) Jordan-Hore, J. A.; Johansson, C. C. C.; Gulias, M.; Beck, E. M.; Gaunt, M. J., Oxidative Pd(II)-Catalyzed C-H Bond Amination to Carbazole at Ambient Temperature., *J. Am. Chem. Soc*., **2008**, *130* (48), 16184-16186.

(410) Thu, H. Y.; Yu, W. Y.; Che, C. M., Intermolecular Amidation of Unactivated Sp2 and Sp3 C-H Bonds via Palladium-Catalyzed Cascade C-H Activation/Nitrene Insertion., *J. Am. Chem. Soc*., **2006**, *128* (28), 9048-9049.

(411) Kalyani, D.; Deprez, N. R.; Desai, L. V.; Sanford, M. S., Oxidative C-H Activation/C-C Bond Forming Reactions: Synthetic Scope and Mechanistic Insights., *J. Am. Chem. Soc*., **2005**, *127* (20), 7330-7331.

(412) Deprez, N. R.; Sanford, M. S., Reactions of Hypervalent Iodine Reagents with Palladium: Mechanisms and Applications in Organic Synthesis, *Inorg. Chem*., **2007**, *46* (6), 1924-1935.

(413) Daugulis, O.; Zaitsev, V. G., Anilide Ortho-Arylation by Using C-H Activation Methodology., *Angew. Chemie - Int. Ed*., **2005**, *44* (26), 4046-4048.

(414) Spencer, J.; Chowdhry, B. Z.; Mallet, A. I.; Rathnam, R. P.; Adatia, T.; Bashall, A.; Rominger, F., C-H Activations on a 1H-1,4-Benzodiazepin-2(3H)-One Template., *Tetrahedron,* **2008**, *64* (26), 6082-6089.

(415) Hull, K. L.; Lanni, E. L.; Sanford, M. S., Highly Regioselective Catalytic Oxidative Coupling Reactions: Synthetic and Mechanistic Investigations., *J. Am. Chem. Soc*., **2006**, *128* (43), 14047-14049.

(416) Boele, M. D. K.; Van Strijdonck, G. P. F.; De Vries, A. H. M.; Kamer, P. C. J.; De Vries, J. G.; Van Leeuwen, P. W. N. M., Selective Pd-Catalyzed Oxidative Coupling of Anilides with Olefins through C-H Bond Activation at Room Temperature., *J. Am. Chem. Soc*., **2002**, *124* (8), 1586-1587.

(417) Wang, J. R.; Yang, C. T.; Liu, L.; Guo, Q. X., Pd-Catalyzed Aerobic Oxidative Coupling of Anilides with Olefins through Regioselective C-H Bond Activation., *Tetrahedron Lett*., **2007**, *48*

(31), 5449-5453.

(418) Chen, X.; Li, J. J.; Hao, X. S.; Goodhue, C. E.; Yu, J. Q., Palladium-Catalyzed Alkylation of Aryl C-H Bonds with Sp_3 Organotin Reagents Using Benzoquinone as a Crucial Promoter., *J. Am. Chem. Soc*., **2006**, *128* (1), 78-79.

(419) Shi, B. F.; Maugel, N.; Zhang, Y. H.; Yu, J. Q., Pd(II)-Catalyzed Enantioselective Activation of C(Sp 2)-H and C(Sp_3)-H Bonds Using Monoprotected Amino Acids as Chiral Ligands., *Angew. Chemie - Int. Ed*., **2008**, *47* (26), 4882-4886.

(420) Tobisu, M.; Ano, Y.; Chatani, N., Palladium-Catalyzed Direct Alkynylation of C-H Bonds in Benzenes., *Org. Lett*., **2009**, *11* (15), 3250-3252.

(421) Daugulis, O.; Do, H.; Shabashov, D. Palladium- and Copper-Catalyzed Arylation of Carbon−Hydrogen Bonds, *Acc. Chem. Res*., **2009**, *42*, 1074-1086.

(422) Wendlandt, A. E.; Suess, A. M.; Stahl, S. S., Copper-Catalyzed Aerobic Oxidative C-H Functionalizations: Trends and Mechanistic Insights., *Angew. Chemie - Int. Ed*., **2011**, *50* (47), 11062-11087.

(423) Gandeepan, P.; Müller, T.; Zell, D.; Cera, G.; Warratz, S.; Ackermann, L., 3d Transition Metals for C-H Activation., *Chem. Rev*., **2019**, *119* (4), 2192-2452.

(424) Björklund, C.; Nilsson, M., Preparation of 2,6-Dinitrobiphenyls from m-Dinitrobenzene and Iodoarenes with Copper(I) Oxide in Quinoline., *Acta.Chem.Scand*., **1968**, *22*, 2338-2346.

(425) Guo, X.; Gu, D.; Wu, Z.; Zhang, W., Copper-Catalyzed C–H Functionalization Reactions: Efficient Synthesis of Heterocycles, *Chem. Rev*., **2015**, *115*, 1622-1651.

(426) Bhadra, S.; Dzik, W. I.; Gooßen, L. J., Synthesis of Aryl Ethers from Benzoates through Carboxylate-Directed C-H-Activating Alkoxylation with Concomitant Protodecarboxylation., *Angew. Chemie - Int. Ed*., **2013**, *52* (10), 2959-2962.

(427) Bhadra, S.; Matheis, C.; Katayev, D.; Gooßen, L. J., Copper-Catalyzed Dehydrogenative Coupling of Arenes with Alcohols., *Angew. Chemie - Int. Ed*., **2013**, *52* (35), 9279-9283.

(428) Wang, Z.; Kuninobu, Y.; Kanai, M., Copper-Mediated Direct C(Sp_3)-H and C(Sp_2)-H Acetoxylation., *Org. Lett*., **2014**, *16*, 4790-4793.

(429) Wu, X.; Zhao, Y.; Ge, H., Copper-Promoted Site-Selective Acyloxylation of Unactivated C(Sp_3)-H Bonds,. *Chem. - An Asian J*., **2014**, *9* (10), 2736-2739.

(430) Wang, F.; Hu, Q.; Shu, C.; Lin, Z.; Min, D.; Shi, T.; Zhang, W., Copper-Catalyzed Direct

Acyloxylation of C(Sp_2)-H Bonds in Aromatic Amides., *Org. Lett*., **2017**, *19* (13), 3636-3639.

(431) Tran, L.D., Popov, I., Daugulis, O., Copper-Promoted Sulfenylation of sp_2 C–H Bonds, *J. Am. Chem. Soc*., **2012**, *134*, 18237-18240.

(432) Rao, W. H.; Shi, B. F., Copper(II)-Catalyzed Direct Sulfonylation of C(Sp_2)-H Bonds with Sodium Sulfinates., *Org. Lett*., **2015**, *17* (11), 2784-2787.

(433) Shuai, Q.; Deng, G.; Chua, Z.; Bohle, D. S.; Li, C. J., Copper-Catalyzed Highly Regioselective Oxidative C-H Bond Amidation of 2-Arylpyridine Derivatives and 1-Methylindoles., *Adv. Synth. Catal*., **2010**, *352* (4), 632-636.

(434) John, A., Nicholas, K.M., Copper-Catalyzed Amidation of 2-Phenylpyridine with Oxygen as the Terminal Oxidant, *J. Org. Chem*., **2011**, *76*, 4158-4162.

(435) Tran, L. D.; Roane, J.; Daugulis, O., Directed Amination of Non-Acidic Arene C-H Bonds by a Copper-Silver Catalytic System., *Angew. Chemie - Int. Ed*., **2013**, *52* (23), 6043-6046.

(436) Zhu, C.; Yi, M.; Wei, D.; Chen, X.; Wu, Y.; Cui, X., Copper-Catalyzed Direct Amination of Quinoline N-Oxides via C-H Bond Activation under Mild Conditions., *Org. Lett*., **2014**, *16* (7), 1840-1843.

(437) Peng, J.; Xie, Z.; Chen, M.; Wang, J.; Zhu, Q., Copper-Catalyzed C(Sp2)-H Amidation with Azides as Amino Sources., *Org. Lett*., **2014**, *16* (18), 4702-4705.

(438) Kim, H.; Heo, J.; Kim, J.; Baik, M. H.; Chang, S., Copper-Mediated Amination of Aryl C-H Bonds with the Direct Use of Aqueous Ammonia via a Disproportionation Pathway., *J. Am. Chem. Soc*., **2018**, *140* (43), 14350-14356.

(439) Phipps, R. J.; Grimster, N. P.; Gaunt, M. J., Cu(II)-Catalyzed Direct and Site-Selective Arylation of Indoles under Mild Conditions., *J. Am. Chem. Soc.,* **2008**, *130* (26), 8172-8174.

(440) Wang, T.; Zhou, L.; Yang, Y.; Zhang, X.; Shi, Z.; Wu, Y. D., Directing Effects on the Copper-Catalyzed Site-Selective Arylation of Indoles., *Org. Lett*., **2018**, *20* (20), 6502-6505.

(441) Yang, Y.; Li, R.; Zhao, Y.; Zhao, D.; Shi, Z., Cu-Catalyzed Direct C6-Arylation of Indoles., *J. Am. Chem. Soc*., **2016**, *138* (28), 8734-8737.

(442) Yang, Y.; Gao, P.; Zhao, Y.; Shi, Z., Regiocontrolled Direct C−H Arylation of Indoles at the C4 and C5 Positions,. *Angew. Chemie - Int. Ed*., **2017**, *56* (14), 3966-3971.

(443) Zhang, G.; Ma, Y.; Cheng, G.; Liu, D.; Wang, R., A Unique Combined Source of “CN” from 1,2-Dichloroethane and $TMSN_3$ in the Copper-Catalyzed Cyanation of a C(sp_3)–H Bond Adjacent

to a Nitrogen Atom, *Org. Lett*., **2014**, *16*, 656-659.

(444) Wang, T.; Schrempp, M.; Berndhäuser, A.; Schiemann, O.; Menche, D., Efficient and General Aerobic Oxidative Cross-Coupling of THIQs with Organozinc Reagents Catalyzed by $CuCl_2$: Proof of a Radical Intermediate., *Org. Lett*., **2015**, *17* (16), 3982-3985.

(445) Dong, Y. X.; Li, Y.; Gu, C. C.; Jiang, S. S.; Song, R. J.; Li, J. H., Copper-Catalyzed Three-Components Intermolecular Alkylesterification of Styrenes with Toluenes and Peroxyesters or Acids., *Org. Lett*., **2018**, *20* (23), 7594-7597.

(446) Ackermann, L.; Althammer, A., Domino N-H/C-H Bond Activation: Palladium-Catalyzed Synthesis of Annulated Heterocycles Using Dichloro(Hetero)Arenes., *Angew. Chemie - Int. Ed*., **2007**, *46* (10), 1627-1629.

(447) Ackermann, L.; Born, R.; Álvarez-Bercedo, P., Ruthenium(IV) Alkylidenes as Precatalysts for Direct Arylations of Alkenes with Aryl Chlorides and an Application to Sequential Catalysis., *Angew. Chemie - Int. Ed*., **2007**, *46* (33), 6364-6367.

(448) Ackermann, L.; Potukuchi, H. K.; Landsberg, D.; Vicente, R., Copper-Catalyzed “Click” Reaction/Direct Arylation Sequence: Modular Syntheses of 1,2,3-Triazoles., *Org. Lett*., **2008**, *10* (14), 3081-3084.

(449) Feldman, A. K.; Colasson, B.; Fokin, V. V., One-Pot Synthesis of 1,4-Disubstituted 1,2,3-Triazoles from in Situ Generated Azides., *Org. Lett*., **2004**, *6* (22), 3897-3899.

(450) Wei, F., Li, H., Song, C., Ma, Y., Zhou, L., Tung, C. H., Xu, Z., Cu/Pd-Catalyzed, Three-Component Click Reaction of Azide, Alkyne, and Aryl Halide: One-Pot Strategy toward Trisubstituted Triazoles., *Org. Lett*., **2015**, *17*(11), 2860-2863.

(451) Cai, Q.; Yan, J.; Ding, K., A CuAAC/Ullmann C-C Coupling Tandem Reaction: Copper-Catalyzed Reactions of Organic Azides with N -(2-Iodoaryl)Propiolamides or 2-Iodo- N -(Prop-2-Ynyl)Benzenamines., *Org. Lett*., **2012**, *14* (13), 3332-3335.

(452) He, C.; Ke, J.; Xu, H.; Lei, A., Synergistic Catalysis in the Sonogashira Coupling Reaction: Quantitative Kinetic Investigation of Transmetalation., *Angew. Chemie - Int. Ed*., **2013**, *52* (5), 1527-1530.

(453) Worrell, B. T., Malik, J. A., Fokin, V. V., Direct evidence of a dinuclear copper intermediate in Cu(I)-catalyzed azide-alkyne cycloadditions., *Science*, **2013**, *340* (6131), 457-460.

(454) Rodionov, V. O.; Fokin, V. V.; Finn, M. G., Mechanism of the Ligand-Free CuI-Catalyzed Azide-Alkyne Cycloaddition Reaction., *Angew. Chemie - Int. Ed*., **2005**, *44* (15), 2210-2215.

(455) Chuprakov, S., Chernyak, N., Dudnik, A.S., Gevorgyan, V., Direct Pd-Catalyzed Arylation of 1,2,3-Triazoles, *Org. Lett*., **2007**, *9*, 2333-2336.

(456) Zhu, J.; Kong, Y.; Lin, F.; Wang, B.; Chen, Z.; Liu, L., Copper-Catalyzed Direct Amination of 1,2,3-Triazole N-Oxides by C-H Activation and C-N Coupling., *Eur. J. Org. Chem*., **2015**, *2015* (7), 1507-1515.

(457) Ye, X.; He, Z.; Ahmed, T.; Weise, K.; Akhmedov, N. G.; Petersen, J. L.; Shi, X., 1,2,3-Triazoles as Versatile Directing Group for Selective Sp_2 and Sp_3 C-H Activation: Cyclization vs Substitution., *Chem. Sci*., **2013**, *4* (9), 3712-3716.

(458) Powers, D. C.; Xiao, D. Y.; Geibel, M. a L.; Ritter, T., On the Mechanism of Palladium-Catalyzed Aromatic C−H Oxidation, *J. Am. Chem*. *Soc*., **2010**, *132*, 14530-14536.

(459) Racowski, J. M.; Dick, A. R.; Sanford, M. S., Detailed Study of C-O and C-C Bond-Forming Reductive Elimination from Stable $C_2N_2O_2$-Ligated Palladium(IV) Complexes., *J. Am. Chem. Soc*., **2009**, *131* (31), 10974-10983.

(460) Gou, F. R.; Wang, X. C.; Huo, P. F.; Bi, H. P.; Guan, Z. H.; Liang, Y. M., Palladium-Catalyzed Aryl C-H Bonds Activation/Acetoxylation Utilizing a Bidentate System., *Org. Lett*., **2009**, *11* (24), 5726-5729.

(461) List, B., Introduction: Organocatalysis., *Chem. Rev*., **2007**, *107*, 5413-5415.

(462) Moss, G. P., Basic Terminology of Stereochemistry., *Pure Appl. Chem*.,**1996**, *68* (12), 2193-2222.

(463)Schreiner, P.R., Metal-Free Organocatalysis through Explicit Hydrogen Bonding Interactions., *Chem. Soc. Rev*., **2003**, *32* (5), 289-296.

(464) Schuster, T.; Kurz, M.; Göbel, M. W., Catalysis of a Diels-Alder Reaction by Amidinium Ions., *J. Org. Chem*., **2000**, *65* (6), 1697-1701.

(465) Huang, Y.; Rawal, V.H., Hydrogen-Bond-Promoted Hetero-Diels-Alder Reactions of Unactivated Ketones., *J. Am. Chem. Soc*., **2002**, *124* (33), 9662-9663.

(466) Domingo, L. R.; Andrés, J., Enhancing Reactivity of Carbonyl Compounds via Hydrogen-Bond Formation. A DFT Study of the Hetero-Diels-Alder Reaction between Butadiene Derivative and Acetone in Chloroform., *J. Org. Chem*., **2003**, *68* (22), 8662-8668.

(467) Gröger, H., Wilken, J., The Application of L-Proline as an Enzyme Mimic and Further New Asymmetric Syntheses Using Small Organic Molecules as Chiral Catalysts., *Angew. Chemie* -

Int. Ed, **2001**, *40* (3), 529-532.

(468) Dalko, P. I.; Moisan, L., In the Golden Age of Organocatalysis., *Angew. Chemie - Int. Ed*., **2004**, *43* (39), 5138-5175.

(469) Vose, J. M., Novel Radioimmunotherapy for the Treatment of Low-Grade and Transformed Low-Grade Non-Hodgkin's Lymphoma., *Oncologist*, **2004**, *9* (2), 160-172.

(470) Volkert, W. A., Hoffman, T. J., Therapeutic radiopharmaceuticals., Chem. Rev., **1999**, *99* (9), 2269-2292.

(471) Struthers, H.; Mindt, T. L.; Schibli, R., Metal Chelating Systems Synthesized Using the Copper(I) Catalyzed Azide-Alkyne Cycloaddition., *Dalt. Trans*., **2010**, *39* (3), 675-696.

(472) Bastero, A.; Font, D.; Pericàs, M. A., Assessing the Suitability of 1,2,3-Triazole Linkers for Covalent Immobilization of Chiral Ligands: Application to Enantioselective Phenylation of Aldehydes., *J. Org. Chem*., **2007**, *72* (7), 2460-2468.

(473) Badèche, S.; Daran, J.; Ruiz, J.; Astruc, D., Synthesis and Coordination Chemistry of Ferrocenyl-1,2 ,3-Triazolyl Ligands., *Inorg. Chem*., **2008**, *47* (11), 4903-4908.

(474) Urankar, D.; Pinter, B.; Pevec, A.; De Proft, F.; Turel, I.; Košmrlj, J., Click-Triazole N2 Coordination to Transition-Metal Ions Is Assisted by a Pendant Pyridine Substituent., *Inorg. Chem*., **2010**, *49* (11), 4820-4829.

(475) Hans, M.; Lorkowski, J.; Demonceau, A.; Delaude, L., Efficient Synthetic Protocols for the Preparation of Common N-Heterocyclic Carbene Precursors., *Beilstein J. Org. Chem*., **2015**, *11*, 2318-2325.

(476) Gründemann, S.; Kovacevic, A.; Albrecht, M.; Faller, J. W. R.; Crabtree, H., Abnormal Binding in a Carbene Complex Formed from an Imidazolium Salt and a Metal Hydride Complex., *Chem. Commun*., **2001**, *1* (21), 2274-2275.

(477) Schuster, O.; Yang, L.; Raubenheimer, H. G.; Albrecht, M., Beyond Conventional N-Heterocyclic Carbenes: Abnormal, Remote, and Other Classes of NHC Ligands with Reduced Heteroatom Stabilization., *Chem. Rev*., **2009**, *109* (8), 3445-3478.

(478) Mathew, P., Neels, A., Albrecht, M., 1,2,3-Triazolylidenes as versatile abnormal carbene ligands for late transition metals., *J. Am. Chem. Soc*., **2008**, *130*(41), 13534-13535.

(479) Schaper, L. A.; Ofele, K.; Kadyrov, R.; Bechlars, B.; Drees, M.; Cokoja, M.; Herrmann, W. A.; Kühn, F. E., N-Heterocyclic Carbenes via Abstraction of Ammonia: 'Normal' Carbenes with

'Abnormal' Character., *Chem. Commun*., **2012**, *48* (32), 3857-3859.

(480) Schaper, L. A.; Graser, L.; Wei, X.; Zhong, R.; Öfele, K.; Pöthig, A.; Cokoja, M.; Bechlars, B.; Herrmann, W. A.; Kühn, F. E., Exploring the Scope of a Novel Ligand Class: Synthesis and Catalytic Examination of Metal Complexes with "normal" 1,2,3-Triazolylidene Ligands., *Inorg. Chem*., **2013**, *52* (10), 6142-6152.

(481) Aromí, G.; Barrios, L. A.; Roubeau, O.; Gamez, P., Triazoles and Tetrazoles: Prime Ligands to Generate Remarkable Coordination Materials., *Coord. Chem. Rev*., **2011**, *255* (5-6), 485-546.

(482) Hao, E.; Wang, Z.; Jiao, L.; Wang, S., "Click" Tetradentate Ligands., *Dalt. Trans*., **2010**, *39* (10), 2660-2666.

(483) Correa, A.; Mancheño, O. G.; Bolm, C., Iron–Catalysed Carbon–Heteroatom and Heteroatom–Heteroatom Bond Forming Processes., *Chem. Soc. Rev*., **2008**, 37 (6), 1108-1117.

(484) Talsi, E.P.; Bryliakov, K.P., Chemo- and Stereoselective CH Oxidations and Epoxidations/Cis-Dihydroxylations with H_2O_2, Catalyzed by Non-Heme Iron and Manganese Complexes., *Coord. Chem. Rev*., **2012**, *256* (13-14), 1418-1434.

(485) Yan, W.; Ye, X.; Akhmedov, N. G.; Petersen, J. L.; Shi, X., 1,2,3-Triazole: Unique Ligand in Promoting Iron-Catalyzed Propargyl Alcohol Dehydration., *Org. Lett*., **2012**, *14* (9), 2358-2361.

(486) Chan, T. R.; Hilgraf, R.; Sharpless, K. B.; Fokin, V. V., Polytriazoles as Copper(I)-Stabilizing Ligands in Catalysis., *Org. Lett*., **2004**, *6* (17), 2853-2855.

(487) Donnelly, P.S.; Zanatta, S.D.; Zammit, S.C.; White, J.M.; Williams, S.J., "Click" Cycloaddition Catalysts: Copper(I) and Copper(II) Tris(TriazolylmethyI)Amine Complexes., *Chem. Commun*., **2008**, *233* (21), 2459-2461.

(488) Coelho, A.; Diz, P.; Caamaño, O.; Sotelo, E., Polymer-Supported 1,5,7-Triazabicyclo [4.4.0] Dec-5-Ene as Polyvalent Ligands in the Copper-Catalyzed Huisgen 1,3-Dipolar Cycloaddition., *Adv. Synth. Catal*., **2010**, *352* (7), 1179-1192.

(489) Nakamura, T.; Terashima, T.; Ogata, K.; Fukuzawa, S. I., Copper(I) 1,2,3-Triazol-5-Ylidene Complexes as Efficient Catalysts for Click Reactions of Azides with Alkynes., *Org. Lett*., **2011**, *13* (4), 620-623.

(490) Saleem, F.; Rao, G. K.; Kumar, A.; Mukherjee, G.; Singh, A. K., Half-Sandwich Ruthenium(II) Complexes of Click Generated 1,2,3-Triazole Based Organosulfur/-Selenium Ligands: Structural and Donor Site Dependent Catalytic Oxidation and Transfer Hydrogenation Aspects., *Organometallics*, **2013**, *32* (13), 3595-3603.

(491) Zhang, Y.; Chen, C.; Ghosh, S. C.; Li, Y.; Hong, S. H., Weil-Defined N-Heterocyclic Carbene Based Ruthenium Catalysts for Direct Amide Synthesis from Alcohols and Amines., *Organometallics*, **2010**, *29* (6), 1374-1378.

(492) Prades, A.; Peris, E.; Albrecht, M., Oxidations and Oxidative Couplings Catalyzed by Triazolylidene Ruthenium Complexes., *Organometallics*, **2011**, *30* (5), 1162-1167.

(493) Astruc, D.; Heuzé, K.; Gatard, S.; Méry, D.; Nlate, S.; Plault, L., Metallodendritic Catalysis for Redox and Carbon-Carbon Bond Formation Reactions: A Step towards Green Chemistry., *Adv. Synth. Catal*., **2005**, *347* (2-3), 329-338.

(494) Suzuki, A., Cross-Coupling Reactions of Organoboranes: An Easy Way to Construct C-C Bonds (Nobel Lecture)., *Angew. Chemie - Int. Ed*., **2011**, *50* (30), 6722-6737.

(495) Lebel, H.; Janes, M. K.; Charette, A. B.; Nolan, S. P., Structure and Reactivity of “Unusual” N-Heterocyclic Carbene (NHC) Palladium Complexes Synthesized from Imidazolium Salts., *J. Am. Chem. Soc.*, **2004**, *126* (16), 5046-5047.

(496) Gu, S.; Xu, H.; Zhang, N.; Chen, W., Triazole-Functionalized N-Heterocyclic Carbene Complexes of Palladium and Platinum and Efficient Aqueous Suzuki-Miyaura Coupling Reaction., *Chem. - An Asian J*., **2010**, *5* (7), 1677-1686.

(497) Amadio, E.; Bertoldini, M.; Scrivanti, A.; Chessa, G.; Beghetto, V.; Matteoli, U.; Bertani, R.; Dolmella, A., Synthesis, Crystal Structure, Solution Behavior and Catalytic Activity of a Palladium(II)-Allyl Complex Containing a 2-Pyridyl-1,2,3-Triazole Bidentate Ligand., *Inorg. Chim. Acta*, **2011**, *370* (1), 388-393.

(498) Verma, A.K.; Jha, R.R.; Chaudhary, R.; Tiwari, R.K.; Danodia, A.K., 2-(1-Benzotriazolyl)Pyridine: A Robust Bidentate Ligand for the Palladium-Catalyzed C-C (Suzuki, Heck, Fujiwara-Moritani, Sonogashira), C-N and C-S Coupling Reactions., *Adv. Synth. Catal*., **2013**, *355* (2-3), 421-438.

(499) Detz, R. J.; Heras, S. A.; De Gelder, R.; Van Leeuwen, P. W. N. M.; Hiemstra, H.; Joost, N.; Reek, H.; Van Maarseveen, J. H., “Clickphine”; a Nowel and Highly Versatile P,N Ligand Class via Click Chemistry, *Org. Lett*., **2008**, *10* (6), 1323.

(500) Saravanakumar, R.; Ramkumar, V.; Sankararaman, S., Synthesis and Structure of 1,4-Diphenyl-3-Methyl-1,2,3-Triazol-5-Ylidene Palladium Complexes and Application in Catalytic Hydroarylation of Alkynes., *Organometallics*, **2011**, *30* (6), 1689-1694.

(501) Canseco-Gonzalez, D.; Gniewek, A.; Szulmanowicz, M.; Müller-Bunz, H.; Trzeciak, A. M.; Albrecht, M., PEPPSI-Type Palladium Complexes Containing Basic 1,2,3-Triazolylidene Ligands

and Their Role in Suzuki-Miyaura Catalysis., *Chem. - A Eur. J.*, **2012**, *18* (19), 6055-6062.

(502) Keske, E. C.; Zenkina, O. V.; Wang, R.; Crudden, C. M., Synthesis and Structure of Silver and Rhodium 1,2,3-Triazol-5-Ylidene Mesoionic Carbene Complexes., *Organometallics*, **2012**, 31 (1), 456-461.

(503) Brunel J. M. BINOL: a versatile chiral reagent., *Chem. Rev.*, **2005**, *105* (3), 857-897.

(504) Liu, B.; Jiang, F. Y.; Song, H. Bin; Li, J. S., A Novel Trinuclear Titanium(IV) Complex with a C3 Axis along Ti1-Ti2-Ti3 Containing 3-[(1H-1,2,4-Triazol-1-Yl)Methyl]-BINOLate Ligands: Synthesis, Structure, and Reactivity., *Tetrahedron Asym.*, **2006**, *17* (14), 2149-2153.

(505) Zurro, M.; Mancheño, O.G., 1,2,3,–Triazole-Based Catalysts: From Metal- to Supramolecular Organic Catalysis., *Chem. Rec.*, **2017**, *17* (5), 485-498.

(506) Pu, L.; Yu, H. Bin., Catalytic Asymmetric Organozinc Additions to Carbonyl Compounds., *Chem. Rev.*, **2001**, *101* (3), 757-824.

(507) Neel, A.J.; Hehn, J.P.; Tripet, P.F.; Toste, F.D., Asymmetric Cross-Dehydrogenative Coupling Enabled by the Design and Application of Chiral Triazole-Containing Phosphoric Acids., *J. Am. Chem. Soc.*, **2013**, *135* (38), 14044-14047.

(508) Ohmatsu, K.; Kiyokawa, M.; Ooi, T., Chiral 1,2,3-Triazoliums as New Cationic Organic Catalysts with Anion-Recognition Ability: Application to Asymmetric Alkylation of Oxindoles., *J. Am. Chem. Soc.*, **2014**, *136* (31), 11195.

(509) Beckendorf, S.; Asmus, S.; Mück-Lichtenfeld, C.; García Mancheño, O., “Click” Bis-Triazoles as Neutral C-H···anion-Acceptor Organocatalysts., *Chem. - A Eur. J.*, **2013**, *19* (5), 1581-1585.

(510) Zhang, Z.; Schreiner, P. R., (Thio)Urea Organocatalysis-What Can Be Learnt from Anion Recognition?, *Chem. Soc. Rev.*, **2009**, 38 (4), 1187-1198.

(511) Zhang, Z.; Lippert, K. M.; Hausmann, H.; Kotke, M.; Schreiner, P. R., Cooperative Thiourea-Brønsted Acid Organocatalysis: Enantioselective Cyanosilylation of Aldehydes with TMSCN., *J. Org. Chem.*, **2011**, *76* (23), 9764-9776.

(512) Meudtner, R. M.; Hecht, S., Helicity Inversion in Responsive Foldamers Induced by Achiral Halide Ion Guests., *Angew. Chemie - Int. Ed.*, **2008**, *47* (26), 4926-4930.

(513) Yamaguchi, J.; Yamaguchi, A. D.; Itami, K., C-H Bond Functionalization: Emerging Synthetic Tools for Natural Products and Pharmaceuticals., *Angew. Chemie - Int. Ed.*, **2012**, 51 (36), 8960-

9009.

(514) Chen, D. Y. K.; Youn, S. W., C-H Activation: A Complementary Tool in the Total Synthesis of Complex Natural Products., *Chem. - A Eur. J.*, **2012**, *18* (31), 9452-9474.

(515) Mc Murray, L.; O'hara, F.; Gaunt, M. J., Recent Developments in Natural Product Synthesis Using Metal-Catalysed C–H Bond Functionalisation., *Chem. Soc. Rev*., **2011**, *40* (4), 1885-1898.

(516) Dai, H. X.; Stepan, A. F.; Plummer, M. S.; Zhang, Y. H.; Yu, J. Q., Divergent C-H Functionalizations Directed by Sulfonamide Pharmacophores: Late-Stage Diversification as a Tool for Drug Discovery., *J. Am. Chem. Soc*., **2011**, *133* (18), 7222-7228.

(517) Meyer, C.; Neue, B.; Schepmann, D.; Yanagisawa, S.; Yamaguchi, J.; Würthwein, E. U.; Itami, K.; Wünsch, B., Exploitation of an Additional Hydrophobic Pocket of σ 1 Receptors: Late-Stage Diverse Modifications of Spirocyclic Thiophenes by C-H Bond Functionalization., *Org. Biomol. Chem*., **2011**, *9* (23), 8016-8029.

(518) Roger, J.; Gottumukkala, A. L.; Doucet, H., Palladium-Catalyzed C3 or C4 Direct Arylation of Heteroaromatic Compounds with Aryl Halides by C-H Bond Activation., *Chem.Cat.Chem*., **2010**, *2* (1), 20-40.

(519) List, B., The Direct Catalytic Asymmetric Three-Component Mannich Reaction, *J. Am. Chem. Soc.*, **2000**, *122*, 9336-9337.

(520) Yamasaki, S.; Iida, T.; Shibasaki, M., Direct Catalytic Asymmetric Mannich Reaction of Unmodified Ketones: Cooperative Catalysis of an AlLibis(Binaphthoxide) Complex and $La(OTf)_3 \cdot nH_2O$., *Tetrahedron*, **1999**, *55* (29), 8857-8867.

(521) List, B.; Pojarliev, P.; Biller, W. T.; Martin, H. J., The Proline-Catalyzed Direct Asymmetric Three-Component Mannich Reaction: Scope, Optimization, and Application to the Highly Enantioselective Synthesis of 1,2-Amino Alcohols., *J. Am. Chem. Soc*., **2002**, *124* (5), 827-833.

(522) Bahmanyar, S., Houk, K.N., The Origin of Stereoselectivity in Proline-Catalyzed Intramolecular Aldol Reactions, *J. Am. Chem. Soc*., **2001**, *123*, 12911-12912.

(523) Yamaguchi, M.; Yokota, N.; Minami, T., The Michael Addition of Dimethyl Malonate to α,β-Unsaturated Aldehydes Catalysed by Proline Lithium Salt., *J. Chem. Soc. Chem. Commun*., **1991**, *16*, 1088-1089.

(524) Yamaguchi, M.; Shiraishi, T.; Hirama, M., Asymmetric Michael Addition of Malonate Anions to Prochiral Acceptors Catalyzed by L-Proline Rubidium Salt., *J. Org. Chem*., **1996**, *61* (10), 3520-3530.

(525) Kozikowski, A.P., Mugrage, B.B., Synthesis of Optically Active Thiadecalins and Thiahydrindans by a Proline-Catalyzed Intramolecular Michael Reaction., *J. Org. Chem*., **1989**, *54* (10), 2274-2275.

(526) List, B.; Pojarliev, P.; Martin, H. J., Efficient Proline-Catalyzed Michael Additions of Unmodified Ketones to Nitro Olefins., *Org. Lett*., **2001**, *3* (16), 2423-2425.

(527) Enders, D.; Seki, A., Proline-Catalyzed Enantioselective Michael Additions of Ketones to Nitrostyrene., *Synlett*, **2002**, *1*, 26-28.

(528) Baumann, M.; Baxendale, I. R., An Overview of the Synthetic Routes to the Best Selling Drugs Containing 6-Membered Heterocycles., *Beilstein J. Org. Chem*., **2013**, *9*, 2265-2319.

(529) Zhang, C.; You, L.; Chen, C., Palladium-Catalyzed C-H Arylation of 1,2,3-Triazoles., *Molecules*, **2016**, *21* (10), 1-7.

(530) Slaitas, A.; Yeheskiely, E., A Novel N-(Pyrrolidinyl-2-Methyl)Glycine-Based PNA with a Strong Preference for RNA over DNA., *Eur. J. Org. Chem*., **2002**, *14*, 2391-2399.

(531) Boto, A.; Hernández, D.; Hernández, R.; Montoya, A.; Suárez, E., Synthesis of Alkaloid Analogues from β-Amino Alcohols by β-Fragmentation of Primary Alkoxyl Radicals., *Eur. J. Org. Chem*., **2007**, *2*, 325-334.

(532) Boyle, R.G, Walker, D.W., Boyce, R.J., Peterson, S., Farouz, F., Vo, C.H., (**2015**), *Pharmaceutical Compound*, WO2015120390A1.

(533) Antonioletti, R.; Bovicelli, P.; Malancona, S., A New Route to 2-Alkenyl-1,3-Dicarbonyl Compounds, Intermediates in the Synthesis of Dihydrofurans., *Tetrahedron*, **2002**, *58* (3), 589-596.

(534) Paryzek, Z.; Koenig, H.; Tabaczka, B., Ammonium Formate/Palladium on Carbon: A Versatile System for Catalytic Hydrogen Transfer Reductions of Carbon-Carbon Double Bonds., *Synthesis*, **2003**, *13*, 2023-2026.